HANFORD TANK WASTE REMEDIATION SYSTEM HIGH-LEVEL WASTE CHEMISTRY MANUAL

Prepared for

**Nuclear Regulatory Commission
Contract NRC-02-97-009**

Prepared by

**Roberto T. Pabalan
Mark S. Jarzemba
Teofilo A. Abrajano Jr.
David A. Pickett
D. Stan Moulton
Narasi Sridhar
James Weldy
Christopher S. Brazel
Joseph T. Persyn
Brian Li
J.P. Hsu
Jimell Erwin**

**Center for Nuclear Waste Regulatory Analyses
San Antonio, Texas**

Revision 1

June 1998

ABSTRACT

The U.S. Department of Energy (DOE) plans to privatize the waste treatment and immobilization operations of the Hanford Tank Waste Remediation System (TWRS) program. A Memorandum of Understanding has been established between the DOE and the Nuclear Regulatory Commission (NRC) for the first phase of the TWRS program. To assist the NRC in developing technical and regulatory tools for the TWRS privatization effort, the Center for Nuclear Waste Regulatory Analyses is providing the NRC with information and tools needed to assess the chemical, radiological, and criticality hazards of Hanford tank wastes and operations addressed under the privatization initiative. Of primary concern are those reactions that could occur during waste retrieval and processing, but potential reactions during continued interim storage are also important.

This report reviews the chemistry of processes that could lead to hazardous situations in the storage, retrieval, and processing of Hanford high-level wastes (HLWs). It summarizes the origin, as well as the physical characteristics and chemistry, of the tank wastes. The chemistry of tank wastes relevant to flammable gas generation is discussed, including the mechanisms of gas generation, flammability of gas mixtures, and factors affecting gas retention in and release from tank wastes. The chemistry of reactions relevant to Hanford organic-bearing wastes, including the sources and estimated current inventory of organic complexants and organic solvents in Hanford tanks, thermodynamic calculations and thermoanalytical measurements of reactions involving organics and oxidants, mechanisms that could result in locally elevated concentrations of organics, and organic degradation processes are reviewed. Ferrocyanide-scavenging operations conducted at the Hanford site and the chemistry relevant to ferrocyanide reactions, including ferrocyanide degradation mechanisms, are discussed. The chemistry of Hanford tank wastes relevant to criticality safety is reviewed, including parameters that affect criticality of HLW and mechanisms that could lead to concentration of fissile materials and neutron absorbers, and a relatively simple approach for determining when criticality should be further evaluated for specific Hanford TWRS operations is proposed. Information on radioactive decay that contributes to heat generation is summarized, and a simplified approach for calculating the volumetric heat generation rate of tank wastes based on known or assumed radionuclide inventories is described. Finally, process simulation software that could be useful in evaluating TWRS operations is reviewed, and examples of simulation of chemical processes relevant to the Hanford TWRS are described.

CONTENTS

CONTENTS (cont'd)

CONTENTS (cont'd)

CONTENTS (cont'd)

CONTENTS (cont'd)

Section   Page

FIGURES

FIGURES (cont'd)

FIGURES (cont'd)

FIGURES (cont'd)

TABLES

TABLES (cont'd)

ABBREVIATIONS, SYMBOLS, AND ELEMENTS

Ag	Silver
Å	Angstrom
Al	Aluminum
Am	Americium
As	Arsenic
B	Boron
Ba	Barium
Be	Beryllium
Bi	Bismuth
Bq	Becquerel
Btu	British thermal unit
C	Carbon
C	Celsius
Ca	Calcium
cal	Calories
Cd	Cadmium
Ce	Cerium
Ci/g	Curies per gram
Ci/L	Curies per liter
Ci/m^3	Curies per cubic meter
Cl	Chlorine
cm	Centimeters
Co	Cobalt
cP	Centipoise
Cr	Chromium
Cs	Cesium
Cu	Copper
dpm	Disintegrations per minute
Dy	Dysprosium
eV	Electronvolt
Er	Erbium
Eu	Europium
F	Fahrenheit
F	Fluorine
Fe	Iron
ft/sec	Feet per second
g	Gram
gal.	Gallon
Gd	Gadolinium
Ge	Germanium
gpm	Gallons per minute
H	Hydrogen
Hg	Mercury
Ho	Holmium
hr	Hour

ABBREVIATIONS, SYMBOLS, AND ELEMENTS (cont'd)

Hz	Hertz
I	Iodine
In	Indium
K	Potassium
K	Degrees Kelvin
k_{eff}	Criticality safety factor
kg	Kilogram
kV	Kilovolts
kW	Kilowatt
L	Liter
La	Lanthanum
Li	Lithium
m	Meter
m	Molal (moles per kilogram of water)
M	Molar (moles per liter of solution)
MeV	Million electron volts
Mg	Magnesium
mg	Milligram
mL	Milliliter
Mn	Manganese
Mo	Molybdenum
mRem/hr	Millirem per hour
MT	Metric Ton
MW	Megawatt
N	Nitrogen
Na	Sodium
Nb	Niobium
nCi	NanoCurie
Nd	Neodymium
Ni	Nickel
Np	Neptunium
O	Oxygen
P	Phosphorus
Pa	Pascal
Pb	Lead
pCi	PicoCurie
Pd	Palladium
Pm	Promethium
ppm	Parts per million
Pr	Protactinium
psi	Pounds per square inch
Pu	Plutonium
Rad	Radiation absorbed dose
Rb	Rubidium
Re	Rhenium

ABBREVIATIONS, SYMBOLS, AND ELEMENTS (cont'd)

rem/hr	Roentgen equivalent man per hour
Rh	Rhodium
R/hr	Rad per hour
Ru	Ruthenium
s	Second
S	Sulphur
Sb	Antimony
Se	Selenium
Si	Silicon
Sm	Samarium
Sn	Tin
Sr	Strontium
Ta	Tantalum
Tb	Terbium
Tc	Technetium
Te	Tellurium
Th	Thorium
Ti	Titanium
Tl	Thallium
Tm	Thulium
U	Uranium
V	Vanadium
W	Watt
W	Tungsten
wt %	Percent by weight
Y	Yttrium
Zn	Zinc
Zr	Zirconium
μ	Micro

ACKNOWLEDGMENTS

QUALITY OF DATA: Sources of data are referenced in each chapter. The respective sources of non-CNWRA data should be consulted for determining their levels of quality assurance.

ANALYSES AND CODES: The computer software MCNP, Version 4A, and Environmental Simulation Program (ESP), Version 6, were used in analyses contained in this report. These are commercial software and only object codes are available to the CNWRA. MCNP and ESP are classified in Technical Operating Procedure (TOP)-018, Development and Control of Scientific and Engineering Software, as acquired/existing software that are required to be under CNWRA control. MCNP, Version 4A, is presently under CNWRA configuration control; ESP is currently being placed under TOP-018 control.

EXECUTIVE SUMMARY

The U.S. Department of Energy (DOE) established the Tank Waste Remediation System (TWRS) program at the Hanford site in 1991 to manage the maintenance and cleanup of radioactive waste contained in 177 aging underground storage tanks. The DOE is legally bound to remediate the waste tanks under the Tri-Party Agreement and plans to privatize the waste treatment and immobilization operations of the TWRS program. The privatization process is divided into Phase I, a proof-of-concept phase, and Phase II, a full-scale operations phase. A Memorandum of Understanding has been established between the DOE and the Nuclear Regulatory Commission (NRC) which provides for the NRC to acquire sufficient knowledge of the physical and operational situation at the Hanford waste tanks and the processes, technology, and hazards involved in Phase I activities to enable the NRC to (i) assist the DOE in performing reviews consistent with the NRC regulatory approach and (ii) be prepared to develop an effective regulatory program for the possible licensing of DOE contractor-owned and contractor-operated facilities during Phase II.

To support the NRC in developing technical and regulatory tools for the TWRS privatization effort, a program was established at the Center for Nuclear Waste Regulatory Analyses (CNWRA). A broad objective of CNWRA activities is to provide NRC staff with information and tools needed to assess the chemical, radiological, and criticality hazards of Hanford tank waste remediation system operations addressed under the privatization initiative. A specific objective is to provide the NRC with a reference manual that discusses possible chemical reactions and processes that could lead to hazardous situations, and information and tools available to evaluate these reactions.

Of primary concern, particularly in the context of the regulatory role of the NRC, are reactions that could occur during waste retrieval and processing, as well as during continued interim storage, that could result in radiological risks to the public and workers and to potential release of radioactivity to the environment. For example, the DOE has developed a set of criteria to identify tanks with potential safety concerns during interim storage of wastes as Watch-list tanks. The four Watch-list categories are flammable/hydrogen gas, high organic content, ferrocyanide, and high-heat load. The safety issue associated with the Flammable/Hydrogen Gas Watch-list pertains to the release of flammable gases, mostly hydrogen generated by radiolytic and thermochemical mechanisms, into the dome space of the waste tanks. If ignited, the resulting reactions could cause a radioactive release or provide an energy source that could facilitate other reactions within the tank. The safety concern with respect to the High Organic Content Watch-list tanks is the potential for rapid energetic reactions between organic compounds (fuel) and sodium nitrate/nitrite (oxidant) present in Hanford wastes that could release radioactivity to the environment. The tanks on the Ferrocyanide Watch-list contain sodium or potassium ferrocyanide, which had been added to the waste to scavenge Cs-137, that could explode in the presence of oxidizing materials, such as nitrates or nitrites, if heated to high temperatures or if exposed to an electrical spark of sufficient energy. One tank is on the High-Heat Load Watch-list because of concerns about elevated temperatures from radioactive decay heat of stored waste, primarily Cs and Sr, that can lead to overheating of the waste tank concrete structure and to releasing high-level nuclear waste to the surrounding soil and groundwater. In all, 38 tanks are currently on various Watch-lists, some in more than one Watch-list category. Specifically, 25 tanks are on the Flammable/Hydrogen Gas Watch-list, 20 tanks are on the High Organic Content Watch-list, and one tank is on the High-Heat Load Watch-list. All tanks that were on the Ferrocyanide Watch-list have been removed from the list (Hanlon, 1997).

Although a major part of the information presented in this report is based on published DOE studies relevant to interim storage of high-level waste (HLW) in the Hanford tanks, safety issues associated with tank storage

of wastes are relevant to the retrieval and processing stages of Hanford TWRS operations. For example, chemical reactions resulting in generation of flammable gases and the attendant risk associated with those gases are expected to continue through some stages of waste retrieval and processing. Similarly, exothermic reactions involving organics and nitrates/nitrites will likely remain a possibility unless pretreatment methods are used to eliminate organics from Hanford wastes. High-heat generation will also need to be considered for those wastes or waste feeds with high concentrations of Sr-90 or Cs-137. Moreover, the chemistry of processes specific to retrieval and pretreatment technologies is the subject of a future CNWRA report.

Introduction

In chapter 1 of this report, the origin, physical characteristics, and chemistry of the Hanford tank wastes are briefly summarized. The wastes have been produced over a long period of time by a variety of processes. The primary source is the historical irradiation of metallic uranium fuel and extraction of plutonium from the irradiated fuel through various processes. The Hanford wastes, at the time they were generated, were highly radioactive, acidic liquids that generated heat and required remote handling behind heavy shielding in corrosion-resistant vessels, usually made of stainless steel. Because stainless steel was in short supply when the first storage tanks were built, the wastes were stored in carbon-steel tanks after addition of sodium hydroxide to neutralize the waste and of sodium nitrite for corrosion control. Approximately 1,500,000 m^3 (400 million gal.) of waste were generated from chemical processing at the Hanford site, and more than 1,100,000 m^3 (300 million gal.) of these were sent to underground storage tanks. Through evaporation, concentration, and the past practice of discharging dilute waste to the ground, the waste volume has been reduced to approximately 208,000 m^3 (55 million gal.).

The tanks contain complex mixtures of solids — sludge or saltcake — and liquids — supernatant or interstitial. Of the 132,000 m^3 (35 million gal.) of waste in single-shell tanks (SSTs), 66 percent is wet saltcake and 34 percent is sludge. The SST wastes are 90 percent sodium nitrates and nitrites, and radioactivity is dominated by Sr-90 (75 percent) and Cs-137 (24 percent). Because wastes in double-shell tanks (DSTs) are dominated by supernatant liquids transferred from SSTs, the 76,000 m^3 (20 million gal.) of DST waste are 85 percent water. The waste is thus dominated by liquids and slurries, sometimes with a bottom layer of sludge. The DST wastes are also composed mainly of sodium nitrates and nitrites, and radioactivity is dominated by Cs-137 (72 percent) and Sr-90 (27 percent). The overall site inventories of organic waste constituents show that, on a molar basis, glycolate is the predominant organic complexant, and other organic species — citrate, ethylenediaminetetra-acetic acid (EDTA), N-(2-hydroxyethyl)ethylenediaminetetra-acetate (HEDTA), acetate, oxalate, dibutyl phosphate (DBP), and butane—all have similarly low molar concentrations. On a weight basis, glycolate is rivaled in abundance by HEDTA. There are no major differences in organic inventories between SSTs and DSTs. The key radionuclides for risk assessment at the Hanford site are C-14, Sr-90, Tc-99, I-129, Cs-137, and U. The two radionuclides Sr-90 and Cs-137 have long enough half-lives that make them the dominant sources of radioactivity exposure and heat generation hazard during waste retrieval and solidification. Consideration of longer term risk centers on those radionuclides — C-14, I-129, Tc-99, and U isotopes — that are deemed mobile in groundwater and have sufficiently long half-lives to persist well into the future. The longer term risk pertains to on-site storage of waste forms prior to disposal in a geologic repository and residual waste remaining in the tanks subsequent to remediation.

Tank waste inventories are derived in large part from reconstructions of waste histories, which precludes attaching a high degree of certainty to the estimated inventory because records on the contents and volumes of wastes transferred to the tanks are typically incomplete or nonexistent. Agnew (1997) calculated estimated

uncertainties in concentrations based on variability in knowledge of process and solubilities, and the resultant variabilities for individual tanks ranged up to nearly 100 percent of reported concentrations, though most appear to be in the range of 10 to 50 percent. Tank waste inventory characterization is being undertaken at Hanford to produce a "best-basis" inventory that draws on all available information from estimation methods and tank waste sample measurements. This work is still in progress, and the most recent results may be viewed online at the Pacific Northwest National Laboratory Tank Waste Information Systems web site at http://twins.pnl.gov:8001/TCD/main.html. However, until completion of this best-basis inventory, use of the HDW model (Agnew, 1997) may be preferred.

Uncertainties in tank waste inventories and disparities in waste content between the different tanks may affect the chemical safety and the processing of the wastes. For example, knowledge of the chemical and physical properties of the wastes is needed to determine what, if any, actions are required to assure safe interim storage, retrieval, or processing of each waste tank. Quantification of major organic constituents is needed to evaluate potential hazards associated with flammable gases and oxidizable organic constituents. Similarly, data on the content, distribution, and form of fissile material would be useful for criticality safety analysis. In addition, information concerning the chemical forms and concentrations of matrix components and their radioactive constituents is necessary before adequate waste consolidation protocols and/or separations processes can be engineered. Furthermore, uncertainties in the concentrations of glass-insoluble phases, such as chrome minerals, spinels, and noble metals, may lead to the need for blending different waste types and/or increasing the volume of glass waste forms, both of which are expensive. Also, the presence of a large number of possible solid phases and of aqueous complexants, and the high ionic strength of the waste solutions make it extremely difficult to determine and predict the distribution of radionuclides between the sludges, suspended solids, and aqueous supernatants. Such a lack of fundamental knowledge about the distribution of radionuclides in the HLW stream significantly impacts the numbers of glass logs requiring disposal and as a result the ultimate HLW disposal cost. The large disparity in the tank waste inventories indicates that significant mixing of tank contents is needed to meet the specified waste envelopes. Mixing of tank wastes may result in additional safety hazards through various chemical reactions that are discussed in detail in subsequent chapters. Thus, it is clear that better information on waste constituents in individual tanks is needed.

Chemistry Relevant to Flammable Gas Generation

In chapter 2, topics relevant to flammable gas generation are discussed, including mechanisms of gas generation in Hanford tank wastes, flammability of gas mixtures, and factors affecting gas retention and release in tank wastes. Flammable gas mixtures are generated in Hanford tank wastes by complex chemical reactions arising from radiolysis of water, thermal and radiological decomposition of organic compounds, and corrosion of metallic tank walls. The gases generated by these reactions comprise mainly hydrogen, nitrous oxide, nitrogen, and ammonia, with smaller amounts of methane and other hydrocarbons. In most tanks, the flammable gas generated in the waste is continuously released to the tank headspace. Various studies indicate that the generation rate is so low that ventilation ordinarily is able to keep the flammable gas diluted far below the concentration necessary for ignition. However, some wastes may have enough retained gas to pose a potential for worker injury, damage to equipment, or release of radionuclides to the environment if a significant fraction of the gas were suddenly released into the headspace of storage or process tanks, transfer lines, and process equipment (e.g., pumps) and ignited. The potential for such releases to cause undesirable consequences constitutes the flammable gas safety issue. Even very small releases can collect in equipment or in poorly ventilated tanks and result in a flammable gas hazard.

The evaluation of flammable gas safety issue with respect to continued tank storage or to retrieval and processing of Hanford wastes must consider the cause-and-effect relationship of gas generation, retention, and release. Gas generation must be understood well enough to estimate the generation rate and relative gas composition. Understanding gas retention (i.e., the volume and composition of gas trapped in the waste) is necessary to determine the possible likelihood, rate, and amount of gas release. Gas release represents the proximate hazard; flammable gas cannot create consequences until it is actually released in a closed volume. If the concentration locally exceeds the lower flammability limit and a source of ignition is present at that location, that flammable portion could burn. Damage caused by the elevated pressures in the headspace or other enclosed spaces could result from such a burn and could result in release of radionuclides to the environment.

Various studies during the past few years have provided information on the mechanisms of flammable gas generation, retention, and release. Based on these studies, the three most important gas generation mechanisms are believed to be (i) radiolytic decomposition of water and some organic species, (ii) chemical reactions, mainly involving organics, and (iii) corrosion of the steel tank walls. The first two dominate, and the yield from chemical reactions usually exceeds that from radiolysis, especially at higher temperatures. Several mechanisms may cause gas retention in tank wastes, but gas bubble retention is the primary mechanism for storing large quantities of flammable gases in tank waste that could be released rapidly. Large amounts of soluble gases, mainly ammonia, can also be retained in tank waste, but no credible mechanism for spontaneous release of large amounts of dissolved gas has been identified. Gas release mechanisms currently considered most credible are the buoyancy-induced displacement, percolation of dendritic bubbles, and mechanical disruption, which includes local penetration (e.g., core sampling), removal of waste by salt-well pumping or sluicing, and severe earthquakes. Only buoyant displacement and seismic disruption are believed capable of a rapid release of a major portion (~50 percent) of the stored gas volume. However, energetic displacement can only occur in tanks with a relatively deep layer of supernatant liquid, a condition that exists only in DSTs. No known mechanism for large spontaneous releases in SSTs has been identified.

Some form of flammability control will always be needed to ensure safe operation during continued tank storage of Hanford wastes and during the TWRS operations. For example, sufficient ventilation must be provided to ensure that flammable gases are maintained at a safe level within the headspace of storage or feed tanks, transfer lines, or process equipment. However, controls need to be applied in a graded manner based on the type of activity being conducted. To identify the proper controls required for specific systems of interest, an adequate understanding of the processes and mechanisms for flammable gas generation, retention, and release is necessary.

Chemistry Relevant to Energetic Reactions Involving Organic Complexants and Organic Solvents

Chapter 3 discusses the chemistry of reactions relevant to Hanford organic-bearing wastes, including the sources and estimated current inventory of organic complexants and organic solvents in Hanford tanks, thermodynamic calculations and thermoanalytical measurements of reactions involving Hanford organics and oxidants, mechanisms that could result in locally elevated concentrations of Hanford organics, and organic degradation processes. The presence in Hanford wastes of various organic compounds mixed with oxidizing sodium nitrate and nitrite salts and heat-producing radionuclides is a major safety concern because a potential exists for rapid exothermic reactions that could result in radioactive release to the environment. Such a reaction resulted in a major explosion in a radioactive waste tank in Kyshtym, U.S.S.R. in 1957. The possibility of chemical reactions involving organic compounds is a safety concern at Hanford, not only during continued interim storage of tank wastes, but also during the retrieval, processing, and solidification stages of the TWRS operations.

To assess potential hazards, determination of energies that could be released during chemical reactions involving oxidizable organic compounds is necessary. Heat or energy releases for different reaction pathways and end-products can be estimated using thermodynamic calculations. Calculations discussed in the chapter show that maximum energy is released by organic reactions with nitrates and nitrites when the reaction products are N_2, Na_2CO_3, H_2O, and CO_2. The reaction is more energetic if $NaNO_2$ is the oxidant instead of $NaNO_3$. Production of N_2O in place of N_2, or of CO in place of CO_2, greatly lowers the energy released. In alkaline pH conditions typical of Hanford tank wastes, CO_2 produced from organic oxidation reactions form Na_2CO_3 and H_2O, resulting in more exothermic heat. It should be emphasized, however, that thermodynamic calculations only provide bounding values for energy released from oxidation reactions. With fast exothermic reactions, equilibria will probably not occur and several reaction paths may be taken simultaneously with less total energy being produced. Nevertheless, maximum values calculated by thermodynamic means are useful as conservative estimates of energies that could be released and temperatures that could be achieved during oxidation of tank waste organics.

Thermoanalytical techniques used in the chemical industry for chemical hazards evaluation have been employed in DOE studies to measure the thermal sensitivities and the thermochemical and thermokinetic properties of organic and oxidant mixtures relevant to Hanford organic-bearing wastes. These studies indicate that energetic, self-sustaining exothermic reactions can occur among the salts of acetate, citrate, formate, oxalate, EDTA, and HEDTA, and the oxidants nitrate and nitrite if heated to a sufficiently high temperature under adiabatic conditions. There are significant differences in the thermal reactivities and sensitivities of the organic compounds. The amount of heat produced is dependent on the nature of the organic, with minimal dependence on the organic concentration (per gram of organic salt). The heat produced by reaction of equimolar sodium nitrate and nitrite with the different organics increased in the order Na_3HEDTA>citrate>Na_4EDTA, which is not consistent with the thermodynamically predicted order Na_3HEDTA>Na_4EDTA>citrate. This inconsistency suggests that the actual reaction pathways differ from those postulated strictly from thermodynamic considerations. The observed production of N_2O instead of N_2, and the less-than-theoretical-maximum heats measured by calorimetric techniques also indicate that the exothermic reactions between the organics and oxidants proceed, at least partially, through pathways that produce less than the maximum thermodynamically possible heat. Consequently, hazard assessments using the maximum thermodynamically based energetics will likely overestimate the consequences of a reaction. In addition, the measured activation energies indicate that there is a relatively high energy barrier to the initiation of these reactions. Thus, high temperatures are likely required to initiate the organic oxidation reactions.

The DOE measurements of onset temperatures indicate that the relative order with respect to thermal sensitivity is $Na_3HEDTA \geq$ citrate > formate $\geq Na_4EDTA$ > acetate > oxalate. This relative order indicates that acetate is generally a less conservative model for the organics used at Hanford with respect to susceptibility to hazardous chemical reactions. It also indicates that organic-bearing wastes containing Na_3HEDTA and citrate should be of greatest concern. In addition, the thermoanalytical studies show that the controlling oxidation reaction is that of nitrite with the organic compound. The exothermic onset temperature of mixtures containing only nitrite are similar to that of equimolar sodium nitrate/nitrite mixtures. Reaction mixtures that contain only nitrate have onset temperatures that are considerably higher and, hence, are more stable.

It should be noted that the DOE thermoanalytical studies used simple organic/oxidant mixtures, whereas Hanford tank waste chemistry is much more complex than those considered in the studies. Engineering analyses to assess the thermal hazards associated with the organic-bearing wastes need to consider the

concentration of waste constituents other than the organics and oxidants. The greater reactivity exhibited by the simulated sludge waste compared to the other surrogate waste mixtures suggests that caution must be used in extrapolating the behavior of waste simulants to that of actual wastes with more complex compositions. It is possible that actual Hanford wastes may be more reactive due to the presence of thermally more sensitive organics, the presence of transition metal ions that could act as catalysts, or to synergistic interactions between the organics.

A concern regarding Hanford tank wastes is the possibility of organic concentrations and quantities being elevated to sufficiently high levels as to create a hazard that would not be anticipated if average tank values are used in the analysis. Two processes that could be important are organic concentration in the liquid phase and precipitation of organic compounds in the solid phase. Many of the organic compounds added to the Hanford waste tanks are quite insoluble in water and, depending on the quantity added to a specific tank, it is possible to form a separate organic phase in the tank. The hydrocarbon solvents are the most likely to have been added to the tanks in sufficient volume to create a separate organic layer, as evidenced by the observed presence of a separate organic layer in tank C-103 believed to be predominantly normal paraffinic hydrocarbons and tributyl phosphate. Precipitation of organic compounds from concentrated wastes can result in locally high concentrations of fuel and produce solids with organic-to-oxidant ratios significantly different from the waste tank average value. Organics could form solid mixtures with $NaNO_3$-$NaNO_2$ either by coprecipitation or by drainage of the bulk aqueous phase followed by evaporation of $NaNO_3$-$NaNO_2$-containing interstitial liquid in the already precipitated organics. The Hanford chemicals that could concentrate by this mechanism are the polar, water-soluble compounds that can form metal salts, including sucrose that was used for denitration, and a large number of organic acids or their sodium salts, such as oxalic acid, glycolic acid, citric acid, tartaric acid, gluconic acid, EDTA and HEDTA, that were used for complexation or pH control.

A numerical criterion, based on measured organic fuel content [in terms of total organic carbon, (TOC)] and moisture concentration, is currently used by the DOE to categorize an organic-bearing tank as safe, conditionally safe, or unsafe. For zero free-moisture content, a minimum of 4.5 wt % TOC is considered necessary for a sustained propagating reaction. Higher TOC is required for a propagating reaction to occur if water is present because it dampens organic reactions. DOE tests indicate that about 20 wt % moisture is sufficient to eliminate the potential for sustained combustion altogether independent of fuel type and concentration. Although the criterion was derived for safety assessment of waste storage in Hanford tanks, the same criterion may be useful for evaluating the safety of organic-bearing wastes during the retrieval and processing stages of the Hanford TWRS. Also, the potential of the waste to dry out and thus become unsafe during continued storage or during TWRS processing will need to be evaluated.

An important consideration in safety analysis of organic-bearing Hanford wastes is the degradation of organic constituents. The wastes have been exposed to radiation, temperatures of 20 to 140 °C, and to a reactive chemical environment having high concentrations of active components, including hydroxide, nitrate and nitrite, as well as transition metals that could act as catalysts for decomposition reactions. Various degradation or aging processes, through mechanisms discussed in detail in the chapter, have occurred that changed the nature and quantity of the organics in the tank wastes. Degradation eventually leads to the formation of very simple compounds, such as formate, oxalate, or carbonate, resulting in a net reduction in the amount of energy available for reaction. A decrease in fuel energy due to organic degradation is indicated by the low exothermic values obtained from calorimetric measurements on actual waste samples and by studies on organic speciation in Hanford wastes. However, although organic degradation results in lower

organic fuel value, concurrent production of flammable gas mixtures increases the potential for flammable gas hazard. Because the chemical environment of Hanford wastes is conducive to organic degradation reactions, flammable gas mixtures will likely remain a key safety issue throughout the TWRS operations.

Chemistry Relevant to Ferrocyanide Reactions

Chapter 4 describes ferrocyanide-scavenging operations conducted at the Hanford site and discusses the chemistry relevant to ferrocyanide reactions, including ferrocyanide degradation mechanisms. Although the ferrocyanide safety issue is considered closed by the DOE with respect to interim storage in Hanford tanks, residual exothermic activity might be initiated by solidification operations that can cause waste to be heated by an external source. Thus, the DOE may evaluate, on a case-by-base basis, the possibility and potential effects of a self-heating reaction involving ferrocyanides as part of the safety analysis of proposed retrieval and processing methods. The ferrocyanide safety issue arose because additional tank storage space for HLW was historically generated at the Hanford site by precipitating Cs-137 from tank waste liquids using sodium or potassium ferrocyanide and nickel sulfate and pumping the decontaminated liquids to disposal cribs. In implementing the scavenging process, approximately 140 metric tons (154 tons) of alkali-nickel ferrocyanide were added to waste that was later routed to 18 SSTs. Because the process precipitated ferrocyanide from solutions that had high concentrations of the oxidants nitrate and nitrite, an intimate mixture of ferrocyanides and oxidants is likely to exist in the ferrocyanide waste. The potential for an uncontrolled exothermic reaction was a concern because, in the laboratory, mixtures of ferrocyanides and nitrates or nitrites can be made to explode if heated to over 200 °C.

Studies by the DOE to evaluate the explosive hazard of ferrocyanide wastes showed that the ferrocyanide mixtures were not ignited by standard impact and friction sensitivity tests (Cady, 1992). An external heat source was required in the tests before any exothermic reaction could be observed. Thermal tests indicated major exotherms at temperatures above approximately 260 °C, suggesting the possibility of explosive reactions if mixtures of ferrocyanide and nitrate/nitrite are heated to high temperatures or if there is an electrical spark of sufficient energy to ignite a dry mixture.

Oxidation of ferrocyanide by nitrate and/or nitrite can result in a variety of reaction products with different reaction enthalpies. The most energetic, for a given amount of fuel, is one that produces nitrogen and carbon dioxide (or carbonate salt if there is sufficient hydroxide available to form it). The reaction energy is greatly reduced if a sizable fraction of the carbon goes to CO due to incomplete oxidation, or if appreciable oxides of nitrogen form. On the other hand, a change in the reacting ferrocyanide salt results in a much smaller change in energy released.

The range of compositions of ferrocyanide sludge capable of sustaining a propagating chemical reaction and the safety categories for storage of ferrocyanide wastes have been established by the DOE from experimental measurements supported by theoretical considerations. The theoretical analysis indicates that, for waste with 0 wt % free water, the minimum fuel concentration necessary to sustain a propagating reaction is about 8 wt % sodium nickel ferrocyanide. For waste with greater than 8 wt % sodium nickel ferrocyanide, the mass of free water required to quench reactions increases linearly with ferrocyanide concentration. This relationship can be approximated by a moisture concentration that increases linearly from 0 at 8 wt % $Na_2NiFe(CN)_6$ to 24 wt % water at a ferrocyanide concentration of 26 wt %. The results from theoretical analysis are conservative relative to the results of combustion experiments on mixtures of ferrocyanide waste simulants or pure sodium nickel ferrocyanide and nitrate/nitrite. Tests using the Reactive System Screening Tool (RSST) showed that a fuel concentration of about 15 wt % $Na_2NiFe(CN)_6$ was necessary to support a

propagating reaction, almost twice the 8 wt % theoretical criterion. Tube propagation tests supported the RSST results and also demonstrated that the ferrocyanide concentration required to support propagation increased with the water content of the sludge. A key finding of the tube propagation test is that propagation ceased when the free water concentration was 12 wt % or more at a ferrocyanide concentration of 25.5 wt % (the highest concentration found in the waste simulants). This water concentration was roughly half of the theoretical moisture criterion (23 wt %) for a fuel value of 25.5 wt %. This difference was expected because the thermodynamic calculations are inherently conservative. The results regarding the effect of moisture on propagation are important. Studies indicate that ferrocyanide sludge in the Hanford waste tanks is wet and will stay wet. Dryout by pumping, leakage, hot spots, and surface evaporation has been considered and found to be negligible (Postma and Dickinson, 1995).

Some portion of the ferrocyanide waste in most of the Hanford tanks on the ferrocyanide Watch-list probably exceeded 8 wt % $Na_2NiFe(CN)_6$, the minimum fuel concentration considered necessary to sustain a propagating reaction, when it was originally established. However, ferrocyanide decomposition has resulted in current ferrocyanide concentrations substantially less than the estimated original concentrations. DOE experiments and results of tank waste characterization demonstrated that substantial ferrocyanide decomposition to chemicals that are either inert or have lower energy content has occurred. Degradation processes substantially lower the energy content of tank wastes and ultimately eliminate the hazards associated with ferrocyanide (Babad et al., 1993). The DOE studies showed that the rate of degradation is primarily a function of the waste temperature. Tank records indicate that most tanks were at a sufficiently high temperature for a sufficiently long time that significant aging would be expected. Tank sampling data and waste history data show that the ferrocyanide concentrations have decreased to levels lower than 8 wt % and that the ferrocyanide tanks should be categorized as safe based on the safety criteria established by the DOE.

In October 1996, the DOE closed out the ferrocyanide safety issue with respect to waste storage in Hanford tanks. However, evaluation of potential ferrocyanide reactions are planned on a case-by-case basis as part of the safety analysis of proposed retrieval and processing methods (Postma and Dickinson, 1995) because residual exothermic activity might be initiated by waste processing options that cause waste to be heated by an external source (e.g., during vitrification or other accidental circumstance). DOE studies regarding safety during continued storage of ferrocyanide wastes are also useful for safety analysis of the Hanford TWRS. The results regarding the effect of moisture on propagation are particularly important. Ferrocyanide-containing wastes are expected to contain sufficient moisture during the retrieval and pretreatment stages of the TWRS operations. For example, the low activity waste feed will have an insoluble solids fraction not exceeding 5 volume percent (U.S. Department of Energy, 1996b). Subsequent centrifugation will separate a fraction with a relatively high amount of entrained solids, perhaps to about 70 wt % insoluble solids. However, there may be no mechanism during the retrieval and pretreatment operations that could reduce the water content sufficiently to permit the sludge to become reactive. If such is the case, then ferrocyanide and nitrate/nitrite mixtures will likely not constitute a safety hazard during the TWRS operations.

Chemistry and Approximation Methods Relevant to Criticality Safety Analyses

In chapter 5, information on the principles of criticality safety, factors that affect criticality of HLWs, and chemical mechanisms that could lead to concentration of fissile materials or to redistribution of neutron absorbers are discussed. Although the wastes discharged into the tanks, with the exception of tank SY-102, may be considered to be subcritical by the DOE (U.S. Department of Energy, 1996a), conditions within the

tanks are not static, and the composition of Hanford wastes will change during retrieval and processing operations. A review of the compositions of the wastes indicated that retrieval and subsequent processing of wastes from tanks with high total fissile plutonium nuclide content need to be evaluated (Cragnolino et al., 1997). Because Pu-239 is the only fissile Hanford tank waste component with a reasonable potential to induce criticality, discussion of chemical mechanisms are focused on Pu. The important aqueous Pu reactions are those affecting solubility and aqueous speciation. Available data suggest that Pu may exist in tank liquids as tetravalent hydroxycarbonate species with solubilities (limited by $PuO_2 \cdot xH_2O$) perhaps as high as 10^{-3} M. Oxidation to potentially more soluble Pu(VI) species, however, may be possible if more oxidizing conditions are present or have been induced by, for example, radiolysis or aeration. In addition, colloid formation could lead to Pu liquid concentrations exceeding solubility limits, but no quantitative means for evaluating this mechanism are available.

Consideration of mechanisms for aqueous Pu concentration suggests that it is highly unlikely that criticality levels could be achieved in liquids. However, plutonium concentrations in tank solids typically exceed those in liquids by several orders of magnitude and, consequently, have a greater criticality potential. The important chemical mechanisms for solids concentration are pure Pu phase precipitation, coprecipitation with other solids, and adsorption. Growth of new pure Pu phases would require evaporation or chemical changes resulting in lowered solubility, in competition with coprecipitation and adsorption. Coprecipitation may result from two phenomena, solid solution and coagulation. While it may be possible to predict solid-solution behavior by thermodynamic calculation, understanding of coagulation behavior rests on observation and experimentation. Adsorption of Pu onto tank solids such as hydroxides of iron and other metals is considered by many to be an important means of Pu sequestration in solids. However, available experimental data imply suppression of Pu adsorption at the high pH and high carbonate contents typical of tank liquids, although more experimental studies for conditions relevant to Hanford tank wastes are clearly warranted. From a criticality standpoint, it seems most conservative to assume that Pu precipitation or coprecipitation reactions and adsorption phenomena can result in complete removal of Pu from solution. However, quantitative evaluation of chemical mechanisms for concentrating Pu is difficult due to Pu redox complexity and the paucity of data on Pu behavior in tank-type chemical environments. In attempting to evaluate these mechanisms, it is clear that much more experimental data under tank waste conditions are necessary to gain more confidence in predictive capabilities.

Another aspect of waste chemistry relevant to criticality potential is the fate of neutron absorbers. In Hanford tank wastes, nitrogen is the most important soluble neutron absorber, whereas Fe and Al are the most abundant absorbers in the solids. Model simulations or predictions of waste chemistry should track these and other potentially important neutron absorbers. For example, Fe can undergo redox changes that will affect its aqueous solubility/speciation and solid phase distribution, and Al solubility may be enhanced at high pH.

An approximate method is proposed and discussed in chapter 5 for determining k_{eff} for tank wastes when Pu-239, the primary fissile isotope in the tanks, has been concentrated to levels that approach criticality. This method is intended to allow an investigator to rapidly and conservatively estimate the criticality potential of a process and determine those cases where more detailed investigations into criticality are required.

Radioactive-Decay Heat Generation in Hanford Tank Wastes

Chapter 6 provides information on radioactive decay that contributes to heat generation and describes a simplified approach for calculating the volumetric heat generation rate of tank wastes based on known or assumed radionuclide inventories. Radioactive decay heat of highly radioactive species, such as Sr-90 and Cs-137, are of potential safety concern in the Hanford TWRS because it could result in elevated temperatures

during storage, retrieval or pretreatment operations. For example, radioactive decay heat determines the waste temperature profile and influences the moisture loss rate. Thus, ventilation requirements, whether passive or active, for waste storage and process feed tanks need to consider the effect of radioactive decay heat. For example, tank C-106, the only Hanford tank on the High Heat Watch-list, requires more than active ventilation to keep the temperature below 150 °C (300 °F), which is the maximum temperature limit established in the DOE Operating Safety Document (Wodrich, 1992). In a transfer line containing waste with high heat load due to radioactive decay, problems such as thermal expansion and distortion or rupture of the line could result. Also, degradation of ion exchange resins or other media used in pretreatment of Hanford wastes could be enhanced by high heat generated by radioactive decay. Thus, waste temperature estimates could be useful in anticipating potential problems in TWRS operations.

A simplified method is presented in chapter 6 for calculating the volumetric heat generation rate of tank wastes based on their activity concentrations of Cs-137 and Sr-90. It was found that there can be significant differences in the volumetric heat generation rate for small heat sources versus large heat sources due to the escape of the 0.662 MeV gamma ray emitted by Ba-137m from smaller systems. The equations presented are useful in estimating waste temperatures based on known or assumed inventories of Sr-90 and Cs-137.

Models and Codes for Simulating Hanford TWRS Processes

Chapter 7 provides a general discussion of process simulation software and its potential application to the Hanford TWRS. Because of the complexity and variability in the chemical types, compositions, and concentrations of Hanford tank wastes, as well as in the technologies that will be used to retrieve, pretreat, and solidify the wastes, the identification and evaluation of potential hazards in Hanford TWRS operations will be difficult. Hazard audits of the TWRS facility may fail to identify certain chemical reactions, plant processes, or plant conditions that could lead to a safety problem.

Process simulation is a standard industry tool that is valuable for developing and designing complex processes. It may be possible to use process simulation software, available commercially from several vendors, to enhance the identification and evaluation of plant processes and conditions and chemical reactions that could lead to safety hazards in the Hanford TWRS operations. However, developing a process simulation for the Hanford tank waste system faces the obstacles of process complexity and inadequate data. Previous efforts by DOE investigators in process simulation have concentrated on ways to obtain overall global views of the process because several critical questions require answers at that level before more detailed analysis can be conducted. Thus, the process simulation has been accomplished with some sacrifice of theoretical rigor, which might (though not necessarily) have caused some loss in accuracy. For the Hanford tank wastes, the ability to quickly make changes and obtain numerical solutions is of particular importance to support lengthy, detailed reviews, and to address any potential concerns about the TWRS facility.

A general discussion of a class of simulation software, referred to as flowsheet simulation software, and its application to process development are discussed in this chapter. However, a critical evaluation of the different commercial software available and their possible application to the Hanford TWRS is beyond the scope of this report. A specialized suite of software for chemical process simulation developed by OLI Systems, Inc. and used extensively by Hanford investigators for various applications is also described. Simulation examples were developed for this report using the OLI software as part of a preliminary analysis of its potential use to the Hanford TWRS. These examples are relevant to potential safety issues resulting from (i) flammable gases, (ii) high organic and nitrate contents, and (iii) fissile elements, particularly Pu. Supernatant solutions for three tanks on the DOE Watch-list were used in the simulation examples. The simulation results indicate that the OLI software has the chemical and process modeling capabilities that

could be useful to studies of potential safety issues resulting from waste management operations. However, inclusion of additional species and model parameters not currently in the OLI database is essential for better description and modeling of the chemical processes relevant to the Hanford TWRS.

References

Agnew, S.F. 1997. *Hanford Tank Chemical and Radionuclide Inventories: HDW Model Rev. 4.* LA-UR-96-3860. Los Alamos, NM: Los Alamos National Laboratory.

Babad, H., J.E. Meacham, B.C. Simpson, and R.J. Cash. 1993. *The Role of Aging in Resolving the Ferrocyanide Safety Issue.* WHC-EP-0599. Richland, WA: Westinghouse Hanford Company.

Cady, H.H. 1992. *Evaluation of Ferrocyanide/Nitrate Explosive Hazard.* LA-12589-MS. Los Alamos, NM: Los Alamos National Laboratory.

Cragnolino, G.A., M.S. Jarzemba, J. Ledbetter-Ferrill, W.M. Murphy, R.T. Pabalan, D.A. Pickett, J.D. Prikryl, and N. Sridhar. 1997. *Hanford Tank Waste Remediation System Familiarization Report.* CNWRA 97-001. San Antonio, TX: Center for Nuclear Waste Regulatory Analyses.

Hanlon, B.M. 1997. *Waste Tank Summary Report for Month Ending September 30, 1997.* HNF-EP-0182-114. Richland, WA: Lockheed Martin Hanford Corporation.

Postma, A.K., and D.R. Dickinson. 1995. *Ferrocyanide Safety Program: Analysis of Postulated Energetic Reactions and Resultant Aerosol Generation in Hanford Site Waste Tanks.* WHC-EP-0876. Richland, WA: Westinghouse Hanford Company.

U.S. Department of Energy. 1996a. *Tank Waste Remediation System, Hanford Site, Richland, Washington, Final Environmental Impact Statement.* DOE/EIS-0189, Volumes 1–5. Richland, WA: U.S. Department of Energy.

U.S. Department of Energy. 1996b. *Tank Waste Remediation System Privatization Request for Proposals.* DE-RP06-96RL13308. Richland, WA: U.S. Department of Energy.

Wodrich, D.D. 1992. *Summary of Single-Shell Tank Stability.* WHC-EP-0347, Supplement. Richland, WA: Westinghouse Hanford Company.

1 INTRODUCTION

1.1 OBJECTIVES

The U.S. Department of Energy (DOE) established the Tank Waste Remediation System (TWRS) program at the Hanford site in 1991 to manage the maintenance and cleanup of radioactive waste contained in 177 aging underground storage tanks. The DOE is legally bound to remediate the waste tanks under the Hanford Federal Facilities Agreement and Consent Order of 1989 (Ecology, 1994), also known as the Tri-Party Agreement (TPA). To fulfill the requirements of the TPA, the DOE plans to privatize the waste treatment and immobilization operations of the TWRS program. The TWRS privatization process is divided into two phases, a proof-of-concept or demonstration phase (Phase I) and a full-scale operations phase (Phase II). The Phase I program, scheduled for completion in 2012, is divided into Part A (feasibility study), which is scheduled for completion in January 1998, and Part B (demonstration pilot plant study), which is scheduled for completion in June 2011.

During performance of Part A, the privatization contractor will develop a solution for low-activity waste (LAW) services only or will develop two parallel solutions for LAW and high-level waste (HLW) services. The contractor will establish the technical, operational, regulatory, and financial elements required by privatized facilities to provide waste treatment services. In Part B, LAW services provided by the contractor include (i) receiving batches of three waste envelopes, referred to as waste envelopes A, B, and C and with specifications described in tables A-1 and A-2, into an existing double-shell tank (DST), (ii) retrieving and transferring the waste from the DST to contractor facilities, (iii) separating the waste into low-activity and high-level fractions, and (iv) treating and immobilizing the low-activity fraction into final waste products for return to DOE. If the contractor provides LAW and HLW services, additional services are required to receive batches of the HLW, referred to as waste envelope D and with specifications described in tables A-3 to A-6, and to treat and immobilize the high-level solids and the high-level fraction from LAW services into final waste products for return to DOE. The four waste envelopes described in tables A-1 to A-6 are representative of the range of Hanford tank wastes. Envelopes A, B, and C contain cesium and technetium at concentrations that make it necessary for their removal to ensure that the LAW glass specification can be met. Envelope B contains higher concentrations of cesium than envelopes A and C, as well as higher concentrations of chlorine, chromium, fluorine, phosphates, and sulfates, which may limit the waste loading in the glass. Envelope C contains organically complexed strontium and transuranics (TRUs) that will require removal. Envelope D contains an HLW slurry.

A Memorandum of Understanding has been established between the DOE and the Nuclear Regulatory Commission (NRC)[1] for Phase I activities. The Memorandum of Understanding provides for the NRC to acquire sufficient knowledge of the physical and operational situation at the Hanford waste tanks and the processes, technology, and hazards involved in Phase I activities to enable the NRC to (i) assist the DOE in performing reviews consistent with the NRC regulatory approach and (ii) be prepared to develop an effective regulatory program for the possible licensing of DOE contractor-owned and contractor-operated facilities during Phase II.

---

[1]Memorandum of Understanding Between the Nuclear Regulatory Commission and the U.S. Department of Energy, January 29, 1997, Federal Register, 62(52): 12861. Washington, DC: U.S. Government Printing Office. March 18, 1997.

A program to assist the NRC in developing technical and regulatory tools for the TWRS privatization activities was established at the Center for Nuclear Waste Regulatory Analyses (CNWRA). The program consists of four tasks, of which only task 1 (Familiarization and Regulatory Development and Safety Review) is currently active. A broad objective of the CNWRA activities is to provide NRC staff with information and tools needed to assess the chemical, radiological, and criticality hazards of Hanford tank wastes and operations addressed under the privatization initiative. Of primary concern are those reactions that could occur during waste retrieval and processing, but potential reactions during continued interim storage are also important. A specific objective is to provide the NRC with a reference manual that discusses possible chemical reactions and processes that could lead to hazardous situations and information and tools available to evaluate these reactions.

1.2 TECHNICAL SCOPE

Information on the chemical and physical properties of the contents of the Hanford tank wastes is key to determining the potential chemical reactions that could lead to hazardous conditions. The chemical and physical properties of the tank wastes are discussed in a previous report (Cragnolino et al., 1997) and are summarized in this chapter.

The DOE identified a number of safety issues associated with Hanford waste tanks. Of primary importance, particularly with respect to the regulatory role of the NRC, are those issues involving radiological risks to the public and workers and the potential release of radioactivity to the environment. The DOE developed a set of criteria to identify tanks with potential safety concerns as Watch-list tanks.[2] The four Watch-list categories are flammable/hydrogen gas, high organic content, ferrocyanide, and high-heat load. The safety issue associated with the Flammable/Hydrogen Gas Watch-list pertains to the release of flammable gases, mostly hydrogen generated mainly by radiolytic and thermochemical mechanisms, into the dome space of the waste tanks. The presence of flammable concentrations of gases and an ignition source could lead to reactions that could cause a radioactive release or provide an energy source that could facilitate other reactions within the tank. The safety concern with respect to the High Organic Content Watch-list tanks is the potential for rapid energetic reactions between organic compounds (fuel) and sodium nitrate/nitrite (oxidant) present in Hanford wastes that could release radioactivity to the environment. Such a reaction, for example, resulted in a major explosion in a radioactive waste tank in Kyshtym, U.S.S.R., in 1957 (Medvedev, 1979) causing radiation contamination of an estimated 23,000 sq km. It has been concluded that the design and operation of the tanks at Hanford are quite different from those at Kyshtym (Fisher, 1990). The tanks on the Ferrocyanide Watch-list contained sodium or potassium ferrocyanide that had been added to the waste to scavenge Cs-137. The safety concern associated with these tanks is the potential for exothermic reactions involving ferrocyanides. In the presence of oxidizing materials, such as nitrates or nitrites, ferrocyanide can

---

[2]A separate but related formal administrative DOE program is in place to identify as an Unreviewed Safety Question (USQ) known or suspected operating conditions that have not been analyzed or that fall outside of the established authorization bases. Following identification of a USQ, a review is conducted, and corrective action is taken if applicable. The USQ may be closed from an administrative standpoint, which means that conditions surrounding the safety issue have been analyzed, although the safety issue may still exist and may require mitigation, controls, or corrective action. The safety issues identified under the Watch-list program were also previously analyzed as USQs. Technical evaluation has resulted in closing the USQs on ferrocyanide, floating organic layer, and criticality (U.S. Department of Energy, 1996a). A USQ is associated with the Flammable/Hydrogen Gas Watch-list tanks because of the potential consequences of a radiological release resulting from a flammable gas burn, an event not analyzed in the Single-Shell Tank (SST) Safety Analysis Report. Hanlon (1996) reported that the DOE declared a USQ on some tanks containing dry organic nitrate chemicals because methods for analyzing accident scenarios have become available for these.

explode if heated to high temperatures or if exposed to an electrical spark of sufficient energy. One tank is on the High-Heat Load Watch-list because of concerns about elevated temperatures from radioactive decay heat of stored waste, primarily Cs and Sr, that can lead to overheating of the waste tank concrete structure and to releasing high-level nuclear waste to the surrounding soil and groundwater.

In all, 38 tanks are on various Watch-lists. Some of the tanks are placed in more than one Watch-list category. Specifically, 25 tanks are on the Flammable/Hydrogen Gas Watch-list, 20 tanks are on the High Organic Content Watch-list, and one tank is on the High-Heat Load Watch-list. All tanks that were on the Ferrocyanide Watch-list have been removed from the list (Hanlon, 1997). The Hanford waste tanks identified for each Watch-list are given in table 1-1.

The following sections in this chapter briefly summarize the origin as well as the physical characteristics and chemistry of the tank wastes. The succeeding chapters discuss the chemistry of processes that could lead to hazardous situations in the Hanford TWRS. A major part of information presented in this report is based on published DOE studies relevant to storage of HLWs in the Hanford tanks. However, safety issues associated with storage of wastes in the Hanford tanks may also be relevant to the retrieval and processing stages of Hanford TWRS operations. For example, chemical reactions resulting in the generation of flammable gases and the attendant risk associated with those gases are expected to continue through some stages of the Hanford TWRS program. Similarly, exothermic reactions involving organics and nitrates/nitrites likely will remain a possibility unless pretreatment methods are used to eliminate organics from Hanford wastes. High-heat generation will also need to be considered for those wastes or waste feeds with high concentrations of Sr-90 or Cs-137.

Chapter 2 of this report focuses on the chemistry relevant to flammable gas generation and includes discussions of the mechanisms of gas generation in Hanford tank wastes, the flammability of gas mixtures, and factors affecting gas retention in tank wastes. Chapter 3 discusses the chemistry of reactions relevant to Hanford organic-bearing wastes, including the sources and estimated current inventory of organic complexants and organic solvents in Hanford tanks, thermodynamic calculations and thermoanalytical measurements of reactions involving Hanford organics and oxidants, mechanisms that could result in locally elevated concentrations of Hanford organics, and organic degradation processes. Chapter 4 describes ferrocyanide scavenging operations and discusses the chemistry relevant to ferrocyanide reactions, including ferrocyanide degradation mechanisms. Although the ferrocyanide safety issue is considered closed by the DOE with respect to interim storage in Hanford tanks, residual exothermic activity might be initiated by solidification operations that can cause waste to be heated by an external source. Thus, the DOE may evaluate on a case-by-case basis the possibility and impact of a self-heating reaction involving ferrocyanides as part of the safety analysis of proposed retrieval and processing methods (Postma and Dickinson, 1995).

Although the wastes discharged into the tanks, with the exception of tank SY-102, may be considered to be subcritical by the DOE (U.S. Department of Energy, 1996a), conditions within the tank are not static, and the composition of Hanford wastes will change during retrieval and processing operations. A review of the compositions of the wastes indicated that retrieval and subsequent processing of wastes from tanks with high total fissile plutonium (Pu) nuclide content need to be evaluated (Cragnolino et al., 1997). Thus, chapter 5 focuses on the chemistry of Hanford tank wastes relevant to criticality safety. Discussed in the chapter are the principles of criticality safety, parameters that affect criticality of HLW, and mechanisms that could lead to concentration of fissile materials and neutron absorbers. A relatively simple approach for determining when criticality should be further evaluated for specific Hanford TWRS operations is also proposed and discussed.

Table 1-1. Watch-list tanks, November 30, 1997 (Hanlon, 1998)

Single-Shell Tanks Tank No.	Watch-list	Officially Added to Watch-list	Double-Shell Tanks Tank No.	Watch-list	Officially Added to Watch-list
A-101 (*)	Hydrogen	1/91	AN-103	Hydrogen	1/91
	Organics	5/94	AN-104	Hydrogen	1/91
AX-101	Hydrogen	1/91	AN-105	Hydrogen	1/91
AX-102	Organics	5/94	AW-101	Hydrogen	6/93
AX-103	Hydrogen	1/91	SY-101	Hydrogen	1/91
B-103	Organics	1/91	SY-103	Hydrogen	1/91
C-102	Organics	5/94	6 tanks		
C-103	Organics	1/91			
C-106	High-Heat Load	1/91	Tanks by Watch-list		

Single-Shell Tanks Tank No.	Watch-list	Officially Added to Watch-list	Hydrogen	Organics	
S-102 (*)	Hydrogen	1/91	A-101	A-101	
	Organics	1/91	AX-101	AX-102	
S-111 (*)	Hydrogen	1/91	AX-103	B-103	
	Organics	5/94	S-102	C-102	
S-112	Hydrogen	1/91	S-111	C-103	
SX-101	Hydrogen	1/91	S-112	S-102	
SX-102	Hydrogen	1/91	SX-101	S-111	
SX-103 (*)	Hydrogen	1/91	SX-102	SX-103	
	Organics	5/94	SX-103	SX-106	
SX-104	Hydrogen	1/91	SX-104	T-111	
SX-105	Hydrogen	1/91	SX-105	TX-105	
SX-106 (*)	Hydrogen,	1/91	SX-106	TX-118	
	Organics	1/91	SX-109	TY-104	
SX-109	Hydrogen because other tanks vent through it	1/91	T-110	U-103	
T-110	Hydrogen	1/91	U-103	U-105	
T-111	Organics	2/94	U-105	U-106	
TX-105	Organics	1/91	U-107	U-107	
TX-118	Organics	1/91	U-108	U-111	
TY-104	Organics	5/94	U-109	U-203	
U-103 (*)	Hydrogen	1/91	AN-103	U-204	
	Organics	5/94	AN-104	20 tanks	
U-105 (*)	Hydrogen	1/91	AN-105		
	Organics	5/94	AW-101		
U-106	Organics	1/91	SY-101	High Heat	
U-107 (*)	Organics	1/91	SY-103	C-106	
	Hydrogen	12/93	25 tanks	1 tank	
U-108	Hydrogen	1/91			
U-109	Hydrogen	1/91			
U-111	Organics	8/93	32 Single-Shell tanks		
U-203	Organics	5/94	6 Double-Shell tanks		
U-204	Organics	5/94	38 tanks on Watch-lists		
32 tanks (*)					
(*) Eight tanks are on more than one Watch-list.					

Because radioactive decay heat can result in elevated temperatures of Hanford wastes during storage and possibly during retrieval or processing operations, heat generation by radioactive decay needs to be considered in safety analyses. Chapter 6 provides information on radioactive decay that contributes to heat generation and describes a simplified approach for calculating the volumetric heat generation rate of tank wastes based on known or assumed radionuclide inventories.

The complexity and variability of the Hanford tank wastes and of the technologies to be used in retrieving, pretreating, and solidifying the wastes will make the identification and evaluation of potential hazards in TWRS operations difficult. Process simulation software, a standard industry tool for developing and designing complex processes, could enhance this identification and evaluation of potential hazards. Chapter 7 provides a general discussion of process simulation software and its potential application to the Hanford TWRS. Finally, conclusions derived from information discussed in the first seven chapters of this report are given in chapter 8.

1.3   ORIGINS OF TANK WASTES

The wastes have been produced over a long period of time by a variety of processes, as described in a previous report (Cragnolino et al., 1997). The primary source of the waste at the Hanford site is the historical irradiation of metallic uranium (U) fuel and extraction of Pu from the irradiated fuel through various processes. The metallic U fuel was at first clad with an Al-Si alloy, but was later clad with zirconium. The earliest process for extraction of Pu was the bismuth phosphate (BP) process, which used BP and phosphoric acid to coprecipitate Pu, that was then separated by controlling the redox state of the solution using ferrous salts. The wastes from the BP process, containing Sr, Cs, and U, were sent to the T, TX, TY, B, BX, and BY tank farms. The waste from the BP process was later retrieved from the tanks, and the U was recovered using tributyl phosphate (TBP) solvent extraction in the uranium recovery (UR) process. The wastes from this process went to the U tank farm. Because the volume of wastes was twice as much as the material processed, ferrocyanide was used to scavenge the Cs-137. The sludge from adding ferrocyanide, which contained most of the Cs, was returned to the tanks; the supernatant was discharged to cribs. The tanks also contained some remnant wastes from the BP process, suspected to be mainly U and Pu carbonate. The reduction oxidation (REDOX) process was based on a continuous solvent extraction of U and Pu using methyl isobutyl ketone as the solvent. The wastes from this process went primarily to the S and SX tank farms. The Plutonium Uranium Extraction Plant (PUREX) process replaced the REDOX process. The PUREX process also used TBP/kerosene as the solvent phase for extraction with a mixture of ferric salts, dichromates, and bisulfites to control the REDOX condition. From 1959 to 1961, the wastes from the PUREX process were sent to the A and AX tank farms. The B and C plants were used to recover the Cs and Sr from the wastes because the decay heat from these radionuclides was causing boiling in the tanks (Agnew, 1997). The wastes from the Sr removal process in the C plant were sent to the C tank farm. The B plant was used to remove the Cs and Sr from the PUREX wastes in the A and AX tank farms. The wastes from the B plant, after Cs and Sr recovery, were sent to the B and BL tank farms.

At the time they were generated, the Hanford wastes were highly radioactive, acidic liquids which generated heat and required remote handling behind heavy shielding in corrosion-resistant vessels, usually made of stainless steel. However, because stainless steel was in short supply when the first storage tanks were built, the wastes were neutralized with sodium hydroxide, and sodium nitrite was added for corrosion control so that the wastes could be stored safely in carbon-steel tanks. The use of carbon-steel tanks continued even after stainless steel became more readily available.

Approximately 1,500,000 m^3 (400 million gal.) of waste were generated from chemical processing at the Hanford site, and more than 1,100,000 m^3 (300 million gal.) of these were sent to underground storage tanks. Volume reduction practices were followed to maintain waste volumes within available tank space. Through evaporation, concentration, and the past practice of discharging dilute waste to the ground, the waste volume has been reduced to approximately 208,000 m^3 (55 million gal.) (Hanlon, 1996). Other HLWs are stored in storage tanks at other U.S. facilities, particularly 51 tanks at the Savannah River Site (SRS, Aiken,

South Carolina), 11 tanks at the Idaho National Engineering and Environmental Laboratory (INEEL, Idaho Falls, Idaho), and two tanks at the West Valley Demonstration Project (WVDP, West Valley, New York) (Gephart and Lundgren, 1995). To provide a perspective to the Hanford HLW inventory, the estimated cumulative volume and radioactivity of HLWs stored in storage tanks, bins, and capsules at Hanford, SRS, INEEL, and WVDP are plotted in figure 1-1.

1.4 PHYSICAL CHARACTERISTICS OF TANK WASTES

Hanford Tank Wastes may be considered in the following four categories: single-shell tank (SST) wastes, DST wastes, miscellaneous underground storage tank (MUST) wastes, and future tank waste additions. The discussions of this report emphasize the inventory of SSTs and DSTs, which together comprise greater than 99 percent of the total waste volume and a majority of total radionuclide activity at the Hanford site (U.S. Department of Energy, 1996a). The other major contributors to radioactivity in Hanford wastes are the Cs and Sr capsules, which are not of interest to this report as these wastes are not expected to be retrieved for solidification. The total MUST waste volume is minor and the MUST inventory, while not yet well documented, is expected to differ little in character from the SST and DST inventories (U.S. Department of Energy, 1996a). Unless otherwise noted, the sources for the information contained in this section are Gephart and Lundgren (1995), Golberg and Guberski (1995), Agnew (1997), and the U.S. Department of Energy (1996a).

The tanks contain complex mixtures of solids and liquids. Liquids are either supernatant—easily pumped and floating above settled solids—or interstitial—confined to pore spaces of the solids. Solids are classified as sludge or saltcake (Gephart and Lundgren, 1995). Sludge is a thick, wet layer of settled and precipitated water insoluble solids at the tank bottom, with small pore spaces that do not allow removal of liquids. Saltcake is dryer with larger pore spaces, being a residue after evaporation of supernatant liquid; saltcake components are typically water soluble. Slurry is a liquid/solid mixture that can be pumped.

1.4.1 Single-Shell Tanks

From 1943 to 1964, 149 SSTs were built that hold from 208 to 3,785 m³ (55,000 to 1,000,000 gal.) each. Of the combined 132,000 m³ (35 million gal.) of waste, 66 percent is wet saltcake, predominantly sodium nitrate, and 34 percent is sludge. Nearly all separable liquids have evaporated or been transferred from the SSTs to DSTs, but about 23,000 m³ (6 million gal.) of liquid are not easily pumped and will remain in the tanks. The solids and dissolved constituents of the SSTs are 90 percent sodium nitrates and nitrites, with the remainder consisting mostly of phosphates, carbonates, hydroxides, and sulfates. Radioactivity in the SSTs is dominated by Sr-90 (75 percent) and Cs-137 (24 percent); Sr is concentrated in the sludge, while Cs is located chiefly in the saltcake and interstitial liquids. Because many of the SSTs have been found to be leaking and there is considerable uncertainty regarding the migration of radioactive material to the water table, there is great urgency in retrieving and processing the wastes.

1.4.2 Double-Shell Tanks

The 28 DSTs are newer and larger than the SSTs, having been built between 1968 and 1986, and range in capacity from 3,785 to 4,390 m³ (1 to 1.16 million gal.). Because they are volumetrically dominated by supernatant liquids transferred from SSTs, the 75,700 m³ (20 million gal.) of DST waste are 85 percent

(a)

Hanford
(233.5x10^3 m^3)

WVDP
(2.2x10^3 m^3)

INEEL
(11.2x10^3 m^3)

SRS
(126.5x10^3 m^3)

(b)

INEEL
(49.3x10^6 Ci)

Hanford
(339.9x10^6 Ci)

WVDP
(24.1x10^6 Ci)

SRS
(502.2x10^6 Ci)
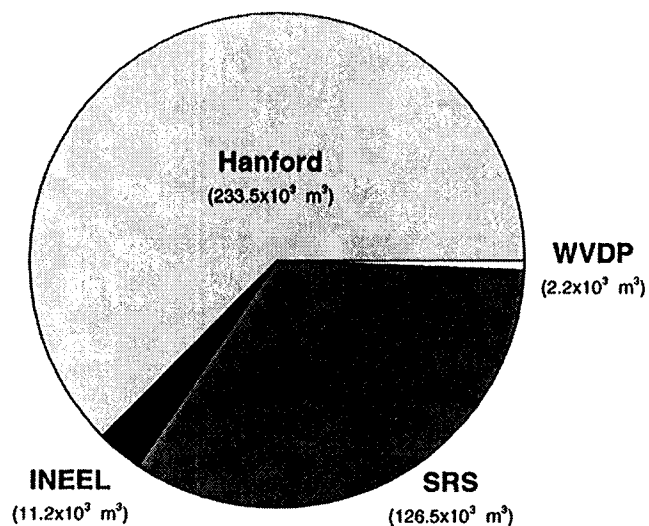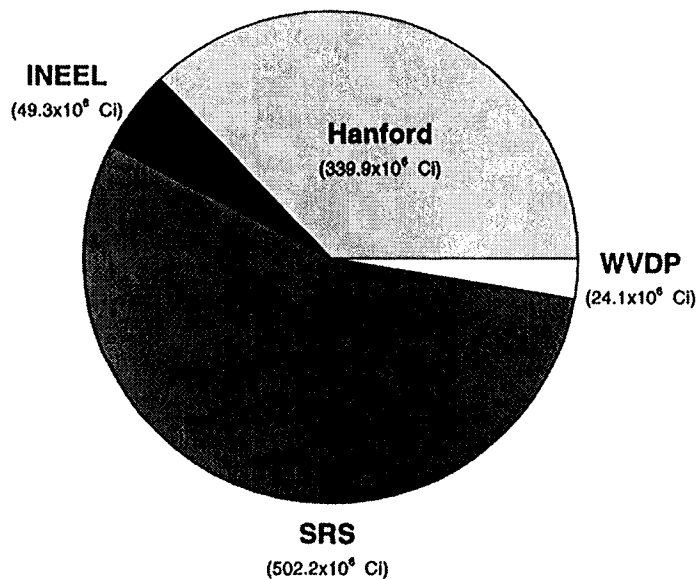
Figure 1-1. Estimated (a) cumulative volume and (b) cumulative radioactivity of HLWs stored in tanks and bins at Hanford, INEEL, SRS, and WVDP for calendar year 1995. Values were taken from the Integrated Data Base Report—1995 (U.S. Department of Energy, 1996c). At Hanford, an additional 146.1 × 10^6 Ci of Cs-137 and Sr-90 are stored in the form of capsules.

water. The waste is thus dominated by liquids and slurries, sometimes with a bottom layer of sludge. DST waste types have been delineated in greater detail than for SSTs. Eight types have been defined, listed here in decreasing order of volume (Gephart and Lundgren, 1995; Hanlon, 1996):

- **Double-shell slurry and double-shell slurry feed (31 percent of total DST waste volume; various sources)**—suspension-rich, high-salt solutions from evaporation of SST and reprocessing plant wastes; includes solids comprising 19 percent of this waste type
- **Concentrated complexant (23 percent; various sources[3])**—liquid and solid alkaline waste with high organic and transuranic contents, resulting from evaporation of dilute complexed waste; includes solids comprising 17 percent of this waste type

- **Dilute noncomplexed waste [21 percent; sources are T, B, REDOX, and PUREX plants, the N Reactor, the 300 Area, and the Plutonium Finishing Plant (PFP)]**—low-radioactivity liquid waste from a variety of processing operations; includes solids comprising 9 percent of this waste type

- **Neutralized current acid waste (9 percent; PUREX)**—93 percent liquid waste generated since 1983

- **Concentrated phosphate waste (6 percent; N Reactor)**—from decontamination of N Reactor; confined to tank AP-102

- **Dilute complexed waste (5 percent; various sources)**—high-organic liquids from the SSTs; includes solids comprising 10 percent of this waste type

- **Neutralized cladding removal waste (4 percent; PUREX)**—thick alkaline sludge, chiefly zirconium hydroxide

- **PFP sludge wash (0.7 percent; PFP)**—sludge from PFP recovery operations; confined to tank SY-102

According to the Westinghouse Hanford Company (WHC) Waste Tank Summary (Hanlon, 1996), most tanks contain only one of these waste types. Exceptions are tanks AW-103, AW-105, and SY-102, which contain neutralized cladding removal waste solids or PFP solids in addition to dilute noncomplexed waste, and tanks SY-101 and SY-103, which both contain concentrated complexant and double-shell slurry.

The chemistry of the solids and dissolved constituents of the DSTs is, like the SSTs, dominated by sodium nitrates and nitrites, with an additional 20 percent metal hydroxides and 10 percent phosphates, carbonates, oxides, and sulfates. Decay of Cs-137 and its short-lived daughters comprises 72 percent of the DST waste radioactivity, while 27 percent is from Sr-90; this contrast with the SST proportions is caused

---

[3]There are differing definitions of concentrated complexant waste in the Hanford literature, but they appear to be compatible. The source definition used here—evaporation of dilute complexed waste, which is itself derived from SSTs—is from Hanlon (1996) and appendix B in the TWRS EIS (U.S. Department of Energy, 1996a). Gephart and Lundgren (1995) and appendix L of the EIS (U.S. Department of Energy, 1996a) define concentrated complexant as being derived chiefly from Sr recovery operations in B Plant. Scheele et al. (1995) suggest that Sr recovery is the chief source of the organic complexants present in the tanks; thus, the definitions are compatible.

by Sr having settled out in the SST solids before waste transfer to the DSTs. The DSTs have not been found to be leaking thus far.

Temperatures are regularly monitored in most tanks, and these temperature data are available in monthly tank waste summary reports [e.g., Hanlon (1997, 1998)] or in the online Tank Waste Information Network System database (TWINS; http://twins.pnl.gov:8001/TCD/main.html). For example, table 1-2 shows the maximum temperatures measured in September 1997 and reported in Hanlon (1997) for tanks on the Flammable Gas Watch-list, High Organic Watch-list, and High Heat Load List. The High Heat Load List, taken from Hanlon (1998), is comprised of SSTs that have high heat loads and for which temperature surveillance requirements have been established by DOE procedures. Note that only one tank on the High Heat Load List, C-106, is on the High Heat Watch-list (Hanlon, 1997). Tank C-106 is on the High Heat Watch-list because in the event of a leak, without water additions the tank temperature could exceed the design limit and result in unacceptable structural damage (Hanlon, 1998). The tank is cooled through evaporation in conjunction with active ventilation, and water is added periodically as evaporation takes place.

Shown in figure 1-2 are recent data for individual tanks, with DSTs distinguished by waste type as described previously, and with SSTs grouped together. Note the range from less than 60 °F (16 °C) to greater than 180 °F (82 °C). Higher temperatures have also been reported. Hanlon (1998) notes that a maximum

Individual tank maxima, January 1998
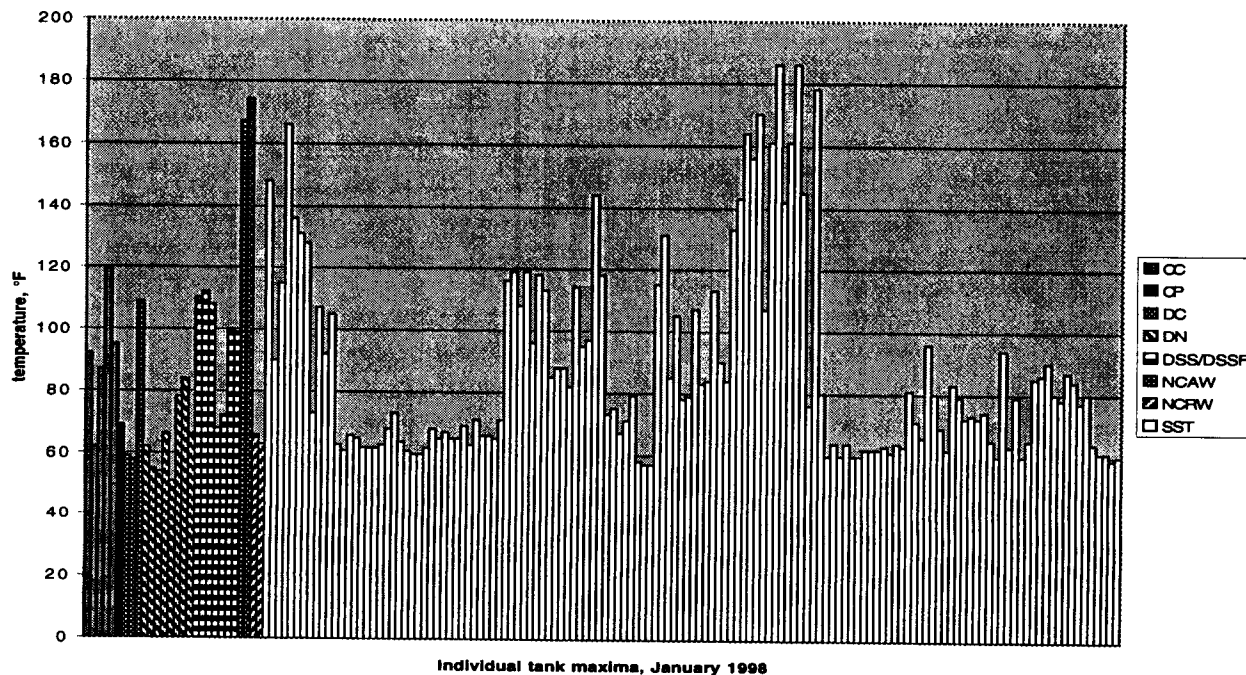
Figure 1-2. Maximum measured temperatures in Hanford tanks in January, 1998, from the TWINS database. Double shell tanks are grouped by dominant waste type as categorized in Hanlon (1998): CC = concentrated complexant, CP = concentrated phosphate, DC = dilute complexed, DN = dilute noncomplexed (includes one tank—SY-102—that also has appreciable PFP sludge), DSS/DSSF = double-shell slurry and slurry feed, NCAW = neutralized current acid waste, NCRW = neutralized cladding removal waste. Single shell tanks are uncategorized and actual tank numbers are not given to improve clarity of the figure. Not all tanks have a complete set of data in the TWINS database.

Table 1-2. Maximum temperatures measured in September, 1997, for tanks on the Flammable Gas Watch-list, High Organic Watch-list, and High Heat Load List (Hanlon, 1997). Note that only one tank on the High Heat Load List, C-106, is on the High Heat Watch-list.

Flammable Gas Watch-list		Organics Watch-list		High Heat Load List	
Tank No.	Temp. (°F)	Tank No.	Temp. (°F)	Tank No.	Temp. (°F)
A-101	162	A-101 (*)	162	A-104	173
AX-101	132	AX-102 (*)	78	A105	148
AX-103	111	B-103 (*)	67	C-106	153
S-102	105	C-102	81	SX-107	168
S-111	89	C-103	116	SX-108	189
S-112	83	S-102	105	SX-109	144
SX-101	133	S-111	89	SX-110	164
SX-102	144	SX-103	166	SX-111	191
SX-103	166	SX-106	107	SX-112	151
SX-104	161	T-111	66	SX-114	181
SX-105	172	TX-105 (*)	95		
SX-106	107	TX-118	73		
SX-109	144	TY-104	66		
T-110	64	U-103	85		
U-103	85	U-105	89		
U-105	89	U-106	80		
U-107	78	U-107	78		
U-108	87	U-111	79		
U-109	82	U-203	65		
AN-103	112	U-204	63		
AN-104	114				
AN-105	108				
AW-101	100				
SY-101	120				
SY-103	96				
(*) All Watch-list tanks are monitored continuously for temperature, except for the tanks identified with an asterisk, which are measured manually on a weekly basis.					

temperature of 238 °F (114 °C) was measured beneath—but not inside—tank A-105 in November 1997; high temperatures at this tank are confirmed in the TWINS database. In addition, inspection of the TWINS data from December 1997 and January 1998 showed reported temperatures from 200 to 399 °F (93 to 204 °C) for tanks BY-111 and T-101. The significance of these unusually high temperatures is not yet known; values of this magnitude are not reported in the Hanlon (1997, 1998) waste tank summaries.

1.5 CHEMISTRY OF TANK WASTES

Records on the contents and volumes of wastes transferred to the tanks are typically incomplete or nonexistent. Chemical and radiological characterizations are therefore challenging tasks, complicated by the inherent difficulties of sampling heterogeneous tank contents. Two approaches to this question have been employed, each complementing the other. The approaches include direct sample measurement (or assay) and estimation based on facility records. The former is limited by the extreme physical and chemical heterogeneity of the tank contents, while the latter may be unreliable due to incomplete or inaccurate documentation of waste transfer transactions. Furthermore, inventories may change due to additions, transfers, radioactive decay, and chemical degradation.

The ongoing Hanford tank waste inventory effort combines both approaches: (i) analytical characterization work is being reported in a Tank Characterization Report for each tank (e.g., Benar and Amato, 1996)—these reports include estimations of total tank inventories based on an informed combination of individual sample results; and (ii) historical characterization is reported in documents termed Historical Tank Content Estimates (HTCE), which are released for quadrant groupings of tank farms (e.g., Brevick et al., 1996) with reference to supporting summaries for each farm (e.g., Brevick and Newell, 1996). The HTCE reports summarize all available historical data on processing and waste transfers and present the waste inventories based on those data.

The complex computational basis for HTCE inventories is being developed at Los Alamos National Laboratory (LANL). This effort, using what is termed the Hanford Defined Waste (HDW) model (Agnew, 1997), compiles historical process and waste transaction records to construct spreadsheets delineating time-dependent inventories of solid and liquid chemical inventories for each tank. In the HDW model, all possible sources of tank contents are classified among 48 different waste types, each with a given chemical/radionuclide profile based on knowledge of the processing from which it originated. Tank contents are then calculated from combinations of these waste types consistent with the historical records. The HDW estimation model for solids compositions is termed the Tank Layer Model and the model for liquids is called the Supernatant Mixing Model. The HDW model compiles estimates for 33 nonradioactive chemical species, 46 radionuclides (decayed to 1994), and four other properties [density, wt % water, total organic carbon (TOC), and sludge void fraction]. The radionuclide estimates are based on ORIGEN2 (Croff, 1980) calculations for all the nuclear fuel batches processed at Hanford, with modifications for extraction and other processing.

1.5.1 Inorganic Chemicals

The analyses outlined above show that, by far, the most abundant cation in the tank wastes is sodium. Na^+ comprises around 80 percent of the cationic content by weight. Figure 1-3 shows average Na^+ concentrations for tanks, with DSTs categorized by dominant waste type. These and other chemical parameters discussed below were obtained by (i) downloading "Tank Results" files for the given parameter from the TWINS database (http://twins.pnl.gov:8001/TCD/main.html), (ii) selecting only results that are
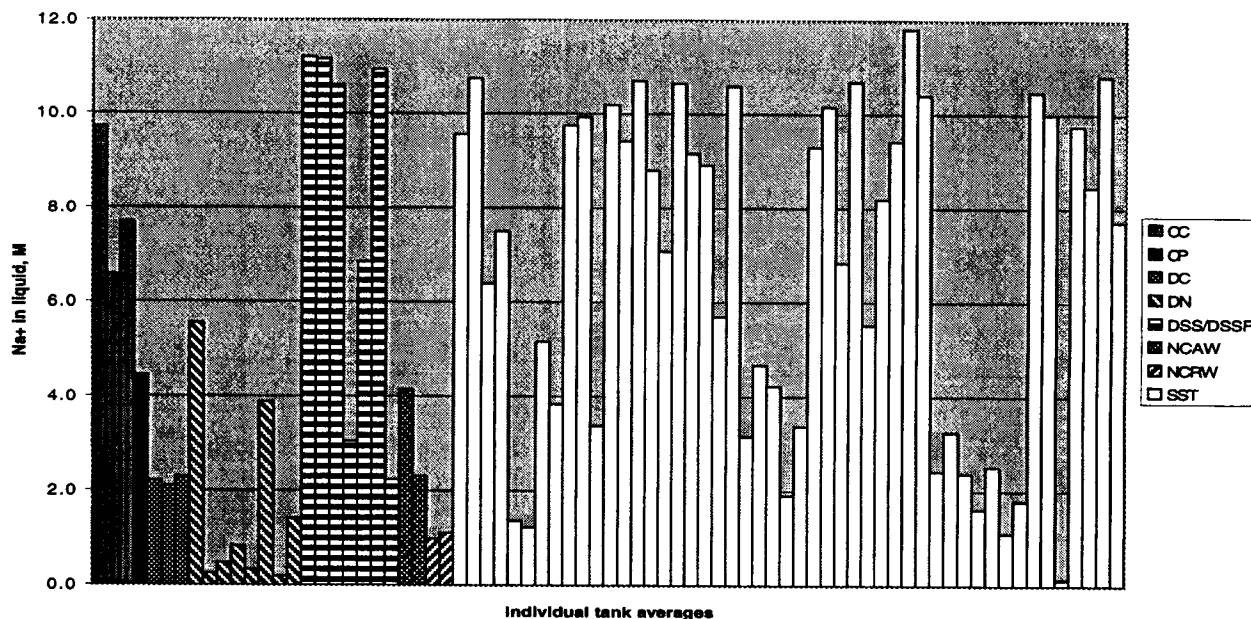
Figure 1-3. Average sodium concentrations (moles per liter) in tank liquids from the TWINS database. Abbreviations as in figure 1-2.

primary (i.e., not duplicate), reviewed, and not "unusable" or below detection limits, (iii) separating liquid and solid sample types, and (iv) calculating average values for each tank. Not all tanks are necessarily represented for a given parameter. Sodium liquid contents range from 0.1 to nearly 12 M. Figure 1-4 shows that solid Na concentrations are also typically substantial. The next most abundant cation overall is aluminum, with approximately 5 wt % of the cationic inventory. Also the tank wastes have relatively large concentrations of cations derived from construction materials, including Fe^{3+}, Ni^{2+}, and Cr^{3+}, and fuel claddings, consisting of Zr^{4+} and Al^{3+} [also present as $Al(OH)_4^-$].

The anionic waste contents are not so dominated by a single constituent. The dominant anion, by weight, is nitrate (NO_3^-) at about 62 percent, and other abundant anions include hydroxide (OH^-), nitrite (NO_2^-), and carbonate (CO_3^{2-}). Liquid and solid abundances of these major anions are shown in figures 1-5 through 1-11. (For compatibility with the available data, carbonate is represented in figures 1-10 and 1-11 by the TWINS value for total inorganic carbon.) However, a number of other anions such as phosphate (PO_4^{3-}), Cl^-, F^-, SiO_3^{2-}, and SO_4^{2-} have significant concentrations and are important to waste chemistry. The Environmental Impact Statement (EIS) (U.S. Department of Energy, 1996a) designates nitrate as the chief inorganic anion of significance to risk, because of its potential to oxidize ferrocyanide as well as organics in the tank, leading to explosion and radionuclide release.

Other parameters that are important to understanding chemical processes in tank wastes include pH, ionic strength, and oxidation potential of the liquids. Tank wastes are typically strongly alkaline, as shown in the tank average pH values of figure 1-12. Ionic strength values are not reported in the TWINS database, but the data illustrated in figures 1-3 to 1-11 suggest that they tend to be high. Calculations performed on a few representative waste analyses suggest that ionic strengths range from around 0.1 to more than 15;
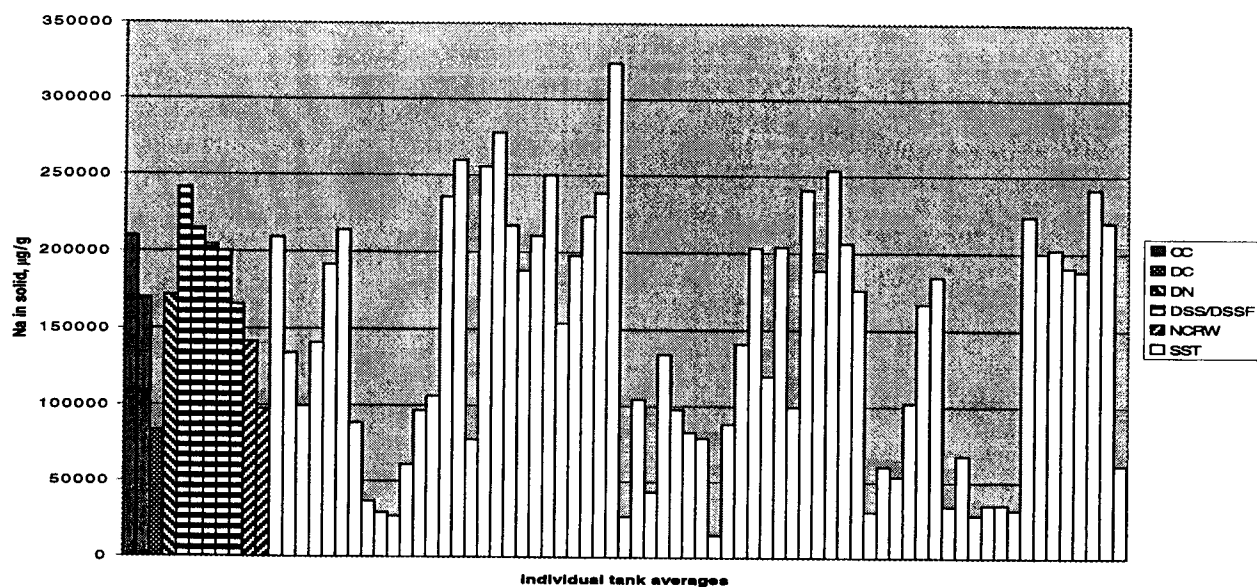
Figure 1-4. Average sodium concentrations (μg/g) in tank solids from the TWINS database. Abbreviations as in figure 1-2.
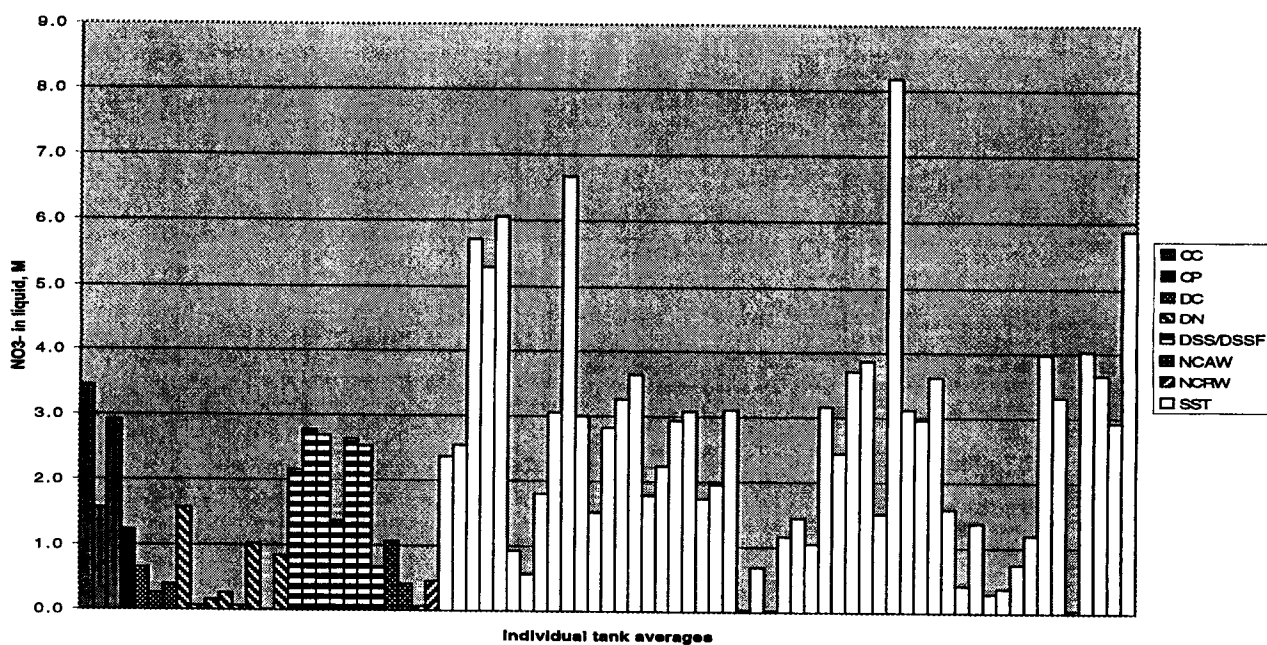
Figure 1-5. Average nitrate concentrations (moles per liter) in tank liquids from the TWINS database. Abbreviations as in figure 1-2.
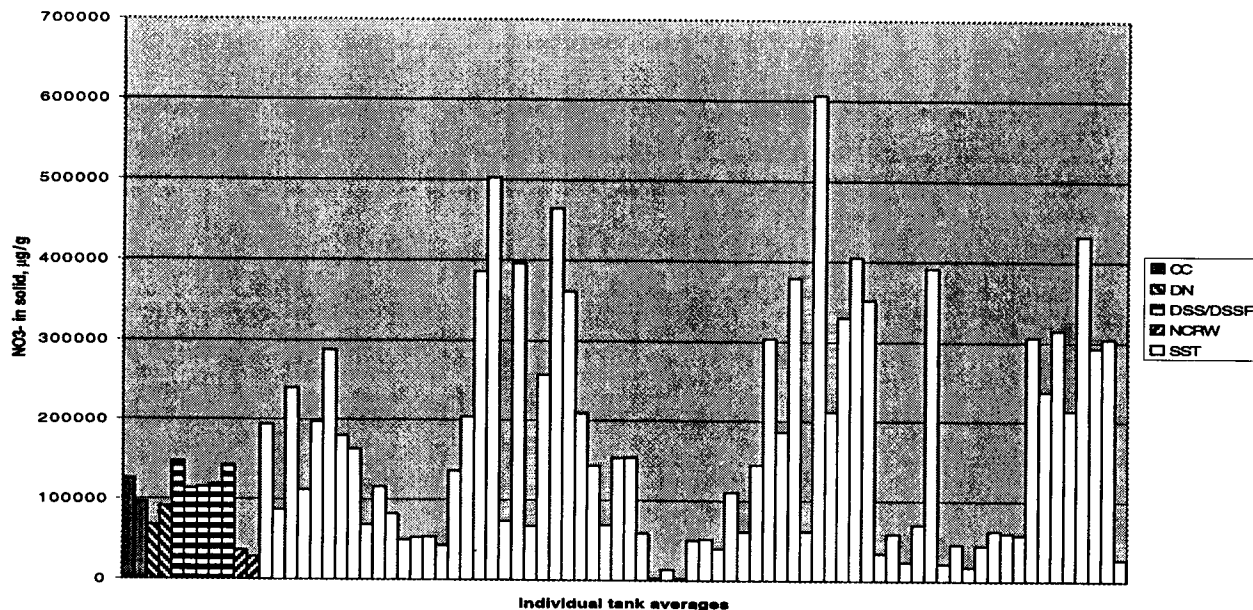
Figure 1-6. Average nitrate concentrations (μg/g) in tank solids from the TWINS database. Abbreviations as in figure 1-2.

inspection of the overall variation suggests that values cluster in the range of 1 to 10. Data on oxidation-reduction potential in tank liquids are not generally available. This lack of data may be addressed by various means, such as direct measurement of oxidation states of redox-sensitive species (e.g., Fe, Pu) and/or by thermodynamic modeling. For example, if it can be assumed that a pair of redox-sensitive constituents, such as nitrate and nitrite, are in equilibrium, then conditions in pH-Eh space may be constrained by measuring nitrate and nitrite concentrations. However, such calculations that rely on an assumption of equilibrium must be used with caution.

1.5.2 Organic Chemicals

Interest in organic waste constituents arises from two considerations (Gephart and Lundgren, 1995; Turner et al., 1995). First, at elevated temperatures, organic compounds can combine with the abundant oxidizing materials in the waste, chiefly nitrates and nitrites, in exothermic reactions that pose risks of fire, explosion, or both. (This issue is discussed in more detail in chapter 3.) Second, organic complexants can bind with waste constituents (e.g., radionuclides) and affect their chemical behavior during waste treatment processes. The overall EIS inventories report organic components only as TOC. Ongoing individual tank inventory efforts such as HDW provide more detailed delineation of organic compound contents by tank and overall for the Hanford site (Agnew, 1997; Cragnolino et al., 1997). The overall site inventories show that, on a molar basis, glycolate is the predominant organic complexant. The other listed organic species—citrate, ethylenediaminetetra-acetic acid (EDTA), N-(2-hydroxyethyl)ethylenediaminetetra-acetate (HEDTA), acetate, oxalate, dibutyl phosphate (DBP), and butane—all have similarly low molar concentrations, ranging from approximately 1/20 to 1/4 of the total site glycolate value. On a weight basis, glycolate is rivaled in

1-14
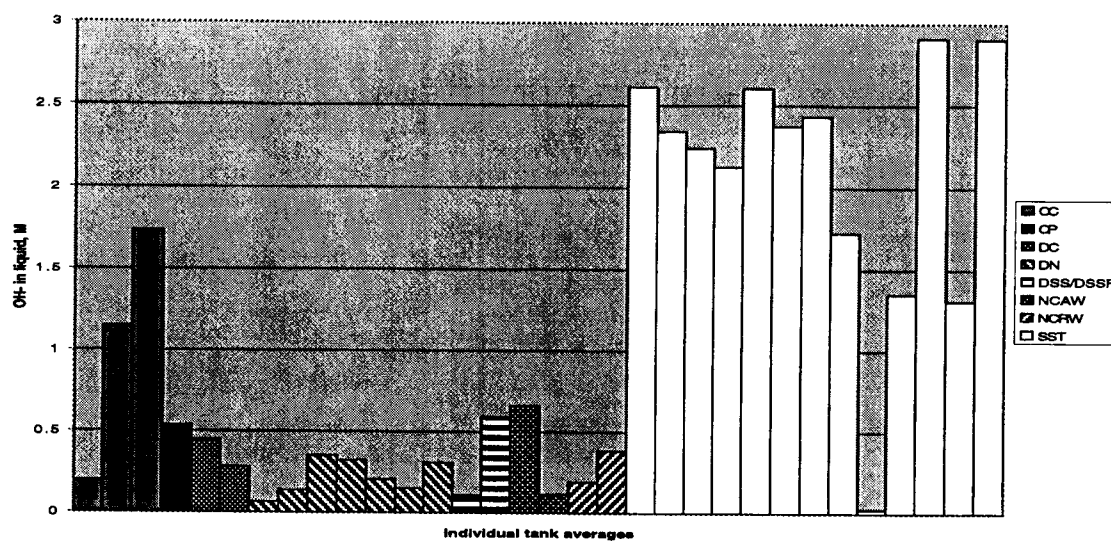
(a)
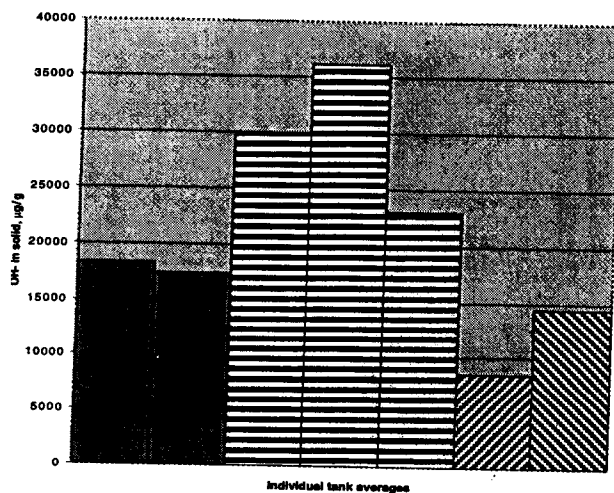
(b)

Figure 1-7. Average hydroxide concentrations in (a) tank liquids (moles per liter) and (b) tank solids (μg/g) from the TWINS database. Abbreviations as in figure 1-2.
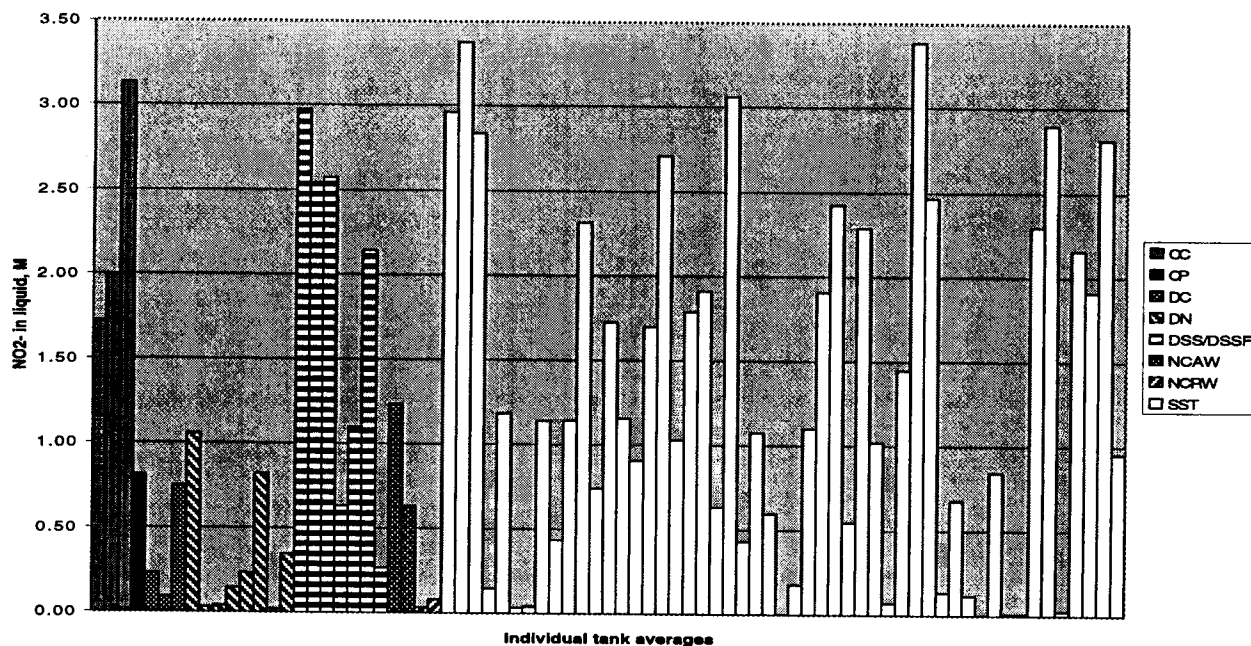
Figure 1-8. Average nitrite concentrations (moles per liter) in tank liquids from the TWINS database. Abbreviations as in figure 1-2.
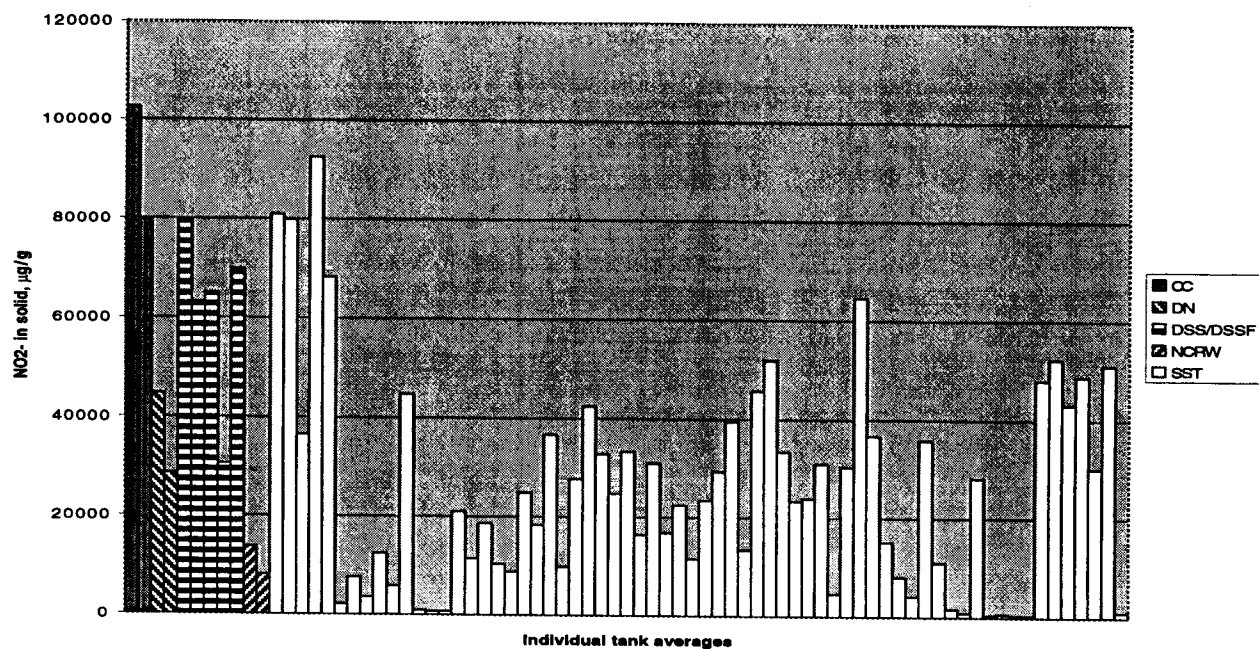
Figure 1-9. Average nitrite concentrations (µg/g) in tank solids from the TWINS database. Abbreviations as in figure 1-2.
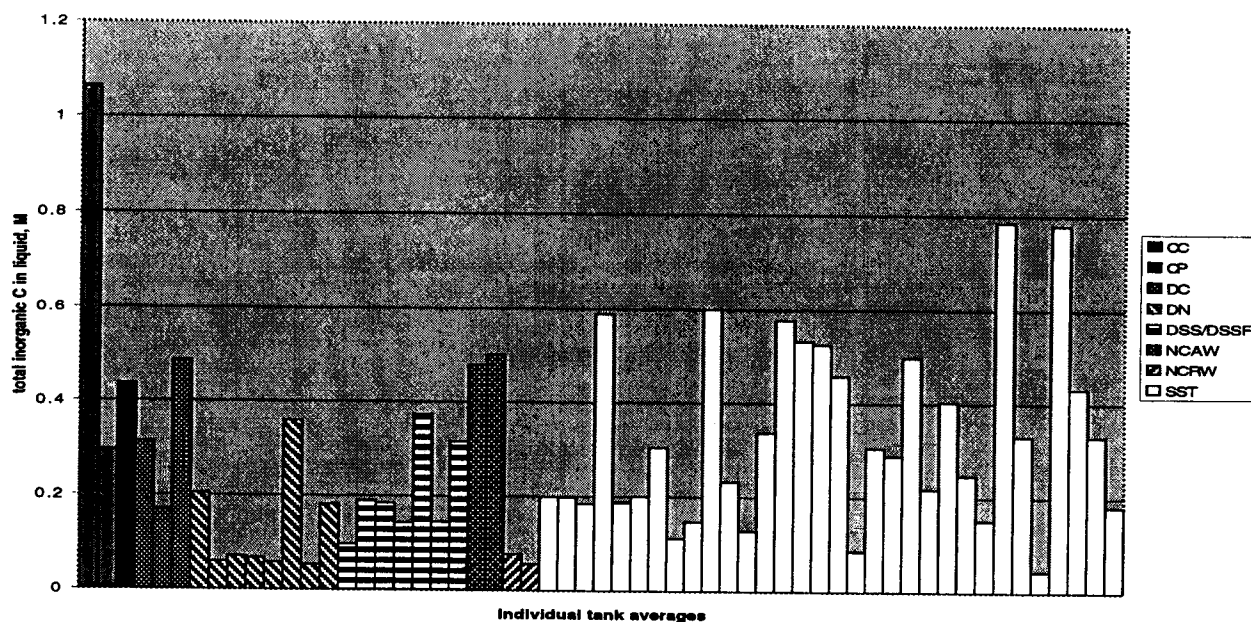
Figure 1-10. Average concentrations of total inorganic carbon (moles per liter) in tank liquids from the TWINS database. Abbreviations as in figure 1-2. The range of variation is consistent with the supernate data compiled by Serne et al. (1996) and shown in figure 5-12 of the present report.
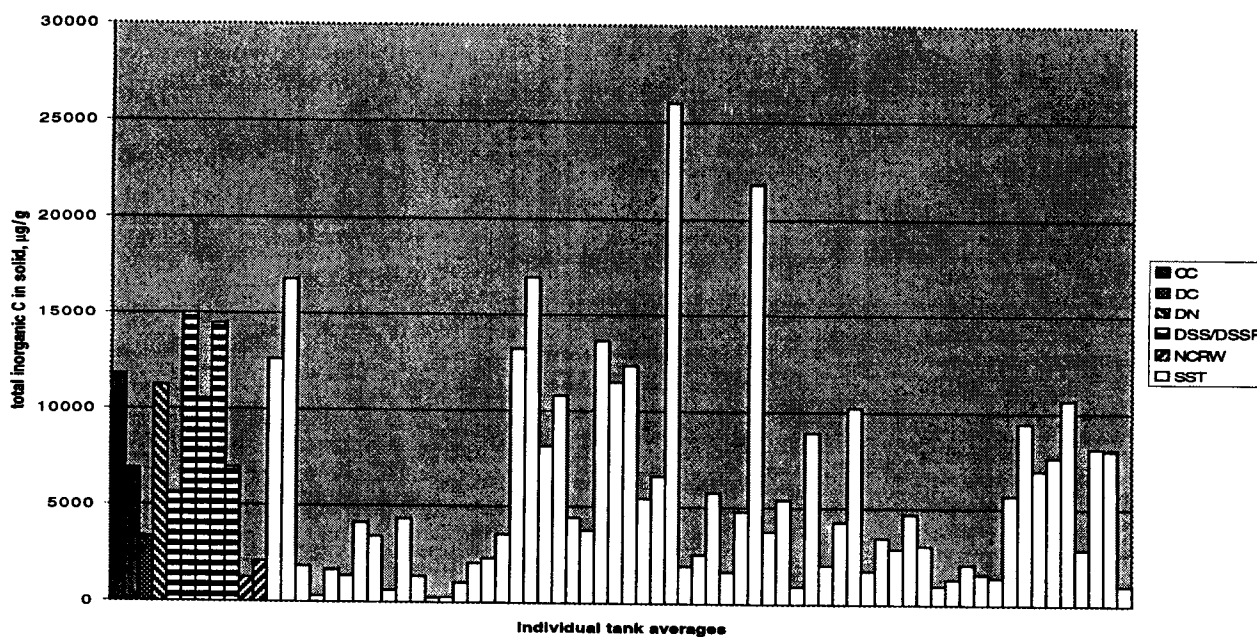
Figure 1-11. Average concentrations of total inorganic carbon (μg/g) in tank solids from the TWINS database. Abbreviations as in figure 1-2.
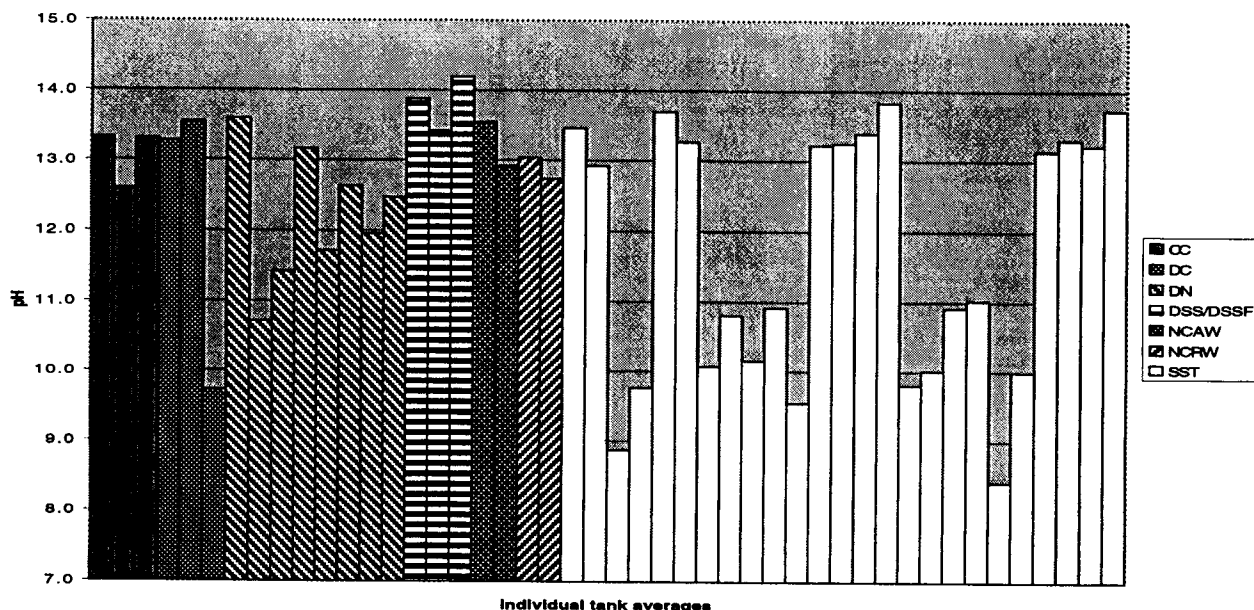
Figure 1-12. Average pH of tank wastes from the TWINS database. Abbreviations as in figure 1-2.

abundance by HEDTA. There are no major differences in organic inventories between SSTs and DSTs. As an illustration of organic content variations among tanks, figures 1-13 and 1-14 show tank average total organic carbon concentrations from the TWINS database. The high organic content of concentrated complexant waste compared to other DST wastes is evident.

1.5.3 Radionuclides

The key radionuclides for risk assessment at the Hanford site are C-14, Sr-90, Tc-99, I-129, Cs-137, and U (U.S. Department of Energy, 1996a). Table 1-3 lists the total tank HDW inventories for these radionuclides on a quadrant basis. Plutonium is added to the table because it is the key element for criticality hazard assessment (see section 5.3). As mentioned previously, Sr-90 and Cs-137 are by far the most abundant radionuclides on an activity basis. The daughters of Sr-90 and Cs-137—Y-90 and Ba-137m, respectively—are at or near a state of transient radioactive equilibrium (i.e., equal radioactivity) with their parents and should be included in the inventory. However, both of these daughters are sufficiently short-lived— they decay away in a matter of days when separated from their parents. Figure 1-15 shows the wide variability of Sr-90 concentrations in the tanks.

Of the six key radionuclides listed in the EIS, C-14, Sr-90, I-129, and Cs-137 are considered to present exposure hazards during remediation (U.S. Department of Energy, 1996a). Although the half-lives of Sr-90 and Cs-137 are short—29 and 30 yr, respectively—relative to the others, they are still long enough that these two radionuclides will remain the dominant sources of radioactivity exposure and heat generation hazard during waste retrieval and solidification. Consideration of longer term risk centers on those radionuclides—C-14, I-129, Tc-99, and U isotopes—which are deemed mobile in groundwater and have
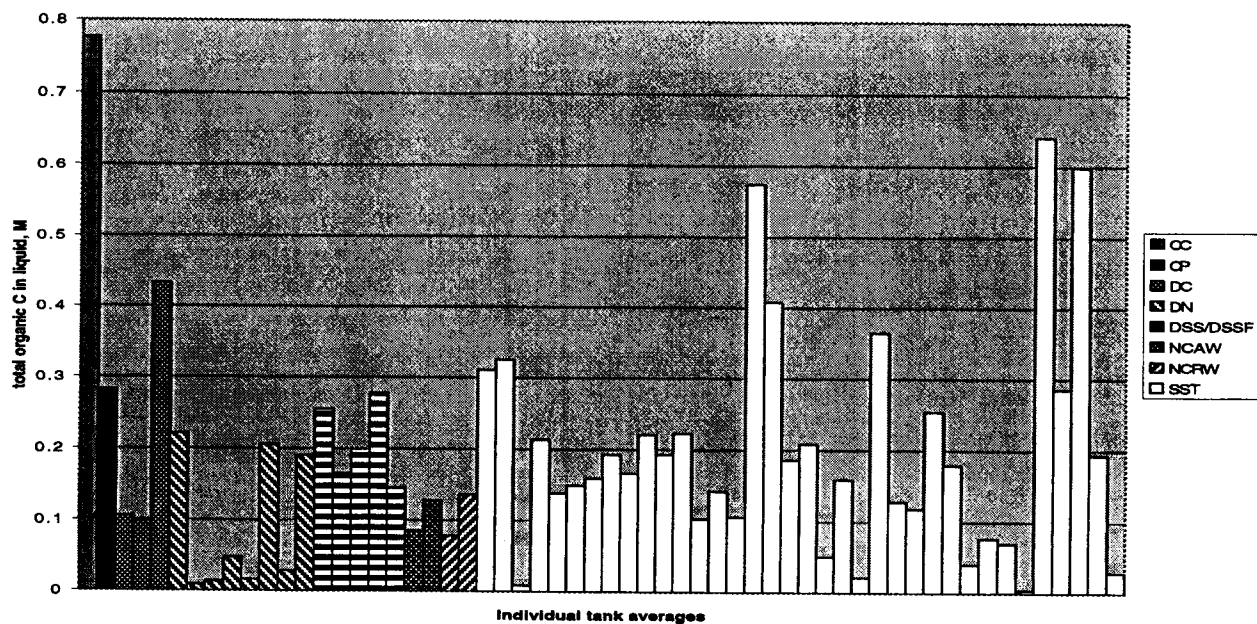
Figure 1-13. Average concentrations of total organic carbon (moles per liter) in tank liquids from the TWINS database. Abbreviations as in figure 1-2.
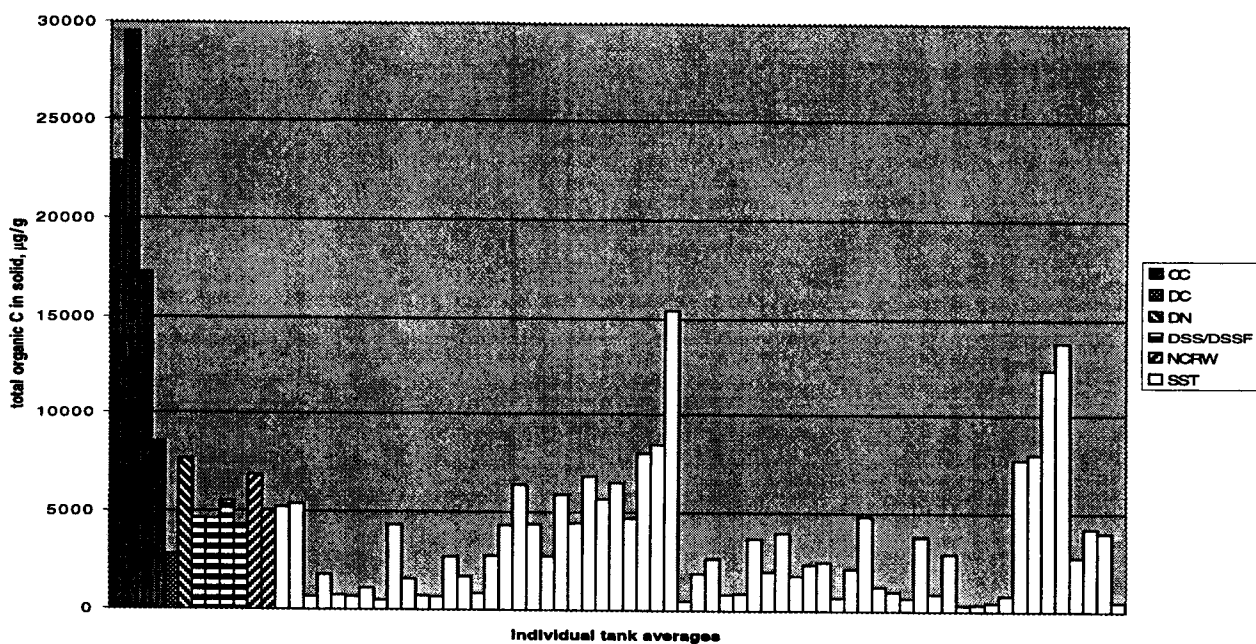
Figure 1-14. Average concentrations of total organic carbon (µg/g) in tank solids from the TWINS database. Abbreviations as in figure 1-2.

Table 1-3. Total Hanford defined waste inventories of key radionuclides in Hanford tanks, listed by quadrant (taken from Cragnolino et al., 1997). Values are in curies, with the exceptions of U and Pu (kg). Although Pu-239 and Pu-241 are the only fissile Pu isotopes, they comprise more than 95 percent of waste Pu by mass. Therefore, total Pu is reasonably representative of the relative fissile Pu content.

Quadrant	C-14	Sr-90	Tc-99	I-129	Cs-137	U (kg)	Pu (kg)
NE	8.4×10^2	2.3×10^7	5.3×10^3	1.0×10^1	6.7×10^6	1.1×10^6	2.7×10^2
SW	1.5×10^3	1.9×10^7	1.1×10^4	2.0×10^1	1.3×10^7	6.2×10^5	1.4×10^2
NW	4.1×10^2	1.9×10^6	2.9×10^3	5.6×10^0	4.5×10^6	4.9×10^5	1.2×10^2
SE	2.1×10^3	1.8×10^7	1.4×10^4	2.7×10^1	2.3×10^7	1.9×10^5	2.5×10^2
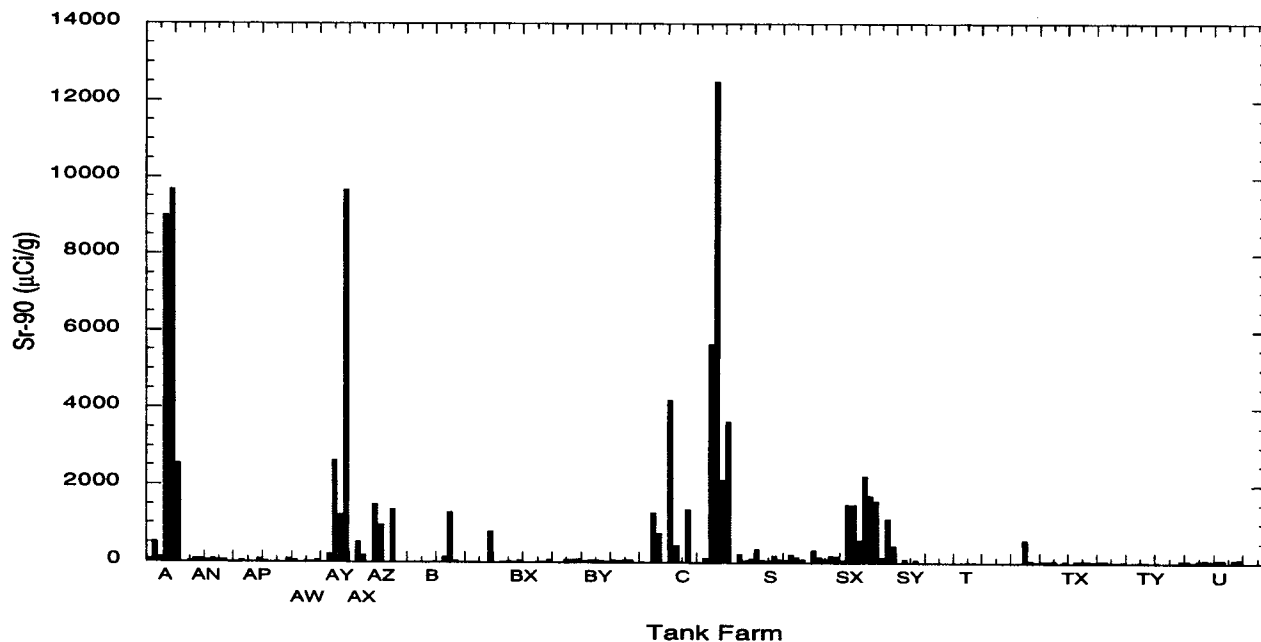
Figure 1-15. Bar chart of Sr-90 concentrations (μCi/g) in Hanford tanks from the Hanford defined waste model (Agnew, 1997). Many values are too small to be visible.

sufficiently long half-lives (5×10^3 to 4×10^9 yr) to persist well into the future. The longer term risk pertains to on-site storage of waste forms prior to disposal in a geologic repository and residual waste in the tank following remediation.

1.6   DISCUSSION

The nature of the tank waste inventories—chiefly their derivation in large part from reconstructions of waste histories—precludes attaching a high degree of certainty to any particular inventory estimation scheme without consideration of the times considered and the methods employed. For example, distribution of Cs-137 between SSTs and DSTs can be appreciably affected by pumping liquids from the former into the latter, which is an ongoing activity. Furthermore, it is projected that the 74,200 m^3 of waste in the DSTs will be augmented by another 12,400 m^3 during future waste transfers; no calculations of the effects on tank inventories were noted in the literature. Individual tank inventories have the highest degree of uncertainty. Agnew (1997) calculated estimated uncertainties in concentrations based on variability in knowledge of process and solubilities. The resultant variabilities for individual tanks based on Agnew (1997) and shown in Cragnolino et al. (1997; tables A-2 to A-7) ranged up to nearly 100 percent of reported concentrations, but most appear to be in the range of 10 to 50 percent. While the overall site tank waste inventories for constituents are subject to less uncertainty, significant differences emerge from one estimation scheme to another. The EIS authors state that it is not possible, considering model complexities, to easily explain the source of these differences.

A higher degree of confidence in individual tank inventories is the goal of the Hanford "best-basis" effort, which is intended to unify results from the HTCE/HDW estimation scheme with analytical data on the wastes themselves. This work is still in progress, and the most recent results may be viewed online at the PNNL Tank Waste Information Systems (TWINS) web site at

http://twins.pnl.gov:8001/TCD/main.html

(Permission for access to this database must be obtained from PNNL). This database also has all available assay data on tank waste samples and should prove to be a valuable resource for ongoing tank waste familiarization. However, until completion of this "best-basis" inventory, use of the HDW model (Agnew, 1997) is generally preferred.

Uncertainties in tank waste inventories and disparity in waste content between tanks may affect the chemical safety and the processing of the wastes. For example, knowledge of the chemical and physical properties of the wastes is needed to determine what, if any, actions are required to assure safe interim storage, retrieval, or processing of each waste tank. Quantification of major organic constituents is needed to evaluate potential hazards associated with flammable gases and oxidizable organic constituents. Similarly, data on the content, distribution, and form of fissile material would be useful for criticality safety analysis. In addition, information concerning the chemical forms and concentrations of matrix components and their radioactive constituents is necessary before adequate waste consolidation (mixing) protocols and/or separations processes can be engineered. Furthermore, uncertainties in the concentrations of glass-insoluble phases, such as chrome minerals, spinels, and noble metals, may lead to the need for blending of different waste types and/or increasing the volume of glass waste forms, both of which are expensive. Also, the presence of a large number of possible solid phases, aqueous complexants, and the high ionic strength (often several molal) of these solutions makes it extremely difficult to determine and predict the distribution of radionuclides among the sludges, suspended solids, and aqueous supernatants. Such a lack of fundamental knowledge about the distribution of radionuclides in the HLW stream significantly impacts the numbers of

glass logs requiring disposal and as a result the ultimate HLW disposal cost. The large disparity in the tank waste inventories indicates that significant mixing of tank contents is needed to meet the specified waste envelopes. Mixing of tank wastes may result in additional safety hazards through various chemical reactions that are discussed in detail in subsequent chapters. Thus, it is clear that better information on waste constituents in individual tanks is needed. Tank waste characterization is an ongoing activity at Hanford, and a strategy for sampling Hanford site tank wastes for development of disposal technology has been described by Slankas et al. (1995).

2 CHEMISTRY RELEVANT TO FLAMMABLE GAS GENERATION

2.1 INTRODUCTION

The risk associated with the release of flammable gases into the dome space of waste tanks at the Hanford site is a top priority safety issue (McDuffie, 1995). Twenty-five tanks are on the DOE Flammable/Hydrogen Gas Safety Program Watch-list as of September 30, 1997 (Hanlon, 1997), and all 177 tanks (Watch-list and non-Watch-list) are under flammable gas controls. This status means that flammable gas may exist in all 177 tanks, and special safety measures will be taken during maintenance, monitoring, and waste transfer activities (Hanlon, 1996; U.S. Department of Energy, 1996a). Although flammable gas production from radiolysis is always a concern for high-level radioactive waste storage, a special problem developed at the Hanford site when wastes were concentrated by evaporation to generate additional storage space in the million-gallon waste tanks. Due to retention of generated gases, the volume of the waste slowly increased after being pumped into the tanks, which defeated the purpose of volume reduction. The real problem became evident when some tanks began to have rather large surface level drops accompanied by release of gas mixtures containing both fuel (hydrogen, H_2) and oxidant (nitrous oxide, N_2O). These gas mixtures are flammable and potentially explosive even if not mixed with oxygen in the ambient air. Tank SY-101, prior to installation of a mixer pump, exhibited the largest cyclic releases (as indicated by tank surface level drop and increase in tank pressure)[1]. Also, hydrogen concentrations in the tank dome space and ventilation header exceeded the lower flammability limit (LFL) for short periods of time (McDuffie, 1994).

The tank wastes at Hanford are known to generate gases, primarily H_2 and N_2O, but also nitrogen (N_2), ammonia (NH_3), and minor gases such as methane (CH_4). The presence of flammable concentrations of gases and an ignition source, such as an electrical discharge, a hot surface, or a hot gas, could result in deflagration or detonation[2]. In a closed system such as a waste storage tank, transfer line, or waste process feed tank, the resulting high pressure from the expanding product gases can compromise the integrity of the tank or transfer line and cause a radioactive release to the environment. The resulting heat could also provide an energy source that could facilitate other reactions within the tank or transfer line.

The processes that result in generation of flammable gases and the attendant risk associated with those gases are expected to continue through the retrieval and processing stages of the Hanford TWRS operations[3]. This chapter provides information that may be useful to NRC staff in conducting safety analyses

---

[1] A summary description of the flammable gas hazard associated with tank SY-101 is given in appendix B.

[2] Deflagration is an exothermic reaction which propagates from the burning gases to the unreacted material by conduction, convection, and radiation (McKinnon and Tower, 1976). In this process the combustion zone progresses at a rate that is less than the speed of sound in the unreacted medium. Detonation is an exothermic reaction characterized by a pressure or shock wave in the material that establishes and maintains the reaction. In contrast to deflagration, the reaction zone in a detonation propagates at a rate greater than the speed of sound in the unreacted material (McKinnon and Tower, 1976; Cote, 1997). A deflagration or a detonation could lead to an explosion, a rapid expansion of gases in a rapidly moving pressure or shock wave that could disrupt enclosing materials or structures.

[3] A separate, but also important, safety issue relates to toxicity of gases or vapors, organic or inorganic, emitted from tank wastes that could lead to adverse health effects on workers. For example, NH_3, a gas produced in tank wastes, is on the Environmental Protection Agency (EPA) list of extremely hazardous substances, and has a National Institute for Occupational Safety and Health (NIOSH) permissible exposure level (PEL) of 50 ppm (Lewis, 1993). This safety issue, which is important to occupational risk and

of the Hanford TWRS with respect to flammable gases. Included in this chapter are discussions regarding flammability of gas mixtures, the mechanisms of flammable gas generation, and the factors affecting gas retention in tank wastes.

2.2   FLAMMABILITY OF GAS MIXTURES

2.2.1   Flammability Limits

Flammability[4] refers to the capability of gas mixtures, once ignited, to support combustion. Gas combustion requires an oxidizing gas, usually oxygen in air, and a reducing gas or fuel, such as methane or hydrogen. An inert gas, such as nitrogen, in the mixture affects flammability indirectly by absorbing the heat of combustion and affecting the flame propagation. Not all gas mixtures support combustion, and the shapes of some combustion chambers are more conducive to combustion than others. A combustion chamber designed to facilitate combustion for a particular fuel or purpose is a combustor. Regardless of the combustor, if a gaseous fuel and oxidizer are mixed in their stoichiometric ratio so that combustion would consume all of both oxidizer and fuel, any flammable gas will ignite when exposed to a small flame or spark. However, if the composition is changed to increase the ratio of oxidizer to fuel above the stoichiometric level, a limit is eventually reached at which there is insufficient fuel to support combustion. Beyond this limit, the composition is too lean for combustion, and the limit is termed the lower, or LFL. The term lean refers to having insufficient fuel for the amount of air or oxidizer present. Proceeding the other way from stoichiometric, if the mixture is changed to decrease the ratio of oxidizer to fuel, another limit is reached at which there is insufficient oxidizer to support combustion. Beyond that limit, the composition is too rich for combustion, and the limit is termed the upper, or rich, flammability limit (UFL). The term rich refers to having excess fuel for the amount of air or oxidizer present.

Common transportation fuels provide examples of using each limit to enhance safety. The diesel fuel manufacturing procedure limits the vapor pressure to a low value, so the vapor space above the fuel in a fuel tank is below the LFL, and a spark would not cause combustion. On the other hand, gasoline is manufactured with a relatively high vapor pressure, so the vapor space above the fuel in a fuel tank remains above the UFL. The published limits in several handbooks are based on work by the U.S. Bureau of Mines in the mid-1950s. The LFL is of primary interest in most attempts to prevent gas combustion, and reported values are generally accurate. The UFL is of less concern, and measured values in the literature are not as consistently accurate.

More recently, Cashdollar et al. (1992), also of the Bureau of Mines, published a detailed study of the flammability of hydrogen, nitrous oxide, and air. They also included some data for ammonia and methane. In the Hanford tanks that produce gas, ammonia is present in significant quantities. By itself, ammonia is more difficult to ignite than hydrogen. Nitrous oxide, an additional oxidizer, is also present, and methane is present in small quantities.

---

safety and is regulated by the Occupational Safety and Health Administration (OSHA), is not addressed in this report.

[4]Note that the term inflammable, encountered more frequently in older literature, has the same meaning as flammable. In current usage, the term nonflammable indicates a mixture that will not burn. The term flammability refers only to the combustion process.

At the stoichiometric ratio, combustion of the fuel and air mixture is not sensitive to the combustor geometry. However, combustion does become sensitive to combustor geometry near either of the flammability limits. Heat produced by the combustion expands the gas and causes it to flow. The flow is affected by the walls of the chamber, which means that different values of the flammability limits are obtained when the measurements are made in different combustors. Precise, valid comparisons can be made only if measurements used combustors with the same shape, size, and point of ignition. As combustor size gets larger, the influence of shape becomes less significant. To provide consistent and useful values of flammability limits, laboratories use either large combustion chambers, or well recognized, standard combustor geometries in which the flammability limits of many other gases have been measured. For example, flammability studies relevant to Hanford gas mixtures were done using a 120-L spherical chamber with an internal diameter of 2 ft (60 cm) (Cashdollar et al., 1992).

The results of flammability limit measurements vary significantly with the measurement conditions. The energy in the ignition source, the flow regime (turbulent, laminar, or quiescent), geometry of the combustion device, and the location of the ignitor all affect the measured value. For example, if a hydrogen-air mixture is ignited at the bottom of a cylindrical tube so the flame travels upward, combustion occurs in compositions down to about 4 percent hydrogen. However, if the mixture is ignited at the top so the flame has to travel downward, the limit is about 9 percent hydrogen. A spherical combustion chamber provides yet a different value. The differences are caused by buoyancy effects and the large disparity in the diffusion rates between hydrogen and air (Cashdollar et al., 1992; Jarosinski et al., 1982; Andrews and Bradley, 1972). Figure 2-1 shows the outlines of the flame front in a burning gas mixture within a large, spherical combustion chamber. (The outlines were drawn from photographs having insufficient contrast for direct reproduction.) As the flame front expanded outward into quiescent gas from the ignition source, it enclosed a bubble containing hot combustion products and began to rise because of the buoyant force. The resulting induced flow around the bubble modified its shape from nearly spherical at 360 msec to the mushroom-top shape at 900 msec (Burgess et al., 1982). The low values of pressure rise, or ΔP in figure 2-1, indicate a combination of incomplete combustion near the LFL and heat loss to the combustor wall. Jarosinski et al. (1982) and Andrews and Bradley (1972) provide detailed flame descriptions and discuss the mechanism of flame extinguishment in both upward and downward propagating flames.

Published LFLs generally reflect the lowest limit observed. This low limit means that, among the different combustor geometries tested, the case most likely to cause combustion was reported. In practice, therefore, a mixture slightly above the published LFL might not burn because of unfavorable geometry, but a mixture slightly below the LFL should not burn in any geometry. Thus, the LFL values tend to be conservative, or they err on the side of safety. The published LFLs are generally measured on homogeneous, quiescent mixtures within cylinders and ignited near the cylinder base. In practice, the common variations of composition in both space and time must be considered in any safety planning.

Another aspect of combustion makes the published LFL values conservative with respect to damage. Gas combustion causes damage because of the sudden increase of temperature, pressure, or both. If the gas mixture is only slightly above the LFL, in the region where the flame travels only upward, combustion produces only a slight pressure increase. This condition could only happen if the combustion were incomplete with only a small fraction of the available fuel actually reacting. The results of Furno et al. (1971), illustrated in figure 2-2, show the pressure rises for a hydrogen-air flame as a function of hydrogen concentration. The calculated values are the pressures that would occur if all available hydrogen were to react. The experimental or measured values begin at the LFL, a little above 4 percent hydrogen, but show much less pressure rise than is calculated. Only near 8 percent hydrogen, where downward flame
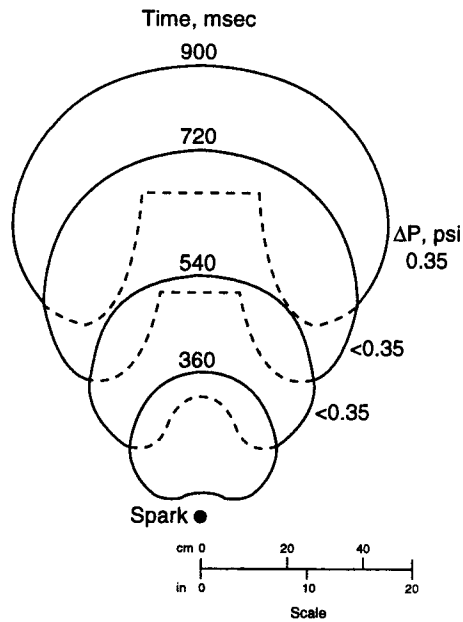
Figure 2-1. Side view of flame profile at four time intervals in millisecond after central ignition of a 6.9% CH$_4$, 65.8% air, and 27.3% N$_2$ mixture in a 3.6-m (12-ft) diameter sphere (redrawn from Burgess et al., 1982)
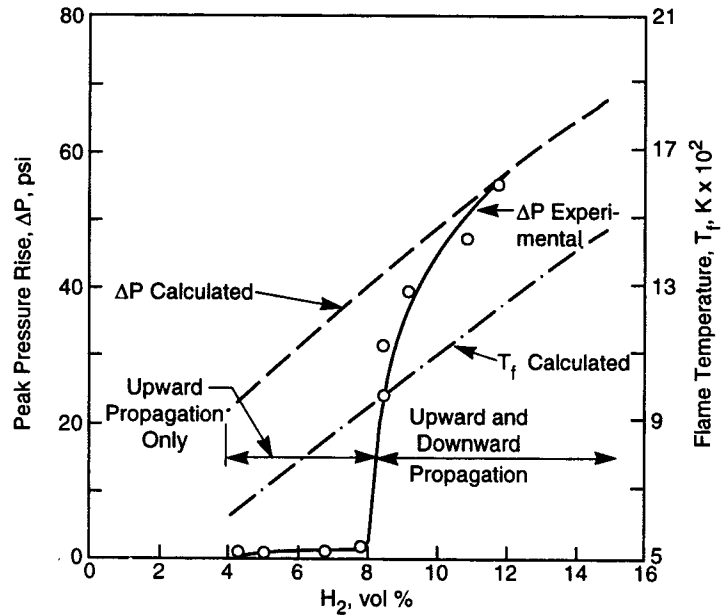
Figure 2-2. Peak pressure rises for ignition of hydrogen-air mixtures in a 3.6-m (12-ft) diameter sphere (redrawn from Furno et al., 1971)

propagation can also occur, does the pressure rise become significant. The pressure then rises steeply, approaching the calculated value at about 10 percent hydrogen.

Values of LFLs for various gases and mixtures of gases found in Hanford tanks are listed in table 2-1[5]. Fire and explosion hazards associated with flammable gases are often minimized by controlling the concentrations of the fuel, the oxidant, and inert gases. The LFLs measured under conditions of upward flame propagation, which are lower and more conservative than those determined with a downward propagating flame, are the values used for mitigating flammable gas hazards. For example, at Hanford, a safety criterion for flammable gas concentration in storage tank domes is 25 percent of the LFL, a value recommended by the National Fire Protection Association (NFPA). DOE Order 5480.4 requires that the NFPA guidelines be used for nuclear facilities. As mentioned previously, instances have occurred at Hanford, specifically at tank SY-101, in which a sudden gas release resulted in a hydrogen gas concentration in the dome space exceeding the 4 percent LFL.

Because of its small molecular size, the diffusion rate of hydrogen is faster than other fuel gases and common inert gases. At flame temperatures, hydrogen preferentially diffuses into the flame so the flame boundary becomes hydrogen enriched with respect to the bulk gas. This property, sometimes called diffusional demixing, is a significant factor in the mechanistic explanation of the low hydrogen LFL value. This also explains why the LFL for various $H_2 + N_2O + NH_3$ mixtures is not significantly different from that of pure H_2 (table 2-1).

Table 2-1. Lower flammability limits for gases found in Hanford tanks

Gas Composition	Lower Flammability Limits in Air at Atmospheric Pressure (Jones, 1954; Burgess et al., 1982; Cashdollar et al., 1992)	
	Upward Propagation, Vol %	Downward Propagation, Vol %
Hydrogen	4.0	8.5
Methane	4.85	5.25
Ammonia	15.5	NA
H_2 - N_2O (1:1 ratio)	4.0% H_2	8.5
H_2 - N_2O (3:2 ratio)	4.0% H_2	8.5
H_2 - N_2O (1:1 ratio) + 1 vol % NH_3	4.0% H_2	8.0% H_2
H_2 - N_2O (1:1 ratio) + 2 vol % NH_3	4.0% H_2	7.5% H_2

---

[5]Note that flammability limits are used interchangeably with explosivity limits.

The mechanism of combustion is complex. A number of chemical reactions involving radicals occur simultaneously in flames. Detailed information on the reactions can be obtained in other texts (e.g., Glassman, 1977) and will not be covered here, but a general understanding provides an explanation of some flame phenomena. Chemical reactions involving radicals are termed chain reactions and may be classified as branching, propagating, or terminating reactions. Branching reactions provide a larger number of radicals in the products than in the reactants, propagating reactions provide the same number of radicals, and terminating reactions provide fewer radicals in the products than in the reactants.

The reactions occurring in flames are strongly temperature dependent. The LFL for given components represents the point at which the combustion temperature allows a balance between chain-branching and chain-terminating reactions. Near the LFL, the flame temperature—called the limit flame temperature—is approximately the same for a variety of hydrocarbon fuels because the same fundamental chemical reactions are involved in each one, with only slight differences in carbon and hydrogen concentrations (Egerton, 1953; Zabetakis et al., 1959). If a different inert gas is substituted for nitrogen, the limit flame temperature changes, and the change can be accounted for entirely by the difference in heat capacity of the inert gases involved. The substituted inert gas must be truly inert—argon, for example—and not a participant in the chemical reactions. While steam and carbon dioxide do not support combustion, their effects on the limit flame temperature cannot be accounted for by differences in heat capacity. Both are reaction products and can function as a source of radicals that participate in the chemical reactions. In high concentrations, they change the chemical equilibrium compositions. This point is illustrated in figure 2-3, which compares some flammability limits obtained with carbon dioxide and nitrogen. Note that the term inert gas in the X-axis label refers to both nitrogen and carbon dioxide although, as the figure shows, carbon dioxide quenches combustion more effectively than nitrogen and, thus, is not truly inert. For a given ratio, in figure 2-3, the lower numerical value is the LFL and the higher value is the UFL. The differences in each pair of curves demonstrate the noninertness of carbon dioxide, but the original tabulated data (Jones, 1929), or more recent data, should be used for applications requiring numeric values. Egerton (1953) also discussed the so-called cool flames, which often involve decomposition reactions and also do not follow the relationship between temperature and reaction kinetics in the expected manner.

In contrast to reaction products, additional reactants affect the reaction only if they are in short supply. Additional fuel gases affect the LFL, but additional oxygen behaves much like an inert gas, causing a small difference in flame temperature accounted for by the slight difference in heat capacity between oxygen and the nitrogen it replaces. At the LFL, air already provides more oxygen than can participate in the reactions, so more oxygen does not significantly increase its participation in the reactions. Thus, the LFL of most gases is about the same whether measured in air or oxygen (Egerton, 1953).

2.2.2   Flammability Limits of Multicomponent Mixtures

The Hanford tanks that contain gas also contain multiple fuel gases and multiple oxidizers. A study of a large body of gas compositions available for tank SY-101 shows the composition given in table 2-2 for a typical gas release event (GRE). Gas samples from other tanks contain the same components, but in different amounts. For example, the ratio of hydrogen to nitrous oxide varies from a high of 33 for tank AW-101 to a low of 0.4 for tank U-105 (Pasamehmetoglu, 1994). However, most available data on flammability limits concern only mixtures of a single fuel and a single oxidizer. Industries commonly deal with multiple fuel components but only infrequently with multiple oxidizers.
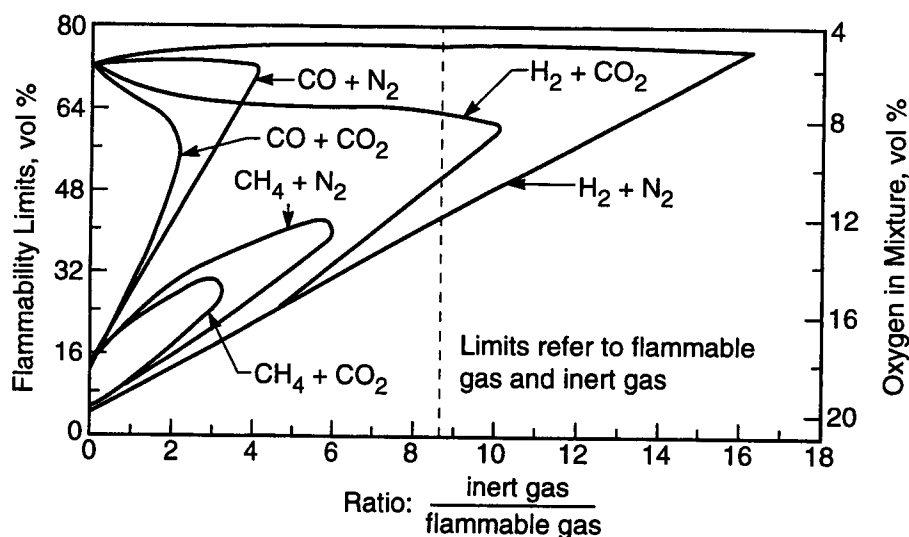
Figure 2-3. Limits of flammability of hydrogen, carbon monoxide, and methane in air with various amounts of carbon dioxide and nitrogen (redrawn from Burgess et al., 1982)

Table 2-2. Estimates of the overall composition of gases at 46 °C in Tank SY-101 (Pasamehmetoglu, 1994)

Component	Estimated Mole Percent
Hydrogen	29
Nitrous oxide	24
Ammonia	11
Nitrogen	33
Methane	0.4
Carbon monoxide	0.2
Water	2.4

Treating the fuel-gas mixture as though its LFL were equal to that of the component with the lowest LFL facilitates a conservative and adequate control method. Using this method requires that the sum of all the flammable gases be monitored; combustion is regarded as possible if the sum exceeds the LFL of the component having the lowest LFL. One industrial practice requires that the sum of all flammable gases be less than some fraction, typically one-fifth, of that limit (i.e., the LFL of the component having the lowest LFL) (Speight, 1987). Since the response, such as turning on a fan or opening vents, is usually convenient and inexpensive, this policy provides an effective strategy for preventing unwanted combustion. For example, in an operation using methane (LFL = 5.0 vol %) and ethane (LFL = 3.0 vol %), a policy may require additional ventilation if the flammable gas concentration were to exceed one-fifth of the LFL of ethane. The policy might be implemented by installing a continuous monitoring system to measure the sum of methane and ethane and automatically turn on additional ventilation fans if the sum exceeded 0.6 vol %. This procedure avoids the more complex necessity of determining the actual value of the mixture LFL.

In some circumstances, knowledge of an LFL value for a mixture may be desired. For example, combustion of a mixture near its LFL may be desired and planned for. The best solution is to obtain

2-7

measurements with the composition in question. However, if the composition changes, or if there are other reasons for needing data on a wide variety of compositions, the requirements for laboratory work may become quite extensive. If measurements cannot be made on the composition in question, a calculated or estimated value may be preferred. A rigorous approach for calculating mixture flammability limits from basic chemical principles would require chemical kinetic modeling using the radical reaction intermediates known to be present in flames. Flame propagation also depends on diffusion rates and the heat capacity of the total mixture including the inerts. Both diffusion and heat capacities are temperature-dependent. The problem would be computationally intensive and should have computer codes written and tested specifically for calculating the flammability limits of mixtures. For safety purposes, the practice of treating a mixture flammability limit as though it were equal to that of its lowest LFL component has generally provided adequate protection, and rigorous calculation procedures have not received much attention. If the mixture is expected routinely to go below its LFL, additional fuel gas may be added.

A simpler approach for making an approximation of the mixture LFL may be sufficient. Many (but not all) fuel gases obey the mixture law of LeChatelier, which states that if one takes several fuel-air mixtures, each containing a single fuel at its LFL, and mix them, the resultant multifuel mixture will also be at its LFL. The comparable version for the upper or rich flammability limit also holds. The equation for the mixture law is written as follows (Jones, 1954; Burgess et al., 1982):

$$L = \frac{100}{(P_1/L_1) + (P_2/L_2) + ... + (P_n/L_n)} \qquad (2\text{-}1)$$

where L is the limit of flammability in the multifuel mixture, P_n is the vol % of the nth component fuel in the final multifuel mixture so the sum of $P_1 + P_2 + ... + P_n$ equals 100 percent on a combustible basis (i.e., excluding air and inerts), and L_n is the flammability limit of the nth component in its single-fuel mixture. Both L and L_n are in vol %. The resultant value of L is an approximation and not as precise as a measured value.

The mixture law holds for mixtures containing hydrogen, carbon monoxide, and paraffinic hydrocarbons (ethane, propane, butane, etc.) in air (Jones, 1954; Burgess et al., 1982). Cashdollar et al. (1992) reported a few mixtures of hydrogen and ammonia for which the mixture law holds. However, the mixture law does not hold for hydrogen with either ethylene or acetylene in air, hydrogen sulfide with methane in air, nor for mixtures containing carbon disulfide. There are also several exceptions for mixtures containing chlorinated hydrocarbons. Thus, LeChatelier's mixture law should be applied with caution. If it can be established that it gives correct results for several mixtures of a given set of components, it should apply to all mixtures of the same set of components (Jones, 1954). Otherwise, experimental means of obtaining the limits may be required.

In the Hanford tanks, the production of nitrous oxide, N_2O, would seem to complicate the flammability question further. However, some studies done with mixtures of components in the Hanford tank gases indicate fairly predictable behavior. For example, Cashdollar et al. (1992) measured the LFL of blends containing either 50 or 60 percent hydrogen with the balance comprising nitrous oxide. The blends were then mixed with air for the flammability measurements. They reported that at up to about 20 percent hydrogen in the fuel-air mixture, the flammability data behaved essentially the same as a hydrogen-air mixture. This result is important because it simplifies the question of flammability limits in the presence of N_2O. Like additional oxygen in the lean region, the added N_2O appears to act much like an inert gas. As the concentration of fuel and N_2O moves away from the LFL toward stoichiometric, however, the N_2O can participate more fully in the reaction. At high concentrations, N_2O increases the explosion hazard

(Cashdollar et al., 1992). However, a significantly higher energy spark is required to initiate combustion/deflagration in $H_2/N_2O/air$ systems as compared to $H_2/O_2/air$ systems.

The result that N_2O at significant concentrations does not affect the LFL is important for another reason. Nitrogen dioxide, NO_2, although not significant in the Hanford tank vapor compositions, can promote the ignition of hydrogen (Ashmore and Tyler, 1963). However, in engine studies, neither NO_2 nor N_2O promoted the ignition of ammonia (Gray et al., 1966). Since NO_2 is not present in significant quantities and N_2O does not promote ignition of either hydrogen or ammonia, it appears that the oxides of nitrogen do not increase the flammability hazard above that which would exist if they were not present. However, if N_2O were allowed to increase to high levels, along with high fuel gas levels, the hazard of detonation with a shock wave rather than ordinary combustion would be increased.

2.3 MECHANISMS OF FLAMMABLE GAS GENERATION

The tank wastes at Hanford are known to generate gases, primarily H_2 and N_2O, but also N_2, NH_3, and minor gases such as CH_4. Flammable gases, such as H_2 and NH_3, are generated by radiolytic processes and thermochemical degradation of tank wastes, with minor contribution from tank corrosion for H_2. The two primary processes may have synergistic relationships such that some thermal breakdown may be enhanced by radiation exposure, and that the rates and mechanisms of radiolytic reactions may be temperature-dependent or involve byproducts of thermal degradation.

A solid understanding of the tank waste composition is a prerequisite to understanding flammable gas generation by radiolytic or thermochemical reactions. First, the mechanism(s) and rate of radiolytic gas generation are functions of the type of radiation and, possibly, the total dose, with both in turn functions of the amount and type of radioactive elements present in the waste. Likewise, heat generated by decaying nuclides also affects the magnitude and direction of thermochemical reactions. Second, the efficiency of radiolytic gas generation (often expressed in terms of the so-called G values; see section 2.3.2.1) depends on the composition of the matrix being irradiated—in this case, primarily the aqueous phase but also the solid and gaseous phases in the tank. Such compositional effects can come in the form of availability of reactant/substrate for radiolysis reactions (e.g., organic compounds for hydrogen abstraction reactions) or availability of scavengers that can nullify reactants in specific radiolytic reactions (e.g., NO_2^- for hydrogen abstraction reactions). Finally, back-reactions involving any radiolytically or thermochemically generated product also depend on the chemical species present in the waste matrix. The composition of tank wastes varies from tank to tank, and the majority of the tanks have poorly defined compositions (Gephart and Lundgren, 1995).

2.3.1 Radiation Sources and Interactions

The principal sources of radiation in Hanford tank waste are the radioactive decays of Sr-90 (half life = 28.8 yr) and Cs-137 (half life = 30.3 yr) and their short-lived daughters, together accounting for about 99 percent of the total radioactivity (measured in curies) in the waste tanks (Gephart and Lundgren, 1995)[6]. In SSTs, it is estimated that Sr-90 is responsible for about 75 percent of the radioactivity, with Cs-137

---

[6]Beta decay of Sr-90, its daughter Y-90, and of Cs-137 produces energetic beta particles (fast electrons) with energy that ranges from zero up to the characteristic energy of the emitting nuclide. This mode of decay also produces low-energy recoil nuclei and could also yield gamma rays (e.g., the isomeric transition from Ba-137m, a daughter of Cs-137, to Ba-137 emits a gamma in the Cs-137 decay scheme). Figures 6-1 and 6-2 in chapter 6 illustrate the decay scheme of Sr-90 and Cs-137, respectively.

accounting for about 24 percent. Conversely, Cs-137 is responsible for about 72 percent of radioactivity in DSTs with only 27 percent attributable to Sr-90. This distribution, however, applies to SSTs and DSTs in general and, hence, may not represent exactly the situation for individual tanks. Furthermore, the importance of specific radiation sources in gas generation is also influenced by their spatial localization in the tanks (Strachan and Schulz, 1993). For example, Sr is much less soluble than Cs in the supernatant and slurry aqueous phase in DSTs, hence most of the Sr-90 is resident in the precipitated sludge at the tank bottom. In contrast, Cs-137 primarily resides in the supernatant and slurry liquid of DSTs or in the saltcake and interstitial liquid of SSTs. Hence, any waste component that resides in the supernatant liquid or the overlying vapor phase is less likely to be directly influenced by beta emission from Sr-90. Depending on the efficiency of advective transport within each tank, the heterogeneous distribution of the primary radiation sources may affect tank-specific production of flammable gases.

Outside of Sr-90 and Cs-137, the balance of radiation is accounted for by other beta and alpha emitters. Alpha decay results in the production of energetic alpha particles ($_2^4\text{He}^{2+}$), energetic recoil nuclei, and gamma rays (Gephart and Lundgren, 1995). Alpha-emitting radionuclides such as Pu-239 and Am-242 will largely reside in the tank sludge, but some could be soluble, depending on the aqueous phase chemistry within individual tanks. In general, alpha emitters will become more important radiation sources only at much longer time frames (greater than ten times the half lives of Sr-90 and Cs-137 or more than 300 yr of storage) and they account for less than 0.1 percent of present radioactivity in Hanford waste tanks. This relatively low contribution of alpha emitters to the total radioactivity is not sufficiently counterbalanced by a higher radiation chemical yield for alpha radiation to make a substantial contribution to radiolytic gas production. For example, the alpha radiation chemical yield of H_2 for the radiolysis of water is only about three times that of its gamma radiation chemical yield.

Minor radiation contributions from spontaneous fission and alpha-neutron reactions are also expected, but their overall contribution to the radiation effects is even less important than alpha emission due to the relatively infrequent occurrence of such decay modes in Hanford tank waste (Spinks and Woods, 1990). Thus, within the time frame of on-site tank storage, waste retrieval, and waste processing, beta and gamma emission of Sr-90 and Cs-137 or their daughters will be the primary sources of radiation.

The energy transfer characteristics of alpha, beta, and gamma rays are such that they are anticipated to interact with the tank waste to produce radiolytic species that include a wide range of molecular, ionic, and radical species, depending on the initial molecular and ionic species present. The extent of this interaction is governed by the linear energy transfer (LET) characteristics of radiation in a given medium (table 2-3). Specifically, LET is defined as the linear rate loss of energy (locally absorbed), dE, of an ionizing particle or photon traversing through a distance, dl, in a material medium:

$$\text{LET} = -\frac{dE}{dl} \qquad (2\text{-}2)$$

Positively charged, short-range alpha particles, which have high LET values, interact very strongly with matter. Hence, they penetrate air through only a few centimeters and are stopped by paper-thin films of solid substances. Negatively charged, intermediate-range beta particles have generally lower LET values (the exact value is dependent on the energy with which it was emitted) and, thus, are able to penetrate a millimeter or more of solid matter or as much as a meter of air. It is reasonable to assume that alpha and beta emission energies are absorbed in wastes (Kasten, 1991).

Table 2-3. Linear energy transfer values for alpha, beta, and gamma emitters (modified from Spinks and Woods, 1990)

Isotope	Type of Radiation	Radiation Energy (MeV) (max. energy is listed for beta emitters)	Average LET in Water (keV/μm)
Ra-226	alpha	4.795	145
Po-210	alpha	5.30	136
H-3	beta	0.018	2.6
Sr-90	beta	0.544	0.27
Cs-137	gamma	0.662	0.52
Co-60	gamma	1.25 (avg.)	0.27

In contrast to alpha and beta particles, gamma radiation is very penetrating, and the energy absorbed by the waste depends on the strength of the gamma emission, the amount of gamma ray energy absorbed by interaction or collision with a waste particle, and the number of particles with which the gamma ray interacts. Gamma energy absorption increases with increasing numbers of waste particles, thus gamma absorption is a function of the waste density and geometry.

The decay of Cs-137 and Sr-90 can result in a substantial rise in the temperature of the tank waste. Chapter 6 provides an estimate of the heat buildup associated with these radioactive elements in the tank waste. The magnitude of the temperature increase depends on the radiation flux, the rheological properties of the waste mixture, the thermal conductivity of the multiphase system, and the heat transfer efficiency in the system environment. Self-heating effects in Hanford tank waste have resulted in a range of tank temperatures from 15 to 93 °C (Gephart and Lundgren, 1995). The specific temperature trends in each tank, of course, depend on the storage configuration, waste loading, and tank history. The heat buildup will affect thermochemical reactions.

2.3.2 Radiolytic Generation of Flammable Gases

2.3.2.1 Pure Water System

The overall chemical changes induced by exposure to ionizing radiation result from the initial formation and subsequent reaction of ionic and excited states along the trajectories or spurs of the charged particles or photons. Figure 2-4 shows the overall radiation products (top), specific ionization reactions involving water molecules (middle), and the physical dimensions of radiation spurs (bottom). The energy transfer from the radiation source to the ionic and excited states is primarily in the form of electronic interaction. The so-called primary products of radiolysis are the molecular and radical species formed as a result of dissociation and ion-molecule reactions involving the excited states. In pure water, the primary products include the radicals e^-_{aq}, H, OH, and HO_2 (or an ionic form of the radicals), molecular hydrogen
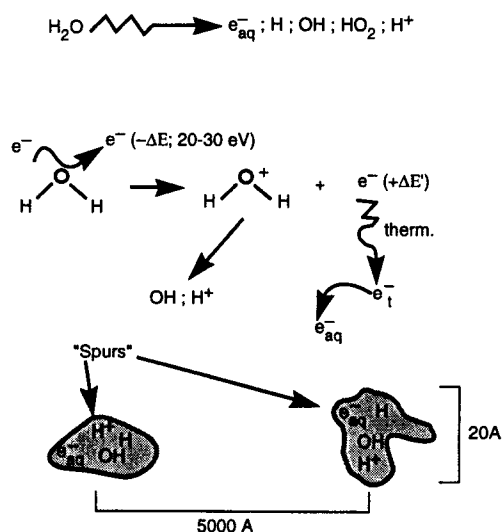
Figure 2-4. Primary radicals produced by the exposure of water to ionizing radiation (redrawn from Meisel et al., 1993)

(H_2), and molecular hydrogen peroxide (H_2O_2). The radicals e^-_{aq} and H are reducing radicals because they bring about reduction in inorganic solutes. Conversely, OH, HO_2 and H_2O_2 are oxidizing products because of their ability to oxidize inorganic solutes.

In the pure water system, H_2 is generated via the following mechanisms (k = reaction rate constant) (Meisel et al., 1993):

$$e^-_{aq} + H + H_2O = H_2 + OH^-$$
$$k = 2.5 \times 10^{10} \ M^{-1}s^{-1}$$

(2-3)

$$e^-_{aq} + e^-_{aq} + 2H_2O = H_2 + 2OH^-$$
$$2k = 1.1 \times 10^{10} \ M^{-1}s^{-1}$$

(2-4)

$$H + H = H_2$$
$$k = 1.55 \times 10^{10} \ M^{-1}s^{-1}$$

(2-5)

2-12

$$e^-_{aq} + H^+ = H$$
$$k = 2.3 \times 10^{10} \ M^{-1}s^{-1}$$

<div align="right">(2-6)</div>
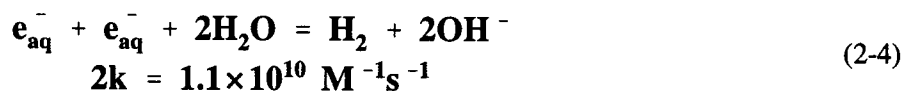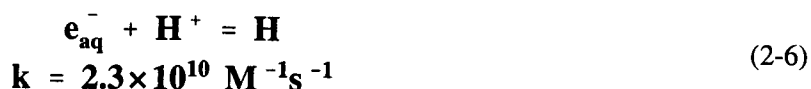
The radiation chemical yield of radicals or molecules in a given medium is expressed as its G value, which arithmetically is the average number of radiolytic species created (positive G) or destroyed (negative G) by the absorption of 100 eV of radiation energy. Compilations of G values are often in units of molecules per 100 eV, whereas the SI unit of the radiation chemical yield is mol/J (1 mol/J = 9.649×10^6 mol/100 eV). It must be recognized that the G values measure the final yield of radiolysis after the radiolytic reactions are complete. In contrast, the radiation chemical yield of radicals and molecules measured before they have had the opportunity to react outside of the radiation spurs or tracks is referred to as the primary yield (g). The latter is usually measured quantitatively using radical- or molecule-specific scavengers (Spinks and Woods, 1990). G values are radiation-specific. For example, gamma radiation is more efficient in producing radical species like e^-_{aq}, OH, and H, whereas alpha yields are greater for molecular HO_2, H_2, and H_2O_2 (table 2-4).

The radiation dependence of G values is related to the LET values discussed earlier in that higher LET values generally lead to higher G values. Compared to the g values, the G values in complex aqueous solutions will be substantially lower for any primary products that can react with other aqueous components. The degree to which such secondary reactions take place depends on the overall chemistry of the aqueous phase. Thus, G values are also matrix-specific in that changes in solution chemistry have the potential to change G values for any radiolytic species.

Given the chemical nature of the primary products of radiolysis, it is not surprising that the G values of some of these species are also a function of pH. Figure 2-5 (Spinks and Woods, 1990) shows, for example, that H and OH production declines substantially above a pH of about 2.5 and 10, respectively. The OH radical in alkaline solutions is converted to its conjugate base, the O^- radical. The conversion of OH to O^- radical could have significant impact on subsequent reactions because the O^- radical reacts much more slowly than the OH radical, and their potential interaction with dissolved organic matter can be quite different [O^- behaves as a nucleophile, whereas OH behaves as an electrophile (Gerber et al., 1992)]. At low pH, e^-_{aq} likewise rapidly is scavenged by the hydrogen ion and converted to H. Note that H_2, a very important byproduct from the standpoint of flammability hazard, is largely unaffected by pH. However, because atomic H is affected, H_2 generation in the presence of organic constituents could be indirectly affected given the role played by H in hydrogen abstraction reactions (see section 2.3.2.3). Table 2-5 shows a compilation of experimentally obtained $G(H_2)$ due to the radiolytic decomposition of water (Kasten, 1991).

Table 2-4. G-values (molecules/100 eV) of principal radiolytic species for gamma and 5 MeV alpha radiation of liquid water (Mendel, 1984)

	Species							
	H^+	e^-_{aq}	H	OH	HO_2^-	H_2	H_2O_2	H_2O
Gamma	2.7	2.7	0.61	2.86	0.03	0.43	0.61	−4.14
Alpha	0.3	0.3	0.3	0.5	0.10	1.4	1.3	−3.3
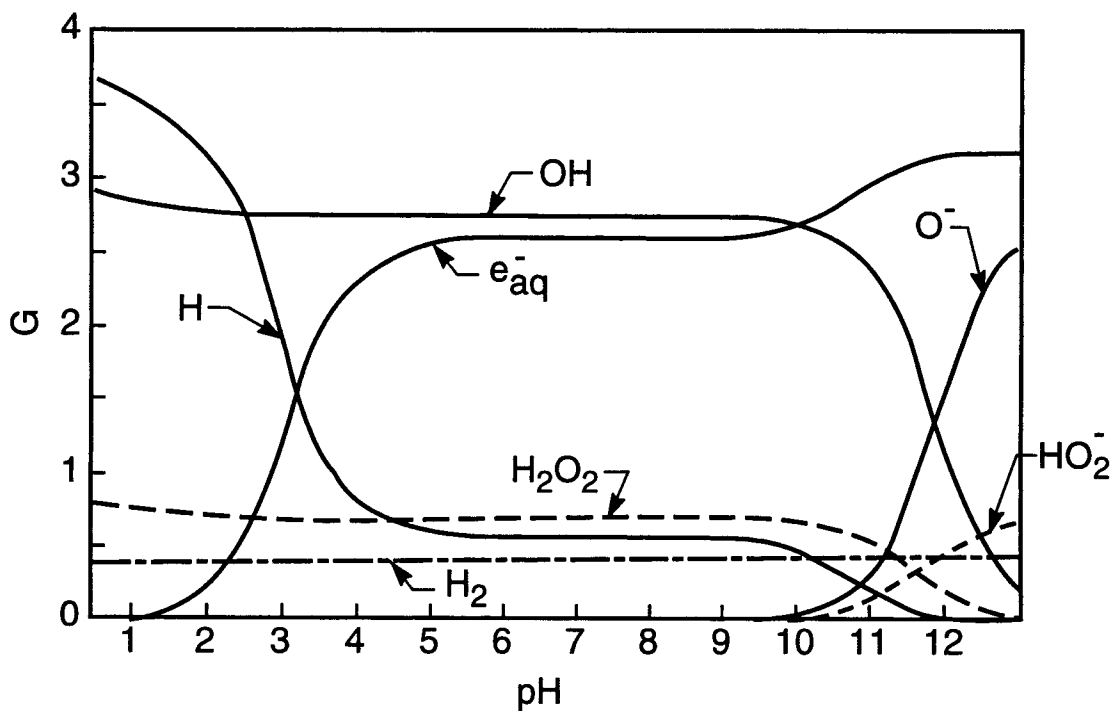
Figure 2-5. Dependence of G values on pH in gamma-irradiated water (redrawn from Spinks and Woods, 1990)

Table 2-5. Experimentally obtained $G(H_2)$ associated with the radiolytic decomposition of water [from Kasten (1991) and references cited therein]

Molecules of H_2 Generated per 100 eV of Radiation Energy Absorbed[a]		
Alpha	**Beta**	**Gamma**
4.6, 4.4, 3.6, 1.8, 1.57[b], 2.0, 1.3, 1.57	1.0, 0.60[c], 0.45, 0.425[g], 0.51	0.6, 0.45, 0.41, 0.45, 0.41, 0.40[b], 0.50[d], 0.55[e], 0.60[f], 0.70[g], 0.42, 0.45, 0.45, 0.425[g], 0.44
[a]The $G(H_2)$ value is determined from water at a pH of 7 unless noted as follows: [b]pH of 0.5; [c]pH of 1.0; [d]pH of 2 to 4; [e]pH of 5; [f]pH of 8; [g]pH of 13.		

2.3.2.2 Water-Inorganic Solute Systems

Most experiments performed by irradiating complex solutions (such as simulated Hanford tank wastes) and analyzing the products (postmortem) necessarily measure only the G values for the product species. The presence of other dissolved solutes in water could dramatically affect the G values because they, themselves, may radiolytically decompose, adding a parallel pathway for product generation. They may also react with the primary products of radiolysis, leading to the formation of so-called secondary radicals. For example, dissolved molecular nitrogen and carbon dioxide in water may undergo radiolytic decomposition involving a several-step recombination of the dissociation products with oxygen, water, and other associated radiolytic products (e.g., N_3, CO_2^-) to ultimately yield nitric and carboxylic acids, respectively. Dissolved O_2 also can scavenge e_{aq}^- and H quickly to produce HO_2 at pH below 4 and O_2^- at neutral to higher pH. The presence of O_2 also can have a dramatic impact on the nature of the radiolytic products formed in the presence of dissolved organic compounds (Meisel et al., 1993).

The predominant dissolved anion in Hanford tank wastes is NO_3^-, the radiation chemistry of which (together with that of NO_2^-) has been studied extensively. The aqueous concentration of NO_3^- is a key factor in H_2 generation because NO_3^- lowers $G(H_2)$. This lowering comes about because NO_3^- can effectively scavenge e_{aq}^- [compare Eqs. (2-3) and (2-4) to Eq. (2-7)] (Meisel et al., 1991) as in:

$$e_{aq}^- + NO_3^- = NO_3^{2-}$$
$$k = 9.7 \times 10^9 \ M^{-1}s^{-1}$$

(2-7)

Likewise, NO_2^- can effectively scavenge H via:

$$H + NO_2^- = NO_2 + OH^-$$
$$k = 7.1 \times 10^8 \ M^{-1}s^{-1}$$

(2-8)
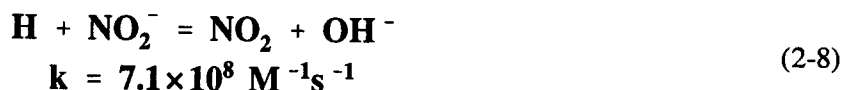
Scavenging of H by NO_2^- also plays a key role in suppressing H_2 generation in systems containing organic compounds because the capture of hydrogen radicals preempts the abstraction of organic hydrogen by H (see section 2.3.2.3). The degree to which NO_3^- and NO_2^- can suppress $G(H_2)$ is a direct function of the concentration of NO_3^-, NO_2^-, and organic compounds, and the respective rate constants. For example, if a simulated tank waste solution similar to that studied by Meisel et al. (1993) had 2 M NO_2^- and 0.1 M EDTA, competition kinetics (Spinks and Woods, 1990) would suggest a ratio of H consumption of 1.42:0.12 in favor of NO_2^- over EDTA. In such a solution, therefore, 92 percent of H will react with NO_2^- rather than participate in a hydrogen abstraction reaction involving EDTA. Interestingly, Meisel et al. (1993) showed that when NO_3^- concentration in tank waste simulant solutions exceeds 0.5 M and NO_2^- concentration exceeds 2 M, additional concentrations of scavengers have little effect on H_2 gas generation at 30 °C (figure 2-6). A series of experiments by Henrie et al. (1986) further supports the experimental observations of Meisel et al. (1993) on the effect of NO_3^- on H_2 generation. Finally, there is also some interest in the possible radiolytic generation of N_2O, an oxidizer, from Hanford tank waste. Whereas aqueous NO_3^- and NO_2^- are believed to provide the source of nitrogen for N_2O generation, the radiolytic formation of N_2O appears to require the presence of organic compounds (see section 2.3.2.3) (Meisel et al., 1993).
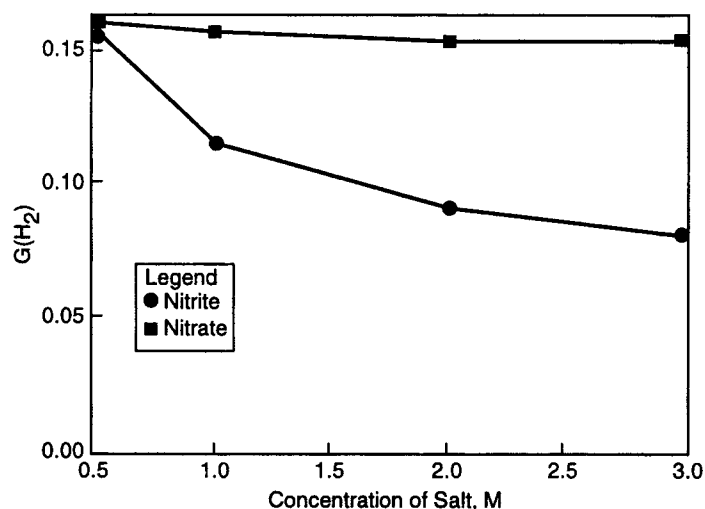
Figure 2-6. Calculated G(H₂) as a function of nitrite or nitrate concentration for gamma-irradiated tank waste simulant solutions (redrawn from Meisel et al., 1991). The symbols represent concentrations for which the calculations were performed. The simulant solutions were assumed to have 1.0 M NaOH. In addition, simulant solutions for which the nitrate effect was evaluated had 0.5 M NaNO₂, whereas solutions for which the nitrite effect was evaluated had 1.0 M NaNO₃.

The presence of other cations and anions in Hanford wastes undoubtedly also affects the generation of radiolytic product species. Changes in $G(H_2)$ can arise from changes in the total concentration as well as the specific nature of the dissolved ions. Multivalent metal ions and complexes could be reduced or oxidized, and unusual valency states may also be generated by reaction with e^-_{aq} and other radicals (Spinks and Woods, 1990).

2.3.2.3 Water-Organic Solute Systems

Radiolysis of water in the presence of dissolved organic compounds is important to flammability hazard assessment of Hanford tank wastes because of the presence of organic complexants, organic acids, and other organic constituents in the waste mixtures. In contrast to the oxidation and reduction reactions characterizing water radiolysis in the presence of inorganic solutes, abstraction and addition reactions are predominant in aqueous-organic systems (Spinks and Woods, 1990; Neta, 1976). The initial products of reaction between the primary radicals and organic solutes are organic radicals, which themselves react further, via addition or disproportion, to yield more stable products.

Hydrogen abstraction leading to the formation of H_2 is a classic radiolytic reaction in water-organic systems, and is also of prime importance in flammable gas generation in Hanford tank wastes. The generic reaction is of the form: $H + RH = H_2 + R$, where RH is an organic reactant, and R is the resulting organic radical. One such reaction, using formic acid as the organic reactant, is

$$H + HCO_2H = CO_2H + H_2 \qquad (2\text{-}9)$$
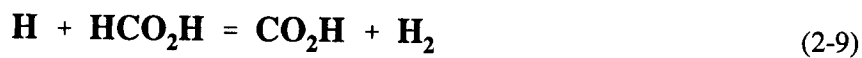
The rate constants for several analogous reactions involving organic compounds, including EDTA, HEDTA, nitrilotriacetic acid (NTA), iminodiacetic acid (IDA), glycolate, and citrate, are summarized in table 2-6 (Meisel et al., 1993).

Meisel et al. (1993) further determined the hydrogen abstraction efficiency at 30 and 60 °C of the organic compounds EDTA, HEDTA, NTA, IDA, citrate, glycine, and glycolate, and of tank SY-101 waste simulant solutions, such as those referred to as POC and POI (with compositions given in table 2-7). They established a correlation whereby the efficiency factor, R_x, when multiplied by the molar concentration of the organic compound in the aqueous solution, gives the increase in $G(H_2)$ above the yield of the same solution without the organic compound [table 2-7 (Meisel et al., 1993)]. The empirical correlation can be summarized as

$$G(H_2) = G(H_2)_{[RH=0]} + (R_x \times [RH]) \qquad (2\text{-}10)$$

where $G(H_2)_{[RH=0]}$ is the G value in the absence of organic compounds [$G(H_2)_{[RH=0]} = 0.03$ molecules/100 eV for simulated tank waste solution without dissolved organic compounds, according to Meisel et al. (1993)], and [RH] is the molar concentration of the organic compound. Furthermore, another correlation was suggested to predict R_x for compounds that were not tested (figure 2-7):

Table 2-6. Rate constants, k_1, and activation energies, E_a, for the hydrogen abstraction reaction: $H + RH \rightarrow H_2 + R$ (Meisel et al., 1993)

RH	$10^{-9} \times k_1$ at 30 °C $(M^{-1} s^{-1})$	$10^{-9} \times k_1$ at 60 °C $(M^{-1} s^{-1})$	E_a (kcal M^{-1})	$10^{-9} \times k_1$ at 25 °C and pH 1
EDTA	1.2	2.7	5.4	0.065
HEDTA	1.4	1.6	0.9	—
NTA	0.6	1.3	5.2	0.0075
IDA	0.55	0.85	2.9	0.00040
Glycolate	—	0.14	—	—
Citrate	≈0.007	≈0.02	7.1	0.00043
OH⁻ᵃ	0.033	0.13	9.2	—
[a]The reaction rate constants in columns 2 and 3 were measured relative to the known literature values of the rate constants for the reaction $H + OH^- \rightarrow e^-_{aq}$ at the two temperatures.				

Table 2-7. Hydrogen abstraction efficiencies, R_x, and yields, $G(H_2)^a$, of select gamma-irradiated organic compounds at 30 and 60 °C (from Meisel et al., 1993)

Organic Additive	[RH] (M)	$G(H_2)$ 30 °C	$G(H_2)$ 60 °C	Ratio $G_{60\ °C}/G_{30\ °C}$	R_x (30 °C)	R_x (60 °C)	Ratio $G_{x,60\ °C}/G_{x,30\ °C}$
None	0	0.031	0.033	1.06	—	—	—
EDTA	0.085	0.045	0.053	1.18	0.167	0.20	1.20
HEDTA	0.085	0.045	0.054	1.20	0.17	0.25	1.45
NTA	0.17	0.047	0.054	1.15	0.094	0.124	1.31
IDA	0.17	0.041	0.045	1.10	0.056	0.071	1.26
Citrate	0.17	0.036	0.037	1.03	0.029	0.024	0.81
Glycine	0.3	0.042	0.045	1.07	0.038	0.040	1.05
Glycolate	0.3	0.048	0.055	1.15	0.055	0.073	1.33
POC	b	0.045	0.063	1.40	—	—	—
POI	c	0.47	0.08	1.7	—	—	—

[a] Samples irradiated to approximately 140 krad in 30-min irradiations.
[b] Mixture of 2.3 M NaOH, 2.8 M $NaNO_3$, 2.2 M $NaNO_2$, 0.86 M $NaAlO_2$, 0.065 M EDTA, 0.065 M HEDTA (sodium salts), and 0.1 M sodium citrate.
[c] Same as b, but received 31.5 Mrad at 0.51 krad/min preirradiation, subsequently degassed, and used as starting material for further irradiation.
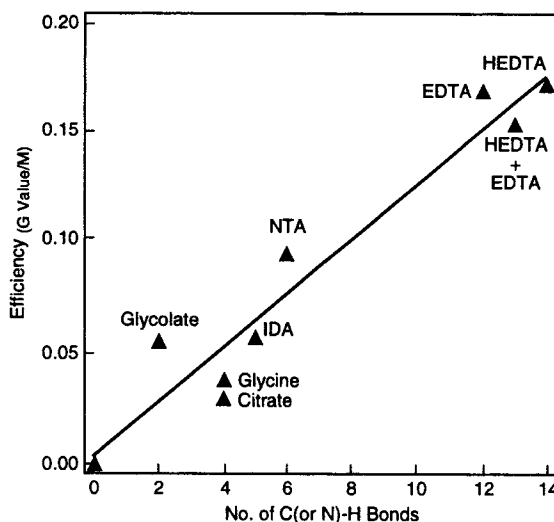
Figure 2-7. Dependence of abstraction efficiencies on number of C-H and N-H bonds in organic structure (Meisel et al., 1991)

2-18

$$R_x = 0.013(n_{x-H})$$ (2-11)

where n_{x-H} is the total number of C-H and N-H bonds in the structure of the organic reactant. Interestingly, there appears to be no dose rate dependence on $G(H_2)$ at 30 °C (Meisel et al., 1993).

One caution in the use of empirical equations, such as Eqs. (2-10) and (2-11), is that they involve an implicit assumption of a linear free-energy relationship applicable to the range of organic compounds available for hydrogen abstraction. Meisel et al. (1993) also pointed out that this empirical relationship applies only to background solution similar to the simulated tank SY-101 waste they tested. We note that the primary radical products of water radiolysis (e^-_{aq}, H, and OH) tend to react with functional groups, rather than the whole organic compound. It is therefore likely that the proportionality constant for Eq. (2-11) applies only to structurally similar series of reactants (Weston and Schwarz, 1972). It is difficult to estimate the impact of this uncertainty in the overall estimate of G values as a function of the amount and type of organic compounds present, although figure 2-7, which shows good correlation between abstraction efficiency and the number of C-H and N-H bonds in the organic structure, supports the validity of Eqs. (2-10) and (2-11).

Organic compounds appear to also play a key role in the radiolytic generation of N_2O. Meisel and others noted that no N_2O was generated in the absence of organic compounds in simulant tank waste solutions. Using N-15 labeled glycine as the organic reactant, they further showed, however, that only a minor proportion (less than 2.6 percent) of N_2O nitrogen actually comes from organic nitrogen, the balance coming from inorganic nitrogen (NO_3^- and NO_2^-). The roles of organic compounds and organic nitrogen were confirmed with the observation that N_2O is generated in the presence of organic compounds that do not contain nitrogen (e.g., glycolate) (Meisel et al., 1993).

2.4 THERMAL AND RADIOLYTICALLY ASSISTED THERMAL DEGRADATION OF ORGANIC COMPOUNDS

A major issue of concern in the formation of flammable gases in the Hanford tank wastes is the direct thermal and radiolytically assisted thermal degradation of organic constituents in the waste. This degradation arises from the simple fact that virtually all forms of organic constituents in the Hanford waste are thermodynamically unstable under present tank storage conditions. The rate and extent of thermal degradation are functions of the chemical nature of the organic constituents and other active chemicals in the waste, temperature, and time. Chapter 3 of this report discusses the sources of organic-bearing Hanford tank wastes and provides estimates of the total amount of organic chemicals introduced into Hanford waste tanks. Estimates of the total inventory of organic chemicals in Hanford tanks are also listed in chapter 3; estimated organic contents of individual Hanford tanks are provided by Agnew (1997).

One key issue of concern is how the organic wastes thermally decompose and generate gases of flammability concern such as H_2 and N_2O. It is noteworthy that the waste tanks known to produce flammable gas primarily received chelators (i.e., EDTA, HEDTA) and low molecular weight carboxylic acids (i.e., methanoic, ethanoic, glycolic, oxalic, succinic, and citric acids). It appears, therefore, that these compounds are the dominant components of concern from the standpoint of H_2 and N_2O generation. Probable reaction pathways and mechanisms for degradation of and gas generation from these organic components are discussed in detail in chapter 3 of this report.

Thermally activated reactions can be characterized using the standard Arrhenius relation:

$$k = Ae^{-\frac{E_a}{RT}}$$

(2-12)

where k is the rate constant, A (the pre-exponential factor) is a constant for a given reaction, R is the universal gas constant, E_a is the activation energy, and T is the temperature (in K). However, it is well known that the degradation rates of organic compounds are also influenced by factors other than temperature. For example, Meisel et al. (1993) have shown that preirradiation could considerably enhance the thermal degradation rates of organic compounds (see solution POI in table 2-7). Other factors that could affect thermal generation rates include TOC load, aluminate content, and the nature of other organic and inorganic species present.

It is useful to bear in mind that the application of an Arrhenius relation to describe the decomposition of organic compounds at various temperatures assumes that the reaction mechanism does not change over the temperature range examined. Where mechanistic changes are involved at different temperatures, separate Arrhenius expressions are required for each temperature range (Camaioni et al., 1994). For example, Barefield et al. (1996) examined the thermal decomposition of HEDTA and its degradation products in simulated tank waste at 90 and 120 °C and showed possible mechanistic changes at the two temperatures. Furthermore, multiple reaction pathways (at the same temperature) could lead to the generation of a single gas (e.g., H_2) from multiple precursors (Meisel et al., 1993). It is thus important to recognize that each of these multiple reaction pathways will have its own set of Arrhenius parameters (A and E_a). Ashby et al. (1994) attempted to extract Arrhenius parameters (pre-exponential and activation energy terms) for initial H_2 generation for simulated tank waste, estimating the activation energy for H_2 generation from HEDTA to be 71 kJ/mol. A similar approach was used for glycolate, for which activation energies for H_2 generation of 113 and 126 kJ/mol in an argon and argon/oxygen atmosphere, respectively, were estimated. For comparison, Meisel et al. (1993) suggested an activation energy for H_2 generation from formaldehyde of 84.8 kJ/mol, and from glyoxylate of 40.9 kJ/mol.

In the experiments performed by Meisel et al. (1993), the radiolytic breakdown products of EDTA and HEDTA were suggested to be the primary reactants leading to the ultimate thermal generation of H_2. This suggestion was confirmed by Ashby et al. (1994), who identified specific breakdown pathways of HEDTA and simpler analogues after irradiation. It was noted that the degradation products were different for samples that were irradiated prior to thermal decomposition versus those samples that were thermally decomposed without irradiation. These differences were primarily caused by the higher concentration of irradiation breakdown products (primarily glyoxylate, $CHOCO_2$, and formaldehyde, $HCHO$) in the irradiated samples.

2.5   MODELING FLAMMABLE GAS GENERATION

Flammable gas generation rates have been reasonably well established for waste compositions similar to those in tanks SY-101 and SY-103 through laboratory studies, such as those discussed in preceding sections, and observations of tank behavior, e.g., changes in waste surface level (Pederson and Bryan, 1996). However, gas generation rates for many other tanks are not known but are desired for analyses of potential flammable gas hazards. Graves (1994) presented an overall approach to estimating hydrogen gas generation

in nonburping Hanford waste tanks as a function of temperature and waste composition. The approach was to use a mass balance equation, which can be expressed in differential form as

$$\frac{dV(t)}{dt} = \dot{V}_{H_2} - (\dot{V}_{H_2} + Q)\frac{V(t)}{V_{cv}}$$

(2-13)

where $V(t)$ is the instantaneous volume of H_2, $\dot{V}_{H_2}$ is the volumetric production rate, V_{cv} is the headspace volume, and Q is the ventilation flow rate. The solution to this equation gives the volumetric concentration of H_2 in the headspace at any given time as

$$\frac{V(t)}{V_{cv}} = \left[\frac{V_o}{V_{cv}} - \frac{\dot{V}_{H_2}}{(\dot{V}_{H_2} + Q)}\right] e^{-(\dot{V}_{H_2} + Q)t/V_{cv}} + \frac{\dot{V}_{H_2}}{(\dot{V}_{H_2} + Q)}$$

(2-14)

where V_o/V_{cv} is the initial concentration of H_2 in the headspace. At steady state H_2 concentration,

$$\frac{\dot{V}_{ss}}{V_{cv}} = \frac{\dot{V}_{H_2}}{(\dot{V}_{H_2} + Q)}$$

(2-15)

Although H_2 is used in Eqs. (2-13) and (2-14), the same mass balance equation applies to the production of N_2O and other gases of concern. From the standpoint of the present report, the key parameter needing accurate prediction is the volumetric production rate of H_2 or any other gas of interest. From the previous review, there are two key generation mechanisms for H_2 production: thermal degradation of organics and radiolysis of water and organic compounds:[7]

$$\dot{V}_{H_2} = \dot{V}_{H_2,R} + \dot{V}_{H_2,T}$$

(2-16)

where $\dot{V}_{H_2,R}$ and $\dot{V}_{H_2,T}$ are the volumetric production rate of H_2 from radiolytic and thermal mechanisms, respectively. The radiolytic generation rate can be estimated from the radiolytic decay heat load (H), G value [$G(H_2)$], and a units conversion factor (F):

$$\dot{V}_{H_2,R}\left(\frac{L}{day}\right) = H \times G(H_2) \times F$$

(2-17)

F is a function of T (in K) and is given by

$$F = 7.35 \times 10^{-4} \times T$$

(2-18)

Chapter 6 provides a method for estimating heat load using Sr-90 and Cs-137 inventory. An alternative approach, using external vapor space temperature profile (where available), was used by others

---

[7]Generation of H_2 from tank corrosion was also considered by Graves (1994), with the essential conclusion that this source could account for up to 10 percent of H_2 production.

2-21

(e.g., Crowe et al., 1993; Graves, 1994). The last remaining obstacle in the accurate prediction of the radiolytic component of $\dot{V}_{H_2}$ is thus the value of $G(H_2)$.

The most quoted $G(H_2)$ value in the literature, and that used by Graves (1994), is 0.45 molecules/100 eV of ionizing radiation (see, for example, table 2-5). The presence of nitrate salts is expected to lower the $G(H_2)$ values as shown in figure 2-6, and Meisel et al. (1993) showed that $G(H_2)$ for simulated tank waste (without organics) is 0.031 at 303 K. Similarly, the effect of organic compounds present in solution on $G(H_2)$ has been formalized by Meisel et al. (1993) as (section 2.3.2.3):

$$G(H_2) = G(H_2)_{[RH=0]} + \sum (R_x \times [RH]_x) \qquad (2\text{-}19)$$

The second term in Eq. (2-19) represents the cumulative effect of all organic compounds on $G(H_2)$.

To estimate $\dot{V}_{H_2}$ from thermal production, Graves (1994) proposed the equation

$$\dot{V}_{H_2,T}\left(\frac{L}{day}\right) = \dot{V}_{H_2,T,POI} \times V_{LIQ} \times C \times (\text{TOC Ratio}) \times e^{-(E_a/R)(1/T_w-1/T_{POI})} \qquad (2\text{-}20)$$

where $\dot{V}_{H_2,T,POI}$ is the H_2 volume production rate (L/day) of preirradiated SY-101 tank waste simulant solution referred to as POI (Meisel et al., 1993), V_{LIQ} is the volume of liquid in the tank, C is a units conversion factor [from M/min (moles of gas per liter of liquid per minute) to L/day], TOC Ratio is the ratio of the TOC in solution relative to that present in POI, T_w is the tank waste temperature, T_{POI} is the solution temperature of POI (60 °C), and all other parameters are as defined previously. POI is the waste simulant solution in the experiments of Meisel et al. (1993) that exhibited the highest gas generation rate at 60 °C (see table 2-7). The total liquid volume is the volumetric sum of the supernatant, slurry, 60 percent of sludge volume, and 40 percent of saltcake volume. The correction for the sludge and saltcake volume is for the volumetric portion occupied by solid. One of the critical parameters in Eq. (2-20) is that of the activation energy for organic H_2 generation. Graves (1994) suggested a value of 40.9 kJ/mole, given that this value is the lowest activation energy yet measured for relevant organic compounds. As noted in section 2.4, this value corresponds to that of glyoxalate, an irradiation breakdown product of original chelators.

The computational method outlined previously makes estimation of flammable gas release rates in tank wastes viable, although it is constrained by limited available data and, to some extent, mechanistic understanding. In theory, the release of other gases (e.g., NH_3, N_2O, CH_4) can be considered in an analogous fashion as that of H_2. However, the scarcity of relevant data (e.g., G values, E_a) for these other gases precludes such calculations at this point (Graves, 1994; Bryan and Pederson, 1996). With respect to the calculation of the H_2 generation rate, the model used to derive the computational method is conservative in that no back-reactions are considered. It is not clear to what extent experimental systems used to simulate radiolytic and thermal effects have realistically included the effects of these back-reactions. One important issue in this regard is the generation of NH_3, which could form, at least in part, by back-reaction of H_2 (Bryan and Pederson, 1996).

Several of the input parameters to the predictive equations discussed previously have to be estimated empirically. Examples include estimation of the effect of NO_3^- and organic content on $G(H_2)$, effect of aluminate and TOC concentration on the rate constant, and estimation of E_a for H_2 generation. A

2-22

serious concern with this empirical approach is that the relationships are really applicable only to the matrix (in this case, solution chemistry) for which the empirical relationship was established. For example, the functional dependence of $G(H_2)$ on organic content (and type) developed by Meisel et al. (1993) [Eq. (2-10)] applies only to solution compositions similar to SY1-SIM-91C (tank SY-101). Caution is therefore required in the use of that formulation for other tank wastes. Similarly, the use of a single E_a value (e.g., for glyoxalate) to estimate the thermal contribution to H_2 generation in tank waste with a large, and yet to be fully characterized, suite of organic compounds may not be fully justified at this point. The use of the lowest activation energy known may indeed be conservative (Graves, 1994), but the resulting H_2 release rates may be too exaggerated to be useful.

The assumed dependence of thermal H_2 generation on other chemical parameters needs to be fully validated. For example, it is known that the reaction rate constant for thermal H_2 generation has a first-order dependence on aluminate concentration and TOC, but the thermal H_2 generation rate [Eq. (2-20)] used by Graves (1994) assumes that the amount of aluminate in the waste is similar to that of the SY-101 waste simulant POI. Hence, if aluminate levels in tank wastes are higher than are present in POI, the thermal H_2 generation rate will be underestimated. Finally, some comments are in order on the suggested relationship between the rate constant and the TOC value. It must be recognized that the thermal generation of H_2 from dissolved organic matter depends not only on TOC, but on the thermal stability of organic compounds present. Since it is likely that the rate constant for H_2 generation depends more on the abundance of thermally labile compounds rather than TOC, caution in the use of TOC ratio in Eq. (2-20) is suggested.

Graves (1994) applied the formulation discussed in preceding paragraphs to SST, DST, and double-contained receiver tanks to examine the full impact of H_2 gas generation from radiolytic and thermal processes. The full application of Eq. (2-14) required knowledge of ventilation methods and rates for each tank. As an example, table 2-8 shows a comparison between estimated and measured H_2 concentration normalized to the LFL (National Fire Protection Association, 1986) for selected SSTs.

In all the tanks examined in table 2-8, the measured values are less than the estimated H_2 values assuming passive breathing. It appears that the assumptions used by Graves (1994) were indeed conservative. More importantly, measured and calculated concentrations of H_2 shown in table 2-8 are all below 25 percent of the LFL. Hence the expected thermal and radiolytic H_2 generation rates are such that they are below the flammable limits with an adequate safety margin for either passive breathing or augmented flow. Additional tank to tank estimates of the input parameters and the calculated radiolytic and thermal H_2 generation rates are compiled in Graves (1994). That compilation shows that augmented ventilation will be required for several DSTs and SSTs with calculated H_2 levels exceeding LFL with only passive ventilation. Analysis of headspace gases in these tanks must be performed to verify the accuracy of model calculations, given that a significant level of conservatism has been built into the calculations. Finally, it should be noted that calculations based on the mass balance imposed by Eq. (2-13) treat the air ventilation as a simple dilution process. However, air ventilation also has an accompanying chemical effect (section 2.3.2.2), and Meisel et al. (1993) noted the enhancement of $G(H_2)$ in air- and O_2-saturated systems. Indeed, this enhancement of $G(H_2)$ by O_2 (present in actual tanks) is a plausible explanation for the higher $G(H_2)$ values observed in tank SY-101 relative to that predicted from Eq. (2-16) [see Section 3.5.1 of Graves (1994)].

2.6   FACTORS AFFECTING GAS RETENTION IN TANK WASTES

Several mechanisms may cause gas retention or immobilization in tank wastes. Immobilization can occur as a result of absorption into a solid or liquid, confinement within stable bubbles or foam, reaction with

Table 2-8. Calculated H_2 concentrations from radiolytic and thermal processes compared to measured H_2 concentrations from tank gas samples (from Graves, 1994)[a]

Tank	Date Sampled	Measured (% LFL)	Calculated	
			Passive Ventilation (% LFL)	Purge Air[b] (% LFL)
BX-106	06/17/93	< 1	2.3	0.7
BY-104	10/30/91	1	11.7	2.9
BY-110	09/27/92	< 1	7.3	1.8
BY-111	10/25/93	< 1	3.1	0.7
C-103	11/93	2.2	24.0	6.0
C-108	07/23/91	< 1	3.5	1.0
C-109	08/26/92	< 1	4.3	1.2
C-111	08/11/93	0.07	3.6	1.0
C-112	03/18/92	< 1	5.6	1.5
T-107	10/23/92	< 1	2.0	0.5
TX-118	07/28/93	< 1	1.29	0.34

[a]Of the tanks included in this table, calculated thermal H_2 generation exceeded radiolytic generation only in tanks BX-106, BY-110, and BY-111, with H_2 generation in the remaining tanks dominated by radiolytic production.
[b]Purge rate of 1.4 m^3/hr (50 ft^3/hr)

a solid or liquid, or adsorption onto the surface of a solid. Of these mechanisms, in the Hanford tank wastes, adsorption provides only a minor quantity of gas immobilization and does not have a significant effect on gas retention. The other mechanisms explain the gas retention behavior, with bubble confinement accounting for the majority of the gas retained (Johnson et al., 1997).

The gases generated in the waste vary in their solubilities in the liquid fraction of the waste. The solubilities of nitrogen and oxygen, entering from atmospheric contact, are also of interest. Gases are less soluble in brines than in water due to a salting-out effect[8], and the Hanford waste liquids have high salt concentrations. Norton and Pederson (1995) found the hydrogen and nitrous oxide solubilities in simulated tank waste (tank SY-101) to be 5 to 7 times lower than their solubilities in pure water. Nitrogen, oxygen, and methane solubilities were 10 times lower than in pure water. Methane is of less concern than hydrogen

---

[8] Salting-out effect refers to a reduction in the solubility of a gas in aqueous solution resulting from addition of another solute, particularly an electrolyte.

because only trace quantities are present. Of these five gases, none of which react with water, nitrous oxide is the most soluble, and the aqueous phase can account for significant quantities. For example, tank SY-101 retains an estimated 6.2 to 15.3 m^3 (220 to 540 standard ft^3) of N$_2$O in solution.

In contrast to the gases mentioned in the previous paragraph, gases that react with water, such as ammonia, have higher solubilities in water and in brine solutions. Ammonia reacts with water via Eq. (2-21):

$$NH_3(g) + H_2O \rightleftharpoons NH_4^+ + OH^- \qquad (2\text{-}21)$$
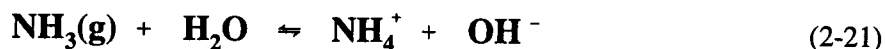
with an equilibrium constant, K, equal to $10^{-2.95}$ at 25 °C (Stumm and Morgan, 1981). Although the above reaction makes the aqueous solubility of ammonia dependent on the basicity or OH$^-$ concentration, which is high in Hanford tank wastes, it also makes ammonia solubility less sensitive to salt concentrations compared to the nonreacting gases. The measured solubility of ammonia in simulated tank waste is only about two times lower than in pure water. Norton and Pederson (1995) used activity models to estimate the quantity of ammonia in tank SY-101 as a function of temperature. The results range from 28,000 to 124,000 m^3 (1 to 4.4 million standard ft^3) as the temperature goes from 60 to 20 °C. The relatively high solubility of ammonia in solution mitigates the potential hazard involving this gas because no known mechanism could cause a sudden release of such large quantities from the aqueous phase. Further, although the ammonia released during GREs at Hanford has resulted in ammonia concentrations in the headspace as high as 1.3 percent, versus the 0.0035 to 0.005 percent during the interim or quiescent periods, the quantities released have been much less than the amount estimated to be in solution (Alleman, 1994; Norton and Pederson, 1995).

Any mechanism for causing a sudden release of ammonia from solution must accomplish the reversal of Eq. (2-21). The forward reaction is favored, even in brines, so equilibrium requires a relatively high concentration of ammonia in the liquid compared to the concentration in the vapor phase. Because gas solubilities in the aqueous phase decrease with increasing temperature, heating can cause reversal of Eq. (2-21). However, the tank waste volumes make rapid heating difficult to accomplish, whether intentionally or due to any unintentional actions. Also, the tank geometries, the presence of surface crusts or other solids, and tank ventilation makes a "Lake Nyos effervescent release," or limnic eruption, very unlikely (Palmer et al., 1996).

Tank ventilation constantly removes some ammonia from solution, so the liquid remains below the ammonia saturation limit. Palmer et al. (1996) developed ammonia concentration profiles for various tank waste configurations that agree with the available measurements. The concentration of ammonia in the headspace is a function of the concentration in the liquid near the surface, the amount of surface area exposed to the ventilation air, and the diffusional resistance across the boundary between them. A set of conditions such that the three factors could combine to produce ammonia concentrations higher than normal has been suggested by Stewart et al. (1996b) as a possible means of generating a rapid ammonia release. The suggested scenario applies to the SSTs, which are more likely than the DSTs to have a thick solids layer that sometimes exceeds the thickness of the liquid above it. This scenario could operate if the solid material had large pores that would allow the liquid to drain away quickly and, at the same time, a large surface area in the pores such that draining the liquid would expose a large, wetted surface area to the air in the headspace. If an event causes sudden draining of such a tank, the exposed liquid surface area would suddenly be increased to many times the geometric surface area of the original tank liquid. This process could then allow a large increase in the ammonia concentration in the vapor phase, assuming no change in the tank ventilation rate.

The above scenario is complex and difficult to model. Whenever there is a crust layer or other porous solid above any exposed liquid in the tank, it presents a diffusional resistance between the headspace and the liquid. Thus, although draining would cause the surface area to increase, favoring faster ammonia release, the diffusional resistance would also increase and restrict the rate of release. The gas release mechanism requires a large surface area, and a large number of small pores generally provides a larger surface area than a small number of large pores. However, as pore size decreases, the draining rate becomes smaller due to capillary forces and rapid draining of the liquid becomes less likely. Within a fixed volume, the pore size also affects the amount of diffusional resistance. Therefore, any model of ammonia release during draining must account for several variables that interact in complex ways and may be difficult to measure. For example, a rigorous accounting of pore size effects includes the pore size distribution, the wetted pore surface area after draining, and how both of these change with depth in the tank. Stewart et al. (1996b) reported on preliminary models, indicating that the tank headspace could experience a large increase in ammonia concentration from draining caused by salt-well pumping. However, the authors noted disagreement with salt-well pumping experience, and a remeasurement of some model parameters provided a revised ammonia concentration only 1/15 as high as previously calculated (Stewart et al., 1996b).

A simpler model of ammonia release, concentrating on the diffusional resistance, may be useful. It should be possible, for example, to show that some level of diffusional resistance would prevent a hazardous ammonia release from a hypothetical "instantly drained" tank. Then it may be possible to show that any credible pore size distribution would present a diffusional resistance as great or greater than the required diffusional resistance. In any event, a satisfactory resolution of this potential route to ammonia release requires further modeling and experimental verification of the model results. Johnson et al. (1996) noted that additional measurements of the liquid ammonia concentration are needed.

As indicated above, the ammonium ion in the brine should not be expected to be in equilibrium with the ammonia gas in the headspace if there is a crust on the surface of the liquid. A floating crust presents a diffusional barrier that is just as effective as a solid layer supported from the bottom of the tank and extending above the liquid level. The liquid composition will only be in equilibrium with gas that is trapped (i.e., gas moving slowly in and out of the pore compared to diffusion rates) within the pore spaces contacting the liquid surface. Those pore spaces should have higher concentrations of ammonia than in the headspace that is subject to ventilation. The crust layer is discussed further at the end of section 2.6.3.

Because temperature affects gas solubility in both water and brine, tank temperatures also affect the quantity of gas that is held in solution. Many of the Hanford tanks have elevated temperatures (up to 90 °C) (Hanlon, 1996) due to radioactive decay heat, so that dissolved gas concentration in these tanks is lower than if the tank temperatures were determined solely by the ambient weather conditions

2.6.1 Gas Retained in Bubbles

Ashby et al. (1992) have shown convincing evidence that gas retained in bubbles accounts for the majority of gas released in the occasional GREs. The chemistry of gas retention in bubbles and foams involves both the liquid and solid components of the material surrounding the bubbles. Without solids present, bubbles generally are not in thermodynamic equilibrium. A bubble in pure water will rise to the surface and burst within a few seconds. Bubbles persisting significantly longer are said to be stabilized. In most situations, they are stabilized by the presence of surface-active molecules or surfactants, such as soaps or detergents. These solutes act to change the rate of bubble bursting, not the equilibrium. Over a sufficiently long period of time, water gradually drains away from the bubble interfaces in the upper layers of a

surfactant-stabilized foam, and the bubbles eventually coalesce and burst. The slow rates permit such surfactant-stabilized foams to persist for months.

The presence of solids, on the other hand, can affect the equilibrium. Solidification of a polymer foam by cooling or reaction provides an extreme example. In those tanks at Hanford that generate gas, the bubbles are produced throughout the volume, and some of them contain chelating agents or organic complexants with surface-active properties (Ashby et al., 1992). Solid particles are usually present and may grow by crystallization processes or by adhesion to other particles. Thus, all necessary conditions are present for bubble stabilization and gas retention.

Surfactants affect both direct bubble stabilization and bubble stabilization with solids. In direct bubble stabilization without solids, the surfactant action dominates. Upon bubble formation, the surfactant concentration at the gas-liquid interface increases to a significantly higher value than in the bulk liquid. Surfactant molecules have a polar end, often containing oxygen atoms, and a nonpolar end, which is usually a hydrocarbon chain. The nonpolar end, by itself, would be insoluble in the liquid. The surfactant molecules align on the surface with their polar ends toward the water and their nonpolar ends toward the gas. The nonpolar ends associate strongly with each other and strengthen the film or surface. The migration of surfactant molecules to the interface occurs quickly, aided by the flow of liquid around the rising bubble; in water, it occurs while the bubble rises a distance equal to only a few of its diameters.

In stabilizing bubbles, surfactants act through a series of mechanisms. Reduction of surface tension reduces the energy required for bubble formation and is the best understood mechanism. Surface tension reduction alone, however, does not account for the observed stabilities. A related mechanism applies when gradients in the surface tension, which could arise around a thin spot in the bubble wall, induce flow toward the thin area. The gradient is referred to as the Gibbs Elasticity, and the flow as a Marangoni Flow. The chemistry and theory of these and other surfactant effects, including electrostatic interactions, are discussed in texts on surfactant chemistry and summarized by Durian and Weitz (1995).

2.6.2 Physical Gas Retention

Bubbles, with or without surfactants, adhere to hydrophobic surfaces. The hydrophobic nature of the solid surface may be a natural property corresponding to the bulk chemical composition, or it may be induced by treatments altering the surface chemistry or by certain surfactants, sometimes in conjunction with activators. For example, coal particles are naturally hydrophobic when freshly ground; after prolonged exposure to air, the surface becomes partially oxidized and less hydrophobic. Induced hydrophobicity is commonly used in mineral separations. The mineral and associated refuse are powdered, and the surfactant molecules adsorb onto the surface of the desired mineral with the polar ends toward the solid and the nonpolar ends toward the liquid. Bubbles are produced, possibly stabilized by another surfactant, to make a froth containing the mineral, which can be separated from the refuse by skimming. Thus, bubble attachment to solids is a common, easily produced phenomenon (Somasundaran and Grieves, 1975).

Gauglitz et al. (1994) discussed bubble entrapment in sludge, the forces involved, and the effect on tensile strength. Two types of bubbles are formed in sludge, depending on the relative strength of the forces involved in holding the sludge together. Near the top of the sludge where the weight of overlying particles is relatively small, bubbles can move individual particles and tend to conform approximately to their natural, spherical shape. Such bubbles may become entrapped in the sludge, but entrapment is more likely in more cohesive sludges.

To form a cohesive material, the particles may adhere to each other to form a floc, which is an interconnected network of particles with considerable liquid-filled void space among the particles. In common terms, most flocs would be referred to as sludge. Flocs often have open structures somewhat like sponges. Flocculants are surfactants that enhance the stability of flocs or facilitate the formation of flocs from suspensions of unconnected particles. A floc differs from a slurry in its rheological behavior. Since the particles in a slurry are unconnected, its flow properties differ little from that of the liquid, and liquid flows are generally Newtonian. In Newtonian flow, the viscosity is constant and the rate of shear is proportional to the stress—the more force pushing the liquid, the faster it flows. Flocs, however, are non-Newtonian. Subject to very small forces, their particles remain connected, and the floc does not flow at all. When the shearing force exceeds the forces holding the particles together, the particles disconnect and begin to flow. This transition is the yield value. At a stress below the yield value, the viscosity is infinite (no flow) but as the stress increases, the viscosity diminishes, ultimately approaching the viscosity of the particle-free liquid. Variations in the viscosity of the particle-free liquid affect both bubbles and flocs. At high viscosity, bubbles rise more slowly, and particles settle and adhere to each other more slowly. Since the time spent during bubble rise is normally very short compared to the time spent entrapped, only an extremely high viscosity could increase the overall amount of gas retained. The same argument applies to floc formation. The time required for a particle to settle and connect into a floc is very short compared to the floc "lifetime" or interval between GREs. Again, only an extremely high viscosity could decrease the rate of sludge formation to significantly extend the time between GREs.

Within the sludge layer, branched, or dendritic, bubbles are more common in the lower layers below the region containing spherical bubbles. At greater depth, the weight of overlying particles or interparticle forces inhibit particle motion, and the bubble can only displace liquid. The bubble takes on a branched, dendritic shape by extending into the space between particles. Liquid within the small pores of the floc is held in place by capillary forces stronger than the buoyant force of the bubbles and by the yield strength of the material. Gas bubbles within a sludge layer therefore are inhibited from traveling through the capillary-size spaces and may not have any sufficiently large escape paths. Percolation occurs when dendritic bubbles can grow into each other, connect, and rise toward the surface. Johnson et al. (1997) note that this mode of release is limited to relatively small quantities. More frequently, the bubble is entrapped within the floc, held in place by the capillary forces. Gauglitz et al. (1994) and the summary of their work included in Johnson et al. (1997) provide the mathematical relationships useful for modeling.

Gas generation throughout the bulk of a deep liquid/particle layer such as those found in Hanford waste tanks resembles boiling in porous media. Dhir and Catton (1982) have described experiments to determine the heat needed to dry out deep beds of porous media by boiling. The bed separates into a lower fixed bed in which bubbles move only through channels, and a higher fluidized bed which is continuously mixed. McDuffie (1994), building on earlier studies by Ashby et al. (1992), presents convincing evidence for similar layering in tank SY-101. The temperature profiles of the tank show the layers distinctly; the temperature data indicate a bottom layer at a nonuniform temperature termed the nonconvecting layer under a cooler layer with no significant variation of temperature with height. Heat transfer apparently keeps the second convective layer well stirred. Tank SY-101 and others also have a third crust layer floating on the surface of the liquid.

In other experimental work, Gauglitz et al. (1994) induced bubble generation and growth in simulated Hanford tank sludges. Their results showed that dendritic bubbles increased the sludge shear strength over that of the bubble-free sludge. This increased shear strength would contribute to the stability of the lowest layers of the tank sludge during the quiescent periods between GREs (Gauglitz et al., 1994).

2.6.3 Gas-Release Events

A significant quantity of the gas generation in Hanford tanks occurs within the bottom, nonconvecting floc or sludge layer in which gas becomes entrapped and accumulates. However, the bubble volume is small relative to its mass because of the hydrostatic pressure at the bottom of the tank. A GRE occurs when the trapped gas volume becomes so great that the bulk density becomes lower than the density of the overlying convective layer. Much of the whole bottom layer may then rise at once, or within a short period of time, through the liquid to the surface where the trapped gas is released. The observation that a large portion of the tank waste rises, or turns over together, indicates that the floc is metastable. It has either a small tensile strength or (because of its buoyancy) has become sensitive to a disturbance such as a minor pressure fluctuation. In any event, initiation of a GRE in one part of the tank seems to trigger similar behavior throughout much of the nonconvective layer. In addition to the gas traveling upward while trapped within large aggregates of the sludge, other bubbles are almost certainly freed from the floc as the disturbance temporarily opens channels to the convecting layer.

Johnson et al. (1997) note that, for typical tank conditions, the convective, or liquid, layer must be at least half the thickness of the bottom solids layer for a significant GRE to occur. This finding has been confirmed analytically and experimentally. Since this condition exists only in the DSTs, it undoubtedly explains why the GRE phenomena is limited to those tanks.

Gas accumulation disturbs the sludge layers and causes a GRE. When a GRE begins, a quantity of sludge at the bottom of the tank has only enough buoyant force to overcome its weight plus the forces of attachment to either the tank or some less buoyant section of sludge. However, the sludge is dynamically unstable; as soon as it begins to rise, the entrapped gas volume increases in response to the decreased hydrostatic pressure, which further increases the buoyant force. As a result, the sludge quantity accelerates as it travels upward. At the same time, the growing bubbles force the sludge particles apart until many of the bubbles break free to travel independently of the sludge, which may then decelerate. When the sludge has lost a sufficient quantity of gas so that the buoyant force becomes negative, it reverses direction and begins to sink. If it still contains some gas, it again becomes dynamically unstable as compression by the increasing hydrostatic force decreases the volume of the entrained gas and makes its buoyant force increasingly negative. At the initiation of a GRE, it seems likely that a relatively small part of the sludge breaks loose from its surroundings and begins to travel upward. Some aspect of either its separation, its travel upward, the bubble release, or its return to the bottom causes sufficient disturbance to induce other sections of buoyant sludge to break loose and propagate the event.

The occurrence of a GRE requires that the sludge layer, or a major portion of it, acquires enough trapped gas to become buoyant. Otherwise, disturbances cause gas release only from within the local area disturbed. For example, local penetrations, such as core sampling, cause gas release only from the material actually disturbed by the penetration. No disturbance or gas release occurs from the surrounding material (Johnson et al., 1997).

An exception to the buoyancy requirement for a GRE could occur if the entire sludge layer were disturbed at one time. This disturbance could occur as a result of a seismic event. Johnson et al. (1997) compared the energy involved in a GRE with that available from earthquakes and found that the GRE energy was comparable to that of a "...100-yr earthquake (0.22 g)...," and noted that for SST waste with its higher yield strength, a more severe "...1,000-yr earthquake (assumed to be 0.35 g)..." would be required to deposit the same relative energy. The cited figures refer to the maximum acceleration of the ground, relative to g or

the acceleration of gravity, occurring during an earthquake. Housner (1970) discussed this method of indicating earthquake intensity and seismic energy. The ground acceleration is measured at the location of concern and is a function of the inherent energy, or magnitude, of the earthquake, the distance from the epicenter, and the properties of the material carrying the seismic wave. He tabulated maximum accelerations for several earthquakes and the horizontal distances between the measurement and the slipped fault. Housner (1985) also summarizes the distance-acceleration relationships developed for evaluating the effects of earthquakes. The work of Johnson et al. (1997) is most useful for making general comparisons between single- and double-shelled tanks. For any individual tank, the disturbing energy required to initiate a GRE would be higher immediately following a GRE and decreases to near zero immediately before the next GRE.

Some quantity of gas is also retained in the crust layer, but it is not a major contributor to the quantity of gas released during a GRE. The crust material has a greater density than the brine, but floats because of the gas trapped within and beneath it. The mechanism of crust formation is not well known, but it may have formed from individual particles or small groups of particles that were floated to the surface by attached bubbles. If crystal growth by evaporation resulted in enclosed spaces holding gas, the aggregated particles could float permanently. Similarly, a section of sludge might conceivably reach the surface without losing its bubbles and remain sufficiently intact to float permanently. It could then become strengthened by evaporative crystal growth. However this layer originated, the crust always retains some gas and acts as a diffusion barrier to gas coming continuously from the convecting layer. In addition, the observed surface disturbances occurring during GREs may cause a small amount of gas release or exchange from affected parts of the crust to the headspace above the crust.

Studies to date make it clear that, with the exception of ammonia, the mechanism of bubble entrapment in the nonconvective sludge layer is the primary means of gas retention. Stewart et al. (1996a) have measured the void fractions with a void fraction instrument (VFI) at specific locations within several tanks and used the information to calculate the total gas volume. Table 2-9 shows the results for six Flammable/Hydrogen Gas Watch-list DSTs. These tanks are the only ones for which direct measurements are available. Stewart et al. (1996a) also provide supporting data and related evidence to support their results.

2.6.4 Summary of Gas Retention Mechanisms

Table 2-10 lists the possible mechanisms of gas retention in Hanford tank wastes. It is intended to summarize the preceding material and provide one or two common examples of each mechanism. Where significant, the examples were drawn from investigations of the Hanford tank wastes; otherwise, they came from common industrial applications. Those examples believed to apply significantly to the Hanford tank

Table 2-9. Calculated gas volume in six Flammable/Hydrogen Gas Watch-list tanks[a] (after Johnson et al., 1997)

Tank	SY-101	SY-103	AW-101	AN-103	AN-104	AN-105
Gas Volume (m³ at STP) from VFI measurements[b]	218 ± 52	192 ± 73	209 ± 46	464 ± 30	213 ± 41	180 ± 26

[a]These double-shell tanks have the same total capacity of 4,391 m³ (1,160,000 gal).
[b]STP = standard temperature and pressure; VFI = void fraction instrument.

Table 2-10. Gas retention mechanisms and examples for Hanford tank wastes

Mechanism	Example
*Absorption or solution in a solid or liquid.**	*NH₃ in liquid tank waste.**
	*N₂O in liquid tank waste.**
Adsorption or attachment to a solid surface.	Activated carbon for air or water purification.
	Solid chemical catalysts.
Retention in bubbles stabilized by:	
Surfactants	Long-lasting foams, detergent solutions.
Surfactant/particle combination	Possible step in the formation and growth of a floating crust.*
	Mineral separations.
Entrapment between particles of a floc (sludge) and held by capillary forces.	*Gases generated in bottom sludge of tank waste retained until a GRE.**
	Possible step in the formation and growth of a floating crust.*
Gas held in porous media by diffusional resistance.	Causes higher concentrations of non-atmospheric gases in the crust layer than in the vapor space above the crust.*
*Makes a significant contribution to gas retention in the Hanford tank wastes.	
Italic type indicates largest contributors to gas retention.	

wastes are marked with an asterisk (*), and the major contributors to gas retention at Hanford are in italic font.

2.7   SUMMARY

Essentially all radioactive wastes generate flammable gas mixtures by complex chemical reactions arising from radiolysis of water, thermal and radiological decomposition of organic compounds, and corrosion of metallic tank walls. The gases generated by these reactions comprise mainly hydrogen, nitrous oxide, nitrogen, and ammonia, with smaller amounts of methane and other hydrocarbons. In most tanks, the flammable gas generated in the waste is continuously released to the tank headspace. Various studies indicate that the generation rate is so low that ventilation ordinarily is able to keep the flammable gas diluted far below the concentration necessary for ignition. However, some wastes may have enough retained gas as to pose a potential for worker injury, damage to equipment, or release of radionuclides to the environment if a significant fraction of the gas were suddenly released into the headspace of storage or process tanks, transfer lines, or process equipment (e.g., pumps) and ignited. The potential for such releases to cause undesirable consequences constitutes the flammable gas safety issue. Even very small releases can collect in equipment or in poorly ventilated tanks and result in a flammable gas hazard.

Evaluation of the flammable gas safety issue with respect to continued tank storage or to retrieval and processing of Hanford wastes must consider the cause-and-effect relationship of gas generation, retention, and release. Gas generation is the ultimate source of the hazard. It must be understood well enough to estimate the generation rate and relative gas composition. Gas retention (i.e., the volume and composition of gas trapped in the waste) is a direct measure of the potential flammable gas hazard. Its understanding is necessary to determine the possible likelihood, rate, and amount of gas release. Gas release represents the proximate hazard. Flammable gas cannot create consequences until it is actually released in a closed volume at a composition that can be ignited. If the peak concentration of fuel gas released into the headspace of tanks, transfer lines, and process equipment is everywhere below the LFL, the gas will not ignite. If the concentration locally exceeds the LFL and a source of ignition is present at that location, that flammable portion could burn. Damage caused by the elevated pressures in the headspace or other enclosed spaces could result from such a burn and could result in release of radionuclides to the environment.

Various studies during the past few years have provided information on the mechanisms of flammable gas generation, retention, and release. Based on these studies, the three most important gas generation mechanisms are believed to be (i) radiolytic decomposition of water and some organic species, (ii) chemical reactions, mainly involving organics, and (iii) corrosion of the steel tank walls. The first two mechanisms dominate, and the yield from chemical reactions usually exceeds that from radiolysis, especially at higher temperatures. Several mechanisms may cause gas retention in tank wastes, but gas bubble retention is the primary mechanism for storing in tank waste large quantities of flammable gases that could be released rapidly. Large amounts of soluble gases, mainly ammonia, can also be retained in tank waste, but no credible mechanism for spontaneous release of large amounts of dissolved gas has been identified. Gas release mechanisms currently considered most credible are buoyancy-induced displacement, percolation of dendritic bubbles, and mechanical disruption, which includes local penetration (e.g., core sampling), removal of waste by salt-well pumping or sluicing, and severe earthquakes. Only buoyant displacement and seismic disruption are believed capable of a rapid release of a major portion (~50 percent) of the stored gas volume. However, energetic displacement can only occur in tanks with a relatively deep layer of supernatant liquid, a condition that exists only in DSTs. No known mechanism for large spontaneous releases in SSTs has been identified.

Some form of flammability control will always be needed to ensure safe operation during continued tank storage of Hanford wastes and during the TWRS operations. For example, sufficient ventilation must be provided to ensure that flammable gases are maintained at a safe level within the headspace of storage or feed tanks, transfer lines, or process equipment. However, controls need to be applied in a graded manner based on the type of activity being conducted. To identify the proper controls required for specific systems of interest, an adequate understanding of the processes and mechanisms for flammable gas generation, retention, and release is necessary.

3 CHEMISTRY RELEVANT TO ENERGETIC REACTIONS INVOLVING ORGANIC COMPLEXANTS AND ORGANIC SOLVENTS

3.1   INTRODUCTION

Various organic compounds were used at the Hanford site during fuel reprocessing, metal-recovery operations, and waste-management operations. In addition to the organic compounds, the Hanford tank wastes contain large amounts of sodium nitrate and nitrite, with the nitrite arising principally from radiolysis of nitrate and from nitrite addition for corrosion control (Agnew, 1997)[1]. Since these organic-bearing wastes are mixtures of organic compounds[2], strong inorganic oxidants, and heat-producing radionuclides, the potential exists for rapid energetic reactions that could result in radioactive release to the environment. Such a reaction resulted in a major explosion in a radioactive waste tank in Kyshtym, U.S.S.R. in 1957 (Fisher, 1990), resulting in radiation contamination of an estimated 23,000 km^2. The Kyshtym explosion occurred when the tank cooling system failed and the radioactive decay heat raised the temperature of a sodium acetate-sodium nitrate radioactive waste mixture to the point at which a thermal-runaway reaction occurred between acetate and nitrate. Another explosion occurred in 1975 at the DOE Savannah River Plant when excessive amounts of organic material were transferred to a denitrator during the conversion of liquid uranyl nitrate to solid U oxide (Gary, 1978). More recently, in 1997, an autocatalytic chemical reaction caused approximately 20 gal. of hydroxylamine nitrate and nitric acid stored in a 400-gal. storage tank at the Hanford Plutonium Reclamation Facility to explode (U.S. Department of Energy, 1997).

The possibility of analogous exothermic reactions to the ones cited above occurring at Hanford due to the presence of organic waste components mixed with oxidizing salts is a major safety concern, not only during continued storage of tank wastes, but also during the retrieval, processing, and solidification stages of the Hanford TWRS operations. For example, a potential for an uncontrollable exothermic reaction between nitrate and organic salts during preparation of a HLW melter feed was identified in the Hanford Waste Vitrification Plant Preliminary Safety Analysis Report (Herborn, 1992). Evaluation of potentially hazardous reactions is needed such that necessary mitigating actions can be determined and implemented (e.g., controlling the rate and quantity of melter feed, temperature ramps, and diluents). Additional information that could aid in this evaluation will be provided in a future CNWRA report on the chemistry of processes relevant to proposed Hanford processing technologies.

Chemical reactivity hazards associated with organic-bearing Hanford wastes depend on specific factors including fuel[2] concentration, the specific identity of the organic constituents, oxidant concentration, the strength of the oxidant(s), and the reaction mechanism (Scheele et al., 1995). This chapter provides information relevant to the chemistry of Hanford organic compounds and their potential chemical reactions with inorganic oxidants. It reviews the sources of the various organic chemicals introduced into the Hanford

---

[1]According to S.F. Agnew (Los Alamos National Laboratory. Personal Communication to R. Pabalan, December 11, 1997), the amount of nitrite produced by radiolysis of nitrate overwhelms the nitrite added to tank wastes for corrosion control by about three orders of magnitude. For example, concentrated waste that initially had about six molar nitrate would now have more than half the nitrate converted to nitrite by radiolysis.

[2]In this chapter, all organics are regarded as potential fuels for autogenic combustion and may be referred to as fuels in the text.

waste tanks, their estimated current inventory, and tabulates the thermophysical properties of the organics, if known. Thermodynamic calculations of energies of possible reactions involving organics and nitrates/nitrites as well as results of thermoanalytical studies of organic/oxidant mixtures reported in the literature are discussed. Processes that may result in locally high concentrations of organics, which would enhance tank waste chemical reactivity, and processes that lead to decomposition or aging of organics, which would result in lower fuel value and reduced chemical hazard, are also reviewed. Finally, numerical criteria used by the DOE in assigning the safety category for organic-bearing Hanford waste tanks are discussed. These criteria may be useful in estimating chemical reactivity hazards of organic-bearing wastes in future TWRS operations.

The chemistry of Hanford tank wastes is complex, with large uncertainties regarding the organic chemical inventory of individual tanks. During HLW processing at Hanford, 229 raw material chemicals (63 of which were organic in nature) and 68 chemical products (23 organic) were used. Many of the chemicals ended up in the underground storage tanks (Klem, 1990). This chapter focuses on the organic chemicals that have been identified as having the highest concentrations or the greatest likelihood of participating in energetic exothermic reactions.

3.2   SOURCES OF ORGANIC-BEARING HANFORD TANK WASTES

The principal sources for the majority of the organics were the solvent-extraction processes used to recover Pu and U, particularly the UR, REDOX, and PUREX processes. The UR process involved solvent extraction of U from nitric acid solutions into a mixture of TBP and normal paraffinic hydrocarbon (NPH) or kerosene (Cragnolino et al., 1997). The REDOX process is based on continuous solvent extraction of Pu and U from an aqueous nitrate solution into methyl isobutyl ketone (MIBK), also known as hexone. The PUREX process involved extracting Pu and U from a nitric acid solution into an organic phase comprised of 30 vol % TBP in various organic diluents—Soltrol-170 (Phillips) was first used, followed by E-2342 (Shell), and finally NPH or kerosene (Sederburg and Reddick, 1994).

The other major source of organic-bearing wastes at the Hanford site was the waste-management operations to remove Sr-90 and Cs-137, the main sources of radioactive decay heat, from wastes produced by PUREX operations. There were three primary types of PUREX wastes (Buckingham, 1967), namely, (i) the PUREX acid waste (PAW), which resulted from processing aluminum-clad fuel; (ii) the zirconium acid waste (ZAW), which resulted from processing zirconium-jacketed fuel elements; and (iii) PUREX acidified sludge (PAS), which was stored, alkaline PAW that had been redissolved using nitric acid. Two significantly different chemical processes were used at the Hanford B Plant to remove Cs and Sr from the PUREX wastes. Cesium was removed using a phosphotungstate precipitation process that used little or no organics. Removal of Sr, which produced the largest volume of organic-bearing wastes currently stored in Hanford waste tanks (Scheele et al., 1995), was accomplished using a solvent-extraction process, shown schematically in figure 3-1. Prior to solvent extraction, the PAS feed stream (stream 1 in figure 3-1) was pretreated to remove the bulk of Fe and Al by precipitation (stream 2 in figure 3-1), whereas the PAW and ZAW feeds were pretreated to leach and recover the Sr and Pm from the feed stream solids. Subsequently, organic complexants such as trisodium hydroxyethylenediaminetriacetate (Na_3HEDTA) and tetrasodium ethylenediaminetetraacetate (Na_4EDTA) was added (stream 3 in figure 3-1) to the solution to complex the metallic ions in the feed. The complexants helped obtain the desired distribution ratios in the solvent-extraction column for the different metals in the feed. Excess complexant was usually added to the feed to ensure adequate complexing and to account for fluctuations in feed composition. Because the metallic
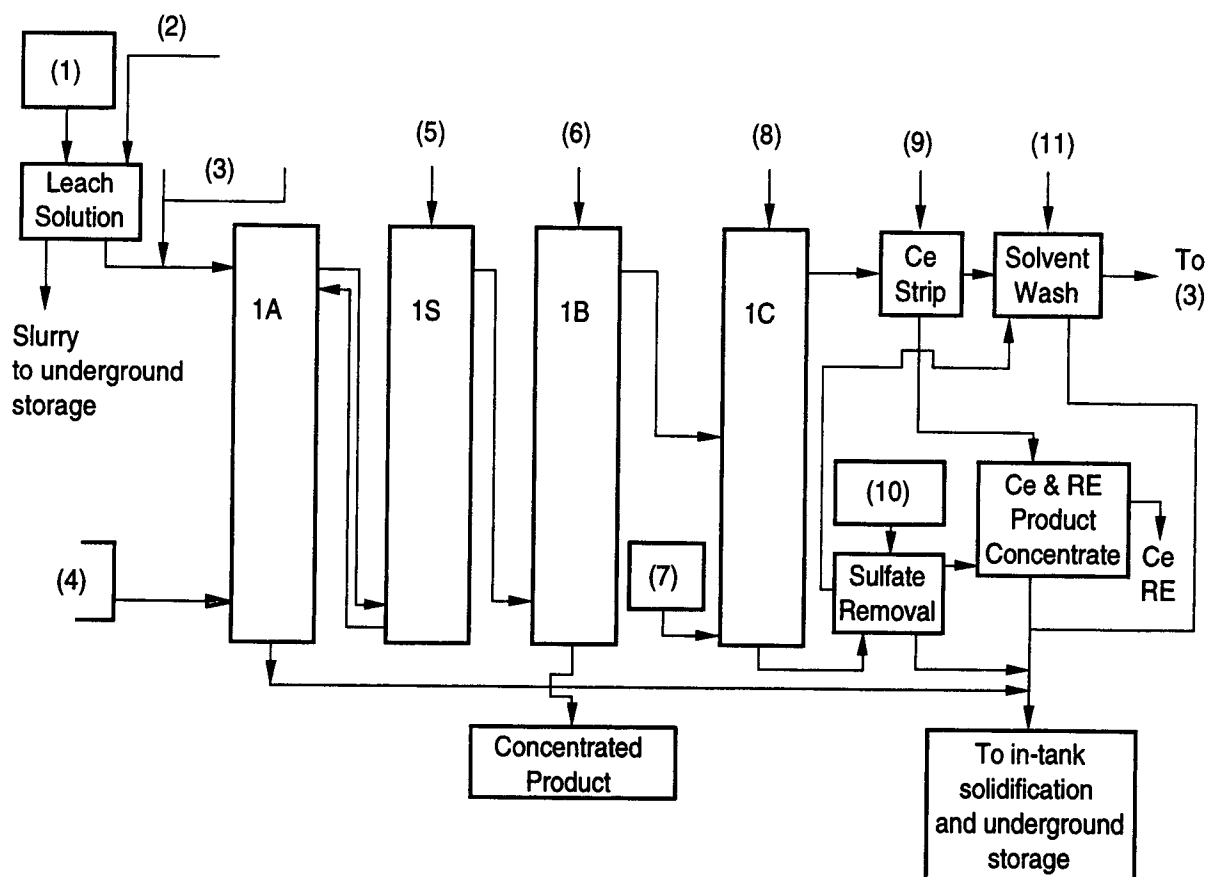
Figure 3-1. Schematic of the B Plant solvent extraction process (redrawn from Scheele et al., 1995)

ion distribution ratio is very pH-dependent, hydroxyacetic acid (HAcOH) was added to buffer the pH throughout the entire extraction process.

The solvent-extraction process consisted of a battery of four columns (Buckingham, 1967): 1A, 1S, 1B, and 1C. The feed entered column 1A where mixing occurred with the organic extractant (stream 4 in figure 3-1). This extractant was composed of TBP and di-(2-ethylhexyl) phosphoric acid (D2EHPA) in NPH diluent. The D2EHPA served as a metallic ion extractant, and the TBP acted as a solvent modifier to prevent third-phase formation and to increase the Sr organic-to-aqueous distribution ratio. In the 1A column, Sr, Ca, Mn, Mg, Y, rare earths, and U were extracted into the organic phase, whereas the bulk of the cations and other fission products remained in the aqueous phase and were sent to interim waste storage. A small amount of tartaric acid was added to the feed to enhance the extraction kinetics in column 1A. The organic solvent leaving column 1A was transferred to the 1S column where Na, trace Fe, and Al were stripped from the organic solvent with a solution of HAcOH and Na_3HEDTA (stream 5 in figure 3-1). The organic material from column 1S was pumped to the bottom of the 1B column where the Sr, some of the Ca, and the remaining divalent cations were stripped with a nitric acid solution (stream 6 in figure 3-1). The aqueous solution from the bottom of 1B, highly concentrated in Sr, was stored for further purification followed by encapsulation. The organic effluent from 1B was transferred to the 1C column where it was combined with additional organic extractant (stream 7 in figure 3-1) to maximize decontamination from Ce. The rare earths and the balance of calcium were stripped from the organic phase with a nitric acid solution that contained persulfate and silver ions (stream 8 in figure 3-1), which prevented Ce from leaving the organic phase.

The organic effluent from column 1C containing Ce, Y, and other tightly held ions was then stripped with a nitric acid solution (stream 9 in figure 3-1) leaving an ionically clean solvent, which was sent to solvent treatment. Sulfate, derived from the decomposition of persulfate by radiation and reaction with water, was removed (stream 10 in figure 3-1) to prevent precipitation of rare earth sulfates and to allow the concentration of rare earths and Am to volumes small enough for storage. All organic extractants used to recover Sr, rare earths, and Am were washed with sodium hydroxide and citric acid (stream 11 in figure 3-1) to remove any contaminant from the solutions. Nitric acid was then added to the cleaned extractant to adjust the Na/H mole ratio before the extractant was recycled to the 1A column. A more detailed discussion of B Plant solvent extraction operations is given in Buckingham (1967) and in Scheele et al. (1995).

Other processes also involved organic solvents and organic phosphate extractants, although less is known about the quantities used. D2EHPA diluted with hydrocarbon solvent was used in the waste fractionation and encapsulation process. Considerable quantities of hexone were used in the REDOX process as both extractant and solvent. For example, Gerber et al. (1992) reported 55 metric tons of hexone as having been retrieved from one storage tank, treated, and disposed in 1990 to 1991. However, an estimate of the total amount sent to Hanford tanks is not available. Oxalic acid was used in the BP process as a reducing agent (Gerber, 1996). Sugar and formaldehyde were added in the PUREX process to denitrate a portion of the nitric acid. These chemicals were largely consumed in the process (Gerber et al., 1992). Other organic chemicals used in quantity in the PUREX process were sodium gluconate and sodium acetate. Carbon tetrachloride, the only halogenated material used as a process solvent on-site, was used in the Reflux Solvent Extraction process (RECUPLEX) that produced purified Pu metal in the PFP, also known as the Z plant, and later in the plutonium reclamation facility (PRF). The RECUPLEX process used 15 percent TBP diluted in carbon tetrachloride to extract Pu from solution (Cleveland, 1967), followed by extraction of Am using 30 percent dibutyl butyl phosphonate (DBBP) in carbon tetrachloride (Kingsley, 1965).

Large quantities of organic compounds were also added to the tanks from plant decontamination operations. These operations used large quantities of cleaning agents, including organic surfactants, solvents, and chelating agents. For example, one N-Reactor decontamination campaign in FY83 used 20,000 gal. of Turco 4512-A[3] containing over 10 wt % organics (Gerber et al., 1992). Organic components found in concentrations of 5 weight percent or greater in the various detergents used in decontamination operations are diethylene glycol monobutyl ether, monohydroxyethyltrihydroxy-propylethylenediamine, triethanolamine, dichloromethane, toluene, butyl benzyl phthalate, isopropanol, acetone, and octylphenoxypoly(ethyleneoxy) ethanol (Gerber et al., 1992).

Table 3-1 lists the major organic compounds used at Hanford, the originating processes that used the chemicals, and the estimated amounts of the chemicals placed in the waste tanks. Thermophysical properties of these compounds, if known, are listed in table 3-2, as compiled from various sources (Lide, 1991; Lewis, 1993; Sederburg and Reddick, 1994; Burger, 1995).

3.3 ESTIMATED INVENTORY OF ORGANIC CHEMICALS IN HANFORD WASTE TANKS

Estimates of the organic inventory of the HLW tanks are based on either a review of the available processing histories, direct analytical measurements, or a combination thereof. The TOC inventory for all

---

[3]Turco 4512-A is a proprietary material containing about 70 wt % H_3PO_4 with added inhibitors and wetting agents (Kratzer, 1967). It was a commercially available decontamination chemical that was specifically tailored for the cleaning and decontamination needs of the nuclear industry and previously marketed by the TURCO Company of Cincinnati, Ohio.

Table 3-1. List of principal organic chemicals introduced into Hanford waste tanks

Chemical	Originating Process or Operation	Approximate Amount Placed in HLW Tanks (if known)
Solvents		
Carbon tetrachloride	Z plant	
NPHs (e.g., kerosene, Soltrol)	PUREX & B plant	1,310 metric tons
Oils and degreasers	Z plant	
Extractants		
Hexone or MIBK	REDOX	
TBP	PUREX, B, C, and Z plants	722 metric tons
D2EHPA	B plant	10 metric tons
DBBP	Z plant	480 metric tons
Complexing Agents and Organic Acids		
EDTA	B plant	166 metric tons
HEDTA	B plant	745 metric tons
Glycolic acid	B plant, PUREX	684 metric tons
Citric acid	B plant, N-Reactor	633 metric tons
Oxalic acid	Bismuth process	
Acetic acid	PUREX	
Formaldehyde	PUREX	
Process Chemicals		
Ferrocyanide	Cs-137 scavenging	(see chapter 4)
Various organics	RECUPLEX	

HLW tanks has been estimated to be between 1,500 and 1,800 metric tons, or less than 1 weight percent of the 357,000 metric tons of waste. However, organic concentrations vary widely between tanks. Using processing histories, Agnew (1997) developed the Hanford Defined Waste (HDW) model to predict the concentrations of a limited number of organics on a per tank basis. The HDW model is described briefly in section 1.5, and the total inventory for some organics estimated from the model is listed in table 3-3. A detailed description of the model and the estimated constituent inventories for each of the 177 tanks are given in Agnew (1997). Note that the HDW estimates listed in table 3-3 are different from the tank organic

Table 3-2. Thermophysical properties of principal high-level waste tank organic chemicals[*]

Physical Property	Acetic Acid[d]	Butanol[c]	Carbon Tetrachloride[c]	Citric Acid[a]	Dibutyl Butyl Phosphonate[c]	Dibutyl Phosphate (DBP)[b]	Ethylenediamine tetraacetic acid[c]	Glycolic Acid[a]	Hexone (MIBK)[c]
Formula	$C_2H_4O_2$	$C_4H_{10}O$	CCl_4	$C_6H_8O_7$	$C_{12}H_{27}O_3P$	$(C_8H_{19})PO_4$	$C_{10}H_{16}N_2O_8$	$C_2H_4O_3$	$C_6H_{12}O$
Molecular weight	60.1	74.1	153.81	192.1	250.4	210.2	292.3	76.05	100.2
Density (g/mL at 25 °C)	1.049 (at 20 °C)	0.810 (at 20 °C)	1.597	1.665	8.62	1.065	—	—	0.796 – 0.799
Melting point (°C)	16.7	-90[a]	-22.6	153[c]	—	—	240 (decomposes)	80	-80.2
Boiling point (°C at 1 atm)	118	117.5	76.8	decomposes	128 (at 2.5 mm Hg)	190 (decomposes)	—	decomposes	118
Flash point (°C)	43	35 – 38	none	100[c]	311	—	—	—	17
Viscosity (cp at 25 °C)	1.31 mPa s (at 15 °C)[d]	2.85 mPa s[d]	0.97 mPa s (at 20 °C)[d]	—	—	—	—	—	0.54 mPa s[d]
Aqueous solubility (g/L at 25 °C)	∞	91[a]	0.79[a]	59.2 wt % (at 20 °C)	—	18	510[h]	∞[f]	1.91 wt %[a]
Vapor pressure (mm Hg at 25 °C)	11.4 (at 20 °C)	5.5 (at 20 °C)	110 (at 23 °C)	—	—	—	—	—	16 (at 20 °C)
Flammability range (vol %)	5.4–16.0 (at 100 °C)	1.4–11.2	—	—	—	—	—	—	1.4 – 7.5
Heat capacity at 25 °C (cal/mol °C)	29.7[g]	—	31.49 (l)[g] 19.91 (g)[g]	—	—	—	—	—	—
Heat of formation (kJ/mol)	-484.5[c,g]	-327.4[c]	-135.44(l)[g] -102.9(g)[g]	-1,543.9[c]	—	-1,500 (Na-DBP)[b]	-1,759[c]	-664[c]	-322[d]
Heat of vaporization (kcal/mol)	5.67[d]	10.36[d]	7.78[g]	—	—	—	—	—	8.25[d]

[*]Values were taken from the reference identified in the column heading, except where noted for specific values.

[a]Budavari et al. (1996); [b]Sederburg and Reddick (1994); [c]Lewis (1993); [d]Lide (1991); [c]Burger (1995); [f]Perry et al. (1984); [g]Wagman et al. (1982); [h]Barney (1994).

Table 3-2. Thermophysical properties of principal high-level waste tank organic chemicals[*] (cont'd)

Physical Property	Hydroxyethylene diamine triacetic acid[b]	Isobutyric Acid[a]	Monobutyl Phosphate (MBP)[b]	Normal Paraffinic Hydrocarbon (NPH)[b,i]	Oxalic Acid[a]	Shell E-2342[b,i]	Sodium Acetate[d]	Sodium Citrate[a]
Formula	$C_{10}H_{15}N_2O_7$	$C_4H_8O_2$	$(C_4H_{11})PO_4$	—	$C_2H_2O_4$	—	$NaC_2H_3O_2$	$C_6H_5Na_3O_7$
Molecular weight	275.2	88.1	154.1	—	90.0	—	82.0	258
Density (g/mL at 25 °C)	—	0.95 (at 20 °C)	1.220	0.76 (max)	1.653 (at 18.5 °C)	0.801	1.528	—
Melting point (°C)	212 (decomposes)[j]	−47	—	—	101 – 102 (sublimes)	—	324	—
Boiling point (°C at 1 atm)	—	152–155	105 (decomposes)	174 – 252	—	—	—	—
Flash point (°C)	—	77	—	80	—	74	—	—
Viscosity (cp at 25 °C)	—	—	—	1.8	—	1.7	—	—
Aqueous solubility (g/L at 25 °C)	—	160	—	<0.005	140	< 0.004	119 (at 0 °C)	72 (solub. of dihydrate)[d]
Vapor pressure (mm Hg at 25 °C)	—	1 (at 14.7 °C)[c]	—	—	0.0065 (at 55 °C, solid to gas)[d]	—	—	—
Flammability range (vol %)	—	—	—	0.77–5.35 (Decane)[d]	—	—	—	—
Heat capacity at 25 °C (cal/mol °C)	—	—	—	55.7 (Decane)[d]	28.0[g]	—	19.1[g]	—
Heat of vaporization (kcal/mol)	−1,552[e] (−2,247 Na₃)[e]	−774 (Na-butyrate)[e]	—	−301 (Decane)[d]	−827.2[g]	—	−708.8[e,g]	−2,260[e]
Heat of formation (kJ/mol)	—	—	11.4[b]	9.27 (Decane)[d]	—	—	—	—

[*]Values were taken from the reference identified in the column heading, except where noted for specific values.

[a]Budavari et al. (1996); [b]Sederburg and Reddick (1994); [c]Lewis (1993); [d]Lide (1991); [e]Burger (1995); [f]Perry et al. (1984); [g]Wagman et al. (1982); [h]Barney (1994).

[i]Shell E-2342 is about 80 vol % of 5 and 6 carbon cycloparaffins (cyclopentane, cyclohexane); NPH is a mixture of C10 to C14 straight chain (normal) aliphatic hydrocarbons (Sederburg and Reddick, 1994).

Table 3-2. Thermophysical properties of principal high-level waste tank organic chemicals[*] (cont'd)

Physical Property	Sodium Glycolate[a]	Sodium Oxalate[c]	Sodium Tartrate[a]	Soltrol-170[h,j]	Tartaric Acid[a]	Tributyl Phosphate (TBP)[a]
Formula	$NaC_2H_3O_3$	$Na_2C_2O_4$	$C_4H_4Na_2O_6$	—	$C_4H_6O_6$	$(C_4H_9)_3PO_4$
Molecular weight	98	134.0	194.1	—	150.1	266.32
Density (g/mL at 25 °C)	—	2.34	1.82	0.773	1.760 (at 20 °C)	0.976
Melting point (°C)	—	250 – 270 (decomposes)	—	—	168 – 170	< -80
Boiling point (°C at 1 atm)	—	—	—	208 – 239	—	289 (decomposes)
Flash point (°C)	—	—	—	89	—	146
Viscosity (cp at 25 °C)	—	—	—	2.3	—	—
Aqueous solubility (g/L at 25 °C)	—	3.7 (at 20 °C)	29 (for dihydrate at 6 °C)[d]	v. slight	1,390 (at 20 °C)	5.9
Vapor pressure (mm Hg at 25 °C)	—	—	—	—	—	0.006[b]
Flammability range (vol %)	—	—	—	—	—	—
Heat capacity at 25 °C (cal/mol °C)	—	—	—	—	43.2	109.2[b]
Heat of vaporization (kcal/mol)	-900.8[e,g]	-1,318[e,g]	-1,771[e]	—	—	-1,456[e]
Heat of formation (kJ/mol)	—	—	—	—	—	14.68[b]

[*]Values were taken from the reference identified in the column heading, except where noted for specific values.
[a]Budavari et al. (1996); [b]Sederburg and Reddick (1994); [c]Lewis (1993); [d]Lide (1991); [e]Burger (1995); [f]Perry et al. (1984); [g]Wagman et al. (1982); [h]Barney (1994).
[j]Soltrol-170 is a mixture of highly branched aliphatic hydrocarbons (Sederburg and Reddick, 1994).

Table 3-3. Total inventory of organic chemicals in Hanford SSTs and DSTs estimated from the HDW model (Agnew, 1997)

Organic Chemical Compound	Total Mass (metric tons)
DBP	562
Butanol	198
EDTA	619
HEDTA	1,030
Oxalate	114
Citrate	678
Glycolate	1,100
Acetate	99

inventory estimates given in table 3-1. As pointed out by Cragnolino et al. (1997), significant differences emerge from one estimation scheme of tank inventory to another, and it is not possible to easily explain these differences due to the assumptions used and the complexities of various estimation methods.

It should be emphasized that deriving tank waste inventories from reconstructions of waste histories, as in the HDW model, leads to large uncertainties, particularly with respect to the organic species. In large part, the uncertainties arise from incomplete or inadequate process or waste transfer records, but the uncertainties also result from chemical processes that are not accounted for in the model. For example, various thermal and radiolytic processes lead to decomposition of organic compounds as discussed in chapter 2 and in section 3.6 of this report, but Agnew's model made assumptions to simplify the description of organic degradation.

Hexone and TBP were used in large quantities at the Hanford site. Hexone is extremely volatile (see table 3-2) and is very reactive with nitric acid, which precluded the use of hexone with concentrated nitric acid process solutions. Isobutyric acid is a relatively stable decomposition product of hexone (Burger, 1995). Because of the volatility and reactivity of hexone, Agnew (1997) assumed that any hexone that reached the waste tanks would not have remained long. Thus, hexone concentrations are assumed to be nil in the HDW model. TBP is insoluble in aqueous solutions, but the TBP phase absorbs 2 to 3 percent water at its saturation point. Thus, TBP is subject to hydrolysis during nuclear fuel reprocessing as well as during storage in contact with aqueous solutions, degrading to DBP and butanol, which are both much more soluble in the aqueous phase (Agnew, 1996a). The HDW model assumes a certain fraction of TBP is lost during processing as DBP + butanol, and that the latter species are in the waste streams going to the tanks. Butanol oxidizes slowly, eventually forming carbon dioxide and water. This reaction is not accounted for in the HDW model. Also, the HDW model does not track the loss of separable organic solvents, such as TBP or NPH. Agnew (1996a) assumed that the volatility of NPH and the hydrolysis of TBP resulted in relatively short lifetimes in the waste tanks. Furthermore, the HDW model does not include certain organic species, such as D2EHPA, assuming that those species can be represented by surrogate species (Agnew, 1996a).

Ideally, analyses of organic concentration and identity would be conducted for individual tanks. However, detailed organic analyses during characterization of Hanford tank wastes are not planned. Instead, decisions on safety of organic-bearing wastes will rely on measurements of TOC and moisture concentration of tank wastes (Turner et al., 1995) (see section 3.7). The TOCs have been measured for Hanford site tanks, but only a few tanks have been studied in enough detail to evaluate the types and amounts of organic components present in tank supernate and sludge (e.g., Campbell et al., 1994a,b,c, 1995a,b; Lokken et al., 1986; Pool and Bean, 1994; Wahl et al., 1995; and Westinghouse Hanford Company, 1995a). However, much

of the material in these references involves development of analytical procedures for measuring selected organic compounds in the complex tank waste matrix. For the most part, extensive lists of tank sample analyses are not available. Analysis of organic species in the complex highly radioactive tank phases is very difficult. The organic analyses that have been conducted have emphasized measuring chelating agents, chelating agent fragments, butyl phosphates, low-molecular weight water-soluble organic acids, and NPH.

To evaluate how well the organic analyses have identified the major organic compounds present in the tank materials, the sum of organic carbon mass in the identified species can be compared with the measured TOC of the tank samples. Results of mass balance checks on Hanford tank waste analyses range from 50 and 90 percent, with an average in the 80- to 90-percent range (Serne et al., 1996). The relatively high average percentage of agreement between detailed speciation techniques versus TOC reflects recent improvements in cation exchange techniques used to remove radioactive constituents, especially Cs-137 and Sr-90, from tank samples. Separation of radioactive constituents permit transferring the samples from the hot cell to fume hoods, where more detailed organic analyses can be performed.

To provide examples of organic constituents found in Hanford tank wastes, the results of organic speciation measurements on tank samples from DSTs SY-101 and SY-103 are shown in tables 3-4 through 3-6. Results for SST C-103 are shown in tables 3-7 and 3-8. Tanks SY-101, SY-103, and C-103 are on the High Organic Watch-list (Hanlon, 1997). According to Serne et al. (1996), the data in tables 3-4 to 3-6 suggest the following conclusions for the two DSTs:

- Oxalate, the predominant low-molecular weight acid, is present at much higher levels in the sludge solids than in the supernate solution. This condition may be caused by the insolubility of many metal oxalates.

- Proportionately more chelators and chelator fragments are found in the supernate solution than in the solids. However, because the solids in the tanks can have higher TOC, the absolute concentration of chelators in the solids can be as high or higher than in the supernate solution. EDTA is the predominant chelator present. The NPH content in the tank samples analyzed is small (less than 7 percent of the TOC).

Lokken et al. (1986) performed organic analyses of supernate solutions, which were classified as concentrated complexant waste, from DSTs AN-107 and AZ-102 using gas chromatography/mass spectrometry (GC/MS) and gas chromatography/Fourier transform infrared spectrometry (GC/FTIR). NTA, HEDTA, EDTA, and citric acid were identified at millimolar concentrations, but the mass balance of TOC was only 40 percent. Using high-performance liquid chromatography techniques, some other classes of organic compounds, such as mono- and di-carboxylic acids, long-chained alkanes ranging from C_{23} to C_{35}, and phthalate esters, were identified. Mass balance was subsequently improved to 75 percent. The final results for the AN-107 supernate waste solution are shown in table 3-9.

Characterization of the speciation of organic carbon in Hanford tank wastes is an ongoing activity. In the first of a planned series of reports on the subject, Carlson (1997) compiled the available organic carbon data for the Hanford tanks. Oxalate data were found to have been reported for 33 tanks, TOC data were found to have been reported for 82 tanks, and both oxalate and TOC data were found to be available for 27 tanks. Of these 27 tanks, eight tanks (BY-104, BY-105, BY-106, BY-110, C-103, C-106, S-109, and SX-108) were found to have greater than 80 percent of the TOC identified as oxalate. Of the remaining 19 tanks, seven (AN-107, AW-101, BY-108, S-101, S-102, S-107, and U-107) had between 40 and 80 percent of the TOC identified as oxalate, and twelve (A-101, A-102, AP-102, AP-105, AP-106, B-106, BX-109, U-102, U-105, U-106, U-108, and U-109) had less than 35 percent of the TOC identified. For most of the latter tanks, the

Table 3-4. Average organic content of tank SY-101 core samples in milligrams of carbon, C, per gram of sample (from Serne et al., 1996)

Constituent	Drainable Liquid (mg C/g)	Solids (mg C/g)
TOC	10.9	11.1
Nitroimidazole (NIDA)	1.04	0.82
NTA	0.33	0.22
Citric acid	0.32	0.31
ED3A	0.30	0.28
EDTA	2.23	0.80
HEDTA	—	—
Other fragments	0.61	0.42
Succinic acid	0.07	0.05
Oxalic acid	1.8	5.7
Acetic acid	—	—
Formic acid	1.4	0.62
Glycolic acid	0.54	—
NPH	0.80	0.02
Mass balance on C	79%	83%

only organic carbon identified is oxalate, although EDTA, HEDTA, citrate, and glycolate were also found in tanks AP-102, AP-105, and AP-106. Carlson (1997) identified several problems in the reproducibility of the data. Differences in concentrations from duplicate measurements were as high as two orders of magnitude in some cases. In addition, in some samples, the carbon values from oxalate were much higher than the TOC values. These variations may have been caused by precipitation of crystals of sodium oxalate. Additional evaluation of organic speciation in Hanford tank wastes is planned (Carlson, 1997).

3.4 POTENTIAL HAZARDOUS CHEMICAL REACTIONS

Hazards associated with chemical reaction between a fuel, such as organics, and an oxidant, such as nitrate or nitrite, are functions of several interrelated factors, including the amount of heat produced, the rate at which heat is produced, and the thermal absorption and transfer properties of the physico-chemical

Table 3-5. Organic carbon analyses for tank SY-103 (from Serne et al., 1996)

Constituent	Drainable Liquid (mg C/g)	Solids (mg C/g)
TOC	6.4	10.5
NIDA	0.2	0.16
NTA	0.14	0.16
Citric acid	0.42	0.56
ED3A	0.25	0.16
EDTA	0.55	0.65
HEDTA	0.03	<0.01
Other fragments	<0.01	0.14
Succinic acid	0.02	0.02
Oxalic acid	—	6.0
Acetic acid	0.6	0.7
Formic acid	1.2	0.9
Glycolic acid	—	tbd
NPH	tbd*	tbd
Mass balance on C	53%	90%
*Listed as to be determined in original reference		

system. The reaction pathway will control the amount of heat produced; the rate at which heat is produced depends on the reaction pathway and kinetics. The heat capacities of chemical components, thermal conductivities of mixture components, and the heat absorbed by endothermic reactions will control the temperature to which a certain amount of heat will raise the temperature of the reaction mixture, which in turn will control the reaction rate. The effects and interactions of these different factors need to be taken into account in a complete hazards assessment—a detailed activity beyond the scope of this report.

To assess potential hazards associated with a chemical system, the approach commonly used in the chemical industry consists of (i) estimation of heat or energy releases using thermodynamic calculations or literature information; (ii) performance of experimental measurements to screen for exothermic behavior, to determine thermal stability or system reactivity (e.g., minimum onset temperature for exothermic reactions), and to determine heats of reaction using calorimetric methods; and (iii) evaluation of the

Table 3-6. Summary of organic types in tank samples (wt % of TOC) (from Serne et al., 1996)

Type	Tank SY-101		Tank SY-103	
	Supernate	Solids	Supernate	Solids
Chelators	44	26	23.4	18.3
Low-molecular weight organic acid	35	57	28.1	72.4
NPH	7	4	tbd*	tbd
Organic Carbon Mass Balance	86%	87%	51.5%	90.7%
*Listed as to be determined in original reference				

consequences of an exothermic reaction considering the thermodynamics, kinetics, and heat transfer of the total system process (Gygax, 1990; Sharkey et al., 1992; West, 1993).

The approach in the previous paragraph is typically employed by chemical manufacturing and processing industries to assess the safety of different chemical systems as most processes for manufacturing chemicals are being developed. The compositions of the chemical systems of interest are usually well known, can be controlled, and are composed of few constituents, factors that help simplify the hazard evaluation process. In contrast, the Hanford tank wastes have varied and, in many cases, unknown compositions, and various types of technologies will be used in the processing and solidification of the wastes. Thus, safety assessments of the Hanford TWRS with respect to organic-bearing wastes is a complex problem. Studies have been conducted by the DOE to address the safety aspects of interim storage of Hanford organic-bearing wastes using many of the tools and methodologies employed in the chemical industry (e.g., Turner and Miron, 1994a,b; Fauske, 1992; Fauske et al., 1995b; Scheele et al., 1995). Because of the complexity of Hanford waste chemistry and the lack of available samples of tank wastes, many of those studies were designed to provide an understanding of the behavior of individual organic and oxidant mixtures or of simulated tank waste. However, those studies provide information that could be useful for safety analysis of the Hanford TWRS operations.

Determination of energy releases during reactions involving oxidizable compounds is an important component of safety analysis of the Hanford TWRS storage, retrieval, and process operations. Experimental determinations of energy releases and general thermal behavior as a function of temperature have been reported by Scheele et al. (1995), Fauske (1992), and Fauske et al. (1995b). Some of the results from these studies are discussed in section 3.4.2. A complementary approach to experimental measurements is the calculation of heat released when various organic compounds that may exist in tank wastes react with nitrate or nitrite salts. Calculations can be made using available thermodynamic data and considering different pathways and end-products to determine differences in energy released and the reaction pathways that yield large amounts of energy. From the results, it would be possible to predict the adiabatic rise in temperature that would occur for various oxidation reactions in different waste mixtures. It would also be possible to

Table 3-7. Organic compounds and inorganic species found in organic layer of tank C-103 (from Serne et al., 1996)

Species	Wt %, unless noted
TBP	47.2
Tridecane (C_{13})	11.4
Tetradecane (C_{14})	6.0
Dodecane (C_{12})	2.8
DBBP	1.9
Pentadecane (C_{15})	0.9
Various branched alkanes	3.5
Water	1.3
Ammonia	<0.003
Water-soluble anions	<0.005
Water-soluble cations	<0.010
Gross alpha emitters	550 pCi/g
Plutonium	2.43×10^{-3} ppm
Gross beta emitters	1.05×10^{5} pCi/g
Sr-90	5.5×10^{5} pCi/g
Cs-137	4.1×10^{4} pCi/g
Others	$\sim 1.0 \times 10^{3}$ pCi/g
Total mass identified	75.0

predict the effect of the concentration of both oxidants and diluents on the temperature rise. Such an approach, based on the work by Burger (1995), is discussed in the next section.

3.4.1 Calculated Reaction Energies of Organic Oxidation Reactions

The nitrate and nitrite salts present in the Hanford waste tanks can oxidize organic compounds to produce heat and gases. It is important to determine the energies that can be released when organic chemicals are oxidized by sodium nitrate or sodium nitrite. Burger (1995) calculated these energies using standard enthalpies of formation available in the literature for various chemical species.

Table 3-8. Organic carbon analyses on tank C-103 samples (from Serne et al., 1996)

Sample Identification	Solids	
	TOC (mg C/g)	Oxalate (mg C/g)
Core 63-seg. 2 (upper)	8.5	2.66
Core 63-seg. 2 (lower)	10.2	—
Core 63-seg. 3 (upper)	7.6	1.94
Core 63-seg. 3 (lower)	8.9	—
Core 63-seg. 4	4.5	2.32
Core 66-seg. 3 (upper)	8.9	3.92
Core 66-seg. 3 (lower)	—	2.96
Core 66-seg. 4	9.2	2.96
	Liquids	
	TOC (mg C/mL)	Oxalate (mg C/mL)
Core 63-seg. 1	7.71	3.36
Core 63-seg. 2	7.61	—
Core 63-seg. 4	—	3.36
Core 66-seg. 1	—	3.14
Core 66-seg. 2	—	3.1
Core 66-seg. 3	—	2.96
Core 66-seg. 4	—	2.73

Maximum energy is released by organic reactions with nitrates and nitrites when the reaction products are nitrogen, Na_2CO_3, H_2O, and CO_2 (Burger, 1995). Typical reactions involving TBP and acetate as examples are

$$TBP + 14.4\,NaNO_3 = Na_3PO_4 + 5.7\,Na_2CO_3 + 6.3\,CO_2 + 13.5\,H_2O + 7.2\,N_2 \qquad (3\text{-}1)$$
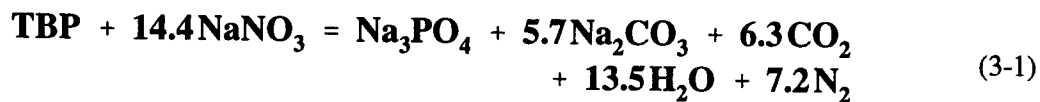
and

Table 3-9. Organic species identified in tank AN-107 supernate solution (from Serne et al., 1996)

Compound	mM	mg C/mL
Chelates/Complexants		
Citric acid	64.39	4.61
HEDTA	37.53	4.53
EDTA	31.41	3.77
Methane tricarboxylic acid*	17.32	1.45
NTA	7.33	0.53
Chelator Fragments		
ED3A	17.91	1.72
HEDDA	2.39	0.26
E2DTA	2.28	0.23
HEIDA	2.14	0.18
MeEDDA	1.02	0.08
others	—	0.14
Carboxylic Acids		
Docos-13en-oic	2.50	0.67
Hexanedioic	2.04	0.15
Hexadecanoic	2.04	0.39
Phthalic	1.10	0.10
Nonanedioic	0.83	0.07
Tetradecanoic	0.68	0.12
Pentanedioic	0.60	0.04
Octadecanoic	0.54	0.11
Hydroxybutanedioic	0.33	0.01
Butanedioic	0.10	0.01
Alkanes		
C_{23} to C_{35}	7.77	2.50
Phthalate esters	—	—
Dibutylphthalate	1.24	0.23
Dioctylphthalate	0.05	0.01
Total organic carbon	—	44.0
*Identification of this species is now considered erroneous (Serne et al., 1996)		

$$\begin{aligned} NaCH_3COO + 1.6NaNO_3 &\rightleftharpoons 1.3\,Na_2CO_3 + 0.7\,CO_2 \\ &\quad + 1.5H_2O + 0.8N_2 \end{aligned} \qquad (3\text{-}2)$$
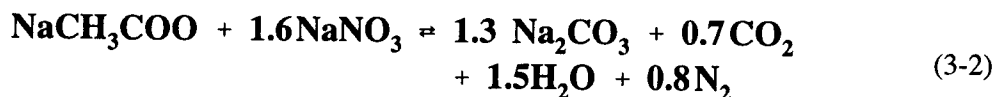
Production of nitrogen oxides in place of nitrogen, or CO in place of CO_2, greatly lowers the energy release (Burger et al., 1991). Table 3-10 presents the stoichiometries and the enthalpies of reaction (ΔH_{rxn}) for the oxidation of organic compounds of greatest concern in the Hanford waste tanks. Theoretical energies are compared in the table for organic oxidation reactions involving two oxidants (nitrate versus nitrite), as is the effect of producing N_2O in place of N_2. As mentioned previously, the most energetic reactions between nitrate or nitrite and organics are those that produce N_2, Na_2CO_3, H_2O, and CO_2, thus the reactions listed in table 3-10 represent conservative scenarios. Data for possible reactions of sodium acetate, which would produce different gaseous products, are shown in table 3-11.

The calculated enthalpies vary greatly with the assumed reaction products; values in table 3-10 illustrate the decrease in heat production when N_2O is formed instead of N_2. The table also shows the effect of excess NaOH on the oxidation reactions. In a neutral environment, CO_2 is produced; however, when excess NaOH is present, it can react with CO_2 to form sodium carbonate and H_2O. There is an increase in the exothermic heat released due to the formation of more sodium carbonate.

According to the theoretical energies calculated in table 3-10, the most energetic reactions are the oxidation of the organics by $NaNO_2$ in the presence of NaOH to produce Na_2CO_3, H_2O, and N_2. It should be emphasized that the ideal oxidation reactions listed in the table are limiting cases (Burger, 1995). The calculated enthalpies of reaction are for the maximum energy pathways. It is recognized that with fast exothermic reactions, equilibria will probably not occur. In addition, several reaction paths may be taken simultaneously with less total energy being produced, so the energies presented in the table are seldom fully realized. Nevertheless, the maximum values are useful as conservative estimates of energies that could be released and temperatures that could be achieved during oxidation of tank waste organics. An example is presented in the following paragraphs.

To get a rough estimate of the potential effect of exothermic reactions involving organic compounds on Hanford waste tanks, heat generation and temperature rise were calculated for three HLW tanks: A-101, an SST on both the Flammable/Hydrogen Gas Watch-list and the High Organic Content Watch-list, and SY-101 and SY-103, DSTs on the Flammable/Hydrogen Gas Watch-list (Hanlon, 1997). The calculations assumed an initial temperature of 25 °C, complete combustion of organic material, and dissipation of the generated heat to a surrounding liquid phase comprised only of water. It was also assumed that water acts as a heat sink but does not dampen fuel reactivity. Using organic chemical concentrations in HLW tanks estimated from the HDW model (Agnew, 1997), the enthalpies of reaction for the organic compounds of interest were calculated assuming the most energetic pathway listed for that compound in table 3-10. The calculations were conservative because of the use of the most energetic reaction pathways and because actual tank liquids, as well as many of the tank solids, have high heat capacities and could dissipate more heat than water dissipates.

The estimated amounts of water and of organic constituents in tanks A-101, SY-103, and SY-101 taken from Agnew (1997) are listed in tables C-1, C-2, and C-3 (appendix C), respectively. Agnew (1997) attempted to account for variabilities in the calculated waste composition and included values for the upper and lower limits for species concentrations. The upper and lower limit (at the 95 percent confidence interval)

Table 3-10. Enthalpies of reaction for the oxidation of organics by sodium nitrate and sodium nitrite[a]

Compound	Reaction	ΔH_{rxn} (kJ/Mole)	ΔH_{rxn} (kJ/g)
Sodium EDTA ($Na_4C_{10}H_{12}O_8N_2$) (MW = 380 g/mol)	$Na_4C_{10}H_{12}O_8N_2 + 8\ NaNO_3 \rightleftharpoons 6\ Na_2CO_3 + 4\ CO_2 + 6\ H_2O + 5\ N_2$	$-3,350$	-8.82
	$Na_4C_{10}H_{12}O_8N_2 + 10\ NaNO_3 \rightleftharpoons 7\ Na_2CO_3 + 3\ CO_2 + 6\ H_2O + 5\ N_2O + N_2$	$-2,740$	-7.21
	$Na_4C_{10}H_{12}O_8N_2 + 8\ NaNO_3 + 8\ NaOH \rightleftharpoons 10\ Na_2CO_3 + 10\ H_2O + 5\ N_2$	$-3,860$	-10.2
	$Na_4C_{10}H_{12}O_8N_2 + 10\ NaNO_3 + 6\ NaOH \rightleftharpoons 10\ Na_2CO_3 + 9\ H_2O + 5\ N_2O + N_2$	$-3,130$	-8.22
	$Na_4C_{10}H_{12}O_8N_2 + 13.3\ NaNO_2 \rightleftharpoons 8.67\ Na_2CO_3 + 1.33\ CO_2 + 6\ H_2O + 7.65\ N_2$	$-4,270$	-11.2
	$Na_4C_{10}H_{12}O_8N_2 + 20\ NaNO_2 \rightleftharpoons 10\ Na_2CO_3 + 4\ H_2O + 4\ NaOH + 10\ N_2O + N_2$	$-2,980$	-7.83
	$Na_4C_{10}H_{12}O_8N_2 + 13.33\ NaNO_2 + 2.667\ NaOH \rightleftharpoons 10\ Na_2CO_3 + 7.33\ H_2O + 7.667\ N_2$	$-4,450$	-11.7
Sodium HEDTA ($Na_3C_{10}H_{15}O_7N_2$) (MW = 344 g/mol)	$Na_3C_{10}H_{15}O_7N_2 + 8.8\ NaNO_3 \rightleftharpoons 5.9\ Na_2CO_3 + 4.1\ CO_2 + 7.5\ H_2O + 5.4\ N_2$	$-3,710$	-10.8
	$Na_3C_{10}H_{15}O_7N_2 + 11\ NaNO_3 \rightleftharpoons 7\ Na_2CO_3 + 3\ CO_2 + 7.5\ H_2O + 5.5\ N_2O + N_2$	$-3,040$	-8.83
	$Na_3C_{10}H_{15}O_7N_2 + 8.8\ NaNO_3 + 8.2\ NaOH \rightleftharpoons 10\ Na_2CO_3 + 11.6\ H_2O + 4.4\ N_2$	$-4,230$	-12.3
	$Na_3C_{10}H_{15}O_7N_2 + 11\ NaNO_3 + 6\ NaOH \rightleftharpoons 10\ Na_2CO_3 + 10.5\ H_2O + 5.5\ N_2O + N_2$	$-3,420$	-9.94
	$Na_3C_{10}H_{15}O_7N_2 + 14.667\ NaNO_2 \rightleftharpoons 8.833\ Na_2CO_3 + 1.167\ CO_2 + 7.5\ H_2O + 8.33\ N_2$	$-4,730$	-13.7
	$Na_3C_{10}H_{15}O_7N_2 + 22\ NaNO_2 \rightleftharpoons 10\ Na_2CO_3 + 5\ NaOH + 5\ H_2O + 11\ N_2O + N_2$	$-3,600$	-10.5
	$Na_3C_{10}H_{15}O_7N_2 + 14.667\ NaNO_2 + 2.33\ NaOH \rightleftharpoons 10\ Na_2CO_3 + 8.667\ H_2O + 8.33\ N_2$	$-4,880$	-14.2
Sodium Glycolate ($NaC_2H_3O_3$) (MW = 98 g/mol)	$NaC_2H_3O_3 + 1.2\ NaNO_3 \rightleftharpoons 1.1\ Na_2CO_3 + 0.9\ CO_2 + 1.5\ H_2O + 0.6\ N_2$	-498	-5.08
	$NaC_2H_3O_3 + 1.5\ NaNO_3 \rightleftharpoons 1.25\ Na_2CO_3 + 0.75\ CO_2 + 1.5\ H_2O + 0.75\ N_2O$	-407.2	-4.15
	$NaC_2H_3O_3 + 1.2\ NaNO_3 + 1.8\ NaOH \rightleftharpoons 2\ Na_2CO_3 + 2.4\ H_2O + 0.6\ N_2$	-613.4	-5.26
	$NaC_2H_3O_3 + 1.5\ NaNO_3 + 1.5\ NaOH \rightleftharpoons 2\ Na_2CO_3 + 2.25\ H_2O + 0.75\ N_2O$	-503.0	-5.13

Table 3-10. Enthalpies of reaction for the oxidation of organics by sodium nitrate and sodium nitrite (cont'd)[a]

3-19

Compound	Reaction	ΔH_{rxn} (kJ/Mole)	ΔH_{rxn} (kJ/g)
Sodium Oxalate $(Na_2C_2O_4)$ (MW = 134 g/mol)	$NaC_2H_3O_3 + 2\ NaNO_2 \rightleftharpoons 1.5\ Na_2CO_3 + 0.5\ CO_2 + 1.5\ H_2O + N_2$	−418.1	−4.26
	$NaC_2H_3O_3 + 3\ NaNO_2 \rightleftharpoons 2\ Na_2CO_3 + 1.5\ H_2O + 1.5\ N_2O$	−195.7	−2.00
	$NaC_2H_3O_3 + 2\ NaNO_2 + NaOH \rightleftharpoons 2\ Na_2CO_3 + 2\ H_2O + N_2$	−482.0	−4.92
	$Na_2C_2O_4 + 0.4\ NaNO_3 \rightleftharpoons 1.2\ Na_2CO_3 + 0.8\ CO_2 + 0.2\ N_2$	−166.6	−1.24
	$Na_2C_2O_4 + 0.5\ NaNO_3 \rightleftharpoons 1.25\ Na_2CO_3 + 0.75\ CO_2 + 0.25\ N_2O$	−136.0	−1.01
	$Na_2C_2O_4 + 0.4\ NaNO_3 + 1.6\ NaOH \rightleftharpoons 2\ Na_2CO_3 + 0.2\ N_2 + 0.8\ H_2O$	−268.8	−2.01
	$Na_2C_2O_4 + 0.5\ NaNO_3 + 1.5\ NaOH \rightleftharpoons 2\ Na_2CO_3 + 0.25\ N_2O + 0.75\ H_2O$	−232.0	−1.73
	$Na_2C_2O_4 + 0.667\ NaNO_2 \rightleftharpoons 1.33\ Na_2CO_3 + 0.67\ CO_2 + 0.33\ N_2$	−213.8	−1.60
	$Na_2C_2O_4 + NaNO_2 \rightleftharpoons 1.5\ Na_2CO_3 + 0.5\ CO_2 + 0.5\ N_2O$	−175.2	−1.31
	$Na_2C_2O_4 + 0.667\ NaNO_2 + 1.333\ NaOH \rightleftharpoons 2\ Na_2CO_3 + N_2 + 0.657\ H_2O$	−298.2	−2.22
	$Na_2C_2O_4 + NaNO_2 + NaOH \rightleftharpoons 2\ Na_2CO_3 + 0.5\ N_2O + 0.5\ H_2O$	−239.1	−1.78
Sodium Acetate $(NaCH_3CO_2)$ (MW = 82 g/mol)	$NaCH_3CO_2 + 1.6\ NaNO_3 \rightleftharpoons 1.3\ Na_2CO_3 + 0.7\ CO_2 + 1.5\ H_2O + 0.8\ N_2$	−650	−7.94
	$NaCH_3CO_2 + 2\ NaNO_3 \rightleftharpoons 1.5\ Na_2CO_3 + 0.5\ CO_2 + 1.5\ H_2O + N_2O$	−530	−6.45
	$NaCH_3CO_2 + 1.6\ NaNO_3 + 1.4\ NaOH \rightleftharpoons 2\ Na_2CO_3 + 2.2\ H_2O + 0.8\ N_2$	−740	−9.02
	$NaCH_3CO_2 + 2\ NaNO_3 + NaOH \rightleftharpoons 2\ Na_2CO_3 + 2\ H_2O + N_2O$	−580	−7.11
	$NaCH_3CO_2 + 2.67\ NaNO_2 \rightleftharpoons 1.83\ Na_2CO_3 + 0.17\ CO_2 + 1.5\ H_2O + 1.33\ N_2$	−840	−10.2
	$NaCH_3CO_2 + 4\ NaNO_2 \rightleftharpoons 2\ Na_2CO_3 + NaOH + H_2O + 2\ N_2O$	−620	−7.58
	$NaCH_3CO_2 + 2.667\ NaNO_2 + 0.333\ NaOH \rightleftharpoons 6\ Na_2CO_3 + 1.667\ H_2O + 1.33\ N_2$	−860	−10.5

Table 3-10. Enthalpies of reaction for the oxidation of organics by sodium nitrate and sodium nitrite (cont'd)[a]

Compound	Reaction	ΔH_{rxn} (kJ/Mole)	ΔH_{rxn} (kJ/g)
Sodium Citrate $(Na_3C_6H_5O_7)$ (MW = 258 g/mol)	$Na_3C_6H_5O_7 + 3.6\ NaNO_3 \rightleftharpoons 3.3\ Na_2CO_3 + 2.7\ CO_2 + 2.5\ H_2O + 1.8\ N_2$	−1,460	−5.66
	$Na_3C_6H_5O_7 + 4.5\ NaNO_3 \rightleftharpoons 3.75\ Na_2CO_3 + 2.25\ CO_2 + 2.5\ H_2O + 2.25\ N_2O$	−1,190	−4.60
	$Na_3C_6H_5O_7 + 3.6\ NaNO_3 + 5.4\ NaOH \rightleftharpoons 6\ Na_2CO_3 + 5.2\ H_2O + 1.8\ N_2$	−1,805	−7.00
	$Na_3C_6H_5O_7 + 4.5\ NaNO_3 + 4.5\ NaOH \rightleftharpoons 6\ Na_2CO_3 + 4.75\ H_2O + 2.25\ N_2O$	−1,470	−5.71
	$Na_3C_6H_5O_7 + 6\ NaNO_2 \rightleftharpoons 4.5\ Na_2CO_3 + 1.5\ CO_2 + 2.5\ H_2O + 3\ N_2$	−1,880	−7.28
	$Na_3C_6H_5O_7 + 9\ NaNO_2 \rightleftharpoons 6\ Na_2CO_3 + 2.5\ H_2O + 4.5\ N_2O$	−1,540	−5.96
	$Na_3C_6H_5O_7 + 6\ NaNO_2 + 3\ NaOH \rightleftharpoons 6\ Na_2CO_3 + 4\ H_2O + 3\ N_2$	−2,070	−8.02
Sodium Tartrate $(Na_2C_4H_4O_6)$ (MW = 194 g/mol)	$Na_2C_4H_4O_6 + 2\ NaNO_3 \rightleftharpoons 2\ Na_2CO_3 + 2\ CO_2 + 2\ H_2O + N_2$	−823	−4.25
	$Na_2C_4H_4O_6 + 2.5\ NaNO_3 \rightleftharpoons 2.25\ Na_2CO_3 + 1.75\ CO_2 + 2\ H_2O + 1.25\ N_2O$	−670	−3.45
	$Na_2C_4H_4O_6 + 2\ NaNO_3 + 4\ NaOH \rightleftharpoons 4\ Na_2CO_3 + 4\ H_2O + N_2$	−1,076	−5.54
	$Na_2C_4H_4O_6 + 2.5\ NaNO_3 + 3.5\ NaOH \rightleftharpoons 4\ Na_2CO_3 + 3.75\ H_2O + 1.25\ N_2O$	−892	−4.60
	$Na_2C_4H_4O_6 + 3.33\ NaNO_2 \rightleftharpoons 2.667\ Na_2CO_3 + 1.3\ CO_2 + 2\ H_2O + 1.667\ N_2$	−1,055	−5.44
	$Na_2C_4H_4O_6 + 5\ NaNO_2 \rightleftharpoons 3.5\ Na_2CO_3 + 0.5CO_2 + 2\ H_2O + 2.5\ N_2O$	−868.8	−4.48
	$Na_2C_4H_4O_6 + 3.33\ NaNO_2 + 2.667\ NaOH \rightleftharpoons 4\ Na_2CO_3 + 3.337\ H_2O + 1.667\ N_2$	−860	−4.43
	$Na_2C_4H_4O_6 + 5\ NaNO_2 + NaOH \rightleftharpoons 4\ Na_2CO_3 + 2.5\ H_2O + 2.5\ N_2O$	−933	−4.80
Sodium Formate $(NaCHO_2)$ (MW = 68 g/mol)	$NaCHO_2 + 0.4\ NaNO_3 \rightleftharpoons 0.7\ Na_2CO_3 + 0.3\ CO_2 + 0.5\ H_2O + 0.2\ N_2$	−176.3	−2.59
	$NaCHO_2 + 0.5\ NaNO_3 \rightleftharpoons 0.75\ Na_2CO_3 + 0.25\ CO_2 + 0.5\ H_2O + 0.25\ N_2O$	−146.4	−2.15
	$NaCHO_2 + 0.4\ NaNO_3 + 0.6\ NaOH \rightleftharpoons Na_2CO_3 + 0.8\ H_2O + 0.2\ N_2$	−214.3	−3.15

Table 3-10. Enthalpies of reaction for the oxidation of organics by sodium nitrate and sodium nitrite (cont'd)[a]

Compound	Reaction	ΔH_{rxn} (kJ/Mole)	ΔH_{rxn} (kJ/g)
	$NaCHO_2 + 0.5\ NaNO_3 + 0.5\ NaOH \rightleftharpoons Na_2CO_3 + 0.75\ H_2O + 0.25\ N_2O$	−178.3	−2.62
	$NaCHO_2 + 1.667\ NaNO_2 \rightleftharpoons 0.833\ Na_2CO_3 + 0.167\ CO_2 + 0.5\ H_2O + 0.33\ N_2$	−223.2	−3.28
	$NaCHO_2 + 0.667\ NaNO_2 + 0.33\ NaOH \rightleftharpoons Na_2CO_3 + 0.667\ H_2O + 0.33\ N_2$	−243.9	−3.58
	$NaCHO_2 + 1.667\ NaNO_2 \rightleftharpoons Na_2CO_3 + 0.5\ H_2O + 0.5\ N_2O$	−184.9	−2.72
Sodium Dibutylphosphate $(NaO(C_4H_9O)_2PO)$ (MW = 232 g/mol)	$NaO(C_4H_9O)_2PO + 9.6\ NaNO_3 \rightleftharpoons 3.8\ Na_2CO_3 + 4.2\ CO_2 + 9\ H_2O + Na_3PO_4 + 4.8\ N_2$	−3,952	−17.0
	$NaO(C_4H_9O)_2PO + 12\ NaNO_3 \rightleftharpoons 5\ Na_2CO_3 + 3\ CO_2 + 9\ H_2O + Na_3PO_4 + 6\ N_2O$	−3,222	−13.9
	$NaO(C_4H_9O)_2PO + 9.6\ NaNO_3 + 8.4\ NaOH \rightleftharpoons 8\ Na_2CO_3 + 13.2\ H_2O + Na_3PO_4 + 4.8\ N_2$	−4,489	−19.3
	$NaO(C_4H_9O)_2PO + 12\ NaNO_3 + 6\ NaOH \rightleftharpoons 8\ Na_2CO_3 + 12\ H_2O + Na_3PO_4 + 6\ N_2O$	−3,605	−15.5
	$NaO(C_4H_9O)_2PO + 16\ NaNO_2 \rightleftharpoons 7\ Na_2CO_3 + CO_2 + 9\ H_2O + Na_3PO_4 + 8\ N_2$	−5,066	−21.8
	$NaO(C_4H_9O)_2PO + 16\ NaNO_2 + 2\ NaOH \rightleftharpoons 8\ Na_2CO_3 + 10\ H_2O + Na_3PO_4 + 8\ N_2$	−4,536	−19.5
	$NaO(C_4H_9O)_2PO + 24\ NaNO_2 \rightleftharpoons 8\ Na_2CO_3 + 6\ NaOH + 6\ H_2O + Na_3PO_4 + 12\ N_2O$	−3,777	−16.3
Sodium Butyrate $(NaC_4H_7O_2)$ (MW = 110 g/mol)	$NaC_4H_7O_2 + 4\ NaNO_3 \rightleftharpoons 2.5\ Na_2CO_3 + 1.5\ CO_2 + 3.5\ H_2O + N_2$	−1,615	−14.7
	$NaC_4H_7O_2 + 5\ NaNO_3 \rightleftharpoons 3\ Na_2CO_3 + CO_2 + 3.5\ H_2O + 2.5\ N_2O$	−1,309	−11.9
	$NaC_4H_7O_2 + 4\ NaNO_3 + 3\ NaOH \rightleftharpoons 4\ Na_2CO_3 + 5\ H_2O + 2\ N_2$	−1,804	−16.4
	$NaC_4H_7O_2 + 5\ NaNO_3 + 2\ NaOH \rightleftharpoons 4\ Na_2CO_3 + 4.5\ H_2O + 2.5\ N_2O$	−1,436	−13.0
	$NaC_4H_7O_2 + 6.67\ NaNO_2 \rightleftharpoons 3.83\ Na_2CO_3 + 0.17\ CO_2 + 3.5\ H_2O + 3.33\ N_2$	−2,073	−18.8
	$NaC_4H_7O_2 + 10\ NaNO_2 \rightleftharpoons 4\ Na_2CO_3 + 3\ NaOH + 2\ H_2O + 5\ N_2O$	−1,510	−13.7
	$NaC_4H_7O_2 + 6.67\ NaNO_2 + 0.33\ NaOH \rightleftharpoons 4\ Na_2CO_3 + 3.667\ H_2O + 3.33\ N_2$	−2,099	−19.1

3-21

Table 3-10. Enthalpies of reaction for the oxidation of organics by sodium nitrate and sodium nitrite (cont'd)[a]

Compound	Reaction	ΔH_{rxn} (kJ/Mole)	ΔH_{rxn} (kJ/g)
Butanol ($C_4H_{10}O$) (MW = 74 g/mol)	$C_4H_{10}O + 4.8\ NaNO_3 \rightleftharpoons 2.4\ Na_2CO_3 + 1.6\ CO_2 + 5\ H_2O + 2.4\ N_2$	−2,199	−29.7
	$C_4H_{10}O + 6\ NaNO_3 \rightleftharpoons 3\ Na_2CO_3 + CO_2 + 5\ H_2O + 3\ N_2O$	−1,834	−24.8
	$C_4H_{10}O + 4.8\ NaNO_3 + 3.2\ NaOH \rightleftharpoons 4\ Na_2CO_3 + 6.6\ H_2O + 2.4\ N_2$	−2,474	−33.4
	$C_4H_{10}O + 6\ NaNO_3 + 2\ NaOH \rightleftharpoons 4\ Na_2CO_3 + 6\ H_2O + 3\ N_2O$	−2,006	−27.1
	$C_4H_{10}O + 12\ NaNO_2 \rightleftharpoons 4\ Na_2CO_3 + 3\ H_2O + 4\ NaOH + 6\ N_2O$	−1,959	−26.5

[a]With the exception of butanol, the data presented are from Burger (1995), with corrections made to the reaction enthalpies for DBP and sodium glycolate .

Table 3-11. Reactions of sodium acetate (from Burger, 1995)

	Reactants, moles				Products, moles[a]								
Oxidant	H_2O	NaOH	Na_2CO_3	CO_2	H_2O	N_2	N_2O	NO	NH_3	NaOH	CO	$Na_2C_2O_4$	$-\Delta H_{rxn}$, kJ
NaNO_3													
1.6	—	—	1.3	0.70	1.50	0.80	—	—	—	—	—	—	651
2.0	—	—	1.5	0.50	1.50	—	1.00	—	—	—	—	—	529
2.00	—	1.00	2.00	—	2.00		1.00	—	—	—	—	—	583
1.60	—	1.40	2.00	—	2.20	0.80	—	—	—	—	—	—	740
2.67	—	—	1.833	0.167	1.50	—	—	2.67	—	—	—	—	304
2.67	—	0.333	2.00	—	1.667	—	—	2.67	—	—	—	—	324
1.00	—	—	1.00	1.00	—	—	—	—	—	1.00	—	—	394
1.00	—	2.00	2.00	—	1.00	—	—	—	—	1.00	—	—	522
0.80	—	—	—	—	—	—	—	—	—	—	2.0	—	49
1.20	—	—	—	—	1.40	0.60	—	—	—	0.20	—	1.00	472
1.60[b]	—	—	—	2.00	0.20	0.80	—	—	—	2.60	—	—	485
2.00[b]	—	—	—	2.00	—	—	1.00	—	—	3.00	—	—	337
1.60[b]	—		—	2.00	1.20	0.80	—	—	—	1.60	—	—	525
NaNO_2													
2.666	—	—	1.833	0.17	1.50	1.333	—	—	—	—	—	—	836
2.666	—	0.333	2.00	—	1.667	1.333	—	—	—	—	—	—	858
4.00	—	—	2.00	—	—	—	2.00	—	—	1.00	—	—	620
8.00	1.00	—	2.00	—	—	—	—	8.00	—	5.00	—	—	-46

[a] Na_2CO_3 is the assumed product until either carbon or sodium is consumed. At that point, either CO_2 or NaOH is formed. The carbonates of the heavy metals are unstable at the temperatures of interest.
[b] Hypothetical reaction, assumes CO, liberated.

for the amounts of organic constituents and water, respectively, of tanks A-101, SY-103, and SY-101 given in the Agnew (1997) report are also listed in tables C-1 to C-3.

The results of the calculations for tank A-101 indicate that complete oxidation of the organics in the tank would yield a total energy of 1.96×10^9 kJ, sufficient to heat the water content of the waste to 100 °C and vaporize 24 weight percent of the water (for calculations, see appendix C). If the upper estimate of organic chemical concentrations and the lower estimate of water content are used in the calculations, the results indicate an energy yield of 2.98×10^9 kJ, sufficient to volatilize 47 weight percent of the water. The temperature would remain at the boiling point of water, 100 °C, but the evaporation of such large volumes of water (550,000 to 1,076,000 L) could lead to high, and potentially explosive, pressures in a closed tank or to volatilization of other tank waste components.

Heat balance calculations for tank SY-103 show results similar to those for tank A-101. Complete oxidation of the organic constituents yields about 1.07×10^9 kJ, evaporating 18 weight percent of the water content. When the upper and lower estimates of organic and water content, respectively, are used in the calculations, the energy yield increases to 1.60×10^9 kJ and the fraction of water vaporized increases to 38 weight percent. Compared to the results for tanks A-101 and SY-103, oxidation of organic constituents in tank SY-101 yields much higher energy (2.36×10^9 kJ), sufficient to evaporate about 52 weight percent of the water content. If the upper estimate of organic content and lower estimate of water content are used, the energy yield is 3.43×10^9 kJ, sufficient to evaporate 100 weight percent of the water content and to raise the SY-101 waste temperature to 436 °C.

The examples discussed in the preceding paragraphs indicate that the energy given off by oxidation reactions involving organic compounds in HLW tanks could be significant and could cause the temperature to rise to at least 100 °C and to vaporize the water. Generation of steam and other gases (e.g., CO_2 and N_2) could also result in pressure build-up that could damage the tank and release radionuclides to the environment.

3.4.2 Thermoanalysis of Organic/Oxidant Mixtures

Various thermoanalytical techniques are used in the chemical industry for chemical hazards evaluation. Studies by the DOE employed the same techniques to measure the thermal sensitivities and thermochemical and thermokinetic properties of organic and oxidant mixtures relevant to Hanford organic-bearing wastes (e.g., Turner and Miron, 1994a,b; Scheele et al., 1995; Fauske et al., 1995a,b). Scheele et al. (1995) reported measurements of the energy release and thermal behavior of mixtures of selected organics and sodium nitrate and/or nitrite and a simulated Hanford organic-bearing waste. The analytical instruments used to determine the thermal sensitivities, energies, and chemical reactivity information were differential scanning calorimetry (DSC), thermogravimetric analysis (TGA), differential thermal analysis (DTA), accelerating rate calorimetry (ARC), and a reactive system screening tool (RSST). To characterize the gases evolved during TGA experiments, infrared (IR) spectrophotometry or mass spectroscopy (MS) were used.

For the experiments performed by Scheele et al. (1995), DSC and DTA were used to screen for exothermic behavior, provide preliminary information about reaction onset temperature, and provide a measure of the heat of reaction. Both instruments observe the release or absorption of heat as the temperature is increased at a constant rate. However, DSC measures enthalpy change, whereas DTA observes temperature differences between the sample and an inert reference material. Due to the wide variety of constituents in Hanford wastes, multiple reactions can occur simultaneously. For example, an endothermic process

(i.e., melting of a solid) occurring simultaneously with an exothermic reaction could cause the heat of reaction measured by the DSC to be misleading. The use of additional instruments, such as TGA, can overcome this problem. TGA helps to interpret the DSC results and identify exothermic reactions. TGA measures the weight change of the sample as the temperature is increased at a constant rate. Thus, chemical reactions that result in gas evolution, such as exothermic reactions between organics and nitrate, are detectable by TGA. To help interpret the TGA results, the evolved gases can be analyzed by IR or MS or both.

Scheele et al. (1995) used two adiabatic calorimeters, the ARC and RSST, in their study. Adiabatic calorimeters can provide more accurate onset temperatures than DSC or DTA, can measure reaction enthalpies, and can provide thermokinetic parameters. The ARC operates in a heat-wait-search mode, while monitoring the sample and container temperature and the system pressure at adiabatic conditions. The sample and container are heated to a set temperature, the system is allowed to come into thermal equilibrium, and then the temperatures of the sample and container are monitored and compared (Scheele et al., 1995). If no temperature difference is detected, then the ARC increases the temperature and repeats the heat-wait-search cycle until an exothermic reaction is detected. The RSST is similar to the ARC and can be used to measure onset temperatures, reaction enthalpies, gas production rates based on pressure, and selected reaction thermokinetic properties. A difference is that the RSST uses a continuous heat rate to induce reactions, whereas the ARC uses the heat-wait-search mode.

The goal of Scheele et al. (1995) was to measure the thermal behavior and heats of reactions of waste mixtures containing organic salts and sodium nitrate or nitrite. The organic compounds used for the study were sodium acetate, sodium citrate, Na_4EDTA, and Na_3HEDTA, all of which are of potential concern for the safety analysis of Hanford organic-bearing waste. The experiments included the use of DSC, ARC, TGA, and IR evolved-gas analyses of the selected organic mixed with nitrate or nitrite. The compositions used were a 6 wt % TOC mixture of the selected organic compound and sodium nitrate, a 6 wt % TOC mixture of the selected organic compound and sodium nitrite, and 2, 6, and 10 wt % TOC mixtures of the selected organic compound and equimolar sodium nitrate and nitrite. The latter mixtures containing equimolar amounts of sodium nitrate and nitrite as the oxidant most closely represent the organic-bearing wastes found at Hanford.

3.4.2.1 Thermal Reactivity of Sodium Acetate

Many of the organic complexants used at Hanford contain acetate groups, and sodium acetate is a common complexant component. Thus, sodium acetate was considered by Fisher (1990) as a useful energetics reference and model organic for Hanford organic-bearing wastes. DOE thermoanalytical measurements have been reported for this chemical. For example, Turner and Miron (1994b) performed experiments on the thermal behavior of sodium acetate, sodium nitrate, sodium nitrite, and sodium hydroxide mixtures using DSC and TGA. They reported exothermic onset temperatures ranging from 213 to 235 °C. Scheele et al. (1995) reported that the reaction between sodium acetate and equimolar sodium nitrate and nitrite (6 wt % TOC) shows an exotherm near 325 °C. A comparison to Turner and Miron's (1994b) reported onset temperature of 213 to 235 °C suggests that sodium hydroxide increases the thermal sensitivity of the reaction mixture.

Scheele et al. (1995) reported that the reactions, as measured by TGA, of the 2, 6, and 10 wt % TOC mixtures of sodium acetate and equimolar sodium nitrate and nitrite all begin at the same temperature (~330 °C), independent of the concentration of the organic. In contrast to the TGA results, the onset temperatures measured by ARC showed that the thermal behavior of acetate and nitrate/nitrite mixtures is dependent on organic concentration. Increasing the organic concentration from 2 to 6 to 10 wt % TOC decreased the ARC-measured onset temperature from 284 to 274 to 250 °C, respectively

(Scheele et al., 1995). The ARC results are more consistent with the expectation that observed onset temperatures would decrease with increasing organic concentration up to the concentration where a stoichiometric mixture (~ 9 wt % TOC for reactions between sodium acetate and sodium nitrate/nitrite) is reached.

The results of the thermal analysis study of sodium acetate and equimolar sodium nitrate and nitrite mixtures suggest that rapid energetic reactions will occur around 270 °C under adiabatic conditions (ARC), and at 325 °C if the sample is heated at a rate of 5 °C/min (TGA). The IR evolved-gas analysis indicates that the reactions proceed, at least partially, by a reaction mechanism other than the most energetic.

3.4.2.2 Thermal Reactivity of Sodium Citrate

To obtain an understanding of the behavior and potential hazards associated with Hanford wastes containing citrate, Scheele et al. (1995) performed measurements on mixtures of sodium citrate dihydrate and equimolar sodium nitrate and nitrite. The results of the DSC, TGA, and ARC thermal studies indicate that citrate and nitrate and nitrite can react exothermically at a detectable rate (0.025 °C/min) if heated to 190 °C. The studies found little difference in the qualitative thermal behavior of the mixtures containing different amounts of citrate. Quantitatively in terms of weight loss, the measured changes are consistent with postulated reaction pathways that produce nitrogen or nitrous oxide. Evolved gas IR analysis indicates the evolution of N_2O, supporting the inference that the reaction proceeds at least partially by a mechanism other than the most energetic (Scheele et al., 1995).

3.4.2.3 Thermal Reactivity of Na_4EDTA

Sodium EDTA was one of the primary organic complexants used to remove Sr-90 during waste-management operations at the Hanford B Plant. Turner and Miron (1994a) determined the thermal sensitivity of reactions of Na_4EDTA with nitrate and with nitrate/nitrite mixtures using DSC and TGA. The reported onset temperatures for exothermic behavior of EDTA with nitrate are about 300 to 305 °C as measured in the DSC, and approximately 295 °C or slightly higher when measured in the TGA. For mixtures with sodium nitrate/nitrite, onset temperatures determined with DSC by Turner and Miron (1994a) clustered near 290 °C, but TGA measurements showed low onset temperatures that ranged from 235 to 254 °C. It appears that the presence of nitrite lowers the onset temperature for exothermic reaction of sodium EDTA. Additional data are given by Scheele et al. (1995), who reported an onset temperature around 250 °C for 6 wt % TOC mixture of Na_4EDTA and equimolar sodium nitrate and nitrite. The gases evolved (CO_2, N_2O) indicate a less than maximum energetic path was followed. The ARC analysis of the same reaction mixture showed a self-heating exotherm at 210 °C at adiabatic conditions. The ARC analysis of the 10 wt % TOC mixture indicated an onset temperature 10 to 15 °C less than the 6 wt % TOC mixture.

3.4.2.4 Thermal Reactivity of Sodium Oxalate and Sodium Formate

Turner and Miron (1994a) determined the onset temperatures for the reaction of sodium oxalate with sodium nitrate and sodium nitrite using DSC and TGA. Their results indicate evidence for an exothermic reaction between sodium oxalate and sodium nitrate, and between the oxalate and a mixture of the two oxidants. The onset temperatures for exothermic behavior, determined in the DSC tests, varied from about 395 to 420 °C with sodium nitrate as the oxidant, and from 355 to 385 °C with a sodium nitrate/nitrite mixture as the oxidant. The results show that the oxidant mixture is more reactive toward the oxalate compared to sodium nitrate alone. Also, in general, the onset temperatures decreased with increasing amounts of oxidant(s). Similar trends were observed in the TGA tests, whereby onset temperatures for

exothermic behavior decreased with increasing oxidant(s) concentration and lower onset temperatures were observed in tests that used a mixture of two oxidants. The onset temperatures measured with TGA for oxalate-nitrate mixtures ranged from 310 to 420 °C. For mixtures of sodium oxalate and sodium nitrate/nitrite, the TGA onset temperatures ranged from 275 to 345 °C.

Additional data on mixtures of sodium oxalate (10 wt % TOC) with equimolar sodium nitrate/nitrite were obtained by Sills (1995) using DSC. The measured onset temperature was ~365 °C. Sills (1995) also measured the onset temperature of exothermic behavior for mixtures of sodium formate (10 wt % TOC) with equimolar sodium nitrate/nitrite. The measured onset temperature was ~250 °C.

3.4.2.5 Thermal Reactivity of Na$_3$HEDTA

Sodium HEDTA was also one of the primary organic complexants used to remove Sr-90 during waste-management operations at the Hanford B Plant. Results of thermoanalytical studies on 2, 6, and 10 wt % TOC mixtures of Na$_3$HEDTA and equimolar sodium nitrate and nitrite indicate that significant exothermic reactions will occur beginning at temperatures as low as 180 °C at adiabatic conditions (ARC), depending on the organic concentrations (Scheele et al., 1995). Detection of the gases N$_2$O and CO$_2$ by IR analysis indicates the reaction proceeds by an energetic path less than the maximum possible value.

3.4.2.6 Thermal Reactivity of Simulated Hanford Organic-Bearing Waste

The Hanford tank wastes are complex mixtures of organic complexants and solvents, organic degradation products, sodium nitrate, sodium nitrite, sodium hydroxide, and a variety of other inorganic materials. To determine the thermal behavior of complex chemical mixtures approximating those in Hanford waste tanks, Scheele et al. (1995) used DTA, TGA, ARC, and RSST to measure the thermal sensitivity and reactivity of a simulated neutralized PUREX acid sludge waste. The simulated waste was prepared by mixing sodium hydroxyacetate, Na$_3$HEDTA, sodium citrate, sodium tartrate, sodium di-(2-ethylhexyl) phosphate, and NPH with equimolar sodium nitrate and nitrite. The prepared simulated waste contained around 9.5 wt% TOC.

The results of the DTA, TGA, ARC, and RSST tests indicate that exothermic reactions can occur when the waste is heated to 150 °C. ARC analysis suggests that this self-sustaining exothermic reaction will lead to a second, more rapid reaction. The RSST analysis indicates that a propagating reaction will occur if the sample is heated to 200 °C. This simulated waste was the most thermally sensitive mixture tested by Scheele et al. (1995). Scheele et al. (1995) proposed the following explanations to account for the observed greater sensitivity of the simulant sludge waste compared to the other surrogate wastes: (i) an untested organic in the simulant waste is more thermally susceptible than any of the organics that were tested, (ii) interactions among the different organics increased thermal susceptibility, (iii) the reaction was catalyzed by a material in the simulated sludge waste, and (iv) organic complexing of metals in the waste increased thermal sensitivity. Scheele et al. (1995) suggested that components in complex mixtures will not behave independently of the other constituents.

3.4.2.7 Summary of Thermoanalytical Studies

The thermal behavior of the various organic compounds shows significant differences in terms of thermal reactivity and sensitivity. DSC and ARC analyses indicate that the amount of heat produced by reactions between the oxidants sodium nitrate and sodium nitrite and the organics studied are dependent on the nature of the organic, with minimal dependence on the organic concentration (per gram of organic salt).

Based on the ARC-measured reaction heats, the heat produced (per gram of fuel) by reaction of equimolar sodium nitrate and nitrite with the different organics increased in the order Na_3HEDTA > citrate > Na_4EDTA, which is not consistent with the thermodynamically predicted order Na_3HEDTA > Na_4EDTA > citrate. This inconsistency suggests that the reaction pathways differ from those postulated strictly from thermodynamic considerations.

The thermoanalytical studies indicate that dried simulated PUREX sludge waste and dried surrogate waste mixtures containing 2, 6, and 10 wt % TOC of the sodium salts of acetate, citrate, EDTA, and HEDTA and the oxidants sodium nitrate or nitrite will support self-sustaining exothermic reactions (self-heat rate $\geq$ 0.025 °C/min) if heated to a sufficiently high temperature under adiabatic conditions: $\geq$140 °C for the simulated sludge waste and $\geq$180 °C for the surrogate waste mixtures. The onset temperatures measured by Scheele et al. (1995) using ARC indicate that acetate is the most resistant of the tested organics to oxidation by nitrate or nitrite; Na_3HEDTA and citrate are the least resistant. The DSC and TGA results of Turner and Miron (1994a), as well as the DSC data of Sills (1995), indicate that oxalate is more thermally resistant than acetate. The data on formate is very limited, but the DSC results of Sills (1995) suggest that the thermal sensitivity of formate is somewhat higher than that of sodium EDTA. Thus, the thermoanalytical data suggests the following relative order of the tested organics with respect to thermal sensitivity: Na_3HEDTA $\geq$ citrate > formate $\geq$ Na_4EDTA > acetate > oxalate. This relative order indicates that acetate is generally a less conservative model for the organics used at Hanford with respect to susceptibility to hazardous chemical reactions. It also indicates that organic-bearing wastes containing Na_3HEDTA and citrate should be of greatest concern.

Average activation energies of reactions between the different organics and equimolar mixtures of sodium nitrate and sodium nitrite determined from ARC data ranged between 125 and 405 kJ/mole, depending upon the organic material in the order Na_4EDTA>acetate>Na_3HEDTA>citrate. The simulated PUREX sludge waste had the lowest activation energy of the mixtures tested, consistent with its having the highest thermal sensitivity.

From the results presented by Scheele et al. (1995), it appears the controlling oxidation reaction is that of nitrite with the organic compound. Comparison of the exothermic onset temperature indicates that the reaction mixtures containing only nitrite are similar to the equimolar sodium nitrate/nitrite mixtures. Reaction mixtures that contain only nitrate have onset temperatures that are considerably higher and, hence, are more stable.

In summary, thermoanalytical studies conducted by the DOE indicate that energetic, self-sustaining exothermic reactions can occur at adiabatic conditions among the salts of acetate, citrate, formate, EDTA, HEDTA, oxalate, and nitrate and/or nitrite and among the organics and nitrate and/or nitrite in the PUREX simulated waste. The evolved-gas analyses from the TGA and ARC experiments showing production of nitrous oxide instead of nitrogen, and the less-than-theoretical-maximum measured heats by DSC, ARC, and RSST indicate that the exothermic reactions between different organics and sodium nitrate and/or nitrite proceed at least partially by reaction pathways that produce less than the maximum possible heat. This indication suggests that hazard assessments using the maximum thermodynamically based energetics (as in section 3.4.1) will likely overestimate the consequences of a reaction, assuming that the reaction(s) in the waste proceeds as in the TGA and ARC. In addition, the measured activation energies indicate that there is a relatively high energy barrier to the initiation of these reactions. Thus, high temperatures are likely required to initiate the organic oxidation reactions.

It should be noted that the thermoanalytical studies reviewed above used dried organic/oxidant mixtures and, thus, did not take into account the heat-absorption properties of water, which in most cases is present in Hanford wastes. On the other hand, most of the studies did not consider conditions that could result in higher reaction enthalpies due to the formation of carbonate as a reaction product (see, for example, table 3-10). Thus, engineering analyses to assess the thermal hazards associated with the organic-bearing wastes need to consider the concentration of waste constituents other than the organics and oxidants. Also, the greater reactivity exhibited by the simulated sludge waste compared to the other surrogate waste mixtures suggests that caution must be used in extrapolating the behavior of waste simulants to that of actual wastes with more complex compositions. It is possible that actual Hanford wastes may be more reactive due to the presence of thermally more sensitive organics, the presence of transition metal ions that could act as catalysts, or to synergistic interactions between the organics. The potentially higher thermal sensitivity of Hanford wastes is supported by the lower onset temperatures of exothermic reactions of sodium acetate in mixtures containing sodium hydroxide compared to mixtures without sodium hydroxide (Turner and Miron, 1994b).

3.4.3 Discussion of Organic Chemical Reactivity

Reactivity, as a general term, refers to the threshold (either thermal or concentration) for chemical decomposition or heteromolecular combination. By this definition, a scale of intensity, rather than extent, is inferred when reactivity is mentioned. Reactivity implies the ease of reaction, instead of the quantity of heat given off or amount of product liberated once a reaction takes place. It relates to initiation and self-sustainability of chemical processes.

It is useful to have heuristic guides when considering the relative reactivity of materials that have not been tested for reactivity by the same methods. Although detailed and sophisticated theories of organic chemical reaction mechanisms might be applied by experienced organic chemists, some rules of thumb can be applied by any worker who needs to compare potential reactivity on a differential basis. Further, mixtures of complex molecules and their fragments, which may defy rigorous theoretical analysis of specific reaction pathways because of their complexity, may be considered from the point of view of aggregate molecular types or predominant carbon bonding patterns.

Frequently, a molecule containing carbon-carbon double bonds (e.g., -HC=CH-, so called alkenes or dienes, in the case of two double bonds in one molecule) heads the list of increasing reactivity. The more double bonds there are per noncyclic molecule, the more reactive is the organic material. The presence of carbon atoms bonded to three other carbon atoms(e.g., $-c-\overset{c}{c}-c-$), so called tertiary carbon atoms, is also a reactive feature, but less so than alkenes. A list, in decreasing reactivity, of easily identified features is: (i) molecular fragments (free radicals), (ii) multiple double bonds, (iii) alternating double bonds, (iv) individual double bonds, (v) tertiary carbon atoms, and (vi) straight chain molecules. Individual aromatic rings are themselves more stable than linear structures containing the above features, but one or more aromatic rings acting as a side group may weaken adjacent points in a molecule.

As molecules increase in size and length, they present more places to react than the more compact molecules. Hence, among similar molecules, molecular weight correlates positively with reactive propensity toward degradation. Degradation could be oxidation (such as with oxygen or nitrates/nitrites), but it could also be polymerization or pyrolysis (thermal decomposition). In that pyrolysis frequently gives off hydrogen gas as a product, it is important to remember that reactivity can change as a reaction mixture begins to undergo chemical change. Hydrogen is itself readily permeating and possesses a low specific energy of ignition.

Atoms other than carbon and hydrogen can increase or decrease the average reactive strength of organic substances. Molecules held together by metals are frequently fragile. Organic chains and rings containing heteroatoms (i.e., sulfur, nitrogen, and oxygen) offer variations in molecular strength that can be used to estimate their relative likelihood to react. The more centrally placed a heteroatom is in a molecule, the stronger its attachment. For example, amines ($R-\overset{R}{\underset{}{N}}-R$) are more reactive than pyridines (⬡). Similar patterns exist for oxygen and sulfur in organic compounds.

When complex inorganic anions and cations are bonded into organic molecules, they usually remain intact when a reaction of the organic molecule occurs. Hence, reactivity is enhanced by large ionic substituents. Organic molecules are more often affected by the number and size of inorganic groups than by the particular inorganic atoms involved because ionic (inorganic) bonding within ions is comparatively stronger than organic bonding to the ion for most molecules.

In crucial comparisons, no estimate should replace physical measurements of potential reactivity. Although not as generalizable as a theoretical approach, well selected tests hold the greatest promise for accurately assessing the potential for exotherms in complex mixtures of organics and oxidizers such as nitrates and nitrites. Several techniques for thermoanalysis are discussed in section 3.4.2. There are, however, surrogates for rigorous thermal measurements when differential reactivity may need to be assessed. Two such methods are Bromine Number (ASTM D 1159) and Aniline Point (ASTM D 611). For differential estimates, or for ranking reactivity, these American Society for Testing and Materials (ASTM) guides provide a starting point.

Bromine Number is a particularly sensitive test for assessing the extent of reactive double bonds (such as from hydrogen-generating thermal decomposition or cracking) in organic mixtures. ASTM D 1159, "Standard Test Method for Bromine Numbers of Petroleum Distillates and Commercial Aliphatic Olefins by Electrometric Titration," can be applied readily to wastes or surrogates of interest. In this method, bromine is added slowly to samples to assess the number of grams that will be taken up by 100 g of sample through chemical reactions of all kinds. Heteroatom compounds (e.g., those containing sulfur) and some aromatic compounds will take up bromine, but the predominant class of compounds that take up bromine is olefins. Taken as an indicator of reactivity, higher bromine numbers indicate greater propensity to react. Taken as an indication of the extent of reaction, higher bromine numbers signal more pyrolysis with attendant double-bond formation. As cracking occurs, first olefins then aromatics form in product liquids as the extent of cracking increases and off-gases (usually hydrogen) are produced. As such, olefins are an early indicator of the onset of cracking. The range of values for bromine number is 0 to ~240, spanning pure, unreactive compounds to highly reactive, neat olefins. Usual cracked stocks, such as those produced during petroleum refining, would be in the range 10–20.

Aniline Point is not a direct measure of reaction but of the similarity of test samples to aromatic hydrocarbons. Aniline point is not as direct a measure as Bromine Number for reactivity and must be used more carefully. In ASTM D 611, "Standard Test Method for Aniline Point and Mixed Aniline Point of Petroleum Products and Hydrocarbon Solvents," equal volumes of sample and aniline are mixed and heated until they are miscible. The temperature is then lowered in a controlled way until two phases again form. That temperature is designated the aniline point. Special provisions are made for dark, volatile, or small samples. Aromatic hydrocarbons have the lowest aniline point temperature followed by cycloparaffins, olefins, and normal paraffins. This listing is roughly the order of resistance to thermal cracking of the named species.

All the guidelines for relative reactivity or surrogate tests to delineate sequences of particular samples depend on the threshold energy for reaction to take place. This threshold is the activation energy for reaction, which is distinct from the energy bound up in a molecule or group of molecules via the enthalpy of reaction or decomposition. Enthalpies of reaction are extensive values relating to the quantity of energy available to be liberated. Activation energy is an intensive quantity that establishes a minimum limit that must be achieved to initiate reaction. Thermal analysis methods that find a temperature of decomposition or reaction help to determine activation energy.

3.5 CONCENTRATION MECHANISMS FOR ORGANIC CHEMICALS IN HANFORD TANK WASTES

As pointed out in section 3.3, the organic carbon inventory for the HLW tanks at the Hanford site constitutes less than 1 weight percent of the 357,000 metric tons of waste. Therefore, it was previously assumed that, even though organic reactions could take place, no significant heat would be generated by the reactions. For example, studies by Beitel (1976a,b,c; 1977) concluded that uncontrolled reactions between organics and nitrates/nitrites would not occur in Hanford waste tanks because the concentrations of organics were too low to sustain a reaction and because the tank temperatures were well below those required to initiate a reaction. However, the organic content of individual tanks varies widely because different processes generated the wastes in each tank. In addition, information released in 1989 regarding a major explosion that occurred in 1957 in a radioactive waste tank in Kyshtym, U.S.S.R., showed that the tank contained a mixture of oxidizing salts and organics, primarily sodium nitrate and sodium acetate. The mixture was allowed to dry out, concentrate, then self-heat to an explosion-initiation temperature estimated to be 380 °C (Borsheim and Kirch, 1991). A concern regarding Hanford tank wastes is the possibility of organics being elevated to concentrations and total quantities sufficiently high to create a hazard that would not be anticipated if average tank values are used in the analysis. Two processes that could be important to safety assessments of Hanford TWRS operations are organic concentration in the liquid phase and precipitation of organic compounds in the solid phase.

3.5.1 Liquid Phase Concentration Mechanisms

Many of the organic compounds added to the Hanford waste tanks are quite insoluble in water, including the hydrocarbons, ion-exchange resins, halogenated solvents, and the higher alkyl amines. Depending on the quantity added to a specific tank, it is possible to form a separate organic phase in the tank. Of the various organic compounds, the hydrocarbon solvents are the most likely to have been added to the tanks in sufficient volume to create a separate organic layer, as evidenced by the observed presence of a separate organic layer in tank C-103 believed to be predominantly NPH and TBP.

Organic compounds that are slightly water soluble (solubility less than 1 g/L) include the phosphorus-containing solvents, most of the chlorinated compounds, and most alkyl amines (Gerber et al., 1992). The higher alcohols and ethers (e.g., dibutyl carbitol) have somewhat higher solubility, with ethers having a solubility in water of 2.7 g/L. Hexone (MIBK) is more soluble, 17 g/L in water at 25 °C. The sparingly water-soluble organics, by the very nature of their hydrophobic character, will tend to partition to the organic phase if one is present.

The organic acids, including the carboxylic amine derivatives such as NTA, are soluble in water; their sodium salts are slightly to moderately soluble. Formation of some form of sodium salt may occur in tank wastes due to evaporation of the aqueous phase. These salts are generally not highly crystalline compounds, and the sodium salts of the larger organic acids are essentially soaps. These organic salts are

3-31

generally soluble in water, exhibiting micelle formation, with the solubility increasing rapidly as the temperature is raised. For example, sodium decanoate has a solubility of 2.1 weight percent at 24 °C, 42 weight percent at 50 °C, and 60 weight percent at 60 °C (Stephen and Stephen, 1963). The salts are relatively insoluble in nonpolar solvents (an organic phase), but the presence of alcohols or other very polar compounds greatly increases their solubility in the organic phase.

There is little reason to expect more than one liquid organic phase (Gerber et al., 1992). The possible exception might result from a large amount of metal salts of long-chain carboxylic acids or organophosphorus acids, which can form a separate organic phase under some conditions. Solvent-extraction systems containing D2EHPA, for example, can form a separate phase slightly more dense than the hydrocarbon layer if a sufficient modifier, such as a polar organic, is not present to increase D2EHPA solubility in the hydrocarbon phase (Richardson and Schulz, 1967). However, TBP is expected to be present wherever D2EHPA is present and will modify the solubility of D2EHPA. Alcohols, esters, and ethers are also excellent solubilizing agents (Gerber et al., 1992).

Density is an important parameter because it not only determines the location of the organic phase, perhaps as a layer if enough organic compounds are present, but along with viscosity and interfacial tension, it determines the ease and degree of phase separation. Most of the organic compounds present in significant quantity in Hanford tank wastes have densities ranging from 0.8 to 1.1 g/mL, except for the halogenated solvents. The solubility of sodium compounds varies, from 2.27 (sodium oxalate) and 1.53 (sodium acetate) to about 1.2 g/mL for the higher organic salts. However, sodium oxalate is insoluble, and sodium acetate has a low solubility in the organic phase. Thus, it is reasonable to expect that a liquid organic phase would have a density of about 1.0 g/mL or, at a maximum, less than that of the aqueous phase (Gerber et al., 1992). The density of the latter would be about 1.4 g/mL at the minimum, equivalent to the density of a 40 wt % NaOH solution. Actual data for tank SY-103, for example, show a density of 1.54 g/mL (Bryan et al., 1992). Thus, a liquid organic layer would be expected to be at the upper surface of a waste tank unless it is trapped by solids.

The solubilities of organics in the aqueous phase are greatly diminished by the presence of electrolytes, an effect called salting out. This trend has been shown for various ethers, carbitols, ketones, and aromatics (Marcus and Kertes, 1969). The decrease in solubility normally follows the Setchenow rule:

$$\ln \frac{S}{S_0} = -kC \qquad (3\text{-}3)$$

where S is the solubility in a salt solution of concentration C, and S_0 is the solubility in pure water. The value of the constant k varies with the organic of interest, but is much more dependent on the particular salt in the aqueous phase. As an approximation, there is a factor of two reduction in solubility at an ionic strength of about three compared to that in pure water (Harned and Owen, 1950). The sodium salt of D2EHPA presents an extreme illustration of the Setchenov relation. The salt is soluble in water, but its solubility in a 0.38 M Na^+ solution is only 0.325 g/L and 0.007 g/L in a 2.8 M Na^+ solution (Richardson and Schulz, 1967).

A number of studies on the solubility of TBP have been reviewed by Burger (1984). Higgins et al. (1959) measured Setchenov constants for TBP in a variety of electrolyte solutions, but only data on NaOH are applicable to Hanford tank wastes. Data from Higgins et al. (1959) indicate TBP solubility will decrease by a factor of 400 for a 1-M solution and by a factor greater than 10^5 for an 8-M solution. Alcock et al. (1955) measured the solubility of TBP in sodium nitrate solutions and obtained a k value equal to 0.81 for concentrations up to 5-M. Extrapolation to higher ionic strengths (to 10 or 15 M) using the reported k

indicates reductions in the solubility of TBP of 10^4 to 10^5. Unfortunately, k values for most of the other organic compounds are not available.

3.5.2 Solid Phase Concentration Mechanisms

Precipitation of organic compounds from concentrated wastes is a mechanism that can result in locally high concentrations of fuel and produce solids with organic-to-oxidant ratios significantly different from the waste tank average value. Precipitated organics could form mixtures with $NaNO_3$-$NaNO_2$ either by crystallization of $NaNO_3$-$NaNO_2$ simultaneously with precipitation of the organics or by drainage of the bulk aqueous phase followed by evaporation of $NaNO_3$-$NaNO_2$-containing interstitial liquid in the already precipitated organics. The Hanford chemicals that could concentrate by this mechanism are the polar, water-soluble compounds that can form metal salts. These compounds include sucrose that was used for denitration, and a large number of organic acids or their sodium salts that were used for complexation or pH control. These acids include oxalic, glycolic, citric, tartaric, gluconic, EDTA, and HEDTA.

Oxalic acid is an important constituent of Hanford tank wastes. For example, it was the most abundant organic compound identified in tank AN-103, constituting about half (by weight) of the approximately 40 organic compounds identified (Hendrickson, 1990). Oxalic acid was used as a reducing agent in the BP process, but its abundance in tank wastes results from degradation of other organics (Gerber et al., 1992). It is produced by nitrate oxidation of sugar and is a likely product of degradation (radiolytic and chemical) of tartrate, citrate, glycolate, and perhaps of aminopolyacetate chelating agents (Gerber et al., 1992). The solubility of its sodium salt, $Na_2C_2O_4$, in water is 37 g/L at 20 °C. However, sodium oxalate solubility in aqueous solution is lower in the presence of excess Na^+ due to the common ion effect.[4] For example, sodium oxalate solubilities calculated from experimental data listed in Seidell (1953) and using density data from Hodgman (1947) are 0.0052 M $Na_2C_2O_4$ at 7.43 M $NaNO_3$ at 15 °C and 0.0051 M $Na_2C_2O_4$ at 9.05 M $NaNO_3$ at 50 °C. Many of the waste tanks are saturated with $NaNO_3$ and $NaNO_2$, and also contain significant amounts of dissolved $NaOH$ and $NaAlO_2$. Thus, many of the Hanford tanks will have high Na^+ concentration. For example, the reported concentration of Na^+ in the interstitial liquid of tank SY-103 is 11.3 M (Bryan et al., 1992). Sodium oxalate solubilities in these tanks will be very low.

Other cations such as Ca^{2+}, Mg^{2+}, Sr^{2+}, Ba^{2+}, and lanthanides form even less soluble oxalates. However, these other metals are present in much smaller quantities than Na^+, and they form other low-solubility compounds with other anions present in Hanford tank wastes, such as phosphate, carbonate, and hydroxide. Thus, metals other than Na^+ will probably have little effect on the solubility of oxalate.

The solubilities of salts of other organic acids derived from complexing agents, buffering agents, and diluents are harder to predict. The solubilities of the sodium salts of many of these acidic materials are high, and many are present in considerably smaller amounts compared to oxalate. Sodium salts of chelating agents such as EDTA and HEDTA have high solubilities, and sodium citrate, tartrate, glycolate, butyrate, and salts of longer chain mono- and dicarboxylic acids are generally quite soluble. Data are limited or nonexistent for other organic compounds present in Hanford wastes, particularly for high ionic strength solutions. The solubility of alkaline earth, uranyl, and other polyvalent cation salts of long-chain carboxylate acids (soaps) is quite low, although it is doubtful that these solids would form because these metals may be preferentially tied up with phosphate, carbonate, or chelating agents.

---

[4] Additive effect on solubility of two compounds sharing a common cation or anion

3.6 ORGANIC WASTE DEGRADATION MECHANISMS

The chemical reactivity hazards associated with organic-bearing wastes at Hanford depend on the concentration and chemical nature of the organic fuels and oxidants present in the wastes. However, the wastes have been exposed to radiation, temperatures of 20 to 140 °C, and to a reactive chemical environment having high concentrations of active components, including hydroxide, nitrate and nitrite, as well as transition metals that could act as catalysts for decomposition reactions. Thus, various degradation or aging processes must have occurred that have changed the nature and quantity of the organics in the tank wastes. For example, organic aging studies performed by Lokken et al. (1986) on simulated organic-bearing waste for 85 days at room temperature and in the absence of radiation showed that, even under the mild conditions of the experiment, chelators such as EDTA and HEDTA exhibited significant degradation (approximately 70 percent), citric acid showed 18 percent degradation, and NTA showed no degradation. The chelator fragments identified were similar to those found in actual Hanford waste, suggesting that EDTA and HEDTA in Hanford tank wastes had similarly exhibited appreciable degradation. The aging products accounted for only 41 percent of the loss of EDTA and HEDTA, which suggests that other fragments not amenable to GC/MS analysis, such as amines, had also been formed.

Campbell et al. (1995a,b) described several aging mechanisms that should change the nature and quantity of organics in Hanford tanks. The high caustic content of the tanks should result in saponification of TBP to DBP and, because DBP is much more soluble than TBP, it should be extracted from discrete organic phases into the aqueous fluids. Also, TBP undergoes radiolytic decomposition. NPH is somewhat volatile under tank heat conditions, and the passive ventilation systems of some Hanford tanks has allowed some NPH to escape from the tank headspace. In addition, NPH decomposes radiolytically to carboxylic acids that are much more soluble than NPH. Therefore the carboxylic acids will migrate toward the aqueous layers, and some of the long-chained acids perhaps precipitate and coat the inorganic sludges.

The high-radiation field provides the energy necessary to break chemical bonds that otherwise would be unaffected at ambient conditions (Gerber, 1994). In the organic phase, radiation causes dehydrogenation and cleavage that result in the degradation of high-fuel-value organics. With this degradation process, there could be considerable loss due to the formation of volatile fragments, an increase of lower-fuel-value carboxylates (e.g., oxalates), and some polymer formation (Gerber, 1994). A probable result of the degradation process is an increased organic solubility in the aqueous phase, although this effect is likely counterbalanced by the salting-out effect due to the high ionic strength of the aqueous phase.

In the aqueous phase, radiolysis will convert nitrate (NO_3^-) to nitrite (NO_2^-) with an equilibrium composition around 30 to 40 percent nitrite and with O_2 also being produced (Gerber, 1994). This reaction leads to the chemical oxidation of both parent and intermediate organic compounds (including ketones, aldehydes, and alcohols) with carboxylic acids being a reasonably stable end product. An oxidative environment may also be produced by the radiolytic degradation of H_2O since the product formed is the OH radical (O^- at high pH). See chapter 2 for additional discussions on radiolysis effects.

The following sections provide additional information regarding the degradation reactions that organic compounds in the Hanford wastes can undergo. For discussion purposes, the organics were grouped into complexing agents, low-molecular weight carboxylic acids (e.g., glycolic, oxalic, citric acids), phosphate ester extractants, and solvents. As pointed out in section 2.4, waste tanks known to produce flammable gas mixtures primarily received chelators and low-molecular weight carboxylic acids, which suggests that these compounds are the dominant components of concern from the standpoint of H_2 and N_2O generation. Thus, the discussions of reaction mechanisms in the following sections are focused on these compounds.

3.6.1 Degradation of Complexing Agents/Organic Acids

Table 3-1 lists the major organic complexants and the approximate quantities placed in the Hanford waste tanks. The list includes EDTA, HEDTA, glycolic acid, citric acid, tartaric acid, oxalic acid, and acetic acid. Extensive studies of degradation mechanisms for complexants have been performed by Argonne National Laboratory (Meisel et al., 1993), Georgia Institute of Technology (Ashby et al., 1994), Pacific Northwest Laboratory (Bryan and Pederson, 1994), and Westinghouse Hanford Company (Delegard, 1987a). The primary focus of these studies was to determine the degradation pathways and the role of complexing agents in producing gases such as H_2, N_2, and N_2O. As discussed in chapter 2, degradation of Hanford waste organics and production of flammable gas mixtures result from thermal and radiolytic processes.

Thermal degradation of chelators such as EDTA and HEDTA, which results in generation of hydrogen gas, involves extensive fragmentation of those molecules (Ashby et al., 1994; Barefield et al., 1996). The aluminate and nitrite ions are believed to play an important role in initiating the decomposition reaction through formation of a trihydroxynitritoaluminum complex (Pederson and Bryan, 1996). The coordinated nitrito ligand is expected to be much more electrophilic than the free nitrite ion and more reactive toward HEDTA. In addition to dependence on aluminate, hydroxide, and nitrite ion concentrations, as well as on the identity and concentration of organic components, organic thermal degradation and hydrogen generation also depended on the presence and concentration of minor components, such as transition metals and chloride ions (Bryan and Pederson, 1994). Thus, rates of thermal degradation and gas generation for a given waste are not easily predicted based on studies using waste simulants.

Early studies by Delegard (1980, 1987) indicated that HEDTA and EDTA were degraded by losing one and two carbon atoms from the moiety, yielding ethylenediaminetriacetate (ED3A). Later studies confirmed that these organics decompose by losing one- and two-carbon fragments from the molecule (Strachan, 1991, 1992a, 1992b; Schulz and Strachan, 1992). Breakdown products of HEDTA include ED3A, glycine, asymmetric ethylenediaminediacetic acid (u-EDDA), symmetric ethylenediaminediacetic acid (s EDDA), formaldehyde, formate, and acetate (Pederson and Bryan, 1996). These fragments ultimately yield oxalate and formate, plus H_2 and CO_2, which, in strongly alkaline environments, is converted immediately to CO_3^{2-}. Oxalate and formate are reasonably stable degradation products and would exist as sodium salts in the Hanford tank wastes. Other gases (e.g., N_2O, NH_3, and N_2) are also produced during the decomposition of the organics.

Formaldehyde, a byproduct of several fragmentation steps, is believed to be among the most important hydrogen-producing species. It is known to react in basic solutions to form hydrogen as in:

$$HCHO + H_2O(OH^-) \rightarrow HCOO^- + H_2 \qquad (3\text{-}4)$$

Similar reactions will occur with other aldehydic aging products such as glyoxylate. The importance of fragments such as formaldehyde as a source of hydrogen is consistent with the induction period commonly observed in tests using simulated wastes (Pederson and Bryan, 1996).

3.6.1.1 Aluminate Catalytic Decomposition of Organic Complexants

As mentioned previously, thermal decomposition of organic complexants was demonstrated to be catalyzed by aluminate ion. Ashby et al. (1994) postulated that the function of aluminate is to complex nitrite and, thus, activate it for reaction with nucleophilic groups in organic complexants, such as alcohol and amine

groups, as shown in figure 3-2. As shown in this figure, both amino and hydroxy groups can react with nitrilo aluminum tri-hydroxide or aluminum dioxide to form N-nitroso amine (or N-nitroso-ammonium ion for tertiary amine) or nitrite ester, respectively. It has been demonstrated that the nitrite ester of β-hydroxy amine is in equilibrium with N-nitroso ammonium ion through intramolecular reactions (Wolf, 1964). The decomposition of the N-nitroso amine or the nitrite ester of β-hydroxy amine has been proposed by Wolf (1964) and is represented as Mechanisms a through c in figure 3-3. However, decomposition of N-nitroso ammonium ion may follow Mechanism d, generally known as Hofmann elimination, shown in figure 3-3. The various mechanisms illustrated in figure 3-3 can be described as:

Mechanism a: Elimination of the nitroso group by base removal of α-hydrogen and subsequent hydroxylation of the imine formed

Mechanism b: Elimination of the nitroso group of nitrite ester of β-hydroxy amine and subsequent hydroxylation of the imine formed

Mechanism c: Decarboxylation and elimination of the nitroso group of α-carboxyl N-nitroso amine and subsequent hydroxylation of the imine formed

Mechanism d: Hofmann elimination of quaternary ammonium hydroxide

Mechanism e: Mixed Cannizzaro reaction to form carboxylate and hydrogen

Except for Mechanism d, the above mechanisms have been evaluated or proposed in previous studies (e.g., Ashby et al., 1994). These various mechanisms play a role in the complete decomposition of organic complexants. It is important to note that hydrogen gas is produced through Mechanism e, which is the major route for hydrogen gas formation.

3.6.1.2 Oxidation of Organic Complexants by Oxygen

The presence of oxygen has a significant effect on the reaction rate of some organic complexants, in the reactivity order of glycolate > HEDTA >> EDTA, and on the amount of some gaseous products, such as hydrogen. The oxidation of these organic complexants by oxygen (autoxidation) is not catalyzed by aluminate ion. The possible mechanisms for decomposition of glycolate, HEDTA, and EDTA are detailed in the following paragraphs.

Decomposition of Glycolate

The decomposition of glycolate is shown in figure 3-4a. As shown in this figure, glycolate undergoes nitrosation to form nitrite ester. The nitrite ester undergoes further oxidation via two routes to produce the final products carbon dioxide, hydrogen, formate, and oxalate:

Route 1:   Decarboxylation and elimination of the nitroso group; similar to Mechanism c in figure 3-3, and followed by a Cannizzaro reaction to form carbon dioxide, formate, and hydrogen

Route 2:   Elimination of the nitroso group by base removal of α-hydrogen; similar to Mechanism a, and followed by a Cannizzaro reaction to form hydrogen and oxalate
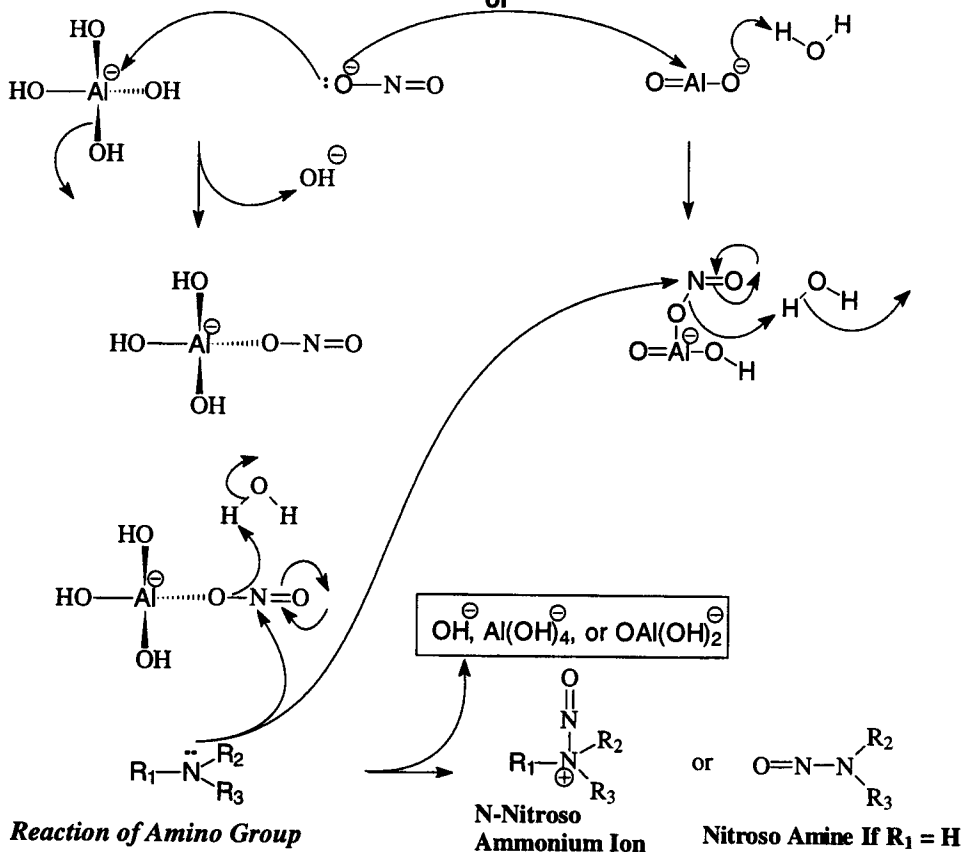
For β-hydroxy amine, the nitrosation of the hydroxy group will form nitrite ester, which is in equilibrium with the corresponding N-nitroso ammonium ion, as shown below:
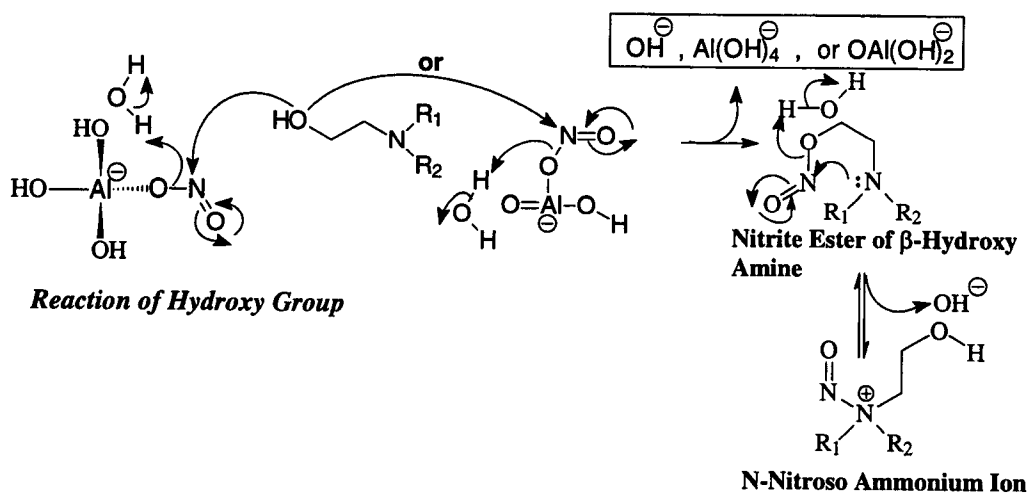
Figure 3-2. Nitrosation of amines and alcohols catalyzed by aluminate in the presence of nitrite

Mechanism a:

Elimination of Nitroso Group of N-Nitroso Amine by Base and Subsequent Hydroxylation of Imine Group
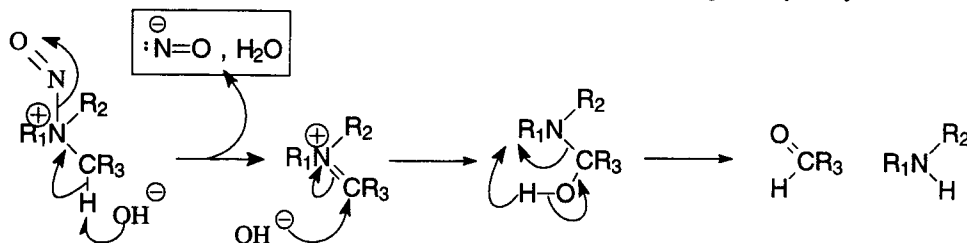
Mechanism b:

Elimination of Nitroso Group of Nitrite Ester and Subsequent Hydroxylation of Imine Group
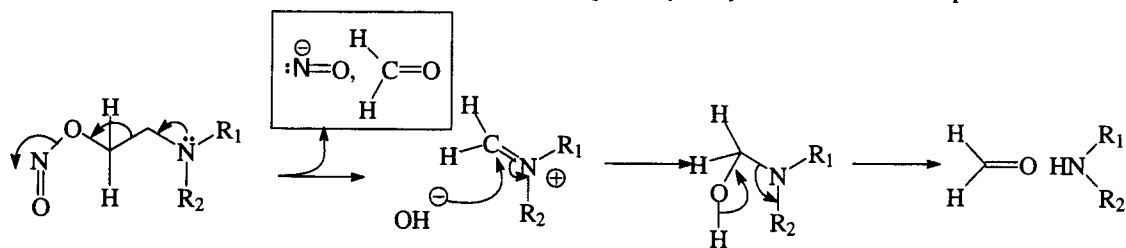
Mechanism c:

Decarboxylation of α-Carboxyl N-Nitroso Amine and Subsequent Hydroxylation of Imine Group
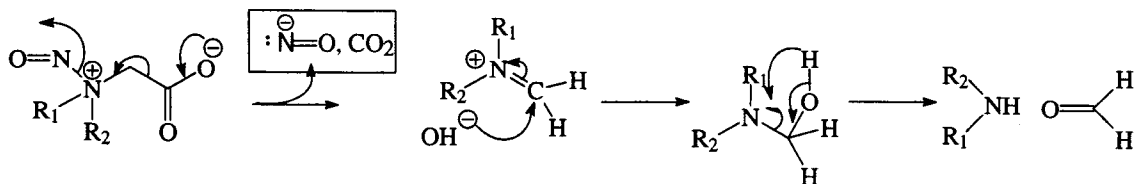
Mechanism d (Possible Reaction):

Hofmann Elimination of Quaternary Ammonium Hydroxide
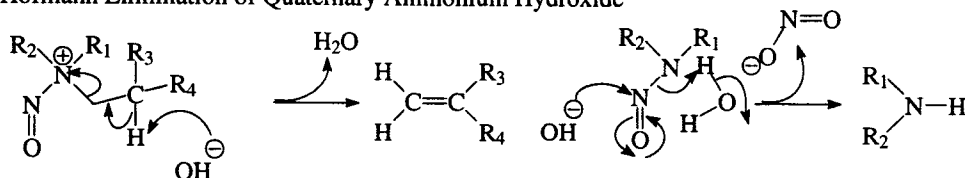
Mechanism e (Mixed Cannizzaro Reaction)
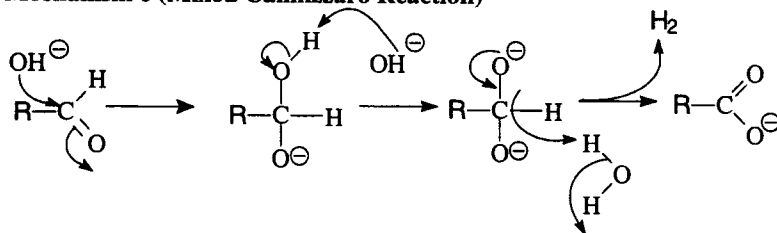
Figure 3-3. Decomposition of N-nitroso amine and nitrite ester of β-hydroxy amine

(a)

(b)

(c)

(d)
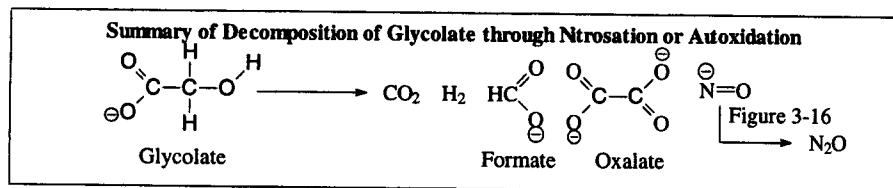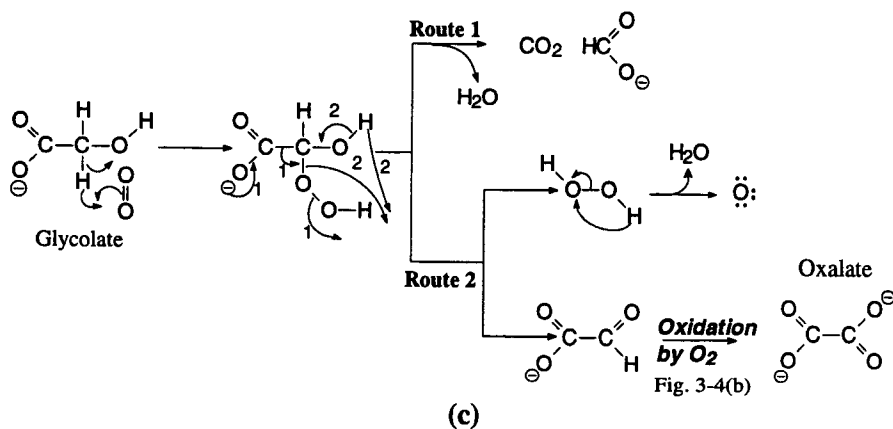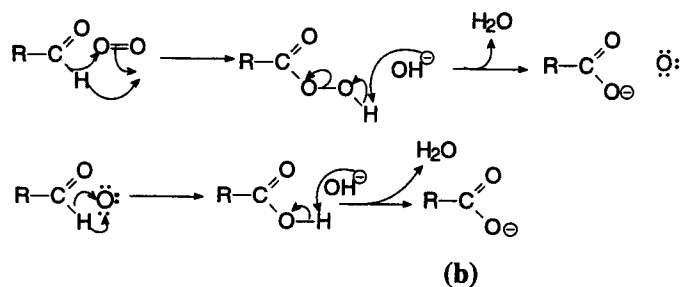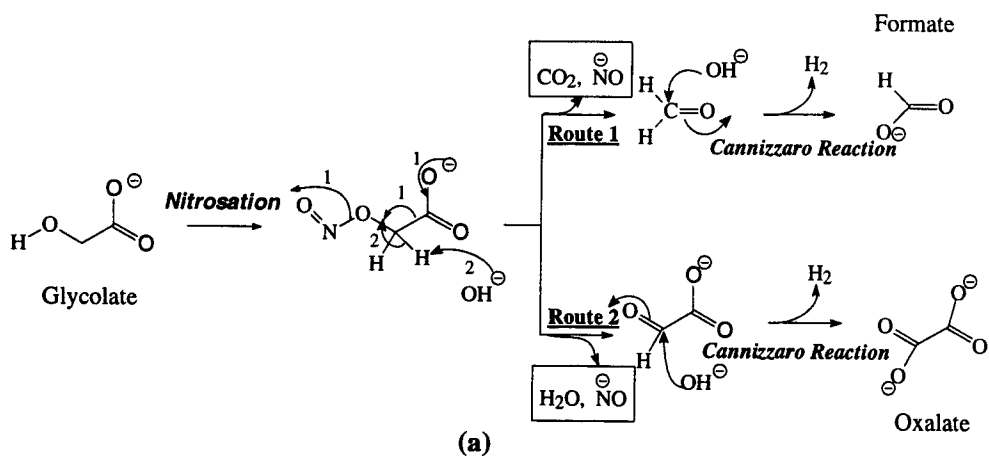
Figure 3-4. (a) Decomposition of glycolate through nitrosation; (b) oxidation of aldehydes by oxygen; (c) oxidation of glycolate by oxygen; and (d) summary of decomposition of glycolate

3-39

As shown in figure 3-4c, the autoxidation of glycolate, in the absence of sodium nitrite, forms the final products carbon dioxide and formate (Route 1, figure 3-4c) or oxalate (Route 2, figure 3-4c) through an intermediate of aldehyde, which is probably autoxidized by the mechanism shown in figure 3-4b.

In summary (figure 3-4d), the decomposition of glycolate forms carbon dioxide, hydrogen, formate, oxalate, and nitrous oxide. The carbon dioxide formed may dissolve in the basic aqueous wastes to form carbonate or partition into the headspace.

Decomposition of Citrate and Isocitrate

As shown in figure 3-5, the citrate is decomposed in the basic solution without either aluminate-catalyzed nitrosation or autoxidation, and without aldehydes as reaction intermediates. Therefore, no hydrogen or nitrous oxide is formed from citrate decomposition because of the absence of aldehydes, a source of hydrogen, and the absence of nitroso ion, a source of nitrous oxide formed in a subsequent reaction after nitrosation. Nitrous oxide formation will be described in the section on gas formation. Also note from figure 3-5 that no formate results from degradation of citrate.

In summary, decomposition of citrate forms oxalate and acetate, which are stable in simulated wastes under waste storage conditions. No further decomposition of these products occurs. Formate is also stable in simulated wastes under waste storage conditions.

The decomposition of the isomer of citrate – isocitrate – is also illustrated in figure 3-5. The isocitrate may have been present as an impurity in the citrate reagent used in Hanford processing, or may have formed from citrate after long storage in caustic conditions. As shown in figure 3-5 (Route 1), the isocitrate may either be decomposed directly to oxalate and succinate, or converted to citrate (Route 2), which is further decomposed to acetate and oxalate.

Decomposition of HEDTA and EDTA

The decomposition of HEDTA through nitrosation is shown in figures 3-6 to 3-10. One of the routes of nitrosation of HEDTA is shown in figure 3-6, in which HEDTA undergoes nitrosation to form the nitrite ester of HEDTA [labeled (1) in figure 3-6], which becomes ED3A after following Mechanism b in figure 3-3. The nitrosation of ED3A forms N-nitroso ED3A, which follows Mechanisms a (also a_1 and a_2), c, and d, to eventually form hydrogen, nitrous oxide, ammonia, carbon dioxide, formate, and oxalate.

The other routes of the nitrosation of HEDTA is the formation of N-nitroso HEDTA with the nitroso group attached to either nitrogen of HEDTA. The subsequent decomposition of N-nitroso HEDTA is similar to those in figures 3-6 to 3-10, with the identical final products as those from the nitrite ester of HEDTA.

The proposed autoxidation of HEDTA is shown in figure 3-11, in which oxygen insertion occurs into two types of α-C-H bonds next to either nitrogen or oxygen on a hydroxyethyl group in HEDTA. The hydroperoxides formed by these two types of autoxidation undergo decomposition and hydrolysis and yield carbon dioxide, formate, oxalate, ED3A, and EDTA. Without a hydroxyethyl group, both EDTA and ED3A undergo the proposed autoxidation and, following decomposition and hydrolysis through mechanisms f and g as shown in figure 3-12, to carbon dioxide, formate, oxalate, ammonia and hydroxide, as shown in figure 3-13.

The decomposition of EDTA through nitrosation is shown in figure 3-14, and its autoxidation is shown in figure 3-13.
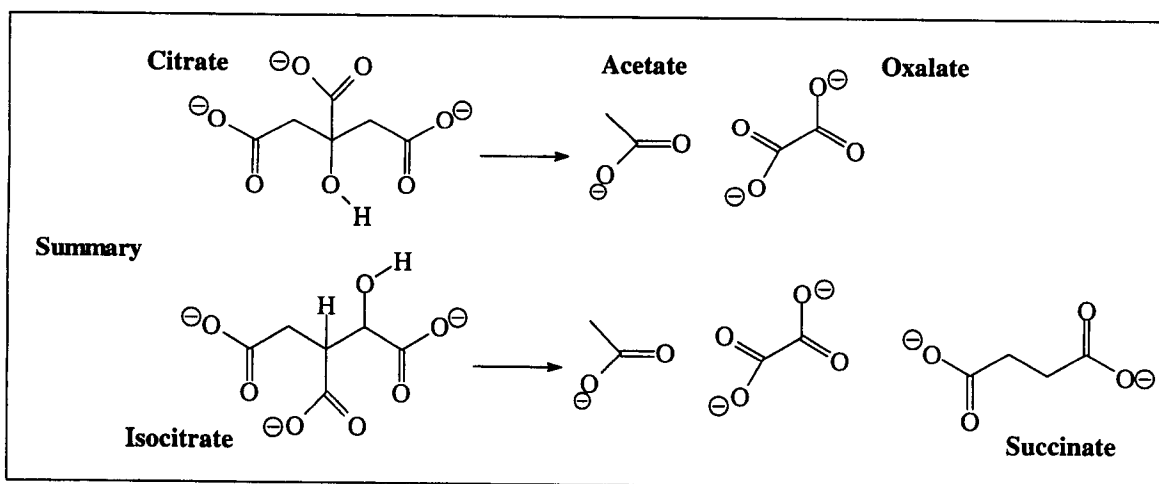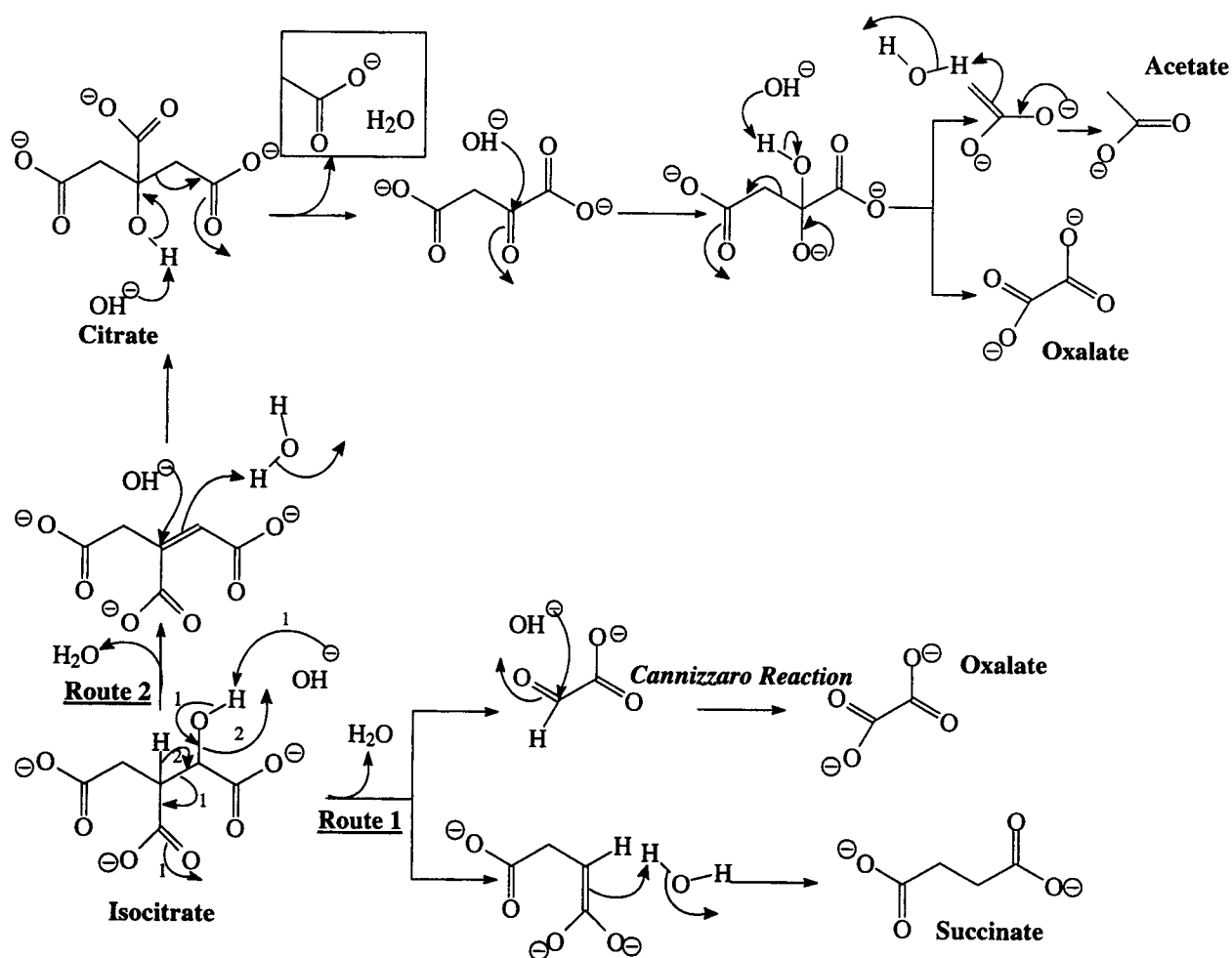
Figure 3-5. Decomposition of citrate and isocitrate

Figure 3-6. Decomposition of HEDTA through mechanisms a, b, c, and d
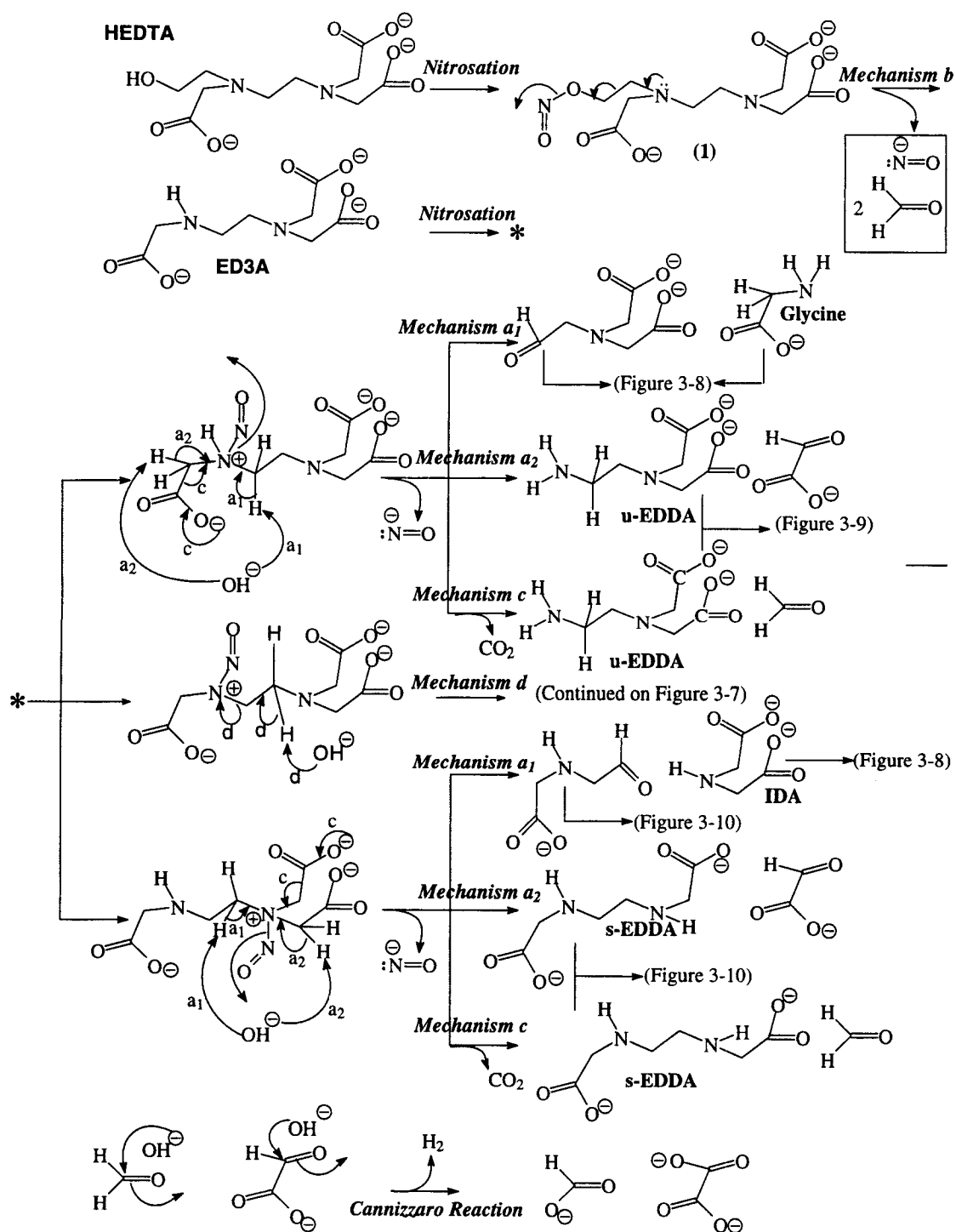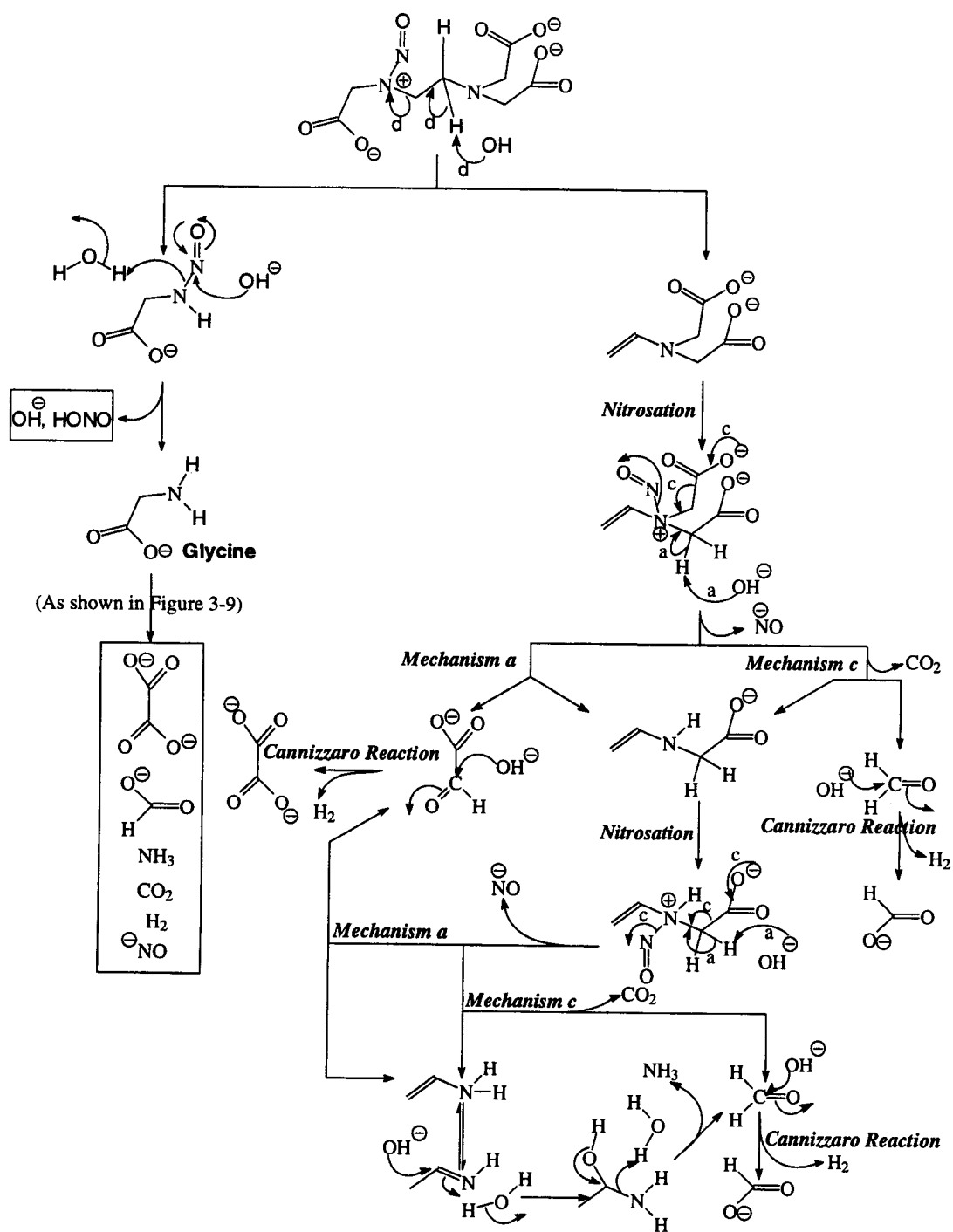
Figure 3-7. Decomposition of N-nitroso-ED3A by mechanism d
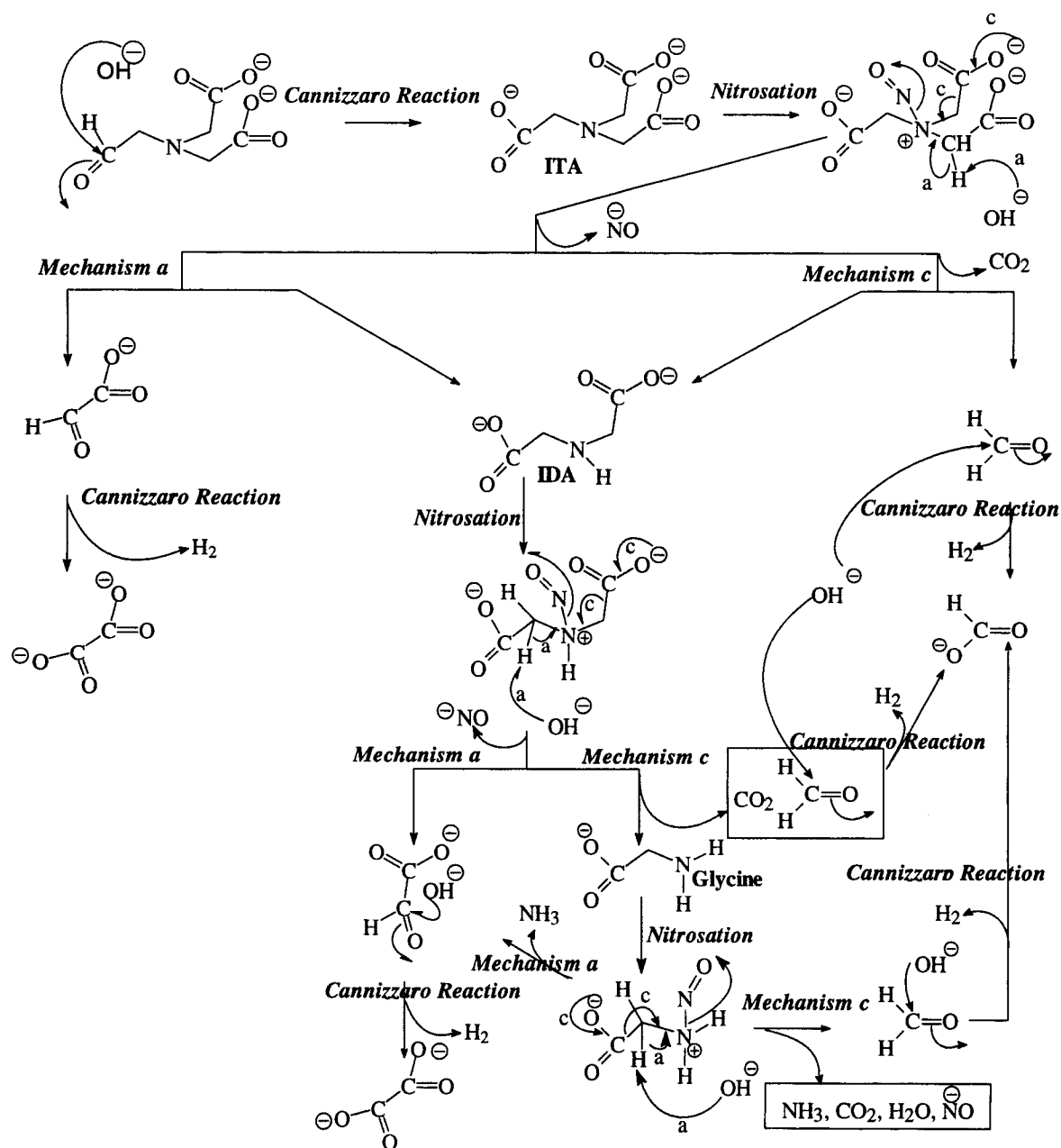
Figure 3-8. Decomposition of imito dialdehyde diacetate through ITA, IDA, and glycine

Figure 3-9. Decomposition of u-EDDA
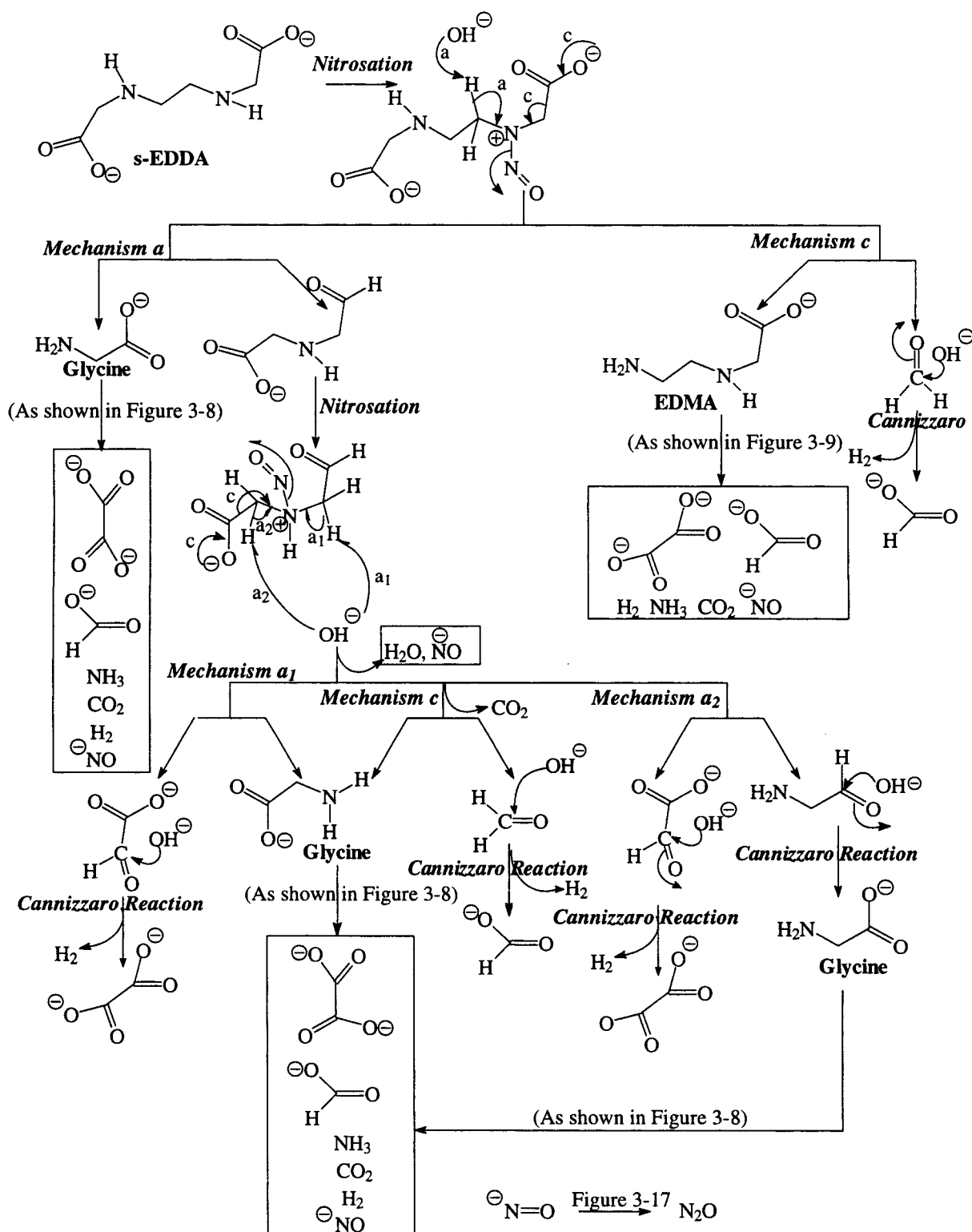
3-10. Decomposition of s-EDDA
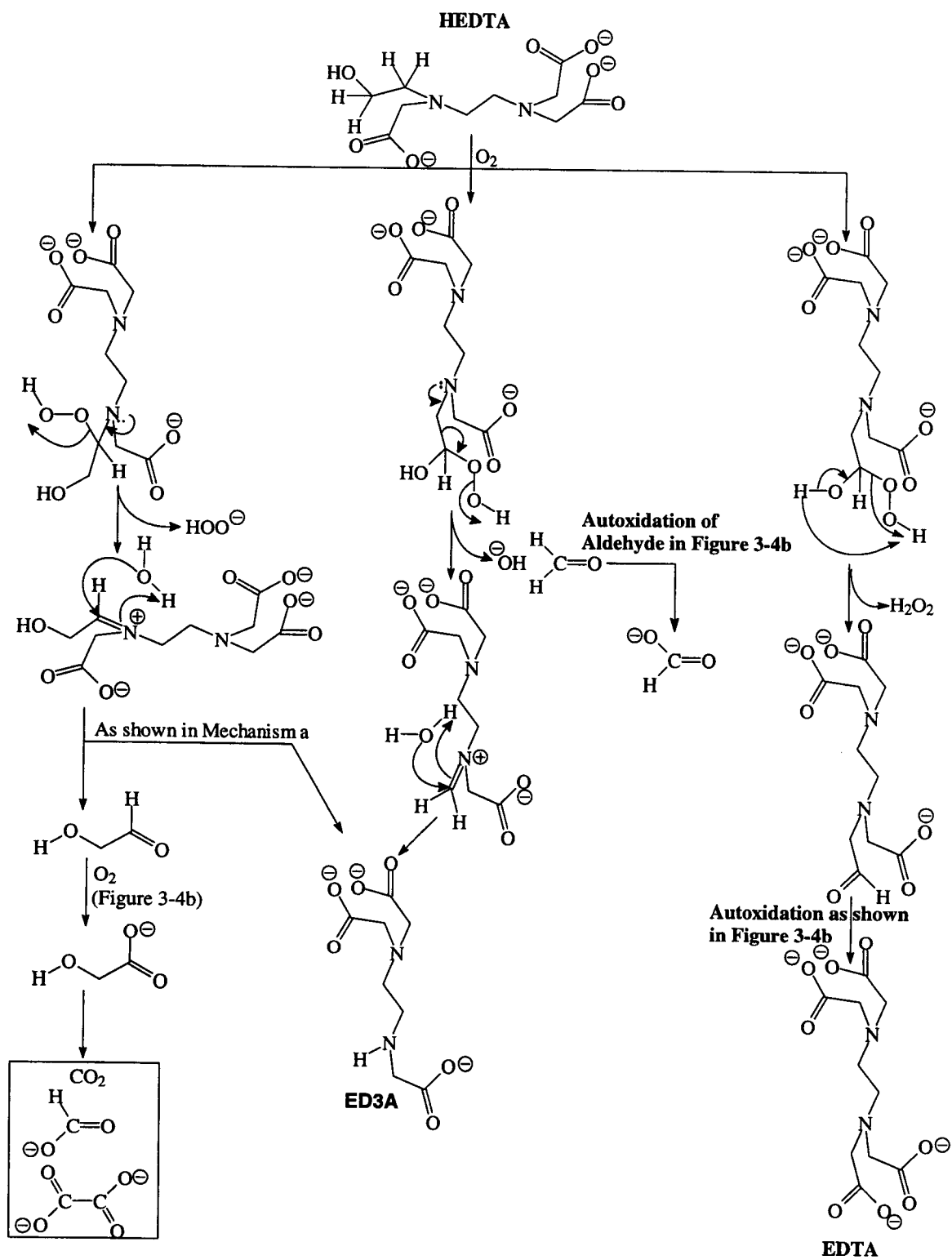
Figure 3-11. Autoxidation of HEDTA
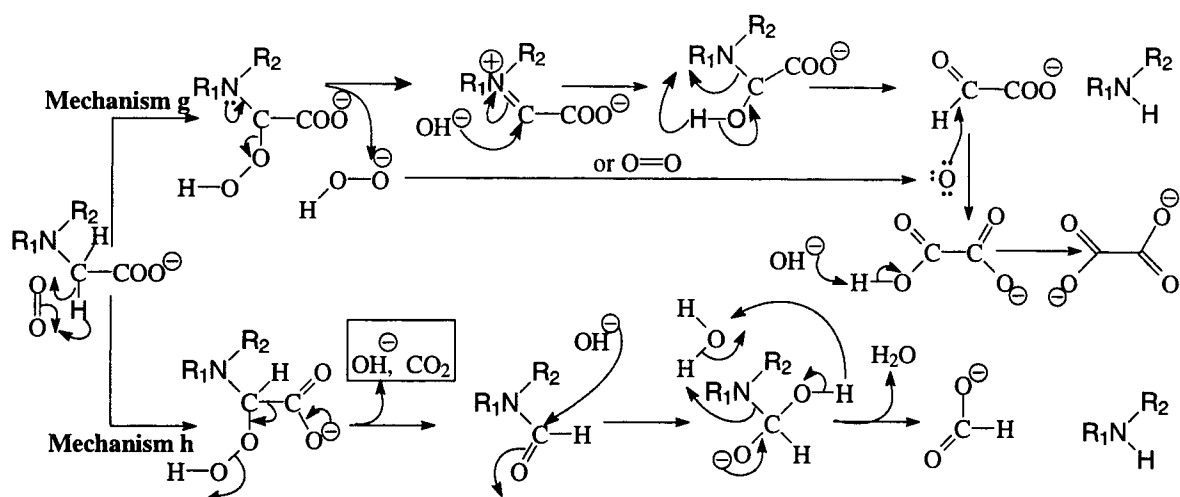
Figure 3-12. Autoxidation of amine
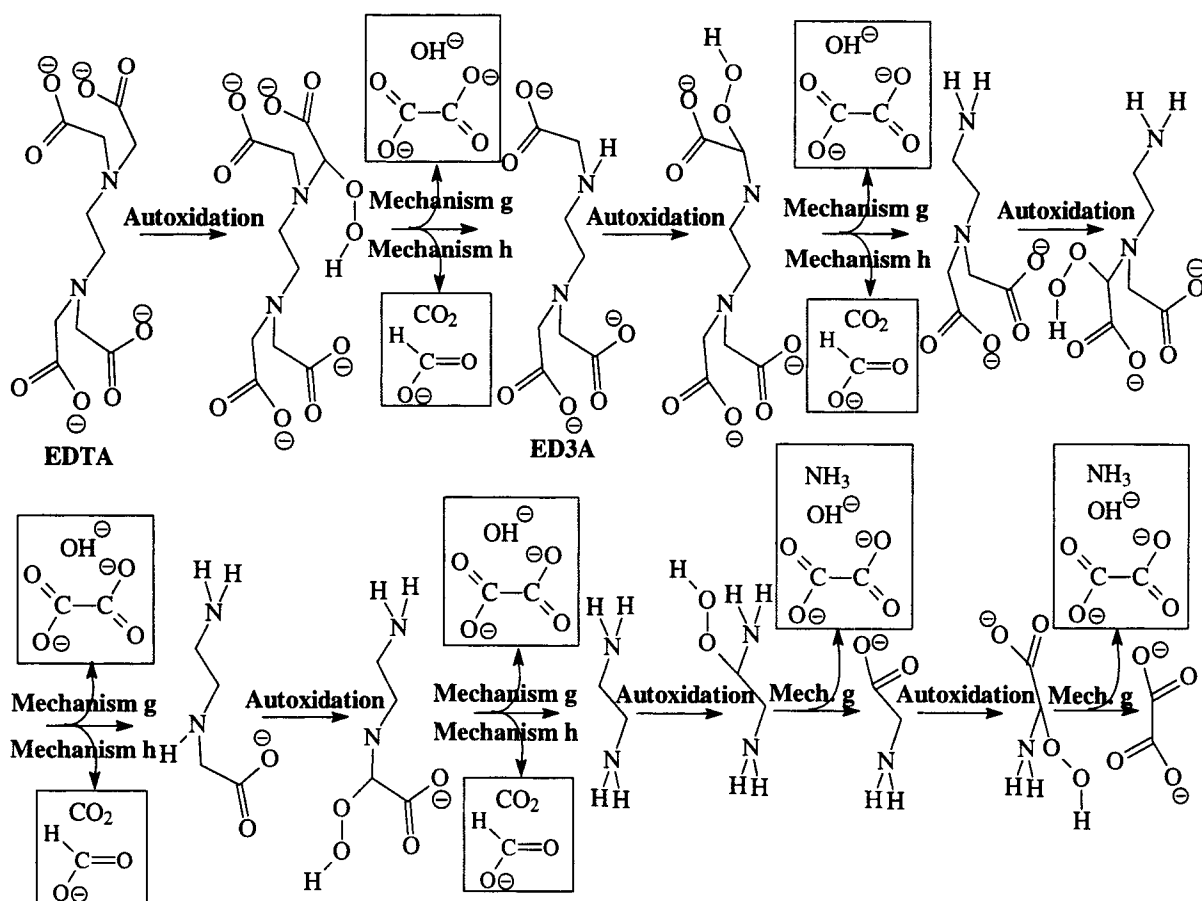
Figure 3-13. Autoxidation of EDTA

In summary, both HEDTA and EDTA decompose through the proposed mechanisms of nitrosation and autoxidation to yield as final products hydrogen, carbon dioxide, ammonia, formate, oxalate, peroxide, and hydroxide, as shown in figure 3-14.

3.6.1.3 Formation of Nitrous Oxide, Nitrogen, and Ammonia

Nitrous oxide and nitrogen are formed completely from nitrite ion in the waste, as the is majority of ammonia. As shown in figure 3-15, nitrous oxide can be formed from the dimerization of NO$^-$ and the subsequent hydrolysis of the dimer. Thermal decomposition of nitrous oxide will lead to nitrogen (figure 3-16).

The nitroso ion, NO$^-$, is one of the products from the decomposition of the nitrosated intermediates, as shown in Mechanisms a, b, and c in figure 3-3. The nitroso ion can also react with formaldehyde to form hydroxyamine, as shown in figure 3-17. The hydroxyamine reacts further either with formaldehyde to form hydrogen cyanide or cyanide, which then further hydrolyzes to form formate and ammonia (figure 3-17), or with itself (figure 3-16), eventually forming nitrogen.

The formation of cyanide or hydrogen cyanide in the waste may be important to evaluating the safety of waste processing.

3.6.2 Degradation of Phosphate Ester Extractants

In alkaline solution, phosphate esters are hydrolyzed to phosphates and alcohols. The following reaction shows the hydrolysis of TBP.

$$O=P-(OC_4H_9)_3 + OH^- \rightarrow (HO)(C_4H_9O)_2P=O + C_4H_9OH \qquad (3-5)$$
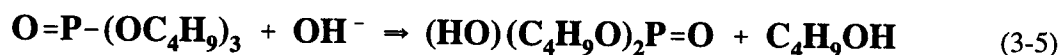
The radiolytic degradation of TBP produces the same initial products as the hydrolytic degradation. The DBP formed may be a stable product in alkaline medium since hydrolysis tends to stop after the first alkyl group is cleaved (Gerber, 1994). However, radiolytically induced decomposition of DBP can occur. The subsequent radiolytic degradation products of TBP include DBP, MBP, butanol, and phosphoric acid (H_3PO_4). Since TBP contains alkyl groups, radiolysis can also lead to the production of H_2, methane, and other low molecular weight hydrocarbons. Polymeric materials are also formed from the radiolysis of TBP.

DBBP has nearly the same degradation products as TBP. First, monobutyl butylphosphonate would form, which would then degrade radiolytically to H_2, methane, butane, butanol, and other low molecular weight organics. The major decomposition product of D2EHPA is the mono-(2-ethylhexyl) phosphoric acid ester (Gerber, 1994). Its radiolytic degradation products should be similar to TBP, presumably with ethylhexyl alcohol being formed.

Camaioni et al. (1994) provided a brief review of free radical reactions with alkyl phosphates such as TBP. Alkyl radicals readily add to the P=O bond to form phosphoranyl radical intermediates that subsequently cleave one of the O-R bonds and reform the P=O bond (Eq. 3-5). When R = H, this reaction explains the formation of DBP during the radiolytic decomposition of TBP. DBP and MBP probably follow the same radiolytic degradation path, which explains the decomposition of these hydrolytically stable phosphate esters.
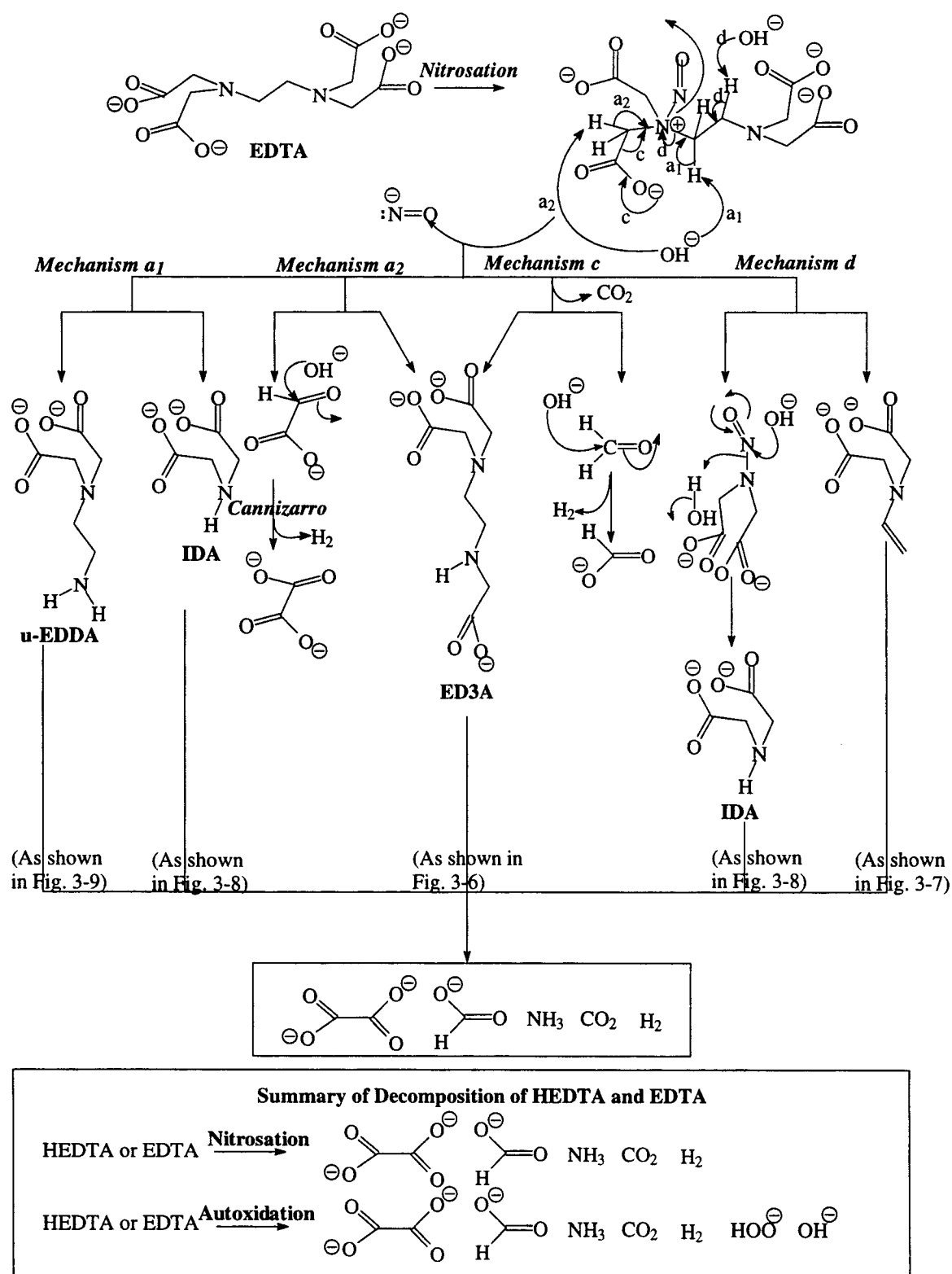
Figure 3-14. Decomposition of EDTA

$^{\ominus}$NO can be formed from any nitrosation reaction

Figure 3-15. Formation of nitrous oxide

Figure 3-16. Formation of nitrogen and ammonia
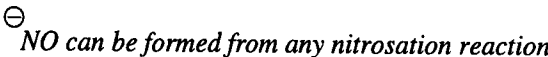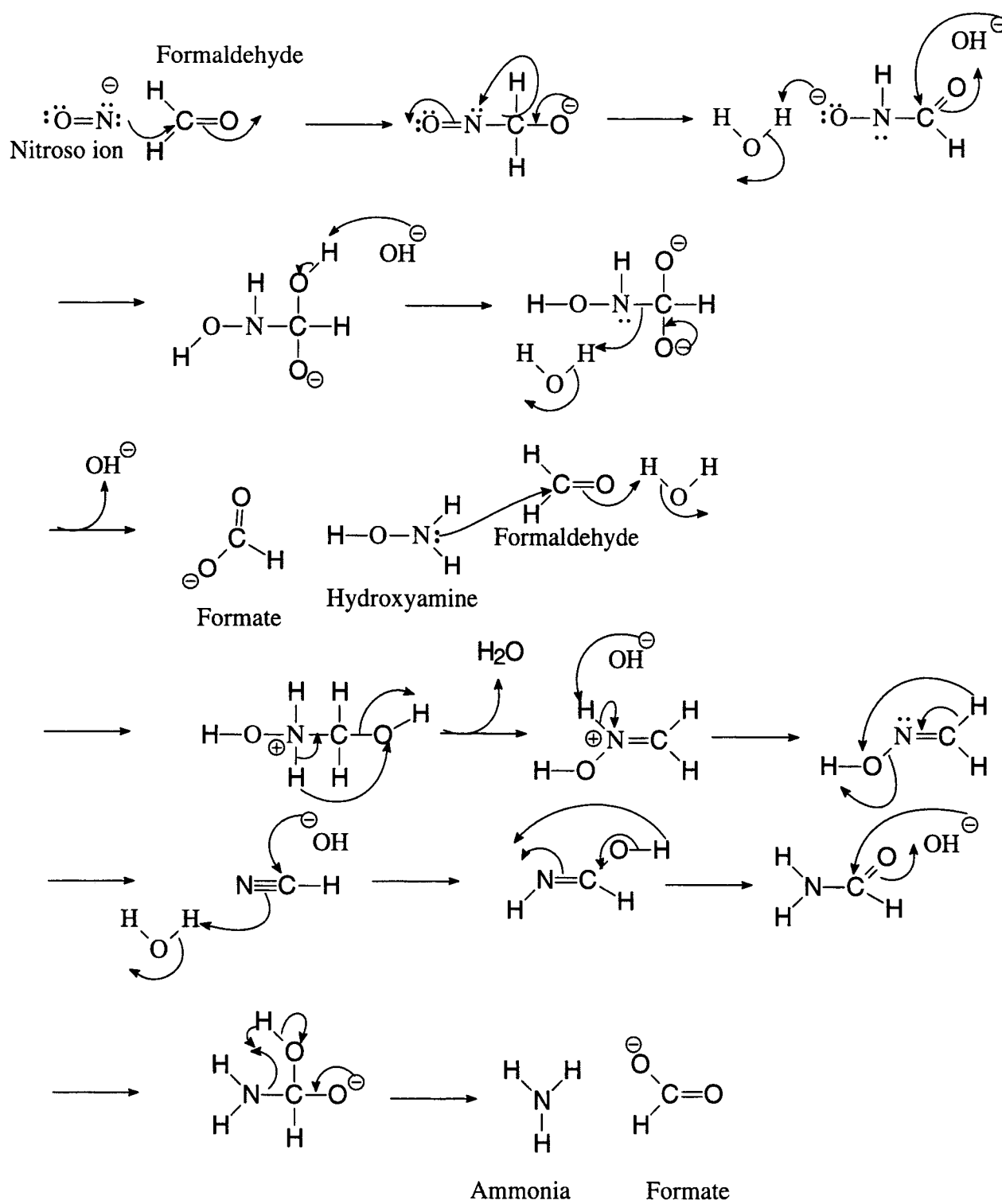
Figure 3-17. Formation of ammonia and formate

$$O = P(OC_4H_9)_3 + R \cdot \rightarrow ROP(OC_4H_9)_3 \cdot \rightarrow (RO)(C_4H_9O)_2P = O + C_4H_9 \cdot \quad (3\text{-}6)$$
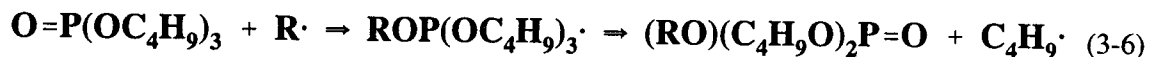
Another means of phosphate ester degradation is through oxidation reactions. TBP was added in significant quantities to the Hanford tank waste. However, since the TBP was in contact with the aqueous phase during storage, it is assumed to have completely hydrolyzed to DBP and butanol, which could slowly be oxidized by sodium nitrate and nitrite. Table 3-10 presents the theoretical energies that can be released by the oxidation of DBP and other TBP degradation products.

3.6.3 Degradation of Organic Solvents

The largest quantity of hydrocarbon solvents added to the Hanford waste tanks is probably the NPHs (n-dodecane and kerosene) used as diluents for TBP and D2EHPA. The chemical reactivity of these hydrocarbons in the highly alkaline aqueous environment should be relatively small. However, radiolysis may have rearranged many of the compounds. Oxidation of the radiolysis fragments produces alcohols and aldehydes, which would ultimately form more stable carboxylic acids and CO_2 (Gerber, 1994).

Hexone was used in large quantities in the REDOX process as both an extractant and solvent. Due to the volatility (BP = 115.9 °C) and reactivity of hexone, little should remain in the Hanford waste tanks (Burger, 1995). Hexone can degrade to isobutyric acid, isovaleric acid, acetic acid, and CO_2 under the harsh conditions that exist in the waste tanks.

3.7   SAFETY CATEGORIES FOR ORGANIC WATCH-LIST TANKS

Because intimate mixtures of organic complexants and oxidizing nitrate/nitrite may exist in some Hanford waste tanks, controls are in place to prevent propagating any exothermic reactions that may arise (Westinghouse Hanford Company, 1995b). The chemical reactivity of organic chemicals stored in Hanford waste tanks was classified into three safety categories: safe, conditionally safe, or unsafe (Turner et al., 1995), using numerical criteria derived from experimental data (Fisher, 1990; Babad and Turner, 1993). Tanks categorized as safe contain insufficient organic fuel and will not support a propagating reaction. Tanks categorized as conditionally safe contain organic waste that will not support a propagating reaction under current storage conditions, but may require periodic monitoring. Unsafe tanks have sufficient organic fuel levels that controls are necessary to avoid conditions that could lead to reaction ignition.

Data on fuel and moisture concentration are necessary to categorize an organic complexant tank as safe, conditionally safe, or unsafe. The waste must exceed a minimum fuel concentration to support a propagating reaction. This minimum fuel concentration, based on empirical data (Fisher, 1990), is 3 wt% TOC on a dry-weight basis, or an energy equivalent (based on sodium acetate) of 480 J/g. To judge if waste exceeds this minimum value, the TOC concentration or the exothermic energy (in J/g) must be determined experimentally (Turner et al., 1995). Direct persulfate oxidation is recommended to determine TOC (Turner et al., 1995), although other techniques that meet the desired analytical uncertainty are also acceptable. The TOC may also be determined by furnace oxidation to provide corroborative data on the fuel content of the waste.

In sufficient quantity, moisture can prevent a propagating reaction. Since water is a major component in all the HLW tanks at Hanford, analysis of water damping of organic reactions helps determine if the tanks are being operated under safe conditions. Test tube propagation tests using organic complexant waste

surrogates have shown that propagating reactions do not occur if the moisture exceeds 17 weight percent (Babad and Turner, 1993). Moisture content of tank wastes can be determined by TGA.

The current TOC threshold of 3 weight percent is based on the TOC fuel concentration for identifying organic tanks (Fisher, 1990) that has been incorporated into the Interim Safety Basis for Hanford storage tanks (Westinghouse Hanford Company, 1994b). However, recent experiments indicate that at least 4.5 wt % TOC (1,200 J/g energy equivalent as sodium acetate) is required to support a propagating reaction (Fauske et al., 1995b). The theoretical TOC envelope, including the effect of moisture, proposed by Fauske et al. (1995b) and currently under consideration by the DOE as the new safety criterion (Turner et al., 1995) is given by:

$$\text{wt \% TOC} > 4.5 \text{ wt \%} + 0.17 \times (\text{wt \% } H_2O) \tag{3-7}$$

Equation (3-6) is valid only to 20 wt % H_2O (Fauske et al., 1995b). For zero free-moisture content (wt % $H_2O = 0$), Eq. (3-6) predicts a lower bound value of 4.5 wt % TOC for sustained propagation. For comparison, the lowest measured TOC that resulted in sustained combustion of nonvolatile salt organic complexants, including Na_3HEDTA, is about 6 wt % TOC (Fauske et al., 1995b). Thus, the use of 4.5 wt % TOC represents a margin of safety of about 30 percent, which is well in excess of experimental measurement uncertainties (< 5 percent) (Fauske et al., 1995b). The theoretical heats of reaction for the volatile organic substances such as TBP and DBP, including their sodium and aluminum salts, are still higher than those of the nonvolatile organic complexants. However, none of those volatile organics exhibited propagating characteristics (Fauske et al., 1995b).

Consistent with the above TOC criterion, Fauske et al. (1995b) proposed and the DOE is considering the following lower bound theoretical chemical energy release (ΔH_{min}) envelope:

$$\Delta H_{min} \text{ (kJ/g)} > 1.2 + 4.5 x_w \tag{3-8}$$

where x_w is the moisture weight fraction.

It follows from Eq. (3-7) that exothermic reactions must exceed endothermic processes, such as water evaporation, by an amount at least equal to 1,200 J/g (~290 cal/g) in actual waste mixtures to indicate a potential for propagating reaction.

Finally, studies by Fauske et al. (1995b) show that the presence of about 20 wt % moisture is sufficient to eliminate the potential for sustained combustion altogether independent of fuel type and concentration. However, the potential of the tank waste to dry out and thus become *unsafe* will need to be evaluated based on the waste temperature, heat load, "tank breathing rate," and the chemical, physical, and rheological properties of the waste (Turner et al., 1995).

Although the numerical safety criteria discussed in this section were derived for safety assessment of waste storage in Hanford tanks, the same criteria may be useful for evaluating the safety of organic-bearing wastes during the retrieval and processing stages of the Hanford TWRS.

3.8 SUMMARY

The presence in Hanford wastes of various organic compounds mixed with oxidizing sodium nitrate and nitrite salts and heat-producing radionuclides is a major safety concern because a potential exists for rapid exothermic reactions that could result in radioactive release to the environment. Such a reaction resulted in a major explosion in a radioactive waste tank in Kyshtym, U.S.S.R. in 1957, and in an explosion and fire at the DOE Savannah River Plant in 1975. More recently, in 1997, an autocatalytic chemical reaction involving hydroxylamine nitrate and nitric acid resulted in an explosion at the Hanford Plutonium Reclamation Facility. The possibility of chemical reactions involving organic compounds is a safety concern at Hanford, not only during continued interim storage of tank wastes, but also during the retrieval, processing, and solidification stages of the TWRS operations. Evaluation of potentially hazardous reactions is needed such that necessary mitigating actions can be determined and implemented (e.g., using diluents, destroying the organics, controlling the rate and quantity of process feed, controlling process temperature).

To assess potential hazards, determination of energies that could be released during chemical reactions involving oxidizable organic compounds is necessary. Heat or energy releases for different reaction pathways and end-products can be estimated using thermodynamic calculations. Calculations discussed in this chapter show that maximum energy is released by organic reactions with nitrates and nitrites when the reaction products are N_2, Na_2CO_3, H_2O, and CO_2. The reaction is more energetic if $NaNO_2$ is the oxidant instead of $NaNO_3$. Production of N_2O in place of N_2, or of CO in place of CO_2, greatly lowers the energy released. In alkaline pH conditions typical of Hanford tank wastes, CO_2 produced from organic oxidation reactions form Na_2CO_3 and H_2O, resulting in more exothermic heat.

Thermodynamic calculations can be used to predict the adiabatic rise in temperature that could occur for various oxidation reactions in different waste mixtures, and to predict the effect of the concentration of both oxidants and diluents on the temperature rise. For example, estimates of heat generation and temperature rise for the HLW tanks A-101, SY-101, and SY-103 indicate that the energy given off by organic oxidation reactions could cause the temperature to rise to at least 100 °C and to vaporize the water in the waste. The resulting pressure build-up could damage the tank and release radionuclides to the environment. It should be emphasized, however, that the oxidation reactions considered in the calculations are limiting cases and are for the maximum energy pathways. With fast exothermic reactions, equilibria will probably not occur and several reaction paths may be taken simultaneously with less total energy being produced. Thus, the maximum energies are seldom fully realized.

Thermoanalytical techniques used in the chemical industry for chemical hazards evaluation have been employed in DOE studies to measure the thermal sensitivities and the thermochemical and thermokinetic properties of organic and oxidant mixtures relevant to Hanford organic-bearing wastes. These studies indicate that energetic, self-sustaining exothermic reactions can occur among the salts of acetate, citrate, formate, oxalate, EDTA, and HEDTA, and the oxidants nitrate and nitrite if heated to a sufficiently high temperature under adiabatic conditions. There are significant differences in the thermal reactivities and sensitivities of the organic compounds. The amount of heat produced is dependent on the nature of the organic, with minimal dependence on the organic concentration (per gram of organic salt). The heat produced by reaction of equimolar sodium nitrate and nitrite with the different organics increased in the order Na_3HEDTA > citrate > Na_4EDTA, which is not consistent with the thermodynamically predicted order Na_3HEDTA > Na_4EDTA > citrate. This inconsistency suggests that the actual reaction pathways differ from those postulated strictly from thermodynamic considerations. The observed production of N_2O instead of N_2, and the less-than-theoretical-maximum heats measured by calorimetric techniques also indicate that the exothermic reactions between the organics and oxidants proceed, at least partially, through pathways that

produce less than the maximum thermodynamically possible heat. Consequently, hazard assessments using the maximum thermodynamically based energetics will likely overestimate the consequences of a reaction. In addition, the measured activation energies indicate that there is a relatively high energy barrier to the initiation of these reactions. Thus, high temperatures are likely required to initiate the organic oxidation reactions.

The DOE measurements of onset temperatures indicate that the relative order with respect to thermal sensitivity is $Na_3HEDTA \geq$ citrate > formate $\geq Na_4EDTA$ > acetate > oxalate. This relative order indicates that acetate is generally a less conservative model for the organics used at Hanford with respect to susceptibility to hazardous chemical reactions. It also indicates that organic-bearing wastes containing Na_3HEDTA and citrate should be of greatest concern. In addition, the thermoanalytical studies show that the controlling oxidation reaction is that of nitrite with the organic compound. The exothermic onset temperature of mixtures containing only nitrite is similar to that of equimolar sodium nitrate/nitrite mixtures. Reaction mixtures that contain only nitrate have onset temperatures that are considerably higher and, hence, are more stable.

It should be noted that the DOE thermoanalytical studies used simple organic/oxidant mixtures, whereas Hanford tank waste chemistry is much more complex than the chemistries considered in the studies. Engineering analyses to assess the thermal hazards associated with the organic-bearing wastes need to consider the concentration of waste constituents other than the organics and oxidants. The greater reactivity exhibited by the simulated sludge waste compared to the other surrogate waste mixtures suggests that caution must be used in extrapolating the behavior of waste simulants to that of actual wastes with more complex compositions. It is possible that actual Hanford wastes may be more reactive due to the presence of thermally more sensitive organics, the presence of transition metal ions that could act as catalysts, or to synergistic interactions between the organics.

A concern regarding Hanford tank wastes is the possibility of organic concentrations and quantities being elevated to sufficiently high levels as to create a hazard that would not be anticipated if average tank values are used in the analysis. Two processes that could be important are organic concentration in the liquid phase and precipitation of organic compounds in the solid phase. Many of the organic compounds added to the Hanford waste tanks are quite insoluble in water and, depending on the quantity added to a specific tank, it is possible to form a separate organic phase in the tank. The hydrocarbon solvents are the most likely to have been added to the tanks in sufficient volume to create a separate organic layer, as evidenced by the observed presence of a separate organic layer in tank C-103 believed to be predominantly NPH and TBP. Precipitation of organic compounds from concentrated wastes can result in locally high concentrations of fuel and produce solids with organic-to-oxidant ratios significantly different from the waste tank average value. Organics could form solid mixtures with $NaNO_3$-$NaNO_2$ either by coprecipitation or by drainage of the bulk aqueous phase followed by evaporation of $NaNO_3$-$NaNO_2$-containing interstitial liquid in the already precipitated organics. The Hanford chemicals that could concentrate by this mechanism are the polar, water-soluble compounds that can form metal salts, including sucrose that was used for denitration and a large number of organic acids or their sodium salts, such as oxalic acid, glycolic acid, citric acid, tartaric acid, gluconic acid, EDTA and HEDTA, that were used for complexation or pH control.

A numerical criterion, based on measured organic fuel content (in terms of TOC) and moisture concentration, is currently used by the DOE to categorize an organic-bearing tank as safe, conditionally safe, or unsafe. For zero free-moisture content, a minimum of 4.5 wt % TOC is considered necessary for a sustained propagating reaction. Higher TOC is required for a propagating reaction to occur if water is present because it dampens organic reactions. DOE tests indicate that about 20 wt % moisture is sufficient to

3-56

eliminate the potential for sustained combustion altogether independent of fuel type and concentration. Although the criterion was derived for safety assessment of waste storage in Hanford tanks, the same criterion may be useful for evaluating the safety of organic-bearing wastes during the retrieval and processing stages of the Hanford TWRS. Also, the potential for the waste to dry out and thus become unsafe during continued storage or during TWRS processing will need to be evaluated.

An important consideration in safety analysis of organic-bearing Hanford wastes is the degradation of organic constituents. Because the wastes have been exposed to radiation, temperatures of 20 to 140 °C, and to a reactive chemical environment having high concentrations of active components, including hydroxide, nitrate and nitrite, as well as transition metals that could act as catalysts for decomposition reactions, various degradation or aging processes have occurred that changed the nature and quantity of the organics in the tank wastes. Degradation eventually leads to the formation of very simple compounds, such as formate, oxalate, or carbonate, resulting in a net reduction in the amount of energy available for reaction. Although the total amount of carbon in a tank, measured as TOC, would not change, the energy available for release during oxidation reactions with nitrates and nitrites would be reduced because the degradation products, such as oxalate and formate, have a low energy content per carbon atom. A decrease in fuel energy due to organic aging is indicated by the low exothermic values obtained from calorimetric measurements on actual waste samples and by studies on organic speciation in Hanford wastes. However, although organic degradation results in lower organic fuel value, concurrent production of flammable gas mixtures increases the potential for flammable gas hazard. Because the chemical environment of Hanford wastes is conducive to organic degradation reactions, flammable gas mixtures will likely remain a key safety issue throughout the TWRS operations.

4 CHEMISTRY RELEVANT TO FERROCYANIDE REACTIONS

4.1 INTRODUCTION

During the 1950s, additional tank storage space for HLW from defense operations was generated using precipitation processes for scavenging cesium and other soluble radionuclides from tank waste liquids. In the Cs-137 scavenging processes, waste solutions were adjusted to a pH between 8 and 10, and sodium or potassium ferrocyanide and nickel sulfate were added to coprecipitate cesium with the insoluble alkali-metal nickel ferrocyanide [$Na_2NiFe(CN)_6$ or $K_2NiFe(CN)_6$]. After allowing the radioactive precipitates to settle, the decontaminated solutions were pumped to disposal cribs, thereby providing additional tank storage volume. Later, when some tanks were found to be leaking, pumpable liquids were removed from these tanks, leaving behind a wet solid (sludge) residue containing the ferrocyanide precipitates (Burger et al., 1991).

In implementing the scavenging process, approximately 140 metric tons (154 tons) of ferrocyanide [calculated as $Fe(CN)_6^{4-}$] were added to waste that was later routed to 18 SSTs. Because the scavenging process precipitated ferrocyanide from solutions that had high nitrate and radiolytically produced nitrite concentrations, an intimate mixture of ferrocyanides and nitrates or nitrites is likely to exist in the ferrocyanide waste. The potential for an uncontrolled exothermic reaction involving ferrocyanides was a concern because, in the presence of oxidizing materials such as nitrates or nitrites, ferrocyanide can be made to explode if heated to high temperatures (approximately 250 °C) or if exposed to an electrical spark of sufficient energy (Cady, 1992).

This chapter provides information relevant to the chemistry of ferrocyanides historically used in processing nuclear wastes contained in the Hanford tanks and to potential chemical reactions involving these compounds. This information is useful in understanding the technical bases for safety concerns regarding ferrocyanides and may be useful in safety assessments of Hanford TWRS operations with respect to potential ferrocyanide chemical reactions. The safety criteria determined by the DOE for storage of ferrocyanide wastes are also provided. In addition, processes relevant to degradation of ferrocyanides are discussed because decrease of the ferrocyanide concentrations to levels considered below the safety criteria is the main technical basis used by the DOE in closing out the Ferrocyanide Safety Issue with respect to Hanford waste tanks. Although uncontrolled ferrocyanide-nitrate/nitrite reactions are believed by the DOE not to be credible during continued storage, residual exothermic activity might be initiated by processing options that cause waste to be heated by an external source (e.g., during vitrification or other accidental circumstance). Thus, the DOE will evaluate, on a case-by-case basis, the possibility and impact of a self-heating reaction as part of the safety analysis of proposed retrieval and processing methods (Postma and Dickinson, 1995).

4.2 DESCRIPTION OF THE FERROCYANIDE SCAVENGING OPERATIONS

4.2.1 The Bismuth Phosphate and Uranium Recovery Processes

The primary source of Hanford site tank wastes is the irradiation and processing of U fuel to extract Pu. The various Hanford reprocessing operations are discussed in Agnew (1995) and Cragnolino et al. (1997). The wastes treated with the cesium scavenging process resulted from the BP and UR processes. The BP process used in the B and T Plants was a Pu recovery/purification process that did not recover U from its waste streams. The extraction waste, called metal waste (MW), contained the U and

approximately 90 percent of the fission products. This waste was stored in underground waste tanks in the 200 Area. First decontamination cycle (1C) waste, which contained approximately 10 percent of the fission products, was also stored in 200 Area tanks separate from those containing MW. Sodium nitrate is a major component of the stored wastes, resulting from the addition of sodium hydroxide (NaOH) to the liquid waste to neutralize the nitric acid (HNO_3).

The U Plant was originally built as a third BP plant. However, it was never used as such and was instead converted to a solvent extraction UR plant. The alkaline MW solution was sluiced from the 200 area waste tanks, acidified, and transferred to the UR plant for processing and recovery of U. The UR plant waste was then neutralized with caustic and returned to the underground waste tanks.

Although the UR process efficiently removed U from the sluiced, acidified MW, the overall process generated almost 2 m^3 of waste to be stored for every 1 m^3 of stored MW processed. This excess waste necessitated the implementation of the ferrocyanide scavenging process to precipitate and remove the soluble, relatively long-lived fission product, Cs-137 (half-life 30.2 yr), from the UR and 1C wastes. Removal of the cesium thus permitted disposal of the supernate to cribs reducing the stored waste volume in the tanks.

4.2.2 Scavenging Process Description

The potential hazard posed by the ferrocyanide-bearing wastes can differ depending on the waste composition. The composition of the ferrocyanide sludges, as they were originally formed, varied as a function of the different processes that produced them. Three principal scavenging processes—the U Plant, the T Plant, and the In-Farm processes—were used in the decontamination of aqueous wastes (Borsheim and Simpson, 1991). In general, the aqueous waste was pumped to process tanks in which the pH was adjusted and precipitating agents were added. The slurry was then transferred to an underground storage tank for settling of the solids and disposal of the supernatant liquid to cribs.

The U Plant process was used to treat acid solvent extraction waste after the U had been removed from the BP MW using the TBP process. The U Plant scavenging process consisted of adding $Fe(CN)_6^{4-}$ ion [as $K_4Fe(CN)_6$ in initial batches, but subsequently as $Na_4Fe(CN)_6$] to the acid MW, adjusting the waste pH to 9 ± 1, and then adding an equimolar amount (0.005 M) of Ni^{2+} ion (as $NiSO_4$) to produce a $Cs_2NiFe(CN)_6$ precipitate and/or coprecipitate Cs-137 with other nickel ferrocyanides such as $Ni_2Fe(CN)_6$ and $Na_2NiFe(CN)_6$ (Scheele et al., 1991). The precipitated solids formed a sludge that constituted the ferrocyanide waste. The U Plant process is named as such because it was performed at the U Plant facility. Similarly, the T Plant process originally was used to treat 1C waste from the BP process at the T Plant facility. Approximately 66 and 8 percent (by mass) of the total ferrocyanide used at the Hanford site were used in the U Plant and T Plant processes, respectively.

The In-Farm process was used to treat unscavenged UR waste recovered from the 200 area underground tanks. The liquid wastes were treated in the CR Process Vault facility adjacent to the C Farm tanks in the 200-E Area. The In-Farm scavenging process treated the basic waste from recovery of uranium by adjusting the pH with HNO_3 and/or NaOH to pH 9.3 ± 0.7 and adding $Fe(CN)_6^{4-}$ and Ni^{2+} (generally to 0.005 M each). Calcium nitrate was also added if laboratory analysis of the feed tank indicated additional Sr-90 decontamination was necessary. Note that this procedure may have left much of the original, alkaline-insoluble solids [e.g., $Fe(OH)_3$] produced from neutralizing the UR waste in the original UR waste storage tanks. The In-Farm process consumed approximately 26 percent of the ferrocyanide used at Hanford.

The U and T Plants processes produced precipitates that contained relatively large percentages of inert diluents[1] and thus produced sludge that contained relatively low concentrations of ferrocyanide. Simulant sludges produced in laboratory studies using procedures analogous to the U and T Plant processes contained approximately 8.3 and 8.8 wt % sodium nickel ferrocyanide on a dry weight basis, respectively (Postma and Dickinson, 1995). On the other hand, the In-Farm process contained lower concentrations of inert diluents, and therefore resulted in sludge that contained relatively higher concentrations of ferrocyanide. Simulant sludge that was made using methods analogous to this process contained up to 25.8 wt % sodium nickel ferrocyanide (Postma and Dickinson, 1995). All the simulated sludges retained relatively high moisture contents (35 to 69 wt % water) after centrifuging in the laboratory for a time that corresponded to a gravity-time product of 30 yr (Postma et al., 1994).

A more detailed review of ferrocyanide waste production is presented by Postma et al. (1994) and by Jeppson and Wong (1993). Historical records were used to determine which tanks contained ferrocyanide waste and to estimate the original ferrocyanide inventories and concentrations (Borsheim and Simpson, 1991; Jeppson and Wong, 1993; Agnew, 1995). These estimates are summarized in table 4-1. It is important to note that each of the ferrocyanide sludge types settled in layers, and the layers contained a distribution of sodium nickel ferrocyanide. Therefore, a single ferrocyanide concentration is not presented for each process. The ferrocyanide sludge types are more accurately depicted as a range of concentrations as shown in table 4-1.

4.3 FERROCYANIDE CHEMISTRY AND REACTIONS

4.3.1 Metal Cyanide Complexes

Nearly all the d-transition metals form cyanide complexes in a wide range of metal-ligand ratios and in a variety of configurations including linear, triangular, square, octahedral, and dodecahedral geometries. The hexacyanoferrate(II) [$Fe(CN)_6^{4-}$] ion, commonly called ferrocyanide, is a very stable complex of ferrous and cyanide ions that is considered nontoxic because it does not dissociate in aqueous solutions. In contrast, the ferricyanide ion [$Fe(CN)_6^{3-}$], a complex of ferric ion and cyanide, is quite poisonous; for kinetic reasons, $Fe(CN)_6^{3-}$ dissociates and reacts rapidly, whereas $Fe(CN)_6^{4-}$ is not labile (Cotton and Wilkinson, 1980). Both complexes liberate HCN upon addition of acids (Kroschwitz, 1995). Ferrocyanide is probably the best known metal cyanide complex, having been studied for well over 200 yr (American Cyanamid Company, 1953). Several structures for ferrocyanide have been suggested over the years, but the octahedral configuration proposed by Werner (1907) and supported by Pauling (1939) has been accepted.

4.3.2 Ferrocyanide Solids and Possible Tank Precipitates

Basic chemical data on some ferrocyanide solids are presented in table 4-2. Alkali or alkaline earth salts of ferrocyanide are quite soluble in water except for barium ferrocyanide. Transition metal ferrocyanides are fairly insoluble, with reported solubilities in the order of 10^{-5} g-ion/L (Tananaev et al., 1956). The alkali and alkaline earth salts of ferrocyanide are yellow in color, but transition metal ferrocyanides typically have other characteristic colors. Many ferrocyanide solids have commercial

---

[1] Diluents likely to be present in the ferrocyanide waste tanks include water, excess sodium nitrate and nitrite, aluminates, and a mix of lesser components such as silicates, sulfates, phosphates, carbonates, and metal ions such as iron and bismuth (Scheele et al., 1991). These diluents may change the thermal conductivity of the tank waste, thus influencing the propagation of exothermic reactions, and also introduce additional heat capacity that will control the temperature rise during an adiabatic process (Scheele et al., 1991).

Table 4-1. Estimated original ferrocyanide concentrations and sludge heights for Hanford tanks that were on the ferrocyanide Watch-list (taken from Meacham et al., 1996)

Tank Number	Scavenging Process	Estimated Original Concentration of $Na_2NiFe(CN)_6$ (wt%, dry)	Original Sludge Height (meters)
BY-103	U Plant	6.0–8.3	2.1
BY-104	U Plant	4.0–8.3	2.6
BY-105	U Plant	4.0–8.3	1.1
BY-106	U Plant	5.2–8.3	2.3
BY-107	U Plant	5.0–8.3	1.6
BY-108	U Plant	5.0–8.3	2.1
BY-110	U Plant	5.7–8.3	2.3
BY-111	U Plant	6.3–8.3	0.3
BY-112	U Plant	3.5–8.3	0.2
C-108	In-Farm	10.4–22.6	0.9
C-109	In Farm	14.0–22.6	1.2
C-111	In-Farm	8.9–22.6	1.1
C-112	In-Farm	16.1–25.5	1.0
T-107	U Plant	6.3–8.3	2.1
TX-118	a	a	a
TY-101	T Plant	1.6–10.7	1.6
TY-103	T Plant	1.6–10.7	1.8
TY-104	T Plant	1.6–10.7	0.9

[a]Historical records show that no significant quantity of ferrocyanide sludge was stored in this tank (Borsheim and Simpson, 1991; Agnew, 1995). The tank was erroneously identified as a ferrocyanide tank because of a transcription error in the track radioactive components (TRAC) calculations (Jungfleisch, 1984).

applications, although the majority of industrial production of iron cyanide complexes is of iron blues, such as Prussian Blue, used as pigments (Kroschwitz, 1995). A large number of insoluble or slightly soluble mixed salts of the general formula $K_2M^{II}Fe(CN)_6$, where M^{II} is a transition metal ion (Ni^{2+}, Co^{2+}, Cu^{2+}, Mn^{2+}), are known (Kroschwitz, 1995). These salts have polymeric structures that contain bridging Fe-CN-M units.

Table 4-2. Basic chemical data on some ferrocyanide solids (Lide, 1991)

Name	Formula	Molecular Weight	Crystalline form, color	Density (g/ml)	Solubility, g per 100 ml (except as noted)	
					Cold Water	Hot Water
Sodium ferrocyanide	$Na_4Fe(CN)_6$ •$10H_2O$	484.07	monoclinic, pale yellow color	1.458	31.85 (at 20 °C)	156.5 (at 98 °C)
Potassium ferrocyanide	$K_4Fe(CN)_6$ •$3H_2O$	422.39	monoclinic, lemon yellow color	1.85	27.8 (at 12 °C)	90.6 (at 96 °C)
Ammonium ferrocyanide	$(NH_4)_4Fe(CN)_6$ •$3H_2O$	338.15	monoclinic, yellow color, turns blue in air		soluble	decomposes
Cesium ferrocyanide[a]	$Cs_4Fe(CN)_6$	743.58	yellow color		soluble	
Thallium ferrocyanide	$Tl_4Fe(CN)_6$ •$2H_2O$	1065.52	triclinic, yellow color	4.641	0.37 (at 15 °C)	3.93 (at 101 °C)
Magnesium ferrocyanide	$Mg_2Fe(CN)_6$ •$12H_2O$	476.75	pale yellow color		33	
Calcium ferrocyanide	$Ca_2Fe(CN)_6$ •11 or $12H_2O$	490.28 or 508.30	triclinic, yellow color	1.68	86.8 (at 25 °C)	115 (at 65 °C)
Strontium ferrocyanide	$Sr_2Fe(CN)_6$ •$15H_2O$	657.42	monoclinic, yellow color		50	100
Barium ferrocyanide	$Ba_2Fe(CN)_6$ •$6H_2O$	594.70	monoclinic, yellow color	2.666	0.17 (at 15 °C)	0.9 (at 100 °C)
Nickel ferrocyanide	$Ni_2Fe(CN)_6$ •xH_2O		greenish white color	1.982	insoluble; 2×10^{-5} g-ion Ni/L[b]	
Copper(II) ferrocyanide	$Cu_2Fe(CN)_6$ •xH_2O		red brown color		insoluble; 1×10^{-5} g-ion Cu/L[b]	
Iron(II) ferrocyanide	$Fe_2Fe(CN)_6$	323.65	amorphous, bluish white color	1.601	insoluble	
Lead ferrocyanide	$Pb_2Fe(CN)_6$ •$3H_2O$	680.40	yellowish white powder		insoluble; 3×10^{-5} g-ion Pb/L[b]	
Manganese(II) ferrocyanide	$Mn_2Fe(CN)_6$ •$7H_2O$	447.94	greenish white powder		insoluble; 4×10^{-5} g-ion Mn/L[b]	
Zinc ferrocyanide	$Zn_2Fe(CN)_6$	342.71	white powder	1.85	insoluble; 1.5×10^{-5} g-ion Zn/L[b]	
Cobalt ferrocyanide	$Co_2Fe(CN)_6$ •xH_2O		grayish green color		insoluble; 2.4×10^{-5} g-ion Co/L[b]	

[a] From American Cyanamid Company (1953).
[b] Values at 25 °C reported by Tananaev et al. (1956).

Mixed ferrocyanide salts containing alkali metal and transition metal cations often have nonstoichiometric compositions (Loos-Neskovic et al., 1984, 1989). Thus, the composition of ferrocyanide precipitates depends on the relative concentrations of reagents added, the order in which the reagents were added, the solubilities of endmember ferrocyanide components, and probably also on the solution pH and temperature. In the case of alkali metal nickel ferrocyanides, phases that are likely to be in Hanford ferrocyanide wastes, solubility decreases with increasing alkali atomic number. Because no information on the solubility of sodium nickel salts was found in the literature (Scheele et al., 1991), experiments were conducted by the DOE to measure the solubility of sodium nickel ferrocyanide.

The major ferrocyanide precipitates in Hanford ferrocyanide wastes have not been identified. However, considering that the tank wastes to which nickel and ferrocyanide ions were added during cesium scavenging operations had 3 to 6 M sodium nitrate/nitrite concentrations, the precipitates that originally formed in the waste treatment process have been inferred by Scheele et al. (1991) to be mainly $Na_2NiFe(CN)_6$, $Ni_2Fe(CN)_6$, small amounts of $K_2NiFe(CN)_6$ and $Cs_2NiFe(CN)_6$, and large amounts of a mixed salt, $Na_xNi_y[Fe(CN)_6]_z$, where $4z = x + 2y$. Attempts made at the PNL to prepare various ferrocyanide forms resulted in sodium nickel ferrocyanide as the predominant phase (Scheele et al., 1991). The precipitates that formed in these tests were very fine grained, and washing with water tended to produce colloids.

4.3.3 Reactions Involving Ferrocyanides

Pyrolysis of the sodium and potassium ferrocyanide salts in air at 400 °C or slightly higher temperatures results in a mixture of products including the cyanate salt, nitrogen, carbon, and, at much higher temperatures, some free alkali metal. Pyrolysis in an oxygen atmosphere yields similar products and sodium carbonate (American Cyanamid Company, 1953). Experiments at PNL using DSC and scanning thermogravimetric analyses suggest that complete oxidation to nitrogen and CO_2 or carbonates may occur at about 500 °C, although the products have not been confirmed (Scheele et al., 1991).

Prior to the DOE studies, data on thermal decomposition of alkali metal nickel ferrocyanides were not available. However, Wirta and Koski (1957) found the thermal decomposition of cesium zinc ferrocyanide to be exothermic, and Hepworth et al. (1957) observed decomposition of the cesium zinc compound beginning at 480 °C. DSC tests performed at PNL on cesium nickel ferrocyanide indicate a reaction starting at about 230 to 260 °C, with a maximum in the exotherm at about 305 to 330 °C (Burger and Scheele, 1990). Preliminary data for the sodium nickel ferrocyanides and ferricyanides suggest that the oxidation reaction may start at a temperature below 200 °C.

Cyanides are relatively strong reductants, and some literature information indicates that ferrocyanides react explosively with nitrates, nitrites, chromates, and other strong oxidants. For example, Hepworth et al. (1957) reported that cesium zinc ferrocyanide can be explosive when samples that were wet with nitrate solutions were allowed to dry. Other studies indicate that the explosion threshold temperature of the material in contact with sodium nitrate is 375 °C (Cooper, 1957). The latter study showed that if solid nitrates were heated in the presence of dry ferrocyanide compound, explosions accompanied by dense white fumes occurred. The explosive reaction of molten sodium nitrate and sodium cyanide was noted by Sax (1957) and by the National Board of Fire Underwriters (1950). In addition, there is an Austrian explosives patent that is based on mixtures of nitrites and cyanides or ferrocyanides (Eiter et al., 1954).

The DOE conducted tests on ferrocyanide wastes to evaluate their explosive hazard (Cady, 1992). Results of these studies showed that the ferrocyanide mixtures were not ignited by standard impact and friction sensitivity tests. An external heat source was required in the tests before any exothermic reaction could be observed. Thermal tests indicated significant exothermic reactions were initiated after melting endotherms[2] that were evident above approximately 220 °C. Major exotherms were evident at temperatures above approximately 260 °C, suggesting the possibility of explosive reactions if mixtures of ferrocyanide

---

[2] In differential thermal analysis, a graph of the temperature difference between a sample compound and a thermally inert reference compound (commonly aluminum oxide) as the substances are simultaneously heated to elevated temperatures at a predetermined rate and the sample undergoes endothermal processes, is referred to as an endotherm (Parker, 1994). The graphical plotting of heat rise and fall versus time for an endothermic reaction or process is the exotherm.

and nitrate/nitrite are heated to high temperatures or if there is an electrical spark of sufficient energy to ignite a dry mixture.

Small-scale explosive testing at PNL, involving a time-to-explosion technique similar to the standard test Henkin and McGill (1952) used to evaluate explosives, confirmed that explosive reactions do occur under certain conditions. Some conclusions derived from the tests are as follows (Scheele et al., 1991):

- Sodium nickel ferrocyanides and ferricyanides or ferrocyanides with a high nickel content were more reactive than cesium nickel ferrocyanide.

- Reactions involving nitrites were more vigorous than those with nitrates.

- Maximum explosive behavior was probably exhibited by near-stoichiometric mixtures of ferrocyanide and nitrate/nitrite, but large excesses of either the ferrocyanide or the oxidant may still produce explosions.

- The explosive tests were not always reproducible with respect to either time or temperature. This nonreproducibility is characteristic of explosive reactions.

- Samples of dried, settled solids prepared using the In-Farm process produced explosions when heated (no added nitrate or nitrite). A sample of dried, settled precipitate prepared using the U Plant process (using dilute ferrocyanide, 0.0025 M) did not explode.

- The violence of the observed reactions leaves no doubt that an explosion will result if a mix of ferrocyanides and nitrate or nitrite salts is rapidly heated. However, it is possible that slow heating may produce slower and less exothermic reactions.

The enthalpies of reaction for oxidation of ferrocyanide compounds were estimated by Scheele et al. (1991) from the enthalpies of formation of the reactants and products. Because no data were found for the nickel ferrocyanides, these authors assumed ΔH_f values for di-nickel ferrocyanide and sodium nickel ferrocyanide equal to 200 and 0 kJ/mol, respectively, based on known enthalpies and free energies of formation for other cyanide compounds (e.g., Wagman et al., 1982; Barin, 1989). These assumed values of ΔH_f are uncertain to at least $\pm$ 200 kJ/mol. Scheele et al. (1991) considered several combinations of reactants and products in their analysis. Basically, 6 moles of nitrate or 10 moles of nitrite are required for the complete oxidation of 1 mole of ferrocyanide to N_2 and CO_2. The products of the reaction with either nitrate or nitrite salts may include N_2, CO_2, CO, NO, Na_2O, NaOH, Na_2CO_3, NiO, FeO, and traces of carbon and other compounds. Some water is assumed to be present when NaOH is formed. The heats of reaction for the different reactions are shown in table 4-3. The results indicate that the energetics of the postulated reaction is highly sensitive to the products formed. The reaction energy is greatly reduced if a sizable fraction of the carbon goes to CO due to incomplete oxidation, or if appreciable oxides of nitrogen form. On the other hand, a change in the reacting ferrocyanide or cyanide salt results in a much smaller change in energy released.

The sensitivity of calculated reaction energies to the combination of reactants and products assumed in the calculations suggests it would be difficult to estimate the energetics of chemical reactions that could occur in actual ferrocyanide wastes. However, analyses of solid and gas reaction products from experiments using ferrocyanide simulants could help identify the reaction stoichiometry. For example, Jeppson and Simpson (1994) analyzed gases produced from reacting an In-Farm simulant mixture of ferrocyanide and nitrate/nitrite at an initial temperature of 61 °C. The solid reaction products were also

4-7

Table 4-3. Calculated heats of reaction for oxidation of some cyanides and ferrocyanides (from Scheele et al., 1991)

Compound	Oxidant	Products*	ΔH_R, kJ/mole
$Na_2NiFe(CN)_6$	$NaNO_3$	Na_2CO_3, CO_2, N_2	$-3,012$
$Na_2NiFe(CN)_6$	$NaNO_3$	Na_2O, CO_2, N_2	$-1,722$
$Na_2NiFe(CN)_6$	$NaNO_3$	Na_2O, CO, N_2	-240
$Na_2NiFe(CN)_6$	$NaNO_3$	Na_2CO_3, Na_2O, NO	$+230$
$Na_2NiFe(CN)_6$	$NaNO_2$	Na_2CO_3, N_2	$-3,708$
$Na_2NiFe(CN)_6$	$NaNO_2$	Na_2CO_3, CO_2, N_2	$-3,480$
$Ni_2Fe(CN)_6$	$NaNO_3$	Na_2CO_3, CO_2, N_2	$-2,880$
$NaCN$	$NaNO_3$	Na_2CO_3, N_2	$-3,450$
*Other products are FeO and NiO			

determined by x-ray diffraction methods as well as by inductively coupled plasma emission spectrometry and x-ray fluorescence. Based on the reaction products, Jeppson and Simpson (1994) approximated the overall chemical reaction as

$$Na_2NiFe(CN)_6 + 6NaNO_3 + 2NaNO_2 \rightarrow 0.7NaFeO_2 + 3.8Na_2CO_3 + Na_2O + 0.3Ni_3Fe + 2.2CO_2 + 2.6NO + 5.6N_2 \qquad (4\text{-}1)$$
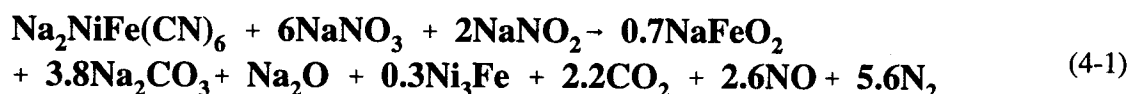
Jeppson and Simpson (1994) also determined the overall heat of the ferrocyanide-nitrate/nitrite reaction in ferrocyanide simulants at temperatures up to 620 °C by measuring waste temperature increases and using appropriate heat capacity values for the reaction constituents. A value of $-1,900$ kJ/mol (-6.0 MJ/kg) of $Na_2NiFe(CN)_6$ for the overall heat of reaction was measured using a U Plant simulant, whereas a value of $-1,930$ kJ/mol (-6.1 MJ/kg) of $Na_2NiFe(CN)_6$ was measured from a test using an In-Farm simulant. These measured net energies released are consistent with theoretical exothermic values reported by Burger (1993). For reactions giving N_2 and CO_2 as gas reaction products, Burger (1993) calculated values of $-3,600$ and $-3,700$ kJ/mol (-9.5 and -11.7 MJ/kg) of $Na_2NiFe(CN)_6$ for reactions involving nitrate and nitrite, respectively. On the other hand, Burger (1991) reported an endothermic value of $+630$ kJ/mol ($+2.0$ MJ/kg) of $Na_2NiFe(CN)_6$ when NO is produced along with N_2 and CO_2 from ferrocyanide reactions with nitrate.

4.3.4 Accident Scenario

The postulated accident of concern associated with ferrocyanide wastes is the occurrence of a sustainable, rapid exothermic ferrocyanide-nitrate (or nitrite) reaction in the stored waste (Meacham et al., 1996). A sustainable reaction is one that can spread beyond a local ignition source. A rapid reaction is one that generates heat faster than it can be removed; it excludes the slow degradation reactions that occur over a period of years. Such a sustainable, rapid exothermic reaction could produce sufficient heat and evolved

gases to pressurize the tank headspace, releasing aerosolized waste from tank vents and potentially damaging the tank structure. Similar reactions that may occur during retrieval and processing of tank wastes could damage transfer pipes and equipment and release radionuclides to the environment.

For a propagating reaction accident to occur, several conditions would be necessary:

- Tank waste would need a ferrocyanide (fuel) concentration sufficient to support a sustainable rapid exothermic reaction (propagating reaction).

- Sufficient oxidizer would need to be well mixed and in contact with the fuel.

- The water (moisture) content of the sludge would need to be sufficiently low (the sludge must be relatively dry) to prevent quenching of initiated reactions by wet material.

- The reaction would need to be initiated by heating a portion of the waste to the reaction ignition temperature.

If the previous conditions are met or exceeded, a reaction could propagate through additional reactive sludge until materials not meeting these conditions are encountered (Meacham et al., 1996).

4.4   FERROCYANIDE SAFETY CRITERIA

The range of compositions of ferrocyanide sludge capable of sustaining a propagating chemical reaction has been established by experimental measurements supported by theoretical considerations. The derivation is described in Postma et al. (1994) and provides the bases used to determine safe storage criteria. The same criteria could be used in safety evaluation of waste retrieval and processing methods.

4.4.1   Theoretical Analysis

The theoretical approach used to identify waste compositions that could or could not support a propagating reaction is based on an enthalpy balance. A necessary condition for propagation is that the reaction generate enough energy to heat adjacent unreacted fuel to its ignition temperature. The condition is satisfied when the potential reaction enthalpy is greater than the endothermic capacity of the waste from ambient temperature to a reaction threshold temperature [Eq. (4-2)].

$$\Delta H_M + \Delta H_R < 0 \tag{4-2}$$

where

ΔH_M —   change in enthalpy of waste upon heating from initial temperature to reaction onset temperature (positive term)

ΔH_R —   enthalpy of reaction (negative term).

As discussed in section 4.3.3, the oxidation of ferrocyanide by nitrate and/or nitrite can result in a variety of reaction products with different reaction enthalpies. The most energetic, for a given amount of fuel, is one that produces nitrogen and carbon dioxide (or carbonate salt if there is sufficient hydroxide available to form it). A representative equation with nitrate is

4-9

$$\text{Na}_2\text{NiFe(CN)}_6 + 6\text{NaNO}_3 \rightarrow \text{FeO} + \text{NiO} + 4\text{Na}_2\text{CO}_3 + 6\text{N}_2 + 2\text{CO}_2 \qquad (4\text{-}3)$$

The calculated ΔH_R value for this exothermic reaction is approximately -3,014 kJ/mol (-9.52 MJ/kg) of $\text{Na}_2\text{NiFe(CN)}_6$ at 25 °C.

DOE studies indicate that oxides of nitrogen are formed in slow, low-temperature reactions between ferrocyanide and nitrate/nitrite mixtures. Calculated ΔH_R values are lower for reactions that produce nitrogen oxides. The theoretical enthalpy available from the reactions decreases to -2,100 kJ/mol (-6.6 MJ/kg) when N_2O is the product. If NO is produced, the reaction is endothermic with a calculated ΔH_R of 230 kJ/mol (0.73 MJ/kg) of $\text{Na}_2\text{NiFe(CN)}_6$.

To determine the ferrocyanide safety criteria, Meacham et al. (1996) assigned to the reaction enthalpy a value of -1,900 kJ/mol (-6 MJ/kg) of $\text{Na}_2\text{NiFe(CN)}_6$ based on three independent experimental determinations on waste simulants (Postma et al., 1994). This value corresponds to 63 percent of the theoretical value for Eq. (4-3) and 90 percent of the calculated enthalpy with N_2O as the product gas. The threshold temperature for waste simulants has been measured to be in the range of 220 to 270 °C (Cady, 1992), and was selected as 250 °C by Meacham et al. (1996).

Postma et al. (1994) determined the minimum theoretical fuel concentration necessary to sustain a propagating reaction based on enthalpy balance calculations and assuming a ΔH_R of -1,900 kJ/mol (-6 MJ/kg) of $\text{Na}_2\text{NiFe(CN)}_6$, an initial waste temperature of 30 °C, and a reaction threshold temperature of 250 °C. For waste with 0 wt % free water, the minimum fuel concentration is about 8 wt % sodium nickel ferrocyanide. In terms of safe storage, the fuel criterion is therefore

$$\text{Na}_2\text{NiFe(CN)}_6 \text{ Concentration} \le 8 \text{ wt \%} \qquad (4\text{-}4)$$

As shown in table 4-1, some portion of the ferrocyanide waste in most of the Hanford tanks on the ferrocyanide Watch-list probably exceeded the 8 wt % $\text{Na}_2\text{NiFe(CN)}_6$ fuel criterion when it was originally established. However, as discussed in section 4.5, ferrocyanide decomposition has resulted in current ferrocyanide concentrations substantially less than the estimated original concentrations.

For waste with greater than 8 wt % sodium nickel ferrocyanide, the mass of free water required to quench reactions increases linearly with ferrocyanide concentration. This relationship can be approximated by a moisture concentration that increases linearly from 0 at 8 wt % $\text{Na}_2\text{NiFe(CN)}_6$ to 24 wt % water at a ferrocyanide concentration of 26 wt %. Thus, in terms of safe storage, the moisture criterion is

$$\text{Water Concentration (wt\%)} \ge (4/3)\,\text{Fuel}\,[\text{dry wt \% Na}_2\text{NiFe(CN)}_6] \\ - 10.7\,\text{wt\%} \qquad (4\text{-}5)$$

The safety criteria derived from this theoretical approach are conservative relative to the results of combustion experiments on ferrocyanide waste simulants. Results from this testing are described in the next section.

4.4.2   Experimental Results

Combustion experiments using ferrocyanide waste simulants and pure sodium nickel ferrocyanide were conducted by the DOE to corroborate the safe storage criteria derived from theoretical analyses (e.g., Fauske et al., 1995a,b). The simulants were prepared by reproducing the three process recipes (In-Farm, U Plant, and T Plant), not including the radioactive constituents. The precipitates were centrifuged to simulate approximately 40 yrs of settling. Typically, two or three layers of precipitates (discernible by color) were formed at the bottom of the settling and centrifuging containers. The bottom layer of the U Plant and In-Farm simulants and the top layer of the T Plant simulant contained the higher ferrocyanide concentrations.

A number of tests were conducted on mixtures of ferrocyanide and $NaNO_3/NaNO_2$ using the RSST[3] (Fauske and Leung, 1985). In these tests, sizeable samples (10 and 70 g) were heated at 10 °C/min under low heat loss conditions. As the sample was heated to above the reaction onset temperature, the thermal energy produced by the reaction caused the sample to self-heat. The rate and extent of this self-heating provide direct evidence of the character of the reaction that has taken place. A summary of the test results is given in table 4-4.

Two distinct types of behavior were seen depending on sample reactivity (i.e., ferrocyanide concentration): (i) a relatively slow heat-up rate that is typical of an Arrhenius or runaway reaction (any material that contains chemicals that react exothermally will exhibit this behavior), and (ii) a sharp transition to a very high self-heating rate indicating ignition and the passing of a reaction front. For materials that exhibit this behavior, a propagating reaction is possible, given a sufficient initiator.

The RSST test results (table 4-4) showed that a fuel concentration of about 15 wt % $Na_2NiFe(CN)_6$ was necessary to support a propagating reaction, almost twice the 8 weight percent theoretical criterion. It is interesting to note that only the In-Farm ferrocyanide waste simulants (representing waste from the four C Farm tanks) supported a propagating combustion. These results suggest that the U Plant and T Plant process sludges never contained sufficient fuel to propagate.

Another type of test, the tube propagation test, was used to evaluate the effect of moisture on ferrocyanide reactions. The test apparatus consisted of a thin, insulated stainless steel cylinder, 25 mm in diameter and 100 mm tall, that was filled with the test material (Fauske, 1992). The test material was ignited at the top by a BaO_2-Al mixture. The progress of the reaction, if any, was monitored by four thermocouples spaced 20 to 30 mm apart. Similar to the RSST tests, one of two distinct behaviors was observed. In samples capable of supporting a propagation reaction, the reaction proceeded to the bottom of the cylinder. On the other hand, the test material either did not ignite or failed to sustain combustion if the sample is not capable of supporting a propagating reaction. Several compositions with varying ferrocyanide and water concentrations were tested by this method. Test compositions, test conditions, and results are summarized in table 4-5.

The results of the tube propagation tests supported the RSST results that showed that $Na_2NiFe(CN)_6$ concentrations of about 15 weight percent were required to support a propagation reaction. The ferrocyanide concentration required to support propagation increased with the water content of the

---

[3]The RSST is a widely used industry tool implementing the AIChE-DIERS (American Institute of Chemical Engineers Design Institute for Emergency Relief Systems) methods to quantify runaway reactions to support safe design and operation in the commercial chemical industry.

Table 4-4. Summary of reactive system screening tool tests of ferrocyanide reaction propagation using waste simulants[a]

Measured Na$_2$NiFe(CN)$_6$ (wt%, dry)	Description	Propagation Observed	Ignition Temperature (°C)
2.5	Mixtures[b] of pure Na$_2$NiFe(CN)$_6$	No	NA[d]
4.6	U Plant 1[c]	No	NA
5.0	Mixtures of pure Na$_2$NiFe(CN)$_6$	No	NA
6.3	U Plant 2[c] top layer	No	NA
8.2	U Plant 2 bottom layer	No	NA
8.8	T Plant	No	NA
10.0	Mixtures of pure Na$_2$NiFe(CN)$_6$	No	NA
14.0	Mixtures of pure Na$_2$NiFe(CN)$_6$	No	NA
15.5	Mixtures of pure Na$_2$NiFe(CN)$_6$	Yes	275
15.6	In-Farm + NaNO$_2$ diluent	Yes	270
18.2	In-Farm 1[c] top layer	Yes	254
18.6	In-Farm 2[c] top layer	Yes	278
18.6	In-Farm + NaNO$_3$ diluent	Yes	260
20.0	Mixtures of pure Na$_2$NiFe(CN)$_6$	Yes	240
22.6	In-Farm 2 bottom layer	Yes	244
25.5	In-Farm 1 bottom layer	Yes	250

[a]Data from Fauske (1992) and Fauske et al. (1995a,b).
[b]Mixtures were comprised of a combination of pure Na$_2$NiFe(CN)$_6$ and excess NaNO$_3$.
[c]Two variations of U Plant and In-Farm simulants were prepared (Jeppson and Simpson, 1994). U Plant 2 and In-Farm 1 simulants represent wastes with ferrocyanide concentrations typical of Hanford ferrocyanide sludge.
[d]NA = Not applicable, sample did not propagate.

sludge. A stoichiometric mixture of fuel and oxidizer failed to propagate when 20 wt % free water was present. A key finding of the tube propagation test is that propagation ceased when the free water concentration was 12 weight percent or more at a ferrocyanide concentration of 25.5 weight percent (the highest concentration found in the waste simulants). This water concentration was roughly half of the theoretical moisture criterion (23 wt %) for a fuel value of 25.5 weight percent. This difference was expected because the thermodynamic calculations are inherently conservative.

Table 4-5. Summary of ferrocyanide tube propagation tests (from Meacham et al., 1996)

Measured Na$_2$NiFe(CN)$_6$ Concentration (wt%, dry basis)	Free Water Concentration (wt%)	Initial Temperature (°C)	Propagation Observed	Propagation Velocity (cm/min)	Notes
12	0	30	No	NA	a
12	0	130	No	NA	a
14	0	30	No	NA	a
14	0	130	Partial	NA	a
15.5	0	30	Yes	2	a
26	0	26	Yes	10	b
26	8	26	Yes	5.3	b
26	12	26	No	NA	b
26	14.6	26	No	NA	b
26	50	26	No	NA	b
29.5	0	60	Yes	9	c
35	0	~25	Yes	20	d
35	15	~25	Yes	7.8	d
35	20	~25	No	NA	d

NA = Not applicable, mixture failed to propagate.
[a]In-Farm simulant (Fauske et al., 1995a).
[b]Mechanical mixture representing In-Farm 1 process (Fauske, 1992).
[c]Mixture of 30 percent Na$_2$NiFe(CN)$_6$ with 70 percent NaNO$_3$/NaNO$_2$ oxidizer (Fauske, 1992).
[d]Stoichiometric mixture of pure Na$_2$NiFe(CN)$_6$ with NaNO$_3$ (Fauske et al., 1995a).

The results regarding the effect of moisture on propagation are important. As mentioned previously (section 4.2.2), simulated ferrocyanide sludges retained relatively high moisture contents (35 to 69 wt % water) after centrifuging in the laboratory for a time that approximated 30 yr of gravity settling. Additional studies indicate that ferrocyanide sludge in the Hanford waste tanks is wet and will stay wet. Dryout by pumping, leakage, hot spots, and surface evaporation has been considered and found to be negligible (Postma and Dickinson, 1995). For example, surface evaporation would not cause dryout of the waste because water would be wicked to the sludge surface much faster than it could evaporate. Dryout due to an internal hot spot cannot occur because the concentration of radionuclides required to even reach the boiling point from the current maximum temperature of 54 °C is too great to be credible. Water loss through a tank leak or pumping

would be distributed uniformly over the sludge volume and would not reduce the water content sufficiently to permit the sludge to become reactive (Postma and Dickinson, 1995).

4.4.3 Waste Safety Categories

Based on theoretical analyses and supported by experimental studies described previously, the DOE has defined safety categories for ferrocyanide-containing wastes. The criterion that defines the safe category is as follows:

- Fuel concentration $\leq$ 8 wt % $Na_2NiFe(CN)_6$ (temperature, oxidizer, and water concentration are not limiting).

The category safe defines waste that cannot burn or explode because it contains too little ferrocyanide as fuel. This conclusion is valid even for waste that contains optimum concentrations of oxidizer or no free water. A small amount of bound water (4.6 molecules of H_2O per molecule of sodium nickel ferrocyanide) has been identified through testing and is credited as being present in ferrocyanide waste that meets safe criteria (Postma et al., 1994).

The criterion that defines the conditionally safe category is as follows:

- Water concentration (wt %) $\geq$ 4/3 Fuel [in wt % $Na_2NiFe(CN)_6$] $-$ 10.7 wt % (Temperature and oxidizer are not limiting).

The conditionally safe category defines waste that cannot burn or explode because, although it may contain sufficient fuel and oxidizer, it contains sufficient water (moisture) to quench any reaction that may be initiated, and thus propagating reactions are prevented. This safety category is valid even for waste that contains optimum concentrations of oxidizer.

The category unsafe defines waste that does not meet the criteria for the safe or conditionally safe categories.

4.5 FERROCYANIDE DEGRADATION

Whether an exothermic reaction can occur or not in stored waste depends on the relative concentrations of the reactants, inert solid diluents (e.g., excess sodium nitrate and nitrite, aluminates, silicates, phosphates, sulfates, and carbonates), and water. In early DOE studies, analyses of core samples taken from three tanks showed ferrocyanide concentrations about a factor of 10 lower than predictions based on the scavenging process used, suggesting that degradation of the ferrocyanide matrix may have occurred during the more than 35 yr the wastes have been stored at the Hanford site (Meacham et al., 1994). To better understand processes that may have occurred during extended storage of ferrocyanide waste, the DOE initiated ferrocyanide degradation experiments in October 1992. The experiments were designed to investigate the effects of temperature, pH, and radiation on degradation of ferrocyanides. The parameters that affect the rate of degradation were examined through tests using ferrocyanide waste simulants. In addition, tank waste histories and tank sample data were evaluated to bound the amount of degradation that has occurred in all the ferrocyanide tanks.

The results of these experiments and tank waste characterization demonstrated that substantial ferrocyanide decomposition to chemicals that are either inert or have lower energy content has occurred. For example, experiments showed that the cyanide complex decomposes to a lower energy compound such as formate ($HCOO^-$), which further decomposes to carbon dioxide or carbonate (Lilga et al., 1996). The carbonate is inert and will not combust. Thus, degradation processes substantially lower the energy content of tank wastes and ultimately eliminate the hazards associated with ferrocyanide (Babad et al., 1993). In October 1996, the DOE closed out the ferrocyanide safety issue with respect to waste storage in Hanford tanks. However, evaluation of potential ferrocyanide reactions are planned on a case-by-case basis as part of the safety analysis of proposed retrieval and processing methods because residual exothermic activity might be initiated by disposal options that cause waste to be heated by an external source (Postma and Dickinson, 1995).

4.5.1 Mechanisms of Ferrocyanide Degradation

The primary degradation route for ferrocyanide waste is dissolution of alkali metal nickel ferrocyanides. Sodium nickel ferrocyanide, the major component of ferrocyanide sludges, is insoluble in water, but will dissolve in a caustic solution [e.g., 0.1 M hydroxide (Babad et al., 1993; Lilga et al., 1992)]. Dissolution of sodium nickel ferrocyanide results in soluble sodium ferrocyanide and a nickel hydroxide precipitate as described by Eq. (4-6):

$$Na_2NiFe(CN)_6(s) + 2OH^- \rightleftharpoons Fe(CN)_6^{4-} + 2Na^+ + Ni(OH)_2\downarrow \qquad (4\text{-}6)$$
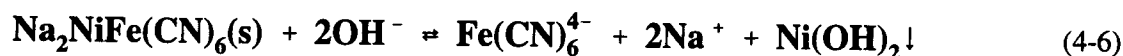
Soluble ferrocyanide is a byproduct of many industries, including aluminum manufacturing, iron and steel making, metal finishing (Robuck and Luthy, 1989), and chemical manufacturing. Thus, several papers have been written on alkaline hydrolysis reactions involving ferrocyanide. For example, Robuck and Luthy (1989) conducted experiments using spent potlining leachate and demonstrated that ferrocyanide will hydrolyze to form formate, ferric oxide, and ammonia as represented in

$$Fe(CN)_6^{4-} + 2OH^- + 11H_2O + \frac{1}{6}O_2 \rightleftharpoons 6HCO_2^- + \frac{1}{3}Fe_3O_4\downarrow + 6NH_3\uparrow \qquad (4\text{-}7)$$
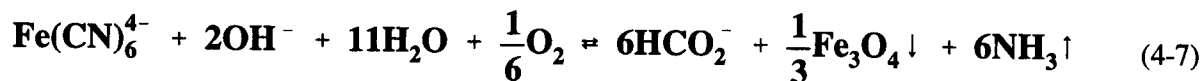
Reactions similar to Eq. (4-7) should be possible in the alkaline conditions found in ferrocyanide waste tanks.

The work by Wiegand and Tremelling (1972) suggests that hydrolysis is actually a two-step process. The ferrocyanide dissociates to free cyanide, which is then hydrolyzed to form formate and ammonia:

$$Fe(CN)_6^{4-} + H_2O \rightarrow [Fe(CN)_5H_2O]^{3-} + CN^- \qquad (4\text{-}8)$$

$$CN^- + 2H_2O \rightarrow HCO_2^- + NH_3\uparrow \qquad (4\text{-}9)$$

The dissolution of sodium nickel ferrocyanide initially leads to precipitation of $Ni(OH)_2$ [Eq. (4-6)]. However, as hydrolysis of the ferrocyanide ion occurs, cyanide ions are liberated [Eq. (4-8)]. Some of the cyanide ions are converted to ammonia and formate ions [Eq. (4-9)], but some redissolves nickel as $Ni(CN)_4^{2-}$:

$$Ni(OH)_2(s) + 4CN^- \rightleftharpoons Ni(CN)_4^{2-} + 2OH^- \tag{4-10}$$
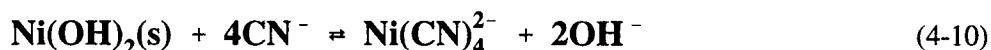
Equation (4-10) is a reaction with a very negative free energy and an equilibrium constant, K_R, of 7.95×10^{12} (Lilga et al., 1995).

In DOE ferrocyanide degradation studies, atomic absorption (AA) spectrometry and FTIR were used to analyze reaction solutions from simulant experiments. FTIR results showed that the soluble iron and soluble nickel existed principally as $Fe(CN)_6^{4-}$ and $Ni(CN)_4^{2-}$ species, respectively. Concentrations determined by AA were close to concentrations using FTIR, indicating that essentially all the soluble iron and nickel were present as the cyano-complexes (Lilga et al, 1996).

4.5.2   Parameters Affecting the Rate of Degradation

Literature information (MacDiarmid and Hall, 1953; Masri and Haissinsky, 1963; Hughes and Willis, 1961; Ohno and Tsuchihasi, 1965; Robuck and Luthy, 1989) indicates that various parameters can affect the rate of ferrocyanide degradation including pH, radiation dose rate, and temperature. For example, Robuck and Luthy (1989) found that Eq. (4-7) was zero-order with respect to hydroxide concentration for pH values greater than 10 and first-order with respect to ferrocyanide concentration. The work by Wiegand and Tremelling (1972) indicates that the hydrolysis of cyanide [Eq. (4-9)] is very temperature-dependent. The reaction proceeds slowly at room temperature, but the reaction rate increases three-fold for every 10 °C rise in temperature.

The DOE studied the effects of pH, radiation dose rate, and temperature on the degradation of Hanford ferrocyanide wastes (Lilga et al., 1992, 1995, 1996). Experimental data indicate that the rate of dissolution of sodium nickel ferrocyanide [Eq. (4-6)] increases with increasing hydroxide concentration. However, the rate does not increase further at pH greater than 9.0. Although Cs-137 scavenging with ferrocyanide was done at pH~8 to 10, the ferrocyanide tanks were used for a variety of waste management operations that resulted in wastes of higher pH (Anderson, 1990). Available historical pH and hydroxide data for the eighteen ferrocyanide tanks show that all the tanks had pH values greater than 9 (Wodrich et al., 1992). An excerpt of alkalinity data for some ferrocyanide tanks taken from Wodrich et al. (1992) is presented in table 4-6. Thus, waste pH does not appear to be a limiting factor for ferrocyanide waste degradation in Hanford waste tanks.

Experiments conducted on ferrocyanide waste simulants at various gamma dose rates indicate that the rate of degradation is not much affected by dose rate except at the highest values [100 Gy/hr (10,000 Rad/hr)] used in the study (Lilga et al., 1996). There was little effect of dose rates between 0 and 10 Gy/hr (1,000 Rad/hr). Dose rates calculated for the ferrocyanide waste tanks are in the 10 Gy/hr (1,000 Rad/hr) range, and none approached 100 Gy/hr (10,000 Rad/hr) (Parra, 1994). Consequently, dose rates in the ferrocyanide tanks most likely had only a second-order effect on the rate of degradation (Meacham et al., 1996).

Table 4-6. Alkalinity of some ferrocyanide tank wastes (Wodrich et al., 1992)

Tank	pH[a]	OH⁻ Concentration (M)	Sample Date	Notes
BY-105	13.3	0.78	11/90	Supernatant
BY-111	9.60	Not available	6/56[b]	
C-108	11.8	0.48	9/75	Supernatant
C-109	13.7	0.50	11/90	Supernatant
C-112	12.1 11.9 9.0–10.5	0.67 0.49 Not available	11/74 6/75 3/92	Water leach of core segments[c]
T-107	13.2 12.3 11.1	0.160 0.080 0.025	3/65 9/75 9/89	Supernatant
TY-101	12.7 10.0	0.05 Not available	12/82 9/85	Water leach of core composite
TY-103	12.0 11.7 9.5–12.2	0.24 Not available 0–0.017	3/65 2/72 9/85	Supernatant Drainable liquid
TY-104	12.0 12.1 12.1–12.2	0.32 Not available 0.013–0.016	3/65 2/72 8/85	 Drainable liquid

[a]There is considerable error in pH values due to the high ionic strength (>4.0 M) of the supernatant and drainable liquid samples. The OH⁻ concentrations, which were measured by direct potentiometric titration of the solutions with a standardized acid, are a more reliable measure of alkalinity.
[b]A more recent sample has not been found.
[c]Water leach of 1 g of core sample with 100 g of water.

In contrast, experiments that investigated the effect of temperature showed that the rate of degradation was strongly affected by temperature (Lilga et al., 1996). For example, results shown in table 4-7 indicate that the rate of degradation increased dramatically with increasing temperature. These data suggest that the extent of ferrocyanide degradation in Hanford site tanks was likely determined by the individual tank temperature histories. This conclusion is important because it allows a method for selecting those tanks that bound ferrocyanide degradation. Tanks with the lowest temperature histories would have the least amount of degradation. Therefore, analytical data for the coolest ferrocyanide tanks can be extrapolated to provide estimates of the extent of degradation for unsampled tanks with higher temperature histories.

Table 4-7. Degradation rate as a function of temperature determined from experiments using waste simulants (Lilga et al., 1996)

Temperature °C (°F)	Reaction Rate [g $Na_2NiFe(CN)_6$/100 g dry solids/yr]
40 (104)	0.04
50 (122)	0.19
60 (140)	0.90
70 (158)	3.90
80 (176)	15.50
90 (194)	57.0

4.5.3   Confirmation of Ferrocyanide Degradation in Hanford Wastes

Ferrocyanide degradation can be confirmed by examining nickel and cyanide concentrations in waste or simulant solutions. Nickel is a signature analyte of the nickel ferrocyanide scavenging process (the major source of high nickel concentrations) and indicates how much ferrocyanide was originally present. Analyses of cyanide concentrations give an indication of how much ferrocyanide is remaining.

Meacham et al. (1996) evaluated tank sampling and waste history data for Hanford tanks on the ferrocyanide Watch-list. Nine of the 18 tanks on the Watch-list have been sampled full depth (i.e., to the bottom of the tank) and one tank (BY-106) has been partially sampled. Sample data for these 10 tanks are listed in table 4-8. The range in extent of degradation was calculated from the measured nickel concentration (a measure of the amount of original ferrocyanide) and cyanide concentration (a measure of the amount of ferrocyanide remaining). The lower limit of extent of degradation was determined from the lowest value of original concentration and the highest concentration of ferrocyanide remaining, whereas the upper limit was calculated from the highest original concentration and the lowest concentration of ferrocyanide remaining. For example, the lowest original $Na_2NiFe(CN)_6$ concentration in BY-108 was 5.0 and the highest measured concentration was 0.5; this implies 90 percent degradation. The results listed in table 4-8 confirm that ferrocyanide degradation is significant and pervasive. The measured ferrocyanide concentrations are more than an order of magnitude lower than the original concentrations and significantly below the 8 weight percent safe criterion.

4.5.4   Estimates of Ferrocyanide Degradation for Unsampled Watch-list Tanks

The extent of ferrocyanide degradation for tanks on the ferrocyanide Watch-list that have not been sampled was estimated by Meacham et al. (1996) based on the results of ferrocyanide degradation studies and from tank temperature histories. Current ferrocyanide concentrations for the unsampled tanks were estimated based on the relationship between extent (percent) of degradation and temperatures observed in the sampled tanks and the measured temperatures of the unsampled tanks. The estimated current ferrocyanide concentrations for the unsampled tanks are listed in table 4-9.

Table 4-8. Sample data confirming ferrocyanide degradation (from Meacham et al., 1996)

Tank	Original $Na_2NiFe(CN)_6$ (wt %)	Measured $Na_2NiFe(CN)_6$ (wt %)	Extent of Degradation (%)
BY-104	4.0–8.3	<0.01	>99
BY-106	5.2–8.3	<0.01	>99
BY-108	5.0–8.3	0.01–0.5	90 to >99
BY-110	5.7–8.3	0.00–0.4	98 to >99
C-108	10.4–22.6	0.3–1.1	89 to 99
C-109	14.0–22.6	0.7–1.6	89 to 97
C-111	8.9–22.6	0.02–0.05	>99
C-112	16.1–25.5	1.2–1.5	91 to 95
T-107	6.3–8.3	0.00–0.02	>99
TY-104	1.6–10.7	0.00–0.03	98 to >99

Table 4-9. Estimated current ferrocyanide concentrations in unsampled ferrocyanide tanks (from Meacham et al., 1996)

Tank	Estimated Current $Na_2NiFe(CN)_6$ Concentration (wt %, dry)
BY-103	0.6–0.8
BY-105	0.4–0.8
BY-107	0.5–0.8
BY-111	0.6–0.8
BY-112	0.4–0.8
TY-103	0.0–0.2
TY-104	0.0–0.2

The unsampled tanks have similar or higher waste temperatures than the sampled tanks. All the BY ferrocyanide tanks had temperatures higher or equal to tank BY-108, which showed a minimum of 90 percent degradation (table 4-8). All the TY tanks had temperatures greater than TY-104, which showed a minimum of 98 percent degradation. The estimated concentrations shown in table 4-9 were generated using the minimum percent degradation calculated for the BY and TY ferrocyanide tanks, which is 90 and 98 percent, respectively.

4.5.5 Conclusion on Ferrocyanide Waste Degradation

Meacham et al. (1996) concluded that, based on tank sampling and waste history data, as well as laboratory experiments with simulated ferrocyanide-bearing tank waste materials, conditions existed within the tanks that promoted ferrocyanide degradation. Tank sampling data and waste history data indicate that the ferrocyanide concentrations have decreased to levels substantially lower than 8 weight percent and that the ferrocyanide tanks should be categorized as safe based on the safety criteria discussed in a previous section.

4.6 SUMMARY

Historically, additional tank storage space for HLW at the Hanford site was generated by precipitating cesium from tank waste liquids using sodium or potassium ferrocyanide and nickel sulfate and pumping the decontaminated liquids to disposal cribs. In implementing the scavenging process, approximately 140 metric tons (154 tons) of alkali-nickel ferrocyanide were added to waste that was later routed to 18 SSTs. Because the process precipitated ferrocyanide from solutions that had high concentrations of the oxidants nitrate and nitrite, an intimate mixture of ferrocyanides and oxidants is likely to exist in the ferrocyanide waste. The potential for an uncontrolled exothermic reaction was a concern because, in the laboratory, mixtures of ferrocyanides and nitrates or nitrites can be made to explode if heated to over 200 °C.

Studies by the DOE to evaluate the explosive hazard of ferrocyanide wastes showed that the ferrocyanide mixtures were not ignited by standard impact and friction sensitivity tests (Cady, 1992). An external heat source was required in the tests before any exothermic reaction could be observed. Thermal tests indicated major exotherms at temperatures above approximately 260 °C, suggesting the possibility of explosive reactions if mixtures of ferrocyanide and nitrate/nitrite are heated to high temperatures or if there is an electrical spark of sufficient energy to ignite a dry mixture.

Oxidation of ferrocyanide by nitrate and/or nitrite can result in a variety of reaction products with different reaction enthalpies. A comparison of enthalpies of reaction for several combinations of reactants and products, estimated by Scheele et al. (1991) from the enthalpies of formation of the reactants and products, shows that the energetics of the postulated reaction is highly sensitive to the products formed. The most energetic, for a given amount of fuel, is one that produces nitrogen and carbon dioxide (or carbonate salt if there is sufficient hydroxide available to form it). The reaction energy is greatly reduced if a sizable fraction of the carbon goes to CO due to incomplete oxidation, or if appreciable oxides of nitrogen form. On the other hand, a change in the reacting ferrocyanide salt results in a much smaller change in energy released.

The range of compositions of ferrocyanide sludge capable of sustaining a propagating chemical reaction and the safety categories for storage of ferrocyanide wastes have been established by the DOE from experimental measurements supported by theoretical considerations. The theoretical approach, based on an enthalpy balance and assuming a ΔH_R of $-1,900$ kJ/mol (-6 MJ/kg) of $Na_2NiFe(CN)_6$, an initial waste

temperature of 30 °C, and a reaction threshold temperature of 250 °C, indicates that, for waste with 0 wt % free water, the minimum fuel concentration necessary to sustain a propagating reaction is about 8 wt % sodium nickel ferrocyanide. For waste with greater than 8 wt % sodium nickel ferrocyanide, the mass of free water required to quench reactions increases linearly with ferrocyanide concentration. This relationship can be approximated by a moisture concentration that increases linearly from 0 at 8 wt % $Na_2NiFe(CN)_6$ to 24 wt % water at a ferrocyanide concentration of 26 weight percent.

The safety criteria derived from the theoretical approach are conservative relative to the results of combustion experiments. These experiments, which used mixtures of ferrocyanide waste simulants or pure sodium nickel ferrocyanide and nitrate/nitrite, were conducted by the DOE to corroborate the safe storage criteria derived from theoretical analysis. Tests using the RSST showed that a fuel concentration of about 15 wt % $Na_2NiFe(CN)_6$ was necessary to support a propagating reaction, almost twice the 8 weight percent theoretical criterion. Tube propagation tests, which were used to evaluate the effect of moisture on ferrocyanide reactions, supported the RSST results and also demonstrated that the ferrocyanide concentration required to support propagation increased with the water content of the sludge. A stoichiometric mixture of fuel and oxidizer failed to propagate when 20 wt % free water was present. A key finding of the tube propagation test is that propagation ceased when the free water concentration was 12 weight percent or more at a ferrocyanide concentration of 25.5 weight percent (the highest concentration found in the waste simulants). This water concentration was roughly half of the theoretical moisture criterion (23 weight percent) for a fuel value of 25.5 weight percent. This difference was expected because the thermodynamic calculations are inherently conservative. The results regarding the effect of moisture on propagation are important. Studies indicate that ferrocyanide sludge in the Hanford waste tanks is wet and will stay wet. Dryout by pumping, leakage, hot spots, and surface evaporation has been considered and found to be negligible (Postma and Dickinson, 1995).

Some portion of the ferrocyanide waste in most of the Hanford tanks on the ferrocyanide Watch-list probably exceeded 8 wt % $Na_2NiFe(CN)_6$, the minimum fuel concentration considered necessary to sustain a propagating reaction, when it was originally established. However, ferrocyanide decomposition has resulted in current ferrocyanide concentrations substantially less than the estimated original concentrations. DOE experiments, designed to investigate the effects of temperature, pH, and radiation on degradation of ferrocyanides in contact with highly caustic solutions, and results of tank waste characterization demonstrated that substantial ferrocyanide decomposition to chemicals that are either inert or have lower energy content has occurred. Degradation processes substantially lower the energy content of tank wastes and ultimately eliminate the hazards associated with ferrocyanide (Babad et al., 1993). The DOE studies showed that the rate of degradation is primarily a function of the waste temperature. Records indicate that most tanks were at a sufficiently high temperature for a sufficiently long time such that significant ferrocyanide degradation would be expected. Tank sampling data and waste history data show that the ferrocyanide concentrations have decreased to levels significantly lower than 8 weight percent and that the ferrocyanide tanks should be categorized as safe based on the safety criteria established by the DOE.

In October 1996, the DOE closed out the ferrocyanide safety issue with respect to waste storage in Hanford tanks. However, evaluations of potential ferrocyanide reactions are planned on a case-by-case basis as part of the safety analysis of proposed retrieval and processing methods (Postma and Dickinson, 1995) because residual exothermic activity might be initiated by processing options that cause waste to be heated by an external source (e.g., during vitrification or other accidental circumstance). DOE studies regarding safety during continued storage of ferrocyanide wastes are also useful for safety analysis of the Hanford TWRS. The results regarding the effect of moisture on reaction propagation are particularly important. Ferrocyanide-containing wastes are expected to contain sufficient moisture to prevent a

propagating reaction during the retrieval and pretreatment stages of the TWRS operations. For example, the low activity waste feed will have an insoluble solids fraction not exceeding 5 volume percent (U.S. Department of Energy, 1996b). Subsequent centrifugation will separate a fraction with a relatively high amount of entrained solids, perhaps to about 70 wt % insoluble solids. However, there may be no mechanism during the retrieval and pretreatment operations that could reduce the water content to a level that would permit the sludge to become reactive. If such is the case, then ferrocyanide and nitrate/nitrite mixtures will likely not constitute a safety hazard during the TWRS operations.

5 CHEMISTRY AND APPROXIMATION METHODS RELEVANT TO CRITICALITY SAFETY ANALYSES

5.1 INTRODUCTION

An important consideration in safety evaluations of the Hanford TWRS is the potential for nuclear criticality due to the presence of fissile material in the tank wastes. Defense operations at the Hanford site since the 1940s have resulted in the transfer of a significant quantity of the fissile isotopes of Pu and U to the underground waste storage tanks. Collectively, the SSTs and DSTs contain an estimated 500 to 1,000 kg of Pu, which is associated almost exclusively with the sludge phase (Bratzel et al., 1996). It is necessary to ensure that the tank wastes remain subcritical with a sufficient margin of safety during continued storage, as well as during retrieval, pretreatment, and solidification of tank wastes.

Past waste management operations at the Hanford site required that waste be transferred to the storage tanks only after low concentrations of Pu were verified. Based on available Hanford records, Braun et al. (1994) inferred that criticality control limits on waste transfers have been met since initial operation of the Hanford tank farms, although the limits were not formalized until 1967 (Oberg, 1979). The key criticality control limits are: (i) the maximum Pu concentration in the waste mixture routed to the waste tank shall be 0.013 g/L (0.05 g/gal), and (ii) the maximum concentration of Pu allowed in a waste tank shall be 1.0 g/L in the waste tank solids (Oberg, 1979). Based on a criticality safety assessment of Hanford waste tanks, Braun et al. (1994) concluded that the tanks have a large margin of subcriticality.

Although discharged wastes may be subcritical, conditions within the tanks are not static because various processes could lead to locally high concentrations of Pu in the tank wastes. For example, settling of particulates suspended in a waste mixture is the most obvious and, perhaps, the most effective mechanism for concentrating Pu. In addition, evaporation of waste liquid leads to higher concentrations and to possible precipitation of fissile material and/or neutron absorbers. Furthermore, the composition of Hanford wastes will change during waste retrieval and processing operations. Chemical processes during waste retrieval and pretreatment, such as precipitation of fissile material or dissolution of neutron absorbers, could lead to elevated and localized concentration of Pu in the waste. Thus, an important concern in safety evaluations of the Hanford TWRS is the identification and evaluation of processes that may lead to criticality during TWRS storage, retrieval, and processing operations. For example, subprocesses or mechanisms that may lead to criticality that Ha et al. (1996) considered in studying the potential for accidental criticalities at the defense waste-processing facility at the Savannah River Site are (i) chemical reactions that concentrate U and Pu with respect to iron and manganese neutron absorbers, (ii) fissile material adsorbed onto monosodium titanate, (iii) fissile material entrained in the sludge solids, (iv) Pu solubility in mercury, (v) process cleaning procedures, and (vi) melter accumulation. Similar processes or mechanisms may need to be examined for their potential significance to Hanford TWRS operations.

Understanding Pu distribution is particularly important. Unfortunately, there is relatively little information on the effects of possible chemical or physical tank processes on Pu distribution. For example, while Pu chemistry has been well studied for decades, there is a paucity of experimental data on solubility and solid-liquid partitioning in high-pH, high ionic strength systems characteristic of Hanford tank wastes. Therefore, models for Pu concentration mechanisms in the wastes must be used with caution because they are not properly benchmarked to an extensive set of data. Nevertheless, some idea of the relative importance of processes may be obtained.

To aid the NRC in conducting criticality safety evaluations of the Hanford TWRS, information is provided in this chapter on the principles of criticality safety, parameters that affect criticality of HLW, and mechanisms that could lead to concentration of fissile materials and neutron absorbers. A relatively simple approach for determining when criticality may be a problem for Hanford TWRS operations is also proposed and discussed.

5.2   PRINCIPLES OF CRITICALITY SAFETY

Before a self-sustained neutron chain reaction, or critical state, can be achieved, a number of physical conditions must exist. One required condition is the presence of a sufficient amount of fissile material to absorb neutrons and undergo fission. Each fission event generates several high-energy neutrons. These neutrons undergo interactions in which they either lose energy, are absorbed, or are lost from the system by leakage. The critical state of a system is determined by the number of neutrons lost by absorption or leakage relative to the number of neutrons from fission events that are available to produce subsequent fissions. If more neutrons are absorbed or lost by leakage than are produced by fission, then the system is considered to be subcritical. If an equal number of neutrons are produced as are lost or absorbed, then the system is considered to be critical. If more neutrons are produced than are lost or absorbed, then the system is considered to be supercritical.

The critical state is mathematically represented by a parameter called k_{eff}, which is defined as the number of neutrons in one generation divided by the number of neutrons in the preceding generation. A critical state has a neutron population that remains constant, and the value of k_{eff} is equal to one. A subcritical system has a neutron population that decreases in time, and the value of k_{eff} is less than one. A supercritical system has a neutron population that increases in time, and the value of k_{eff} is greater than one. If the size of the system is effectively infinite and has no neutron leakage, the parameter of interest is called k_{∞}. The value of k_{eff} is always less than or equal to the value of k_{∞}. Typically, an upper bound for subcritical conditions used by DOE is to have a calculated k_{eff} less than 0.95, with a 95-percent confidence level, after any postulated event (Westinghouse Hanford Company, 1994a).

Fission occurs more readily after neutrons have undergone several scattering reactions and their energy has decreased such that the neutrons are in thermal equilibrium with the scattering medium. The process of reducing the neutron energy, known as "slowing down" or "moderation," is most effectively accomplished by materials with low atomic masses and high ratios of neutron scattering to absorption coefficients, such as hydrogen. These materials are called moderators. At optimum moderation, a minimum amount of fissile material is required to sustain a chain reaction. At other than optimum moderation, more fissile material is required to reach criticality. The amount of fissile material required for criticality is also affected by the concentration of the fissile material, the geometry of the system containing the fissile material, and the presence (or absence) of other materials that compete with the fissile material for absorption of neutrons.

5.3   PARAMETERS THAT AFFECT CRITICALITY

To prevent inadvertent criticality in a system, specific controls and limitations are placed on the factors that affect criticality. For TWRS operations, the factors most important to criticality are (i) concentration of fissile material, principally Pu-239, (ii) the amount and property of neutron absorbers or moderators present with the fissile material, (iii) the geometry of the system containing the fissile material, and (iv) the presence or absence of neutron reflectors adjacent to the system. Each of these parameters is discussed in more detail in the following sections. The prevention of criticality in Hanford waste tanks relies

on the dilution of fissiles due to the presence of other materials in the waste matrix. For most in-tank waste solids, water present either as interstitial water or as hydration waters of metal hydroxides is the predominant constituent that provides dilution. A second independent factor that can result in subcriticality is the presence of neutron-absorbing elements as soluble and insoluble compounds admixed during precipitation of Pu compounds. Because the wastes were maintained at alkaline conditions, most of the Pu is in the solids (Rai and Serne, 1978).

5.3.1 Fissile Material Concentration

In order to achieve criticality, the fissile material must be present in certain concentrations, regardless of the size of the system. For the Hanford tank wastes, DOE analyses indicate that the plutonium concentration must be at least 2.6 g Pu/L before criticality is possible, even in an unlimited volume of waste (Rogers et al., 1996). This value, which was calculated using the conservative waste model (CWM), is based on a uniform mixture of plutonium, waste solids, and water. The CWM, which was developed by Rogers (1993), is used to calculate the critical plutonium concentrations and to determine the minimum critical dimensions. It is based on a waste model with component concentrations derived from the maximum reported values for tank solids materials that are good neutron reflectors and the minimum reported values for tank solids materials that are good neutron absorbers. The CWM also assumes the water content is optimized. Note that the use of the CWM results in a minimum critical plutonium concentration that is well below the value of 7.2 g/L, which is generally reported as the minimum critical concentration of plutonium in water (Knief, 1992). This difference in minimum critical concentrations is primarily due to the density of water in which the plutonium resides in the CWM. The value of g/L is derived based on water in the system having a density of one, but with no other neutron poisons in the system.

5.3.2 Neutron Absorbers

Neutron absorbers reduce the reactivity of any fissile mixture by reducing the thermal neutron flux in the mixture. These materials generally absorb neutrons and release gamma or alpha particles, which do not contribute to further fission events. There is a unique minimum absorber-to-plutonium mass ratio for all absorbers above which the system will remain subcritical, independent of any other influences. Section 5.4 presents results of a study designed to determine the minimum absorber-to-plutonium mass for various waste components.

Two of the most effective absorber materials, boron and cadmium, are often excluded from modeling because their concentration and distribution in the waste form cannot be ensured for all waste streams, and waste samples are not routinely analyzed for these elements. However, some waste streams are known to have substantial quantities of these excellent neutron absorbers in the waste solids. Boron and cadmium are such strong absorbers that their contribution would dominate those of almost all of the other neutron absorbers. The exclusion of boron and cadmium in a criticality safety analysis leads to a conservative estimate of the subcritical margin of safety.

5.3.3 Geometry

Geometry plays a role in determining subcritical limits because of its influence on neutron leakage. Neutrons that leak out of the system will not contribute to any further fissions. Therefore, reducing the number of neutrons that escape the system will increase the reactivity of the system. Because of the immense size of the Hanford waste tanks, the geometry is normally considered to be essentially infinite, at least in the lateral direction (i.e., slab geometry). If the tanks can be shown to be subcritical for infinite conditions, any tank of finite size will be even more subcritical.

The effects of geometry are typically discussed in terms of a sphere. This is because a sphere is the ideal geometry for achieving criticality and, thus, constitutes the bounding case. For plutonium in concentrations that are relatively low, but still higher than is currently found in the tanks, the critical sphere size is very large (on the order of meters in diameter). From a practical perspective, it is difficult to visualize a credible mechanism by which fissile material could be configured into a sphere of this size. The most probable configuration of the waste form is an approximation of a slab, although other waste form shapes (e.g., hemispheres and cylinders) could exist (Rogers et al., 1996).

5.3.4 Neutron Reflectors

Neutron reflectors surrounding the fissile material may increase the reactivity of the system by returning neutrons that have leaked out of the system to the fissile material where they are able to contribute to further fissions. The reflectors will only reduce the losses from geometry effects, so for conservative calculations that assume absorber-free infinite dimensions, reflectors will have no effect. Although it is not known whether reflectors will be present around the fissile material, calculations that take credit for neutron leakage losses must take into account the effect of neutron reflectors that surround the system on any side, if they are present.

5.4 PUBLISHED STUDY ON HANFORD CRITICALITY SAFETY ANALYSES

Braun et al. (1994) presented results of criticality analyses that were conducted to determine the subcritical nature of tank wastes. The analyses were based on calculating the minimum absorber-to-plutonium (X/Pu) mass ratio necessary to ensure subcriticality of the wastes assuming optimum moderation as calculated with the EGGNIT code. Table 5-1 presents minimum subcritical mass ratios for various waste components taken from Braun et al. (1994). The minimum subcritical ratios determine the minimum relative concentrations of the absorber materials which, if present individually with the Pu, would assure subcriticality for any degree of moderation.[1] In the case of Hanford wastes, which are multicomponent systems containing two or more neutron absorbers, DOE studies indicate that subcritically is guaranteed if the sum of the fractions of the minimum X/Pu subcritical ratios for the various neutron absorbers present in the waste is greater than 1 (e.g., a system with a mass ratio of Mn-to-Pu of 16 and a mass ratio of Fe-to-Pu of 81 would be subcritical).[2]

A problem with the approach presented by Braun et al. (1994) for criticality analysis of TWRS retrieval, processing, and solidification operations is that if a mechanism for concentrating Pu exists that can

---

[1] Waste systems are composed of many components, and it is appropriate to take into account the presence of all neutron absorbers to demonstrate the margin of subcriticality. This procedure can be accomplished by defining a parameter, referred to as the *fraction of the actual-to-minimum subcritical ratios*, that assigns a value to the relative worth of each component as a neutron absorber. This parameter is defined as the actual X/Pu mass ratio for a neutron absorber divided by the corresponding minimum subcritical mass ratio (e.g., table 5-1). The resulting fraction is a measure of the quantity of absorber present relative to that required to ensure subcriticality. The larger the fraction of the actual-to-minimum subcritical ratio, the more subcritical is the waste composition. When the fraction of the actual-to-minimum subcritical ratios exceeds unity, subcriticality is ensured regardless of the degree of moderation and reflection (Braun et al., 1994).

[2] Mathematically, the sum of the fractions is given by the formula

$$\sum_{j=1}^{N} \frac{(X_j/Pu)_{actual}}{(X_j/Pu)_{subcritical}} \geq 1$$

Table 5-1. The minimum subcritical ratio for various waste components (from Braun et al., 1994)

Component (X)	Minimum Subcritical Ratio (mass of X/mass of Pu-239)
Al	910
Cr	135
Ni	105
N	61
Nitrate	270
Na	360
Si	1400
Mn	32
Fe	160
U (natural)	770

lead to Pu concentrations above the 7.2 g/L required for a k_∞ of 1 for a pure water-Pu-239 system (Knief, 1992), the required absorber concentration to guarantee subcriticality becomes quite large. For example, for a mixture composed solely of iron, Pu-239, and water for a situation that has concentrated Pu-239 to a level of 10.0 g/L, an iron concentration of 1,600 g/L is necessary to ensure subcriticality. This required amount of iron would increase for larger Pu concentrations.

The approach discussed by Braun et al. (1994) was not intended to replace detailed criticality investigations, but rather to outline a method for determining those cases for which detailed investigations are not required based solely on information on the absorber content of the waste. The following sections describe another method for accomplishing the same task, which may be of greater utility for determining when criticality may be a problem in Hanford TWRS operations.

5.5   ALTERNATIVE METHOD FOR HANFORD CRITICALITY ANALYSES[3]

This section presents the results of calculations that allow an investigator to rapidly determine if a given process may have a criticality control problem. These calculations are designed such that determinations using their results will be conservative in nature, meaning that the method may indicate a problem when none is present. The method presented in this section should be considered to determine when criticality may be a problem and where more detailed investigations are required. Discussions of the primary

---

[3]The method discussed in this section is for illustrative purposes and may or may not be acceptable to the NRC to demonstrate the criticality safety of tank wastes or other licensed material, and may or may not be used by the NRC for license application review.

fissile isotopes, their enrichment in tank wastes, and the important neutron absorbers present are also provided.

5.5.1 Mass Inventory and Enrichment of Fissile Materials

Three of the important parameters for criticality safety with respect to tank wastes are the concentration, mass inventory, and enrichment of the U and Pu in their fissile isotopes (U-233, U-235, Pu-239, and Pu-241). Figures 5-1 to 5-4 are histograms showing the number of Hanford tanks with the specified range of concentration of fissile materials among all 177 tanks.[4] The values presented in the figures are based on the HDW model of Agnew (1996b) and assume that the fissiles are uniformly distributed throughout the waste volume. These average concentrations are well below the minimum critical Pu concentration of 2.6 g Pu/L (Rogers et al., 1996). However, a significant amount of the Pu is expected to have settled to the sludge at the bottom of the tanks where the concentrations may be greater than the average tank concentration. Therefore, using tank-averaged Pu concentrations cannot assure that subcritical conditions exist in the tanks.

For this report, a study was performed to determine if there is a risk of nuclear criticality based on U as the primary fissile material from processing the tank wastes. The relative isotopic abundances of U in tank AW-104 were used in the study because the U in this tank has the highest enrichment in fissile isotopes (0.866 percent) (Agnew, 1996b). All criticality calculations were performed using the Monte Carlo N-Particle Version 4A (MCNP4A) code (Briesmeister, 1993) with the assumption that the waste would not experience any process that would raise its enrichment (e.g., addition of U-235, or more highly enriched U, from another waste stream). It was found that, for a system composed solely of U and water in optimal concentrations, k_∞ was equal to 0.94, meaning that nuclear criticality of tank wastes based solely on U is not possible with light water as a moderator. This study also showed that discounting the presence of U in criticality calculations where Pu is the primary fissile material is a conservative assumption. The reason is U, with the enrichments found in the tanks, has a net poisoning effect on critical systems.

Based on the above reasoning, the following sections will focus on Pu as the primary fissile material of concern in tank wastes. Table 5-2 lists the tanks that exceed a mass inventory of 200 and 1,000 g of total Pu.

5.5.2 Important Neutron-Absorbing Materials

The TWRS tank contents include numerous isotopes and elements that are known neutron absorbers. These isotopes and elements are both naturally occurring and fission products. Agnew (1996b) shows the tank inventories of numerous constituents, and a list of the isotopes and elements tracked in this report is shown in table 5-3, along with their microscopic thermal neutron absorption cross sections (σ_a^{th}). Isotopes of U and Pu have been excluded from this list because these elements will likely be included in criticality calculations of the tank wastes. To make criticality calculations that are not overly conservative, it is presumed that the presence of key neutron absorbers needs to be taken into account. A key neutron absorber is defined as an absorber whose macroscopic absorption cross section ($\sum_a^{th}$, the product of σ_a^{th} and the

---

[4]The mass inventory of each of the tanks for the fissile isotopes U-233, U-235, Pu-239, and Pu-241, and the enrichments of U and Pu in their fissile isotopes (e.g., atomic number density of fissile Pu divided by atomic number density of total Pu) based on the HDW model (Agnew, 1996b) are listed in table D-1 in the appendix.
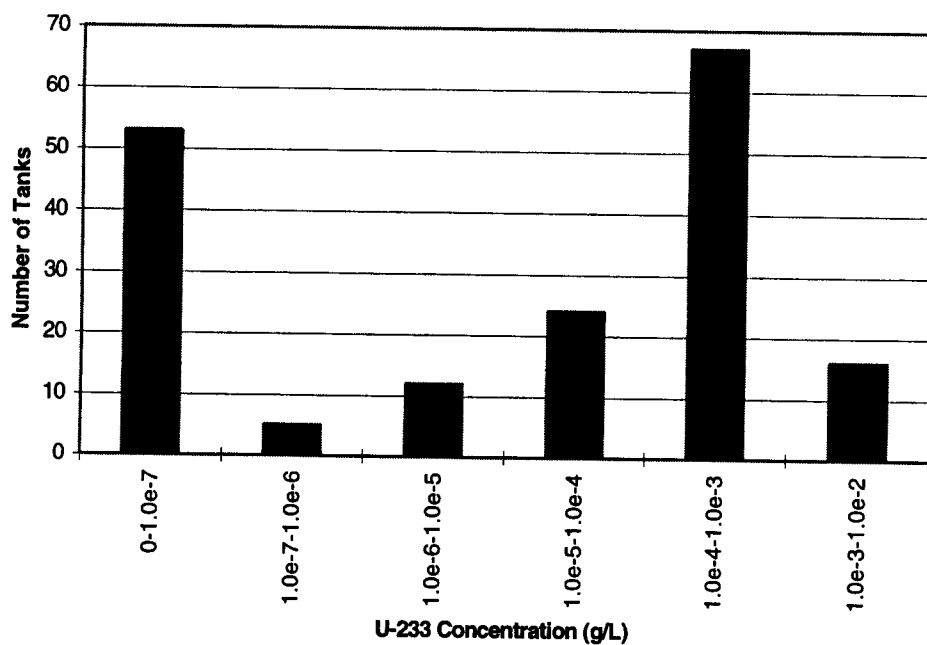
Figure 5-1. Histogram of the number of Hanford waste tanks versus U-233 concentration. Values are based on the HDW model (Agnew, 1996b).
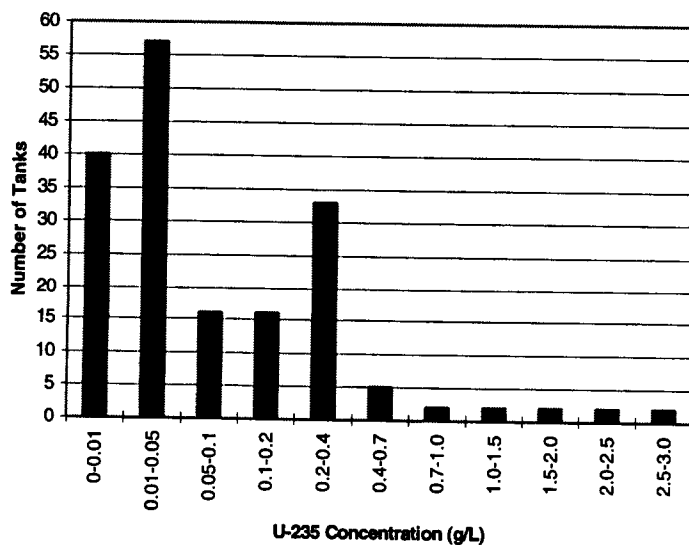
Figure 5-2. Histogram of the number of Hanford waste tanks versus U-235 concentration. Values are based on the HDW model (Agnew, 1996b).
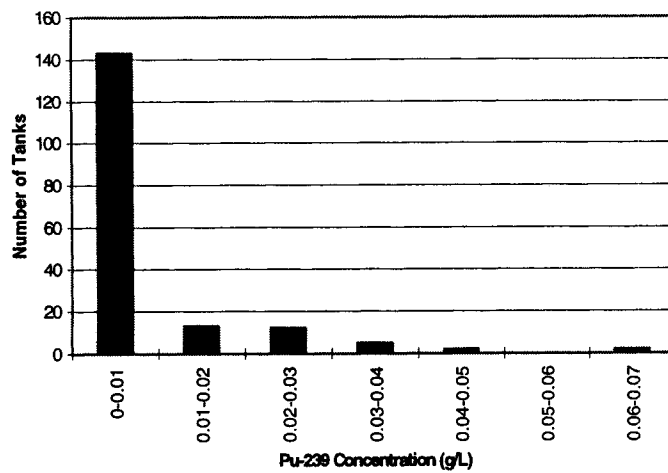
Figure 5-3. Histogram of the number of Hanford waste tanks versus Pu-239 concentration. Values are based on the HDW model (Agnew, 1996b).
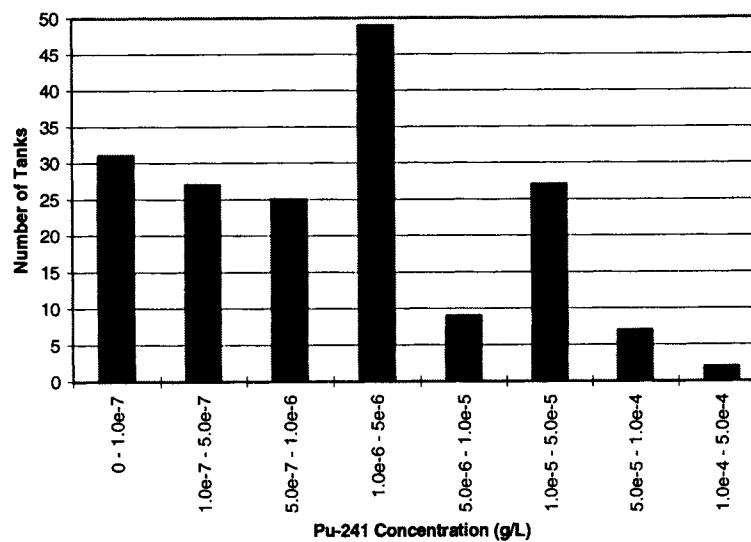
Figure 5-4. Histogram of the number of Hanford waste tanks versus Pu-241 concentration. Values are based on the HDW model (Agnew, 1996b).

5-8

Table 5-2. Listing of the Hanford tanks by total quantity of plutonium based on Agnew (1997)

Tanks with less than 200 grams of Pu	Tanks with 200 to 1000 g of Pu	Tanks with more than 1000 g of Pu		
AN-106	A-104	A-101	BY-106	SY-101
AP-104	AN-101	A-102	BY-109	SY-102
AP-107	AP-101	A-103	BY-110	SY-103
AX-103	AP-103	A-105	BY-111	T-101
B-103	AP-108	A-106	BY-112	T-102
B-107	B-102	AN-102	C-101	T-103
B-112	B-105	AN-103	C-102	T-104
B-201	B-106	AN-104	C-103	T-106
B-202	B-108	AN-105	C-104	T-110
B-203	BX-102	AN-107	C-105	T-111
B-204	BX-107	AP-102	C-106	TX-101
BX-104	BX-110	AP-105	C-107	TX-105
BX-105	BX-112	AP-106	C-109	TX-112
BX-106	BY-107	AW-101	C-111	TX-113
BX-108	BY-108	AW-102	C-112	TX-114
BX-109	C-201	AW-103	S-101	TX-115
C-108	C-202	AW-104	S-103	TX-116
C-110	C-203	AW-105	S-104	TX-117
SX-113	C-204	AW-106	S-105	TX-118
T-107	S-102	AX-101	S-106	U-102
T-108	SX-115	AX-102	S-107	U-103
T-201	T-105	AX-104	S-108	U-105
T-202	T-109	AY-101	S-109	U-107
T-203	T-112	AY-102	S-110	U-108
T-204	TX-102	AZ-101	S-111	U-109
TX-103	TX-106	AZ-102	S-112	U-111
TX-104	TX-108	B-101	SX-101	
TX-107	TX-109	B-104	SX-102	
TY-102	TX-110	B-109	SX-103	
TY-105	TX-111	B-110	SX-104	
TY-106	TY-101	B-111	SX-105	
U-101	TY-103	BX-101	SX-106	
U-104	TY-104	BX-103	SX-107	
U-110	U-106	BX-111	SX-108	
	U-112	BY-101	SX-109	
	U-201	BY-102	SX-110	
	U-202	BY-103	SX-111	
	U-203	BY-104	SX-112	
	U-204	BY-105	SX-114	

Table 5-3. A listing of the microscopic thermal neutron absorption cross section for the elements and isotopes listed in Agnew (1996b), excluding uranium and plutonium. Natural relative abundances given in parentheses (Parrington et al., 1996).

Element/ Isotope	Thermal Neutron Microscopic Absorption Cross Section (barns[a])	Element/ Isotope	Thermal Neutron Microscopic Absorption Cross Section (barns[a])	Element/ Isotope	Thermal Neutron Microscopic Absorption Cross Section (barns[a])
H-1 (0.99985)	0.333	Fe-58 (0.0028)	0.28	113m-Cd[b]	20,600
H-3	6E-06	Co-60	2	Sb-125	—
C (nat)	0.0035	Ni-58 (0.6808)	4.6	I-129	30
C-14	<1E-06	Ni-59	94	Cs-134	140
N-14 (0.9963)	1.89	Ni-60 (0.2622)	2.9	Cs-137	0.25
O-16 (0.9976)	0.00019	Ni-61 (0.0114)	2.5	Ba-137m[c]	5.1
F (nat)	0.009	Ni-62 (0.0363)	14.5	Sm-151	15,200
Na-23 (1.0000)	0.53	Ni-63	24	Eu-152	11,000
Al-27 (1.0000)	0.23	Ni-64 (0.0093)	1.8	Eu-154	1,400
Si (nat)	0.168	Bi-209 (1.0000)	0.034	Eu-155	3,900
P (nat)	0.17	La-139 (0.9991)	9.0	Ra-226	13
S (nat)	0.52	Hg (nat)	374	Ra-228	36
Cl (nat)	33.5	Zr (nat)	0.184	Ac-227	900
K (nat)	2.1	Pb (nat)	0.171	Pa-231	200
Ca (nat)	0.43	Se-79	—	Th-229	60
Cr-50 (0.0435)	15.5	Sr (nat)	1.2	Th-232	737
Cr-52 (0.8379)	0.8	Sr-90	0.01	Np-237	150
Cr-53 (0.0950)	18	Y-90	<7	Am-241	600
Cr-54 (0.0236)	0.36	Zr-93	1	Am-243	78
Mn-55 (1.0000)	13.3	Nb-93m	15.4	Cm-242	20
Fe-54 (0.0585)	2.3	Tc-99	20	Cm-243	130
Fe-56 (0.9175)	2.6	Ru-106	0.15	Cm-244	15
Fe-57 (0.0212)	2.5	—	—	—	—

[a]1 barn = 10^{-24} cm^2
[b]data for Cd-113
[c]data for Ba-137

isotopic number density) is above a threshold value. Since the tank inventories are highly variable from tank to tank and the macroscopic absorption cross section is dependent on the number density of the isotope (i.e., the tank inventory homogeneously mixed with the tank volume), an average number density of each of the isotopes and elements in table 5-3 was calculated based on the inventories and tank volumes of one representative tank from each farm. The tanks that were used to calculate the average number densities are AX-102, BX-102, C-202, SX-113, U-106, TX-101, and SY-101. These tanks were chosen because their wastes contained the lowest fraction of water and, presumably, the highest fraction of contaminants. The tank average nuclide densities used for calculating $\sum_a^{th}$ are shown in table 5-4 and the resultant values of $\sum_a^{th}$ are shown in table 5-5.

A conservative threshold level of 10^{-6} cm^{-1} for the macroscopic absorption cross section is chosen to reflect the fact that some tanks may contain greater amounts of individual poisons than shown by the tank-averaged values in table 5-4. Given this threshold, the list of important isotopes and elements is H-1, N-14, O-16, Na-23, Al-27, Mn-55, Co-60, C, Si, P, S, Cl, K, Ca, Cr, Fe, Ni, Sm-151, Hg, and Pb. It is assumed that the important elements exist in their natural isotopic abundances.

ENDF/B-VI-based cross section files are available for use with Monte Carlo N Particle (MCNP) (Hendricks et al., 1994) for all of the important isotopes and elements with the exceptions of Sm-151, Co-60, Pb, and Hg. For Sm-151, ENDFB-V cross sections are available. However, no cross section files are available for Co-60, Pb, and Hg, hence these isotopes and elements were not included in the analyses. Data in table 5-5 would seem to indicate that the noninclusion of Co-60, Pb, and Hg in criticality analyses would have little effect on calculations of k_{eff} since their tank averaged macroscopic cross-sections are at least two orders of magnitude below those of other nuclides (e.g., Na-23) included in the analyses.

5.5.3 Approximation of Criticality Potential Based on One-Speed Reactor Theory

The definitions for parameters such as k_∞ and k_{eff} based on one-speed reactor theory are summarized in this section (LaMarsh, 1983). In one-speed reactor theory, all parameters whose values vary depending upon neutron energy (e.g., cross-sections) are assumed to be well approximated by constant values. These constant values could be energy-averaged values, however, because situations encountered in TWRS operations would likely be highly moderated. Discussions in this section assume that neutrons travel at 2,200 m/s (i.e., neutrons have a kinetic energy dictated by thermal equilibrium with media nuclei).

The definition for k_∞ is given as follows

$$k_\infty = \eta f p \varepsilon \qquad (5\text{-}1)$$

where

η — neutron reproduction factor $= \nu \dfrac{\sum_f^F}{\sum_a^F}$

ν — average number of neutrons per fission

$\sum_f^F$ — macroscopic cross section for fission in fuel isotopes

$\sum_a^F$ — macroscopic cross section for absorption in fuel isotopes

5-11

Table 5-4. A listing of the tank-averaged number densities for the isotopes and element shown in table 5-3 (Agnew, 1997). Natural relative abundances given in parentheses.

Element/ Isotope	Tank-Averaged Number Density (moles/cm³)	Element/ Isotope	Tank-Averaged Number Density (moles/cm³)	Element/ Isotope	Tank-Averaged Number Density (moles/cm³)
H–1 (0.99985)	4.45E–02	Fe–58 (0.0028)	2.81E–06	Cd–113m	5.29E–12
H–3	4.56E–12	Co–60	2.70E–06	Sb–125	3.47E–12
C (nat)	2.80E–03	Ni–58 (0.6808)	2.53E–05	I–129	9.43E–15
C–14	6.84E–13	Ni–59	6.98E–13	Cs–134	5.54E–14
N–14 (0.9963)	4.73E–03	Ni–60 (0.2622)	9.76E–06	Cs–137	5.05E–09
O–16 (0.9976)	2.23E–02	Ni–61 (0.0114)	4.24E–07	Ba–137m	4.78E–09
F (nat)	3.22E–05	Ni–62 (0.0363)	1.35E–06	Sm–151	7.21E–10
Na–23 (1.0000)	1.12E–02	Ni–63	6.85E–11	Eu–152	1.22E–12
Al–27 (1.0000)	1.80E–03	Ni–64 (0.0093)	3.46E–07	Eu–154	6.45E–11
Si (nat)	1.39E–03	Bi–209 (1.0000)	6.44E–07	Eu–155	6.67E–11
P (nat)	6.81E–05	La–139 (0.99910)	2.30E–08	Ra–226	6.25E–17
S (nat)	1.43E–04	Hg (nat)	4.86E–08	Ra–228	3.32E–15
Cl (nat)	1.34E–04	Zr (nat)	1.10E–07	Ac–227	3.48E–16
K (nat)	4.51E–05	Pb (nat)	2.47E–05	Pa–231	3.08E–15
Ca (nat)	7.67E–05	Se–79	2.34E–13	Th–229	8.37E–17
Cr–50 (0.0435)	3.44E–06	Sr (nat)	0.00E+00	Th–232	2.71E–16
Cr–52 (0.8379)	6.62E–05	Sr–90	5.13E–08	Np–237	1.77E–14
Cr–53 (0.0950)	7.50E–06	Y–90	5.13E–08	Am–241	5.31E–11
Cr–54 (0.0236)	1.86E–06	Zr–93	1.06E–12	Am–243	5.10E–15
Mn–55 (1.0000)	2.05E–06	Nb–93m	7.28E–13	Cm–242	7.25E–14
Fe–54 (0.0585)	5.87E–05	Tc–99	4.89E–12	Cm–243	8.06E–15
Fe–56 (0.9175)	9.21E–04	Ru–106	1.96E–14	Cm–244	3.01E–13
Fe–57 (0.0212)	2.13E–05	—	—	—	—

Table 5-5. A listing of the macroscopic absorption cross sections generated from the tank-averaged number densities (table 5-4) and the thermal macroscopic absorption cross sections (table 5-3)

Element/ Isotope	Thermal Neutron Macroscopic Absorption Cross Section (cm⁻¹)	Element/ Isotope	Thermal Neutron Macroscopic Absorption Cross Section (cm⁻¹)	Element/ Isotope	Thermal Neutron Macroscopic Absorption Cross Section (cm⁻¹)
H–1	8.93E–03	Fe–58	4.74E–07	Cd–113m	6.56E–08
H–3	1.65E–17	Co–60	3.25E–06	Sb–125	NA
C	5.91E–06	Ni–58	7.02E–05	I–129	1.70E–13
C–14	4.12E–19	Ni–59	3.95E–11	Cs–134	4.67E–12
N–14	5.39E–03	Ni–60	1.70E–05	Cs–137	7.60E–10
O–16	2.55E–06	Ni–61	6.39E–07	Ba–137m	1.47E–08
F	1.75E–07	Ni–62	1.18E–05	Sm–151	6.60E–06
Na–23	3.57E–03	Ni–63	9.91E–10	Eu–152	8.05E–09
Al–27	2.49E–04	Ni–64	3.75E–07	Eu–154	5.44E–08
Si	1.41E–04	Bi–209	1.32E–08	Eu–155	1.57E–07
P	6.97E–06	La–139	1.25E–07	Ra–226	4.89E–16
S	4.48E–05	Hg	1.09E–05	Ra–228	7.20E–14
Cl	2.71E–03	Zr	1.22E–08	Ac–227	1.89E–13
K	5.70E–05	Pb	2.54E–06	Pa–231	3.71E–13
Ca	1.99E–05	Se–79	NA	Th–229	3.02E–15
Cr–50	3.21E–05	Sr	0.00E+00	Th–232	1.20E–13
Cr–52	3.19E–05	Sr–90	3.09E–10	Np–237	1.60E–12
Cr–53	8.13E–05	Y–90	2.16E–07	Am–241	1.92E–08
Cr–54	4.04E–07	Zr–93	6.37E–13	Am–243	2.40E–13
Mn–55	1.65E–05	Nb–93m	6.76E–12	Cm–242	8.74E–13
Fe–54	8.14E–05	Tc–99	5.89E–11	Cm–243	6.31E–13
Fe–56	1.44E–03	Ru–106	1.77E–15	Cm–244	2.72E–12
Fe-57	3.21E–05	—	—	—	—

$$f \quad - \quad \text{thermal utilization factor} = \frac{\sum_{a}^{F}}{\sum_{a}^{T}}$$

$\sum_{a}^{T}$ — total macroscopic cross section for the composite material (fuel, moderator, and absorbers)

p — resonance escape probability

ε — fast fission factor.

The macroscopic cross section for a reaction (i.e., absorption, fission) and element is the product of the atom number density and the microscopic cross section (σ). For example, $\sum_{a}^{F}$ for a Pu-239–light water system would be the product of the atom number density of Pu-239 (n^F) and the microscopic cross section for absorption for Pu-239 (σ_{a}^{F}). Also, the macroscopic cross sections are additive, so for this system, $\sum_{a}^{T}$ is the sum of $\sum_{a}^{F}$ and $\sum_{a}^{H_2O}$. It is noted that, for systems with a large amount of hydrogen (i.e., highly moderated), p and ε approach unity and that k_∞ is strictly a function of material properties.

The definition of k_{eff} is as follows

$$k_{\text{eff}} = k_\infty \, P_{\text{NL}-t} \, P_{\text{NL}-f} = k_\infty \, P_{\text{NL}} \qquad (5\text{-}2)$$

where

$P_{\text{NL}-t}$ — probability of nonleakage from the finite system for thermal neutrons

$P_{\text{NL}-f}$ — probability of nonleakage from the finite system for fast neutrons

P_{NL} — total nonleakage probability

The total nonleakage probability is given by

$$P_{\text{NL}} = \frac{\exp\left(-\tau_{th} B_g^2\right)}{1 + L^2 B_g^2} \qquad (5\text{-}3)$$

where

B_g — material buckling

L — thermal neutron diffusion length

— $\sqrt{\dfrac{1}{3\Sigma_a^T\left(\Sigma_a^T + \sum_i \left(1 - \overline{\mu}_{0-i}\right) \Sigma_s^i\right)}}$

$\overline{\mu}_{0-i}$ — 2/(3A) where A is the number of nucleons in isotope i

$\sum_s^i$ — macroscopic scattering cross section of isotope i

τ_{th} — fermi-age corresponding to thermal energies.

Data values for cross sections, average number of neutrons per fission, and others can be found in numerous sources including Duderstadt and Hamilton (1975) and LaMarsh (1983). Methods to calculate fermi-ages can also be found in numerous references. The value of B_g for several common shapes is presented in table 5-6. The parameter B_g, which represents the ratio of the curvature of the neutron flux profile to the magnitude of the flux, is needed to calculate the non-leakage probability [Eq. (5-3)] and k_{eff} [Eq. (5-2)] of a system in one-speed reactor theory.

One-speed reactor theory could be used to make rough estimates of k_{eff} for situations arising during continued storage, retrieval, and processing the Hanford tank wastes to determine where more detailed analyses are required. This approach has at least two limitations: (i) the results of these approximations could not be guaranteed to be conservative; and (ii) considering the number of calculations required (e.g., cross sections for numerous isotopes and especially fermi-ages), the rough estimates may be more cumbersome than performing more detailed analyses using codes such as MCNP. The next sections outline an approximate method for determining where criticality may be a problem based on MCNP code runs, which is much less cumbersome than performing calculations based on one-speed reactor theory.

5.5.4 An Approximate Method for Rapidly Determining k_{eff} for Tank Wastes with Concentrated Plutonium

This section presents an approximate method, based on MCNP4A code runs, that will allow an investigator to rapidly and conservatively assess the criticality potential of tank wastes under several geometries when the Pu in the waste has been concentrated (e.g., via a precipitation mechanism). The calculations described in this section are rough, conservative estimates and are not intended to replace detailed, but more computationally intensive, analyses that calculate k_{eff} from direct solution of the Boltzmann equation for neutron transport (Duderstadt and Hamilton, 1975). They are, however, designed to aid in determining where more detailed analyses are required.

5.5.4.1 k_∞ for Several Tank Wastes

To rapidly assess the criticality potential of tank wastes, the k_∞ of the waste must be estimated. This section describes calculations made to determine the significance of poisons with respect to k_∞ and determine k_∞ for a water-plutonium system.

Table 5-6. Values of geometric buckling, B_g, for several common shapes (Knief, 1992)

Shape	Geometric Buckling
sphere (radius = R)	$(\pi/R)^2$
finite cylinder (radius = R, height = H)	$(2.405/R)^2 + (\pi/H)^2$
infinite cylinder (radius = R)	$(2.405/R)^2$
Cuboid (rectangular parallelepiped) (length = A, width = B, height = C)	$(\pi/A)^2 + (\pi/B)^2 + (\pi/C)^2$
infinite slab (thickness = A)	$(\pi/A)^2$

The k_∞ values of selected tank wastes were calculated using the MCNP4A code. Along with the k_∞ values, a multiplicative factor for the increase in Pu concentration necessary for a k_∞ value equal to 1 and the corresponding Pu-239 concentration were calculated. These multiplicative factors indicate the minimum concentration increase of Pu-239 required to make criticality possible. These results are shown in table 5-7. It is noted that the Pu-239 concentrations required for a k_∞ of 1 are not greatly different than the 7.2 g/L required for a pure Pu-239–water system (Knief, 1992), implying that poisons at the present tank concentrations are not extremely effective at preventing criticality. This result is probably due to the high enrichment of Pu in the tank (i.e., a small amount of Pu can add a significant amount of reactivity to a system). Since criticality of the tank wastes will probably become an issue only if Pu concentrating mechanisms (relative to other tank wastes) such as precipitation are realized, neglecting the presence of poisons in criticality calculations is not as overly conservative as one would expect. An anomaly shown in table 5-7 is the relatively high value of k_∞ for the waste in tank BX-103 in its current condition. This anomaly is due to the U present in the tank. As discussed earlier, U at this enrichment has a net poisoning effect on critical systems. A plot of k_∞ as a function of Pu-239 concentration in a Pu-239–light water system is shown in figure 5-5. The plot was generated using MCNP4A. This information will be used later in this chapter for estimating k_{eff}.

An alternate approach to neglecting the presence of neutron absorbers in determining k_∞ for tank wastes is to determine k_∞ analytically using energy-averaged (more accurate) or thermal neutron (less accurate) cross section data as described in the preceding section. Due to limited availability of energy-averaged cross sections for some of the important absorbers, thermal neutron cross sections were used for these calculations. This approach was used for analytically calculating k_∞ for the tanks listed in table 5-7 with Pu concentrations multiplied by the factor necessary for a k_∞ of 1. The results of these calculations, along with the percent difference from the value calculated using MCNP4A, are shown in table 5-8. A problem with this approach is that the estimates cannot be guaranteed to be conservative.

5.5.4.2 Leakage Probabilities for Several Common Shapes

Although the previous information concerning k_∞ is useful, real systems are finite and will have some neutron leakage out of the system. Because very little is known about the configurations to which tank wastes may be exposed, nonleakage probabilities have been calculated for several common shapes and sizes. These

Table 5-7. A listing of the values of selected tank wastes along with the factor increase in the plutonium concentration required for a $k_\infty = 1$ and the corresponding Pu-239 concentration

Tank	k_∞ (present concentrations)	Plutonium Multiplicative Factor Necessary for $k_\infty \approx 1$	Corresponding Pu-239 Concentration (g/L)
241-AW-104	0.00200 + 0.00004	2,300	7.67
241-BX-103	0.29946 + 0.00074	1,430	7.27
241-TX-118	0.01619 + 0.00010	133	8.17
241-SY-102	0.00395 + 0.00020	530	7.94
241-C-102	0.05244 + 0.00021	210	7.44
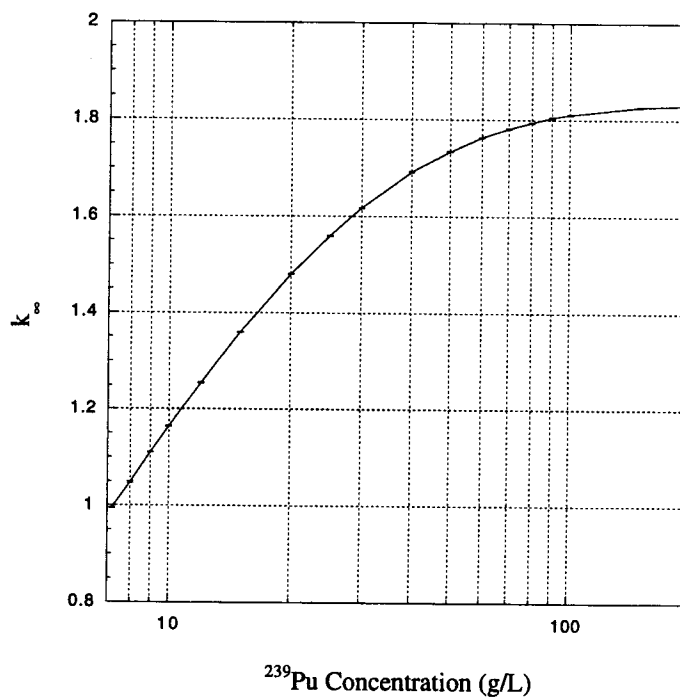
Figure 5-5. A plot of k_∞ as a function of Pu-239 concentration for a Pu-239-water system

Table 5-8. The value of k_∞ for tank wastes as calculated using analytical methods and Monte Carlo N-Particle Version 4A code, and the percent difference between the two methods

Tank	Plutonium Multiplicative Factor Necessary for $k_\infty \approx 1$	k_∞ (analytical)	k_∞ (MCNP4A)	Percent Difference (from the MCNP4A value)
241-AW-104	2,300	0.97261	1.00691 ± 0.00124	3.4
241-BX-103	1,430	1.05631	1.00352 ± 0.00313	5.2
241-TX-118	133	0.96629	0.99548 ± 0.00213	-2.9
241-SY-102	530	0.98416	1.01167 ± 0.00184	-2.7
241-C-102	210	1.00267	1.01585 ± 0.00187	-1.3

nonleakage probabilities (P_{NL}) were calculated as the ratio of k_{eff}/k_∞ for a material with the composition of the waste in tank TX-118 (a high poison bearing tank) with the Pu concentration multiplied by a factor of 133 (i.e., the factor increase in concentration necessary for k_∞ to equal 1). Both k_{eff} and k_∞ were calculated using MCNP4A.

The calculated values are conservative only for compositions that are less dense, because a greater density would shorten the neutron diffusion length (L in equation 5-3) and thus increase P_{NL}. For this reason, a density of 2.0 g/cm^3 with the relative isotopic abundances of the waste in tank TX-118 was used. It is noted that k_∞ for this mixture is still approximately equal to one.

Figure 5-6 shows a plot of P_{NL} for an infinite cylinder (a reasonable analogue for a pipe or conduit) as a function of radius for both a reflected and unreflected cylinder. Figure 5-7 shows a similar plot of P_{NL} for a right, square, circular cylinder as a function of radius, and figure 5-8 shows a similar plot of P_{NL} for an infinite slab as a function of thickness. If a situation arises that is not well described by any of the shapes mentioned in the previous paragraph, a value of P_{NL} can be conservatively approximated by determining P_{NL} for a sphere with an equivalent volume as the shape in question. This method would be guaranteed to be conservative because a sphere has the smallest surface area for a given volume and hence the largest value of P_{NL} for that volume. Figure 5-9 shows a plot of P_{NL} for a sphere as a function of radius for both a reflected and unreflected sphere.

5.5.4.3 Estimating k_{eff}

Equation (5-2) describes how k_{eff} can be calculated as the multiplication of k_∞ and P_{NL} for finite systems. The most conservative method to rapidly assess k_∞ is to neglect the presence of poisons and determine k_∞ directly from figure 5-5. Calculating k_∞ based on Eq. (5-1) may reduce some of this conservatism for tank wastes where a significant poison has been concentrated along with Pu; however, these calculations could not be guaranteed to be conservative. As noted previously, at the current tank concentrations, poisons are not effective at preventing criticality.

Figures 5-6 through 5-9 show conservative estimates for P_{NL} for various geometries. By multiplying the estimate of k_∞ by the appropriate estimate of P_{NL} (e.g., use figure 5-7, which plots P_{NL} estimates for a finite cylinder, to estimate P_{NL} for a 55-gal. drum), an estimate for k_{eff} can be found.

5.5.4.4 Example Calculations and Determination of the Level of Conservatism in the Approximate Method

To determine the level of conservatism in the approximate method, a few sample calculations were performed in which k_{eff} was calculated by (i) the approximate method and (ii) by the MCNP4A code runs. The k_{eff} value was calculated by multiplying k_∞ for a Pu-239–light water system by the appropriate value of P_{NL} from figures 5-6 through 5-9, as described in sections 5.5.4.2 and 5.5.4.3. Table 5-9 contains the results of these calculations. A great deal of the conservatism in the approximate method for estimating k_{eff} in this section results from the calculated values of P_{NL} due to the assumption that the waste has a density of 2.0 g/cm^3. It is noted that, for situations in which the poisons have also been significantly concentrated, the approximate method may become quite conservative.
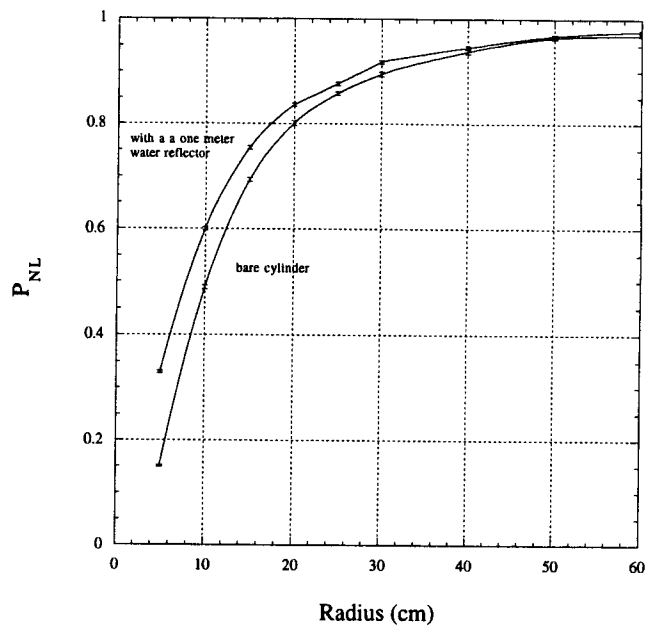
Figure 5-6. A plot of P_{NL} as a function of radius for a bare and water-reflected infinite cylinder
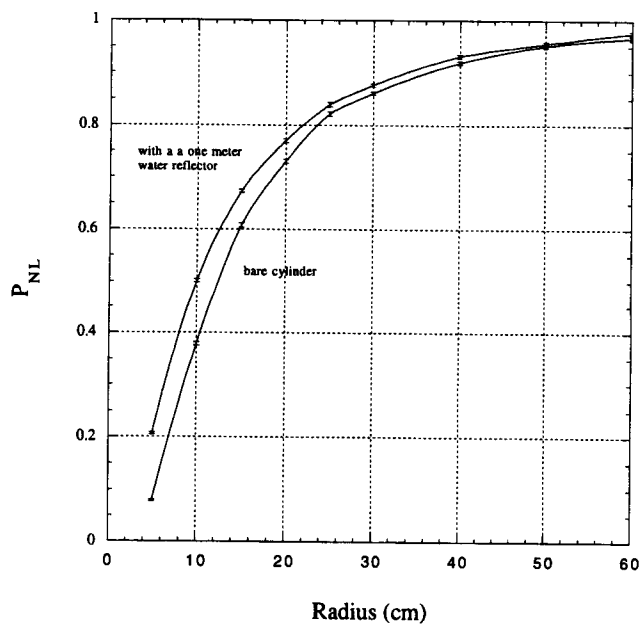
Figure 5-7. A plot of P_{NL} as a function of radius for a right, square circular cylinder
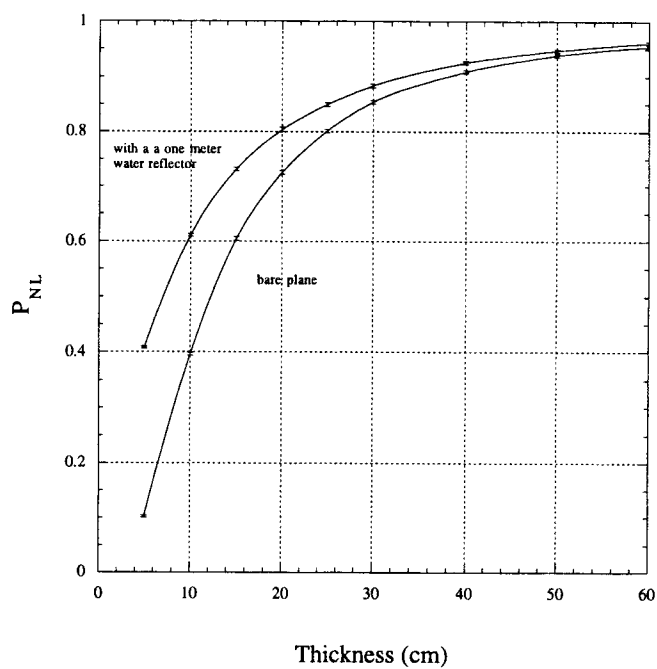
Figure 5-8. A plot of P_{NL} as a function of thickness for a bare and water-reflected infinite plane
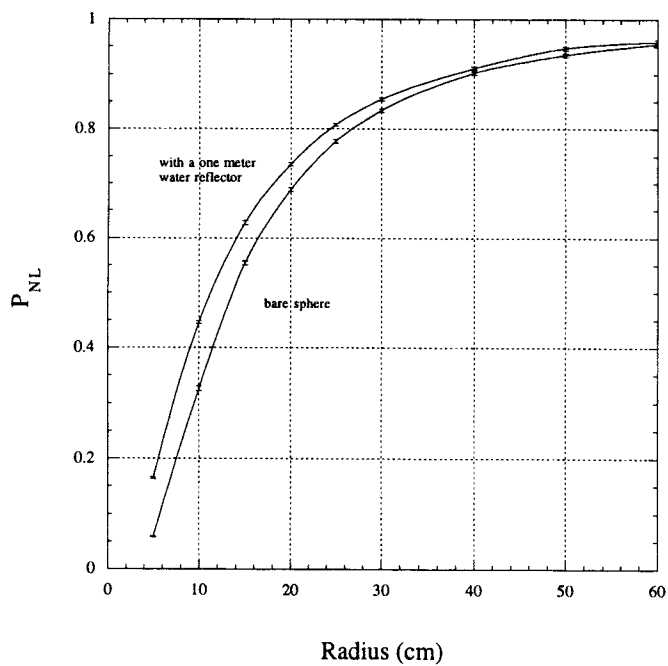
Figure 5-9. A plot of P_{NL} as a function of radius for a bare and water-reflected sphere

Table 5-9. Sample calculations to determine the conservatism in the approximate method

Description	k_{eff} (MCNP4A)	k_{eff} (approximate method)
Tank BX-103 waste with the Pu concentration multiplied by 1,575[a] (8.0 g/L of Pu-239); right, square, reflected cylinder with a radius of 20 cm	0.68741	0.81
Tank BX-103 waste with the Pu concentration multiplied by 1,575[a] (8.0 g/L of Pu-239); right, square, reflected cylinder with a radius of 60 cm	0.94687	1.02
Tank SY-102 waste with the Pu concentration multiplied by 670[a] (10.0 g/L of Pu-239); right, square, reflected cylinder with a radius of 30 cm	0.83975	1.02
Tank SY-102 waste with the Pu concentration multiplied by 6,700[a] (100.0 g/L of Pu-239); right, square, reflected cylinder with a radius of 10 cm	0.65244	0.91
Tank C-102 waste with the Pu concentration multiplied by 283[a] (10.0 g/L of Pu-239); infinite plane 10 cm thick with reflector	0.60420	0.71
Tank C-102 waste with the Pu concentration multiplied by 283[a] (10.0 g/L of Pu-239); infinite plane 50 cm thick with reflector	1.05134	1.09
Tank AW-104 waste with the Pu concentration multiplied by 3,000[a] (10.0 g/L of Pu-239); infinite cylinder of 10 cm radius with reflector	0.45895	0.70
Tank AW-104 waste with the Pu concentration multiplied by 3,000[a] (10.0 g/L of Pu-239); infinite cylinder of 50 cm radius with reflector	1.03259	1.13

[a]These factors represent the increase in Pu concentrations necessary for k_∞ to become equal to 1. A $k_\infty = 1$ is necessary for criticality to be possible, regardless of system geometry.

5.6 MECHANISMS FOR CONCENTRATION OF FISSILE MATERIAL

As discussed in section 5.5.1, Pu (in particular, the isotope ^{239}Pu) is the only fissile element in Hanford tank wastes that poses a potential criticality hazard. In this section, the range of chemical processes that may lead to the concentration of Pu above critical levels is discussed; physical mechanisms for concentrating Pu-rich solids are not discussed. Inclusion in this section of a particular process does not imply that it is a likely mechanism of attaining criticality—it is merely an attempt to survey several possible mechanisms. For example, the 7.2 g/L Pu criticality threshold mentioned in section 5.3 coincides with a solution concentration of 3×10^{-2} M; it is recognized that this would be an unusually high dissolved Pu content. Nevertheless, knowledge of aqueous Pu chemistry in waste systems is useful not only for criticality considerations, but also for issues such as human health and environmental protection, and Pu fate during separation of HLW and low-level waste (LLW) components. In this section, consideration is given to processes in the tanks in their present condition, as well as those resulting from processing (including

retrieval and sludge washing). Also included is a brief discussion of chemical processes potentially affecting the fate of important neutron absorbers.

5.6.1 Plutonium Speciation

5.6.1.1 Oxidation State

Plutonium has a complex redox chemistry, with possible oxidation states ranging from +3 to +6 in aqueous solutions (Newton and Baker, 1967; Choppin, 1983; Seaborg, 1993; and many others). The oxidation state (or states) of Pu in a particular chemical setting has a fundamental influence on its chemical behavior. This is because the different oxidation states will show differing tendencies to form complexes with particular chemical species or compounds, and so will differ in what solid phases they will form and in how much will be present in solution. For example, as will be discussed in section 5.6.2, it is possible that Pu(VI) may achieve higher solubility-limited dissolved concentrations than Pu(IV) at high pH. If this is so, then oxidation of tank wastes during waste retrieval and pretreatment could result in some transfer of Pu from solid to liquid. Also, oxidation state will directly affect the extent of sorption or coprecipitation of Pu with tank waste solids, as well as the fate of Pu during any processing that changes the chemistry of the wastes.

Many studies have been conducted on the chemical properties of Pu. Unfortunately, the majority are centered on acidic systems relevant to Pu separation processes. The Hanford tank waste liquids (Agnew, 1997) are characterized by high ionic strength and high pH, the latter due to addition of NaOH for acid neutralization prior to transfer to the tanks (Gephart and Lundgren, 1995). Very few studies have been carried out on the chemical behavior of Pu in such systems.

Acknowledging this lack of data, Serne et al. (1996), in their analysis of criticality potential in Hanford tanks, concluded on the basis of several lines of evidence that Pu(IV) was likely to be the dominant oxidation state for aqueous Pu. The evidence included (i) experimental work in highly alkaline, reducing systems (Yamaguchi et al., 1994; Delegard, 1995), (ii) the fact that Pu(IV) forms stronger complexes than other oxidation states (figure 4 in Kim, 1986), and (iii) the relatively low Eh in Hanford tanks due to the presence of reductants such as sodium nitrite and organic compounds.

This conclusion is consistent with previous work which, though emphasizing more dilute environmental aqueous systems, implies the dominance of Pu(IV) at high pH in reducing systems. Figure 5-10 shows two illustrative examples (Allard et al., 1980; Paquette and Lemire, 1981). It is important to note, however, that these studies rest on thermodynamic calculations that relied on meager data on Pu carbonate speciation.

The high pH values expected in tank supernates were checked by inspection of the current tabulation of tank sample pH measurements in the TWINS database (http://twins.pnl.gov:8001/TCD/main.html). Including all 436 values reported (which include replicate analyses), the mean pH is 11.8, the median is 12.3, and the range is 6.9 to 14.2 (the single 6.9 value is the only one below 8 reported). Counting only the 397 measurements that have been critically reviewed and accepted, the mean is 11.9, median 12.4, and range 8.0 to 14.2. Therefore, the premise of high pH in tank liquids appears valid.

Furthermore, inspection of nitrite analyses in the TWINS database suggests that it is always present above minimum detection limits, supporting the premise that conditions are generally reducing in tank liquids. Consistent with this observation are the significant contents of organic species (Agnew, 1997).

Pu(IV)

$a = Pu(OH)_5^-$

$b = Pu(OH)^{3+} = Pu(HPO_4)_3^{2-}$

$d = Pu(HPO_4)_4^{4-}$

$h = Pu(OH)_4(aq)$

Pu(III)

$c = Pu(H_2PO_4)^{2+}$

$e = Pu^{3+}$

$f = Pu(OH)^{2+}$

$g = PuSO_4^+$
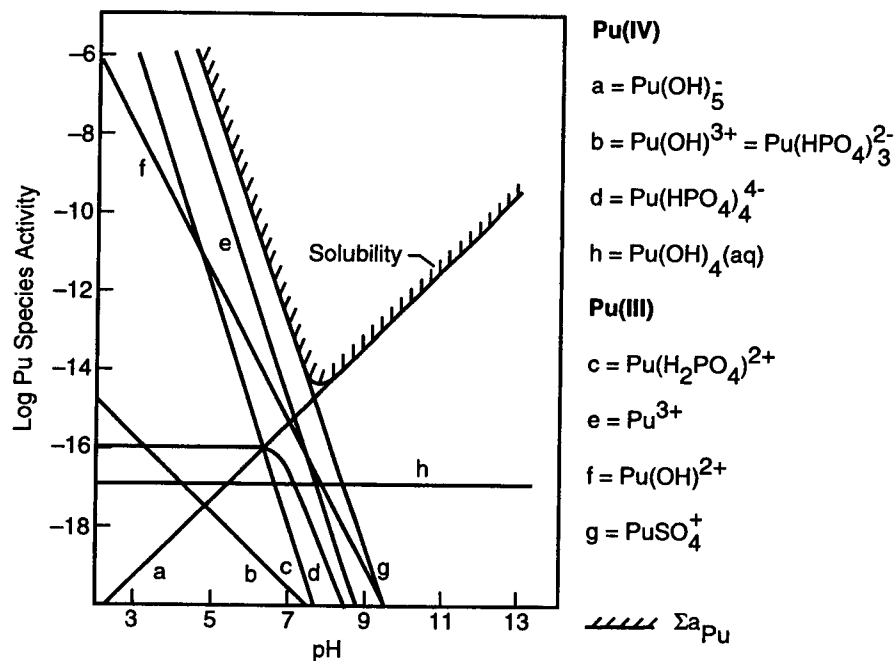
(a)
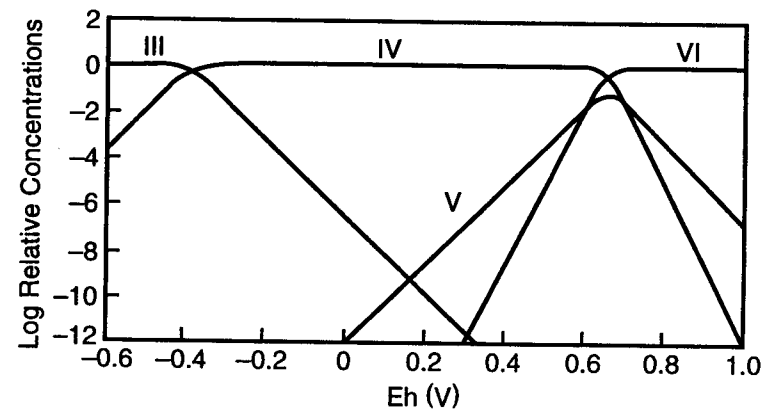
(b)

Figure 5-10. Pu speciation diagrams for dilute aqueous systems. These calculations did not include consideration of the hydroxycarbonate Pu(IV) species discussed in the text and are only illustrative of earlier studies suggestive of dominance of Pu(IV) stability fields. Diagram (a), modified from Paquette and Lemire (1981), shows Pu species distribution in a model groundwater assuming equilibrium with PuO_2 solid and reduction potential set by the hematite/magnetite buffer: $3Fe_2O_3 + 2H^+ + 2e^- = 2Fe_3O_4 + H_2O$. Valence state is shown in brackets next to species; at pH > 8, the tetravalent species $Pu(OH)_5^-$ and $Pu(OH)_4^0$ dominate. Diagram (b) shows Pu valence distribution as a function of Eh at pH = 8, calculated using only hydrolysis constants (after Allard et al., 1980).

Support for the conclusion that these conditions favor Pu(IV) species in Hanford tank liquids is demonstrated graphically in figure 5-11, which is a modified reproduction of figure 5 of the Yamaguchi et. al. (1994) experimental study. The plot shows calculated stability fields of aqueous Pu species in Eh(pe) versus pH space with total carbonate set to 4×10^{-3} M, and includes consideration of hydroxycarbonate species that were not recognized by most earlier studies. The dashed line represents Eh-pH conditions imposed by equilibrium between equal concentrations of nitrate and nitrite (see previous text), and it lies within two fields representing proposed Pu(IV) species (discussed in more detail in the following section). Other experimental work showing Pu(IV) dominance in alkaline, carbonate-rich solutions include Delegard (1995) and Tait et al. (1995). In the former study, conventional spectroscopic analyses suggested Pu(IV) carbonate species of unspecified stoichiometry in reductant-containing, high-ionic strength $NaOH/Na_2CO_3$ solutions. Tait et al. (1995) used photoacoustic spectroscopy to confirm the existence of Pu(IV) hydroxycarbonate species at high pH over a range of total carbonate concentrations of 0.003–1.0 M.

5.6.1.2 Speciation

The conclusion of Serne et al. (1996) that Pu(IV) is likely dominant in Hanford tank waste liquids appears reasonable. To further characterize the chemical behavior of Pu, it is necessary to understand the particular Pu complexes that are most abundant. Table 5-10 shows stability constants for a variety of complexes of Pu with ligands of potential importance to Hanford waste, as compiled by Serne et al. (1996). The stability constants are the equilibrium constants of the reactions of formation of the complexes from their base constituents, for example,

$$Pu^{4+} + NO_3^- \rightleftharpoons PuNO_3^{3+} \tag{5-4}$$

$$Pu^{4+} + 4OH^- + 2CO_3^{2-} \rightleftharpoons Pu(OH)_4(CO_3)_2^{4-}. \tag{5-5}$$
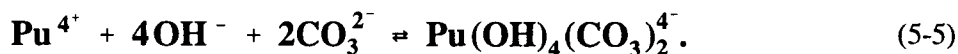
Serne et al. (1996) have shown that, for Hanford tank supernates, the hydroxycarbonate species as identified by Yamaguchi et al. (1994) may dominate the Pu(IV) budget. Calculations showed that concentrations of Pu(IV) complexes with organic ligands such as EDTA (which can exceed carbonate in abundance in tank liquids) with high stability constants nevertheless will be dwarfed by the hydroxycarbonate complexes. Inspection of the hydrolysis constant for $Pu(OH)_4^0$ in table 5-10 would suggest that it would be important in the high OH^- tank liquids; however, Yamaguchi et al. (1994) showed that the two hydroxycarbonate complexes are favored by total carbonate concentrations greater than 10^{-4} M (pH = 9–10) or 10^{-3} M (pH = 12–13). Hanford tank liquid total carbonate concentrations typically far exceed these values (Serne, et. al., 1996; Agnew, 1997). In the Yamaguchi et al. (1994) model, at lower total carbonate concentrations, $Pu(OH)_4^0$ is the dominant species in this pH range. The existence of the $Pu(OH)_5^-$ species—suggested by the calculations of Paquette and Lemire (1981) and others to be dominant at high pH and low carbonate (figure 5-10a)—remains an open issue (Serne et al., 1996). Given the evidence for hydroxycarbonate species under high-carbonate tank waste conditions, the question of the existence of $Pu(OH)_5^-$ may be irrelevant.

The effects of radiolysis, high ionic strengths, and elevated temperature on Pu(IV) speciation have not been well studied. Serne et al. (1996) addressed these issues and concluded that, while temperature and ionic strength effects in the tanks will certainly affect Pu complex stability, the limited available data suggest that the relative importance of complexes is unlikely to be significantly altered. Similarly, they
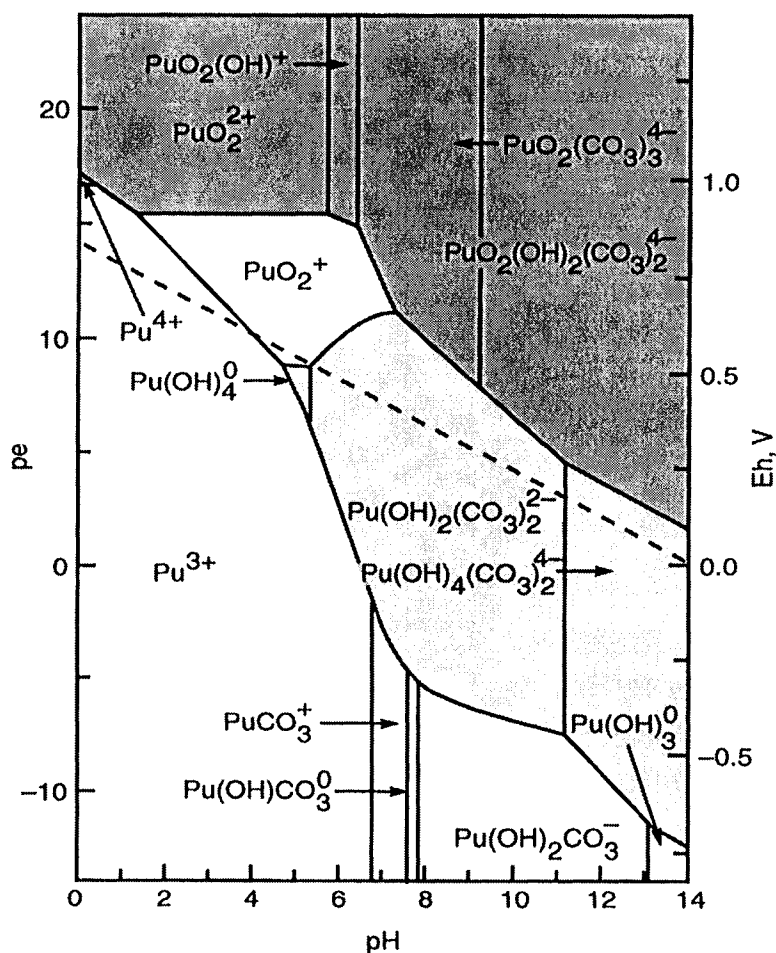
Figure 5-11. Eh-pH diagram of Pu at a total carbonate concentration of 4×10^{-3} M, modified from Yamaguchi et al. (1994). The dashed line represents conditions imposed at equal concentrations of nitrate and nitrite by the following half reaction: $\frac{1}{2} NO_2^- + \frac{1}{2} H_2O = \frac{1}{2} NO_3^- + H^+ + e^-$; conditions will vary negligibly when the concentrations of these two anions are within two orders of magnitude, as they typically are in Hanford supernates (Agnew, 1997). The light shading denotes Pu(IV) species dominance, while the heavier shading represents Pu(VI) fields.

Table 5-10. Stability constants for Pu(IV) complexes (Serne et al., 1996; Allard et al., 1980; value for Pu(OH)$_2$(CO$_3$)$_2^{2-}$ corrected to that published by Yamaguchi et al., 1994). Reported values are for ionic strength (I) of zero, except for species marked with an asterisk (*), which are for I = 0.1. Also listed are log Ks (I = 0.1) for the solubility reactions shown in Eqs. (5-7), (5-8), and (5-9).

Species	log K	Species	log K
Pu(OH)$^{3+}$	13	Pu(HPO$_4$)$_3^{2-}$	33
Pu(OH)$_2^{2+}$	26	Pu(HPO$_4$)$_4^{4-}$	43
Pu(OH)$_3^+$	37	Pu(OH)$_2$(CO$_3$)$_2^{2-}$	44*
Pu(OH)$_4^0$	47	Pu(OH)$_4$(CO$_3$)$_2^{4-}$	50*
PuCl^{3+}	0.9	Pu(citrate)$^{3+}$	~16
PuF^{3+}	8	Pu(citrate)$_2^{2+}$	~30
PuNO$_3^{3+}$	1.8	PuOH(EDTA)$^{2+}$	~17
PuSO$_4^{2+}$	6	Pu(C$_2$O$_4$)$^{2+}$	~9
Pu(SO$_4$)$_2^0$	3.5	Pu(C$_2$O$_4$)$_2^0$	~8
PuHPO$_4^{2+}$	13	Pu(C$_2$O$_4$)$_3^{2-}$	~7
Pu(HPO$_4$)$_2^0$	24	Pu(C$_2$O$_4$)$_4^{4-}$	~4
PuO$_2$ • xH$_2$O solubility Eq. (5-7)	-2.7*	Pu(OH)$_4$(s) solubility Eq. (5-9)	-10.14*
PuO$_2$ • xH$_2$O solubility Eq. (5-8)	-4.98*		

concluded—chiefly on the basis of a lack of overwhelming evidence to the contrary—that radiolysis is more likely to maintain the reducing conditions that favor Pu(IV). Serne et al. (1996) cite a study suggesting radiolytic oxidation of Pu in near neutral solutions (Sullivan, 1983) and two suggestive of net reducing effects in more alkaline systems (Pikaev, 1996; Camaioni et al., 1994). Experiments by Karraker (1994, 1995) on simulations of alkaline Savannah River wastes (similar to Hanford wastes) showed gamma-induced radiolytic increases in Pu solubility—interpreted as resulting from oxidation from Pu(IV) to Pu(VI)—at NaOH concentrations above ~3 M. The effect was greater with increasing hydroxide content, suggesting that higher OH$^-$ contributes to the radiolytic production of oxidizing species such as H$_2$O$_2$. On the other hand, experiments with beginning Pu(VI) solutions showed some decrease in solubility. The evidence for radiolytic effects does not appear to be conclusive, but the potential for oxidation to Pu(VI) should be considered. Oxidation/reduction reactions induced by radiolysis can be highly localized in their effects, with migration of oxidants and/or reductants, as well as kinetic constraints on redox reactions, potentially leading to nonequilibrium conditions. More confidence may be gained from Pu speciation determinations on actual Hanford tank wastes, as well as from radiolysis experiments on same.

Serne et al. (1996) assert that the key factors for Pu speciation are free carbonate and hydroxide concentrations in the liquid. Due to the sparseness of available data, it appears that more confident arguments presently may not be made for or against this conclusion.

It is important to note that, although the evidence appears strong that Pu(IV) will likely form dominantly hydroxycarbonate species under typical tank conditions (Yamaguchi et al., 1994; Delegard, 1995; Tait et al., 1995), there is a great deal of uncertainty in the precise stoichiometries and stability constants of the species. For example, the more generalized stoichiometries proposed by Tait et al. (1995) [e.g., $Pu(OH)_x(CO_3)_{y+1}^{(2-x-2y)}$] are not directly compatible with those interpreted by Yamaguchi et al. (1994). Accurate stoichiometric characterization, of course, is necessary for accurate thermodynamic analysis, but there is not yet consensus on the issue.

5.6.1.3 Other Oxidation States

It cannot be stated with certainty whether Pu oxidation states other than Pu(IV) will be important. Dominance of aqueous Pu(VI) and Pu(V) have been reported in both experimental (e.g., Nitsche et al., 1995) and observational (e.g., Nelson and Lovett, 1978; Orlandini et al., 1986) studies of Pu distribution in environmental waters. However, the chemical conditions in these studies (e.g., pH, ionic strength) differ markedly from those in the Hanford tanks, pointing once again to the paucity of data on Pu chemistry from appropriate systems. This lack of data limits the confidence with which chemical models may be applied to predicting Pu behavior.

Standard potentials for the four key Pu valences are shown in table 5-11; calculation of potentials at high pH is dependent on the speciation scheme used. Note that in figure 5-11, Pu(VI) species $[PuO_2(OH)_2(CO_3)_2^{4-}$ and $PuO_2(CO_3)_3^{4-}]$ occur at higher Eh-higher pH than the hypothesized Pu(IV) species $[Pu(OH)_2(CO_3)_2^{2-}$ and $Pu(OH)_4(CO_3)_2^{4-}]$. Therefore, in this model, chemical conditions varying relatively little from the nitrite/nitrate Eh-pH buffer could effect oxidation to Pu(VI). For example, enhanced sludge washing is a proposed method for waste treatment (U.S. Department of Energy, 1996a); it involves leaching tank sludges in NaOH solutions to remove nonradioactive components from tank solids, resulting in pH near 14. The stability fields of figure 5-11 suggest that increasing pH under oxidizing conditions (e.g., in air) could move Pu into the Pu(VI) stability field by a half reaction such as

$$Pu^{IV}(OH)_4(CO_3)_2^{4-} + 2OH^- = Pu^{VI}O_2(OH)_2(CO_3)_2^{4-} + 2e^- + 2H_2O$$
$$K = 10^{-3.0}$$

(5-6)
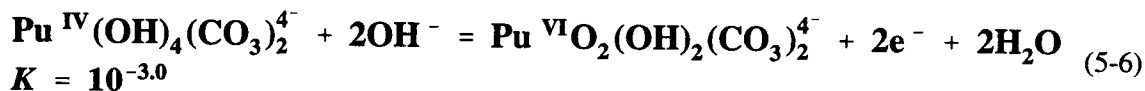
Table 5-11. Standard potentials for Pu oxidation states (Allard et al., 1980)

Valence Change	Reaction	$E^0(V)$
VI ↔ V	$PuO_2^{2+} + e^- = PuO_2^+$	0.933
VI ↔ IV	$PuO_2^{2+} + 4H^+ + 2e^- = Pu^{4+} + 2H_2O$	1.024
V ↔ IV	$PuO_2^+ + 4H^+ + e^- = Pu^{4+} + 2H_2O$	1.115
IV ↔ III	$Pu^{4+} + e^- = Pu^{3+}$	1.017

K was calculated from (i) the stability constant for $Np^{VI}O_2(OH)_2(CO_3)_2^{4-}$ in Yamaguchi et al. (1991) as an analog for the Pu(VI) species, (ii) the stability constant for $Pu^{IV}(OH)_4(CO_3)_2^{4-}$ in Yamaguchi et al. (1994), and (iii) the Pu(VI)–Pu(IV) standard potential in Allard et al. (1980). In low-carbonate systems at pH 14, this oxidation of the dominant Pu(IV) is predicted to occur at Eh = 0.34 V (Allard et al., 1980). It is difficult to quantify the likelihood of the Pu(IV)–Pu(VI) oxidation in Hanford tank liquids, but the possible effects of this process should be considered. The present report, following Serne et al. (1996), emphasizes Pu(IV) reactions, but considers, where appropriate, the possible effects of the presence of higher valence Pu.

5.6.2 Concentration of Plutonium in Liquids

There are two chief chemical mechanisms by which Pu concentration could increase in the liquid wastes: evaporation and dissolution of Pu-bearing solids. In either case, the simplest means of evaluating the potential for critical levels of aqueous Pu concentration is to assess solubility limits. The most conservative approach to solubility determination is to assume control by a relatively pure solid phase; this assumption can be made because other mechanisms for removing Pu from solution, such as coprecipitation and adsorption, will tend to keep liquid concentrations below pure phase solubility limits.

Serne et al. (1996) concluded from a critical review of a number of published studies (e.g., Rai et. al., 1980; Delegard, 1987b; Yamaguchi et al., 1994) that a hydrated Pu(IV) oxide of the general form $PuO_2 \bullet xH_2O$ is the solubility-controlling phase in Hanford tank wastes. They also concluded with less confidence, as discussed in section 5.6.1.2, that the key solution species are (i) $Pu(OH)_2(CO_3)_2^{2-}$ at pH less than around 11 and (ii) $Pu(OH)_4(CO_3)_2^{4-}$ at higher pH. This conclusion is based chiefly on the experimental work of Yamaguchi et al. (1994), in which the following solubility reactions are proposed:

$$PuO_2 \cdot xH_2O + 2HCO_3^- = Pu(OH)_2(CO_3)_2^{2-} + xH_2O$$
$$K = 10^{-2.7 \pm 0.5}$$
(5-7)

$$PuO_2 \cdot xH_2O + 2CO_3^{2-} = Pu(OH)_4(CO_3)_2^{4-} + (x-2)H_2O$$
$$K = 10^{-4.98 \pm 0.31}$$
(5-8)
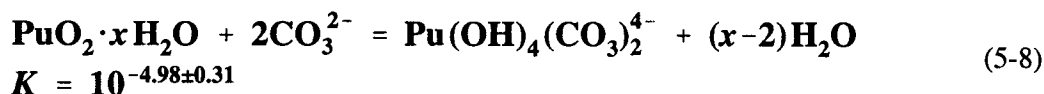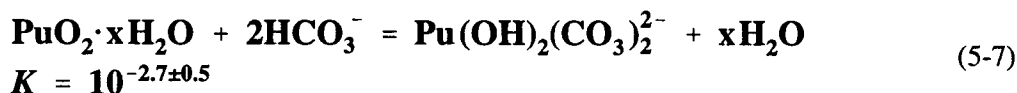
Note that the dominant Pu hydroxycarbonate species reflects the shift in carbonate species from bicarbonate to carbonate with higher pH. Total carbonate in the experiments ranged from 10^{-4} to 10^{-1} M, ionic strength (I) was 0.1, and Eh ranged from approximately 140-350 mV. At lower total carbonate concentrations (i.e., $<10^{-4}$ M for pH <11, $<10^{-3}$ M for pH >11), solubility is controlled by

$$Pu(OH)_4(s) = Pu(OH)_4^0$$
$$K = 10^{-10.14 \pm 0.28} \text{ (Ewart et al., 1985)}$$
(5-9)
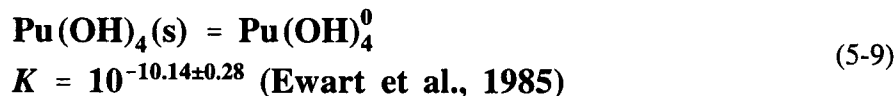
with $Pu(OH)_4^0$ constrained by the hydrolysis reaction

$$Pu^{4+} + 4OH^- = Pu(OH)_4^0$$
$$K = 10^{44.56 \pm 0.46} \text{ (Yamaguchi et al., 1994; calculated for I = 0.1)}$$
(5-10)
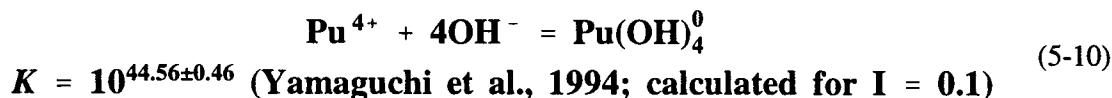
The $Pu(OH)_5^-$ species, the existence of which is in doubt (Serne et al., 1996), is neglected in this model. $Pu(OH)_4(s)$ is equivalent to $PuO_2 \cdot xH_2O$ when $x = 2$; the more general formula has been adopted in several studies (e.g., Rai et al., 1980; Delegard, 1987b; Yamaguchi et al., 1994) due to uncertainty in the specific stoichiometry of the solubility-limiting solid phase.

The Yamaguchi et al. (1994) solubility limits are plotted against total carbonate in figure 5-12, modified from Serne et al. (1996). The two curves show total Pu(IV) concentration at experimentally determined $PuO_2 \cdot xH_2O$ saturation for different pH ranges. Also plotted are measured Pu and carbonate data from actual Hanford tank supernates. Most supernates have elevated total carbonate concentrations of up to 1 M, which the experimental curves suggest increases Pu solubility. However, most supernate carbonate concentrations are above those of the experimental studies. All of the plotted supernate samples had pH $\geq$ 11.9, and thus should be compared with the pH = 12–13 solubility curve. Several samples plot substantially above this solubility curve or the extrapolation of the curve to higher carbonate, suggestive of Pu supersaturation and/or the inadequacy of the experimentally-based model.

Oxidation of dissolved Pu(IV) at high pH, according to the Yamaguchi et al. (1994) model, would lead to formation of the $Pu^{VI}O_2(OH)_2(CO_3)_2^{4-}$ species mentioned previously [Eq. (5-6)]. A solubility reaction for this species in equilibrium with $PuO_2 \cdot xH_2O$ can be written as follows, with K calculated from the data in Yamaguchi et al. (1994) and the constant calculated for Eq. (5-6):

$$PuO_2 \cdot xH_2O + 2CO_3^{2-} + 2OH^- = PuO_2(OH)_2(CO_3)_2^{4-} + 2e^- + xH_2O \tag{5-11}$$
$$K = 10^{-8.0}$$
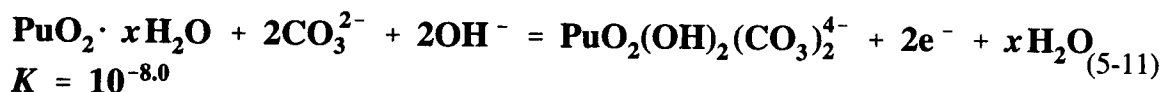
At pH = 12 and Eh = 0.25 V, this solubility relationship coincides graphically (figure 5-12) with that for Pu(IV) at lower pH. However, at pH = 14, calculated Pu(VI) solubilities are more than two orders of magnitude higher than the pH = 12-13 Pu(IV) curve of figure 5-12. Application of these relationships, however, requires some confirmation—now lacking—that the solubility-limiting solid has been properly assigned.

Aside from uncertainties in oxidation state, stoichiometries, ionic strength effects, equilibrium constants, and nonequilibrium effects, predicting dissolved Pu concentrations from these solubility models is dependent on the assumption that there are no other means for removing Pu from solution (e.g., coprecipitation). In light of this preponderance of uncertainty, it seems prudent to predict Pu concentrations based on empirical data. Lacking a more extensive thermodynamic database for Pu, experiments on actual simulated tank wastes are the only available means for prediction with a reasonable degree of confidence. Calculations based on thermodynamic models are useful for guiding discussion and investigations and for interpreting experimental data, but they must not be applied without careful consideration of the uncertainties.

In Delegard (1987b) (as reinterpreted by Delegard, 1995), Pu solubility in $NaOH/Na_2CO_3$ simulated waste supernates was measured as high as 2×10^{-5} M, and the data were found by Delegard (1995) to be consistent with the Yamaguchi et al. (1994) model of Pu(IV) solubility. Hobbs and Karraker (1996) performed experiments on simulations of waste supernate from tanks at Savannah River with similar chemical characteristics to the Hanford tank supernates. Solubilities were measured at varying ligand concentrations and statistical models were fit to the data. Solubilities determined in these experiments and in evaporation experiments ranged up to 2×10^{-4} M, increasing with NaOH concentrations above 2 M. They speculated that this increase could be related to oxidative solubility enhancement.
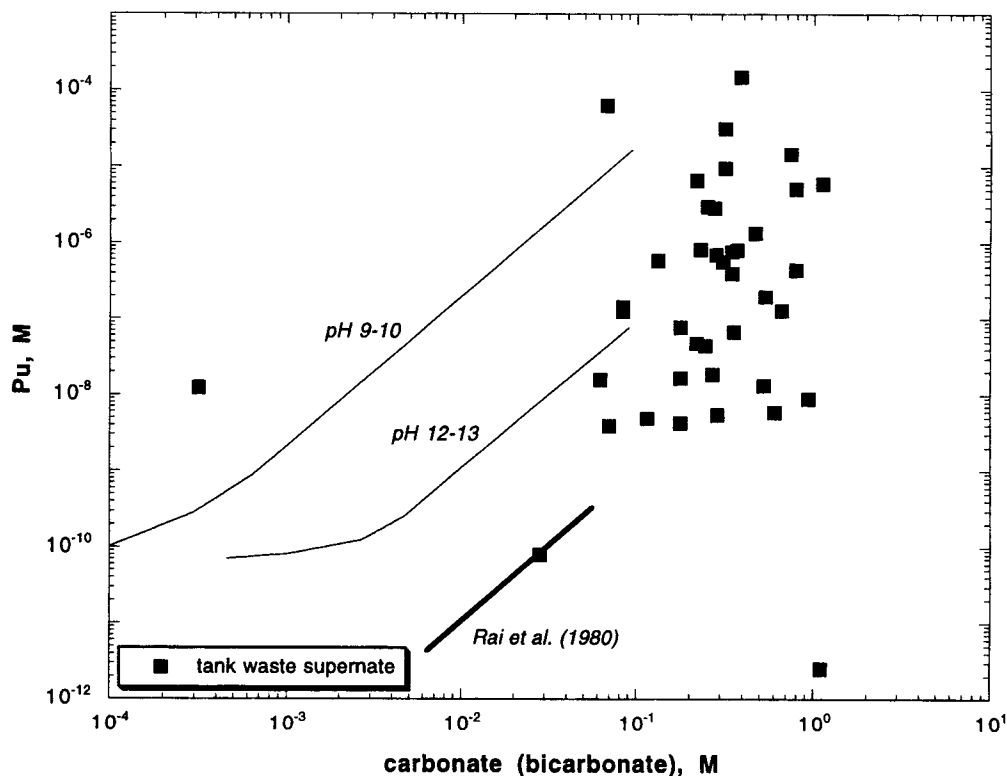
Figure 5-12. Plutonium solubility curves and Hanford tank waste supernate Pu concentration data as a function of carbonate concentration, modified from Serne et. al. (1996). Supernate data from Serne et al. (1996) Table 7-5 have been replotted; these are total Pu measurements with oxidation state unspecified. The two labeled thin curves are Pu(IV) solubility limits from Yamaguchi et al. (1994) at pH = 9–10 and 12–13 for fresh $PuO_2 \cdot xH_2O$ precipitate. For the pH 9–10 curve, the x axis plots bicarbonate (HCO_3^-) concentration, while carbonate (CO_3^{2-}) is plotted for the pH 12–13 curve. The tank supernate data were reported as total carbonate. The thick curve of Rai et al. (1980) represents solubility of a supposedly more crystalline Pu(IV) phase as a function of total carbonate.

Delegard (1987b) also studied the effect on Pu of sludge washing by NaOH (0.01 M followed by 3 M), finding that less than 3 percent (and typically <1 percent) of the Pu contained in actual tank waste sludges was dissolved in the NaOH wash solutions; it should be noted that the reductant $NaNO_2$ was added as part of the experiments. These results suggest that additions of NaOH solutions to tank wastes will not increase Pu solubility, consistent with the downward shift in the experimental solubility curve at pH 12–13 relative to the pH 9–10 curve in figure 5-12.

Finally, it should be noted that Pu colloid formation cannot be discounted as a mechanism for elevating Pu liquid concentrations without regard to solubility limits. However, there are presently no quantitative means for accurately evaluating this process in Hanford wastes.

5.6.3 Concentration of Plutonium in Solids

Because thermodynamic and empirical analyses indicate that solution Pu concentrations remain below critical concentrations, the only likely process for effecting criticality in Hanford tank wastes is by

concentrating Pu in solids. Inspection of Tank Characterization Reports for a sample of tanks (Herting et al., 1995; Kelly, 1995; Baldwin et al., 1995; Hodgson, 1995a,b) demonstrates that, on an activity-per-unit- volume basis, Pu is concentrated in the solids relative to the liquids by a ratio of 10^2 to 10^5. The plausible chemical means for concentrating Pu in solid phases are precipitation of a pure Pu phase, coprecipitation, and adsorption. Plutonium phase precipitation results from solution Pu concentrations in excess of Pu solid phase solubility limits, such as might occur from changes in solution chemistry (e.g., resulting from waste transfer, retrieval, or pretreatment) that decrease solubility limits. Coprecipitation, as discussed here, is the incorporation of Pu into solids—other than those in which Pu is a stoichiometric constituent—as they precipitate from waste liquids, by solid solution or coagulation. This process presupposes active precipitation processes in the wastes, such as (again) might accompany chemical changes. Adsorption is the binding of Pu to the surfaces of solid particles in the waste. As in the preceding discussion of solution concentration mechanisms, quantitative data on these Pu chemical processes are sparse.

5.6.3.1 Plutonium Phase Precipitation

New growth of a pure Pu solid could result from changes in chemistry (e.g., due to sludge washing) or temperature that lower Pu solubility. These processes will be governed by solubility reactions such as those discussed above [Eqs. (5-7), (5-8), (5-9), and (5-11)]. For example, as shown in figure 5-12, Pu solubility limits from Eqs. (5-7) and (5-8) are strongly dependent on total carbonate concentration. If total carbonate concentration is reduced by, for example, addition of a large amount of water or an NaOH sludge wash solution, Pu(IV) solubility would be reduced; this conclusion is experimentally based and independent of the particular stoichiometries chosen. The figure also suggests that evaporation, which would initially yield higher total carbonate concentrations, would increase Pu(IV) solubility. This response to evaporation was observed in the experiments of Hobbs and Karraker (1996), although in that case it was attributed to increasing NaOH concentration. Of course, continued evaporation will eventually lead to Pu precipitation regardless of the solubility. As noted above, the sensitivity of Pu solubility to temperature cannot be quantified yet, but Serne et al. (1996) concluded on the basis of sparse data that there is unlikely to be a large effect.

Another possible effect that could lower Pu solubility and lead to Pu phase precipitation is aging of the likely $PuO_2 \cdot xH_2O$ waste solids. Pu solubility studies by Rai et al. (1980) and Kim and Kanellakopulos (1989) suggested that a more crystalline, stable Pu solid would have lower solubility than young, more amorphous $PuO_2 \cdot xH_2O$. A curve from Rai et al. (1980) is shown in figure 5-12, suggesting that solubility could be lowered by two orders of magnitude by Pu solid aging.

5.6.3.2 Coprecipitation

There are two coprecipitation mechanisms to consider—solid solution and coagulation. Based on consideration of ionic radius differences and coordination numbers, Serne et al. (1996) asserted that only the following elements are likely to form true solid solutions with Pu(IV) in tank wastes: Bi, Ce, La, Th, U(IV), and Zr. In fact, Pu solid solution with Bi and La has been exploited in the past in Pu recovery operations. There are no data, however, on Pu solid solution reactions in actual or simulated Hanford tank wastes. Hodgson et al. (1985) performed experiments on cladding removal wastes, one of the Hanford waste streams. They found, for example, that Pu formed a solid solution with $Zr(OH)_4$ on treatment of the waste with NaOH. In a simple system, this process can be expressed by Eq. (5-9), with the activity of $Pu(OH)_4(s)$ being less than one and approximately equal to the mole fraction of Pu in the $Zr(OH)_4$ solid. It is clear from Eq. (5-9) that, in equilibrium systems, solid solutions will suppress Pu liquid concentrations below pure phase solubility limits. The equilibrium assumption is an important constraint—one not likely to be consistently met between early formed solids and supernates in complex tank waste systems. Nevertheless, it is possible that upon

neutralization of wastes before storage in the tanks, Pu formed a variety of solid solutions in wastes with appreciable amounts of Bi, Ce, La, and Zr.

Experimental observation of coprecipitation of Pu with Al and Fe hydroxides from alkaline solutions similar to Hanford supernates may be found in Hobbs et al. (1993) and Hobbs (1995). However, as pointed out by Serne et al. (1996), Pu(IV) should not form solid solutions with these two elements. Coprecipitation in this case is most likely a coagulation phenomenon, in which pure Pu solids (perhaps $PuO_2 \cdot xH_2O$) form colloids that are enclosed in the hydroxides as they precipitate. This belief is supported in the Hobbs experiments by the observation that Pu(IV) concentrations were consistent with $PuO_2 \cdot xH_2O$ solubility limits [i.e., they represented equilibrium with pure $PuO_2 \cdot xH_2O$ rather than with solid solutions (Serne et al., 1996)]. However, Pu concentrations of the solids resulting from coagulation are not calculable by thermodynamic means.

In summary, considering the high solids contents of most tanks and the physical disruption of tank contents during future treatment (Gephart and Lundgren, 1995; U.S. Department of Energy, 1996), it appears possible that Pu will be affected by coprecipitation involving the more abundant elements mentioned (Bi, Ce, La, Zr, Fe and Al; U is not included in this list because it is thought to exist in tank wastes chiefly in the hexavalent form). For example, using predictions of (i) precipitation of $Zr(OH)_4$ and (ii) Pu concentrations in the liquid during sludge washing, it would be possible to calculate an expected mole fraction of Pu(IV) in $Zr(OH)_4$ using Eq. (5-9). In general, if Pu contents of specific waste solid phases were measurable, it may be possible to estimate changes in Pu distribution resulting from reactions affecting the solids.

5.6.3.3 Adsorption

Although adsorption has been traditionally an empirically defined process, it is, theoretically, a thermodynamically quantifiable chemical process (e.g., Turner, 1995). Models may be developed that describe adsorption at solid surfaces due to electrostatic attraction (e.g., Westall and Hohl, 1980). For example, Sanchez et al. (1985) proposed reactions such as

$$>\text{SOH} + \text{Pu}^{4+} + 4\text{H}_2\text{O} = >\text{SO}-\text{Pu(OH)}_4^0 + 5\text{H}^+$$
$$K = 10^{-12.0}$$

(5-12)

which, together with Pu hydrolysis constants, can be used successfully to model Pu(IV) adsorption on goethite, an iron oxyhydroxide mineral, over a pH range of 2 to 9 in carbonate-free systems. ("S" signifies surface, such that SOH is a surface site and $SO-Pu(OH)_4^0$ is a sorbed species of Pu^{4+}.) Therefore, for predicting Pu adsorption behavior in Hanford tank waste systems, it would be preferred that such thermodynamic models could be incorporated and utilized.

Unfortunately, there are no data on Pu adsorption in chemical environments similar to those that exist in the Hanford waste tanks or that may arise during subsequent processing, and extrapolations from available data are uncertain. As discussed by Serne et al. (1996), the majority of solids in Hanford tanks are oxyhydroxides (dominantly of Fe and Al) that were precipitated on sodium hydroxide neutralization of acidic liquids. Therefore, data on oxyhydroxides and hydroxides are most pertinent to tank waste solid/liquid systems. The most complete published report on pH-dependent Pu sorption on these types of materials is Sanchez et al. (1985), which details experiments on Pu(IV) and Pu(V) adsorption on goethite. Some of their results are shown in figure 5-13, which is taken from presentations of the Sanchez et al. (1985) data by Turner (1995). This plot is for a carbonate-free system, which limits its direct applicability to carbonate-rich tank systems, but it is useful for understanding pH effects. The experimental data show that Pu(IV)
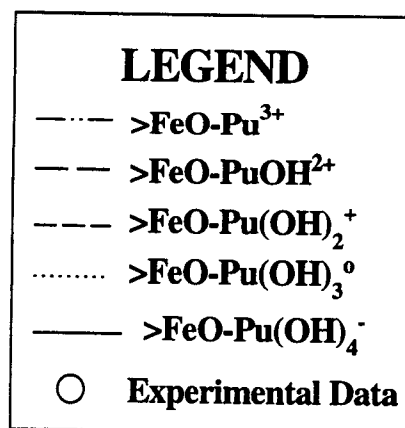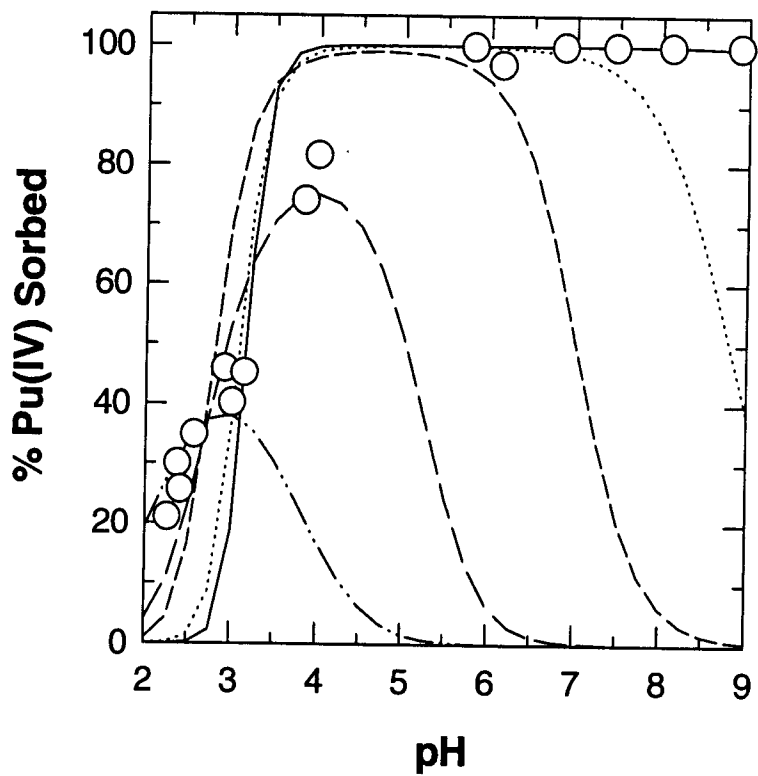
Figure 5-13. Plot of Pu(IV) sorption on goethite. Experimental data are from Sanchez et al. (1985), and curves represent diffuse layer models of several Pu surface complexes taken from Turner (1995).

adsorption is a strong function of pH, rising to a plateau of ~100 percent sorbed at around pH 6. The data do not show a desorption edge at higher pH, but the superimposed surface complexation modeling results of Turner (1995) suggest that it may exist. In the diffuse layer model used to generate the curves shown in figure 5-13, the adsorption reaction that best fits the data at pH > 6 (i.e., it does not show desorption in the plot) is:

$$>FeOH^0 + Pu(OH)_4^0 = >FeO-Pu(OH)_4^- + H^+$$
$$K = 10^{-8.33}$$

(5-13)
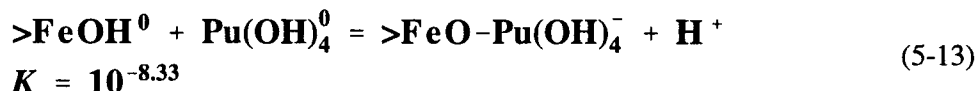
At pH < 6, the relative stability of Pu hydroxy species changes and formation of the $>FeO-Pu(OH)_4^-$ surface complex becomes less important compared to the formation of other Pu surface complexes (see figure 5-13). As pointed out by Sanchez et al. (1985), several adsorption reactions are required to model Pu(IV) adsorption over the full range of experimental pH.

In the same study, Sanchez et al. (1985) measured the effect of increasing carbonate concentration on Pu adsorption on goethite at pH 8.6. In figure 5-14, it can be seen that carbonate has a large effect, leading to essentially no adsorption at a total carbonate alkalinity of 1,000 meq/L. Sanchez et al. (1985) attributed this suppression to the formation of hydroxycarbonate species. This result is consistent with the evidence discussed above for the dominance of such species in carbonate-rich systems such as Hanford tank waste supernates.

Sanchez et al. (1985) also studied Pu(V) adsorption on goethite and found similar results for pH and carbonate dependence, except that the Pu(V) sorption edge was at higher pH compared to Pu(IV). Similar results on the adsorption edge were noted by Righetto et al. (1991) for Pu(V) sorption experiments with alumina. These results suggest that there is some suppression of sorption at a higher oxidation state, which should be considered in scenarios of processes that could affect the Pu oxidation state. On the other hand, experiments on Pu(V) sorption onto minerals from groundwater at pH 7 (Triay et al., 1996) showed strong sorption in contrast to Np(V), which led the authors to speculate that sorbed Pu may have been tetravalent due to effects of the solid phases on Pu redox.

Serne et al. (1996) summarize the available sorption data and assert that "increasing total carbonate and hydroxyl solution concentrations significantly decrease tetravalent actinide adsorption. . . ." On that basis, they construct an adsorption envelope reflecting this dual dependence, which suggests that, at the high pH and high total carbonate typical of tank wastes, there will be essentially no adsorption of Pu. While the case for the carbonate effect is strong, there are no corresponding results on the suppression of Pu adsorption due to increased pH to back up this claim. The highest pH attained in Pu(IV) studies is 9 (Sanchez et al., 1985; Barney et al., 1992), but no desorption edges were evident. The only supporting data cited by Serne et al., (1996) for desorption at high pH were data showing a decrease of adsorption on alumina of analog Th(IV) from pH 8.5 to 9.8 (Righetto et al., 1988). Some of the chemists on the team that prepared the Serne et al. (1996) report disagreed with the conclusion of minimal Pu adsorption under tank waste conditions, citing the very high pH, the high solids contents, and "hydroxyl bridging of mixed oxides during aging" as factors that favor Pu adsorption. This issue is still open, and the true nature of Pu adsorption under high-pH, high-carbonate conditions is not yet understood.

Clearly, processes during initial waste neutralization led to dominant sequestration of Pu in the tank waste solids. Furthermore, subsequent processes have apparently not caused significant desorption or dissolution. Thus, in terms of evaluating criticality potential of solids, the conservative approach of assuming 100 percent Pu in the solids is reasonable. Under this assumption, proposed sludge washing could lead to
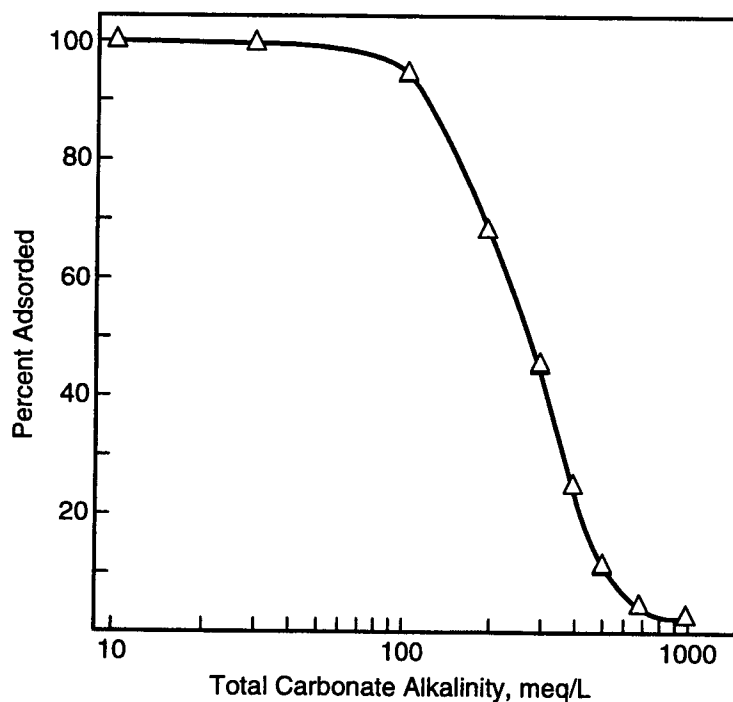
Figure 5-14. Modified Sanchez et al. (1985) plot of percent sorbed Pu(IV) on goethite at pH 8.6 as a function of total carbonate alkalinity. Pu(IV) solution concentration was 10^{-11} M. Results of 96-hr experiments are shown, except for 1-hr results represented by the two lowest carbonate data points.

greater criticality potential were solids to be rearranged into more Pu-rich materials. Such rearrangement would require physical processes the delineation of which is beyond the scope of this section.

Regarding criticality potential in tank liquids, however, the most conservative approach would be to assume complete desorption of Pu with solubility alone controlling solution concentration. During retrieval and sludge washing, for example, it could be argued that the physical disruption of tank wastes would allow re-equilibration of Pu-bearing solids with the supernate, additional retrieval liquids (probably water), and the NaOH wash solutions. If Pu adsorption were indeed suppressed at high pH, sludge washing could thus cause desorption. In this regard, it may be useful to evaluate and apply models that predict desorption at high pH (e.g., Turner, 1995).

As is the case for other chemical processes affecting Pu in tank wastes, there is a lack of data that would allow confident thermodynamic modeling of adsorption. Modeling would serve as a guide to understanding available empirical data and for setting bounds on possible processes.

5.6.4 Chemistry Affecting Neutron Absorbers

As discussed in section 5.5.2, the following elements or isotopes can be considered important neutron absorbers and are thus favorable for preventing criticality: H-1, N-14, O-16, Al-27, Mn-55, Co-60, C, Si, P,

S, Cl, K, Ca, Cr, Fe, Ni, Hg, and Pb. A complete discussion of the chemical processes affecting the fate of all these materials in tank wastes will not be attempted here. Rather, the discussion will be limited to general comments on the important absorbers, without delineation of specific reactions, which are understood well enough that they are likely incorporated into available chemical modeling codes [e.g., Environmental Simulation Program (OLI Systems, Inc., 1996)].

Serne et al. (1996) adopted an upper concentration limit of Pu of 2.6 g/L in both solids and liquids to ensure subcriticality. As tabulated by Serne et al. (1996), the key soluble neutron absorber for tank waste conditions is nitrogen, with a minimum subcriticality mass ratio of 61 (i.e., the N/Pu mass ratio above which criticality is suppressed in a N-Pu system). Nitrogen is a major constituent of some of the most abundant dissolved substances in waste supernates ($NaNO_3$, $NaNO_2$), so it is difficult to envision processes that could significantly reduce its aqueous concentration while increasing that of Pu. For example, the most obvious means for reducing N concentration is dilution, such as during waste retrieval. As discussed above, water dilution leads to decreased Pu solubility or concentration or both. Neutron absorptive properties of the aqueous phase may be important, however, in considerations of the potential for solid-phase criticality because of the intimate solid-liquid mixtures common in tank wastes.

In tank solids, a number of neutron absorbers are present in significant amounts (Serne et al., 1996). In general, sludge solids are dominated by iron and aluminum oxyhydroxides, and these two elements are important neutron absorbers. Other potentially important absorbers having significant concentrations in some waste solids are Mn and Cr (Serne et al., 1996). For these two insoluble neutron absorbers and others (see table 9-3 in Serne et al., 1996), there are no identifiable chemical processes at high pH ($\geq$ 8) that significantly affect solubility; thus, they are expected to remain in the solid phases. However, it is possible to envision processes affecting the solubilities of the two most abundant absorbers, Fe and Al. In the case of iron, it is well established that hydroxides of Fe(II) are more soluble than those of Fe(III); therefore, reduction of Fe in the solids [which is in the Fe(III) form; Agnew, 1997] could lead to liberation of Fe out of the solids into solution. The possible effects of this potential redox transformation on Fe contents of waste solids should be addressed.

Serne et al. (1996) state that aluminum may be relatively solubilized at pH of 14 or greater, and they account for this by reducing Al concentrations in solids by 30 percent in calculations of neutron-absorbing properties. This potential increase in Al solubility should be included in chemical models.

5.7 SUMMARY

This chapter presented information on the principles of criticality safety, factors that affect criticality of HLWs, and chemical mechanisms that could lead to concentration of fissile materials or to redistribution of neutron absorbers. An approximate method was proposed and discussed for determining k_{eff} for tank wastes when Pu-239, the primary fissile isotope in the tanks, has been concentrated to levels that approach criticality. This method is intended to allow an investigator to rapidly and conservatively estimate the criticality potential of a process and determine those cases where more detailed investigations into criticality are required.

Because Pu-239 is the only fissile Hanford tank waste component with a reasonable potential to induce criticality, chemical processes affecting Pu are important to criticality considerations during continued interim storage and also during retrieval, pretreatment, and solidification of Hanford wastes. However, quantitative evaluation of chemical mechanisms for concentrating Pu is difficult due to Pu redox complexity and the paucity of data on Pu behavior in tank-type chemical environments. In attempting to evaluate these

mechanisms, it is clear that much more experimental data under tank waste conditions are necessary to gain more confidence in predictive capabilities.

Consideration of mechanisms for aqueous Pu concentration suggests that it is highly unlikely that criticality levels could be achieved in liquids; nevertheless, it is useful to understand Pu aqueous chemistry. The important aqueous Pu reactions are those affecting solubility and aqueous speciation. Available data suggest that Pu may exist in tank liquids as tetravalent hydroxycarbonate species with solubilities (limited by $PuO_2 \bullet xH_2O$) perhaps as high as 10^{-3} M. Oxidation to potentially more soluble Pu(VI) species, however, may be possible if more oxidizing conditions are present or have been induced by, for example, radiolysis or aeration. In addition, colloid formation could lead to Pu liquid concentrations exceeding solubility limits, but no quantitative means for evaluating this mechanism are available. Furthermore, Pu data from tank samples do not show such elevated concentrations.

Plutonium concentrations in tank solids typically exceed those in liquids by several orders of magnitude and, consequently, have a greater criticality potential. The important chemical mechanisms for solids concentration are pure Pu phase precipitation, coprecipitation with other solids, and adsorption. Growth of new pure Pu phases would require evaporation or chemical changes resulting in lowered solubility, in competition with coprecipitation and adsorption. Coprecipitation may result from two phenomena, solid solution and coagulation. While it may be possible to predict solid-solution behavior by thermodynamic calculation, understanding of coagulation behavior rests on observation and experimentation. Adsorption of Pu onto tank solids such as hydroxides of iron and other metals is considered by many to be an important means of Pu sequestration in solids. However, available experimental data imply suppression of Pu adsorption at the high pH and high carbonate contents typical of tank liquids, although more experimental studies for conditions relevant to Hanford tank wastes are clearly warranted. From a criticality standpoint, it seems most conservative to assume that Pu precipitation or coprecipitation reactions and adsorption phenomena can result in complete removal of Pu from solution.

Another aspect of waste chemistry relevant to criticality potential is the fate of neutron absorbers. In Hanford tank wastes, nitrogen is the most important soluble neutron absorber, whereas Fe and Al are the most abundant absorbers in the solids. Model simulations or predictions of waste chemistry should track these and other potentially important neutron absorbers. For example, Fe can undergo redox changes that will affect its aqueous solubility/speciation and solid phase distribution, and Al solubility may be enhanced at high pH.

6 RADIOACTIVE-DECAY HEAT GENERATION IN HANFORD TANK WASTES

6.1 INTRODUCTION

Radioactive decay can result in elevated temperatures of Hanford wastes during storage and possibly during retrieval or processing operations. For example, 10 SSTs (A-104, A-105, C-106, SX-107, SX-108, SX-109, SX-110, SX-111, SX-112, and SX-114) have high-heat loads [>42,000 kJ/hr (>40,000 Btu/hr)] (Hanlon, 1996). Maximum temperatures measured in these tanks in September, 1997, are listed in table 1-2. These tanks, with the exception of A-104 and A-105, are on active ventilation (Hanlon, 1997). One specific tank, C-106, requires more than active ventilation to keep the temperature below 150 °C (300 °F), which is the maximum temperature limit established in the DOE Operating Safety Document (Wodrich, 1992). The rate of heat generation in tank C-106 is estimated at more than 105,000 kJ/hr (100,000 Btu/hr) and arises primarily from radioactive decay of Sr-90 waste that was transferred into the SST in the late 1960s. For this tank, water is periodically added to maintain a liquid cover (supernate) over the liquid sludge for enhanced thermal conductivity and evaporative cooling (DeFigh-Price and Wang, 1993).

Radioactive decay heat needs to be considered in safety analyses primarily because it determines the waste temperature profile, and secondarily because it influences the moisture loss rate. For example, the maximum temperature that can be achieved due to radiolytic decay in a dried-out slurry receipt and adjustment tank of a vitrification facility was calculated by Dukas and Slaughterbeck (1991) in connection with analysis of potential reactions involving nitrate and nitrite in Hanford waste vitrification process feed. Also, estimates of waste temperature are needed to account for temperature effects on chemical reactions that may occur in tank wastes such as thermochemical generation of flammable gas and ferrocyanide aging (see chapters 2 and 4). For example, Graves (1994) had to calculate the radioactive heat load in waste tanks in order to estimate the amount of flammable gas generated in nonburping waste tanks. Furthermore, high-heat generation could lead to problems such as self-boiling or thermal expansion and possible distortion or rupture of Hanford tanks and TWRS process pipelines. Thus, waste temperature estimates could be useful in anticipating potential problems in TWRS operations.

This chapter provides information on radioactive decay that contributes to heat generation and describes a simplified method for calculating the volumetric heat generation rate of tank wastes based on known or assumed radionuclide inventory. The method assumes that the only heat generation mechanism in the source material is from self-absorption of radiation from Sr-90 and Cs-137, or their short-lived daughters, in the material. Because the radioactivity of Hanford wastes is, in most cases, dominated by these two radionuclides, this assumption seems reasonable (Agnew, 1997).

6.2 DECAY SCHEMES FOR Sr-90 AND Cs-137

The predominant heat-generation mechanism for tank wastes is the emission, and subsequent absorption in the waste, of radiation from radionuclides contained in the waste. As mentioned previously, Sr-90 and Cs-137, and their short-lived daughters, are the dominant sources of radiation in TWRS wastes. The Sr-90 and Cs-137 decay schemes are given in figures 6-1 and 6-2. The 0.662 MeV gamma radiation from Ba-137m (the longest ranged particle in either decay chain) presents a problem for modeling the waste as a heat source. Since gamma radiation at this energy has an unscattered mean free path of about 11 cm and a half value layer for energy deposition of about 21 cm in water (Chilton et al., 1984), a significant amount of

$$^{90}\text{Sr} \xrightarrow[\substack{t_{1/2} = 28.78 \text{ yr} \\ E_{\beta av} = 0.194 \text{ MeV} \\ E_{\beta endpoint} = 0.546 \text{ MeV}}]{\beta \quad (100\%)} {}^{90}\text{Y} \xrightarrow[\substack{t_{1/2} = 2.67 \text{ days} \\ E_{\beta av} = 0.930 \text{ MeV} \\ E_{\beta endpoint} = 2.281 \text{ MeV}}]{\beta \quad (99+\%)} {}^{90}\text{Zr}$$
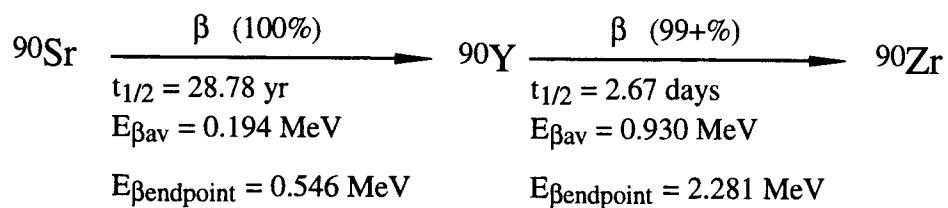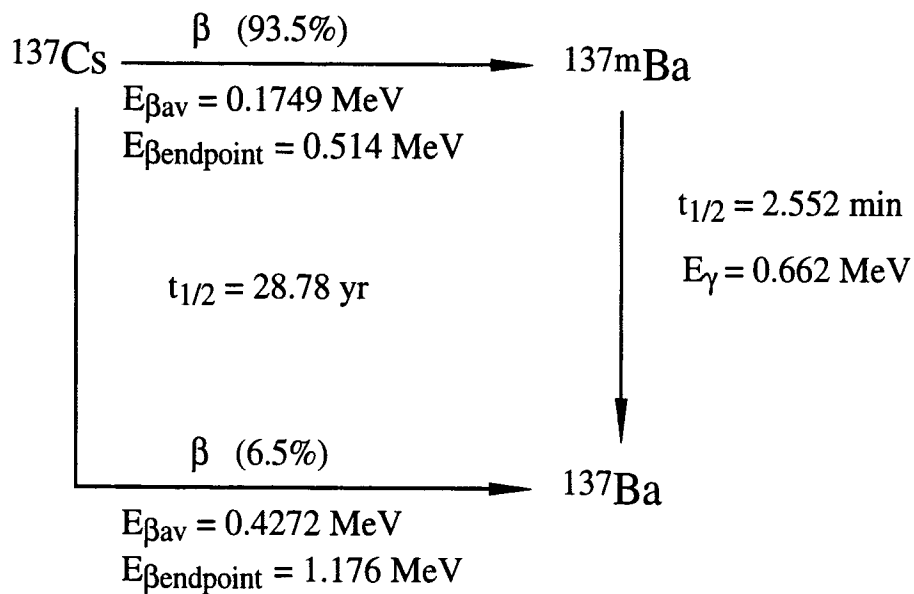
Figure 6-1. The decay scheme of Sr-90

Figure 6-2. The decay scheme of Cs-137

energy from this radiation may be deposited outside of the source. Since the amount of energy deposited in the heat source material from the 0.662 MeV gamma ray is dependent on the size and shape of the source, there is no way of exactly calculating the heat-generation rate of the source for all situations. To compensate for this effect, two estimates of the volumetric heat generation rate are made, one for which it is assumed that the 0.662 MeV gamma ray deposits all its energy in the source material ($\Uparrow \dot{q}$) and one for which it is assumed that the 0.662 MeV gamma ray deposits none of its energy in the source material ($\Downarrow \dot{q}$). These two estimates effectively define the range of the volumetric heat generation rate. It is noted that $\Uparrow \dot{q}$ is accurate for large sources and $\Downarrow \dot{q}$ is accurate for small sources. Since the range of a 2.281 MeV beta particle from Y-90 (the beta particle with the greatest energy in either decay chain) in water is only 1.2 cm, assuming that all beta particles in these analyses deposit their energy in the source material is justifiable.

6.3 EQUATIONS FOR CALCULATING VOLUMETRIC HEAT GENERATION RATE

Equation (6-1) presents an expression for calculating the volumetric heat generation of the waste assuming the emitted gamma and beta particles deposit their energy in the source material:

$$\dot{q} \text{ [W/L]} = 0.00666\left(a_{Sr-90}[\text{Ci/L}]\right) + 0.00593 \cdot \text{FACTOR} \cdot \left(a_{Cs-137}[\text{Ci/L}]\right) \quad \text{(6-1)}$$

where

a_{Sr-90} —   activity concentration of Sr-90 in Ci per liter

a_{Cs-137} —   activity concentration of Cs-137 in Ci per liter

FACTOR   —   0.8103 MeV/s/Bq absorbed by the surrounding material if the 0.662 MeV gamma ray is completely absorbed;
0.1913 MeV/s/Bq absorbed by the surrounding material if the 0.662 MeV gamma ray escapes the material without interaction.

The leading coefficient in the first term of Eq. (6-1) is the power liberated per decay of Sr-90 (in W per Ci) assuming an equilibrium concentration of Y-90. Similarly, the leading coefficient times FACTOR in the second term is the power liberated per decay of Cs-137 (in W per Ci) that is subsequently absorbed in the material assuming an equilibrium concentration of Ba-137m.

Extending Eq. (6-1), one finds an expression for $\Uparrow \dot{q}$:

$$\Uparrow \dot{q} \text{ [W/L]} = 0.00666\left(a_{Sr-90}[\text{Ci/L}]\right) + 0.00480\left(a_{Cs-137}[\text{Ci/L}]\right) \quad \text{(6-2)}$$

and an expression for $\Downarrow \dot{q}$:

$$\Downarrow \dot{q} \text{ [W/L]} = 0.00666\left(a_{Sr-90}[\text{Ci/L}]\right) + 0.00113\left(a_{Cs-137}[\text{Ci/L}]\right) \quad \text{(6-3)}$$

To check the validity of the above equations, the total heat generation rate ($\dot{Q}$) was calculated for several tanks and compared to values listed in Agnew (1997). Due to the large size of the tanks (i.e., millions of gallons), Eq. (6-2) was used to estimate the volumetric heat generation rate. The volumetric heat

Table 6-1. A listing of the heat generation rates of the tank wastes as calculated by Eq. (6-2), as listed in Agnew (1997), and their percentage difference

Tank	$\dot{Q}$ (W) (Eq. 6-2)	$\dot{Q}$ (W) (Agnew, 1997)	Percentage Difference (relative to Agnew, 1997)
C-106	4.04×10^4	4.07×10^4	−0.7
TX-117	2.09×10^3	2.06×10^3	1.5
BY-112	1.78×10^3	1.77×10^3	0.6
AP-108	1.01×10^3	9.93×10^2	1.4

generation rate was then multiplied by the total tank volume (Agnew, 1997) to obtain the estimates of $\dot{Q}$ found in column one of table 6-1. As can be seen from table 6-1, the values are in good agreement. Table 6-1 lists the values $\dot{Q}$ as calculated by Eq. (6-2) ($\Uparrow\dot{q}$ times the waste volume) using activity concentration data listed in Agnew (1997), the heat generation rate value as listed in Agnew (1997), and their percentage difference for several tanks.

6.4 RANGE OF VOLUMETRIC HEAT GENERATION RATE FOR SELECTED TANKS

As a demonstration of the possible range of volumetric heat generation rate due to incomplete absorption of the 0.662 MeV gamma ray in the source material, values of $\Uparrow\dot{q}$ and $\Downarrow\dot{q}$ were calculated for selected tank contents with relatively large activity concentrations of Cs-137 relative to Sr-90. Due to the large dimensions of the tanks compared to the mean free path of the 0.662 MeV gamma ray, it is expected that $\Uparrow\dot{q}$ would be a much better estimate of the volumetric heat generation rate. This is demonstrated by the agreement between the values in Agnew (1997)[1] and the values calculated using $\Uparrow\dot{q}$ in table 6-1. However, as the contents of the tanks are removed and stored in smaller volumes, $\Downarrow\dot{q}$ may become a better estimate of heat generation. Table 6-2 lists the calculated volumetric heat generation rates, $\Uparrow\dot{q}$ and $\Downarrow\dot{q}$, along with their percentage differences to show the effect that storing the wastes in smaller volumes (e.g., for transfers to the vitrification facility) may have on the heat generation rate of the wastes. An estimate of $\Uparrow\dot{q}$ based on data in Agnew (1977) is included for reference. As can be seen in table 6-2, a factor of two difference between the low and high estimates is possible for tank waste source materials. Of course, the differences in table 6-2 would increase for larger activity concentrations of Cs-137 relative to Sr-90.

---

[1]Agnew (1997) did not state how $\dot{Q}$ was estimated.

Table 6-2. A listing of the high and low volumetric heat generation rates for the contents of selected tanks along with their percentage differences

Tank	⇧q̇ (W/L) (Agnew, 1997)	⇧q̇ (W/L)	⇩q̇ (W/L)	Percentage Difference (relative to the low value)
BX-104	0.00112	0.00113	0.00059	91.5
S-106	0.00201	0.00204	0.00102	100.0
AN-102	0.00266	0.00269	0.00144	86.8

6.5   SUMMARY

Radioactive decay heat of highly radioactive species, such as Sr-90 and Cs-137, are of potential safety concern in the Hanford TWRS because it could result in elevated temperatures during storage, retrieval or pretreatment operations. For example, radioactive decay heat determines the waste temperature profile and influences the moisture loss rate. Thus, ventilation requirements, whether passive or active, for waste storage and process feed tanks need to consider the effect of radioactive decay heat. For example, tank C-106, the only Hanford tank on the High Heat Watch-list, requires more than active ventilation to keep the temperature below 150 °C (300 °F), which is the maximum temperature limit established in the DOE Operating Safety Document (Wodrich, 1992). Tank C-106 is cooled through evaporation in conjunction with active ventilation, and water is periodically added as evaporation takes place (Hanlon, 1998). In a transfer line containing waste with high heat load due to radioactive decay, problems such as thermal expansion and distortion or rupture of the line could result. Also, degradation of ion exchange resins or other media used in pretreatment of Hanford wastes could be accelerated by high heat generated by radioactive decay. Thus, waste temperature estimates could be useful in anticipating potential problems in TWRS operations.

A simplified method was presented in this chapter for calculating the volumetric heat generation rate of tank wastes based on the activity concentrations of Cs-137 and Sr-90. It was found that there can be significant differences in the volumetric heat generation rate for small heat sources versus large heat sources due to the escape of the 0.662 MeV gamma ray emitted by Ba-137m from smaller systems. The equations presented are useful in estimating waste temperatures based on known or assumed inventories of Sr-90 and Cs-137.

7 MODELS AND CODES FOR SIMULATING HANFORD TANK WASTE REMEDIATION SYSTEM PROCESSES

7.1 INTRODUCTION

Hazard evaluation is an organized effort to identify and analyze the significance of hazardous situations and to pinpoint weaknesses in the design of a facility. As defined by the American Institute of Chemical Engineers (1992) guidelines, a hazard is a physical or chemical characteristic of a material, system, process, or plant that has a potential for causing harm. From an NRC perspective, the hazards of concern in NRC-licensed nuclear facilities are related to: (i) radiation risk from radioactive materials, (ii) chemical risk from radioactive materials, and (iii) plant conditions that affect the safety of radioactive materials and, thus, present an increased radiation risk to workers and to the public (Ayres, 1997). For example, certain plant conditions might produce a fire or an explosion and, thereby, cause a release of radioactive materials. The OSHA deals with a fourth type of hazard—plant conditions that result in an occupational risk, but do not affect the safety of licensed radioactive materials, such as exposure to toxic nonradioactive materials.

The NRC does not regulate chemicals per se; rather, the NRC determines whether interactions of chemicals with NRC-licensed nuclear materials and/or with equipment that processes, transports, or stores these licensed materials have been appropriately considered in the design of the equipment and facilities and in the operating and maintenance procedures (Ayres, 1997). Hazard identification for a process or facility requires identification of materials, systems, processes, and plant characteristics that can produce those consequences. Thus, safety analysis requires information about the process and about the chemicals used in the process (including chemical intermediates, process parameter limits, etc.).

Because of the complexity and variability in the chemical types, compositions, and concentrations of Hanford tank wastes, as well as in the technologies that will be used to retrieve, pretreat, and solidify the wastes, a comprehensive identification and evaluation of potential hazards in Hanford TWRS operations will be difficult. Hazard audits of the TWRS facility may fail to identify certain chemical reactions that could lead to a safety problem. A good example of an audit failure is the unanticipated rapid decomposition of sodium tetraphenylborate, a chemical used to precipitate Cs-137 from tank wastes, that occurred at the In-Tank Precipitation Facility at the Savannah River Site. The decomposition resulted in the generation and release of the flammable gas benzene into the tank vapor space (Defense Nuclear Facilities Safety Board, 1997). Although radiolytic decomposition of tetraphenylborate is known to produce benzene at a slow rate, rapid tetraphenylborate decomposition, catalyzed by metal ions in the waste, was not anticipated.

Identification and evaluation of plant processes and conditions and of chemical reactions that could lead to safety hazards may be enhanced through the use of computer software for simulating processes relevant to the Hanford TWRS operations. Several commercial software that may be useful for simulating these processes are available. A critical evaluation of these software and their application to Hanford TWRS is beyond the scope of this report. However, a general discussion of flowsheet simulation software and its application to process development is included in this chapter. A specialized suite of software for chemical process simulation developed by OLI Systems, Inc. (Morris Plains, New Jersey) has been used by Hanford investigators for various applications. The OLI software is described in some detail in this chapter, and simulation examples, developed as part of a preliminary analysis of the potential use of the software for the Hanford TWRS, are discussed.

7.2 FLOWSHEET SIMULATION SOFTWARE

A class of software, typically referred to as flowsheet simulation software, performs complex mass and energy balances using thermodynamic equilibrium algorithms. This type of software can handle multiple recycle streams and contain built-in codes that simulate typical processing equipment such as distillation columns, heaters, reactors, pumps, and filters. The individual pieces of equipment are "piped" together to create the overall flowsheet, and modifications can be made by changing equipment blocks, redefining feed streams, and repiping the connecting streams. Commercial software packages, such as ASPEN PLUS (Aspen Technology, Inc., Cambridge, Massachusetts), HYSIM (Hyprotech, Inc., Calgary, Alberta, Canada), and PRO/II (Simulation Sciences, Inc., Brea, California), usually have a large chemical property database supplied (typically containing over 2,000 components), and the user usually can provide data for components not in the database.

7.2.1 The Use of Simulation in Process Development

A process simulation is a model of a complex sequence of chemical or physical processes. It provides results similar to the actual process results. Process simulation provides an engineering tool for developing and designing processes and a management tool for both operational and strategic planning. It provides information about the dynamic operation of a process and the response of the process to various disturbances, without the expense of building and operating an actual or pilot facility.

A classic example illustrates several ways that process simulation can benefit a project. The American Oil Company (now Amoco), Whiting, Indiana, refinery provided an early example of a successful process simulation. The refinery used an electric analog to simulate their fire water distribution system (Rudd and Watson, 1968). The physical process was moving water through an elaborate, interconnected system of pumping stations and pipes to the hose stations. The electric analog contained voltage sources to represent the pumping stations, light bulbs to provide electric resistance and visual indication of current flow to the pipelines, and connections to ground via resistors to represent the hose stations or points of water usage. The model worked visually by indicating current flow (lights on) for any given combination of pumping stations and hose stations in use. In addition, electric current measurements related directly to the actual water flow measurements. The results of the model provided answers to such questions as:

- Will there be enough water to fight two simultaneous fires?

- Should old water lines be discarded as the refinery changes—new units added and old units torn down?

- Which pumps should be operated for fires in any given area?

- Will emergency pumps be adequate?

- Can plugged lines be found with only limited testing?

- Can fire-fighting crews be trained prior to the emergency?

Use of the model saved the company considerable expense on several occasions. The model had the characteristics most useful for process simulation and its accuracy provided numeric values directly related

to the real process. Its predictive ability allowed case studies and trials of preliminary plans prior to making any significant investment. This ability also enhanced confidence in the overall process by enabling crew training without having to turn on the water. The model's flexibility permitted modifications to the model as the real process changed in response to refinery developments.

Modern computers and software development have made mathematical process simulation models routine and indispensable tools for process engineers. A global examination of the overall task of process engineering shows the benefit of process simulation. Process engineering work includes: (i) defining a processing concept, (ii) designing the process, (iii) evaluating the process, and (iv) operating the process while dealing with real-world changes and uncertainties that might easily get overlooked in simpler mathematical models.

7.2.2 Defining the Processing Concept

To define the processing concept, the process engineer determines the basic physical and chemical principles needed. The engineer selects among alternatives derived from previous experience, gleaned from the literature, or obtained in the laboratory. Process simulation has only a limited application until the concept becomes defined, but a simulation of small parts of some suggested processing concept may provide useful insights. For example, the choice between a flash separator and a more expensive multistage distillation column may impact a project economically, and a flash simulation should reveal if the flash separator would perform adequately. When the processing concept has been defined, the kinds of unit operations and their relationships to the major material flows are established.

In some cases, models applied to existing processes or situations provide highly useful information. For any number of reasons, plants are constructed without process simulation, but operators may desire to plan additions or modifications, or to explain some unexpected result. Questions such as "Will our present utilities suffice for a planned addition during all phases of plant operation?", "What caused a line to become plugged?", or "Why does a reactor occasionally overheat?" are asked frequently. In some cases, the process in question may not involve an industrial plant at all. Process simulations can also answer some important questions about environmental effects. For example, the public or governmental bodies frequently ask questions such as, "What would happen if this waste tank were spilled?" A process simulation could provide information about which component would evaporate first and which would dissolve in groundwater most readily. Even in existing, or naturally occurring processes, a process simulation could provide diagnostic information for planning changes and dealing with potential problems.

7.2.3 Designing the Process

After a processing concept has been selected, process design can begin. Process design uses process simulations extensively. Using the simulation, the engineer links up the unit operations on a flow sheet to represent the steady-state plant operation. At steady-state, the plant operates as expected and does not change significantly with time. In addition to the processing concept, the process simulation needs other inputs, including the overall production goals and plant specifications, requirements for each unit operation, and key physical or chemical process parameters. The process engineer next uses the model software to calculate important details, such as:

•   Required capacity for each unit operation

- Utility requirements and thermal loads for each unit operation

- Flow rates, heat content, and chemical composition of each stream

- Temperature, pressure, and vapor fraction for each stream

- Main control systems required for safe and efficient plant operation

- Plant and unit descriptions required for obtaining permits and licenses

- Characteristics of an optimal design, often determined using case studies

A detailed design of the more complex units frequently uses additional specialty simulations. Equipment suppliers often perform this step, but information from the overall plant simulation normally provides many of the inputs needed for the specialty simulation. These simulations are sometimes made with custom or optional software separate from the overall plant simulation software, or they may be made with subroutines. They provide detailed information on such units as distillation columns, heat exchange networks, and individual heat exchangers, compressors, waste, and byproduct-handling systems, biochemical operations, and batch operations. The typical goal is to provide a sufficiently detailed description of each unit operation to obtain accurate cost information and place orders for their construction.

7.2.4 Cost Estimation

Although the capability is not of direct relevance to a hazard analysis, various simulation software can provide cost estimation. A detailed cost estimate is typically the final, major piece of information required to determine whether or not to proceed with a project. Furthermore, cost estimates may provide a useful basis for making regulatory judgments regarding features that will maintain radiation risks as low as reasonably achievable (ALARA). The information obtained from the steady-state and special equipment simulations can provide the data used for conventional plant cost estimation methods. However, many process simulation systems available today have optional software for plant-cost estimation that take data directly from the flow sheet simulations and, with additional data, estimate a project cost. The added information typically includes site information, materials of construction selections, and financing and construction time assumptions. Information from the steady-state flow sheet simulation may also be used in determining manufacturing costs for the product made by the process. A final optimization of the plant configuration and design may take place at this point, particularly if the economic evaluation should differ significantly from earlier expectations.

During project construction, steady-state process simulation is generally not developed further. Exceptions might include unexpected construction problems that force a change in the plant configuration, or changes in product requirements dictated by a rapidly changing market. In a normal situation, the results of the simulation remain unchanged and serve as an important reference and standard for the construction.

7.2.5 Operating the Process

For most plants, start-up is a difficult and complex operation. During start-up, all the errors in design or construction come to light and need to be corrected, special operations required only for start-up need to function properly, and interdependent operations need to come into full operation in the selected, organized

manner. A new category of process simulation called dynamic simulation, or nonsteady-state simulation, may also provide start-up assistance, particularly when all the unit operations are functioning, though not necessarily at their design conditions. However, dynamic simulation requires additional data for calculating the types and rates of changes the plant unit operations and process streams experience in response to changes in controller settings and other parts of the plant. Plant operation during start-up may provide important data for making the dynamic simulation accurately reflect the actual plant operation.

A well-configured dynamic simulation can model the plant operation as it responds to changes. For example, suppose a plant needs to change to a feedstock with a lower concentration of reactant than used previously. The lower concentration may dictate changes in the flow rates needed to meet requirements at a later stage, or it may cause a commensurate slowdown in other parts of the plant to compensate. In addition, the heat derived from (or required by) reactions will be different than with the concentration used earlier. Rerunning the steady-state simulation with the new feed composition describes the plant operation after the change is made. The new simulation would answer some basic questions (e.g., do the pumps, heat exchangers, and other units have sufficient capacity to operate with the new feed?). However, a new steady-state simulation does not answer questions about what happens during the transition (e.g., do the controllers of the flow rates, heat exchangers, and other units have sufficient dynamic response to make the needed changes without plant modification?). These questions are typically answered using dynamic process simulations. In general, dynamic simulations model the plant as it actually operates, including upset conditions, and help the plant operators deal with uncertainties or changes due to new developments (as in the case of the new plant feed stock), data errors, specification tolerances, variations induced by ordinary fluctuations in feeds, and erroneous or unsteady operation in local areas within the plant. The ability to conduct dynamic simulations could help identify potential safety problems, such as process upsets that could lead to out-of-specification conditions for a facility equipment.

An approximation of a dynamic operation can sometimes be made by using a case study approach with the steady-state process simulation software. A procedure involving parameterizing the variable of interest with repeated solution provides this result. The steady-state simulation is solved repeatedly, with each solution differing from the previous one by only a small, step-change in a single parameter. The repeated simulations show how the plant will change in response to changes in the parameter of interest.

Dynamic process simulators assist process engineering in two other major ways. Ideally, the plant operator can make a change in the simulator and observe its effects throughout the simulated plant before making the change in the real plant. The dynamic simulation thus becomes an important aid to planning and decision-making at the plant operation level. A related function enables training of plant operators using the simulator. The operators can learn how to make changes, what circumstances require changes, and then see the effects—good or bad—of their choices, all with the simulator alone. The training of plant operators without incurring any financial risk has become one of the most popular applications of dynamic process simulation.

The benefits of process simulation, both steady-state and dynamic, accrue because a good model is accurate, has predictive capability, and is flexible. Several software packages are available for process simulation. They differ in many respects, however, and like all software, are in a constant state of developmental flux with new enhancements continually being added. Tables 7-1 and 7-2 summarize information available from brochures and internet web pages provided by some companies who supply process simulation software. The information in the tables show those capabilities that might be of interest for operations that could be involved in tank waste remediation system pretreatment. Also, the material was selected from information readily at hand, rather than from interviews with experienced users. Considerable

Table 7-1. Flowsheet simulators—overall capabilities

Features*	CHEMCAD	ASPEN	HYSYS	SIMSCI
Steady-state Flowsheet Simulation:				
Operations				
Recycle	●	●	●	●
Controller, Types[a]	2	15	●	●
Heat Exchangers	●	●	●	●
Tray Distillation, Types[b]	5	4	●	●
Packed Column Distillation	●	●	●	●
Batch Distillation	●	●	●	●
Reactive Distillation	●	●		
Flash, Types[c]	3	3	3	3
Chemical Reactors, Types[d]	4	5	5	4
User Stoichiometry and Rate Expressions				●
Compressors and Pumps	●	●	●	●
Liquid-liquid Extraction	●	●	●	●
Depressuring	●		●	●
Relief Valve Sizing	●	●	●	
Solids Handlers, Types[e]	7	6	6	
Turbines		●		
Thermodynamic Models for K-value[f], Enthalpy and Entropy (see table 7-2):	●	●	●	●
Component Data Library:				
Pure Components (Thousands)		37	2	
Binary Mixtures (Thousands)		5	16	
Aqueous Ionic Reactions Constants (Thousands)		1		

7-6

Table 7-1. Flowsheet simulators—overall capabilities (cont'd)

Features	CHEMCAD	ASPEN	HYSYS	SIMSCI
DIPPR (by Design Institute for Physical Property Data)	●		●	
DETHERM (by DECHEM, Frankfurt, Germany)		●	h	
TRC (Thermodynamic Research Center, Texas A&M)			●	
Dortmund			●	
PPDS			●	
User Input	●	●	●	
Regress User Supplied Data For:				
Activity coefficients in non-ideal models	●	●	●	●
Binary vapor-liquid equilibria	●	●	●	●
Ternary vapor-liquid	●	●	●	●
Pure component physical properties	●	●	●	●
Oil or hydrocarbon pseudocuts[g]	●	●	●	●
User Interactions				
Tabular input, pull-down tables	●	●	●	●
Graphic input, icon click and drag, tabular details	●	●	●	●
Missing data error check	●	●	●	●
Over-specification error check	●	●	●	●
Interrupt for intermediate results	●		●	
Calculate individual units separately	●		●	
Distillation output: profiles and tray details	●	●	●	●
Dynamic simulation capability	●	●	●	●
Dynamic simulation/plant control interface			●	●
Additional, supporting software available:				

Table 7-1. Flowsheet simulators—overall capabilities (cont'd)

Features	CHEMCAD	ASPEN	HYSYS	SIMSCI
Detail design package:				
Shell and tube heat exchange	●	●	●	●
Mixers	●			
Distillation column internals	●	●	●	
Batch stills and separators	●	●	●	●
Adsorption columns		●	●	
Batch reactors	●	●	●	●
Valve and minor component sizing	●	●	●	
Network Design and Analysis:				
Heat exchanger networks	●	●	●	●
Pipe networks for two-phase, liquid-gas	●			●
Pipe networks for liquid and slurries	●			●
Hydraulics in pipe networks	●		●	●
Software Supporting or Extending the Flowsheet:				
Physical property prediction, properties	●	●	●	●
Psychrometric, for air and water mixtures	●			
Euler and Runga Kutta Integrators		●		
Fault tree analysis	●			
Process hazards analysis	●			
Detailed process diagrams and charts	●			
Specification sheets	●		●	
Nonlinear equation solvers				
Process equipment cost estimates	●		●	

Table 7-1. Flowsheet simulators—overall capabilities (cont'd)

Features	CHEMCAD	ASPEN	HYSYS	SIMSCI
Plant upgrade cost estimates	●			
Plant cost estimate from simulator	●			
Plant project management	●			
Plant rating (minimum capital and operating costs)			●	
Heat exchanger optimization			●	
Specialty Process Flow Simulators:				
Biochemical, food, and drug processes	●			
Waste handling processes	●			
Polymer processes			●	
Flare and vent systems			●	
Batch processes			●	

*The ● symbol indicates that the feature is available in the specified flowsheet simulation software. The numbers refer to the number of feature or data type available in the software.

a. Controller types modeled include feedback and feed forward.

b. Distillation types modeled include shortcut, one or two rigorous models, absorber or stripper, and crude oil still.

c. Flash units separate the equilibrium vapor and liquid components based on adiabatic or isothermal conditions with a second liquid phase present.

d. Chemical reactors include kinetic, equilibrium, stoichiometric, or Gibbs types.

e. Solids handling models include filters, crushers, centrifuges, washers, dryers, hydroclones, and others.

f. The K-value is the mole fraction of a component in the vapor phase divided by its mole fraction in the liquid phase and is a measure of the component's tendency to concentrate in the vapor phase.

g. Oils and other hydrocarbons with a boiling range can be characterized as a mixture of, typically, 10 to 50 narrow-boiling fractions called "pseudocuts." Process simulation software with this capability calculates the properties of each of the pseudocuts, then treats them somewhat like pure components.

h. Does not access the database, but it provided the data for the internal library.

Table 7-2. Thermodynamic models and thermophysical property methods

Model	Type of Method*	CHEMCAD	ASPEN	HYSYS	SIMSCI
Amines Properties	K			●	●
Amines (Kent-Eisenberg)	K		●		
Antoine (Usually with Modifications)	K			●	
API Soave	K	●		●	
Benedict-Webb-Rubin (BWR)	EoS	●			
Benedict-Webb-Rubin-Starling (BWRS)	EoS		●		●
Braun K10 (BK10)	G		●	●	
Bromley-Zemaitis (Ionic Activity Coefficients)	A				●
Chao-Seader	F	●	●	●	
Chao-Seader/Prausnitz-Shair	F		●		
Chen NRTL (Non-random, Two Liquid)	A				●
Chien Null	A		●	●	
Debye-Huckel (Ionic Activity Coefficients)	A				●
Electrolytes, Solids, and Biological	S	●		●	●
ESSO Tabular	G			●	
Flory-Huggins (for Polymers)	S	●			
General Polynomial	A		●		
Grayson-Streed	F		●		●
Grayson-Streed Erbar	F				●
Grayson-Streed, Improved	F				●
Hayden-O'Connell	EoS		●		
Hydrogen Fluoride/HEXAMER	EoS	●	●		●
Ideal Gas	EoS	●	●	●	●
Ideal Solution	A	●	●	●	●

Table 7-2. Thermodynamic models and thermophysical property methods (cont'd)

Model	Type of Method*	CHEMCAD	ASPEN	HYSYS	SIMSCI
Lee-Kesler	EoS	●	●	●	
Local Composition Electrolyte	A		●		
Margules	A	●	●	●	●
Maxwell-Bonner K-values (for Heavy Crude Oils)	K	●			
Meissner & Kusik (Water Activity)	A				●
Methods for Aqueous Systems	A	●			●
Methods for Ammonia and Mineral Acids	A	●			●
Nonrandom, Two Liquid (NRTL)	A	●	●	●	●
Nothnagel	EoS		●		
Peng-Robinson (PR)	EoS	●	●	●	●
Peng Robinson, Stryjek-Vera Modification (PRSV)	EoS			●	
Perturbed-Hard-Chain	EoS		●		
Pitzer (Ionic Activity Coefficients)	A		●		●
Polynomial, Modified	K		●		
Redlich-Kister	A		●		
Redlich-Kwong (RK)	EoS		●	●	
Redlich-Kwong-ASPEN	EoS		●		
Redlich-Kwong-UNIFAC	EoS		●		
Scatchard-Hildebrand	A	●	●		
Soave-Redlich-Kwong (SRK)	EoS		●	●	●
SRK with Lee-Kesler Enthalpies (SRK-LK)	EoS			●	
SRK with Kabadi Danner Modification (SRKKM)	EoS			●	●
Sour, API	K		●		

Table 7-2. Thermodynamic models and thermophysical property methods (cont'd)

Model	Type of Method*	CHEMCAD	ASPEN	HYSYS	SIMSCI
Sour, PR	K			●	
Sour, SRK	K			●	●
Standard State Aqueous Equilibrium Constants	A				●
Steam	EoS		●	●	
Tanger and Helgeson Heat Capacity	S				●
T-K Wilson	A	●			
UNIFAC	A	●	●		
UNIQUAC	A	●	●	●	
UNIWAAL	A				●
Van Laar	A	●	●	●	
Virial	EoS			●	
Wagner Interaction Parameter	A		●		
Water-Hydrocarbon 3-Phase	S	●		●	●
Wilson	A	●	●	●	●

*A = liquid activity coefficients; EoS = equation of state; F = fugacity coefficient correlation;
G = general correlation method; K = vapor liquid ratio correlation.

variation exists among companies with respect to the level of detail included in what are, mostly, promotional rather than instructional materials. Thus, the tables are not completely inclusive; they do not include everything the software will do, and some related topics are combined. Similarly, lists of this sort do not always indicate the extent that calculated results will be useful, complete, or directly applicable to any particular system.

After the simulation objective has been well defined, more detailed information should be obtained from prospective suppliers prior to making decisions about software acquisition. If the suppliers permit, a review of the instructional manuals would provide an in-depth understanding of the capabilities and limitations of each software package, well beyond the scope of what can be presented in this report. Interviews with experienced users would also be helpful. Nevertheless, these tables illustrate the range of capabilities available and show, in a general way, some of the variations between software suppliers.

The software discussed in this section is available from some of the largest suppliers. The omission of the smaller, newer suppliers does not reflect negatively on them. Some provide high-quality software for niche markets, such as the Bryan Research and Engineering (BR&E) software for processes involving sulfur.

7.2.6 Hanford Tank Wastes and Process Simulation

Several aspects of process simulation software should be of particular interest for tank waste processing. Investigators evaluating waste treatment technologies need to use tools that could help them understand the implications of their approach in terms of secondary and tertiary waste streams or the extent to which a unique new process will affect upstream or downstream processes. To evaluate many aspects of proposed flowsheet designs, flowsheet modeling that can define the internal recycle streams is needed. This ability would make it possible to study the influence of each operation on the whole plant. For example, one can evaluate how offgas levels from one operation could affect the required offgas treatment operation farther downstream, or how much the blowdown generated in the offgas treatment operation affects the throughput of the aqueous liquids treatment section of the plant. In addition, flowsheet modeling can be used to evaluate the sensitivity and range of operating conditions, radioactive criticality, and relative costs of different flowsheet designs.

Since the tanks contain high concentrations of salts and variable concentrations of organics and flammable gases, such as hydrogen and ammonia, software that can simulate concentrated aqueous electrolyte systems would be of benefit. The ability to predict aqueous solubilities and the conditions of solids formation will be important. Much of the transportation involved in waste processing will go through pipelines, so a strength in modeling piping networks, particularly slurry transport, should also be a plus. Heat exchange networks will almost certainly be involved, but for tank waste processing, optimizing network efficiency may be less important than ensuring high-quality, robust designs. As the planning and design process may be lengthy and subject to significant changes along the way, a process simulator that facilitates rapid production of specification sheets, detailed process flow diagrams, cost estimates, and other relatively finished engineering products may provide a significant saving in time. It is quite possible that no single software package will provide a superior product for every area of concern. A combination of packages may provide the best results. Some large chemical and hydrocarbon processing companies use several packages together successfully.

The complexity of the Hanford TWRS program presents a challenge for successful process simulation. While some aspects of the TWRS are unique, there are parallels in other process industries. Some previous work has been done by the DOE in developing approaches for simulating the complex system. The complexity of the TWRS comes from the large number of feed streams, product streams, and recycle streams, the large number of components in the feed streams, and the need to deal with three phases in much of the processing. In addition, some undefined aspects of the system require, for practical purposes, the use of a variety of potential definitions. These undefined, or incompletely defined, aspects include the overall flowsheet configuration, separations methods, and some feed stream compositions or partial compositions. One of the main goals of early, preliminary flowsheet simulations may be to facilitate improved definition for further simulations. Answers to the following questions may provide information useful for that effort:

- Within the range of uncertainty in the feed streams composition, how much difference does composition make to the global simulation?

- Are different unit operations required?

- How does the product distribution change?

- Do the safety requirements change?

- How do some potential flowsheet configurations affect safety, costs, schedule, and products?

- Can realistic performance measures be developed that will help engineers select among the myriad of processing possibilities?

The issue of stream complexity has been dealt with quite successfully in petroleum refining. Crude petroleum contains many thousands of individually identifiable chemical compounds, and modeling the use of each one would overwhelm the simulation effort. Instead, compounds that boil at about the same temperature are grouped together, then the group is treated as though it were a single compound (the so-called "pseudocut"). Since nearly all separations in a refinery depend on boiling point differences, this grouping works well. The data are readily obtained from laboratory distillations in grouped form. That is, the groups and their properties are not built up compound-by-compound, but a laboratory separation is performed using a method similar to the refinery separations. The yields and properties of each increment of separation are determined, and the information provides a basis for accurately simulating the separations.

The use of a single approach to separations in petroleum refining provides a key to the success of the method. In the Hanford TWRS, the means of making the separations are not yet well defined. A variety of methods may be used, and they may rely on different physical properties. In addition, the basis of separation might not be conveniently characterized by a single property like the boiling temperature in oil refining. For example, some separation methods may provide quite different results from a single feed stream, depending on the stream's acidity, which, in turn, could be subject to independent control by the addition of acid or caustic. However, using this approach for a particular separation method requires that the yields and compositions be readily measured as a function of the extent of separation. The term "extent of separation" refers to the parameter(s) of separator operation that controls how the split occurs. For the distillation column, the temperature at the top of the column determines the cut point temperature. For a crystallizer, the percent of liquid evaporated determines the size of the resulting solids product "stream."

Knutson et al. (1994) used a different kind of grouping that has shown promise for reducing the complexity of the Hanford tank waste system. A section of a detailed simulation dealing only with a few feed and product streams and a separation unit was added to a section with similar streams and separation. By repeating the procedure, a simplified, intermediate simulation was developed in which the individual streams represented composites of several streams, and the separation unit operations represented the average effect of several separators. This approach required the use of relatively simple separator unit operations in which the composition of each product stream could be specified either arbitrarily or on some convenient basis. This approach loses the predictive capability of models that could base the composition of product streams on the composition and known physical properties of each component. However, because of ongoing uncertainties in the feed stream compositions, the more rigorous approach was not generally available on the detailed level anyway. The grouping enabled a solution with what otherwise would have been insufficient data, and the global simulation provided insight into large, macro effects. In this case, the results showed that significant reductions in waste glass production could be obtained if certain glass compositional constraints could be relaxed. That is, the presence of certain components were requiring a higher volume of glass production than required by most of the other components. While such constraints cannot be relaxed at will, in this case, research was directed to finding new glass compositions that could accommodate higher loadings

7-14

of the troublesome components. In simulations using groupings of this sort, care must be taken to ensure that the somewhat arbitrary separations can actually be made. Alternatively, it might be shown that separation errors would not affect the capability of the global simulation to provide the intended information.

A more detailed treatment of applying process simulation to the treatment of mixed wastes (i.e., waste containing both hazardous and radioactive contaminants) was provided by Dietsche et al. (1994). They describe the results of developing process simulation flowsheets by two independent groups of people. This approach was taken to provide training, cross-checking, and to obtain the greater insight available from a larger group. After the two flowsheets had been developed fairly well, they were combined into a single process simulation that incorporated the benefits of both approaches. The final result provided a number of valuable observations, including information on the auxiliary heat requirements for several unit operations, and approaches to finding better models for the melters, ion-exchange columns, and solids-handling equipment.

Some problem areas with the simulation itself were clarified. The models had difficulty handling elemental mercury as a liquid and in a distinct separate phase from everything else. To accomplish the simulation, the mercury was occasionally manually classified as a "solid." The simulation also had difficulty integrating batch processes into an overall simulation normally based entirely on continuous flows. The use of batch processes in HLW processing is common when solids are involved, because it is easier to handle solids in batches than in continuous flows. In addition, some special operations need to be accomplished in only small, selected portions of the total waste. In the global view, incorporating short term "campaigns" to accomplish some objectives on part of the waste resembles a batch process because it makes short-term changes or interruptions in the flow.

In some cases, the model of a batch process can be closely approximated by a flow system. To do this, it is necessary to know the results of the batch process on an incremental basis, that is, the modeler needs to know how the results vary as the batch is processed from start to completion. This knowledge may come from laboratory data or from a theoretical calculation. Then the batch is represented in a flowing system as a series of continuous-flow unit operations, all of which are identical in function, but their feed compositions differ. In the first operation, the result of the first increment of the actual batch processing takes place, then the bulk of the material "flows" to the second unit operation. The results of the first operation will have caused slight changes in the properties of the stream to the second operation, with respect to the first operation feed. With this slightly, or incrementally, changed feed stream, the second unit operation produces a slightly different result—it represents the second increment of batch processing. The stream continues through each successive unit operation, each representing another increment of results to the last, which represents the conclusion of the batch process. A useful criterion for determining how many increments are needed is that if a doubling of the number of incremental unit operations does not make a significant difference in the results, the number is sufficient.

Safety will be a paramount issue in designing the Hanford waste treatment process, and an accurate process simulation provides an important tool for safety analysis. The toxicity and reactivity of each process stream depend on its composition, and safe handling practices can be determined accordingly. Also, since improperly specified equipment may lead to unsafe situations, simulation results can be used to avoid such equipment problems as inadequate capacity, temperature or pressure ratings below actual stream conditions, and inability to handle unexpected solids or gases in the feed. Case studies can be particularly valuable in determining "worst case scenarios" that might not be the same in different parts of a large and complicated

process. The entire safety approval process will require flexibility and making quick changes, because many modifications, both minor and major, may be required as a result of the safety reviews. These modifications may require repeating the simulation and another safety review of the modified flowsheet. Involving safety experts in the early stages of flowsheet development can sometimes expedite the safety approval process.

7.3   THERMODYNAMIC MODELING OF AQUEOUS-BASED CHEMICAL SYSTEMS

The complexity and variability in the chemistry of the various Hanford tank wastes result in significant difficulty in assessing processing or criticality hazards or reactions. The chemistry of Hanford tanks is complicated because of the many volume reduction campaigns undertaken during the operating history of the Hanford site that involved chemical additions, inter-tank transfers, and evaporation. The compositions of many of these tanks are therefore quite distinct from one another. Hazard analyses of the Hanford TWRS could be aided by software that can be used to simulate reactions and processes involving complex, multicomponent aqueous systems over wide ranges of chemical composition, concentration, and temperature.

As pointed out in section 7.2, software with the ability to predict aqueous solubilities and the conditions of solids formation is important for evaluating Hanford TWRS processes. Hanford investigators reviewed software products available in the United States for thermodynamic modeling of aqueous-based chemical systems and selected a computer program produced by OLI Systems, Inc. called the Environmental Simulation Program (ESP) (Meng et al., 1994). The ESP has been used by Hanford investigators for various tank waste studies, including modeling of waste evaporation, waste calcine dissolution, and in-tank leaching and washing (Meng et al., 1994). In this section, a description of OLI software products, including ESP, is provided. As part of a preliminary evaluation of the potential use of OLI software for simulating Hanford processes, several simulation examples were developed for this report. These examples are discussed in section 7.3.6.

7.3.1   OLI Systems, Inc. Software

OLI Systems, Inc., software products are built upon the OLI engine, which is supported by a very large, in-place databank and allows the users to predict the chemical and phase behavior (including aqueous, vapor, organic liquid, and multiple solids) of most mixtures of inorganic or organic chemicals in water. The resulting phase separation into aqueous, vapor, organic liquid and multiple solids is performed automatically.

The major components in the OLI Engine include the underlying thermodynamic framework and the supporting OLI databank, a numerical solver, OLI Express, and Water Analyzer. The OLI Express performs single or parametric calculations for investigating chemical speciation changes, pH, solubility, adiabatic or isothermal equilibrium and other phenomena of real and hypothetical samples and process streams. The Water Analyzer can be used to input, store, manipulate, and reconcile laboratory water analyses data, with facilities to export the results to process simulation modules such as ASPEN and PRO/II, which are described in a preceding section.

OLI software products, which all use the OLI Engine, include the ESP, Corrosion Simulation Program (CSP), Scaling Simulation Program (SSP), Remediation Simulation Program (RSP), and Crystallization Simulation Program (CrySP). The ESP, which will be of greatest interest to TWRS operations, can be used to simulate steady-state chemical and environmental processes with control loops

and multiple recycles. Modeling of heterotrophic and autotrophic biological degradation can also be achieved. ESP is a useful tool in understanding complex aqueous problems, investigating and evaluating process alternatives, troubleshooting and optimizing existing processes and discharges. Included with ESP is a dynamic simulator called DynaChem, which calculates time-dependent and transient process responses. It can be used to examine control strategy, controller tuning, startup/shutdown studies, system behavior with respect to process upsets, and operator training.

The CSP predicts corrosion chemistry and corrosion rates under real solution conditions, that is, accounting for ion interactions, ionic strength, and temperature. It makes it possible to predict if a system is susceptible to corrosion, thus allowing preventive actions to be taken (e.g., selecting the correct operating conditions and corrosion-resistant materials). The principal features of CSP include automatic generation of corrosion and redox chemistry, calculation and display of real solution Pourbaix, generalized stability, and yield diagrams, and computation of electrical conductivity and oxidation-reduction potential (ORP) of any multicomponent system.

Another component of OLI software is the SSP, which provides a practical, easy-to-use tool for studying scale formation problems in oil-field production wells over the range of conditions observed by the exploration and production industry. Unlike the other OLI programs, SSP uses a special customized databank with species that are of interest mainly to the petroleum industry.

The CrySP is a specialized program that addresses both the equilibrium and kinetic aspects of a crystallization process. It performs solubility analysis with regard to changes in process conditions such as temperature, pressure, and compositions. Material and energy balance, as well as nucleation and growth kinetics, are taken into account in the modeling of a mixed-suspension, mixed-product-removal crystallizer.
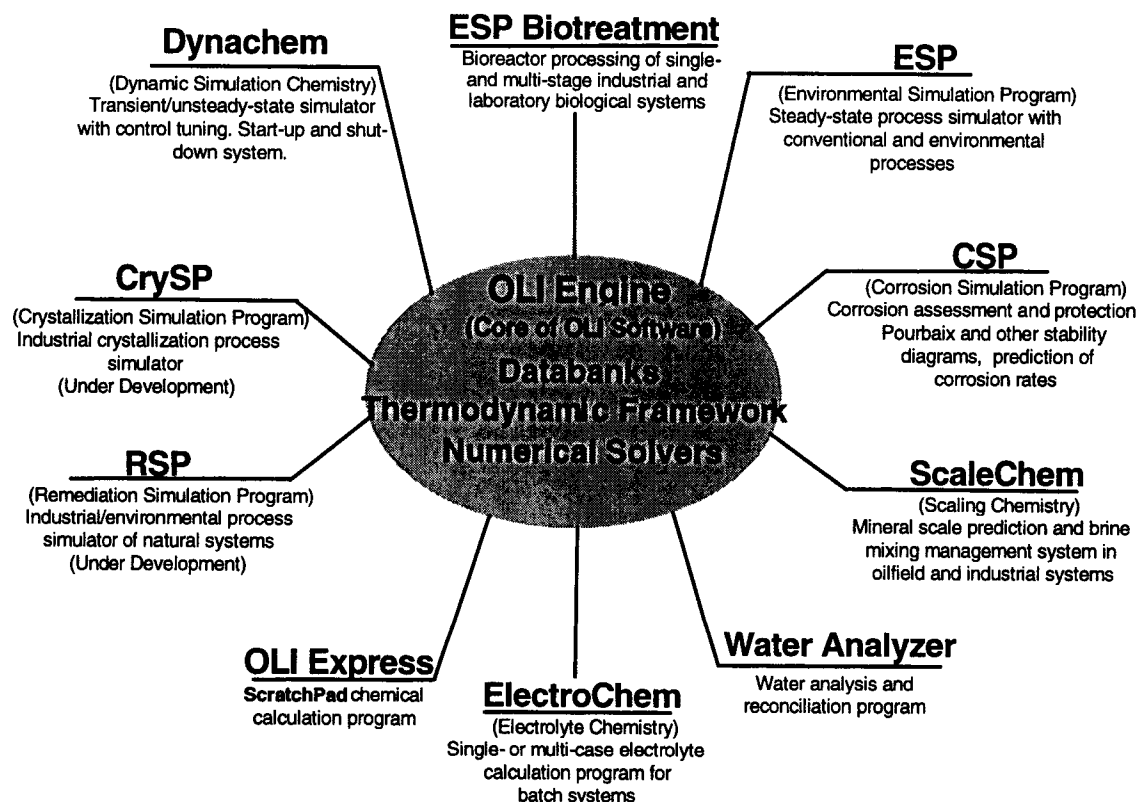
The principal features of the RSP include the Solid Analyzer, toxicity characteristic leaching procedure (TCLP) modeling, step-wise simulator, *in-situ* remediation simulation, and, ultimately, chemical fate modeling. Given the elemental analyses, the Solid Analyzer in RSP calculates thermodynamically stable solid phases at specified conditions in a solid sample. A routine EPA TCLP can be simulated with RSP. The step-wise simulator feature allows the simulation of a sequence of steps involving solids and reagents to answer what-if scenarios. Advanced phenomena such as coprecipitation, surface complexation, and molecular adsorption will also be included in RSP. However, it should be pointed out that RSP, as well as CrySP, are still under development. Commercial releases of this software are due in the near future.

The relationships among various OLI software components and their features can be summarized in figure 7-1. It should be pointed out that CrySP and RSP are still under development. Commercial releases are due in the near future.

7.3.2 Thermodynamic Framework

The underlying thermodynamic framework used in the OLI software combines the Helgeson-Kirkham-Flowers (HKF) (Helgeson et al., 1981) equation of state for standard-state properties with a solution non-ideality model based on the activity coefficient expressions developed by Bromley (1972) and Pitzer (1973, 1991). This framework is coupled with an efficient mathematical algorithm for calculating phase equilibria in multicomponent systems that may contain an aqueous phase, any number of solid phases and, if necessary, a vapor and a nonaqueous liquid phase. The thermodynamic model and the numerical solver form the basis of the aqueous simulation technology in the OLI software.

OLI SOFTWARE COMPONENTS

Dynachem

(Dynamic Simulation Chemistry)
Transient/unsteady-state simulator
with control tuning. Start-up and shut-
down system.

ESP Biotreatment

Bioreactor processing of single-
and multi-stage industrial and
laboratory biological systems

ESP

(Environmental Simulation Program)
Steady-state process simulator with
conventional and environmental
processes

CrySP

(Crystallization Simulation Program)
Industrial crystallization process
simulator
(Under Development)

CSP

(Corrosion Simulation Program)
Corrosion assessment and protection
Pourbaix and other stability
diagrams, prediction of
corrosion rates

OLI Engine
(Core of OLI Software)
Databanks
Thermodynamic Framework
Numerical Solvers

RSP

(Remediation Simulation Program)
Industrial/environmental process
simulator of natural systems
(Under Development)

ScaleChem

(Scaling Chemistry)
Mineral scale prediction and brine
mixing management system in
oilfield and industrial systems

OLI Express

ScratchPad chemical
calculation program

ElectroChem

(Electrolyte Chemistry)
Single- or multi-case electrolyte
calculation program for
batch systems

Water Analyzer

Water analysis and
reconciliation program

Figure 7-1. OLI software components and features

The HKF equation is based on solvation theory and expresses the standard-state thermodynamic functions as sums of structural and solvation contributions, the latter being dependent on the properties of the solvent (i.e., water). Using the HKF equation, standard state properties at any temperature and pressure can be calculated accurately with the knowledge of reference state Gibbs free energy of formation, enthalpy of formation, entropy, and seven equation parameters, which have been tabulated for large numbers of ions, complexes, and inorganic and organic neutrals. The HKF equation is valid for temperatures up to 1,000 °C and pressures up to 5 kbar.

The activity coefficient model used for representing the solution non-ideality is an extended form of an expression developed by Bromley (1972). The Bromley equation is a combination of the Debye-Huckel term for long-range electrostatic interactions and a semi-empirical expression for short-range interactions between cations and anions. Interaction parameters exist only between oppositely charged species. The extended three-parameter form of the Bromley model is capable of reproducing the activity coefficients in solutions with ionic strength up to 30 molal, but it is restricted only to ionic interactions. For aqueous solutions with neutral species, the well-known Pitzer model (1973, 1991) is used to account for the ion-molecule and molecule-molecule interactions.

Accurate representation of the standard state properties by the HKF equation and of the excess properties by the Bromley and Pitzer models enables simulation of aqueous chemical systems using the OLI software for temperatures up to 300 °C, pressures up to 1,500 bar, and concentrations up to 30 molal.

7.3.3 Software Capabilities

In applying the software, the user enters the input values of the desired molecular inflows and the simulation conditions. The software automatically determines the stable phases and the equilibrium distribution of the different phases and species. Phase equilibria, including vapor-liquid, liquid-liquid, and solid-liquid equilibrium, are calculated. These calculations allow prediction of aqueous solubility of inorganic and organic compounds, bubble and dew point temperatures and pressures, and isothermal and adiabatic flash points. Other thermodynamic and transport properties reported in the simulation results include enthalpy, density, pH, oxidation-reduction potential, osmotic pressure, and electrical conductivity.

Special capabilities for modeling coprecipitation, surface complexation, membrane separation using reverse osmosis, ultrafiltration, electrodialysis, and biotreatment process are also available in the OLI software for applications to environmental problems. The coprecipitation model allows the replacement of an ionic element in a crystalline lattice by a foreign ion in the solution. The model is based on the Linear Free Energy method of Sverjensky and Molling (1992) for the standard state properties, in conjunction with either a one-parameter regular solution or a two-parameter Margules activity coefficient model. It currently supports 16 lattice types, including carbonates, sulfates, oxides, and hydroxides. The surface complexation model is based on the work of Dzombak and Morel (1990) and uses a generalized two-layer representation of the solid-water interface. Sorption of twelve cations and ten anions on hydrous ferric oxide can be modeled in the current version of OLI software.

For process simulations, the OLI software has the following chemical and environmental process and control units:

Absorber	Electrodialysis	Neutralizer
Bioreactor	Feedforward	Precipitator
Clarifier	Gibbs Reactor	Reactor
Component Splitter	Heat Exchanger	Saturator
Controller	Incinerator	Sensitivity
Crystallizer	Manipulate	Separator
Dehydrator	Membrane	Splitter
Extractor	Mixer	Stripper

These units make up the building blocks for simulating a simple process (aqueous chemistry-focused) or a complete flowsheet (process-focused).

7.3.4 OLI Databank

Simulations using the OLI thermodynamic framework require the use of reference state and mixture properties stored in the OLI Databank. The OLI Databank contains thermodynamic and physical properties for 78 inorganic elements in the periodic table (including actinides, heavy and precious metals) and their associated aqueous species. Figure 7-2 shows the elements in the periodic table that are covered by the OLI Databank. The databank also includes over 3,000 organic compounds (including organic electrolytes and

Periodic table of the elements

Figure 7-2. Periodic table showing the elements included in the OLI Databank

chelating agents). Thus, the content of the databank represents almost all components of potential interest to a wide variety of industries. However, thermodynamic data for some elements and aqueous/gas/solid species that are of specific interest to the Hanford TWRS may be lacking from the OLI databank, which could limit the applicability of OLI software to Hanford studies. Thus, a critical evaluation of thermodynamic data for use in Hanford simulations would be necessary in any modeling of Hanford TWRS processes.

The OLI Databank consists of different chapters. In the Species Chapter, all the thermophysical properties for each species are stored in three sections: (i) the aqueous phase, (ii) the vapor phase, and (iii) the solid phase sections. All three sections contain published reference state properties, which include Gibbs free energy of formation, enthalpy of formation, entropy, heat capacity, and volume. Governing equilibrium reactions associated with each species are also contained in these sections. For each aqueous species, either neutral or ionic, the HKF parameters are stored in the aqueous phase section. Additional pure component properties stored in the vapor phase section include critical temperature, pressure, volume, acentric factor, normal boiling point, and a vapor pressure correlation based on experimental data.

The Interaction Chapter contains all the interaction parameters used in the OLI thermodynamic models for calculations of thermodynamic and transport properties. These parameters are based either on published mixture data or obtained by available estimation methods. The Electrical Chapter contains values of limiting electrical conductivity of individual species, which are needed for accurate predictions of electrical conductivity of multicomponent solutions. The Coprecipitation and Sorption Chapters provide the necessary parameters to support the coprecipitation and ion exchange modeling.

7-20

The default databank used in the OLI software is called the PUBLIC Databank. In addition to the PUBLIC Databank, there is a special corrosion databank used exclusively for corrosion simulation. It contains all additional species and reactions resulting from corrosion processes. SURCMPX Databank is another special databank used for modeling surface complexation phenomena. Currently, it supports only cation and anion surface complexation on hydrous ferric oxides.

All properties in the OLI Databank come from either the open literature or sponsored research projects. Reference citations can be easily accessed within the software for each stored property.

7.3.5 Simulation Examples Relevant to Hanford TWRS

Hanford investigators have used OLI software for various tank waste studies, including modeling of waste evaporation, waste calcine dissolution, and in-tank leaching and washing (Meng et al., 1994). For example, the Tri-Party Agreement (Ecology, 1994) specifies that the Hanford tank wastes will be pretreated by in-tank caustic leaching and sludge washing to greatly reduce the quantity of solids that must be vitrified as high-level waste. Caustic leaching will dissolve some or all of the aluminum, silicon, chromium, and some other nonradioactive metals, and also metathesize insoluble phosphate that is bound with bismuth to soluble phosphate ions. Washing the sludges will remove the mostly nonradioactive soluble species from the radioactive sludges.

To provide separation factors for tank waste species that can be used to predict results of leaching and washing a waste, PNNL investigators conducted leaching and washing experiments using tank core samples. Because the separation factors derived from these experiments are empirical, the leaching and washing behavior in systems with different chemical compositions that is predicted using these factors may not be accurate. To provide a simulation capability that is based on fundamental thermodynamic principles, ESP was used by PNNL investigators to simulate leaching and washing of tank wastes. The results of computer simulations were compared with laboratory data on sludge washing and leaching. The results from both agreed reasonably well, particularly for those elements that have solid phase data in the ESP Public Databank. The good agreement between experimental and simulation results indicate that ESP could be useful for simulating the aqueous-based waste treatment processing at Hanford.

To assess the chemical and process modeling capabilities of the OLI software for potential use in identifying and evaluating potential safety and operational hazards in Hanford TWRS operations, a number of simulation examples using OLI software were developed for this report. Various components of the OLI software were used in developing the examples. These components include ESP, OLI Databook, and OLI Toolkit. ESP was used for all examples that highlight the process modeling capability of the OLI software. OLI Databook is useful in determining if a Hanford-related species is covered by the supporting databank. OLI Toolkit, which includes OLI Express, Water Analyzer, and ProChem, was used to demonstrate the chemical modeling capability of the OLI software.

Compositions of the Hanford tank wastes were obtained from the HDW model of Agnew (1997). The DOE developed a set of criteria to identify tanks with potential safety concerns as Watch-list tanks, which are further grouped into flammable/hydrogen gas, high organic content, and high-heat load categories. In this report, compositions of tank supernatant solutions for three DSTs, AN-103, SY-101, and SY-103, in the Flammable/Hydrogen Gas Watch-list category, were used in the simulations.

Only major cations, anions, and organics in the tank component list were considered in the simulations. However, most tank components can be found in the OLI Databook, and additional components

can be added if more rigorous simulations are desired. The compositions of the three tank-supernates are shown in table 7-3. Among the organic components, glycolate was chosen for simulations relevant to oxidation reaction by nitrate or nitrite because it has the highest concentrations in all three tank supernatant solutions.

The feed stream compositions listed in table 7-3 in the ionic form cannot be used directly in the simulations. The Water Analyzer in the OLI Toolkit is a useful tool for converting ionic compositions into the corresponding molecular inflows, which can then be used directly in the process modeling. The ionic compositions of the three solutions were fed into Water Analyzer and reconciled for electroneutrality. An additional option for reconciling pH is also available in the Water Analyzer. However, pH reconciliation for the three solutions was not performed as the compositions are approximate and laboratory pH values are not available. After electroneutrality reconciliation, the resulting molecular compositions were sent directly to ESP Process for process modeling. The Water Analyzer also gave scaling tendency reports for the three solutions, which indicate possible solid formation at the specified conditions. The reconciled streams from Water Analyzer were also used in the OLI Express to study the solubilities of various gases, organics, and solids.

Whenever possible, quantitative comparisons of simulation results with literature values are shown in the figures. If literature data are not available, qualitative behavior is illustrated to address the specific chemical phenomenon predicted by the OLI software.

7.3.5.1 Example 1: Waste Compatibility During Mixing of Simulated Hanford Tank Wastes

Waste compatibility is an important issue in Hanford waste transfer operations. Chemical phenomena that can be studied with the OLI software include dissolution/precipitation, coprecipitation and sorption of Pu, flammable gas generation, and changes in organic solubility.

Table 7-3. Compositions of Hanford tank supernatant solutions

Chemical Constituents	SY-101 (ppm)	SY-103 (ppm)	AN-103 (ppm)
Na^+	23,8000	203,000	204,000
Al^{3+}	32,100	28,200	26,300
OH^-	121,000	105,000	99,400
NO_3^-	227,000	190,000	193,000
NO_2^-	81,200	70,700	57,100
CO_3^{2-}	20,200	17,100	25,200
SO_4^{2-}	17,900	15,300	14,700
Cl^-	6,350	5,410	5,350
Glycolate$^-$	5,610	4,750	9,150

In this example, simulation studies at 25 °C and 1 atm were performed for mixing supernatant solutions from tanks AN-103 and SY-103 at various volume ratios. A total volume of 1,000 L was used. The AN-103 volume was varied from 20 to 80 percent, at an increment of 10 percent. In ESP Process, both solutions were first sent to the Separator Block, which separates the inlet streams into different phases. The resulting liquid phases leaving the Separator Block were then mixed isothermally in the Mix Block where equilibrium calculations were carried out to determine the species concentrations and the potential formation of various phases at the specified process conditions.

The resulting simulation results indicate that both solutions are saturated with inorganic salts. The AN-103 solution is saturated with sodium nitrate, whereas the SY-103 solution is saturated with both sodium nitrate and sodium nitrite. For the AN-103 supernatant solution, the simulation results also show a high potential for precipitation of sodium nitrite, aluminum hydroxide, and sodium chloride. For the SY-103 solution, there is potential precipitation of aluminum hydroxide and sodium chloride. No solid formation was predicted for mixtures of AN-103 and SY-103 at all volume ratios. However, sodium nitrate remains the solid with the highest precipitation potential. This particular example illustrates how the OLI software can be used to investigate the potential formation of solids during mixing or transfer operations. The information obtained from the simulation can help determine actions necessary to mitigate plugging of transfer systems.

Pu is the radionuclide of most concern in criticality analyses at Hanford. In addition to precipitation, chemical processes such as coprecipitation and adsorption can lead to locally high concentrations of Pu. It would be useful to study the impact of these processes on the Pu distribution in tank wastes upon mixing. In the highly alkaline Hanford waste solutions, the dominant solids are ferric and aluminum hydroxides. However, as pointed out in section 5.6.3.2, Pu is not likely to form solid solutions with iron and aluminum due to a large difference in their ionic radii. Coprecipitation of Pu with these two elements is most likely a coagulation phenomenon in which Pu forms colloids that are enclosed in the hydroxides as precipitation occurs. Unfortunately, coagulation is not a phenomenon supported by the OLI software. Adsorption phenomena can be simulated with the OLI software, but parameters for simulating Pu adsorption are not in the databank and will need to be derived. For example, experimental data of Sanchez et al. (1985) can be reviewed to determine if they can be used to develop the missing parameters of the surface complexation model in the OLI software.

7.3.5.2 Example 2: Heats of Reaction of Hanford Organics with Nitrate and Nitrite and the Resulting Adiabatic Temperature Rise of Tank Wastes

Major organic compounds used in past Hanford operations are organic complexants and solvents. Due to the extensive use of nitric acid and sodium hydroxide, the Hanford waste tanks also contain large amounts of sodium nitrate and nitrite, with the nitrite arising primarily from radiolysis of nitrate. With the presence of heat-producing radionuclides, there exists a potential for rapid exothermic reactions between the strong inorganic oxidants such as nitrates and nitrites and the organic components. Such reactions could result in radioactive release to the environment.

Supernatant solution from tank SY-101 was used in this example. Thermodynamic heats of reaction of glycolate with nitrate were obtained using ESP Process for reactions with or without hydroxide and also with different end products. These thermodynamic values represent the maximum amount of heat produced from these reactions. Because of reaction kinetics and competing reaction pathways, these reaction heats are seldom fully realized. Nevertheless, the maximum values are useful as conservative estimates of heats that could be released and temperatures that could be achieved during the oxidation of tank waste organic components.

The heat of reaction can be easily calculated from the standard enthalpies of formation of reactants and products, which are stored in the OLI Databook. The OLI software is designed in such a way that it does not report thermodynamic heats of reactions of specific reactions in the simulation. Instead, the values are used internally for calculations of any enthalpy-related properties. The approach adopted here is to use an ESP Mix Block where the reactants, carried in two separate feed streams in approximate stoichiometric amounts, are mixed isothermally. The resulting heat duties of the Mix Block are taken as thermodynamic heats of reactions. Due to the heats of mixing, these values will not be exactly the same as the values calculated directly from standard state thermodynamic data.

The reaction between glycolate and nitrate is a reduction-oxidation (redox) reaction. Although the OLI software allows the inclusion of this type of reaction during the model generation step, redox reactions involving organics are not automatically included because of the use of a single material balance code in the OLI software for organic species. However, this problem can be easily overcome by creating a private database where the organic compounds are represented by elements, each with its unique material balance code.

Table 7-4 lists four reactions between glycolate and nitrate. These reactions are written for reactants and products in their real solution states, and, therefore, are different from those listed in table 3-10. The simulation results shown in table 7-4 are close to the standard state thermodynamic heats of reactions and indicate that the reaction in the presence of sodium hydroxide, with CO_3^{2-} and N_2 as the end products (reaction 3 in table 7-4), produces the maximum amount of energy.

Simulations were also carried out to determine the adiabatic temperature rise of tank wastes due to each of these four reactions. The composition of tank waste SY-101 is presented in table 7-3. A total solution mass of 7.45×10^6 kg, based on the HDW model of Agnew (1997), was used. Supernatant solution from tank SY-101 was first brought to an ESP Separator where phase separation was calculated. Like SY-103 and AN-103 solution, SY-101 was also found to be saturated with sodium nitrate, sodium nitrite, and sodium chloride. The saturated solution leaving the Separator was then split into two streams, each carrying separately the reactants. One feed stream contains most of the tank contents except glycolate. The other feed stream contains sodium glycolate and water. Because sodium ion is not involved in the reaction, it would have been possible to use glycolic acid to provide the glycolate ion reactant in the feed stream. However, glycolic acid would have been a poor choice because it would introduce additional heat of reaction due to acid-base neutralization during mixing of the two feed streams. Again, ESP Mix Block was used with these two feed streams. Adiabatic temperature rise was obtained by selecting the adiabatic calculation option in the ESP Mix Block. The simulation results are shown in table 7-4.

As would be expected, the resulting temperature rise of the tank wastes due to the redox reactions is consistent with the amount of heat released, with the value corresponding to reaction 3 being the highest. Adiabatic temperature rise for reaction three was also calculated for a solution consisting only of water plus the reactants glycolate and nitrate. The resulting temperature is 81.6 °C, which is about 17 °C higher than that in the SY-101 solution. It should be remembered that simulation results shown here considered only the reaction of glycolate with nitrate. Redox reactions involving other Hanford organics can be incorporated into the OLI chemistry model for more realistic calculations of the adiabatic temperature rise due to organic oxidation reactions.

Table 7-4. Enthalpy of reactions for the oxidation of glycolate with nitrate

Reactions	ΔH (kJ/mole) (std. state)	ΔH (kJ/mole) (ESP)	Adiabatic T Rise (°C)
$0.1\text{Glycolate}^- + 0.12NO_3^{-1} = 0.11CO_3^{2-} + 0.09CO_{2,aq}$ $+ 0.15H_2O + 0.06N_{2,aq}$ (1)	-655	-659	59.9
$0.1\text{Glycolate}^- + 0.15NO_3^- = 0.125CO_3^{2-} +$ $0.075CO_{2,aq} + 0.15H_2O + 0.075N_2O_{aq}$ (2)	-576	-575	56.0
$0.1\text{Glycolate}^- + 0.12NO_3^- + 0.18OH^- = 0.2CO_3^{2-} +$ $0.24H_2O + 0.06N_{2,aq}$ (3)	-733	-751	64.4
$0.1\text{Glycolate}^- + 0.15NO_3^- + 0.15OH^- = 0.2CO_3^{2-} +$ $0.225H_2O + 0.075N_2O_{aq}$ (4)	-642	-652	59.2

7.3.5.3 Example 3: Gas Solubilities in Hanford Supernates

Radiolytic processes and thermochemical degradation of Hanford tank wastes can lead to the generation of flammable gas mixtures. The presence of flammable gases and an ignition source could lead to reactions that could cause a radioactive release or provide an energy source that could facilitate other reactions within the tank. Gases produced at Hanford are mainly hydrogen and nitrous oxide. The solubility of these gases in tank wastes depends not only on temperature but also on tank composition. Predictions of gas solubility in the OLI software can be achieved with the use of OLI Express or ProChem.

In figure 7-3, calculated hydrogen solubilities in pure water are compared with the literature values of Wilhelm et al. (1977) over the temperature range of 10–70 °C and at a partial pressure of hydrogen of one atmosphere. Good agreement can be seen in this figure. Gases are less soluble in brines than in pure water due to a salting-out effect, and the Hanford wastes have high electrolyte concentrations of sodium, aluminum, nitrate, nitrite, and hydroxide. Figure 7-4 shows clearly the salting-out effect for hydrogen. The calculated solubility in the caustic solutions at 25 °C decreases as the sodium hydroxide concentration increases.

For gases that are sparingly soluble in liquids, their solubilities are known to follow the Setschenow relation, $\log (S/S_o) = k\,C$, where S and S_o are solubilities in a salt solution of concentration C and in pure water, respectively, and k is the Setschenow constant [see also Eq. (3-3)]. It can be observed in figure 7-4 that the calculated solubilities of hydrogen follow the Setschenow equation. Hydrogen solubilities in the SY-101 solution were also calculated and shown in figure 7-5. The solubility decreases by about 50 percent when the temperature increases from 25 to 100 °C.

For nitrous oxide, the calculated solubility in pure water at a partial pressure of 1 atm is in excellent agreement with the literature values of Wilhelm et al. (1977) shown in figure 7-6. Good agreement with the experimental values of Markham and Kobe (1941) can also be observed in figure 7-7 for nitrous oxide solubilities in sodium and potassium chloride solutions at 25 °C. However, a large disagreement between calculated and experimental values is observed for potassium nitrate solutions. Unfortunately, experimental values are not available for solutions containing the hydroxide ion, which is the dominant anion in Hanford tank wastes. In the SY-101 solution, the calculated solubility was found to decrease by about 85 percent when the temperature changes from 25 to 100 °C.
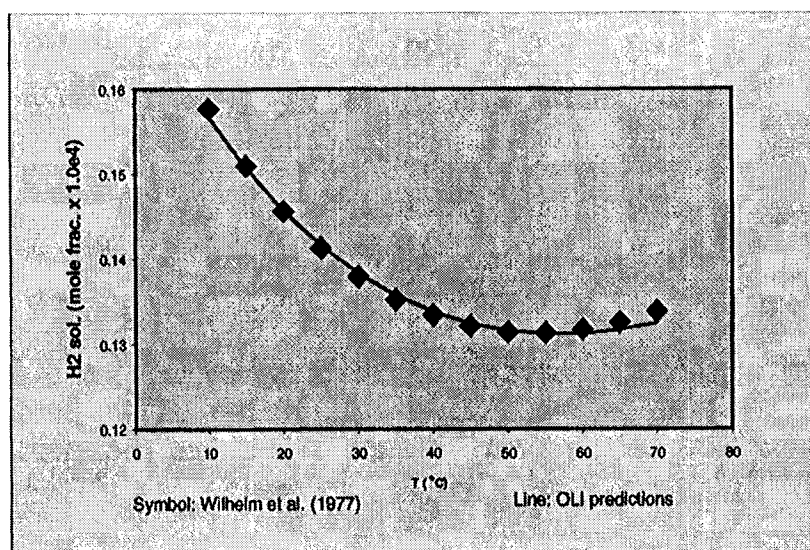
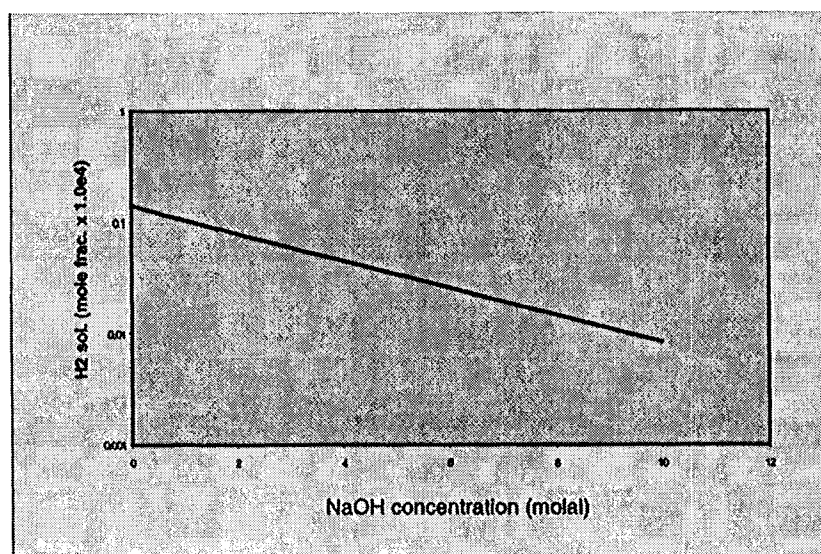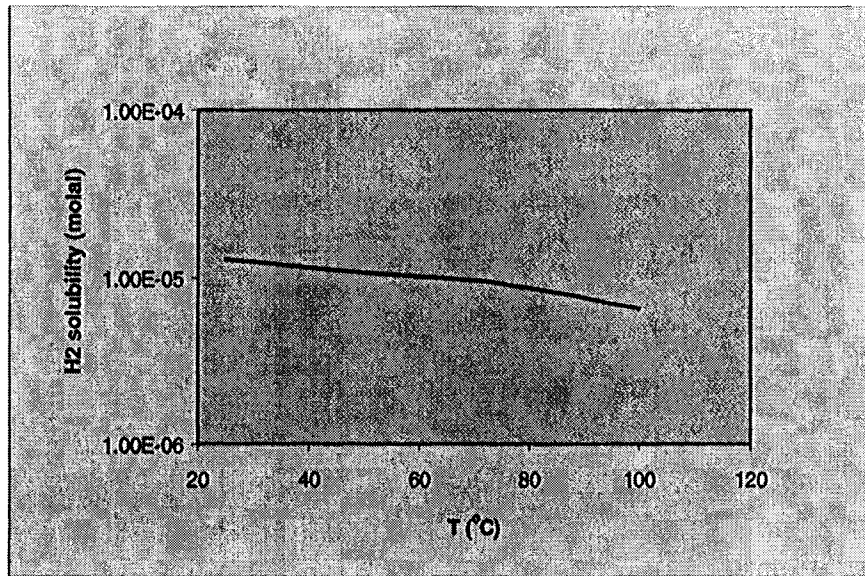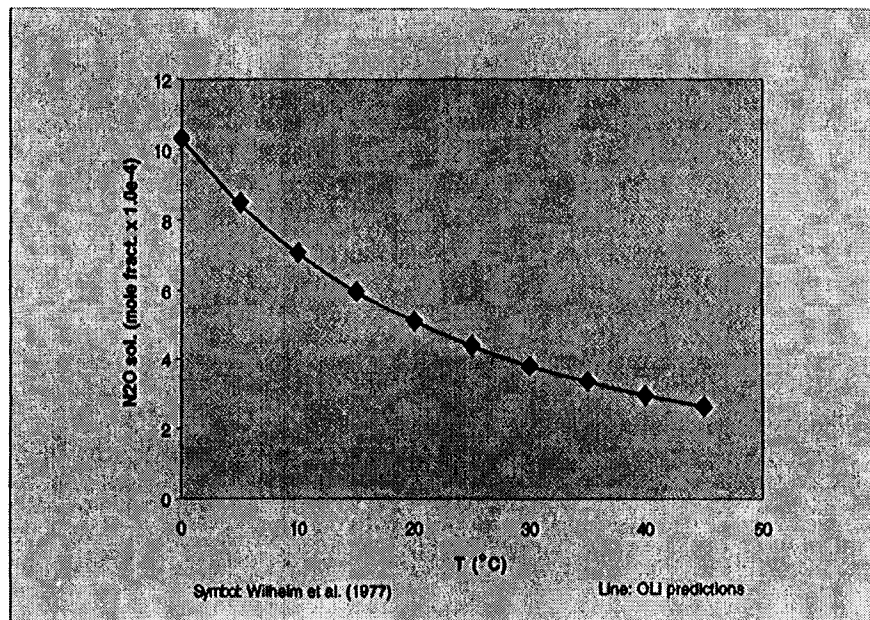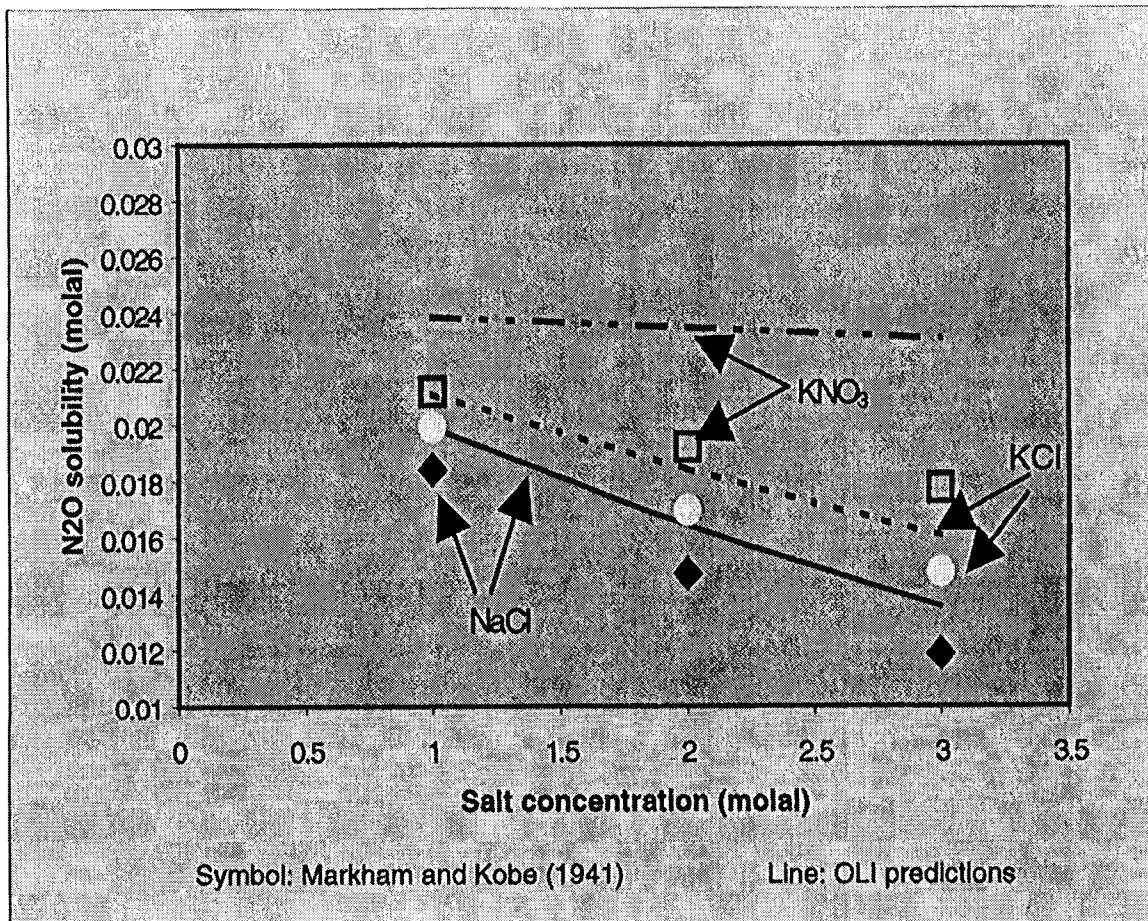**Figure 7-3. Hydrogen solubility in water**

Figure 7-4. Hydrogen solubility at 25 °C as a function of NaOH concentration

Figure 7-5. Hydrogen solubility in SY-101 solutions as a function of temperature

Figure 7-6. N₂O solubility in water as a function of temperature

Figure 7-7. N₂O solubility in salt solutions at 25 °C as a function of salt concentration

The simulation results presented here indicate both quantitative and qualitative agreement with the limited literature data. Although only single gas solubilities were calculated, predictions of gas mixture solubilities can be obtained without difficulty.

7.3.5.4 Example 4: Solubility of Organic Solvents in Hanford Supernates

Although the organic content in Hanford tank wastes is low, there is the possibility of organics being elevated to concentrations and total quantities sufficiently high to create a safety hazard. One of the mechanisms that can result in locally high concentrations of organics is dependent on organic compound solubility in the liquid wastes.

Hexone and TBP were used in large quantities at Hanford. Hexone is extremely volatile and is very reactive with nitric acid. Because of the volatility and reactivity of hexone, concentrations of this organic compound were assumed to be negligible in the HDW model of Agnew (1997). TBP is subject to hydrolysis, degrading to DBP (dibutylphosphate) and butanol, which are both much more soluble in the aqueous phase. It was found that OLI Databook does not contain, at present, any organic phosphate species. As a result, solubility prediction cannot be made for both TBP and DBP.

7-28

Other organic solvents that were used extensively in the solvent-extraction processes used to recover Pu and U are normal paraffinic hydrocarbons (NPHs), which are quite insoluble in the aqueous phase and likely to form a separate liquid phase. Results of detailed organic speciation measurements on tank C-103 samples (see table 3-7) indicate that, among all NPHs identified, tridecane has the highest concentrations, followed by tetradecane and dodecane.

As in example 3, OLI Express and ProChem were used to calculate organic solubilities in pure water and salt solutions. It is necessary to include the organic liquid phase option during the chemistry model generation. This option enables the program to determine if an organic phase is present and to calculate the species distribution between the aqueous and organic phases.

In the solubility data series compiled by Shaw et al. (1989), dodecane solubility in water at 25 °C reported by Franks (1966) is 8.9×10^{-10} mole fraction. However, a value of 4.0×10^{-10} by Sutton and Calder (1974) at the same temperature is also cited. The OLI calculated value is 5.4×10^{-10} mole fraction. In the same data compilation, Franks (1966) reported a value of 2.5×10^{-9} mole fraction for decane in water, whereas McAuliffe (1969) obtained a solubility of 6.58×10^{-9} mole fraction. The corresponding OLI calculated value is 7.2×10^{-9} mole fraction. It is apparent that there is a large amount of uncertainty in the experimental solubility values of the heavy alkanes.

For tridecane, no solubility data in water are available. Calculated water solubilities in the organic phase are plotted against temperature in figure 7-8. Also plotted are experimental values of Schatzberg (1963). Considering the scatter of the literature data for decane and dodecane, the agreement could be considered reasonable. The sparingly soluble organics in the aqueous phase exhibit the same salting-out effect as gases. Figure 7-9 shows this effect due to sodium nitrate.

7.3.5.5 Example 5: Solubility of Organic Salts in Hanford Supernatant Solutions

In addition to the organic solvents, organic complexants or acids were used frequently at Hanford. Another safety concern is the precipitation of organic salts together with sodium nitrate or nitrite, which could lead to energetic redox reactions. The organic salts are soluble in water; their metal salts are slightly to moderately soluble.

Oxalic acid is an important constituent in the Hanford tank wastes. It was used in the Bismuth Phosphate process as a reducing agent to separate the radiochemicals in the spent fuel. It also results from degradation of other organics in the tank wastes.

The same OLI software components for examples 3 and 4 were used for predicting the solubility of organic salts. Figure 7-10 compares the calculated solubility of oxalic acid (di-hydrate form) with the literature values of Seidell (1941). Good agreement can be seen. Similar agreement between calculated values and literature data of Linke and Seidell (1965) can be observed in figure 7-11 for sodium oxalate solubility in water. The common ion effect on sodium oxalate solubility can be clearly seen in figure 7-12 as the solubility decreases with increasing sodium nitrate concentrations. Solubility predictions of sodium oxalate can be easily made for solutions saturated with sodium nitrate at various sodium hydroxide concentrations. Figure 7-13 presents the simulation results. Again, the common-ion effect is correctly predicted.
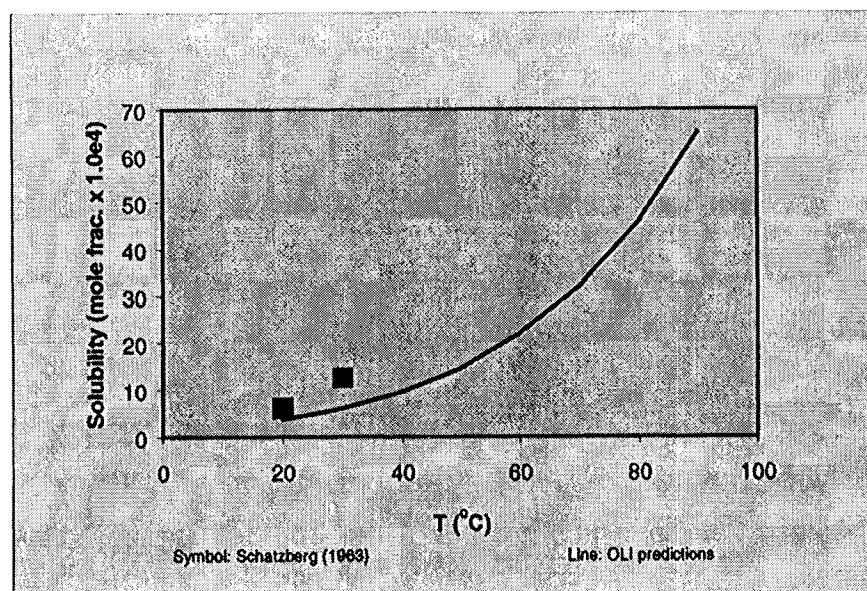
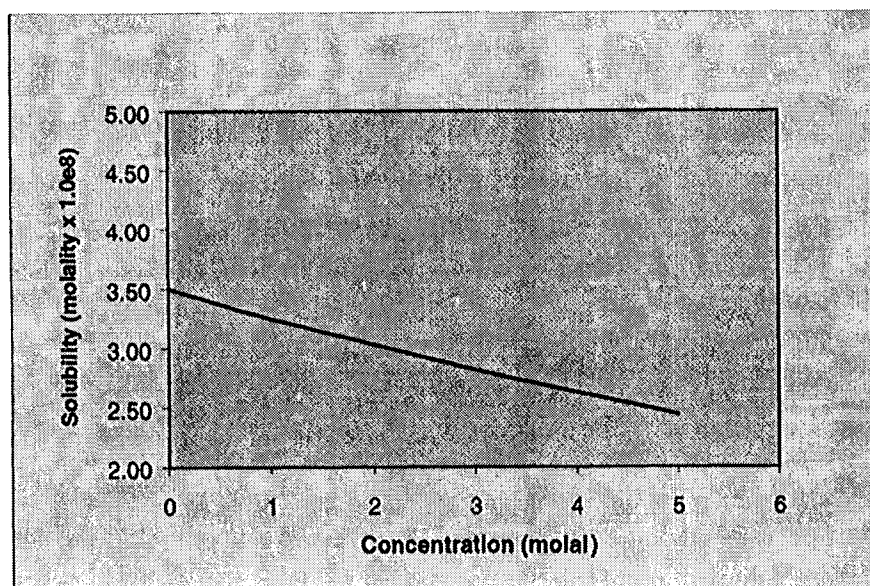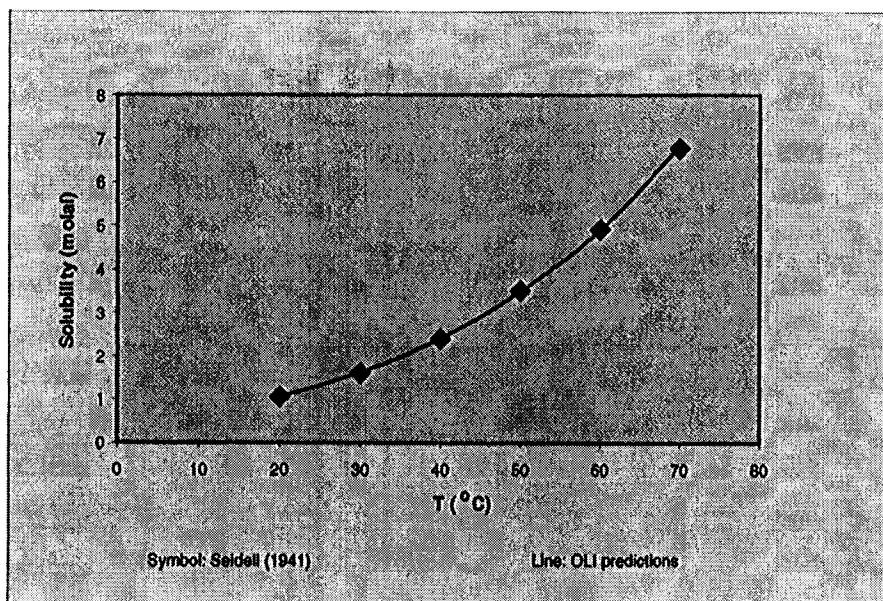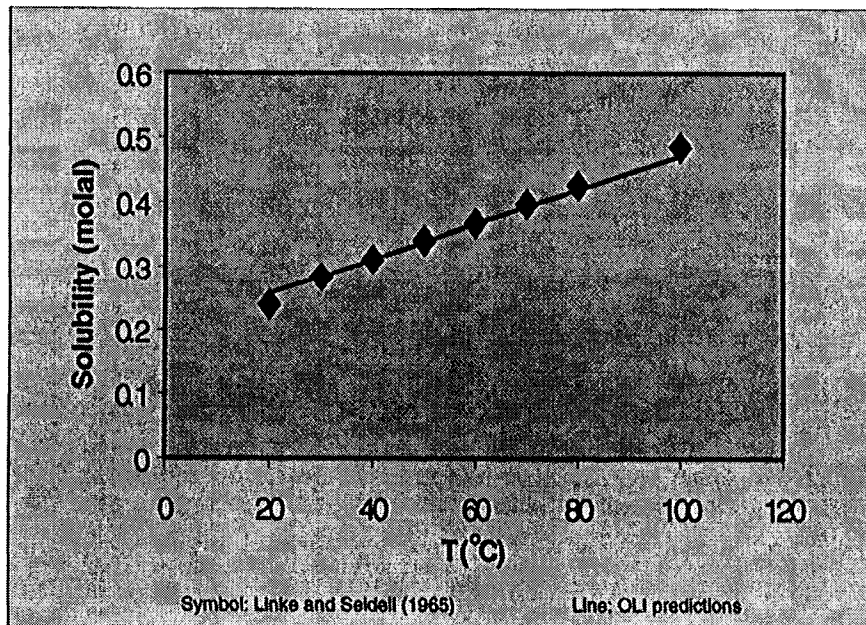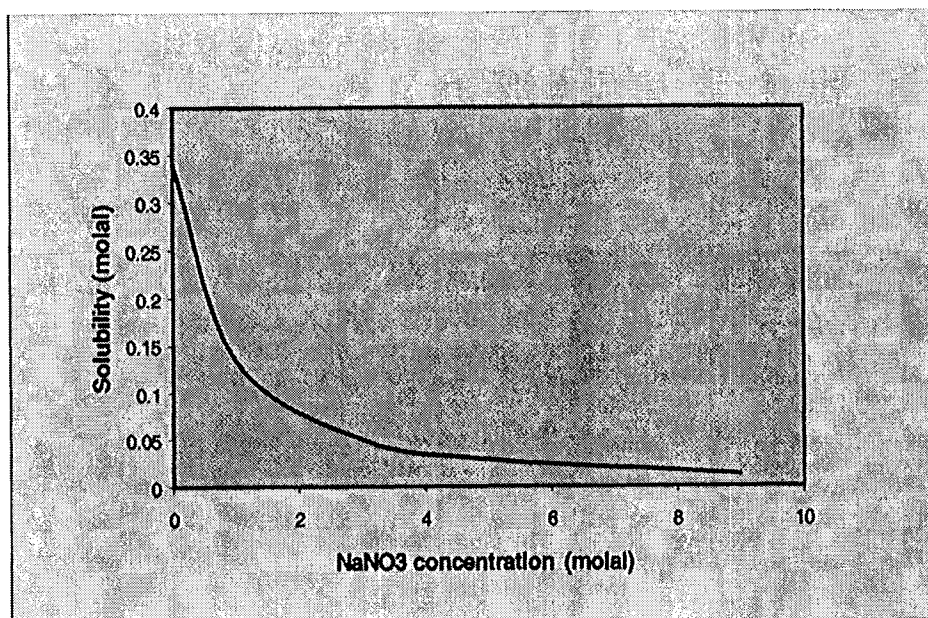**Figure 7-8. Solubility of water in tridecane**

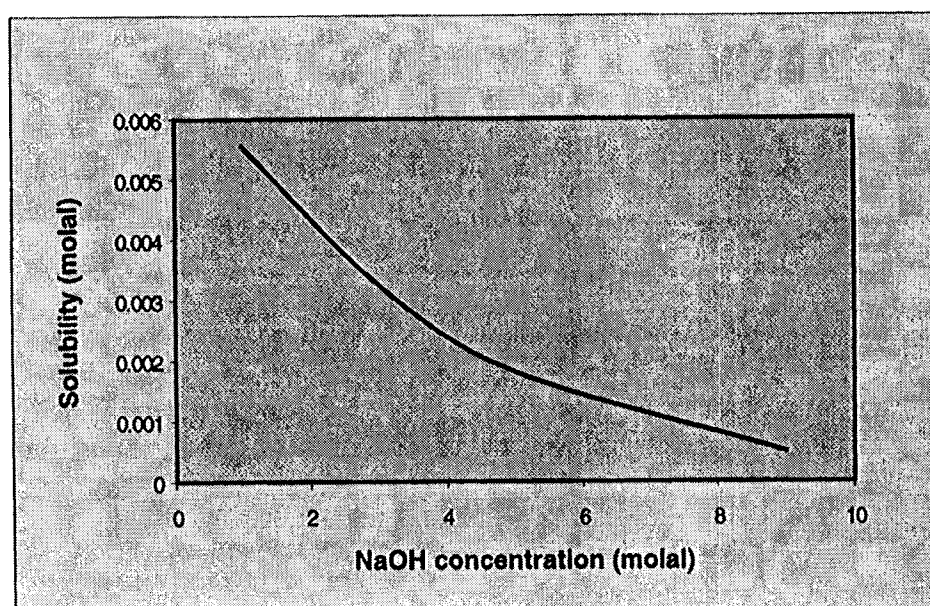**Figure 7-9. Solubility of tridecane in NaNO₃ solutions as a function of NaNO₃ concentration**

Figure 7-10. Solubility of oxalic acid in water as a function of temperature

Figure 7-11. Solubility of sodium oxalate in water as a function of temperature

Figure 7-12. Solubility of sodium oxalate in $NaNO_3$ solutions at 50 °C as a function of $NaNO_3$ concentration

Figure 7-13. Solubility of sodium oxalate at 50 °C in $NaNO_3$-saturated NaOH solutions as a function of NaOH concentration

The solubility of sodium oxalate in SY-101 solution was also calculated for various temperatures. The simulation results show a gradual increase from 1.22×10^{-4} molal at 25 °C to 1.92×10^{-3} at 100 °C. Compared to that in pure water, the calculated solubilities in SY-101 solutions are lower by several orders of magnitude, which is apparently due to the high concentration of sodium ion in the wastes.

Simulation results presented here illustrate how the OLI software can be used to study organic concentration processes resulting from precipitation in complex Hanford supernatant solutions.

7.3.5.6 Example 6: Aqueous Pu Chemistry

Plutonium is the primary fissile element in Hanford tank wastes that poses a potential nuclear criticality hazard. The OLI software can be utilized to study two parameters that are important to nuclear criticality, namely, the concentration of fissile material and the amount of neutron absorbers present in the tank wastes. Pu can exist in different oxidation states. However, as discussed in section 5.1.1.1, the Pu (IV) species is favored in Hanford wastes.

One mechanism by which Pu can be concentrated in the wastes is through precipitation as a pure solid. Assuming Pu concentration is controlled by a pure solid phase represents the most conservative approach because other controlling phenomena, such as coprecipitation and adsorption, will keep Pu concentration in the liquid below the pure phase solubility limit.

Figure 7-14 shows that Pu solubilities, assumed to be controlled by the $Pu(OH)_4$ solid, in water are extremely small and increase with increasing temperature. Calculated Pu solubilities at 25 °C are shown in figure 7-15 to decrease at increasing sodium hydroxide concentrations. Plutonium solubilities were calculated at 0.5 molal sodium hydroxide and various carbonate concentrations. However, the simulation results do not show an increasing Pu solubility with increasing carbonate concentrations, as seen in the work of Yamaguchi et al. (1994). An explanation for this discrepancy is that the Pu hydroxy-carbonate complexes proposed by Yamaguchi et al. (1994) are not in the OLI Databook. These species can be easily added to the OLI Databook provided that accurate thermodynamic properties are available in the literature.

Potential complexing agents for Pu are present in Hanford tank wastes. Even though these compounds are powerful complexants for Pu in weakly acidic solutions, they are not very effective at the high hydroxide ion concentrations of actual supernatant liquids. Figure 7-16 demonstrates how the OLI software predicts the weakening Pu-complexing power of oxalate when the solution changes from acidic to alkaline conditions. In this figure, PuOxa and PuOH refer to all Pu complexed to oxalate and hydroxide ligands, respectively.

The above results show that the OLI software can be used to study the complex aqueous Pu chemistry of the Hanford tanks. The software can also be used to calculate potential changes in Pu aqueous chemistry that may result during retrieval and processing of tank wastes. However, it is apparent that some additional input into the databank will be required to better describe the Pu speciation.

7.4 SUMMARY

The complexity and variability in the chemical types, compositions, and concentrations of Hanford tank wastes, as well as in the technologies that will be used to retrieve, pretreat, and solidify the wastes, make the identification and evaluation of potential hazards in the Hanford TWRS difficult. Consequently, conventional hazard audits of the TWRS facility may fail to identify a certain chemical reaction, plant
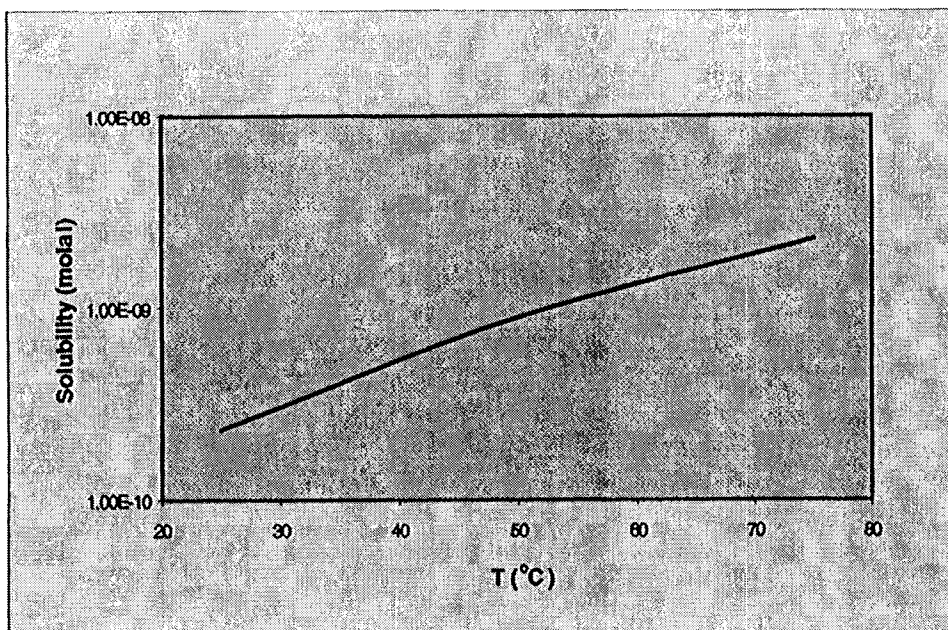
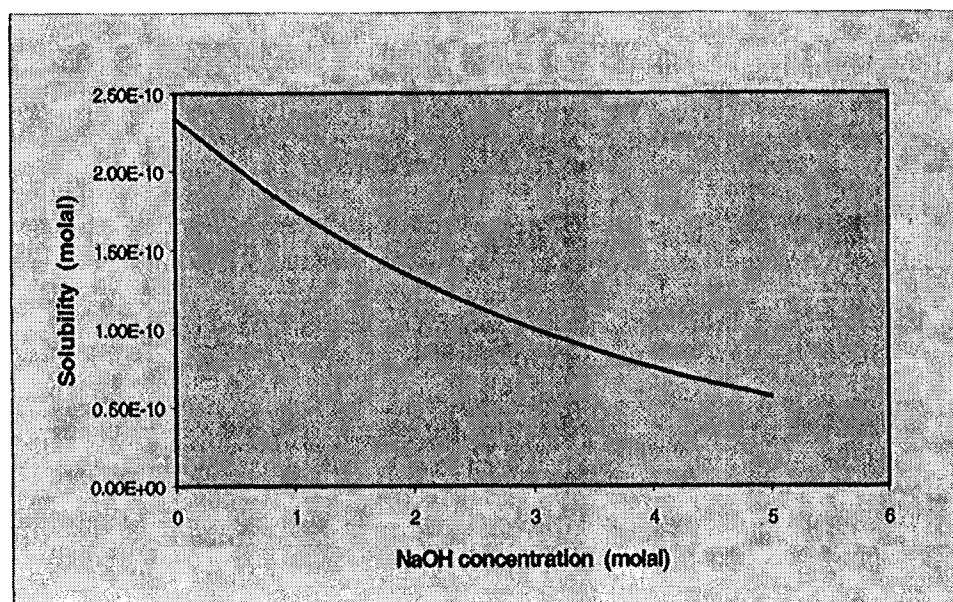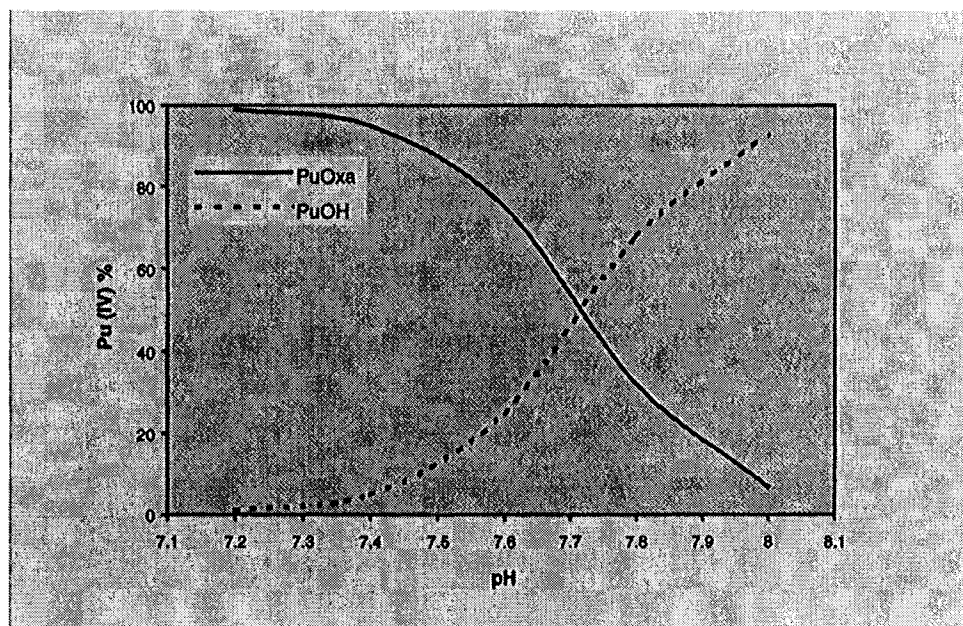Figure 7-14. Solubility of Pu(OH)$_4$ in water as a function of temperature

Figure 7-15. Solubility of Pu(OH)$_4$ in NaOH solutions at 25 °C as a function of NaOH concentration

Figure 7-16. Relative distribution of Pu(IV) species between Pu-oxalate complexes (PuOxa) and Pu-hydroxy complexes (PuOH) as a function of pH

process, or plant condition that could lead to a safety problem. Process simulation is a standard industry tool that is valuable for developing and designing complex processes and assessing factors that could cause safety problems. Several software programs for process simulation are available from commercial vendors, and each has its own areas of specialty and strengths. Flowsheet simulation software and their applications to process development were discussed in this chapter, but a critical evaluation of the different commercial software available is beyond the scope of this report.

It may be possible to use process simulation software to enhance the identification and evaluation of plant processes and conditions and chemical reactions that could lead to safety hazards in the Hanford TWRS operations. However, developing a process simulation for the Hanford TWRS faces the obstacles of process complexity and inadequate data. Previous efforts in process simulation by DOE investigators have concentrated on ways to obtain overall global views of the process because several critical questions require answers at that level before more detailed analyses can be conducted. Thus, the process simulation has been accomplished with some sacrifice of theoretical rigor, which might (though not necessarily) have caused some loss in accuracy. For the Hanford tank wastes, the ability to quickly make changes and obtain numerical solutions is of particular importance to support lengthy, detailed reviews, and to address any potential concerns about the TWRS facility.

A specialized suite of software for chemical process simulation developed by OLI Systems, Inc. has been used by Hanford investigators for various applications. Simulation examples were developed for this report using the OLI software as part of a preliminary analysis of its potential use for the Hanford TWRS. These examples are relevant to potential safety issues resulting from (i) flammable gases, (ii) high organic and nitrate contents, and (iii) fissile elements, particularly Pu. Supernatant solutions for three tanks on the DOE Watch-list, with compositions derived from the HDW model of Agnew (1997), were used in the

simulation examples. Three components of the OLI software—ESP Process, OLI Databook, and OLI Toolkit—were used in generating the examples. The simulation results indicate that the OLI software is able to provide the chemical and process modeling capabilities that could be useful to studies of potential safety issues resulting from waste management operations. However, inclusion of additional species and model parameters not currently in the OLI database is essential for better description and modeling of the chemical processes relevant to the Hanford TWRS.

8 CONCLUSIONS

This report provides information that could be useful to NRC staff in their assessment of chemical, radiological, and criticality hazards of the Hanford TWRS. Important hazards, particularly with respect to the regulatory role of the NRC, are those involving radiological risks to the public and workers, and the potential release of radioactivity to the environment. Current safety concerns of the DOE for continued interim tank storage of Hanford wastes are associated with the presence of flammable gas mixtures, high organic content, and heat-producing radionuclides in tank wastes. Based on the information discussed in this report, it is likely that the same safety issues would be of concern during the retrieval and processing stages of the TWRS program. In addition, the potential for nuclear criticality, considered by the DOE to be negligible during interim storage, needs to be considered during retrieval and processing of Hanford wastes. Furthermore, although the ferrocyanide safety issue has been closed by the DOE with respect to interim storage, this issue may also need to be reevaluated for the retrieval and processing stages of the TWRS program.

8.1   CHEMICAL AND PHYSICAL PROPERTIES OF TANK WASTES

Information on the chemical and physical properties of the Hanford tank wastes, summarized in chapter 1 of this report, is key to determining potential chemical reactions that could lead to hazardous conditions upon retrieval and processing. However, there is a high degree of uncertainty regarding these properties. Tank waste inventories are chiefly derived from reconstructions of waste histories and depend on the methods employed by the particular estimation scheme. Individual tank inventories have the highest degree of uncertainty. Although the overall site tank waste inventories for constituents are subject to less uncertainty, significant differences emerge from one estimation scheme to another.

Uncertainties in tank waste inventories and disparities in waste content between tanks may affect the chemical safety and the processing of the wastes. For example, knowledge of the chemical and physical properties of the wastes is needed to determine what, if any, actions are required to ensure safe interim storage, retrieval, or processing of each waste tank. Quantification of major organic constituents is needed to evaluate potential hazards associated with flammable gases and oxidizable organic constituents. Similarly, data on the content, distribution, and form of fissile material would be useful for criticality safety analysis. In addition, information concerning the chemical forms and concentrations of matrix components and their radioactive constituents is necessary before adequate waste consolidation (mixing) protocols and/or separation processes can be engineered. Furthermore, uncertainties in the concentrations of glass-insoluble phases, such as chrome minerals, spinels, and noble metals, may lead to the need for blending different waste types and/or increasing the volume of glass waste forms, both of which are expensive. Also, the presence of a large number of possible solid phases, aqueous complexants, and the high ionic strength (often several molal) of these solutions makes it extremely difficult to determine and predict the distribution of radionuclides between the sludges, suspended solids, and aqueous supernatants. Such a lack of fundamental knowledge about the distribution of radionuclides in the HLW stream significantly impacts the numbers of vitrified waste solids requiring disposal and, as a result, the ultimate HLW disposal cost. The large disparity in the tank waste inventories indicates that significant mixing of tank contents is needed to meet the specified waste envelopes. Mixing of tank wastes may result in additional safety hazards through various chemical reactions that are discussed in this report.

It is clear that better information on waste constituents in individual tanks is needed. Tank waste characterization is an ongoing activity at Hanford. A higher degree of confidence in individual tank

inventories is the goal of the Hanford "best-basis" effort, which is intended to unify results from the HTCE/HDW estimation scheme with analytical data on the wastes themselves. However, this work is still in progress, and the most recent results may be viewed online at the PNNL TWINS web site at http://twins.pnl.gov:8001/TCD/main.html. This database has all available assay data on tank waste samples, which should be a valuable resource for ongoing tank waste familiarization activities. However, until completion of this best-basis inventory, use of the HDW model (Agnew, 1997) may be preferred.

8.2 FLAMMABLE GAS SAFETY ISSUE

As discussed in chapter 2, the risk associated with flammable gas mixtures is a top priority safety issue with respect to interim storage of Hanford wastes. It is also likely to be a major safety concern during retrieval and processing of tank wastes because the processes that result in generation of flammable gases are expected to continue through the retrieval and processing stages of the Hanford TWRS operations. Essentially all radioactive wastes generate flammable gas mixtures by complex chemical reactions arising from radiolysis of water, thermal and radiological decomposition of organic compounds, and corrosion of metallic tank walls. The gases generated by these reactions comprise mainly hydrogen, nitrous oxide, nitrogen, and ammonia, with smaller amounts of methane and other hydrocarbons. In most tanks, the flammable gas generated in the waste is continuously released to the tank headspace. Various studies indicate that the generation rate is so low that ventilation ordinarily is able to keep the flammable gas diluted far below the concentration necessary for ignition. However, some wastes may have enough retained gas to pose a potential for worker injury, damage to equipment, or release of radionuclides to the environment if a significant fraction of the gas were suddenly released into the headspace of storage or process tanks, transfer lines, and process equipment (e.g., pumps) and ignited by an electrical discharge, a hot surface, or a hot gas. In a closed system, such as a waste storage tank, transfer line, or waste process feed tank, the resulting high pressure from the expanding product gases can compromise the integrity of the tank or transfer line and cause a radioactive release to the environment. The resulting heat could also provide an energy source that could facilitate other reactions within the tank or transfer line. Even very small gas releases can collect in equipment or in poorly ventilated tanks and result in a flammable gas hazard.

Various studies during the past few years have provided information on the mechanisms of flammable gas generation, retention, and release. Based on these studies, the three most important gas generation mechanisms are believed to be (i) radiolytic decomposition of water and some organic species, (ii) chemical reactions, mainly involving organics, and (iii) corrosion of the steel tank walls. The first two dominate, and the yield from chemical reactions usually exceeds that from radiolysis, especially at higher temperatures. Several mechanisms may cause gas retention in tank wastes, but gas bubble retention is the primary mechanism for storing in tank waste large quantities of flammable gases that could be released rapidly. Large amounts of soluble gases, mainly ammonia, can also be retained in tank waste, but no credible mechanism for spontaneous release of large amounts of dissolved gas has been identified. Gas release mechanisms currently considered most credible are the buoyancy-induced displacement, percolation of dendritic bubbles, and mechanical disruption, which includes local penetration (e.g., core sampling), removal of waste by salt-well pumping or sluicing, and severe earthquakes. Only buoyant displacement and seismic disruption are believed capable of a rapid release of a major portion (~50 percent) of the stored gas volume. However, energetic displacement can only occur in tanks with a relatively deep layer of supernatant liquid, a condition that exists only in DSTs. No known mechanism for large spontaneous releases in SSTs has been identified.

Some form of flammability control will always be needed to ensure safe operation during continued tank storage of Hanford wastes and during the TWRS operations. For example, sufficient ventilation must be provided to ensure that flammable gases are maintained at a safe level within the headspace of storage or feed tanks, transfer lines, or process equipment. However, controls need to be applied in a graded manner based on the type of activity being conducted. To identify the proper controls required for specific systems of interest, an adequate understanding of the processes and mechanisms for flammable gas generation, retention, and release is necessary.

8.3   HIGH ORGANIC SAFETY ISSUE

The possibility of exothermic reactions involving organic compounds mixed with oxidizing sodium nitrate and nitrite salts and heat-producing radionuclides is a major safety concern because rapid exothermic reactions can result in radioactive release to the environment, with attendant radiological exposure of workers and the public. Evaluation of potentially hazardous organic oxidation reactions is needed such that necessary mitigating actions can be determined and implemented (e.g., using diluents, destroying the organics, controlling the rate and quantity of process feed, controlling process temperature).

To assess potential hazards, it is necessary to determine the energies that could be released during chemical reactions involving oxidizable organic compounds. Heat or energy releases for different reaction pathways and end-products can be estimated using thermodynamic calculations. The calculated values can be used to predict the adiabatic rise in temperature that could occur for various oxidation reactions in different waste mixtures and to predict the effect of the concentration of both oxidants and diluents on the temperature rise. Calculations discussed in chapter 3 show that maximum energy is released by organic reactions with nitrates and nitrites when the reaction products are N_2, Na_2CO_3, H_2O, and CO_2. The reaction is more energetic if $NaNO_2$ is the oxidant instead of $NaNO_3$. Production of N_2O in place of N_2, or of CO in place of CO_2, greatly lowers the energy released. In alkaline pH conditions typical of Hanford tank wastes, CO_2 produced from organic oxidation reactions forms Na_2CO_3 and H_2O, resulting in more exothermic heat. Bounding estimates of heat generation and temperature rise for three HLW tanks discussed in chapter 3 indicate that the energy given off by organic oxidation reactions could cause the temperature to rise to at least 100 °C and to vaporize the water in the waste. The resulting pressure build-up could damage the tank and release radionuclides to the environment.

Thermoanalytical techniques used in the chemical industry for chemical hazards evaluation have been employed in DOE studies to measure the thermal sensitivities and the thermochemical and thermokinetic properties of organic and oxidant mixtures relevant to Hanford organic-bearing wastes. These studies indicate that energetic, self-sustaining exothermic reactions can occur among the salts of acetate, citrate, formate, oxalate, EDTA, and HEDTA, and the oxidants nitrate and nitrite if heated to a sufficiently high temperature under adiabatic conditions. There are significant differences in the thermal reactivities and sensitivities of the organic compounds. The amount of heat produced is dependent on the nature of the organic, with minimal dependence on the organic concentration (per gram of organic salt). The heat produced by reaction of equimolar sodium nitrate and nitrite with the different organics increased in the order $Na_3HEDTA > citrate > Na_4EDTA$, which is not consistent with the thermodynamically predicted order $Na_3HEDTA > Na_4EDTA > citrate$. This inconsistency suggests that the actual reaction pathways differ from those postulated strictly from thermodynamic considerations. The observed production of N_2O instead of N_2, and the less-than-theoretical-maximum heats measured by calorimetric techniques also indicate that the exothermic reactions between the organics and oxidants proceed, at least partially, through pathways that produce less than the maximum thermodynamically possible heat. Consequently, hazard assessments using

the maximum thermodynamically based energetics will likely overestimate the consequences of a reaction. In addition, the measured activation energies indicate that there is a relatively high energy barrier to the initiation of these reactions. Thus, high temperatures are likely required to initiate the organic oxidation reactions.

The DOE measurements of onset temperatures indicate that the relative order with respect to thermal sensitivity is $Na_3HEDTA \geq$ citrate > formate $\geq Na_4EDTA$ > acetate > oxalate. This relative order indicates that acetate is generally a less conservative model for the organics used at Hanford with respect to susceptibility to hazardous chemical reactions. It also indicates that organic-bearing wastes containing Na_3HEDTA and citrate should be of greatest concern. In addition, the thermoanalytical studies show that the controlling oxidation reaction is that of nitrite with the organic compound.

It should be noted that the DOE thermoanalytical studies used simple organic/oxidant mixtures, whereas Hanford tank waste chemistry is much more complex than those considered in the studies. Engineering analyses to assess the thermal hazards associated with the organic-bearing wastes need to consider the concentration of waste constituents other than the organics and oxidants. The greater reactivity exhibited by the simulated sludge waste compared to the other surrogate waste mixtures suggests that caution must be used in extrapolating the behavior of waste simulants to that of actual wastes with more complex compositions. It is possible that actual Hanford wastes may be more reactive due to the presence of thermally more sensitive organics, the presence of transition metal ions that could act as catalysts, or to synergistic interactions between the organics.

A concern regarding Hanford tank wastes is the possibility of organic concentrations and quantities being elevated to sufficiently high levels as to create a hazard that would not be anticipated if average tank values are used in the analysis. Two processes that could be important are organic concentration in the liquid phase and precipitation of organic compounds in the solid phase. Many of the organic compounds added to the Hanford waste tanks are quite insoluble in water and, depending on the quantity added to a specific tank, it is possible to form a separate organic phase in the tank. The hydrocarbon solvents are the most likely to have been added to the tanks in sufficient volume to create a separate organic layer, as evidenced by the observed presence of a separate organic layer in tank C-103 believed to be predominantly NPH and TBP. Precipitation of organic compounds from concentrated wastes can result in locally high concentrations of fuel and produce solids with organic-to-oxidant ratios significantly different from the waste tank average value. Organics could form solid mixtures with $NaNO_3$-$NaNO_2$ either by coprecipitation or by drainage of the bulk aqueous phase followed by evaporation of $NaNO_3$-$NaNO_2$-containing interstitial liquid in the already precipitated organics. The Hanford chemicals that could concentrate by this mechanism are the polar, water-soluble compounds that can form metal salts and organic acids or their sodium salts, such as oxalic acid, glycolic acid, citric acid, tartaric acid, gluconic acid, EDTA, and HEDTA.

A numerical criterion, based on measured organic fuel content (in terms of TOC) and moisture concentration, is currently used by the DOE to categorize an organic-bearing tank as safe, conditionally safe, or unsafe. For zero free-moisture content, a minimum of 4.5 wt % TOC is considered needed for a sustained propagating reaction. Higher TOC is required for a propagating reaction to occur if water is present because it dampens organic reactions. DOE tests indicate that about 20 wt % moisture is sufficient to eliminate the potential for sustained combustion altogether, independent of fuel type and concentration. Although the above criterion was derived for safety assessment of waste storage in Hanford tanks, the same criterion may be useful for evaluating the safety of organic-bearing wastes during the retrieval and processing stages of the

Hanford TWRS. Also, the potential for the waste to dry out and thus become unsafe during continued storage or during TWRS processing will need to be evaluated.

Various organic degradation processes have occurred that resulted in the formation of very simple compounds, such as formate, oxalate, or carbonate, and in a net reduction in the amount of energy available for reaction. However, although organic degradation results in lower organic fuel value, concurrent production of flammable gas mixtures increases the potential for flammable gas hazard. Because the chemical environment of Hanford wastes is conducive to organic degradation reactions, flammable gas mixtures will likely remain a key safety issue through most of the TWRS operations.

8.4 FERROCYANIDE SAFETY ISSUE

This safety issue has been closed by the DOE with respect to interim waste storage, but may be evaluated by the DOE, on a case-by-case basis, with respect to retrieval and processing of wastes. Historically, alkali-nickel ferrocyanides were added to Hanford wastes to precipitate Cs-137 and create additional tank storage space. The ferrocyanide safety issue arose because, in the laboratory, mixtures of ferrocyanides and nitrates or nitrites can be made to explode if heated to over 200 °C. As discussed in chapter 4, laboratory studies by the DOE to evaluate the explosive hazard of ferrocyanide wastes showed that an external heat source was required before any exothermic reaction could be observed. Thermal tests indicated major exotherms at temperatures above approximately 260 °C, suggesting the possibility of explosive reactions if mixtures of ferrocyanide and nitrate/nitrite are heated to high temperatures or if there is an electrical spark of sufficient energy to ignite a dry mixture.

Oxidation of ferrocyanide by nitrate and/or nitrite can result in a variety of reaction products with different reaction enthalpies. A comparison of enthalpies of reaction for several combinations of reactants and products shows that the energetics of the postulated reaction is highly sensitive to the products formed. The most energetic, for a given amount of fuel, is one that produces nitrogen and carbon dioxide (or carbonate salt if there is sufficient hydroxide available to form it). The reaction energy is greatly reduced if a sizable fraction of the carbon goes to CO due to incomplete oxidation, or if appreciable oxides of nitrogen form.

The range of compositions of ferrocyanide sludge capable of sustaining a propagating chemical reaction and the safety categories for storage of ferrocyanide wastes have been established by the DOE from experimental measurements supported by theoretical considerations. The theoretical approach indicates that, for waste with 0 wt % free water, the minimum fuel concentration necessary to sustain a propagating reaction is about 8 wt % sodium nickel ferrocyanide. For waste with greater than 8 wt % sodium nickel ferrocyanide, the mass of free water required to quench reactions increases linearly with ferrocyanide concentration. A key finding of the experiments is that propagation ceased when the free water concentration was 12 weight percent or more at a ferrocyanide concentration of 25.5 weight percent (the highest concentration found in the waste simulants). This water concentration was roughly half of the theoretical moisture criterion (23 weight percent) for a fuel value of 25.5 weight percent. This difference was expected because the thermodynamic calculations are inherently conservative.

Although initially some portion of the ferrocyanide waste probably exceeded 8 wt % $Na_2NiFe(CN)_6$, the minimum fuel concentration considered necessary to sustain a propagating reaction, ferrocyanide decomposition has resulted in chemicals that are either inert or have lower energy content. The DOE studies showed that the rate of degradation is primarily a function of the waste temperature, and tank records indicate

that most tanks were at a sufficiently high temperature for a sufficiently long time such that significant ferrocyanide degradation would be expected. Tank sampling data and waste history data show that the ferrocyanide concentrations have decreased to levels significantly lower than 8 wt % $Na_2NiFe(CN)_6$. On this basis, the DOE closed out the ferrocyanide safety issue with respect to waste storage in Hanford tanks.

However, evaluation of potential ferrocyanide reactions may be done on a case-by-case basis as part of the safety analysis of proposed retrieval and processing methods (Postma and Dickinson, 1995) because residual exothermic activity might be initiated by processing options that cause waste to be heated by an external source (e.g., during vitrification or accidental circumstance). The DOE results regarding the effect of moisture on reaction propagation are particularly important in this evaluation because studies indicate that ferrocyanide sludge is wet and will stay wet. Dryout by pumping, leakage, hot spots, and surface evaporation have been considered and found to be negligible during storage (Postma and Dickinson, 1995). Ferrocyanide-containing wastes are expected to contain sufficient moisture during the retrieval and pretreatment stages of the TWRS operations. For example, the low activity waste feed will have an insoluble solids fraction not exceeding 5 volume percent (U.S. Department of Energy, 1996b). Subsequent centrifugation will separate a fraction with a relatively high amount of entrained solids, perhaps to about 70 wt % insoluble solids. However, there may be no mechanism during the retrieval and pretreatment operations that could reduce the water content sufficiently to permit the sludge to become reactive. If such is the case, then ferrocyanide and nitrate/nitrite mixtures will likely not constitute a safety hazard during the TWRS operations.

8.5   NUCLEAR CRITICALITY SAFETY ISSUE

An important consideration in safety evaluations of the Hanford TWRS is the potential for nuclear criticality due to the presence of fissile material in the tank wastes. Collectively, the SSTs and DSTs contain an estimated 500 to 1,000 kg of Pu, which is associated almost exclusively with the sludge phase (Bratzel et al., 1996). It is necessary to ensure that the tank wastes remain subcritical with a sufficient margin of safety during continued storage, as well as during retrieval, pretreatment, and solidification of tank wastes. Based on a criticality safety assessment of Hanford waste tanks, Braun et al. (1994) concluded that the tanks have a large margin of subcriticality. However, conditions within the tanks or during retrieval and processing of wastes are not static, and various processes could lead to locally high concentrations of Pu in the tank wastes. For example, settling of particulates suspended in a waste mixture is the most obvious and, perhaps, the most effective mechanism for concentrating Pu. In addition, evaporation of waste liquid leads to higher concentrations and to possible precipitation of fissile material and/or neutron absorbers. Chemical processes during waste retrieval and pretreatment, such as precipitation of fissile material or dissolution of neutron absorbers, could lead to elevated and localized concentration of Pu in the waste. Thus, an important concern in safety evaluations of the Hanford TWRS is the identification and evaluation of processes that may lead to criticality during TWRS storage, retrieval, and processing operations.

As discussed in chapter 5, understanding chemical processes affecting Pu distribution is particularly important because Pu-239 is the only fissile Hanford tank waste component with a reasonable potential to induce criticality. Unfortunately, there is relatively little information on the effects of possible chemical or physical tank processes on Pu distribution. For example, while Pu chemistry has been well studied for decades, there is a scarcity of experimental data on solubility and solid-liquid partitioning in high-pH, high ionic strength systems characteristic of Hanford tank wastes. Quantitative evaluation of chemical mechanisms for concentrating Pu is difficult due to Pu redox complexity and the lack of sufficient data on Pu behavior in tank-type chemical environments. Therefore, models for Pu concentration mechanisms in the

wastes must be used with caution because they are not properly benchmarked to an extensive set of data. It is clear that much more experimental data under tank waste conditions are necessary to gain more confidence in predictive capabilities.

Nevertheless, some idea of the relative importance of processes may be obtained from the limited experimental and thermodynamic data on Pu. Consideration of mechanisms for aqueous Pu concentration suggests that it is highly unlikely that criticality levels could be achieved in liquids. The important aqueous Pu reactions are those affecting solubility and aqueous speciation. Available data suggest that Pu may exist in tank liquids as tetravalent hydroxycarbonate species with solubilities (limited by $PuO_2 \cdot xH_2O$) perhaps as high as 10^{-3} M. Oxidation to potentially more soluble Pu(VI) species, however, may be possible if more oxidizing conditions are present or have been induced by, for example, radiolysis or aeration. In addition, colloid formation could lead to Pu liquid concentrations exceeding solubility limits, but no quantitative means for evaluating this mechanism are available. Furthermore, Pu data from tank samples do not show such elevated concentrations.

Plutonium concentrations in tank solids typically exceed those in liquids by several orders of magnitude and, consequently, have a greater criticality potential. The important chemical mechanisms for solids concentration are pure Pu phase precipitation, coprecipitation with other solids, and adsorption. Growth of new pure Pu phases would require evaporation or chemical changes resulting in lowered solubility, in competition with coprecipitation and adsorption. Coprecipitation may result from two phenomena, solid solution and coagulation. While it may be possible to predict solid-solution behavior by thermodynamic calculation, understanding of coagulation behavior rests on observation and experimentation. Adsorption of Pu onto tank solids such as hydroxides of iron and other metals is considered by many to be an important means of Pu sequestration in solids. However, available experimental data imply suppression of Pu adsorption at the high-pH and high-carbonate contents typical of tank liquids, although more experimental studies for conditions relevant to Hanford tank wastes are clearly warranted. From a criticality standpoint, it seems most conservative to assume that Pu precipitation or coprecipitation reactions and adsorption phenomena can result in complete removal of Pu from solution.

Another aspect of waste chemistry relevant to criticality potential is the fate of neutron absorbers. In Hanford tank wastes, nitrogen is the most important soluble neutron absorber, whereas Fe and Al are the most abundant absorbers in the solids. Model simulations or predictions of waste chemistry should track these and other potentially important neutron absorbers. For example, Fe can undergo redox changes that will affect its aqueous solubility/speciation and solid-phase distribution, and Al solubility may be enhanced at high pH.

An approximate method was proposed and discussed in chapter 5 for determining k_{eff} for tank wastes when Pu-239, the primary fissile isotope in the tanks, has been concentrated to levels that approach criticality. This method is intended to allow an investigator to rapidly and conservatively estimate the criticality potential of a process and determine those cases where more detailed investigations into criticality are required.

8.6   HIGH HEAT LOAD SAFETY ISSUE

Radioactive decay heat of highly radioactive species, such as Sr-90 and Cs-137, is a potential safety concern in the Hanford TWRS because it could result in elevated temperatures during storage, retrieval or pretreatment operations. For example, radioactive decay heat determines the waste temperature profile and

influences the moisture loss rate. Thus, ventilation requirements, whether passive or active, for waste storage and process feed tanks need to consider the effect of radioactive decay heat. In a transfer line containing waste with high heat load due to radioactive decay, problems such as thermal expansion and distortion or rupture of the line could result. Also, degradation of ion exchange resins or other media used in pretreatment of Hanford wastes could be enhanced by high heat generated by radioactive decay. Furthermore, estimates of waste temperature are needed to account for temperature effects on chemical reactions that may occur in tank wastes such as degradation of organic species, thermochemical generation of flammable gas mixtures, and ferrocyanide degradation. Thus, waste temperature estimates could be useful in anticipating potential problems in TWRS operations.

A simplified method was presented in chapter 6 for calculating the volumetric heat generation rate of tank wastes based on their activity concentrations of Cs-137 and Sr-90. It was found that there can be significant differences in the volumetric heat generation rate for small heat sources versus large heat sources due to the escape of the 0.662 MeV gamma ray emitted by Ba-137m from smaller systems. The equations presented are useful in estimating waste temperatures based on known or assumed inventories of Sr-90 and Cs-137.

8.7 HANFORD TANK WASTE REMEDIATION SYSTEM AND PROCESS SIMULATION

Hazard audits of the TWRS facility may fail to identify certain chemical reactions, plant processes, or plant conditions that could lead to a safety problem because of the complexity and variability in the chemical types, compositions, and concentrations of Hanford tank wastes, as well as in the technologies that will be used to retrieve, pretreat, and solidify the wastes. It may be possible to use process simulation software, a standard industry tool for developing and designing complex processes, to enhance the identification and evaluation of plant processes and conditions and chemical reactions that could lead to safety hazards in the Hanford TWRS operations. For example, the toxicity and reactivity of each process stream depends on its composition, and safe handling practices can be determined with the aid of process simulation. Also, since improperly specified equipment may lead to unsafe situations, simulation results can be used to avoid such equipment problems as inadequate capacity, temperature or pressure ratings below actual stream conditions, and inability to handle unexpected solids or gases in the feed. Case studies can be particularly valuable in determining "worst case scenarios" that might not be the same in different parts of a large and complicated process. The entire safety approval process will require flexibility and the ability to make quick changes, because many modifications, both minor and major, may be required as a result of the safety reviews. These may require repeating the simulation and another safety review of the modified flowsheet. Involving safety experts in the early stages of flowsheet development may help expedite the safety approval process.

Several aspects of process simulation software should be of particular interest for tank waste processing. The waste disposal fractions that must be produced at Hanford need to be less troublesome than the original waste material. Thus, investigators evaluating waste treatment technologies need to use tools that can help them understand the implications of their approach in terms of secondary and tertiary waste streams or the extent to which a unique new process will affect upstream or downstream processes. Flowsheet modeling that has the ability to define the internal recycle streams would make it possible to study the influence of one operation on the whole plant. For example, one can evaluate how offgas levels from one operation could affect the required offgas treatment operation farther downstream, or how much the blowdown generated in the offgas treatment operation affects the throughput of the aqueous liquids treatment

section of the plant. In addition, flowsheet modeling can be used to evaluate the sensitivity and range of operating conditions and the relative costs of different flowsheet designs.

Developing a process simulation for the Hanford tank wastes faces the obstacles of process complexity and inadequate data. Previous efforts by DOE investigators in process simulation have concentrated on ways to obtain overall global views of the process because several critical questions require answers at that level before more detailed analysis can be conducted. Thus, the process simulation has been accomplished with some sacrifice of theoretical rigor, which might have caused some loss in accuracy. For the Hanford tank wastes, the ability to quickly make changes and obtain numerical solutions is of particular importance to support lengthy, detailed reviews, and to address any potential concerns about the TWRS facility. It is quite possible that no single software package will provide a superior product for every area of concern and that a combination of packages may provide the best results. Some large chemical and hydrocarbon processing companies use several packages together successfully.

Software that has the ability to simulate concentrated aqueous electrolyte systems and predict aqueous solubilities and the conditions of solids formation will be important for evaluating Hanford TWRS processes. A specialized suite of software for process simulation of aqueous-based chemical systems developed by OLI Systems, Inc. has been used by Hanford investigators for various applications. Simulation examples were developed for this report using the OLI software as part of a preliminary analysis of its potential use to the Hanford TWRS. These examples, which are discussed in chapter 7, are relevant to potential safety issues resulting from (i) flammable gases, (ii) high organic and nitrate contents, and (iii) fissile elements, particularly Pu. The simulation results indicate that the OLI software can provide the chemical and process modeling capabilities that could be useful to studies of potential safety issues resulting from waste management operations. However, inclusion of additional species and model parameters not currently in the OLI database is essential for better description and modeling of chemical processes relevant to the Hanford TWRS.

9 GLOSSARY

AA—atomic absorption spectrometry

AIChE—American Institute of Chemical Engineers

AIChE-DIERS—American Institute of Chemical Engineers Design Institute for Emergency Relief Systems

ALARA—As low as reasonably achievable

ANL—Argonne National Laboratory

Annulus—The space between the inner and outer shells on DSTs. Drain channels in the insulating and/or supporting concrete carry any leakage to the annulus space where conductivity probes and radiation detectors are installed.

ANS—American Nuclear Society

ARC—Accelerating rate calorimetry

ASTM—American Society for Testing and Materials

B Plant (222-B)—A facility located in the 200-East area of the Hanford site. The $BiPO_4$ process ran in B Plant from April 1945 to October 1952, while Cs/Sr recovery from tank farms ran from 1967–1976, and Cs/Sr recovery from NCAW and CAW ran from 1967–1972, and then from 1983–1991. B Plant's mission from 1967 was to take the acid stream from PUREX through cesium and strontium recovery operations.

BP [Bismuth Phosphate ($BiPO_4$)] Process—First precipitation process used at the Hanford Site for separating plutonium from the irradiated uranium fuels. This process was replaced by REDOX and PUREX processes to gain the advantages of separation and recovery of the uranium and plutonium fission products; 1944–1956. The process left U in the waste.

Burping—Burping is a term commonly used to refer to a rollover event due to gas generation. Hydrogen gas generated, notably in tank SY-101, in a lower layer, makes that layer light enough to roll over to the top, potentially releasing flammable gas.

Canyon—A heavily shielded, partially below grade concrete structure used for remote chemical processing of radioactive fuels or wastes.

$CHOCO_2$—Glyoxylate (also glyoxalate)

CNWRA—Center for Nuclear Waste Regulatory Analyses

Complexants—Organic chemicals that assist in chelating metallic atoms

CPS—DOE criticality prevention specifications

Crib—An underground structure designed to receive liquid waste from tanks or evaporators that can percolate into the soil directly or after traveling through a connected tile field.

Crust—A hard surface layer that has formed in many waste tanks containing concentrated solutions.

CrySP—Crystallization Simulation Program (OLI Systems, Inc.)

CSA—Criticality safety analyses

CSP—Corrosion Simulation Program (OLI Systems, Inc.)

D2EHPA—Di-(2-ethylhexyl) phosphoric acid

DBBP—Dibutyl butyl phosphonate

DBP—Dibutyl phosphate

DOE—U.S. Department of Energy

Dose Equivalent—Product of the absorbed dose, the quality factor, and any other modifying factors to compare the biological effectiveness of different types of radiation on a common scale.

DQO—Data quality objective is a series of planning steps to identify and design more efficient and timely data collection programs.

Drainable Interstitial Liquid—Liquid that is not held in place by capillary forces, and will therefore migrate or move by gravity. Drainable liquid remaining minus supernate. Drainable Interstitial Liquid is calculated based on the salt cake and sludge volumes, using average porosity values or actual data for each tank, when available.

DSC—Differential scanning calorimetry

DST—Double-shell tank; a reinforced concrete underground vessel with two inner steel liners to provide containment and backup containment of liquid wastes; annulus is instrumented to permit detection of leaks from the inner liner. The Hanford Site has 28 double-shell tanks.

DTA—Differential thermal analysis

Ecology—Washington State Department of Ecology

ED3A—Ethylenediaminetriacetate

EDTA—Ethylenediaminetetra-acetic acid

EIS—Environmental impact statement

EPA—Environmental Protection Agency

ESP—Environmental Simulation Program (OLI Systems, Inc.)

FTIR—Fourier transform infrared spectroscopy; technique used to identify molecular species by their vibrational frequencies.

G value—The radiation chemical yield of radicals or molecules in a given medium. It is arithmetically the average number of radiolytic species created (positive G) or destroyed (negative G) by the absorption of 100 eV of radiation energy.

GC/FTIR—Gas chromatography/Fourier transform infrared spectrometry

GC/MS—Gas chromatography/mass spectrometry

GRE—Gas release event

HAcOH—Hydroxyacetic acid

Hanford Site—A 570-square-mile reservation in southeast Washington State owned by the Federal Government. Established in 1943 as part of the Manhattan Project, the Hanford Site's chief mission was to produce plutonium for use in nuclear weapons for the nation's defense. The Site has had nine production reactors and four chemical separation plants. Hanford's current mission is environmental cleanup and developing related technologies.

HCHO—Formaldehyde

HDW—Hanford defined waste

HEDTA—N-(2-hydroxyethyl)ethylenediaminetetra-acetate

HLW—High-level waste (also see Waste, High-Level)

HPLC—High-performance liquid chromatography

HPLC/MS—High-performance liquid chromatography/mass spectrometry

HTCE—Historical tank content estimate

IDA—Iminodiacetate

IHLW—Immobilized high-level waste

ILAW—Immobilized low-activity waste

Immobilization—Immobilization is the act or process of reducing the mobility of waste constituents for long-term transport and subsequent exposure to human, animal, or plant species in the biosphere. Grouting and vitrification are examples of immobilization processes.

INEEL—Idaho National Engineering and Environmental Laboratory [formerly Idaho National Engineering Laboratory (INEL)]

Interstitial Liquor—The liquid within pores of saltcake and sludge. Some of the liquid is capable of drainage, but the rest of the liquid is held by capillary forces.

IR—Infrared

LANL—Los Alamos National Laboratory

LAW—Low activity waste (see Waste, Low-Activity)

LEL—Lower explosive limit

LET—Linear energy transfer; the rate loss of energy (locally absorbed), dE, of an ionizing particle or photon traversing through a distance, dl, in a material medium.

LFL—Lower flammability limit

LLW—Low-level waste (see Waste, Low-Level)

MBP—Monobutyl phosphate

MCNP4A—Monte Carlo N-Particle Version 4A code

MIBK—Methyl isobutyl ketone (also known as hexone) is a solvent that was used in the REDOX plant

Mitigation—Measures taken to reduce adverse impacts on the environment

Monitoring—Periodic or continuous surveillance or testing to determine the level of compliance with statutory requirements, laws, etc.

MOU—Memorandum of understanding

MS—Mass spectrometry

MTU—Metric ton uranium

MUST—Miscellaneous underground storage tanks are relatively small steel or concrete containers ranging in capacity from 3,400 liters to 189,000 liters (900 to 50,000 gallons). These tanks were used for solids settling prior to decanting liquids to cribs, neutralizing acidic process wastes, uranium recovery operations, collecting waste transfer leakage, and waste handling and experimentation. Inactive MUSTS (or IMUSTS) are tanks that are out of service, but may still contain wastes. Active MUSTS are tanks that are still being used to transfer wastes between tanks in tank farms.

MW—Metal waste; extraction waste from the $BiPO_4$ process; contained the U and approximately 90 percent of the fission products.

Na₃HEDTA—Trisodium hydroxyethyl-ethylenediaminetriacetate

Na₄EDTA—Tetrasodium ethylenediaminetetraacetate

NIDA—Nitroimidazole

NIOSH—National Institute of Occupational Safety and Health

NOx—Oxides of nitrogen

NPH—Normal paraffinic hydrocarbons; diluent used in UR and PUREX processes; composition is close to Dodecane, $C_{12}H_{26}$.

NRC—U.S. Nuclear Regulatory Commission

NTA—Nitrilotriacetic acid

NUREG—Nuclear Regulatory Guide

Offgas—Gas evolved or generated during thermal treatment processes such as evaporation, incineration, or solidification. Offgas treatment is a generic name for equipment/system used to clean up these gases.

OSHA—Occupational Safety and Health Administration

PAW—PUREX acidified waste

PAS—PUREX acidified sludge

PFP—Plutonium Finishing Plant (also called Z Plant). Pu Finishing Plant waste

PNNL—Pacific Northwest National Laboratory [formerly Pacific Northwest Laboratory (PNL)]

Pretreatment—Chemical treatment process or a series of processes used to prepare waste for immobilization.

PRF—Plutonium reclamation facility

PUREX—Plutonium Uranium Extraction Plant process which used TBP/kerosene as the solvent phase for extraction of U and Pu. Also refers to the PUREX or A Plant where PUREX process ran from January 1952 to June 1972, then was in standby and ran again from November 1983 to 1991, and is now shut down.

RECUPLEX—Reflux solvent extraction process. A process conducted in the Z plant to recover Pu from the Z plant waste stream. Ended in 1962.

REDOX—Reduction oxidation process based on a continuous solvent extraction of U and Pu using methyl isobutyl ketone (MIBK) as solvent.

RSP—Remediation Simulation Program (OLI Systems, Inc.)

RSST—Reactive system screening tool

Saltcake—Crystallized nitrate and other salts deposited in waste tanks, usually after active measures are taken to remove moisture.

s-EDDA—Symmetric ethylenediaminediacetic acid

Scavenged—Waste that has been treated with ferrocyanide to remove cesium from the supernatant by precipitating it into the sludge.

Sludge—At the Hanford Site, the term is applied to those water-insoluble solids that settle and accumulate at the bottom of a storage tank. Solids are formed by precipitation or self-concentration and are metal hydroxides and oxides precipitated during sodium hydroxide additions to waste.

SRS—Savannah River site

SSP—Scaling Simulation Program (OLI Systems, Inc.)

SST—Single-shell tank

STP—Standard temperature and pressure

Supernate, Supernatant—The liquid layer that is above the solids in the waste storage tanks. Drainable liquid remaining minus drainable interstitial. Supernate is usually derived by subtracting the solids level measurement from the liquid level measurement. In some cases, the supernatant volume includes floating solid crusts because its volume cannot be measured.

T Plant—Decontamination plant for various equipment. Originally built for $BiPO_4$ process, but has since been used only for decontamination. $BiPO_4$ ran from December 1944 to August 1956.

Tank farm—An area containing a number of storage tanks; that is, a chemical tank farm for storage of chemicals used in a plant, or underground waste tank storage of radioactive waste.

Tank waste—Waste currently contained in single-shell and double-shell tanks; all new waste added to double-shell tanks.

TBP—Tributyl phosphate, $OP(OC_4H_9)_3$, which was used in uranium recovery and in PUREX.

TGA—Thermogravimetric analysis

TIC—Total inorganic carbon

TOC—Total organic carbon

TPA—Tri-Party Agreement is also known as the Hanford Federal Facility and Consent Order. It is an agreement signed in 1989 and amended in 1994 by the U.S. Department of Energy, the U.S. Environmental Protection Agency, and the Washington State Department of Ecology that identifies milestones for site cleanup.

Treatment—A method, technique, or process designed to change the physical or chemical character of waste to render it less hazardous for disposal.

TRU—Transuranic; elements of atomic numbers above 92. All are radioactive and are products of artificial nuclear changes. All are members of the actinide group.

TRUEX—Transuranic extraction

TWINS—Tank Waste Inventory Network System is a database managed by PNNL.

TWRS—Tank Waste Remediation System. An integrated waste operations program established by the DOE in December 1991 to retrieve, store, pretreat, immobilize, and either dispose of or prepare for disposal of Hanford radioactive tank waste.

u-EDDA—Asymmetric ethylenediaminediacetic acid

U Plant—Uranium Recovery Plant from March 1952 to January 1958, UO_3 Plant from then until September 1972. Restarted in March 1984, and is now shut down.

UFL—Upper (or rich) flammability limit

UR—Uranium recovery operation; 1952–1957

USQ—Unreviewed safety question. This program aims to identify known or suspected operating conditions outside the known safe limits (also called authorization bases).

UST—Underground storage tank

VFI—Void fraction instrument

VOC—Volatile organic compounds

Waste acceptance criteria—The set of performance requirements established by the DOE that the contractor's waste products must meet before acceptance for storage by the DOE.

Waste envelope—The set of compositional limitations within which the DOE will provide waste feed for processing.

Waste feed tank—The feed tank into which waste will be transferred for subsequent retrieval and treatment by the contractor.

Waste form—The processed radioactive waste immobilized in glass or another substance that meets the requirements specified by the DOE.

Waste Tank Safety Issue—A potentially unsafe condition in the handling of waste material in underground storage tanks that requires corrective action to reduce or eliminate the unsafe condition.

Waste, High-Level (HLW)—High-level radioactive waste or HLW means (i) irradiated reactor fuel, (ii) liquid wastes resulting from the operation of the first cycle solvent extraction system, or equivalent, and the concentrated wastes from subsequent extraction cycles, or equivalent, in a facility for reprocessing irradiated fuel, and (iii) solids into which such liquid wastes have been converted.

Waste, Low-Activity (LAW)—Low-level tank waste that has not yet received the NRC concurrence as incidental.

Waste, Low-Level (LLW)—Waste that contains radioactivity and is not classified as high-level radioactive waste, transuranic waste, spent nuclear fuel, or byproduct material (as defined in Section IIc(2) of the Atomic Energy Act of 1954, {42 USC 2014(e)(2)}).

Waste, Transuranic—Non-high-level radioactive waste that is contaminated with alpha-emitting radionuclides with an atomic number greater than 92 at a concentration of greater than 100 nano Curies per gram.

Watch-list Tank—An underground storage tank containing waste that requires special safety precautions because it may have a serious potential for release of high-level radioactive waste caused by uncontrolled increases in temperatures or pressure. Special restrictions have been placed on these tanks by Safety Measures for Waste Tanks at Hanford Nuclear Reservation, Section 3137 of the National Defense Authorization Act for Fiscal Year 1991, November 5, 1990, Public Law 101-501 (also known as the Wyden Amendment).

WHC—Westinghouse Hanford Company

WVDP—West Valley Demonstration Project

ZAW—Zirconium acid waste; resulted from processing zirconium-jacketed fuel elements.

Z Plant—Pu finishing plant. Operated from 1949 to 1991; now in standby.

10 REFERENCES

Agnew, S.F. 1995. *Hanford Defined Wastes: Chemical and Radionuclide Compositions.* LA-UR-94-2657, Rev. 2. Los Alamos, NM: Los Alamos National Laboratory.

Agnew, S.F. 1996a. *History of Organic Carbon in Hanford HLW Tanks: HDW Model Rev. 3.* LA-UR-96-989. Los Alamos, NM: Los Alamos National Laboratory.

Agnew, S.F. 1996b. *Hanford Tank Chemical and Radionuclide Inventories: HDW Model Rev. 3.* LA-UR-96-3858. Los Alamos, NM: Los Alamos National Laboratory.

Agnew, S.F. 1997. *Hanford Tank Chemical and Radionuclide Inventories: HDW Model Rev. 4.* LA-UR-96-3860. Los Alamos, NM: Los Alamos National Laboratory.

Alcock, K., S.S. Grimley, T.V. Healy, J. Kennedy, and H.A.C. McKay. 1955. The extraction of nitrates by tri-n-butyl phosphate (TBP). *Transactions of the Faraday Society* 52: 39.

Allard, B., H. Kipatsi, and J.O. Liljenzin. 1980. Expected species of uranium, neptunium, and plutonium in neutral aqueous solutions. *Journal of Inorganic and Nuclear Chemistry* 42: 1,015–1,027.

Allemann RT. 1994. *Some Theories of Dissolved Gas Release from Tank 241-SY-101.* PNL-10091. Richland, WA: Pacific Northwest Laboratory.

American Cyanamid Company. 1953. *The Chemistry of the Ferrocyanides.* New York, NY: American Cyanamid Company.

American Institute of Chemical Engineers. 1992. *Guidelines for Hazard Evaluation Procedures. 2nd Edition.* New York, NY: Center for Chemical Process Safety, American Institute of Chemical Engineers.

Anderson, J.D. 1990. *A History of the 200 Area Tank Farms.* WHC-MR-0132. Richland, WA: Westinghouse Hanford Company.

Andrews, G.E., and D. Bradley. 1972. Limits of flammability and natural convection for methane-air mixtures. *Fourteenth International Symposium on Combustion, University Park, Pennsylvania.* Pittsburgh, PA: The Combustion Institute: 1,119–1,128.

Ashby, E.C., C. Jonah, D. Meisel, L.R. Pederson, and D.M. Strachan. 1992. *Gas Generation and Retention in Tank-101-SY: A Summary of Laboratory Studies, Tank Data, and Information Needs.* PNL-8124. Richland, WA: Pacific Northwest Laboratory.

Ashby, E.C., A. Annis, E.K. Barefield, D. Boatright, F. Doctorovich, C.L. Liotta, H.M. Neuman, A. Konda, C.F. Yao, K. Zhang, and N.G. McDuffie. 1994. *Synthetic Waste Chemical Mechanism Studies.* WHC-EP-0823. Richland, WA: Westinghouse Hanford Company.

Ashmore, P.G., and B.J. Tyler. 1963. The nature and cause of ignition of hydrogen and oxygen sensitized by nitrogen dioxide. *Ninth Symposium (International) on Combustion.* Ithaca, NY: Academic Press: 201–209.

Avallone, E.A., and T. Baumeister, III (eds.). 1996. *Marks' Standard Handbook for Mechanical Engineers, 10th Edition.* New York, NY: McGraw-Hill.

Ayres , D.A. 1997. *Chemical Process Safety at Fuel Cycle Facilities.* NUREG-1601. Washington, DC: Nuclear Regulatory Commission.

Babad, H., and D.A. Turner. 1993. *Interim Criteria for Organic Watch List Tanks at the Hanford Site.* WHC-EP-0681. Richland, WA: Westinghouse Hanford Company.

Babad, H., J.E. Meacham, B.C. Simpson, and R.J. Cash. 1993. *The Role of Aging in Resolving the Ferrocyanide Safety Issue.* WHC-EP-0599. Richland, WA: Westinghouse Hanford Company.

Baldwin, J.H., L.C. Amato, and T.T. Tran. 1995. *Tank Characterization Report for Double-Shell Tank 241-AW-101.* WHC-SD-WM-ER-470. Richland, WA: Westinghouse Hanford Company.

Barefield, E.K., D. Boatright, A. Deshpande, F. Doctorovich, C.L. Liotta, H.M. Neumann, and S. Seymore. 1996. *Mechanisms of Gas Generation from Simulated SY Tank Farm Wastes: FY 1995 Progress Report.* PNNL-11247. Richland, WA: Pacific Northwest National Laboratory.

Barin, I. 1989. *Thermochemical Data of Pure Substances.* Weirheim, Germany: VCH Verlagsgesellschaft.

Barney, G.S. 1994. *The Solubilities of Significant Organic Compounds in HLW Tank Supernate Solutions.* WHC-SA-2565, Richland, WA: Westinghouse Hanford Company.

Barney, G.S., K.J. Lueck, and J.W. Green. 1992. Removal of plutonium from low-level process wastewaters by adsorption. *Environmental Remediation.* G.F. Vandergrift, D.T. Reed, and I.R. Tasker, eds. Washington, DC: American Chemical Society.

Beitel, G.A. 1976a. *Final Report on Investigation of Stability of Organic Materials in Salt Cake.* ARH-LD-126. Richland, WA: Atlantic Richfield Hanford Company.

Beitel, G.A. 1976b. *Chemical Stability of Salt Cake in the Presence of Organic Materials.* ARH-LD-119. Richland, WA: Atlantic Richfield Hanford Company.

Beitel, G.A. 1976c. *Sodium Nitrate Combustion Limit Tests.* ARH-LD-123. Richland, WA: Atlantic Richfield Hanford Company.

Beitel, G.A. 1977. *Exothermic Potential of Sodium Nitrate Salt Cake.* ARH-LD-163. Richland, WA: Atlantic Richfield Hanford Company.

Benar, C.J., and L.C. Amato. 1996. *Tank Characterization Report for Double-Shell Tank 241-AN-101.* WHC-SD-WM-ER-578, Rev. 0. Richland, WA: Westinghouse Hanford Company.

Borsheim, G.L., and N.W. Kirch. 1991. *Summary of Single-Shell Tank Waste Stability.* WHC-EP-0347. Richland, WA: Westinghouse Hanford Company.

Borsheim, G.L., and B.C. Simpson. 1991. *An Assessment of the Inventories of the Ferrocyanide Watch List Tanks.* WHC-SD-WM-ER-133, Rev. 0. Richland, WA: Westinghouse Hanford Company.

Bratzel, D.R., W.W. Schulz, and R. Vornehm. 1996. *Tank Farm Nuclear Criticality Review*. WHC-SD-WM-TI-725, Rev. 0. Richland, WA: Westinghouse Hanford Company.

Braun, D.J., L.D. Muhlestein, T.B. Powers, and M.D. Zentner. 1994. *High-Level Waste Tank Subcriticality Safety Assessment*. WHC-SD-WM-SARR-003. Richland, WA: Westinghouse Hanford Company.

Brevick, C.H., and R.L. Newell. 1996. *Supporting Document for the Historical Tank Content Estimate for a Tank Farm*. WHC-SD-WM-ER-308, Rev. 1. Richland, WA: ICF Kaiser Hanford.

Brevick, C.H., R.L. Newell, and J.W. Funk. 1996. *Historical Tank Content Estimate for the Northeast Quadrant of the Hanford 200 East Area*. WHC-SD-WM-ER-349, Rev. 1. Richland, WA: ICF Kaiser Hanford.

Briesmeister, J.F., ed. 1993. *MCNP-A General Monte Carlo N-Particle Transport Code*. LA-12625. Los Alamos, NM: Los Alamos National Laboratory.

Bromley, L.A. 1972. Approximate individual ion values of β (or B) in extended Debye-Huckel theory for uni-univalent aqueous solutions at 298.15 K. *Journal of Chemical Thermodynamics* 4: 669–673.

Bryan, S.A., and L.R. Pederson. 1994. *Composition, Preparation, and Gas Generation Results from Simulated Wastes of Tank 241-SY-101*. PNL-10075. Richland, WA: Pacific Northwest National Laboratory.

Bryan, S.A., and L.R. Pederson. 1996. *Thermal and Combined Thermal and Radiolytic Reactions Involving Nitrous Oxide, Hydrogen, and Ammonia in Contact with Tank 241-SY-101 Simulated Waste*. PNL-10748. Richland, WA: Pacific Northwest Laboratory.

Bryan, S.A., L.R. Pederson, J.L. Ryan, R.D. Scheele, and J.M. Tingey. 1992. *Slurry Growth, Gas Retention, and Flammable Gas Generation by Hanford Radioactive Waste Tanks: Synthetic Waste Studies, FY 1991*. PNL-8169. Richland, WA: Pacific Northwest Laboratory.

Buckingham, J.S. (ed.). 1967. *Waste Management Technical Manual*. ISO-100 DEL. Richland, WA: Isochem, Inc.

Budavari, S., M.J. O'Neil, A. Smith, P.E. Heckelman, and J.F. Kinneary (eds.). 1996. *The Merck Index — An Encyclopedia of Chemicals, Drugs, and Biologicals, 12th Edition*. Whitehouse Station, NJ: Merck and Co., Inc.

Burger, L.L. 1984. Physical Properties. *The Science and Technology of Tributyl Phosphate*. W.W. Schulz and J.D. Navratil, eds. Boca Raton, FL: CRC Publications.

Burger, L.L. 1991. *The Reactivity of Cesium Nickel Ferrocyanide Towards Nitrate and Nitrite Salts*. PNL-7550. Richland, WA: Pacific Northwest Laboratory.

Burger, L.L. 1993. *Calculation of Reaction Energies and Adiabatic Temperatures for Waste Tank Reactions*. PNL-8557. Richland, WA: Pacific Northwest Laboratory.

Burger, L.L. 1995. *Calculation of Reaction Energies and Adiabatic Temperatures for Waste Tank Reactions.* PNL-8557, Rev.1. Richland, WA: Pacific Northwest Laboratory.

Burger, L.L., and R.D. Scheele. 1990. *The Reactivity of Cesium Nickel Ferrocyanide Towards Nitrate and Nitrite Salts.* PNL-7550. Richland, WA: Pacific Northwest Laboratory.

Burger, L.L., D.A. Reynolds, W.W. Schulz, and D.M. Strachan. 1991. *A Summary of Available Information on Ferrocyanide Tank Wastes.* PNL-7822. Richland, WA: Pacific Northwest Laboratory.

Burgess, D.S., A.L. Furno, J.M. Kuchta, and K.E. Mura. 1982. *Flammability of Mixed Gases.* U.S. Bureau of Mines Report of Investigations 8709. Washington, DC: U.S. Bureau of Mines.

Cady, H.H. 1992. *Evaluation of Ferrocyanide/Nitrate Explosive Hazard.* LA-12589-MS. Los Alamos, NM: Los Alamos National Laboratory.

Camaioni, D.M., W.D. Samuels, B.D. Lenihan, S.A. Clauss, K.L. Wahl, and J.A. Campbell. 1994. *Organic Tanks Safety Program Waste Aging Studies.* PNL-10161. Richland, WA: Pacific Northwest Laboratory.

Campbell, J.A., S. Clauss, K. Grant, F. Hoopes, B. Lerner, R. Lucke, G. Mong, J. Rau, and R. Steele. 1994a. *Flammable Gas Safety Program: Analytical Methods Development FY 1993 Progress Report.* PNL-9062. Richland, WA: Pacific Northwest Laboratory.

Campbell, J.A., S. Clauss, K. Grant, F. Hoopes, B. Lerner, R. Lucke, G. Mong, J. Rau, K. Wahl, and R. Steele. 1994b. *Flammable Gas Safety Program: Analytical Methods Development FY 1994 Progress Report.* PNL-10127. Richland, WA: Pacific Northwest Laboratory.

Campbell, J.A., R. Lucke, S. Clauss, G. Mong, K. Grant, J. Rau, F. Hoopes, R. Steele, B. Lerner, and K. Wahl. 1994c. *Waste Tank Organic Safety Program Analytical Methods Development: FY 1994 Progress Report.* PNL-10128. Richland, WA: Pacific Northwest Laboratory.

Campbell, J.A., S. Clauss, K. Grant, F. Hoopes, G. Mong, J. Rau, R. Scheele, and K. Wahl. 1995a. *Flammable Gas Safety Program Organic Analysis and Analytical Methods Development: FY 1995 Progress Report.* PNL-10776. Richland, WA: Pacific Northwest Laboratory.

Campbell, J.A., R. Bean, K. Wahl, G. Mong, K. Bell, K. Wehner, A. Rick, R. Ray, D. Bechtold, B. Wels, R. Schroeder, J. Ball, B. Valenzuela, J. Frye, S. Fitzgerald, P. Bachelor, B. Griffin, R. Fuller, A. Banally, and S. Parong. 1995b. *Analysis of Samples from Hanford Waste Tank 241-C103.* PNL-10531. Richland, WA: Pacific Northwest Laboratory.

Carlson, C.D. 1997. *Speciation of Organic Carbon in Hanford Waste Storage Tanks: Part 1.* PNNL-11480. Richland, WA: Pacific Northwest National Laboratory.

Cashdollar, K.L., M. Hertzberg, I.A. Zlochower, C.E. Lucci, G.M. Green, and R.A. Thomas. 1992. *Laboratory Flammability Studies of Mixtures of Hydrogen, Nitrous Oxide, and Air.* WHC-SD-WM-ES-219, Rev. 0. Richland, WA: Westinghouse Hanford Company.

Chilton, A.B., J.K. Shultis, and R.E. Faw. 1984. *Principles of Radiation Shielding*. Englewood Cliffs, NJ: Prentice-Hall.

Choppin, G.R. 1983. Aspects of plutonium solution chemistry. *Plutonium Chemistry*. W.T. Carnall and G.R. Choppin, eds. Washington, DC: American Chemical Society: 213–230.

Cleveland, J.M. 1967. Plutonium recovery and waste disposal. O.J. Wick, ed. *Plutonium Handbook*. Volume II. New York, NY: Gordon and Breach Science Publishers.

Cooper, V.R. 1957. *Chemical Research and Development Monthly Report and Quarterly Synopsis*. HW-49419C. Richland, WA: Hanford Atomic Works Operation.

Cote, A.E. (ed.). 1997. *Fire Protection Handbook*. 18th edition. Quincy, MA: National Fire Protection Association.

Cotton, F.A., and G. Wilkinson. 1980. *Advanced Inorganic Chemistry—A Comprehensive Text*. New York, NY: John Wiley & Sons, Inc.

Cragnolino, G.A., M.S. Jarzemba, J. Ledbetter-Ferrill, W.M. Murphy, R.T. Pabalan, D.A. Pickett, J.D. Prikryl, and N. Sridhar. 1997. *Hanford Tank Waste Remediation System Familiarization Report*. CNWRA 97-001. San Antonio, TX: Center for Nuclear Waste Regulatory Analyses.

Croff, A.G. 1980. *A User's Manual for the ORIGEN2 Computer Code*. ORNL/TM-7175. Oak Ridge, TN: Oak Ridge National Laboratory.

Crowe, R.D., M. Kummerer, and A.K. Postma. 1993. *Estimation of Heat Load in Waste Tanks Using Average Vapor Space Temperatures*. WHC-EP-0709. Richland, WA: Westinghouse Hanford Company.

Crowl, D.A., and J.F. Louvar. 1990. *Chemical Process Safety: Fundamentals with Applications*. Englewood Cliffs, NJ: Prentice Hall.

Defense Nuclear Facilities Safety Board. 1997. *Savannah River Site In-Tank Precipitation Facility Benzene Generation: Safety Implications*. DNFSB/TECH-14, Rev. 2. Washington, DC: Defense Nuclear Facilities Safety Board.

DeFigh-Price, C., and O.S. Wang. 1993. *High-Heat Tank Safety Issue Resolution Program Plan*. WHC-EP-0532. Richland, WA: Westinghouse Hanford Company.

Delegard, C. 1980. *Laboratory Studies of Complexed Waste Slurry Volume Growth in Tank 241-SY-101*. RHO-LD-124. Richland, WA: Rockwell Hanford Operations.

Delegard, C.H. 1987a. *Identities of HEDTA and Glycolate Degradation Products in Simulated Hanford High-Level-Level Waste*. RHO-RE-ST-55P. Richland, WA: Rockwell Hanford Operations.

Delegard, C.H. 1987b. Solubility of $PuO_2 \cdot xH_2O$ in alkaline Hanford high-level waste solution. *Radiochimica Acta* 41: 11–21.

Delegard, C.H. 1995. *Calcination/Dissolution Chemistry Development Fiscal Year 1995*. WHC-EP-0882. UC-601. Richland, WA: Westinghouse Hanford Company.

Dhir, V.K., and I. Catton. 1982. Boiling in a porous bed. *Applied Scientific Research* 38: 69–76.

Dietsche, L.J., R.S. Upadhye, D.W. Camp, J.A. Pendergrass, L.C. Borduin, and T.K. Thompson. 1994. *ASPEN Computer Simulations of the Mixed Waste Treatment Project Baseline Flowsheet*. UCRL-ID-118122. Livermore, CA: Lawrence Livermore National Laboratory.

Dzombak, D.A., and F.F. Morel. 1990. *Surface Complexation Modeling: Hydrous Ferric Oxide*. New York, NY: John Wiley and Sons, Inc.

Duderstadt, J.J., and L.J. Hamilton. 1975. *Nuclear Reactor Analysis*. New York: John Wiley and Sons, Inc.

Dukas, S., and D. Slaughterbeck. 1991. *Potential for Reactions of Nitrate and Nitrite in the Hanford Waste Vitrification Process Feed*. Prepared for Westinghouse Hanford Company by Science Applications International Corporation, Idaho Falls, ID.

Durian, D.J., and D.A. Weitz. 1995. Foams. *Kirk-Othmer Encyclopedia of Chemical Technology*. 4th Edition. New York, NY: Wiley-Interscience.

Ecology. 1994. *Hanford Federal Facility Agreement and Consent Order, as amended*. Olympia, WA: Washington State Department of Ecology, U.S. Environmental Protection Agency, and U.S. Department of Energy.

Egerton, A.C. 1953. Limits of inflammability. *Fourth Symposium (International) on Combustion (Combustion and Detonation Waves), Cambridge, Massachusetts*. Baltimore, MD: Williams and Wilkins Company: 4–13.

Eiter, K., O. Vogl, and H. Michl. 1954. Cyanide safety explosives. Austrian Patent 176,784 (1953), *Chemical Abstracts* 48: 1,004.

Fauske, H.K. 1992. *Adiabatic Calorimetry and Reaction Propagation Tests with Synthetic Ferrocyanide Materials Including U Plant 1, U Plant 2, In-Farm 1, In-Farm 2, and Vendor-Procured Sodium Nickel Ferrocyanide*. WHC-SD-WM-RDT-054, Rev. 0. Richland, WA: Westinghouse Hanford Company.

Fauske, H.K., and J.C. Leung. 1985. New experimental techniques for characterizing runaway chemical reactions. *Chemical Engineering Progress*. 81: 39.

Fauske, H.K., J.E. Meacham, and R.J. Cash. 1995a. *Ferrocyanide Safety Program: Final Report on Adiabatic Calorimetry and Tube Propagation Tests with Synthetic Ferrocyanide Materials*. WHC-SD-WM-ER-519, Rev. 0. Richland, WA: Westinghouse Hanford Company.

Fauske, H.K., M. Epstein, D.R. Dickinson, R.J. Cash, D.A. Turner, and J.E. Meacham. 1995b. *The Contact-Temperature Ignition (CTI) Criteria for Propagating Chemical Reactions Including the Effect of Moisture and Application to Hanford Waste*. WHC-SD-WM-ER-496, Rev. 0. Richland, WA: Westinghouse Hanford Company.

Fisher, F.D. 1990. *The Kyshtym Explosion and Explosion Hazards with Nitrate-Nitrite Bearing Wastes with Acetates and Other Organic Salts*. WHC-SD-CP-LB-033, Rev. 0. Richland, WA: Westinghouse Hanford Company.

Franks, F. 1966. The solute-water interactions and the solubility behavior of long-chain paraffin hydrocarbons. *Nature* 210: 87–88.

Furno, A.L., E.B. Cook, J.M. Kuchta, and D.S. Burgess. 1971. Some observations on near-limit flames. *Thirteenth Symposium (International) on Combustion, Salt Lake City, Utah*. Pittsburgh, PA: The Combustion Institute: 593–599.

Gary, L.W. 1978. An explosion and fire during conversion of liquid uranyl nitrate to solid uranium oxide. *Nuclear Safety* 19-1: 91–99.

Gauglitz, P.A., L.A. Mahoney, D.P. Mendoza, and M.C. Miller. 1994. *Mechanisms of Gas Bubble Retention*. PNL-10120. Richland, WA: Pacific Northwest Laboratory.

Gephart, R.E., and R.E. Lundgren. 1995. *Hanford Tank Clean Up: A Guide to Understanding the Technical Issues*. PNL-10773. Richland, WA: Pacific Northwest Laboratory.

Gerber, M.A. 1994. *Waste Tank Organic Concentration Mechanisms Task FY 1994 Progress Report*. PNL-10064. Richland, WA: Pacific Northwest Laboratory.

Gerber, M.A. 1996. *The Plutonium Production Story at the Hanford Site: Processes and Facilities History*. WHC-MR-0521, Rev. 0. Richland, WA: Westinghouse Hanford Company.

Gerber, M.A., L.L. Burger, D.A. Nelson, J.L. Ryan, and R.L. Zollars. 1992. *Assessment of Concentration Mechanisms for Organic Wastes in Underground Storage Tanks at Hanford*. PNL-8339. Richland, WA: Pacific Northwest Laboratory.

Glassman, I. 1977. *Combustion*. New York, NY: Academic Press.

Golberg, C.E., and J.D. Guberski. 1995. *Single-Shell and Double-Shell Tank Waste Inventory Data Package for the Tank Waste Remediation System Environmental Impact Statement*. WHC-SD-WM-EV-102, Rev. 0. Richland, WA: Westinghouse Hanford Company.

Graves, R.D. 1994. *Topical Report on Flammable Gases in Non-Burping Waste Tanks*. WHC-SD-WM-SARR-015, Rev. 0. Richland, WA: Westinghouse Hanford Company.

Gray, J.T. Jr., E. Dimitroff, N.T. Meckel, and R.D. Quillian, Jr. 1966. *Ammonia Fuel—Engine Compatibility and Combustion*. SAE Paper No. 660156. Detroit, MI: Society of Automotive Engineers.

Gygax, R.W. 1990. Scale-up principles for assessing thermal runaway risks. *Chemical Engineering Progress* 86: 53–60.

Ha, B.C., T.G. Williams, J.S. Clemmons, and M.C. Chandler. 1996. Criticality assessment of the Defense Waste Processing Facility. *Proceedings of the International Topical Meeting on Nuclear Waste Management—Spectrum 96*. La Grange Park, IL: American Nuclear Society: 2,277–2,281.

Hanlon, B.M. 1996. *Waste Tank Summary Report for Month Ending July 31, 1996*. WHC-EP-0182-100. Richland, WA: Westinghouse Hanford Company.

Hanlon, B.M. 1997. *Waste Tank Summary Report for Month Ending September 30, 1997*. HNF-EP-0182-114. Richland, WA: Lockheed Martin Hanford Corporation.

Hanlon, B.M. 1998. *Waste Tank Summary Report for Month Ending November 30, 1997*. HNF-EP-0182-116. Richland, WA: Lockheed Martin Hanford Corporation.

Harned, H.S., and B.B. Owen. 1950. *The Physical Chemistry of Electrolyte Solutions*. New York, NY: Reinhold.

Helgeson, H.C., D.H. Kirkham, and G.C. Flowers. 1981. Theoretical prediction of the thermodynamic behavior of aqueous electrolytes at high pressures and temperatures: IV. Calculation of activity coefficients, osmotic coefficients, and apparent molal and standard and relative partial molal properties to 600 °C and 5 kb. *American Journal of Science* 281: 1,249–1,516.

Hendricks, J.S., S.C. Frankle, and J.D. Court. 1994. *ENDF/B-VI Data for MCNP*. LA-12891. Los Alamos, NM: Los Alamos National Laboratory.

Hendrickson, D. 1990. *Methods and Data for Use in Determining Source Term for Grout Disposal Program*. WHC-SD-WM-TI-355. Richland, WA: Westinghouse Hanford Company.

Henkin, H., and R. McGill. 1952. Rates and explosive decomposition of explosives. Experimental and theoretical kinetic study as a function of temperature. *Industrial Engineering Chemistry* 44: 1,391–1,395.

Henrie, J.O., D.J. Flesher, and G.J. Quinn. 1986. *Hydrogen Control in the Handling, Shipping and Storage of Wet Radioactive Waste*. RHO-WM-EV-9-P-Rev 1. Hanford, WA: Rockwell Hanford Operations.

Hepworth, J.L., E.D. McClanahan, and R.L. Moore. 1957. *Cesium Packaging Studies—Conversion of Zinc Ferrocyanide to a Cesium Chloride Product*. HW-48832. Richland, WA: Hanford Atomic Works Operation.

Herborn, D.I. 1992. *Hanford Waste Vitrification Plant Preliminary Safety Analysis Report*. WHC-SD-HWV-PSAR-001, Rev. 0. Richland, WA: Westinghouse Hanford Company.

Herting, D.L., T.L. Welsh, R.W. Lambie, and T.T. Tran. 1995. *Tank Characterization Report for Double-Shell Tank 241-SY-101*. WHC-SD-WM-ER-409, Rev. 0. Richland, WA: Westinghouse Hanford Company.

Higgins, C.E., W.H. Baldwin, and B.A. Soldano. 1959. Effects of electrolytes and temperature on the solubility of tributyl phosphate in water. *Journal of Physical Chemistry* 63: 113.

Hobbs, D.T. 1995. *Effects of coprecipitation on the concentrations of uranium and plutonium in alkaline salt solutions*. WSRC-TR-95-0462. Aiken, SC: Westinghouse Savannah River Company.

Hobbs, D.T., and D.G. Karraker. 1996. Recent results on the solubility of uranium and plutonium in Savannah River Site waste supernate. *Nuclear Technology* 114: 318–324.

Hobbs, D.T., T.B. Edwards, and S.D. Fleischman. 1993. *Solubility of plutonium and uranium in alkaline salt solutions.* WSRC-TR-93-056. Aiken, SC: Westinghouse Savannah River Company.

Hodgman, C.D., ed. 1947. *Handbook of Chemistry and Physics,* 13th Edition. Cleveland, OH: Chemical Rubber Publishing Company.

Hodgson, K.M. 1995a. *Tank Characterization Report for Double-Shell Tank 241-AW-103.* WHC-SD-WM-ER-455, Rev. 0. UC-2070. Richland, WA: Westinghouse Hanford Company.

Hodgson, K.M. 1995b. *Tank Characterization Report for Double-Shell Tank 241-AZ-101.* WHC-SD-WM-ER-410, Rev. 0. UC-2070. Richland, WA: Westinghouse Hanford Company.

Hodgson, K.M., D.L. Herting, W.W. Schulz, L.A. Bray, and J.L. Swanson. 1985. Content and removal of TRU elements from aqueous zirconium cladding waste. *Proceedings International Symposium on Actinide/Lanthanide Separations.* G.R. Choppin, J.D. Navratil, and W.W. Schulz, eds. Philadelphia, PA: World Scientific.

Housner, G.W. 1970. Strong ground motion. *Earthquake Engineering.* R.L. Wiegel, ed. Englewood Cliffs, NJ: Prentice Hall.

Housner, G.W., chair. 1985. *Safety of Dams, Flood and Earthquake Phenomena.* Committee on Safety Criteria for Dams, The National Research Council, and the National Academy of Sciences. Washington, DC: National Academy Press: 63–73.

Hughes, G., and C. Willis. 1961. *The Radiolysis of Ferro- and Ferricyanide Solutions.* Liverpool, United Kingdom: Department of Inorganic, Physical and Industrial Chemistry, Liverpool University.

Jarosinski, J., R.A. Strehlow, and A. Azarbarzin. 1982. The mechanisms of lean limit extinguishment of an upward and downward propagating flame in a standard flammability tube. *Nineteenth Symposium (International) on Combustion, Haifa, Israel.* Pittsburgh, PA: The Combustion Institute: 1,549–1,557.

Jeppson, D.W., and B.C. Simpson. 1994. *Characterization and Reaction Behavior of Ferrocyanide Simulants and Hanford Site High-Level Ferrocyanide Waste.* WHC-SA-2190. Richland, WA: Westinghouse Hanford Company.

Jeppson, D.W., and J.J. Wong. 1993. *Ferrocyanide Waste Simulant Characterization.* WHC-EP-0631. Richland, WA: Westinghouse Hanford Company.

Johnson, G.D., W.B. Barton, J.W. Brothers, S.A. Bryan, P.A. Gauglitz, R.C. Hill, L.R. Pederson, C.W. Stewart, and L.M. Stock. 1996. *Flammable Gas Project Topical Report.* HNF-SP-1193, Rev. 1. Richland, WA: Project Hanford Management Contractor.

Johnson, G.D., W.B. Barton, R.C. Hill, J.W. Brothers, S.A. Bryan, P.A. Gauglitz, L.R. Pederson, C.W. Stewart, and L.M. Stock. 1997. *Evaluation of High-Level Nuclear Waste Tanks Having a Potential Flammable Gas Hazard.* HNF-SA-3127-FP. Richland, WA: Project Hanford Management Contractor.

Jones, G.W. 1954. Inflammation limits and their practical application in hazardous industrial operations. *Proceedings of the Second Symposium on Combustion.* Pittsburgh, PA: The Combustion Institute: 248-264.

Jones, G.W. 1929. *Inflammability of Mixed Gases.* U.S. Bureau of Mines Technical Paper 450. Washington, DC: U.S. Bureau of Mines.

Jungfleisch, F.M. 1984. *TRAC: A Preliminary Estimation of the Waste Inventories in Hanford Tanks through 1980.* WHC-SD-WM-TI-057. Richland, WA: Rockwell Hanford Operations.

Karraker, D.G. 1994. *Radiation Effects on the Solubility of Plutonium in Alkaline High Level Waste.* WSRC-MS-94-0278x. Rev. 2. Aiken, SC: Westinghouse Savannah River Company.

Karraker, D.G. 1995. *Plutonium (VI) Solubility Studies in Savannah River Site High-Level Waste Supernate.* WSRC-TR-95-0244. Aiken, SC: Westinghouse Savannah River Company.

Kasten, J.L. 1991. *A Literature Review of Radiolytic Gas Generation as a Result of the Decomposition of Sodium Nitrate Wastes.* DE91-006930; ORNL/TM-11632. Oak Ridge, TN: Oak Ridge National Laboratory.

Kelly, S.E. 1995. *Tank Characterization Report for Single-Shell Tank 241-TY-104.* WHC-SD-WM-ER-481, Rev. 0. Richland, WA: Westinghouse Hanford Company.

Kim, J.I. 1986. Chemical behaviour of transuranic elements in natural aquatic systems. *Handbook on the Physics and Chemistry of the Actinides.* A.J. Freeman, and C. Keller, eds. Amsterdam, Holland: North-Holland. 413–455.

Kim, J.I., and B. Kanellakopulos. 1989. Solubility products of plutonium(IV) oxide and hydroxide. *Radiochimica Acta* 48: 145–150.

Kingsley, R.S. 1965. *Solvent Extraction Recovery of Americium with Dibutyl Butyl Phosphonate.* RL-SEP-518. Richland, WA: Hanford Atomic Products Operation.

Klem, M.J. 1990. *Inventories of Chemicals Used at Hanford Site Production Plants and Support Operations (1944-1980).* WHC-EP-0172. Richland, WA: Westinghouse Hanford Company.

Knief, R.A. 1992. *Nuclear Engineering-Theory and Technology of Commercial Nuclear Power.* 2nd Edition. Washington, DC: Hemisphere Publishing Corporation.

Knutson, B.J., G. Jansen, Jr., B.D. Zimmerman, L.G. Niccoli, and L. Lauerhass. 1994. *Global Modeling of Hanford Tank Waste Pretreatment Alternatives Within a Total Cleanup System Using Aspen plus^{tm}.* WHC-SA-2407. Richland, WA: Westinghouse Hanford Company.

Kratzer, W.K. 1967. *Evaluation of N-Reactor Piping Decontamination Procedure for Effectiveness and Materials Corrosion.* DUN-2938. Richland, WA: Douglas United Nuclear, Inc.

Kroschwitz, J., exec. ed. 1995. *Kirk-Othmer Encyclopedia of Chemical Technology.* 4th Edition. New York, NY: Wiley-Interscience.

LaMarsh, J.R. 1983. *Introduction to Nuclear Engineering.* Reading, MA: Addison Wesley Publishing Inc.

Lewis, R.J., Sr. 1993. *Hazardous Chemicals Desk Reference.* New York, NY: Van Nostrand Reinhold.

Lide, D.R., ed. 1991. *CRC Handbook of Chemistry and Physics.* 72nd Edition. Boca Raton, FL: CRC Press.

Lilga, M.A., M.R. Lumetta, W.F. Riemath, R.A. Romine, and G.F. Schiefelbein. 1992. *Ferrocyanide Safety Project, Subtask 3.4, Aging Studies FY 1992 Annual Report.* PNL-8387, Richland, WA: Pacific Northwest Laboratory.

Lilga, M.A., E.V. Alderson, R.T. Hallen, M.O. Hogan, T.L. Hubler, G.L. Jones, D.J. Kowalski, M.R. Lumetta, G.F. Shiefelbein, and M.R. Telander. 1995. *Ferrocyanide Safety Project: Ferrocyanide Aging Studies FY 1995 Annual Report.* PNL-10713. Richland, WA: Pacific Northwest Laboratory.

Lilga, M.A., E.V. Alderson, R.T. Hallen, M.O. Hogan, T.L. Hubler, G.L. Jones, D.J. Kowalski, M.R. Lumetta, and M.R. Telander. 1996. *Ferrocyanide Safety Project: Ferrocyanide Aging Studies Final Report.* PNL-11211. Richland, WA: Pacific Northwest Laboratory.

Linke, F., and A. Seidell. 1965. *Solubilities of Inorganic and Metal-Organic Compounds,* 4th Edition. Washington, DC: American Chemical Society.

Lokken, R.O., R.D. Scheele, D.M. Strachan, and A.P. Toste. 1986. *Complex Concentrate Pretreatment: FY 1986 Progress Report.* PNL-7687. Richland, WA: Pacific Northwest Laboratory.

Loos-Neskovic, C., M. Federoff, and E. Garnier. 1989. Preparation, composition and structure of some nickel and zinc ferrocyanides. Experimental results. *Talanta* 36: 749–759.

Loos-Neskovic, C., M. Federoff, E. Garnier, and P. Gravereau. 1984. Zinc and nickel ferrocyanides: preparation, composition and structure. *Talanta* 31: 1,133–1,147.

MacDiarmid, A.G., and N.F. Hall. 1953. Illumination-pH effects in solutions of complex cyanides. *Journal of the American Chemical Society* 75: 5,204–5,207.

Markham, A.E., and K.A. Kobe. 1941. The solubility of carbon dioxide and nitrous oxide in aqueous salt solutions. *Journal of the American Chemical Society* 63: 449–454.

Marcus, Y., and A.S. Kertes. 1969. *Ion Exchange and Solvent Extraction of Metal Complexes.* NewYork, NY: John Wiley & Sons.

Masri, E., and M. Haissinsky. 1963. Radiolytic transformations. Gamma-radiolysis of potassium ferro—and ferricyanide solutions. *Chemical Physics* 60: 397–401.

McDuffie, N.G. 1994. *Flammable Gas Generation, Retention, and Release in High-Level Waste Tanks—Physical and Chemical Models*. WHC-SA-2129-FP. Richland, WA: Westinghouse Hanford Company.

McAuliffe, C. 1969. Solubility in water of normal C_9 and C_{10} alkane hydrocarbons. *Science* 163: 478–479.

McDuffie, N.G. 1995. *Flammable Gas Tank Safety Program: Data Requirements for Core Sample Analysis Developed Through the Data Quality Objectives Process*. WHC-SD-WM-DQO-004, Rev. 2. Richland, WA: Westinghouse Hanford Company.

McKinnon, G.P., and K. Tower (eds.). 1976. *Fire Protection Handbook*. 14th Edition. Boston, MA: National Fire Protection Association.

Meacham, J.E., R.J. Cash, and H. Babad. 1994. *Resolving the Ferrocyanide Safety Issue at the Hanford Site*. WHC-SA-2130. Richland, WA: Westinghouse Hanford Company.

Meacham, J.E., R.J. Cash, D.R. Dickinson, and F.R. Reich. 1996. *Assessment of the Potential for Ferrocyanide Propagating Reaction Accidents*. WHC-SD-WM-SARR-038, Rev. 1. Richland, WA: Westinghouse Hanford Company.

Medvedev, Z.A. 1979. *Nuclear Disaster in the Urals*. Translated by G. Saunders. New York, NY: W.H. Norton and Company.

Meisel, D., H. Diamond, E.P. Horwitz, C.D. Jonah, M.S. Matheson, M.C. Sauer, Jr., J.C. Sullivan, F. Barnabas, E. Cerny, and Y.D. Cheng. 1991. *Radiolytic Generation of Gases from Synthetic Waste Annual Report—FY1991*. ANL-91/41. Argonne, IL: Argonne National Laboratory.

Meisel, D., C.D. Jonah, S. Kapoor, M.S. Matheson, and M.C. Sauer, Jr. 1993. *Radiolytic and Radiolytically Induced Generation of Gases from Synthetic Wastes: Final Report*. ANL-93/43. Argonne, IL: Argonne National Laboratory.

Mendel, J. E., compiler. 1984. Radiation effects. *Final Report of the Defense High-Level Waste Leaching Mechanisms Program*. PNL-5157. Richland, WA: Pacific Northwest Laboratory.

Meng, C.D., G.T. MacLean, and B.C. Landeene. 1994. *Computer Simulation of Laboratory Leaching and Washing of Tank Waste Sludges*. WHC-SD-WM-ES-312. Richland, WA: Westinghouse Hanford Company.

National Board of Fire Underwriters. 1950. *Research Report No. 2, Fire Prevention and Engineering Standards. Potential Standards in Molten Salt Baths for Heat Treatment of Metals*. New York, NY: National Board of Fire Underwriters.

National Fire Protection Association. 1986. *Manual for Classification of Gases, Vapors, and Dusts for Electrical Equipment in Hazardous (Classified) Locations*. NFPA 497M. Quincy, MA: National Fire Protection Association.

Nelson, D.M., and M.B. Lovett. 1978. Oxidation state of plutonium in the Irish Sea. *Nature* 276(5688): 599–601.

Neta, P. 1976. *Advances in Physical Organic Chemistry.* Volume 12. V. Gold and D. Bethell, eds. New York, NY: Academic Press.

Newton, T.W., and F.B. Baker. 1967. Aqueous oxidation-reduction reactions of uranium, neptunium, plutonium, and americium. *Lanthanide/Actinide Chemistry.* P.R. Fields, and T. Moeller, eds. Washington, DC: American Chemical Society. 268–295.

Nitsche, H., K. Roberts, K. Becraft, T. Prussin, D. Keeney, S.A. Carpenter, and D.E. Hobart. 1995. *Solubility and Speciation Results from Over- and Undersaturation Experiments on Neptunium, Plutonium, and Americium in Water from the Yucca Mountain Region Well UE-25p#1.* LA-13017-MS. UC-802. Los Alamos, NM: Los Alamos National Laboratory.

Norton, J.D., and L.R. Pederson. 1995. *Solubilities of Gases in Simulated Tank 241-SY-101 Wastes.* PNL-10785. Richland, WA: Pacific Northwest Laboratory.

Oberg, G.C. 1979. *Miscellaneous Facilities Criticality Prevention Specifications.* RHO-MA-149. Richland, WA: Rockwell Hanford Operations.

Ohno, S., and E. Tsuchihasi. 1965. The photochemistry of hexacyanoferrate (II) ions in aqueous solutions. *Bulletin of the Chemical Society* 38: 1,052–1,053.

OLI Systems, Inc. 1996. *OLI Software Manual.* Morris Plains, NJ: OLI Systems, Inc.

Orlandini, K.A., W.R. Penrose, and D.M. Nelson. 1986. Pu(V) as the stable form of oxidized plutonium in natural waters. *Marine Chemistry* 18: 49–57.

Palmer, B.J., C.M. Anderson, G. Chen, J.M. Cuta, T.A. Ferryman, and G. Terrones. 1996. *Evaluation of the Potential for Significant Ammonia Releases from Hanford Waste Tanks.* PNNL-11237. Richland, WA: Pacific Northwest National Laboratory.

Paquette, J., and R.J. Lemire. 1981. A description of the chemistry of aqueous solutions of uranium and plutonium to 200 °C using potential-pH diagrams. *Nuclear Science and Engineering* 79: 26–48.

Parker, S.P., ed. 1994. *McGraw-Hill Dictionary of Scientific and Technical Terms.* 5th Edition. New York, NY: McGraw-Hill.

Parra, S.A. 1994. *Integrated Beta and Gamma Radiation Dose Calculations for Ferrocyanide Waste Tanks.* WHC-SD-WM-TI-634, Rev. 0. Richland, WA: Westinghouse Hanford Company.

Parrington, J.R., H.D. Knox, S.L. Breneman, E.M. Baum, and F. Feiner. 1996. *Nuclides and Isotopes—15th Edition.* San Jose, CA: General Electric, GE Nuclear Energy.

Pasamehmetoglu, K.O. 1994. *Analyses of Gas Composition and Relevant Gas Concentration Measurements for the Release of Gas in Tank 241-SY-101.* N6-CN-WT-SA-GR-004. Los Alamos, NM: Los Alamos National Laboratory.

Pauling, L. 1939. *The Nature of the Chemical Bond.* Ithaca, NY: Cornell University Press.

Pederson, L.R., and S.A. Bryan. 1996. *Status and Integration of Studies of Gas Generation in Hanford Wastes*. PNNL-11297. Richland, WA: Pacific Northwest National Laboratory.

Perry, R.H., D.W. Green, and J.O. Maloney (eds.). 1984. *Perry's Chemical Engineers' Handbook, 6th Edition*. New York, NY: McGraw-Hill Company.

Peterson, R.F., Jr., and R. Wolfgang. 1971. Elementary reactions of atomic carbon. *Advances in High Temperature Chemistry* 4: 43–70.

Pikaev, A. 1996. Gamma radiolysis of alkaline aqueous solutions of neptunium and plutonium. Poster at the *Chemistry of the Actinides and Technetium in Alkaline Media Meeting*, Battelle Auditorium, April 2, 1996. Richland, WA.

Pitzer K. S. 1973. Thermodynamics of electrolytes. 1. Theoretical basis and general equations. *Journal of Physical Chemistry* 77: 268–277.

Pitzer, K.S. 1991. Ion interaction approach: Theory and data correlation. *Activity Coefficients in Electrolyte Solutions*. 2nd Edition. K.S. Pitzer, ed. Boca Raton, FL: CRC Press: 76–153.

Pool, K.H., and R.M. Bean. 1994. *Waste Tank Organic Safety Project: Analysis of Liquid Samples from Waste Tank 241-C-103*. PNL-9403. Richland, WA: Pacific Northwest Laboratory.

Postma, A.K., and D.R. Dickinson. 1995. *Ferrocyanide Safety Program: Analysis of Postulated Energetic Reactions and Resultant Aerosol Generation in Hanford Site Waste Tanks*. WHC-EP-0876. Richland, WA: Westinghouse Hanford Company.

Postma, A.K., J.E. Meacham, G.S. Barney, G.L. Borsheim, R.J. Cash, M.D. Crippen, D.R. Dickinson, J.M. Grigsby, D.W. Jeppson, M. Kummerer, J.M. McLaren, C.S. Simmons, and B.C. Simpson. 1994. *Ferrocyanide Safety Program: Safety Criteria for Ferrocyanide Watch List Tanks*. WHC-EP-0691. Richland, WA: Westinghouse Hanford Company.

Rai, D., and R.J. Serne. 1978. *Solution Species of ^{239}Pu in Oxidizing Environments: I. Polymeric Pu(IV)*. PNL-SA-6994. Richland, WA: Pacific Northwest Laboratory.

Rai, D., R.J. Serne, and D.A. Moore. 1980. Solubility of plutonium compounds and their behavior in soils. *Journal of the Soil Science Society* 44: 490–495.

Reynolds, D.A., D.D. Siemer, D.M. Strachan, and R.W. Wallace. 1991. *A Survey of Available Information on Gas Generation in Tank 241-SY-101*. PNL-7520. Richland, WA: Pacific Northwest Laboratory.

Reynolds, D.A. 1993. *Tank 101-SY Window E Core Sample: Interpretation of Results*. WHC-EP-0628. Richland, WA: Westinghouse Hanford Company.

Richardson, G.L., and W.W. Schulz. 1967. Process chemistry and engineering. *Waste Management Technical Manual*. Chapter VI. J.S. Buckingham, ed. ISO-100 DEL. Richland, WA: Isochem, Inc.

Righetto, L., G. Bidoglio, B. Marcandalli, and I.R. Bellobono. 1988. Surface interactions of actinides with alumina colloids. *Radiochimica Acta* 44/45: 73–75.

Righetto, L., G. Bidoglio, G. Azimonti, and I.R. Bellobono. 1991. Competitive actinide interactions in colloidal humic acid-mineral oxide systems. *Environmental Science and Technology* 25(11): 1,913–1,919.

Robuck, S.J., and R.G. Luthy. 1989. Destruction of iron-complexed cyanide by alkaline hydrolysis. *Water Science and Technology* 21: 547–558.

Rogers, C.A. 1993. *An Analytical Model for Evaluating Subcritical Limits for Waste in Hanford Site Storage Tanks*. WHC-SD-SQA-CSA-20356, Rev. 0. Richland, WA: Westinghouse Hanford Company.

Rogers, C.A., K.N. Schwinkendorf., and H. Harris. 1996. *Criticality Parameters for Tank Waste Evaluation*. WHC-SD-SQA-CSA-507, Rev. 0. Richland, WA: Westinghouse Hanford Company.

Rudd, D.F., and C. C. Watson. 1968. *Strategy of Process Engineering*. New York, NY: John Wiley & Sons, Inc.: 436–439.

Sanchez, A.L., J.W. Murray, and T.H. Sibley. 1985. The adsorption of plutonium IV and V on goethite. *Geochimica et Cosmochimica Acta* 49: 2,297–2,307.

Sax, I.N. 1957. *Dangerous Properties of Industrial Materials*. New York, NY: Reinhold.

Schatzberg, P. 1963. Solubilities of water in several normal alkanes from C_7 to C_{16}. *Journal of Physical Chemistry* 67: 776–779.

Scheele, R.D., L.L. Burger, J.M. Tingey, S.A. Bryan, G.L. Borsheim, B.C. Simpson, R.J. Cash, and H.H. Cady. 1991. *Ferrocyanide Containing Waste Tanks: Ferrocyanide Chemistry and Reactivity*. PNL-SA-19924. Richland, WA: Pacific Northwest Laboratory.

Scheele, R.D., J.L. Sobalik, R.L. Sell, and L.L. Burger. 1995. *Organic Tank Safety Project: Preliminary Results of Energetics and Thermal Behavior Studies of Model Organic Nitrate and/or Nitrite Mixtures and a Simulated Waste*. PNL-10213. Richland, WA: Pacific Northwest Laboratory.

Seaborg, G.T. 1993. Overview of the actinide and lanthanide (the *f*) elements. *Radiochimica Acta* 61: 115–122.

Sederburg, J.P., and J.A. Reddick. 1994. *TBP and Diluent Mass Balances in the Purex Plant at Hanford 1955-1991*. WHC-MR-0483. Richland, WA: Westinghouse Hanford Company.

Seidell, A. 1941. *Solubilities of Organic Compounds*, 3rd Edition, Vol. 2. New York, NY: D. Van Nostrand.

Seidell, A. 1953. *Solubilities of Inorganic and Metal Organic Compounds*, 3rd Edition, Vol. 1. New York, NY: D. Van Nostrand.

Serne, R.J., G.A. Whyatt, S.V. Mattigod, Y. Onishi, P.G. Doctor, B.N. Bjornstad, M.R. Powell, L.M. Liljegren, J.H. Westsik, Jr., N.J. Aimo, K.P. Recknagle, G.R. Golcar, T.B. Miley, G.R. Holdren, D.W. Jeppson, R.K. Biyani, and G.S. Barney. 1996. *Fluid Dynamic Particulate Segregation, Chemical Processes, and Natural Ore Analog Discussions that Relate to the Potential for Criticality in Hanford Tanks*. WHC-SD-WM-TI-757. Richland, WA: Westinghouse Hanford Company.

Sharkey, J.J., R.S. Cutro, W.J. Fraser, and G.T. Wildman. 1992. Plant safety testing program for reducing risks associated with large scale chemical manufacturing operations. *Plant/Operations Progress* 11: 238–246.

Shaw, D., P.M. Haulait, and G. Hefter. 1989. *Hydrocarbons with Water and Seawater, Solubility Data Series*, Vol. 38, Oxford: Pergamon Press.

Sills, J.A. 1995. *Evaluation of Hanford High Level Waste Vitrification Chemistry for an NCAW Simulant—FY 1994: Potential Exothermic Reactions in the Presence of Formic Acid, Glycolic Acid, and Oxalic Acid*. PNL-10564. Richland, WA: Pacific Northwest Laboratory.

Slankas, J.T., M.J. Kupfer, and W.W. Schulz. 1995. *Strategy for Sampling Hanford Site Tank Wastes for Development of Disposal Technology*. WHC-SD-WM-TA-154, Rev. 1. Richland, WA: Pacific Northwest Laboratory.

Smith, J.M., and H.C. Van Ness. 1987. *Introduction to Chemical Engineering Thermodynamics*. 4th Edition. New York, NY: McGraw-Hill Book Company.

Somasundaran, P., and R.B. Grieves, eds. 1975. Interfacial chemistry of particulate flotation. *Advances in Interfacial Phenomena of Particulate/Solution/Gas/Systems: Applications to Flotation Research*. AIChE Symposium Series No. 150, Vol. 71. New York, NY: American Institute of Chemical Engineers: 1–15.

Speight, J.G. 1987. Gaseous fuels. *Marks' Standard Handbook for Mechanical Engineers*. E.A. Avallone and T. Baumeister III, eds. New York, NY: McGraw-Hill: 7-18 to 7-20.

Spinks, J.W., and R.J. Woods. 1990. *An Introduction to Radiation Chemistry*, 3rd Edition. New York, NY: John Wiley & Sons.

Stephen, H., and T. Stephen. 1963. *Solubilities of Inorganic and Organic Compounds*, Volume 1. New York, NY: McMillan.

Stewart, C.W., J.M. Alzheimer, M.E. Brewster, G. Chen, R.E. Mendoza, H.C. Reid, C.L. Shepard, and G. Terrpmes. 1996a. *In Situ Rheology and Gas Volume in Hanford Double-Shell Waste Tanks*. PNNL-11296. Richland, WA: Pacific Northwest National Laboratory.

Stewart, C.W., P.A. Meyer, M.E. Brewster, K.P. Rechnagle, P.A. Gauglitz, H.C. Reid, and L.A. Mahoney. 1996b. *Gas Retention and Release Behavior in Hanford Single-Shell Waste Tanks*. PNNL-11391. Richland, WA: Pacific Northwest National Laboratory.

Strachan, D.M. 1991. *Minutes of the Tank Waste Science Panel Meeting February 7-8, 1991*. PNL-7709. Richland, WA: Pacific Northwest Laboratory.

Strachan, D.M. 1992a. *Minutes of the Tank Waste Science Panel Meeting July 9-11, 1991*. PNL-8048. Richland, WA: Pacific Northwest Laboratory.

Strachan, D.M. 1992b. *Minutes of the Tank Waste Science Panel Meeting November 11-13, 1991*. PNL-8047. Richland, WA: Pacific Northwest Laboratory.

Schulz, W.W., and D.M. Strachan. 1992. *Minutes of the Tank Waste Science Panel Meeting March 25-27, 1992*. PNL-8278. Richland, WA: Pacific Northwest Laboratory.

Strachan, D.M., and W.W. Schulz, comps. 1993. *Minutes of the Tank Waste Science Panel Meeting January 12–13, 1993*. PNL-8845. Richland, WA: Pacific Northwest Laboratory.

Stumm, W., and J.J. Morgan. 1981. *Aquatic Chemistry*. 2nd Edition. New York, NY: John Wiley and Sons.

Sullivan, J.C. 1983. Reaction of plutonium ions with products of water radiolysis. *Plutonium Chemistry*. W.T. Carnall, and G.R. Choppin, eds. ACS Symposium Series 216. Washington, DC: American Chemical Society: 241–249.

Sutton, C. and J.A. Calder. 1974. Solubility of higher-molecular-weight normal-paraffins in distilled water and sea water. *Environmental Science and Technology* 8: 654–657.

Sverjensky, D., and P.A. Molling. 1992. *Nature* 356: 231–234.

Tait, C.D., S.A. Ekberg, P.D. Palmer, and D.E. Morris. 1995. *Plutonium Carbonate Speciation Changes as Measured in Dilute Solutions with Photoacoustic Spectroscopy: Yucca Mountain Site Characterization Program Milestone Report 3350*. LA-12886-MS. UC-802. Los Alamos, NM: Los Alamos National Laboratory.

Tananaev, I.V., M.A. Glushkova, and G.B. Seifer. 1956. The solubility series of ferrocyanides. *Journal of Inorganic Chemisty of the USSR* 1: 72–74.

Triay, I.R., C.R. Cotter, S.M. Kraus, M.H. Huddleston, S.J. Chipera, and D.L. Bish. 1996. *Radionuclide sorption in Yucca Mountain tuffs with J-13 well water: neptunium, uranium, and plutonium. Yucca Mountain Site Characterization Program Milestone 3338*. LA-12956-MS. UC-814. Los Alamos, NM: Los Alamos National Laboratory.

Turner, D.R. 1995. *A Uniform Approach to Surface Complexation Modeling of Radionuclide Sorption*. CNWRA 95-001. San Antonio, TX: Center for Nuclear Waste Regulatory Analyses.

Turner, D.A., and Y. Miron. 1994a. *Testing of Organic Waste Surrogate Materials in Support of the Hanford Organic Tank Program - Final Report*. WHC-MR-0455. Richland, WA: Westinghouse Hanford Company.

Turner, D.A., and Y. Miron. 1994b. *Testing of Organic Waste Surrogate Materials in Support of the Hanford Organic Tank Program - Final Supplementary Report.* WHC-MR-0455-Supp.1. Richland, WA: Westinghouse Hanford Company.

Turner, D.A., H. Babad, L.L. Buckley, and J.E. Meacham. 1995. *Data Quality Objective to Support Resolution of the Organic Complexant Safety Issue.* WHC-SD-WM-DQO-006, Rev. 2. Richland, WA: Westinghouse Hanford Company.

U.S. Department of Energy. 1996a. *Tank Waste Remediation System, Hanford Site, Richland, Washington, Final Environmental Impact Statement.* DOE/EIS-0189, Volumes 1-5. Richland, WA: U.S. Department of Energy.

U.S. Department of Energy. 1996b.*Tank Waste Remediation System Privatization Request for Proposals.* DE-RP06-96RL13308. Richland, WA: U.S. Department of Energy.

U.S. Department of Energy. 1996c. *Integrated Data Base Report—1995: U.S. Spent Nuclear Fuel and Radioactive Waste Inventories, Projections, and Characteristics.* DOE/RW-0006, Rev. 12. Washington, DC: U.S. Department of Energy.

U.S. Department of Energy. 1997. *Accident Investigation Board Report on the May 14, 1997, Chemical Explosion at the Plutonium Reclamation Facility, Hanford Site, Richland, Washington.* DOE/RL-97-59, Revision 0. Richland, WA: U.S. Department of Energy.

Vail, T.S. 1994. *Waste Storage in Double-Shell Tanks and Associated Equipment.* CPS-T-149-00010. Richland, WA: Westinghouse Hanford Company.

Wagman, D.D., W.H. Evans, V.B. Parker, R.S. Schumm, I. Halow, S.M. Bailey, K.L. Churney, and R.L. Nuttall. 1982. The NBS tables of chemical thermodynamic properties. *Journal of Physical and Chemical Reference Data* 11, Supplement 2.

Wahl, K.L., J.A. Campbell, S.A. Clauss, K.E. Grant, B.D. Lerner, G.M. Mong, A.K. Sharma, C.E. Petersen, A.J. Saenz, S.A. Bryan, I.E. Burgeson, R.D. Scheele, and R.L. Sell. 1995. *Advanced Organic Analysis and Analytical Methods Development: FY 1995 Progress Report Waste Tank Organic Safety Program.* PNL-10777. Richland, WA: Pacific Northwest Laboratory.

Werner, A. 1907. The constitution of inorganic compounds. *Berichte* 40: 15–69; *Chemical Abstracts* 1: 823.

West, A.S. 1993. Chemical reactivity evaluation: The CCPS Program. *Process Safety Progress* 12: 55–60.

Westall, J.C., and H. Hohl. 1980. A comparison of electrostatic models for the oxide/solution interface. *Advances in Colloid and Interface Science* 12: 265–294.

Westinghouse Hanford Company. 1994a. *Nuclear Criticality Safety Manual.* WHC-CM-4-29. Release 6. Richland, WA: Westinghouse Hanford Company.

Westinghouse Hanford Company. 1994b. *Interim Safety Basis (ISB) for the Hanford High Level Waste Storage Tanks.* WHC-SD-WM-ISB-001, Rev. 0. Richland, WA: Westinghouse Hanford Company.

Westinghouse Hanford Company. 1995a. *Tank Waste Source Term Inventory, 1995*. WHC-SD-WM-ER-400. Richland, WA: Westinghouse Hanford Company.

Westinghouse Hanford Company. 1995b. *Operating Specifications for Watch List Tanks*. OSD-T-151-00030, Rev. B-8. Richland, WA: Westinghouse Hanford Company.

Weston, R.E. Jr., and H.A. Schwarz. 1972. *Chemical Kinetics*. Englewood Cliffs, NJ: Prentice-Hall.

Wiegand, G.H., and M. Tremelling. 1972. The kinetics and mechanisms of the decomposition of potassium cyanide in aqueous alkaline medium. Hydrolysis of the simplest nitrile, HCN. *Journal of Organic Chemistry* 37: 914–916.

Wilhelm, E., R. Battino, and R.J. Wilcock. 1977. Low-pressure solubility of gases in liquid water. *Chemical Reviews* 77: 219–262.

Wirta, R.W., and O.H. Koski. 1957. *Flowsheet No. 1 Cs Isolation and Packaging*. HW-50241. Richland, WA: Hanford Atomic Works Operation.

Wodrich, D.D. 1992. *Operating Specification of Single-Shell Waste Storage Tanks*. OSD-T-151-0013. Richland, WA: Westinghouse Hanford Company.

Wodrich, D.D., G.S. Barney, G.L. Borsheim, D.L. Becker, W.C. Carlos, M.J. Klem, R.E. Vandercook, and J.L. Ryan. 1992. *Summary of Single-Shell Tank Stability*. WHC-EP-0347, Supplement. Richland, WA: Westinghouse Hanford Company.

Wolf, A.P. 1964. The reactions of energetic tritium and carbon atoms with organic compounds. *Advances in Physical Organic Chemistry* 2: 201–277.

Wolfgang, R. 1965. The hot atom chemistry of gas-phase systems. *Progress in Reaction Kinetics* 3: 97–169.

Yamaguchi, T., M.I. Pratopo, H. Moriyama, and K. Higashi. 1991. Adsorption of cesium and neptunium(V) on bentonite. *Proceedings of the Third International Conference on Nuclear Fuel Reprocessing and Waste Management (RECOD '91), Sendai, Japan*. Atomic Energy Society of Japan: 999–1,004.

Yamaguchi, T., Y. Sakamoto, and T. Ohnuki. 1994. Effect of the complexation on solubility of Pu(IV) in aqueous carbonate system. *Radiochimica Acta* 66/67: 9–14.

Zabetakis, M.G., S. Lambiris, and G.S. Scott. 1959. Flame temperatures of limit mixtures. *Seventh Symposium (International) on Combustion, London and Oxford, England*. London, England: Butterworths Scientific Publications: 484–494.

APPENDIX A

CHAPTER 1 SUPPLEMENTARY TABLES OF CONCENTRATION LIMITS FOR LAW/HLW FEED ENVELOPES AND HLW FEED PHYSICAL PROPERTIES

Table A-1. Concentration limits for the A, B, and C LAW feed envelopes to be transferred by the DOE to the contractor for LAW services (U.S. Department of Energy, 1996b)[1]

Chemical Analyte	Maximum Ratio, analyte (mole) to sodium (mole)		
	Envelope A	Envelope B	Envelope C
Al	1.9E-01	1.9E-01	1.9E-01
Ba	1.0E-04	1.0E-04	1.0E-04
Ca	4.0E-02	4.0E-02	4.0E-02
Cd	4.0E-03	4.0E-03	4.0E-03
Cl	3.7E-02	8.9E-02	3.7E-02
Cr	6.9E-03	2.0E-02	6.9E-03
F	9.1E-02	2.0E-01	9.1E-02
Fe	1.0E-02	1.0E-02	1.0E-02
Hg	1.4E-05	1.4E-05	1.4E-05
K	1.8E-01	1.8E-01	1.8E-01
La	8.3E-05	8.3E-05	8.3E-05
Ni	3.0E-03	3.0E-03	3.0E-03
NO_2	3.8E-01	3.8E-01	3.8E-01
NO_3	8.0E-01	8.0E-01	8.0E-01
OH	1.0E+01	1.0E-01	1.0E-01
Pb	6.8E-04	6.8E-04	6.8E-04
PO_4	3.8E-02	1.1E-01	3.8E-02
SO_4	9.7E-03	7.0E-02	9.7E-03
TIC	3.0E-01	3.0E-01	3.0E-01
TOC	<10g/l	<10g/l	10 to 40 g/l
U	1.2E-03	1.2E-03	1.2E-03

[1]Shading highlights differences among the three LAW envelopes. The waste feed will be delivered with a sodium concentration between 3 and 14 M. The insoluble solids fraction will not exceed 5 volume percent of the waste transferred. Trace quantities of radionuclides, chemicals, and other impurities may be present in the waste feed.

Table A-2. LAW envelope radionuclide content (U.S. Department of Energy, 1996b)[1]

Radionuclide	Maximum Ratio, radionuclide (Bq) to sodium (mole)		
	Envelope A	Envelope B	Envelope C
TRU	6.0E+05	6.0E+05	3.0E+06
Cs-137	4.3E+09	6.0E+10	4.3E+09
Sr-90	5.7E+07	5.7E+07	8.0E+08
Tc-99	7.1E+06	7.1E+06	7.1E+06

[1]Shading highlights differences among the three LAW envelopes. Some radionuclides, such as ^{90}Sr and ^{137}Cs, have daughters with relatively short half-lives. These daughters are not listed in this table, but are present in concentrations associated with the normal decay chains of the radionuclides.

Table A-3. HLW feed composition limits for nonvolatile components (U.S. Department of Energy, 1996b)[1]

Nonvolatile Element	g/L		Nonvolatile Element	g/L	
	Minimum	Maximum		Minimum	Maximum
Ag	NE[2]	0.17	Cu	NE	0.15
Al	1.3	4.3	Dy	NE	0.008
Am	NE	0.02	Eu	NE	0.005
As	NE	0.05	F	NE	1.1
B	NE	0.4	Fe	2.6	8.9
Ba	NE	1.4	Gd	NE	0.003
Be	NE	0.02	Hg	NE	0.03
Bi	NE	0.86	K	NE	0.41
Ca	NE	2.2	La	NE	0.8
Cd	NE	1.4	Li	NE	0.043
Ce	NE	0.25	Mg	NE	0.65
Co	NE	0.14	Mn	NE	2
Cr	NE	0.21	Mo	NE	0.2
Cs	NE	0.18	Na	2.3	6.0
Nb	NE	0.003	Si	NE	5.8
Nd	NE	0.53	Sm	NE	0.053
Ni	0.05	0.73	Sn	NE	0.011
Np	NE	0.03	Sr	NE	0.16
P	NE	0.54	Ta	NE	0.008
Pb	NE	0.34	Tc	NE	0.08
Pd	NE	0.04	Te	NE	0.04
Pm	NE	0.03	Th	NE	0.16
Pr	NE	0.11	Ti	NE	0.4
Pu	NE	0.016	Tl	NE	0.14
Rb	NE	0.06	U	NE	4.2
Re	NE	0.03	V	NE	0.01
Rh	NE	0.04	W	NE	0.074
Ru	NE	0.11	Y	NE	0.05
S	NE	0.20	Zn	NE	0.13
Sb	NE	0.26	Zr	NE	4.6
Se	NE	0.16			

[1]Compositions are defined in terms of elemental or anion concentrations based on an overall waste concentration of 31 gram equivalent nonvolatile oxides per liter. Nonvolatile trace components below 0.001 g/L are not shown.
[2] NE = Not estimated

Table A-4. HLW feed composition limits for volatile components (U.S. Department of Energy, 1996b)

Volatile Components	g/L	
	Minimum	Maximum
Cl	0	0.1
CO_3	0.74	9.3
NO_2^-	0	11.2 (total NO_2^-/NO_3^-) as NO_3^-
NO_3^-	0	
TOC	0	3.4
CN	0	0.5
NH_3	0	0.5

Table A-5. Maximum radionuclide composition of HLW feed (U.S. Department of Energy, 1996b)[1]

Isotope	Ci/L	Isotope	Ci/L	Isotope	Ci/L
H-3	2E−05	Cd-115m	6.55E−10	Eu-152	1.5E−04
C-14	2E−06	Sn-119m	1.0E−08	Eu-154	1.6E−02
Fe-55	1.0E−03	Sn-121m	9.0E−06	Eu-155	9.0E−03
Ni-59	1.4E−05	Sn-126	4.8E−05	U-234	7.7E−07
Co-60	3.0E−03	Sb-124	2.61E−09	U-235	3.2E−08
Ni-63	1.6E−03	Sb-126	4.83E−06	U-236	8.2E−08
Se-79	4.2E−07	Sb-126m	3.43E−05	U-238	5.8E−07
Sr-90	3.1E+00	Sb-125	1.0E−02	Np-237	2.3E−05
Y-90	3.1E+00	Te-125m	3.0E−03	Pu-238	1.1E−04
Nb-93m	8.7E−05	I-129	9.0E−08	Pu-239	9.5E−04
Zr-93	1.4E−04	Cs-134	6.8E−03	Pu-240	2.6E−04
Tc-99	4.5E−03	Cs-135	3.0E−05	Pu-241	6.9E−03
Ru-106	2.0E−04	Cs-137	3.0E+00	Pu-242	7.1E−08
Rh-106	2.0E−04	Ba-137m	3.0E+00	Am-241	4.3E−02
Pd-107	4.0E−06	Ce-144	1.0E−04	Am-242	3.1E−05
Ag-110m	1.0E−08	Pr-144	1.0E−04	Am-242m	3.2E−05
Cd-113m	1.09E−03	Pr-144m	1.0E−07	Am-243	5.0E−06
In-113m	1.88E−06	Pm-147	1.6E−01	Cm-242	3.7E−05
Sn-113	1.88E−06	Sm-151	9.3E−02	Cm-244	9.3E−04

[1]Decay products, such as radon from uranium and trace isotopes below 1.0E−09 Ci/L, are not shown.

Table A-6. HLW feed physical properties (U.S. Department of Energy, 1996b)[1]

Property	Design Range
Total solids (wt %) dried at approximately 100 °C	2.5–13
Total equivalent nonvolatile oxides (g/L)	25–100
Slurry density (g/mL)	1.02–1.10
Settled solids (vol %)	7–95
Apparent viscosity (cP at 25 °C) at 10 s^{-1} (50 rpm agitator) at 25 s^{-1} (130 rpm agitator) at 183 s^{-1}	6–94 3–50 1–50
Yield stress (dyne/cm^2)	1–150
Settled solids shear strength after 2 days (dyne/cm^2)	20–200
Heat capacity (cal/g ·°C)	0.79–0.97
pH	>10

[1]The bulk of the HLW feed components are in the form of insoluble suspended solids in an aqueous slurry.

APPENDIX B

**SUMMARY DESCRIPTION OF FLAMMABLE GAS HAZARDS
ASSOCIATED WITH TANK SY-101**

General Background

Since 1942, liquid and solid wastes from the various processes used at the Hanford Site to separate plutonium from uranium and the fission products in spent metallic uranium fuel were sent to single-shell tanks (SSTs) for storage. In the early 1970s, a decision was made to transfer all liquid waste from SSTs to double-shell tanks (DSTs). Before transferring the wastes to DSTs, the wastes were concentrated using crystallizer-evaporators, resulting in a thick slurry, referred to as "double-shell slurry," consisting of a solution high in NaOH, $NaNO_3$, $NaNO_2$, $NaAlO_2$, dissolved organic complexants (EDTA, HEDTA, NTA, HOAcOH, etc.), and other salts (sulfates and phosphates). Wastes from ongoing processes were similarly concentrated, and the aqueous portions were stored in DSTs.

In the mid 1970s, the first crystallizer-evaporator, referred to as 242-S, was constructed and cold tested. In early April 1977, 242-S was tested with radioactive waste, and the product was pumped to tank SY-101 for storage. Shortly after transferring approximately 250,000 gal. (950 m³) of double-shell slurry to tank SY-101, the waste volume began to increase. Later that year, "complex concentrate" waste, which has lower salt concentration compared to double-shell slurry but has high organic content (~ 6 M organic carbon after leaving the evaporator), was added to the tank in an effort to dilute the waste and quench the slurry growth. Three more waste additions were made between 1977 and 1980 (see table B-1). During this time, a crust developed on the top of the liquid waste that grew in thickness. In March 1981, the first cycle of slurry growth and collapse, which was accompanied by release of flammable gas mixtures, was observed. These cycles continued more or less regularly until a mixer pump was installed in July 1993. The gas release events (GREs), many times accompanied by a barometric depression, went through the following stages (McDuffie, 1994):

(i)   An initial increase in ammonia release over a period of hours or days,

(ii)   A sudden increase in liquid level up to several inches,

(iii)   A "rollover" during which high surface movements, surface level drops, and an inversion in tank temperature were observed. This process was accompanied by the gas release and an increase in tank pressure.

Measurements of tank SY-101 waste volume have been taken using both an automatic Food Instrument Company gauge and a manual tape. The gauge and the tape were used to measure the distance from the top of the tank riser to the surface of the waste. The data show considerable fluctuations in the crust height, time between gas releases, and the volume of waste associated with each gas release. Changes in these parameters associated with major gas release events during 1990–1991 are summarized in table B-2. The average decrease in surface level was 7.3 in. (18.5 cm.), corresponding to an average volume change of 2,670 ft³ (75.6 m³). The largest volume change occurred on October 24, 1990, during which the hydrogen concentration in the headspace reached 4.7 percent, a value higher than the LFL for hydrogen in air.

The composition of gases released from tank SY-101 are quite variable, but the major constituents are hydrogen, nitrogen, nitrous oxide, ammonia, and water vapor. Methane is usually only a trace component. Approximate ranges of gas concentrations during an episodic gas release event are listed in table B-3. Following a gas release event, concentrations of hydrogen, nitrous oxide, and ammonia gradually decreased over a period of days to reach levels as low as 10 ppm (vol) hydrogen, 12 ppm nitrous oxide, and 20–25 ppm ammonia (McDuffie, 1994). However, ammonia concentration increased, up to more than 100 ppm, during

Table B-1. Fill record for tank SY-101 (Reynolds et al., 1991)

	Addition 1	Addition 2	Addition 3	Addition 4	Addition 5
Date	April 1977	November 1977	June 1978	August 1978	October 1980
Volume[a]	275.5	365.6	133.3	59.5	231.3
NaOH[b]	3.02	2.10	2.11	4.50	3.76
NaAlO$_2$	1.46	0.994	0.409	3.28	3.59
NaNO$_2$	2.72	1.86	1.10	5.23	5.47
NaNO$_3$	2.72	3.44	3.92	4.88	4.95
Na$_2$CO$_3$	0.8	0.474	0.932	0.002	0.14
Na$_2$SO$_4$	0.07	0.065	0.07	0.805	0.07
Na$_3$PO$_4$	0.152	0.148	0.066	0.123	0.30
TOC[c]	14.52	26.32	34.27	26.6	18.01
Sr-90[d]	0.013	0.16	0.074	0.45	0.005
Cs-137[d]	0.74	1.76	0.28	0.28	1.11

[a]Volumes are in 1,000s of gallons
[b]Concentrations of Na-salts are in moles per liter
[c]Total organic carbon values are in grams of carbon per liter
[d]Radionuclide concentrations are in curies per liter

pronounced drops in barometric pressure. The pronounced barometric effect on ammonia concentration has been interpreted to indicate that the SY-101 wastes could be saturated with ammonia, a gas with relatively high solubility in aqueous systems (McDuffie, 1994).

Information on the chemical constituents of tank SY-101 waste has been determined from chemical analyses of core samples. The weighted average composition for samples taken in December 1991 is listed in table B-4. The predominant radionuclides, Cs-137 and Sr-90, have average concentrations of 360 and 24 μCi/g, respectively (Reynolds, 1993).

Mitigative action has been implemented for tank SY-101 (U.S. Department of Energy, 1996a). This mitigative action involved installing a mixer pump in July 1993 to control the release of flammable gases by providing a more frequent and gradual release of gases. The action reduced the maximum concentration of flammable gas that can exist in the tank and greatly reduced the potential for an uncontrolled gas burn.

Table B-2. Data summary for tank SY-101 gas release events during the period from January 1990 to May 1991

Event Date	Number of Days Since Last Event	Change in Surface Level (in.)	Change in Waste Volume (ft³)
January 1990	109	−7.7	−2,830
April 19, 1990	110	−8.7	−3,200
August 5, 1990	109	−5.2	−1,910
October 24, 1990	80	−10.3	−3,790
February 13, 1991	110	−5.0	−1,840
May 16, 1991	92	−7.0	−2,580
Mean and Standard Deviation	102±13	−7.3±2.0	−2,670±730

Table B-3. Tank SY-101 gas release components, dry basis (McDuffie, 1994)

Gas	Vol %
H_2	30–35
N_2O	25–30
N_2	20–25
NH_3	12–18
CH_4	<1

Table B-4. Overall average composition of tank SY-101 waste samples taken in December 1991 (McDuffie, 1994)

Constituent	wt %
Na	20.7
Al	3.2
Cr (total)	0.41
Cr (VI)	0.002
Ca (acid digest)	0.023
Fe	0.028
K	0.326
Ni	0.015
Zn	0.002
NO_3^-	11.7
NO_2^-	10.5
OH^-	2.47
TOC	1.53
TIC*	0.68
PO_4^{3-}	0.64
SO_4^{2-}	0.40
Cl^-	0.79
F^-	0.03
H_2O	35.5
*Total inorganic carbon.	

APPENDIX C

ENERGY BALANCE CALCULATIONS FOR TANKS
A-101, SY-103, AND SY-101

ENERGY BALANCE CALCULATIONS FOR TANKS A-101, SY-103, AND SY-101

Energy balance calculations were done to approximate the adiabatic increase in temperature that could arise in three Hanford high-level waste (HLW) tanks due to exothermic oxidation of organic compounds. Two double-shell tanks (DSTs) (SY-101 and SY-103) and one single-shell tank (SST) (A-101) were considered in the calculations using tank organic chemical concentrations estimated by Agnew (1997). SY-101 and SY-103 are on the Hanford Flammable/Hydrogen Gas Watch-list, whereas A-101 is on both the Flammable/Hydrogen Gas Watch-list and the High Organic Content Watch-list (Hanlon, 1997).

The calculations were made based on the exothermic reaction enthalpies tabulated in table 3-10 and using the reaction pathway for each organic constituent that produces the greatest amount of energy. The energy output, ΔH_{tot} (kJ), from the organic reactions is:

$$\Delta H_{tot} = \sum m_i \Delta H_i \, , \tag{C-1}$$

where ΔH_i is the enthalpy change (kJ/g) for the oxidation of an organic constituent, i, to form sodium carbonate and water, and m_i represents the total mass (g) of i in the waste. ΔH_{tot} was equated to the sum of (i) the energy, Q_1, required to raise the temperature of the total mass of water, m_w, from $T_1 = 25\ °C$ to 100 °C, (ii) the energy, Q_2, required to vaporize m_w at 100 °C, and (iii) the energy, Q_3, used to heat the produced steam to a final temperature, T_2:

$$Q = Q_1 + Q_2 + Q_3 \tag{C-2}$$

$$Q_1 = m_w c_{p1} (100 - T_1) \tag{C-3}$$

$$Q_2 = x m_w \Delta H_v \tag{C-4}$$

$$Q_3 = m_w c_{p2} (T_2 - 100) \tag{C-5}$$

where c_{p1} is the heat capacity of liquid water (assumed constant at 4.188 J/g-K), x is the weight fraction of water that is vaporized, and ΔH_v is the latent heat of vaporization of water (equal to 2,260 J/g).

If ΔH_{tot} is less than Q_1, insufficient energy is available to raise the temperature to the boiling point of water, and the final temperature T_2 can be calculated from

$$T_2 = \Delta H_{tot}/m_w c_{p1} + T_1 \tag{C-6}$$

If ΔH_{tot} is greater than Q_1 but less than $Q_1 + Q_2$, then the final temperature is 100 °C, and the fraction of water vaporized, x, can be calculated from

$$x = (\Delta H_{tot} - Q_1)/m_w \Delta H_v \tag{C-7}$$

If ΔH_{tot} is greater than $Q_1 + Q_2$, then sufficient energy is available to vaporize all the water (i.e., x=1) and

raise the temperature above 100 °C. The final temperature, T_2, can then be calculated from

$$T_2 = (\Delta H_{tot} - Q_1 - Q_2)/(m_w c_{p2}) + 100 \ ^\circ C \qquad \text{(C-8)}$$

where c_{p2} is the heat capacity of water vapor (which can be assumed equal to 1.897 J/g-K for a rough estimate). For more accurate final temperature estimates, the heat capacity must be considered as a function of temperature and integration must be carried out using:

$$Q_3 = \Delta H_{tot} - Q_1 - Q_2 = \int m_w \ c_{p2}(T) \ dT \qquad \text{(C-9)}$$

and

$$c_{p2}/R = 3.47 + 1.45 \times 10^{-3}T + 1.21 \times 10^4 T^{-2} \qquad \text{(C-10)}$$

where R is the universal gas constant, and T is in Kelvin. Integral limits are 373 K to T_2. Equation C-10 was taken from Smith and Van Ness (1987).

The calculations assumed that all energy from the organic oxidation reactions was converted to thermal energy in water. Although other components in the tank, primarily solids and sludge, would also help dissipate the heat, they were not considered in the calculations. Thus, values determined from the above equations are likely to be significantly higher than would be observed in actuality.

Values of water and organic content of wastes in tanks A-101, SY-103, and SY-101 taken from Agnew (1997) are listed in tables C-1, C-2, and C-3, respectively. Also listed in the tables are the upper and lower 95 percent confidence interval estimates, respectively, of the organic and water content in the tanks. Calculations using these data yield the highest energy of reaction with the smallest water sink to absorb the heat. The results of the energy balance calculations are given in the tables.

Note that the pressure build-up in a closed tank due to the vaporization of water was not included in this analysis, but may need to be considered as a significant hazard in the event of exothermic reactions involving organic species.

Table C-1. Energy balance calculations for tank A-101

Reactive Organic Constituent	Mass of Tank Constituent (kg)[a]	Maximum Reaction Enthalpy (kJ/g)[b]	Calculated Heat of Reaction (kJ)	Upper Estimate of Constituent Mass (kg)[a]	Upper Calculated Heat of Reaction (kJ)
EDTA	2.97e + 04	-11.70	-3.47e + 08	5.02e + 04	-5.87e + 08
HEDTA	5.08e + 04	-14.20	-7.21e + 08	8.97e + 04	-1.27e + 09
Glycolate	2.87e + 04	-5.26	-1.51e + 08	3.95e + 04	-2.08e + 08
Oxalate	8.12e + 00	-4.92	-4.00e + 04	9.01e + 00	-4.43e + 04
Acetate	3.96e + 03	-10.50	-4.16e + 07	5.22e + 03	-5.48e + 07
Citrate	1.85e + 04	-8.02	-1.48e + 08	2.09e + 04	-1.68e + 08
DBP	1.65e + 04	-21.80	-3.60e + 08	2.06e + 04	-4.49e + 08
Butanol	5.80e + 03	-33.40	-1.94e + 08	7.24e + 03	-2.42e + 08
TOTAL ENERGY FROM ORGANICS			-1.96e + 09		-2.98e + 09
Total mass of water (kg)	2.27e + 06[a]			2.15e + 06[c]	
Energy required to heat the total mass of water from 25 to 100 °C, Q_1 (kJ)			7.12e + 08		6.75e + 08[d]
Heat of vaporization of total mass of water, Q_2 (kJ)			5.13e + 09		4.87e + 09[d]
Fraction of water vaporized, x			0.244		0.474
Final temperature, T_2 (°C)			100		100

[a]Taken from Agnew (1997). Total mass of waste is 5.37e + 06 kg.
[b]Taken from table 3-10
[c]Lower estimate of water content taken from Agnew (1997)
[d]Using the lower estimated water content from Agnew (1997)

Table C-2. Energy balance calculations for tank SY-103

Reactive Organic Constituent	Mass of Tank Constituent (kg)[a]	Maximum Reaction Enthalpy (kJ/g)[b]	Calculated Heat of Reaction (kJ)	Upper Estimate of Constituent Mass (kg)[a]	Upper Calculated Heat of Reaction (kJ)
EDTA	1.68e + 04	−11.70	−1.97e + 08	2.86e + 04	−3.40e + 08
HEDTA	2.96e + 04	−14.20	−4.20e + 08	5.21e + 04	−7.40e + 08
Glycolate	2.15e + 04	−5.26	−1.13e + 08	2.80e + 04	−1.50e + 08
Oxalate	1.22e + 01	−4.92	−6.00e + 04	1.36e + 01	−6.69e + 04
Acetate	1.63e + 03	−10.50	−1.71e + 07	1.89e + 03	−2.00e + 07
Citrate	1.56e + 04	−8.02	−1.25e + 08	1.68e + 04	−1.30e + 08
DBP	2.69e + 03	−21.80	−5.86e + 07	3.09e + 03	−6.70e + 07
Butanol	4.30e + 03	−33.40	−1.44e + 08	4.95e + 03	−1.70e + 08
TOTAL ENERGY FROM ORGANICS			−1.07e + 09		−1.60e + 09
Total mass of water (kg)	1.49e + 06[a]			1.37e + 06[c]	
Energy required to heat the total mass of water from 25 to 100 °C, Q_1 (kJ)			4.66e + 08		4.30e + 08[d]
Heat of vaporization of total mass of water, Q_2 (kJ)			3.36e + 09		3.10e + 09[d]
Fraction of water vaporized, x			0.181		0.380
Final temperature, T_2 (°C)			100		100

[a]Taken from Agnew (1997). Total mass of waste is 4.53e + 06 kg.
[b]Taken from table 3-10
[c]Lower estimate of water content taken from Agnew (1997)
[d]Using the lower estimated water content from Agnew (1997)

Table C-3. Energy balance calculations for tank SY-101

Reactive Organic Constituent	Mass of Tank Constituent (kg)[a]	Maximum Reaction Enthalpy (kJ/g)[b]	Calculated Heat of Reaction (kJ)	Upper Estimate of Constituent Mass (kg)[a]	Upper Calculated Heat of Reaction (kJ)
EDTA	3.04e + 04	−11.70	−3.56e + 08	5.23e + 04	−6.12e + 08
HEDTA	5.45e + 04	−14.20	−7.74e + 08	9.59e + 04	−1.36e + 09
Glycolate	4.18e + 04	−5.26	−2.20e + 08	5.55e + 04	−2.92e + 08
Oxalate	2.95e + 01	−4.92	−1.45e + 05	3.29e + 01	−1.62e + 05
Acetate	2.27e + 03	−10.50	−2.38e + 07	2.68e + 03	−2.81e + 07
Citrate	2.98e + 04	−8.02	−2.39e + 08	3.24e + 04	−2.60e + 08
DBP	2.23e + 04	−21.80	−4.86e + 08	2.61e + 04	−5.70e + 08
Butanol	7.87e + 03	−33.40	−2.63e + 08	9.23e + 03	−3.08e + 08
TOTAL ENERGY FROM ORGANICS			−2.36e + 09		−3.43e + 09
Total mass of water (kg)	1.59e + 06[a]			9.93e + 05[c]	
Energy required to heat the total mass of water from 25 to 100 °C, Q_1 (kJ)			4.97e + 08		3.11e + 08[d]
Heat of vaporization of total mass of water, Q_2 (kJ)			3.59e + 09		2.25e + 09[d]
Fraction of water vaporized, x			0.520		1.000
Final temperature, T_2 (°C)			100		436

[a]Taken from Agnew (1997). Total mass of waste is 7.45e + 06 kg.
[b]Taken from table 3-10
[c]Lower estimate of water content taken from Agnew (1997)
[d]Using the lower estimated water content from Agnew (1997)

APPENDIX D

MASS INVENTORY OF U-233, U-235, PU-239, AND PU-241 IN HANFORD HLW TANKS, AND THE FISSILE ISOTOPE ENRICHMENTS OF U AND PU BASED ON THE HDW MODEL (AGNEW, 1996B)

Table D-1. A listing of the fissile nuclide content of the tanks with the uranium and plutonium enrichment in their fissile isotopes, organized by tank farm. Values of the mass of U-233, U-235, Pu-239, and Pu-241 were taken from Agnew (1996b).

Tank	Mass of U-233 (g)	Mass of U-235 (g)	Mass of Pu-239 (g)	Mass of Pu-241 (g)	Uranium Enrichment	Plutonium Enrichment
A-101	1.35E+03	4.02E+04	2.91E+03	3.41E+00	4.68E-03	9.56E-01
A-102	6.19E+01	1.70E+03	2.45E+03	3.86E+00	4.48E-03	9.52E-01
A-103	5.77E+02	1.62E+04	1.02E+03	1.29E+00	4.60E-03	9.55E-01
A-104	2.16E+00	3.20E+02	2.51E+02	2.09E-01	6.77E-03	9.59E-01
A-105	1.47E-06	1.43E+02	2.83E+03	4.68E+00	6.69E-03	9.50E-01
A-106	1.18E+02	4.81E+03	2.29E+04	3.64E+01	5.17E-03	9.52E-01
AN-101	2.72E+02	1.90E+04	7.98E+02	1.12E+00	5.93E-03	9.55E-01
AN-102	2.11E+03	7.77E+04	4.67E+03	6.52E+00	5.05E-03	9.54E-01
AN-103	1.43E+03	8.74E+04	3.78E+03	1.03E+01	6.21E-03	9.46E-01
AN-104	1.25E+03	6.47E+04	2.77E+03	6.44E+00	5.79E-03	9.49E-01
AN-105	2.51E+03	9.99E+04	4.86E+03	8.92E+00	5.31E-03	9.51E-01
AN-106	2.16E+01	8.18E+02	4.49E+01	5.64E-02	5.07E-03	9.55E-01
AN-107	2.18E+03	4.81E+04	3.01E+03	4.16E+00	4.19E-03	9.54E-01
AP-101	5.56E+01	7.86E+03	2.33E+02	9.70E-01	7.39E-03	9.39E-01
AP-102	7.99E+02	3.03E+04	1.66E+03	2.09E+00	5.07E-03	9.55E-01
AP-103	1.35E+01	2.88E+03	2.90E+02	7.82E-01	7.69E-03	9.41E-01
AP-104	0.00E+00	0.00E+00	0.00E+00	0.00E+00	–	–
AP-105	1.47E+02	8.83E+04	2.51E+03	1.10E+01	7.44E-03	9.38E-01
AP-106	2.03E+02	3.21E+04	1.05E+03	4.28E+00	7.47E-03	9.38E-01
AP-107	0.00E+00	0.00E+00	0.00E+00	0.00E+00	–	–
AP-108	2.16E+00	3.68E+03	2.58E+02	9.02E-01	8.44E-03	9.39E-01
AW-101	1.80E+03	1.80E+05	1.32E+04	8.08E+01	7.01E-03	9.30E-01
AW-102	4.06E+02	6.57E+04	1.85E+03	7.97E+00	7.47E-03	9.38E-01
AW-103	5.29E-01	1.18E+05	2.17E+04	1.65E+02	8.65E-03	9.23E-01
AW-104	7.33E-01	7.26E+04	1.42E+04	1.08E+02	8.66E-03	9.23E-01

Table D-1. A listing of the fissile nuclide content of the tanks with the uranium and plutonium enrichment in their fissile isotopes, organized by tank farm. Values of the mass of U-233, U-235, Pu-239, and Pu-241 were taken from Agnew (1996b) (cont'd)

Tank	Mass of U-233 (g)	Mass of U-235 (g)	Mass of Pu-239 (g)	Mass of Pu-241 (g)	Uranium Enrichment	Plutonium Enrichment
AW-105	1.99E+02	1.15E+05	1.72E+04	1.28E+02	8.30E-03	9.24E-01
AW-106	4.61E+02	7.12E+04	2.32E+03	9.44E+00	7.43E-03	9.39E-01
AX-101	1.19E+03	3.38E+04	5.92E+03	8.83E+00	4.59E-03	9.52E-01
AX-102	5.00E+01	1.83E+03	6.68E+03	4.07E+01	5.02E-03	9.11E-01
AX-103	1.36E+02	4.07E+03	3.73E+00	6.05E-03	4.68E-03	3.01E-02
AX-104	5.43E-07	5.27E+01	1.04E+03	1.73E+00	6.68E-03	9.51E-01
AY-101	2.44E+02	1.96E+04	2.59E+04	1.21E+02	6.09E-03	9.23E-01
AY-102	9.26E-01	2.21E+03	8.26E+03	2.28E+01	8.47E-03	9.43E-01
AZ-101	5.98E+01	7.07E+04	2.33E+04	1.76E+02	8.44E-03	9.24E-01
AZ-102	3.10E+00	3.63E+04	3.33E+04	1.19E+02	8.64E-03	9.41E-01
B-101	2.88E-04	6.66E+04	1.22E+04	5.37E+01	6.91E-03	9.26E-01
B-102	6.27E+00	4.31E+04	2.30E+02	1.92E-01	6.91E-03	9.61E-01
B-103	2.29E-04	5.46E+04	1.66E+02	1.90E-02	6.89E-03	9.79E-01
B-104	9.10E-04	1.67E+05	1.40E+03	1.37E-01	6.79E-03	9.80E-01
B-105	3.42E-04	6.61E+04	4.93E+02	5.44E-02	6.84E-03	9.79E-01
B-106	8.22E-01	4.62E+04	3.43E+02	4.00E-02	6.83E-03	9.79E-01
B-107	1.63E-02	2.06E+05	1.67E+02	3.93E-03	6.96E-03	9.84E-01
B-108	2.73E-04	6.66E+04	2.11E+02	2.11E-02	6.91E-03	9.80E-01
B-109	1.30E+02	4.81E+04	2.32E+03	2.43E+00	6.69E-03	9.56E-01
B-110	2.49E-05	6.24E+03	1.55E+03	8.55E-01	6.92E-03	9.71E-01
B-111	2.15E+00	2.83E+03	4.89E+03	6.62E+00	6.71E-03	9.55E-01
B-112	2.33E+02	2.89E+03	1.58E+02	1.23E-01	3.11E-03	9.63E-01
B-201	2.54E-07	5.50E+01	7.47E-01	1.31E-04	6.87E-03	9.77E-01
B-202	2.49E-07	5.32E+01	7.21E-01	1.26E-04	6.86E-03	9.77E-01
B-203	4.56E-07	9.80E+01	1.33E+00	2.33E-04	6.85E-03	9.77E-01

Table D-1. A listing of the fissile nuclide content of the tanks with the uranium and plutonium enrichment in their fissile isotopes, organized by tank farm. Values of the mass of U-233, U-235, Pu-239, and Pu-241 were taken from Agnew (1996b) (cont'd)

Tank	Mass of U-233 (g)	Mass of U-235 (g)	Mass of Pu-239 (g)	Mass of Pu-241 (g)	Uranium Enrichment	Plutonium Enrichment
B-204	4.46E-07	9.62E+01	1.31E+00	2.29E-05	6.85E-03	9.77E-01
BX-101	1.60E+00	3.14E+05	3.51E+03	8.44E+00	6.94E-03	9.44E-01
BX-102	2.11E+01	2.54E+05	7.92E+02	9.13E-01	6.92E-03	9.54E-01
BX-103	3.84E+01	5.92E+05	1.28E+03	1.46E+00	6.93E-03	9.54E-01
BX-104	5.21E+01	4.46E+05	1.75E+02	2.02E-01	6.92E-03	9.57E-01
BX-105	5.40E+00	4.99E+05	2.25E+01	1.65E-02	6.98E-03	9.67E-01
BX-106	4.19E+02	3.74E+04	1.67E+02	2.03E-01	5.87E-03	9.55E-01
BX-107	7.32E-02	4.15E+05	6.63E+02	1.01E+00	6.88E-03	9.77E-01
BX-108	1.40E-04	3.10E+04	5.73E+01	9.68E-03	6.89E-03	9.76E-01
BX-109	2.18E-04	3.90E+04	1.42E+02	2.86E-02	6.80E-03	9.75E-01
BX-110	5.98E+02	1.91E+05	6.23E+02	3.54E-01	6.52E-03	9.68E-01
BX-111	2.55E+03	6.61E+04	1.10E+03	1.22E+00	4.28E-03	9.57E-01
BX-112	1.87E+00	1.62E+05	5.43E+02	1.09E-01	6.80E-03	9.75E-01
BY-101	4.99E+03	4.59E+05	1.95E+03	2.35E+00	5.90E-03	9.56E-01
BY-102	4.46E+03	2.47E+05	1.74E+03	2.10E+00	5.36E-03	9.55E-01
BY-103	5.61E+03	7.44E+04	3.57E+03	4.27E+00	3.23E-03	9.55E-01
BY-104	2.51E+03	3.01E+04	1.00E+03	1.18E+00	3.06E-03	9.56E-01
BY-105	4.80E+03	2.30E+05	1.90E+03	2.26E+00	5.20E-03	9.56E-01
BY-106	7.75E+03	9.11E+04	3.03E+03	3.65E+00	3.03E-03	9.55E-01
BY-107	2.13E+03	5.23E+04	9.22E+02	1.02E+00	4.18E-03	9.57E-01
BY-108	8.98E+02	1.14E+04	3.83E+02	4.28E-01	3.13E-03	9.57E-01
BY-109	5.52E+03	4.54E+05	2.14E+03	2.59E+00	5.81E-03	9.55E-01
BY-110	2.97E+03	7.72E+04	1.31E+03	1.43E+00	4.28E-03	9.57E-01
BY-111	6.17E+03	3.53E+05	2.40E+03	2.90E+00	5.41E-03	9.55E-01
BY-112	4.03E+03	6.89E+04	1.56E+03	1.90E+00	3.63E-03	9.55E-01

Table D-1. A listing of the fissile nuclide content of the tanks with the uranium and plutonium enrichment in their fissile isotopes, organized by tank farm. Values of the mass of U-233, U-235, Pu-239, and Pu-241 were taken from Agnew (1996b) (cont'd)

Tank	Mass of U-233 (g)	Mass of U-235 (g)	Mass of Pu-239 (g)	Mass of Pu-241 (g)	Uranium Enrichment	Plutonium Enrichment
C-101	1.06E+02	8.28E+04	6.70E+03	6.45E+00	6.77E-03	9.56E-01
C-102	1.45E+03	4.32E+05	5.68E+04	7.66E+01	6.86E-03	9.52E-01
C-103	5.76E+01	3.14E+04	3.62E+03	2.63E+00	6.25E-03	9.60E-01
C-104	7.52E+03	3.20E+05	3.73E+04	6.68E+01	7.47E-03	9.49E-01
C-105	1.01E-03	1.09E+05	1.24E+04	8.50E+00	6.51E-03	9.60E-01
C-106	7.66E+00	2.87E+04	1.75E+04	3.63E+01	6.52E-03	9.47E-01
C-107	1.57E+02	3.12E+05	2.16E+04	3.16E+01	6.95E-03	9.52E-01
C-108	1.30E-04	3.66E+04	3.77E+01	1.93E-03	4.03E-03	9.83E-01
C-109	4.61E-05	1.29E+04	1.63E+03	1.65E+00	8.04E-04	9.58E-01
C-110	8.30E-04	2.35E+05	1.92E+02	4.35E-03	6.97E-03	9.84E-01
C-111	2.80E-04	5.83E+04	1.51E+03	1.01E+00	5.79E-03	9.60E-01
C-112	1.16E+01	3.31E+04	1.93E+03	1.60E+00	1.20E-03	9.58E-01
C-201	3.83E-05	1.08E+04	2.29E+02	2.35E-01	6.96E-03	9.57E-01
C-202	7.96E-10	8.14E-02	2.29E+02	2.35E-01	6.67E-03	9.57E-01
C-203	1.53E-04	4.33E+04	2.29E+02	2.35E-01	6.94E-03	9.57E-01
C-204	7.65E-05	2.16E+04	2.29E+02	2.35E-01	6.97E-03	9.57E-01
S-101	2.22E+02	5.27E+04	6.50E+03	3.93E+00	6.56E-03	9.62E-01
S-102	2.71E+02	1.52E+04	8.73E+02	9.54E-01	5.67E-03	9.57E-01
S-103	3.08E+02	1.65E+04	1.08E+03	1.10E+00	5.62E-03	9.57E-01
S-104	1.70E+01	4.19E+04	6.20E+03	3.51E+00	6.95E-03	9.62E-01
S-105	1.95E+02	2.26E+04	9.79E+02	9.65E-01	6.26E-03	9.58E-01
S-106	2.18E+02	6.10E+04	4.30E+03	2.91E+00	6.58E-03	9.61E-01
S-107	9.28E+01	2.71E+05	2.75E+04	3.79E+01	7.71E-03	9.53E-01
S-108	2.64E+02	3.08E+04	1.46E+03	1.46E+00	6.27E-03	9.58E-01
S-109	2.69E+02	4.44E+04	2.59E+03	2.10E+00	6.43E-03	9.60E-01

Table D-1. A listing of the fissile nuclide content of the tanks with the uranium and plutonium enrichment in their fissile isotopes, organized by tank farm. Values of the mass of U-233, U-235, Pu-239, and Pu-241 were taken from Agnew (1996b) (cont'd)

Tank	Mass of U-233 (g)	Mass of U-235 (g)	Mass of Pu-239 (g)	Mass of Pu-241 (g)	Uranium Enrichment	Plutonium Enrichment
S-110	2.61E+02	4.31E+04	5.70E+03	3.45E+00	6.41E-03	9.62E-01
S-111	3.45E+02	4.46E+04	4.52E+03	3.22E+00	6.28E-03	9.61E-01
S-112	2.82E+02	3.59E+04	1.79E+03	1.68E+00	6.31E-03	9.58E-01
SX-101	9.27E+01	1.97E+04	5.36E+03	3.19E+00	6.76E-03	9.61E-01
SX-102	7.57E+02	3.78E+04	3.62E+03	3.19E+00	5.49E-03	9.59E-01
SX-103	7.98E+02	4.76E+04	2.72E+03	2.97E+00	5.73E-03	9.56E-01
SX-104	5.91E+02	3.85E+04	4.77E+03	3.69E+00	5.80E-03	9.60E-01
SX-105	8.33E+02	4.81E+04	3.70E+03	4.38E+00	5.65E-03	9.55E-01
SX-106	6.27E+02	3.32E+04	1.66E+03	1.97E+00	5.60E-03	9.56E-01
SX-107	1.79E+00	2.32E+03	4.02E+03	4.18E+00	7.13E-03	9.56E-01
SX-108	7.69E-06	7.86E+02	3.57E+03	3.39E+00	6.90E-03	9.57E-01
SX-109	2.01E+01	1.76E+04	3.57E+03	3.61E+00	7.20E-03	9.56E-01
SX-110	3.17E+00	3.00E+03	2.98E+03	4.37E+00	7.29E-03	9.50E-01
SX-111	4.44E+00	4.54E+03	5.04E+03	6.24E+00	7.24E-03	9.53E-01
SX-112	2.43E+00	2.70E+03	3.59E+03	4.05E+00	7.18E-03	9.54E-01
SX-113	1.57E-07	1.79E+01	5.75E+01	2.91E-02	6.60E-03	9.62E-01
SX-114	1.41E+01	1.24E+04	4.22E+03	5.65E+00	7.23E-03	9.52E-01
SX-115	6.34E-01	5.92E+02	2.00E+02	1.14E-01	7.13E-03	9.61E-01
SY-101	1.75E+03	8.88E+04	4.70E+03	5.66E+00	5.52E-03	9.55E-01
SY-102	1.89E+01	1.96E+03	4.25E+04	9.99E-02	5.36E-03	9.36E-01
SY-103	9.56E+02	4.46E+04	2.37E+03	2.86E+00	5.40E-03	9.55E-01
T-101	9.95E-01	1.52E+05	1.11E+04	9.89E+00	8.25E-03	9.57E-01
T-102	7.19E+01	3.93E+04	2.69E+03	3.10E+00	6.91E-03	9.54E-01
T-103	7.23E+01	2.86E+04	2.69E+03	3.11E+00	6.87E-03	9.54E-01
T-104	1.94E+00	5.23E+05	1.06E+03	1.97E-01	6.85E-03	9.76E-01

Table D-1. A listing of the fissile nuclide content of the tanks with the uranium and plutonium enrichment in their fissile isotopes, organized by tank farm. Values of the mass of U-233, U-235, Pu-239, and Pu-241 were taken from Agnew (1996b) (cont'd)

Tank	Mass of U-233 (g)	Mass of U-235 (g)	Mass of Pu-239 (g)	Mass of Pu-241 (g)	Uranium Enrichment	Plutonium Enrichment
T-105	1.73E-04	3.18E+04	4.01E+02	2.58E-02	6.81E-03	9.82E-01
T-106	2.15E-04	2.64E+04	1.36E+03	9.26E-01	7.20E-03	9.60E-01
T-107	7.60E-04	2.15E+05	1.75E+02	3.98E-03	6.91E-03	9.84E-01
T-108	1.44E-04	3.63E+04	1.08E+02	1.19E-02	6.90E-03	9.79E-01
T-109	1.29E-04	2.51E+04	2.17E+02	2.89E-02	6.84E-03	9.78E-01
T-110	3.76E-05	9.57E+03	1.66E+03	1.71E-01	6.92E-03	9.80E-01
T-111	3.71E-05	8.42E+03	1.96E+03	3.05E-01	6.88E-03	9.77E-01
T-112	4.20E-06	7.49E+02	2.91E+02	6.21E-02	6.78E-03	9.74E-01
T-201	2.54E-07	5.50E+01	7.47E-01	1.31E-04	6.87E-03	9.77E-01
T-202	1.90E-07	4.12E+01	5.60E-01	9.80E-05	6.87E-03	9.77E-01
T-203	3.17E-07	6.89E+01	9.34E-01	1.63E-04	6.87E-03	9.77E-01
T-204	3.44E-07	7.44E+01	1.01E+00	1.78E-04	6.84E-03	9.77E-01
TX-101	8.78E+00	3.36E+04	3.73E+03	1.05E+00	6.93E-03	9.50E-01
TX-102	2.74E+02	3.21E+04	4.78E+02	5.52E-01	6.30E-03	9.56E-01
TX-103	8.59E+01	4.76E+03	1.60E+02	1.68E-01	5.70E-03	9.58E-01
TX-104	5.84E+01	1.97E+05	1.05E+02	1.17E-01	6.92E-03	9.57E-01
TX-105	8.13E+02	1.17E+05	1.21E+03	1.33E+00	6.40E-03	9.57E-01
TX-106	4.35E+02	2.76E+04	8.08E+02	8.34E-01	5.85E-03	9.57E-01
TX-107	6.67E+00	8.69E+04	1.30E+01	1.31E-02	6.95E-03	9.60E-01
TX-108	1.44E+02	2.67E+04	1.96E+02	2.14E-01	6.54E-03	9.57E-01
TX-109	2.13E-03	4.54E+05	9.19E+02	1.65E-01	6.85E-03	9.76E-01
TX-110	4.70E+02	6.10E+04	9.19E+02	9.58E-01	6.29E-03	9.58E-01
TX-111	3.92E+02	6.38E+04	8.39E+02	8.33E-01	6.37E-03	9.59E-01
TX-112	8.39E+02	4.24E+04	1.34E+03	1.39E+00	5.61E-03	9.58E-01
TX-113	5.33E+02	2.27E+05	1.49E+03	1.11E+00	6.64E-03	9.64E-01

Table D-1. A listing of the fissile nuclide content of the tanks with the uranium and plutonium enrichment in their fissile isotopes, organized by tank farm. Values of the mass of U-233, U-235, Pu-239, and Pu-241 were taken from Agnew (1996b) (cont'd)

Tank	Mass of U-233 (g)	Mass of U-235 (g)	Mass of Pu-239 (g)	Mass of Pu-241 (g)	Uranium Enrichment	Plutonium Enrichment
TX-114	6.01E+02	5.27E+04	1.21E+03	1.14E+00	6.06E-03	9.60E-01
TX-115	7.55E+02	2.89E+04	1.13E+03	1.25E+00	5.32E-03	9.57E-01
TX-116	3.29E+02	1.51E+05	1.59E+03	5.88E-01	6.65E-03	9.73E-01
TX-117	6.14E+02	1.03E+05	1.32E+03	7.18E-01	6.36E-03	9.69E-01
TX-118	1.57E+02	9.76E+03	6.65E+04	3.83E-01	5.78E-03	9.36E-01
TY-101	1.43E-03	2.58E+05	8.21E+02	1.61E-01	6.78E-03	9.75E-01
TY-102	4.27E+01	1.41E+04	1.72E+02	8.43E-02	6.60E-03	9.70E-01
TY-103	6.03E+01	1.58E+05	5.12E+02	1.78E-01	6.77E-03	9.71E-01
TY-104	5.56E-04	9.94E+04	2.72E+02	5.79E-02	6.79E-03	9.74E-01
TY-105	7.51E-06	1.60E+03	6.21E+01	9.69E-03	6.86E-03	9.77E-01
TY-106	2.00E-08	4.24E+00	1.66E-01	2.58E-05	6.87E-03	9.77E-01
U-101	8.42E-04	2.38E+05	4.44E+00	1.01E-04	6.94E-03	9.84E-01
U-102	4.60E+02	4.90E+05	1.14E+03	1.35E+00	6.89E-03	9.56E-01
U-103	5.92E+02	3.75E+05	1.44E+03	1.71E+00	6.79E-03	9.56E-01
U-104	4.12E+01	4.38E+05	1.29E+02	1.16E-01	6.95E-03	9.61E-01
U-105	5.86E+02	3.75E+05	1.44E+03	1.72E+00	6.79E-03	9.56E-01
U-106	3.30E+02	2.98E+05	9.18E+02	1.13E+00	6.82E-03	9.55E-01
U-107	4.11E+02	1.05E+05	8.53E+03	5.15E+00	6.52E-03	9.62E-01
U-108	5.59E+02	1.60E+05	9.90E+03	9.33E+00	7.40E-03	9.57E-01
U-109	5.92E+02	3.20E+05	4.15E+03	3.44E+00	6.77E-03	9.60E-01
U-110	1.64E-03	4.62E+05	1.71E+02	3.88E-03	6.95E-03	9.84E-01
U-111	2.64E+02	3.09E+04	1.11E+03	1.05E+00	6.24E-03	9.58E-01
U-112	1.99E-04	4.67E+04	8.23E+02	4.08E-01	6.90E-03	9.64E-01
U-201	3.75E-05	4.40E+03	3.91E+02	2.04E-01	6.83E-03	9.63E-01
U-202	3.75E-05	4.40E+03	3.93E+02	2.04E-01	6.83E-03	9.63E-01

D-7

Table D-1. A listing of the fissile nuclide content of the tanks with the uranium and plutonium enrichment in their fissile isotopes, organized by tank farm. Values of the mass of U-233, U-235, Pu-239, and Pu-241 were taken from Agnew (1996b) (cont'd)

Tank	Mass of U-233 (g)	Mass of U-235 (g)	Mass of Pu-239 (g)	Mass of Pu-241 (g)	Uranium Enrichment	Plutonium Enrichment
U-203	1.92E-05	2.25E+03	1.98E+02	1.03E-01	6.80E-03	9.63E-01
U-204	1.88E-05	2.20E+03	1.96E+02	1.02E-01	6.83E-03	9.63E-01